University of Neuchâtel (Switzerland) - Faculty of Sciences

Institute of Geology Hydrogeology Center

Advances in karst groundwater protection strategy using artificial tracer tests analysis and multiattribute vulnerability mapping (EPIK method)

Thesis presented to the Faculty of Sciences of the Neuchâtel University for the obtention of the title of Docteur ès sciences

Nathalie Doerfliger

1996

Geologist, graduated from the University of Fribourg, Switzerland

M.Sc. in Hydrogeology at the University of Neuchâtel

9th July 1996

Members of the Thesis jury:

Prof. F. Zwahlen, Thesis director, University of Neuchâtel
Prof.L. Kiraly, member of the jury, University of Neuchâtel
Prof. N. Crampon, member of the jury, University of Lille-Artois, France
Prof. A. Parriaux, member of the jury, EPFL, GEOLEP, Lausanne
Dr. J-P. Tripet, member of the jury, National Hydrological and Geological Survey, FOEFL, Bern

IMPRIMATUR POUR LA THÈSE

De la protection des eaux souterraines en milieu karstique à partir des essais de traçage artificiels et de la cartographie multicritère de la vulnérabilité (méthode EPIK)

de Mme Nathalie DOERFLIGER

UNIVERSITÉ DE NEUCHÂTEL

FACULTÉ DES SCIENCES

La Faculté des sciences de l'Université de Neuchâtel sur le rapport des membres du jury,

MM. F. Zwahlen (directeur de thèse), L. Kiraly, A. Parriaux (Lausanne), J.-P. Tripet (Berne) et N. Crampon (Lille)

autorise l'impression de la présente thèse.

Neuchâtel, le 21 avril 1997

Le doyen:

R. Dändliker

R. Dändliker

To the memory of my mother

Préface

« Tu es la plus grande richesse qui soit au monde, et tu es aussi la plus délicate toi si pure au ventre de la terre » Antoine St-Exupéry (Terre des Hommes).

Remerciements

Je tiens tout d'abord à exprimer mes remerciements aux institutions suivantes pour leur soutien financier et matériel:

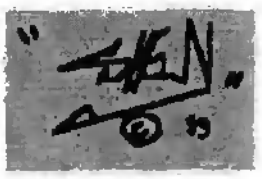

- l'Office fédéral de l'environnement, de la forêt et du paysage (OFEFP) qui e financé un mandat relatif à l'interprétation des essais de traçage en milieu karstique avec l'utilisation d'un modèle boîte noire et une contribution à la recherche dans le domaine de l'hydrogéologie karstique afin de proposer une méthode de cartographie de la vulnérabilité utilisable pour la délimitation des zones de protection.
- l'Office fédéral de la science et de l'éducation (OFES) qui a financé une partie de mon salaire pendant trois ans et demi, ayant assuré des tâches de coordinatrice scientifique de l'action européenne COST 65 relative à la protection des eaux en milieu karstique et également des essais de traçage sur un des sites test, celui de Bure en Ajoie.
- le Fonds National suisse de la Recherche Scientifique qui a financé le projet 20-40419-94, Quantitative interpretation of tracing tests with Bacteriophages in comparison with classical artificial tracers in hydrogeology settings: Karstic and porous aquifers.
- l'Université de Neuchâtel et la République du même nom qui ont financé ces recherches en contre partie du travail d'assistanat que j'ai fourni pendant 3 ans et tout particulièrement le Centre d'Hydrogéologie pour m'avoir accueillie dans son équipe de recherche.

Je remercie sincèrement les personnes qui ont permis la réalisation de ce trevail de recherche

- M. le professeur François Zwahlen, directeur du Centre d'Hydrogéologie et directeur de thèse pour l'intérêt et l'enthousiasme qu'il a montrés pour ces recherhces, sources de motivation et d'encouragement.
- M. le professeur Laszlo Király, directeur de recherche, pour m'avoir suggéré de travailler sur l'interprétation des essais de traçages en milieu karstique par une approche originale, pour ses maintes réflexions et encouragements pour la valorisation des résultats et ses nombreuses suggestions.
- M. le professeur N. Crampon de Lille - Béthunes (France) pour avoir accepté d'être membre du Jury ainsi que M. le professeur A. Parriaux de l'EPFL (Lausanne).
- M. Dr. J-P. Tripet du Service Hydrologique et Géologique National (SHGN) pour avoir été à l'origine de ces projets soumis comme mandats au CHYN, pour avoir accepté d'être membre du Jury et pour avoir toujours porté un vif intérêt aux travaux lors des séances de coordination.
- M. le professeur Imre Müller, requérant principal du projet fonds national sur l'utilisation des bactériophages en milieu karstique en vue d'une interprétation quantitative, pour son enthousiasme vis-à-vis de l'utilisation des bactériophages en hydrogéologie.
- M. le professeur Aragno, directeur du laboratoire de microbiologie de l'université de Neuchâtel co-requérant du projet du fonds national susmentionné, pour avoir mis à disposition son laboratoire ainsi que du personnel qualifié.
- MM. B.Meylan et D. Hartmann de la division pêche et eaux de l'OFEFP pour l'intérêt qu'ils ont apporté au développement de la méthode EPIK et pour nous avoir fait confiance.
- M. Dres Wildberger, Jürg Zobrist, P-Alain Gretillat et G. della Valle (géologue cantonal de Berne), tous quatre membres du groupe de travail karst de la société suisse d'hydrogéologie pour leurs réflexions pertinentes et motivantes lors des séances au SHGN trois à quatre fois par année.
- les bureaux de géologie hydrogéologie conseils tels que le Bureau Clavien à Sion, le bureau MFR SA à Delémont et Bienne et le bureau Dr. von Moos AG á Zürich pour la mise à disposition de données de traçage.

- MM. Joël Pape et Joseph Neppez, agriculteurs au Maira pour les précieux et nombreux trajets de bossettes d'eau nécessaires aux assais de traçage et les nombraux coups de main sur le terrain per tous las temps. Merci pour l'accueil cheleureux de cette région.

Mes sincères remerciements à Fiona Bradford pour evoir corrigè l'anglais de ce manuscrit, ainsi qu'à Keith Kennedy. Leurs contributions ont ètè fort précieuses pour le compréhension du texte. Many many thanks.

Mes remarciements vont ègalement è toutes las personnas du CHYN et du leboratoire de Microbiologie de l'Université de Neuchâtel, sans qui ce travail n'aurait pas vu le jour:

- Olivier Atteia, un grand merci pour les nombreuses critiques lors des relectures de ce manuscrit sens lesquelles il ne serait pas ce qu'il est. Merci d'avoir montré un vif intérét au sujet et émis de nombreuses suggestions quant à l'interprétation et la mise en valeur des résultats.
- Un grand merci également tout particulièrement à Etienne Tâche et á Patrick Adatte pour leur précieuse collaboration dans la phese de test de la méthode EPIK, sur le terrain, sur la table é dessin et á digitaliser, tout comme darrriére l'ordinateur.
- Pierre Rossi pour m'avoir passè le témoin concernant l'utilisation des bactériopheges en miliau karstique et montré un grand enthousiasme vis-à-vis das résultats et promulgué de nombreux encouragements.
- Catharine Gerber, Tong Ettlin pour les analyses des traceurs fluorescents eu CHYN et Magali Grob pour les nombreuses analyses microbiologiques des phages, prèparation, titration et comptage: sans vous les résultats seraient inexistants. Un grand merci pour tout ce travail effectué.
- François Bourret pour les aspects techniques liés aux appareils d'acquisition da données sur le site de Bure.
- Pierre Schnegg et Roberto Costa pour le développemant du fluorimétre de terrain, instrument extrêmement précieux pour les futurs essais da treçage en vue d'una meilleure compréhension des phénomènas de trensport.
- Pierre-Yves, Laurent, Pascal, Denis, Ronald, Reto, Willi, Darko, Olivier, Mahmoud, pour diverses discussions, aides, journées sur la terrain, coups de mains d'ordre informatique, discussions, etc...,sans oublier, Mageli, Elisabeth, Sylvie, Sabina et Michéle pour las pauses cafés, ô combian utiles.
- Un merci tout particulier à ma famille: á mon pére, à Sabine et Bernard at laurs enfants - Aymeric, ton aide sur le terrain, du haut de tes trois ans, m'a été précieusa - : votre présence à vous tous a été source de plus d'un seul encouragament lors de mes visitas éclaires é Fribourg.
- Un merci é tous mes amis qui par le temps d'un souper (une fondue !), d'une partie de squash, de quelques kilomètras de course à pieds en forêt,..., ou d'une rèunion d'Amnesty Intemational ont su me donnar du courage, de la motivation...

ABSTRACT

Key words: Groundwater protection; karst aquifers, artificial tracer tests, input-response model, transfer functions, parametric conceptual model, vulnerability, multiattribute overlay method.

Karst groundwater protection is a major issue in environmental concern at the end of the 20th century. Karst areas provide large quantities of water for water supply at springs and wells in Europe as well as in Switzerland. Karst environment can be troublesome water sources in certain cases, due either to an accident in a very sensitive area or also to inappropriate protection zones and corresponding regulations.

Karst aquifers are characterized generally by on the one hand, highly heterogeneous structure with the existence of a high hydraulic conductivity karst network more or less connected, developed and surrounded by an important volume of fissured rocks with a low hydraulic conductivity. On the other hand, diffuse and concentrated infiltration with limited filtering and auto-purification action of the contaminants occurs.

In matter of karst groundwater protection, therefore, specific strategy has to be developed as required by the Federal Office of the Environment, Forest and Landscape and the dependent Swiss National Hydrological and Geological survey. Two approaches referring to specific conceptual models had been used in the framework of this thesis in order to answer to the following questions on the one hand: does exist a mean transfer function based on artificial tracer tests, that characterizes a given water catchment basin or a part of it and can we use this transfer function to establish some contaminant predicting scheme in the framework of a hydrogeological impact assessment ? And on the other hand, to suggest an appropriated method to outline the groundwater protection zones of karst water catchment basin, as concentric protection zones are not suitable in karst environment due to its specific hydrological features.

Considering the tracing-system (tracing pathway) as an input-response model (black box model), artificial tracer tests are interpreted in terms of transfer functions - impulse response and / or indicial response. The transfer function as impulse response is obtained by deconvolution of the tracer breakthrough curve by its corresponding input function. The indicial response corresponds to the convolution of the impulse response by a step-unit function. In order to determine mean transfer function to specific parts of a water catchment basin or the whole water catchment basin, a study of variability of the transfer functions by variance and multivariance analyses on the gradients at given percentiles of the indicial response and on the modal velocity based on around 100 artificial tracer tests (fluorescent dyes, NaCl salt) carried out in various karst aquifers in Switzerland (Tabular and Folded Jura, Alps (Helvetic realm)) and in various hydrological conditions has been led to, determine the validity of a mean transfer function. The following parameters had been taken into consideration in the variance analysis: geological context, water catchment size, injection site's nature, hydrological conditions, tracing distance and discharge level.

Results of this variability study show that mean transfer functions for a water catchment basin do not exist ! No significant difference of the considered parameters is relevant. Nevertheless, mean transfer functions from tracer tests corresponding to a given geological context or to a given injection point's nature can be differentiated. The validity of the transfer functions intra-water catchment basin is important and depends principally to the injection sites. At the scale of a water catchment basin, tracer tests are not the single tool used to protect the groundwater: a multiattribute approach has to be applied to assess the vulnerability.

In order to outline groundwater protection zones of a water catchment basin an input-response method for tracing-pathway characterizing is not sufficient. An original multiattribute approach based on a parametric conceptual model of the karst aquifer, the EPIK method has been specifically developed for outlining and rating the water catchment basin taking into account the groundwater sensitivity to all kinds of contaminants. EPIK for Epikarst, Protective cover, Infiltration conditions and Karst network development has been applied on two test-sites in the Swiss Jura (St-Imier's springs water catchment basin in the Folded Jura and the Font, Saivu and Bâme's water catchment basin in the Tabular Jura (Bure)) to assess the vulnerability. The resulting vulnerability maps were the basis for outlining the groundwater protection zones according to the Swiss water and environment regulations.

By applying this method on these two test-sites using a GIS, it appears that outlining karst groundwater protection zones from the multiattribute vulnerability mapping is feasible in a reasonable time invest. If the weighting of key attribute into protection factor appears to be logical, the obtained values may dangerously hide the weakness of the method in a simple index. Although the concept underlying these new vulnerability mapping approach is clear nowadays, further developments are still needed to appreciate fully its pertinence, specifically regarding the epikarst, the protective cover attributes and the validation of the weighting system that is still problematic. On critical points in a water catchment basin, tracer tests may be carried out.

In the framework of hydrological impact assessment, it remains useful to carry out repeated tracer tests, at least three, in various and/or extreme hydrological conditions to define characteristic transfer functions, used to establish contaminant forecasting.

RESUME

Mots-clefs: *Protection des eaux souterraines, aquifères karstiques, essais de traçage, fonctions de transferts, vulnérabilité, méthode multicritère.*

A la fin du 20ème siècle, la protection des eaux souterraines d'origine karstique représente un domaine clef s'inscrivant dans le domaine de l'environnement. Les aquifères karstiques contribuent par une quantité d'eau considérable de sources ou captages à l'approvisionnement en eau des communes de Suisse, d'Europe et de part le monde. Ces ressources karstiques peuvent être fregiles dans certains cas, soit dues è un accident dans une zone perticullèrement sensible ou soit è une protection inedaptée - zones de taille et degré inadéquats - .

Les aquifères karstiques de part leur structure spécifique, leur mode de recharge et leur fonctionnement hydrogéologique en découlant, exigent un concept de protection des eaux souterraines tout à fait spécifique. Cette thèse contribue ainsi au développement de cette stratégie de protection telle que requise par l'office fédéral de l'environnement, la forêt et le paysage (OFEFP) et le service hydrologique et géologique national (SHGN). Des réponses aux questions suivantes sont développées dans ce travail: i) existe-t-il une fonction de transfert moyenne établie è partir des essais de traçage, qui caractérise un bassin d'alimentation d'une source ou une partie de celui-ci et ii) peut-on utiliser cette fonction de transfert pour simuler des scénarios de contamination dans le cadre d'étude d'impect ? iii) comme les zones de protection concentriques ne sont pas définissables en milieu karstique, peut-on développer une méthode appropriée pour délimiter les zones de protection en milieu kerstique ?.

Afin de répondre è ces premières questions, quelques 100 essais de traçage ont été effectués dans différents aquifères karstiques en Suisse (Jura tabulaire, Jura plissé et Alpes (domaine helvétique)) et interprétés en termes de fonctions de transfert - réponses impulsionnelles et indicielles - le système traçage étant considéré comme un modèle de type input-réponse. Pour déterminer une fonction de transfert moyenne pour des zones spécifiques ou la totalité d'un bassin d'elimentation, une étude de la variabilité des fonctions de transfert par analyse de la variance et multivariance a été effectuée prenant en considération les variables suivantes: le contexte géologique, la taille du bassin d'alimentetion, la nature du point d'injection, les conditions hydrologiques, la distance de treçage et le débit.

Les résultats de cette étude de la variabilité montrent que des fonctions de transfert moyennes ne peuvent pas être différentiées d'un bassin d'elimentetion è l'autre. Cependant, les fonctions de transfert des essais de traçage relatifs è un contexte géologique ou è la nature du point d'injection peuvent être différentiées. La variabilité des fonctions de transfert à l'intérieur d'un bassin d'alimentation est importante et dépend essentiellement du point d'injection. Par conséquence, dans le cadre d'étude d'impact, il reste toujours nécessaire d'effectuer des essais de traçage répétés, au moins trois, dans des conditions hydrologiques différentes et / ou extrêmes efin de déterminer des fonctions de transfert spécifiques au système-traçage. Du fait de l'importance du poids du point d'injection dans le variabilité des fonctions de transfert, il appareît nécessaire de cartographier les risques potentiels de contamination en relation avec les structures du karst event de procéder è des essais de traçage.

Une approche multicritère basée sur un modèle conceptuel de type paramétrique de l'equifère karstique a été développée pour délimiter des zones de protection prenant en considération la sensibilité à tout type de contaminant de l'aquitère. La méthode EPIK repose sur quatre critères choisis en intégrant les derniers développements de la recherche de l'hydrogéologie karstique, présentés dans la première partie de cette thèse. Les quatra critèras sont l'Epikarst, la couverture Protectrice, les conditions d'Infiltration et le développement du réseau Karstique. Cette méthode a été appliquées sur deux sites dens le Jura suisse (St-Imier et Bure) afin de cartographier la vulnérabilité. Les cartes résultantes ont servies de base pour délimiter les zones de protection en accord avec la législation suisse.

L'application de cette méthode en utilisant un SIG (système d'information géographique) sur ces deux sites-pilotes montre que le délimitation des zones de protection prenant en considération les particularités du karst est faisable avec un investissement en temps raisonnable. Si l'essentiel des carectéristiques du fonctionnement hydrogéologique du karst a été regroupé autour de quatre critères, leur définition reposent sur la recherche en hydrogéologie karstique, la caractérisation de l'épikarst et de la couverture protectrice ont été simplifiées et ceci pour des raisons pratiques. Des recherches supplémentaires dans ces domaines sont encore nécessaires. Le système de pondération et de classificetion peut toujours être remis en question et est difficilement validable. Cependent les facteurs de protection résultant sont classés de manière è refléter l'expérience des personnes travaillant dans le milieu karstique. Une validation finale est souheitée et peut être effectuée de meniére ponctuelle, telle qu'elle a été faite sur les sites-pilotes, è l'aide d'essais de treçage et d'investigation géophysique. La dernière validation de la méthode est inévitablement, la mise en vigueur des zones de protection avec les règlements correspondants ainsi que le contrôle de la qualité de l'eau aux sources concernées.

TABLE OF CONTENTS

General introduction

Chapter 1

Objectives of the thesis

Karst groundwater protection is a major issue of environmental concern at the end of this century. Karst areas provide large quantities of water at springs and wells. These water sources can be severely impacted and at risk following accidents (liquid manure spill, gasoline tank spill) in sensitive areas and due to inappropriate protection zones and regulations.

The karst aquifer is characterized as a **highly heterogeneous structure** with a karst network connected and developed inside the aquifer. The karst network has a high hydraulic conductivity surrounded by a block-type large volume of low hydraulic conductivity fissured rocks. **Diffuee or concentrated surface-recharge** is unique to karst aquifers. Consequently, rapid and concantrated infiltration occurs with which there is only limited filtering and purification of contaminants.

Therefore, a karst aquifer requires a specific subsurface water protection strategy. As used in this thesis, subsurface water protection refers to either hydrogeological impact assessments in karst areas or to dafinition of groundwater protection zones.

Hydrogeological impact assessments in karst areas use various methods including artificial tracer tests. These assessments state the potential of contamination risk related to the activities ongoing in that area. Artificial tracer tests are used to simulate contaminant transport under variable hydrological conditions and from one point to another. To predict transit velocity, the peak concentration and the duration of a contaminant can be estimated analyzing the results of repeated tracer tests provided that the results are for the same tracer system responding under various hydrological conditions (Smoot et al., 1987). Away from this tracer system, another group of tracer tests has to be performed to predict the contaminant transport in the entire or a different karst system. Due to cost, there is commonly little possibility of doing enough tracer tests to adequately characterize the system. However, a tracer system can be characterized using **transfer functions** from **input-response interpretations** of a single tracer test. This is done using a method called deconvolution. In this case, a mean function characterizing a specific part of an aquifer could be used to simulate pollution with error factors.

A statistical approach was used to study the **variability of transfer functions** based on about 100 tracer test experiments done in various karst aquifers of different sizes, geological contexts and hydrological conditions. The validity of this mean transfer function is one of the two major themes of this thesis.

Concentric protection zones are not suitable for karst aquifers. These aquifers can be described with a **deterministic conceptual model** that establishes attributes such as the epikarst (upper part of the aquifer-fissured and well karstified), the protective cover, the

surface recharge conditions and the extent of the karst conduit network development. Each of these attributes contributes to the vulnerability or the protection degree of a part of an aquifer. Based on this conceptual model, a **new multi-attribute approach to assess the vulnerability of the catchment area** of a spring or a well is has been created. The assessment of vulnerability requires the use of an overlay mapping method and a rating system. The resulting vulnerability mapping is a useful tool to define protection zones. This issue is the second major theme of this thesis.

Both issues address specific requirements of the Federal Office of the Environment, Forest and Landscape (FOEFL) and of the associated Swiss National Hydrological and Geological Survey (SNHGS).

Transfer function variability

The research focused on conducting numerous tracer tests in karst aquifers, and using a **black-box model** to calculate, by deconvolution, the transfer function for any of these tests. No software development was required for this research.

The major goal of this part of the work concerned answering the following questions using the data from about 100 tracer tests done mainly in Switzerland:

- Do transfer functions vary according to either catchment size or hydrologic condition (base flow, rising or fall limb)?
- Do transfer functions vary at the aquifer scale or for groups of karst aquifers (geological context)?
- Can mean transfer function be used to accurately and consistently simulate accidental contamination of catchments under specific hydrological conditions?

Transfer function variability can also improve the knowledge of the karst aquifer by determining:

- what knowledge of the karst aquifer and its internal structure can we gain from studying and determining tracer test transfer function variability?

To answer these questions, repeated tracer tests in similar and variable discharge conditions were done. Their variability was studied using transfer functions. To obtain information about the intamal karst structure of the aquifer and the variance of the tracer system, Dzikowski's model CONVOX was used.

In addition, a series of tracer experiments with simultaneous injections of conventional tracers (fluorescent dyes or salt) and microbiological tracers (bacteriophages) were done at three test-sites in the Swiss Jura. Data from these tests were used to compare the resulting breakthrough curves and transfer functions.

Studying transfer function variability identified significant factors including injection points, geological context and hydrological conditions. In this manner, the work contributed to the groundwater protection assessment of specific tracer systems.

Karst aquifer vulnerability mapping

An input-response analysis of tracer systems is not adequate to define catchment protection zones for given karst springs . The spatial dimension has to be considered.

The E P I K method (Epikarst, Protective cover, Infiltration condition and Karst network development) is an unique multi-attribute approach that was developed specifically to define and rate karst catchments. This method takes into account groundwater sensitivity to all contaminants. The approach is based on a relatively typical conceptual model of a karst aquifer (Chapter 2.2. Part I). The approach was developed with the contribution of the Federal Office of Environment, Forest and Landscape (FOEFL) and with the Swiss participation in the European COST Action 65 [Hydrogeological aspects of groundwater protection in karst areas].

Since the seventies, vulnerability maps, mostly at the scale of a country or a province, have been established in many countries of Europe and in the North America. Karst aquifers have been characterized relative to other hydrogeological settings. They are considered more vulnerable than fissured and porous media aquifers. Assessment of the sensitivity of karst spring or well catchments by defining typical attributes is a new approach in vulnerability mapping.

The aim of the research was to produce intrinsic vulnerability[1] maps for springs or wells in a catchment. The resulting vulnerability maps are tools to assist in defining the groundwater protection zones in such cases where the present guidelines to define the protection areas in karst environment are not satisfactory.

The explanation of both the approach based on theory and a weighting system is evaluated using two test site examples in the Swiss Jura - St-Imier (Folded Jura) and Bure, La Milandrine (Tabular Jura).

[1] *Intrinsic vulnerability: vulnerability is an intrinsic or natural property of a groundwater system. This is a general property used for characterizing, with the help of geological and hydrogeological information, the sensitivity of aquifer systems to either an instantaneous (point source) or diffuse contaminant release.*

"General or intrinsic vulnerability" is defined only using hydrogeological factors. The term "specific" vulnerability is used when including potential human impacts on the system. The specific aspect of the vulnerability relates to characteristics of the contaminant and the aquifer properties that play a role in its fate and transport.

Chapter 2

Data base

This chapter describes how the data were used to assess transfer function variability and to validate the EPIK overlay method depicting karst aquifer vulnerability.

2.1. Data for interpreting artificial tracer tests - transfer function variability - .

The greatest number of tracer tests interpreted with a black box model were carried out by the author and other colleagues of the Center of Hydrogeology as part of the Swiss program of COST action 65 at the Bure test site. On the same test site, repeated and double tracer tests using salt (NaCl) and microbiological tracers (marine and fresh water) were done as part of the FN project (number 2000 -040419.94/1.). Some data from tracer test breakthrough curves were provided by R. Attinger in the Alpstein (Attinger, R.,1988). Other test data were from contract work done by geological and hydrogeological consultants (MFR SA, Delémont, Bureau F.Clavien, Sion). Other data came from repetitive and double (fluorescent dye, microbiological tracers) tests done in the L'Areuse spring catchment that were carried out with financial support from the Swiss National Hydrological and Geological Survey (SNHGS) of the Federal Office of the Environment, Forests and Landscape (FOEFL).

2.2. Data for validating vulnerability mapping .

Testing the validity of intrinsic vulnerability mapping was done at both the St-Imier township springs catchment (Folded Jura) and the La Milandrine, La Font, Le Saivu and La Bâme springs in Ajoie (Tabular Jura). Maps of the three principal attributes were made. Tracer tests and geophysical measurements were done with two colleagues, Patrick Adatte and Etienne Tâche. These activities set up the basis of the new vulnerability mapping approach to Swiss karst environments at a catchment scale.

At the first test site, St. Imier, activities were carried out with the support of Canton Bern, St-Imier township and with the collaboration with GEOTEST Consulting (Zollikofen). GEOTEST was contracted to review protection zone activity because of periodic liquid manure contamination at the La Raisette spring.

We chose Bure-Milandrine in Ajoie as the second test site because of the large data base for hydrology, geophysics, boreholes and tracer tests from various research projects (FN and COST 65) and the N16 national road contract. The springs of this water catchment basin are not used directly for water supply with the exception of Saivu and La Font which from time to time are used in summer to artificially recharge the L'Allaine porous aquifer in Boncourt.

Chapter 3

Thesis structure

This thesis consists of an introduction, three detailed parts and a conclusion. Part I contains the theoretical principles related to the specifics of karst aquifer hydraulic behavior that are needed to interpret tracer tests or to map the intrinsic vulnerability in karst aquifers (Figure 1). This part also establishes the reference base upon which the following parts are built.

Chapter 1 of Part II provides a review of the classical qualitative and quantitative interpretation of artificial tracer tests in karst aquifers. Part II emphasizes transfer function variability. This work was based on tracer experiments carried out with variable hydrologic conditions, types of karst aquifers and injection points. A comparison is also made of breakthrough curves and transfer functions from tests using classical tracers (salts such as NaCl, and fluorescent dyes) and microbiological tracers (marine and fresh water bacteriophages).

Part III relates to the intrinsic vulnerability mapping of karst aquifers. An approach is developed that is based on a multi-attribute method in concurrence with a deterministic conceptual model that was defined in Part I. The concept of mapping the aquifer vulnerability, the EPIK method, is explained in theory based on references to previous research. Two examples are used to indicate both the validity and the limitations of the multi-factor approach as a tool to define the karst aquifer catchment protection zones.

The conclusions include a summary of the major results and address the contribution of input-response models to validating vulnerability or protection zones.

Finally a contribution to the development of groundwater protection strategy in karst aquifers is suggested.

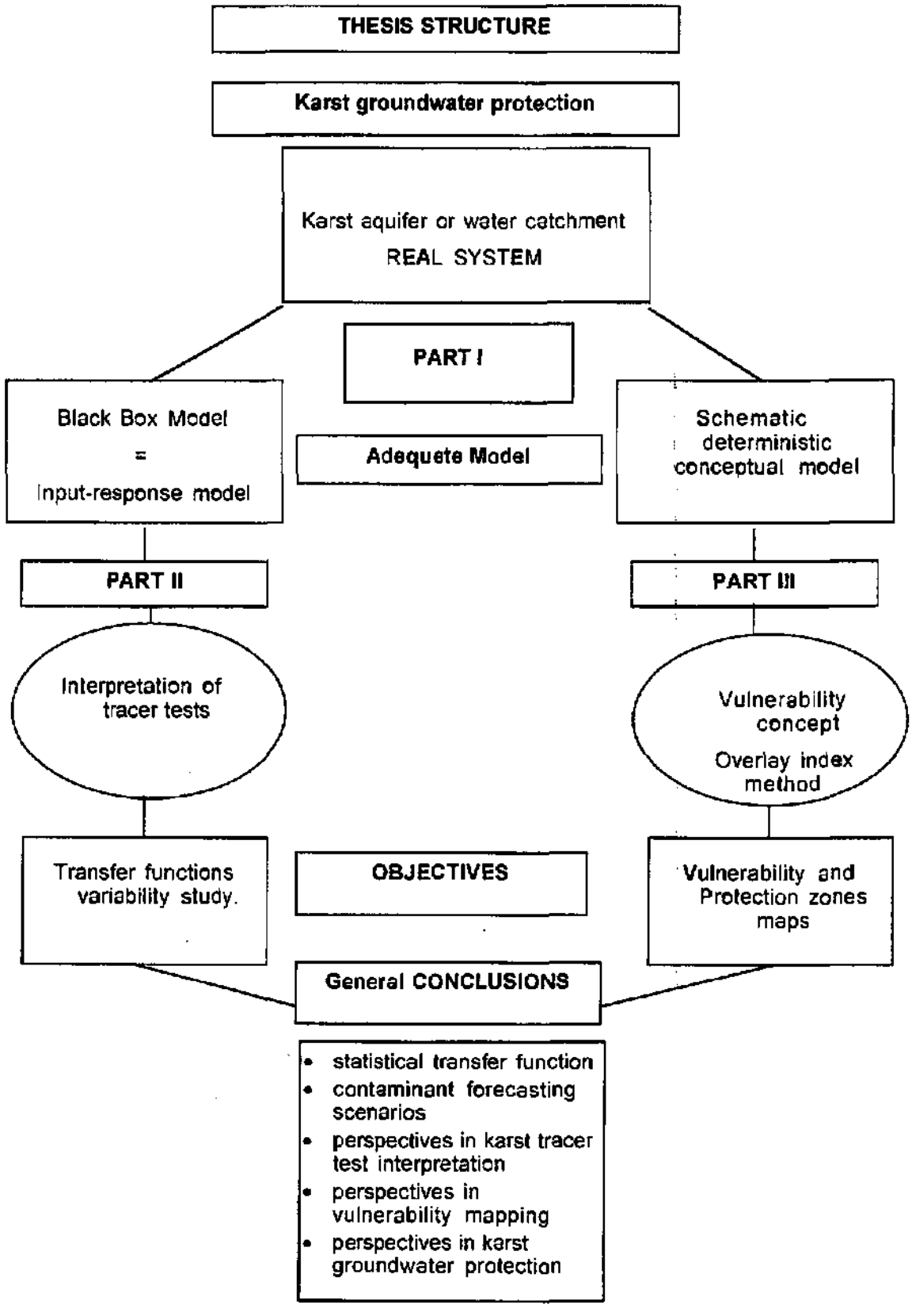
THESIS STRUCTURE
Karst groundwater protection
Karst aquifer or water catchment
REAL SYSTEM
PART I
Black Box Model
=
Input-response model
Adequate Model
Schematic deterministic conceptual model
PART II
PART III
Interpretation of tracer tests
Vulnerability concept
Overlay index method
Transfer functions variability study.
OBJECTIVES
Vulnerability and Protection zones maps
General CONCLUSIONS
• statistical transfer function
• contaminant forecasting scenarios
• perspectives in karst tracer test interpretation
• perspectives in vulnerability mapping
• perspectives in karst groundwater protection

Part I

Theoretical principles of karst hydrogeology and pertinent interpretation models

Chapter 1

Karst aquifers features

Karst is a German word derived from Serbo-Croatian that means stone. It is also the geographical name of a specific limestone terrain region located between Trieste and Ljubljana in Slovenia (Dodge, 1982). Finally, it characterizes a particular morphology that has a specific hydraulic behavior found in geological layers with high rock solubility, such as limestone.

A karst aquifer is defined by Castany and Margat (1977) as an aquifer whose conditions and behavior correspond to karst conditions[1]: heterogeneity, discontinuity, predominance of groundwater flows in channels and conduits of a large size collecting or distributing the water, existence of large cavities. Thus, karst aquifers are characterized by a heterogeneous and contrasted hydraulic conductivity field. The largest part of the aquifer contains low permeability fissured carbonate rock volumes; and within those volumes, there is a network of conduits that are more or less connected and developed. Karst has a hierarchical structure of voids and consequently of flows (Mangin, 1994). This network of conduits behaves either as a discharge form, or as a recharge to, the low permeability rock volume « system », depending on the hydrological conditions. Under base flow conditions, the hydraulic potential may be commonly lowered around the conduits. Consequently, the flow vector is oriented towards the conduits. Therefore, the conduits drain the water from the less permeable rock volume. Under high water level conditions, during the rising limb and falling limb, the hydraulic potential is higher in the channels than in the surrounded blocks. Under these conditions, the flow vector is towards the blocks and the water is drained out the channels to the fissured rocks volume.

The storage capacity and transmissivity of karst aquifers differ throughout the system. The low permeability rock volumes mainly store the water, and it is transmitted under relatively slow drainage conditions into the channel, conduit and cavity network which according to Mangin (1986), is more highly transmissive.

[1] *Karst: according to Paloc (1975) a carbonate rock area with typical surface and subsurface features.*

The karst aquifers are different from porous media aquifers with their morphological features and their particular hydraulic phenomena as pointad previously by several authors and recently summarized by Jeannin et al. (1993).
The major features of karst aquifers are summarized in the following three sections.

1.1. Morphological features

Typical morphological figures such as dolines (swallow holes), karrenfields, dry valleys, poljes (large flat closed depressions or basins) and ouvalas (coalescent dolines) are features of the exokarst. They result from limestone dissolution driven by water infiltration , the bio-chemical and physical processes and the tectonic setting. The intense and high volume of water infiltration in a karst environment allows sinkholes to develop at which point surface water disappears rapidly. The absence of surface drainage may correspond to areas such as dry valleys; areas that may have previously possessed a river that infiltrated and disappeared due to tectonics, dissolution, and the hydrological and climatic conditions.

Shafts and surface water drainege sinkholes (points at which there is concentrated water recharge) allow us to imagine what the underground karst morphology, the endokarst, must be like, whether or not it is accessible by humans. There are channels, conduits, pits, chimneys, covered more or less with dissolution clays or with concretions such as stalactites, stalagmites and others. These conduits build a network of variably dense and connected channels which have sizes on the order of centimeter rather than decameters.

The absence of a surface water drainage system, combined with major individuel springs which occur at the outlet of the large underground drainage systems, characterizes the morphology of karst environment. Therefore, karst aquifers have important individual spring discharge points which are only rarely associated with porous media.

1.2. Hydraulic phenomena

The karst spring responds with rapid and violent flood events. The fast response during the rising limb of a karst spring hydrograph is followed by an equally rapid decrease on the falling limb and thereafter by a slowly declining recession curve during the base flow period. The rapid and violent flood events are directly linked to the movement of groundwater flowing through the interconnected and preferential paths of the more highly permeable conduit network. High flow velocities have been documented as high as 250 m/h using artificial tracers. In porous media, flow velocity values are much lower in the ranga of from 0.05 to 10m/h.

As mentioned by Jeannin and Grasso (1995), rapid water level variations in certain boreholes and slow to insignificant variations in others, demonstrate the heterogeneity of the karst environment. Generally, the borehole hydraulic conductivity as determined from slug-tests isolating specific lengths. A decrease of this property with depth in karst aquifers has been documanted by Drogue (1974).

The spring discharge variations commonly exhibit large fluctuations in chemicel composition and physical properties (temperature, electrical conductivity) of the water.

1.3. Recharge of karst aquifers

Recharge to karst aquifers occurs differently than to porous media aquifers, due principally to the larger degree of karst structural heterogeneity. The surface area of potentiel recharge over the karst surface is made up of varying proportions of swallow holes, karrenfields, dry valleys and, large regions where there is no surface flow. The distribution and proportion of such features depend on tectonics, carbonate (limestone) composition and geological and hydrogeological history.

For this reason, the recharge of the karst is on one hand, concentrated and individual with the loss of a stream into a swallow hole and on the other hand, diffuse in the large closed depressions, in the dry valleys or in tabular or anticline structural features. The diffuse

recharge can also collect and be transferred horizontally, in the upper part of the aquifer, called the epikarst. The epikarst collects the water and, as a perched zone, recharges either slowly into the low permeability volumes by infiltration through cracks and fractures, or into the karst network by rapid infiltration through vertical conduits.

Chapter 2

Conceptual models of the karst aquifer

Two types of models have been considered and adapted to address specific problems that need to be solved and investigated in this thesis. The interpretation of tracing tests in karst environments does not require the same conceptual model as is used for conducting a vulnerability assessment of karst aquifer terrain. The interpretation of tracing tests in terms of transfer functions is based on input-response model, whereas the karst vulnerability assessment is based on deterministic[2] conceptual model.

2.1. Input-response models applied to interpretation of tracing tests

Determining specific characteristics of transport processes in karst aquifer based on a deterministic approach requires a large and commonly quite expensiva data base to characterize the system's flow fields. Today, this data is rarely available. Instead, a global approach is taken that uses knowledge of the input to, and output response from, a system. This technique allows us to improve or understanding of the physical and chemical environment through which the flow occurs without needing the quite extensive and expensive data from the field. Therefore, instead of using documented aquifer properties, the global approach provides an equivalent method, essentially a black box model, to pradict aquifer bahavior.

The global approach is not only pertinent to interpret tracing tests in karst tarrain; it is also used in the fields of logic, rheology, linguistics, chemistry, and hydrology.

Chemists were the first to gather the required information that predicted the resulting impulse responses[3] from documented input and output data (Molinari, 1976). In the 1930's, L.K.Sherman (1932) studied the rainfall-discharge relationship at the outlet of a catchment basin. His work resulted in definition of a « unit hydrograph », an evaluation method that today, still forms the basis for comparing surface water flow system responses.

An input-response model can be used to analyze systems. This model does not take into account the aquifer characteristics at individual points within the system. Instead, the aquifer is considered as a black box. This box has an entrance and an exit and there is a mathematical relationship, reflecting the physical processes taking place within the aquifer, that relates the input at the entrance to the output at the exit. This mathematical relationship, depicting the flow pathway, is called a transfer function. Therefore, the pathway is characterized by this transfer function that converts the input function (e.g. effective precipitation, artificial tracer volume and concentration) into a response, called the output function (e.g. discharge of the system versus time, breakthrough curve of the tracer).

---

[2] *Deterministic modal: when a mathematical modal can be employad for determining exactly all tha states of a system. Modal that prasumes that a system or process operatas such that tha occurrenca of a given set of events leads to a uniquely definable outcome. Tha governing equations dafine precisa causa-and-effact or input-response relationships at each locations.*

[3] *Impulse response: response of a system to an input such as a Dirac, that is an impulse characterized by an intensity to infinity while its duration tends to zero.*

Input-response models have been used for several years to characteriza karst aquifers in term of systems. Mangin (1975) suggested classifying karst aquifers using the density and interconnectivity of the voids (hierarchy) created by the karst processes. To do this, he studied hydrographs and cross-correlated analyses (spectral and correlative) of rainfall and discharge. He concluded that the system is more well developed and interconnected as it moves from its recharge to discharge area.

In 1982, Dreiss developed a method of characterizing karst aquifers using linear transfer functions (kernel functions). The kernel functions are determined using the linear system identification technique proposed by Neuman and de Marsily (1976) for identification of an instantaneous unit hydrograph. The system response (output function) is the spring's rapid discharge resulting from an isolated storm event. The input function is the calculated recharge during that storm.

Interpreting tracing tests in terms of transfer functions is based on having an **input-response conceptual model**. The real system, the karst aquifer, is a closed box with an entrance and an exit. The internal structure of the box is not able to be determined. The aquifer response is accounted for using the transfer function. The function is determined from an equation using the experimental data for the tracer input conditions and breakthrough curves at the sampling point and the discharge flow rate at the spring. The real system, quite different from the box (open system) is described schematically.

One of the main objectives of this work is to predict contaminant transport in karst aquifers, major input to the vulnerability .mapping described in Part III of this thesis. Transfer functions can be readily obtainad from input response modals and their results can be used to predict contamination migration for part or all of karst water catchments.

2.1.1. The black-box model used to interpret tracer tests

Transfer functions can be obtained from tracer breakthrough curves and a black-box input response model. The transfer function can be directly obtained, without any mathematical treatment, from a breakthrough curve if 1) the tracer input is instantaneous, simulating a Dirac[4] [d(t)[type event, and 2) there is a continuous record of the discharge at the sampled spring. In this case, the transfer function is the breakthrough curve. When these conditions exist or are assumed to be true, the normalized breakthrough curve is a transfer function referred to specifically a RTD (Residence time distribution). The breakthrough curve is the output response to this instantaneous input of the injected tracer.

In practice, however, instantaneous injection of tracers is not possible for several technical reasons:

- the tracer injacted does not completely mix with the flow volume at the sinkhole injection point,
- the injection in a casad or uncased borehole is accomplished either in an isolated section or over the total borehole length; and in either case, the injection rate and volume is dependent upon the borehole permeability and therefore, it will not occur instantaneously.
- a tracer injacted into a swallowhole or borehole or on the ground surface, moves towards the groundwater system, but thare is a time lag while it travels through the unsaturated zone. In this case, the tracer does not reach the saturated zone as a single or a short impulse, even flushing with a lot of water (e.g. 3 m^3).

Consequantly, the directly observed response of a tracer system, manifest as the breakthrough curva, usually does not correspond to the impulse response. In that case, the impulse response has to be obtained by a mathematical « treatment » referred as

[4] *A Dirac is an impulse characterized by an intensity tending to infinity while its duration tends to zero.*

deconvolution[5], which relates the output obtained in the breakthrough curve, to the specific input conditions where the tracer was injected.

These following five sections provide the rationale to use input-response models to determine transfer functions from tracing experiments.

2.1.1.1. Introduction: analyses of systems using artificial tracers

Interpreting tracing tests with this type of input response model requires schematically breaking down the real system into a series of steps or pathways depicting the flow of the tracer in the karst or tracing system. However, before describing the typical approaches used within the black-box model to perform deconvolution, it is important to establish the concept of « systems », and the relevance of systems when interpreting tracer tests.

a) systems definitions

A system, as defined by Walliser (1977) is a relatively individual entity that can be separated from its context or environment, even if there is a continuing interchange between the system and its surrounding. A system is an entity independent of its context. The tracing system is similar to its associated karst system and both encompass the surrounding rock volume which contains the matrix, the fractures and the conduit network. Both systems are complex specificelly when one tries to determine the structure over a useful and sufficient schema in order to analyze the consequent relations between the entrance(s) and the exist(s), variable in time and space (Castany and Margat, 1977).

In karst hydrogeology, on the one hand there is the karst system and on the other hand, the tracing system. Both can be characterized as a vector system with several entrances and several exits. The tracing system is defined in our context, as a scalar system with only one entrance and one exit. If an injection point is connected to several springs, each « injection point-spring » system is considered es a separete tracing system (Figure 2.1.)

The tracing system, as shown in Figure 2.1., is a subsystem of the karst system. It is the only part of the hydrogeological system that relates to the pathway and the tracer migration (Lepiller and Mondain, 1986). It has also been referred to as the space occupied by the tracer mass during its transfer (Dzikowski, 1992).

Flow in the tracing system can occur in both the unsaturated and a saturated zone, each of which cen be considered as a subsystem. Thus, the karst system model as a black box, containing the tracing systems, is built up of subsystems. In the non-saturated zone, flow takes piece as the result of infiltration either into the epikarst, or in the low permeability volume of rock. In the saturated zone, water flows in the conduits, in the cracks and fractures of the low permeable surrounding rock, as well as within and throughout these interconnected parts of the network. Finally, the flow reaches the outlet of the system, commonly a spring. Figure 2.2. schematically illustrates potential flow paths within a karst system as well as different suitable tracer injection points. It is important to understand the location of the tracer injection points relative to the karst system in order to be able to characterize the karst aquifer based on the tracing test results (Part II).

[5] *Deconvolution: a mathematical operator that allows to obtain from the input signal - entrance function - and the output signal - the exit -, the transfer function.*

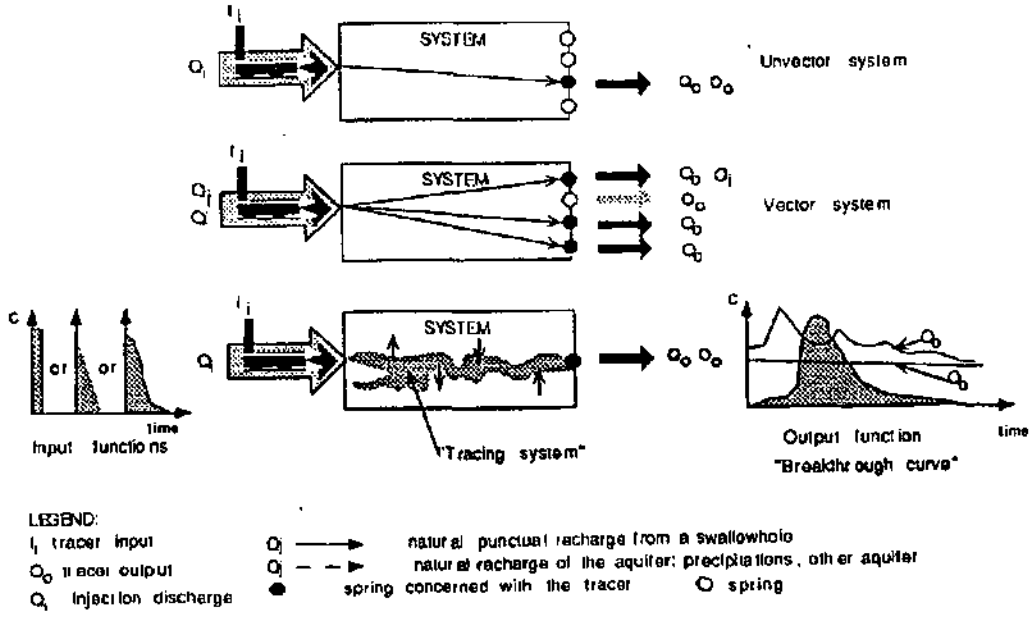

Figure 2.1.: Response of an aquifer system and of a tracing system to artificial tracer (modified after Guizerix and Margrita, 1976).

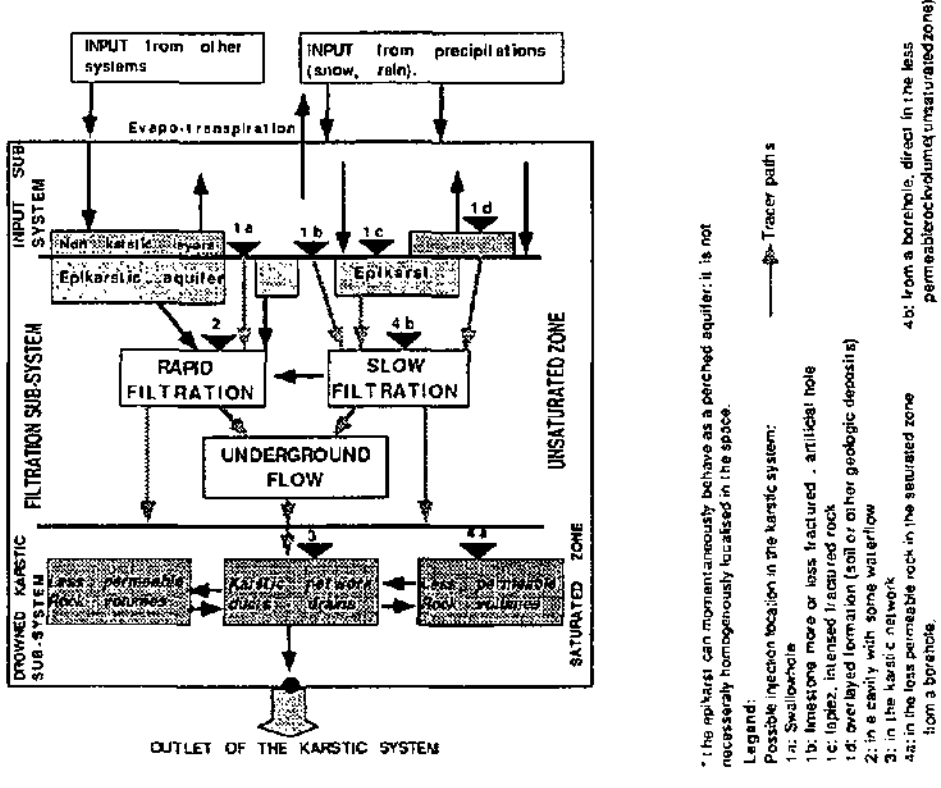

Figure 2.2.: The description of a karst system and the possible location of the trecer input (modified after Mangin, Molinari and Paloc, 1976 and Lepiller and Mondain, 1986).

b) properties of systems

Generally, systems are either scalar or vector systems (Figure 2.1). A scalar or univariable system has one and only one entrance, E(t), and one and only one exit, S(t), that is associated to it. A vector or multivariable system is characterized by several entrances, Ei(t), and several exits, Sj(t) [i and j, from 1 to n and 1 to m, respectivaly]. Only scalar system is considered in this work.

In the real world, hydrogeological systems do not only respond in a linear manner and their behavior is not consistent in time with varying changes, for example, in flow rates. Therefore the systems are not linear and are « time variant ». When conducting tracer tests in karst environments, ideally, to facilitate interpretation, the hydrodynamic conditions should be constant. Dzikowski (1992) as well as Guizerix (1988) proved that the karst systems did not behave in a consistent manner under conditions of variable flow. Both developed calculation methods to transform the system's response as a function of its discharge. This concept will be developed in Chapter 2.1.2. (Part I). Their methods will also be applied in part II (chapter 5I as interpretation techniques for locations where repaated tracing tests have been conducted to get more tracing or even karst system information. Non linear system responses ara found frequently in tracing experiments due in particular to adsorption processes.

However, the black box model being used requiras that the tracer systems be both linear and have consistent and invariant time behavior characteristics (cf. 2.1.1.2.).

Linearity: for a karst tracer system, this means that there is a direct proportion between the flow, as totaled for all the entrances, and the flow from all the system exits:

$$\forall i,\ E_i \Rightarrow S_i$$
$$then \quad E=\sum \lambda_i E_i \Rightarrow S=\sum \lambda_i S_i$$

with S for exit, E for entrance and λ as a constant.

An injected mass E(t) results in a breakthrough curve S(t) at the outlet. If the mass E(t) injected at the entrance, is multiplied by the constant « l », then the breakthrough curve will have a maximum concentration equal to « l » times the maximum concentration of the initial breakthrough curve (Doerfliger, 1994).

A karst system being tested will exhibit a linear characteristic or response if the following conditions are true or assumed to be true: 1) the tracer is a so called perfect tracer and the tracer molecules behave identically to water molecules, 2) the mass transferred is considered conserved, and 3) the recovery of tracer mass at the outlet is equal to the injected mass at the entrance of the system.

Stationary or time-invariant process: for a karst or tracer system, this means that the properties of the system do not change with time. This is equivalant to saying that if S(t) is the response of time system to an input E(t), then S(t+τ) would be the response of the same system to an input E(t+τ) which is E(t) changed by the value τ. The flow patterns are identical at different flow rate; at different steady flow the stream lines are identical and the relative shape of the transfer functions at various flow rates is identical. So stationary assumes that any property of the system does not vary with a translation in time.

2.1.1.2. Definitions and principles

Black box models permit analysis of the karst or the tracing system. As stated previously, the system is considered as a closed box with only one entrance and one exit. The internal structure of the aquifer is not expressly determined. The tracing tests ara interpreted in terms of transfer functions that take in all transport processes and the structural effects.

Considering a linear and steady-state tracing system, transfer functions are obtained using a black box model of **deconvolution**: the output function (breakthrough curve of the tracer) is deconvoluted by the input function. As far as possible, tracing experiments

should be done under steady flow conditions to conform to the invariant characteristic assumptions that are a requirement of the model being used. For the linear condition, it is assumed that the injected mass is equivalent to the recovered one at the sampling point(s).

This term transfer function includes all functions used within the **convolution** operation to transform the input function E(t) into the output function S(t). The use of an operator of convolution or of deconvolution requires the following: the tracing system being studied has to be considered as linear and time invariant (Baudoing et al., 1988, De Marsily, 1978); the hydrological conditions are steady and there is no interference with the tracer. The system has to be conservative.

The transfer function is calculated using the numerical code DYEBOX, a global mass transport FORTRAN 77 code, installed on the VAX at the Center of Calcul, Neuchâtel University (Király and Rossier, 1992) (Appendix I.1). The principle of DYEBOX is based on the mathematical operations of **deconvolution** and **convolution**.

This mathematical operator for convolution is called the DUHAMEL integral:

$$S(t) = i(t) * E(t) = \int_0^t i(t-\tau)E(\tau)d\tau$$

where t is for time and t is an integration variable. Unity: E, S [ML^{-3}]; i [T^{-1}]

The convolution operator can be written in a discretized manner as following:

$$S = \Sigma S_{(j)} = \Delta t\left[i_{(j)} E_{(0)} + \sum_{k=1}^{j} i_{(j-k)} E_{(k)} \right]$$

for j from 0 to N; k variable non equal to 0; Δt is the chosen discretized time step.

The transfer function is calculated using the **deconvolution** operator; the breakthrough curve of the tracer S(t) is deconvoluted by the input function E(t). The discretization of the deconvolution can be written as follows:

$$i_{(j)} = \frac{1}{E_{(0)}}\left[\frac{S_{(j)}}{\Delta t} - \sum_{k=1}^{j} i_{(j-k)} E_{(k)} \right]$$

with j from 0 to N; k a variable different than 0; Dt is the chosen discretization time step.

The term transfer function in its mathematical sense, refers to the Fourier Transform $\phi(\omega) = F(\phi)$ of the impulse response $\phi(t)$ to the system.

In the scope of this thesis and with obvious misuse of language, the term 'transfer function' is used in a more general sense and with the understanding that it represents all functions that transform a system's input signal E(t) into an output function S(t). Schematically, the transfer function is represented as a black box.

Several types of transfer functions (Figure 2.3) can be described:

- the **impulse response** corresponds to the system responding to an impulse with Dirac conditions. The resultant unit response is independent of the injection duration.
- the **indicial response** is the system responding to a step function (or Heaviside function). It is the result of the convolution of the impulse response with a step function. This type of response is used in order to compare transfer functions to each other (Chapter 3, Part II). In this situation, the indicial response is equivalent to a statistical distribution function and the derived indicial response directly defines (or

relates to), the impulse response. For example, the time corresponding to the 0.5 percentile is the time at which 50% of the tracer has passed through the system.

- **a referance response** (Király and Rossier, 1992) is equal to the system responding to a 'reference impulse' which has been or can be characterized with an arbitrary duration and shape. The reference response corresponds to the tracer travel time (RTD-residence time distribution) of a tracing test. This response is opposite to an impulse response, in that it includes the duration of the input. If a tracer test injection duration is not the same from one tracer test to another, this difference invalidates comparison of various tracer tests RTD results.

A referance responsa is used when simple deconvolution of the experimental breakthrough curves is not possible because of errors associated with the input and output conditions , or when the systam does not respond in a linear mannar during the tracing test. A reference response is also called a 'rough transfer function'. (Király et el., 1992).

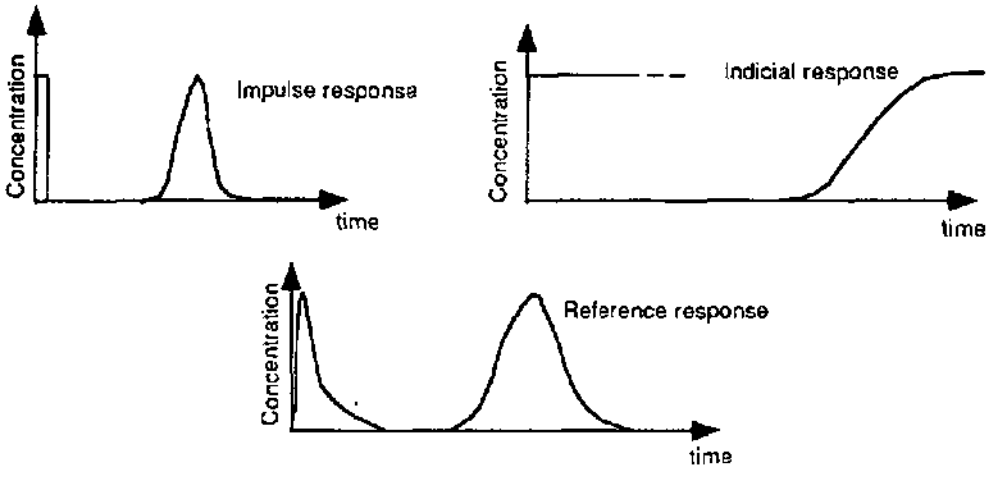

Figure 2.3.: Responses of a system in relation to the type of input function

Commants:

Deconvolution is one of several enalytical methods that ellows relationships within an input-response approach to be demonstrated. Other existing methods have not been developed as part of this thesis. The following is a partial list of the other methods: temporal series analysis(auto-regression models such as ARMA [Auto-Regression Moving Average] and ARIMA [Auto-Regression Integrated Moving Average] (Box and Jenkins, 1976)), optimization methods (multiple and linear regression model by least-squares methods - using error residuals with the discretized convolution integral), the transformation methods (Fourrier or Laplace) and projection methods (Dzikowski, 1992; De Marsily, 1978; Dodge, 1973; Singh et al., 1981; Morel-Seytoux, 1981; Rodriguez-Hernandez, 1989).

2.1.1.3. Practical problems

The daconvolution operation is an unstable mathematical process that is highly sensitive to errors in input and output. These errors can be related to either the shape itself of the input data or function, or to its inappropriata or unsuitable duration (particularly for the input function). The smallest error induces some oscillatory irregularities to the impulse response.

Identification of transfer functions for karst springs or other outlets is difficult due to the basic deconvolution process instability. Since a smooth transfer function is desired, deconvolution involves identification of a realistic or pertinent function that accurately reproduces the system response (i.e. breakthrough curve of the tracing experiment). The

smoothness and the shape of the system response that are to be deconvoluted have to be considered (Dreiss, 1982).

In the following section, the influence of how errors in the input or output function impact the system response will be demonstrated using both theoretical and experimental cases.

Using a black-box model permits comparison of impulse responses. One goal of this work is to determine if there are certain characteristic transfer functions. It is not the issue of this thesis to explain the instability of the deconvolution operation itself . Issues related to numerical instability in parameter identification, such as origin, neture, and effects heve been addressed, by Dietrich et al., 1989.

a) Thaoreticel caeaa

a.1. Convolution with rectangular-shaped input functions with different duration.

Figure 2.4 shows the impulse response (Ri) to a theoretical rectangular input (theo). The output response at different time staps are shown (CA, CB, CC CD). In this case there is a direct correlation between the input and output functions regardless of the length of the time unit (minutes or hours).

When there is an essentially instantaneous input function with Dirac-like conditions, then Ri is essentially equal to the response of the system given by the output function Output (t) as shown on figures 2.4. and 2. 5. A duration of 0.2 was chosen as this duration is still observable on the figure,

Figure 2.4 shows the differances in the convolution of the input function with the theoretical impulse response Ri resulting from changes in the shape and duration of the input function. The input function (t) has a rectangular shape and variable duration times of 0.4 (CA), 1 (CB), 5 (CC), and 10 (CD).

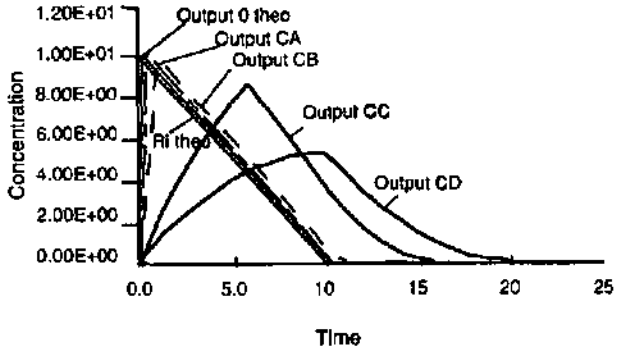

*Figura 2.4.: Theoretical ceses: **Output** functions resulting from the convolution of the above input function (figure 2.5.) with the theoretical impulse response Ri.*

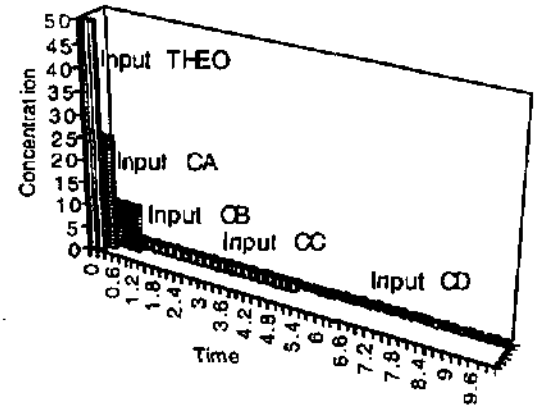

*Figura 2.5.: Theoretical case : Rectangular **Input** functions of variable duration used to convolute the theoretical impulse response Ri.*

Clear differences in the amplitude and in the symmetry of the output functions occur between the initial output function (output 0, theo) and the longer duration time steps of the input functions (CA to CD on figure 2. 4). The more that the input exceeds Dirac, i.e. instantaneous, conditions, the more the breakthrough curve deviates from the system's theoretical impulse response. Beyond a duration of 1 time step, the output function loses its original shape and becomes more symmetric. The amplitude decreases and the recovery duration increases and in all cases, of course, the recovered mass is still conserved (Figure 2.5).

a.2. Deconvolution of a "reference output function" with various shapes in input functions having the same duration

In this case, we took an impulse response Ri, similar to what would typically develop from a tracing test in a karst aquifer (Figure 2.6) and deconvoluted it with differently shaped input functions (Figure 2.7).

The shape of the input function in these cases reflects the field or experimental conditions and therefore corresponds more closely to reality. Field input conditions have a relatively fast injection time (close to 0) with a high concentration of tracer which slowly decreases. According to input conditions measured by Porel (1988), the input function behaves in an exponential decreasing manner and can be written with the equation:

$$C = Co\ t^{-0.485}$$ (time in minutes and C in ppb).

An exponentially decreasing function like this can be approximated by the "quasi-real input function" (4).

The following differently shaped input functions (Figure 2.7.) have been used as input conditions to deconvolute the given referenced output function (in this example). The duration of the referenced input function is defined as 100 time steps with a time step lasting one minute.

(1) triangular input = ***input triangle***

(2) complex triangular input function = ***input Ttriangles***

(3) trapeze input function = ***input trapeze***

(4) decreasing exponential input function (approximated) = ***quasi real input***

The resulting impulse responses are similar to the reference impulse response. The maximum in intensity of the response is slightly shifted along the time steps axis (Figure 2.8.). Regarding the breakthrough duration (3500 minutes), the input function duration (100 minutes) is considered as an impulse duration (ratio of 1 to 35). For this reason, the difference between the various impulse responses is not so important.

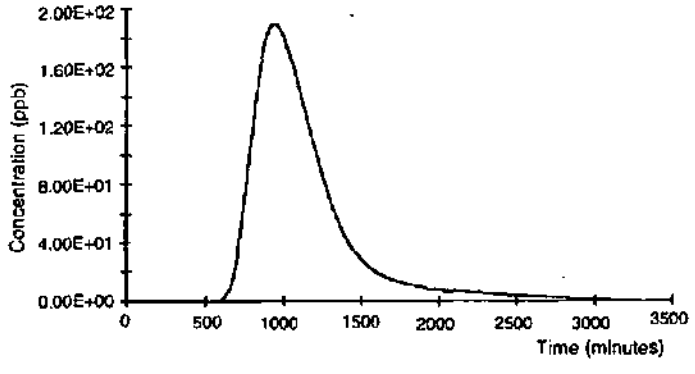

*Figure 2.6.: Reference **output** function [result of the convolution of the theoretical transfer function with the reference rectangular input function]*

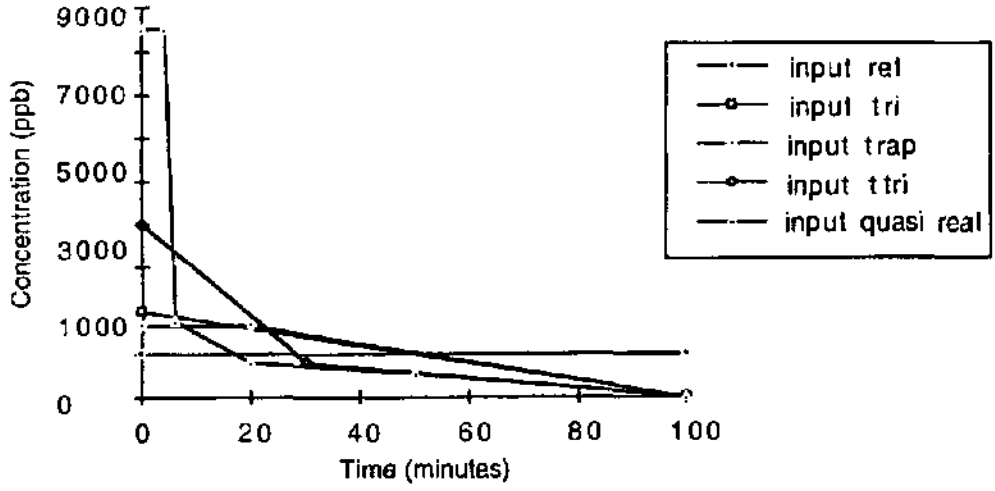

Figure 2.7.: Input functions of different shapes used to deconvolute the reference output function.

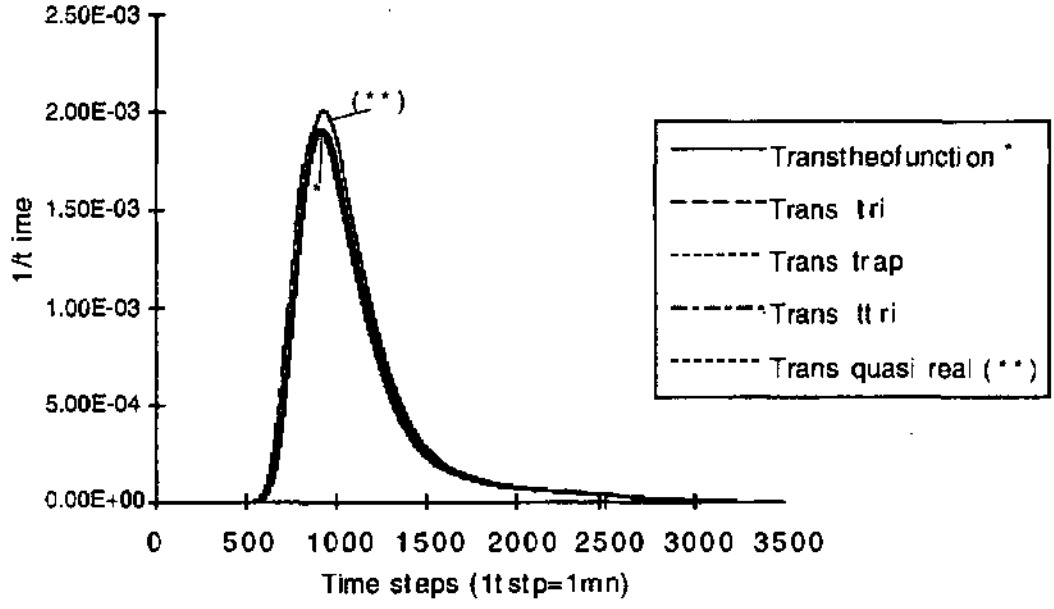

*Figure 2.8.: **Transfer functions - Impulse responses** - results of deconvoluting the reference output function with veriously shaped input functions.*

a.3. Changes in tha impulse responsa from varying the duration of both rectangular and triangular input conditions (functions)

In this situation, we consider the same reference output function as in case a.2 and deconvoluted it, first with rectangular input conditions varying the input duration from 100 (the reference duration) to 600 minutes.

The figures 2.9 and 2.10 illustrate the changes in the impulse response curve when input condition duration extends much beyond the length of the reference conditions. For longer input duration, oscillations begin to appear on the falling limb, and the entire response curve begins to be shifted backwards . The ratio of the input duration to the output duration is about 20.

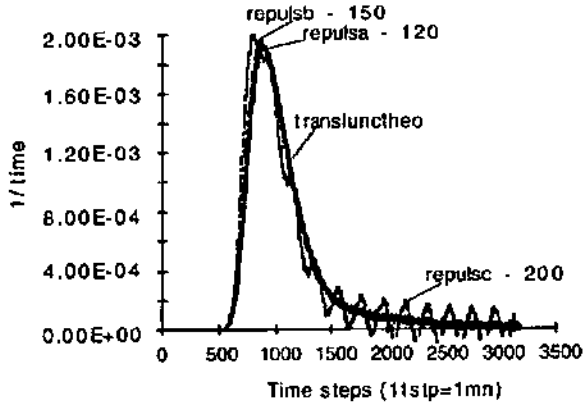

Figure 2.9. : Transfer functions resulting from deconvoluting the reference output function with different rectangular input function duretion.

Figure 2.10. illustretes the increase in oscillation that occurs when the ratio (input duration to output duration) varies between 0.1 and 0.2 (corresponding to an input function time step increase from 300 to 600 minutes). When the oscillations are not important, smoothing the response by additional deconvolution without introducing any major error is possible for situations where forecasting pollution is the required result.

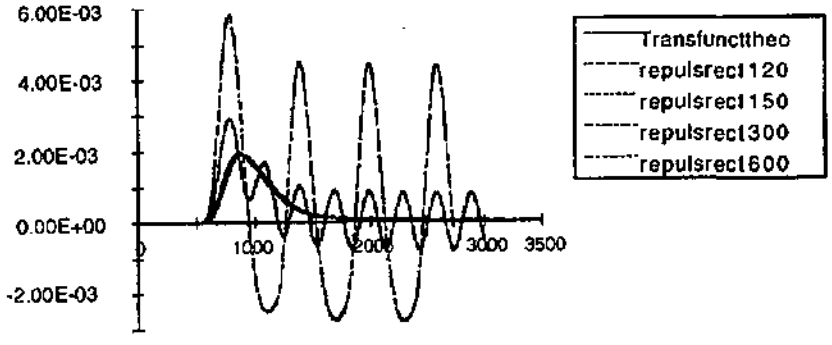

*Figure 2.10.: **Transfer functions** rasulting from deconvoluting the reference output function with rectangular input functions of various duration.*

If triangular, rather than rectangular input functions are used, then the oscillatory effect is not as developed with the referenced output function (Figure 2. 11.. When the ratio of input to output function duration is about 0.1, then the impulse response becomes different than the theoretical transfer function. The peak of Ri shifts backwards and develops a higher intensity. Oscillations also decrease, becoming important only when the input to output duration ratio approaches 0.2.

The oscillation effect due to the duration is stronger for rectangular input functions than for triangular ones as is noticed when comparing figures 2.10. and 2.11.

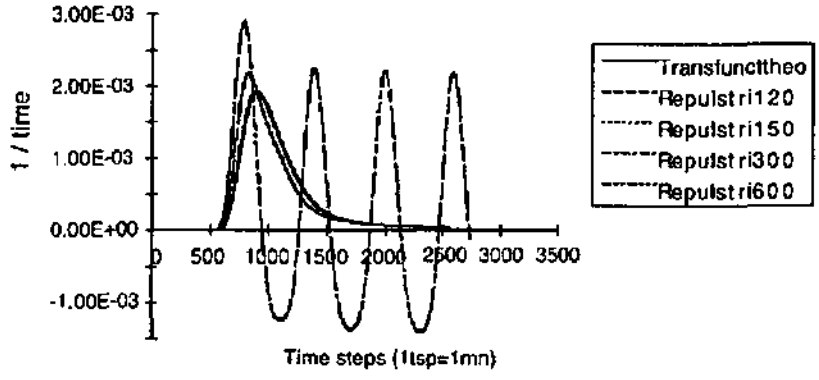

*Figure 2.11.: **Transfer functions** resulting from deconvoluting the reference output function with a triangular input function of various duration.*

a.4. Effect of breakthrough curve data errors on tha impulse responsa

Errors on both the rising and falling limb of the reference output function were introduced (Figure 2.12.) and the result was deconvoluted with both rectangular and triangular input functions.

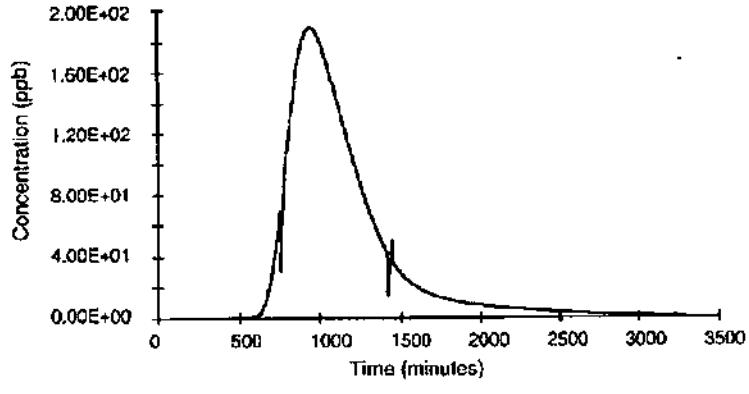

*Figure 2.12.: **Output function** with erroneous data on the rising and falling limbs of the curve.*

The result was that even small to insignificant errors induced significant oscillations on the resulting impulse response (Figures 2.13 and 2.14.). The effect was also stronger for the impulse response being deconvoluted with rectangular rather than triangular input functions.

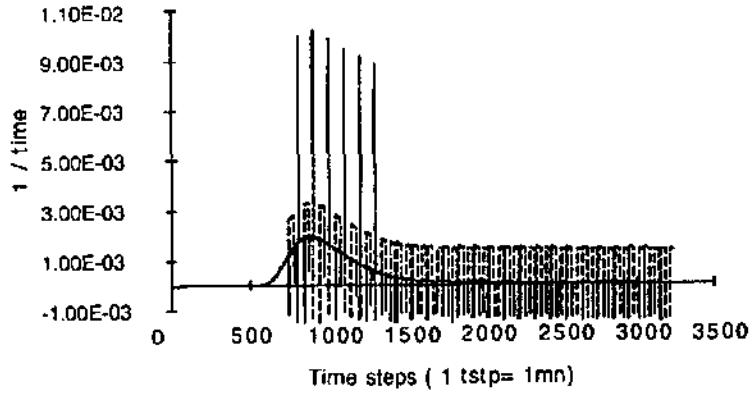

*Figure 2.13.: **Transfer function** resulting from deconvoluting the output function with erroneous data with a rectangular input function duration of 100 minutes.*

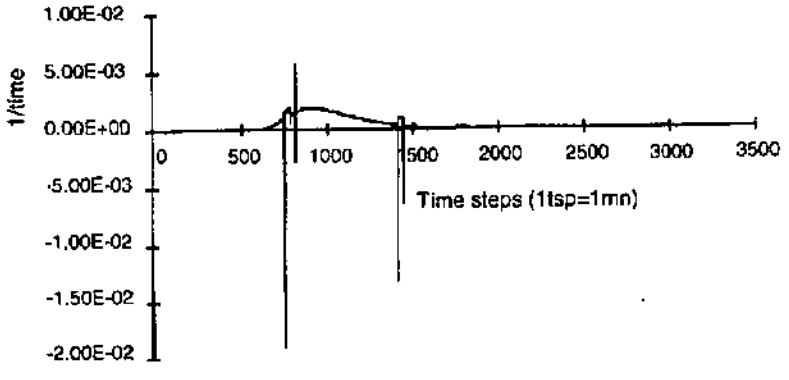

*Figure 2.14.: **Transfer function** resulting from deconvoluting the output function with erroneous data with a triangular input function duration of 100 minutes.*

b) Experimental cases

Experiments were done by Meus (1994), who measured injection well input conditions at the La Milandrine (Bure) test site where two tracing tests were carried out. For both sets of experimental data, we studied the smoothing effect of (1) the breakthrough curve before the deconvolution process and (2) the duration and the shape of the input conditions on the transfer function.

b.1. Measured input functions in Belgium

Input and output functions at Bertrée (uranine) - (Figure 2.15)

Input and output functions at Jandrain (LiCl) - (Figure 2.16.)

Input and output functions at Grand-Hallet (LiCl) - (Figure 2.17.)

For this work, it is clear that, the measured input was not similar to Dirac-type input conditions, and, it was not easy to measure the input function in the field during the injection.

The output function was deconvoluted first, with the measured input function, and second, with an estimated triangular input function and the resulting impulse responses were compared:

Results on figures 2.18 and 2.19 show that the impulse function obtained by deconvoluting the breakthrough curve with an estimated triangular input function is less perturbed by oscillations than convoluting with the measured input function.

Every breakthrough curve except that of Grand-Hallet (LiCl - figure 2.17) is perturbed. Because of this and the irregular input function as measured, the resulting impulse responses have periodically recurring oscillations with a frequency equal to one fifth of the input duration (e.g. Bertrée experiment). The large scale oscillations in the impulse response disappears if we use a triangular input function. The perturbations are still present but with a low amplitude.

The deconvolution process, as it is an instable operation, is sensitive to irregularities in either the output or input functions. The documented input conditions at the Bertrée and Jandrain test sites have some rapidly changing concentrations. In addition, the corresponding output results are irregular and bimodal. Consequently, the impulse responses oscillate considerably.

The Grand-Hallet's experiment is characterized by a highly and naturally smoothed and regular breakthrough curve. Its input function is close to a Dirac-type impulse. In this case, the deconvolution operation produces a regular impulse response.

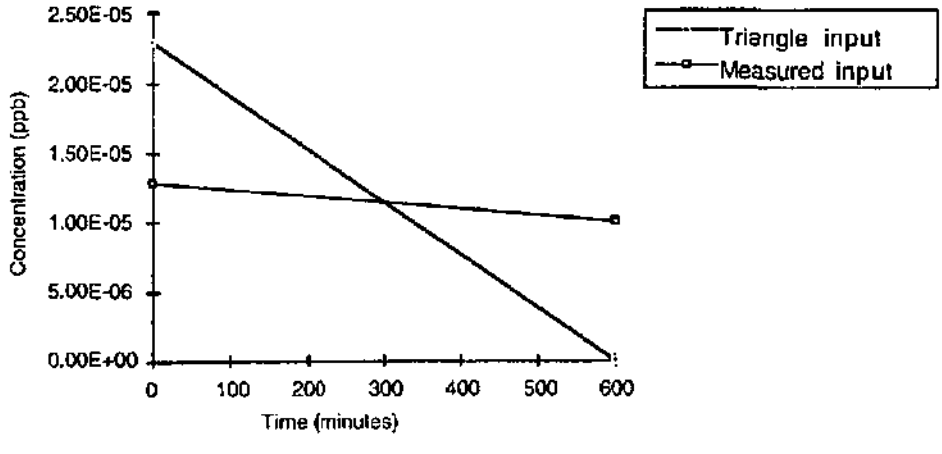

*Figure 2.15 a: **Bertrée input functions:** as measured and as estimated with a triangle.*

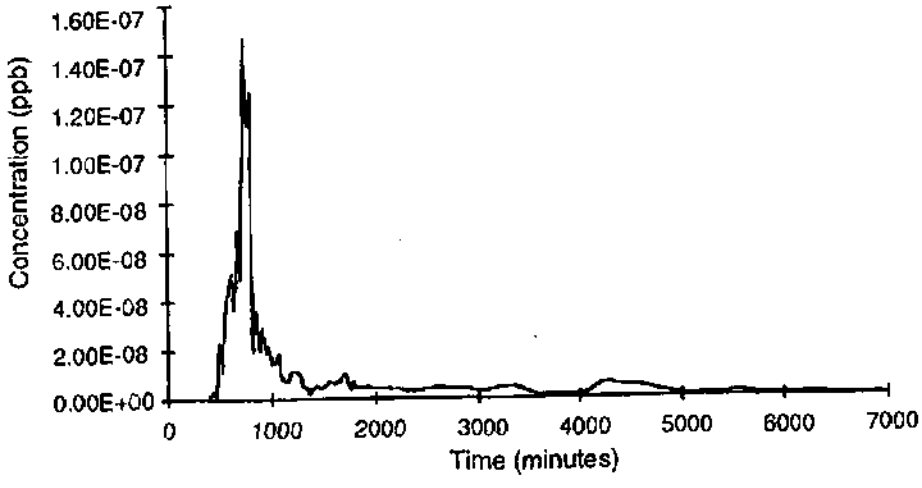

Figure 2.15.b: ***Bertrée output function****: real.*

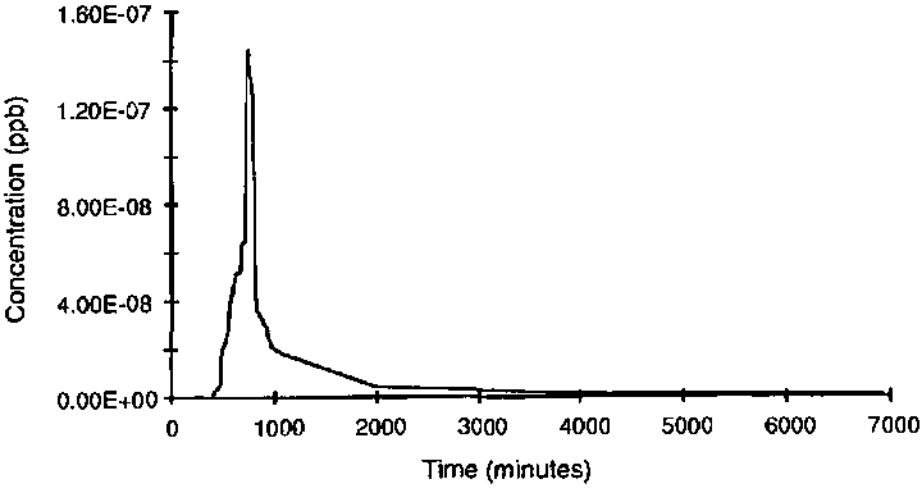

Figure 2.15.c.: ***Bertrée output function****: smoothed (c).*

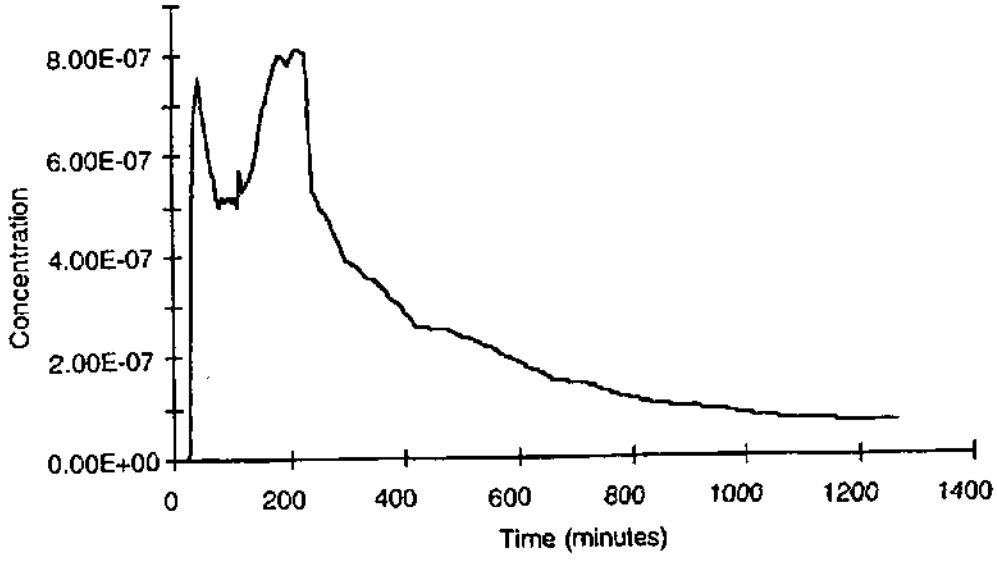

*Figure 2.16.a : **Jandrain output function.***

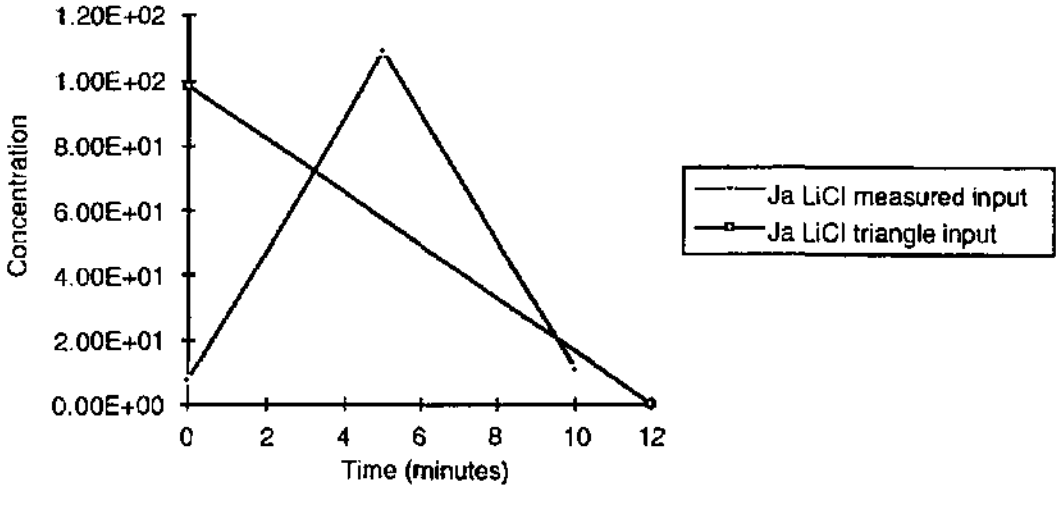

*Figure 2.16. b.: **Jandrain input functions:** measured and estimated with a triangle.*

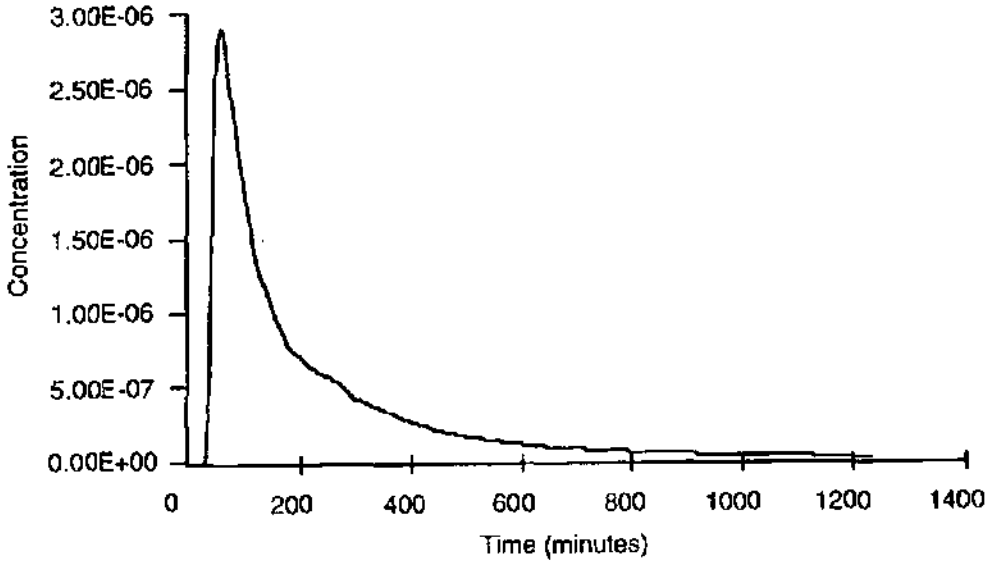

*Figure 2.17 a: **Grand-Hallet output function.***

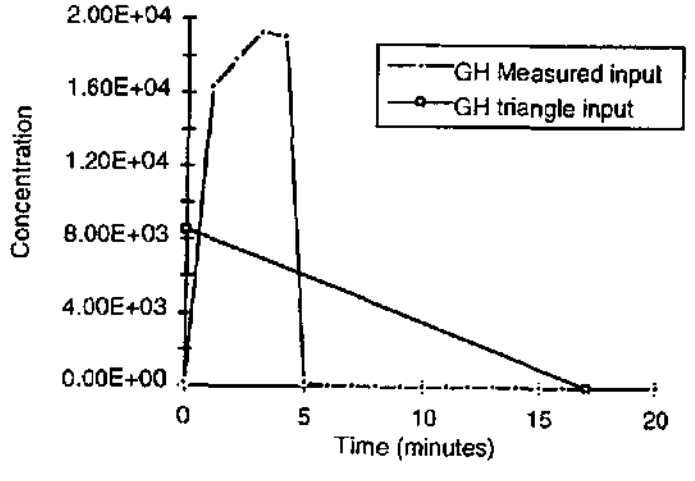

*Figure 2.17. b.: **Grand-Hallat input functions:** measured and estimated with a triangle..*

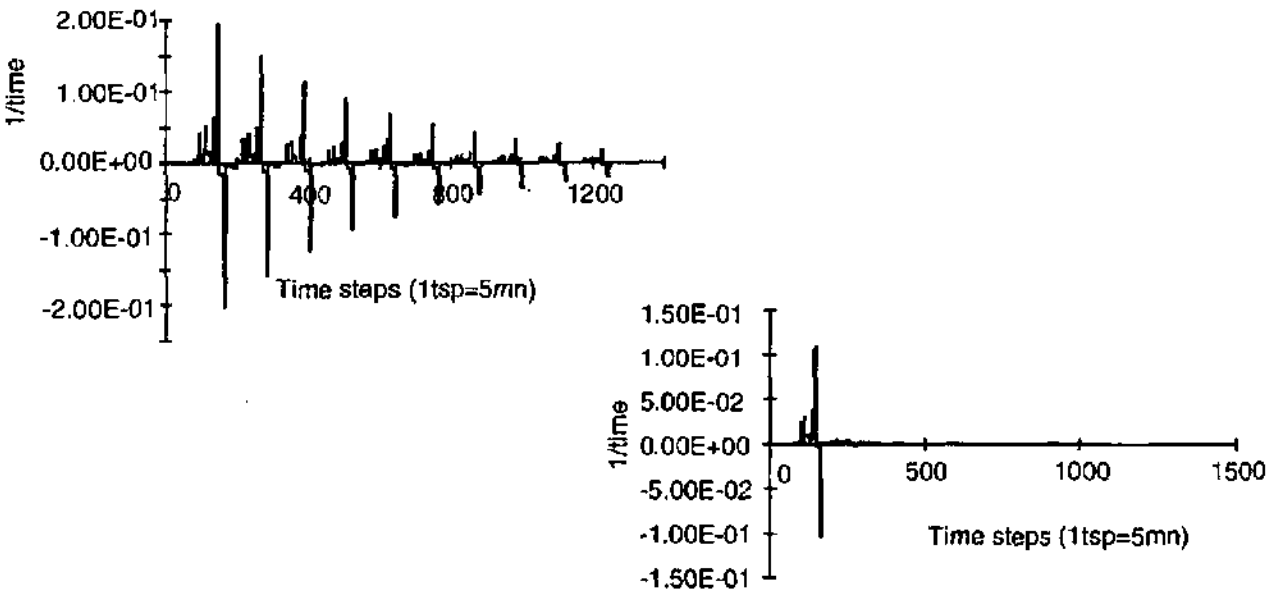

*Figure 2.18.: **Bartrèa** resulting impulse responses: a) with smoothed output and measured input and b) with smoothed output and astimated triangular input.*

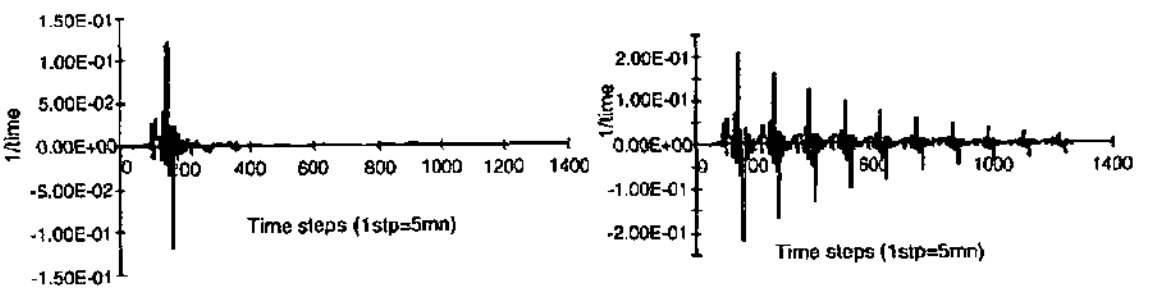

*Figure 2.18.: **Bertrée** resulting impulse responses: c) with measured output and input and d) with measured output and estimated triangular input. .*

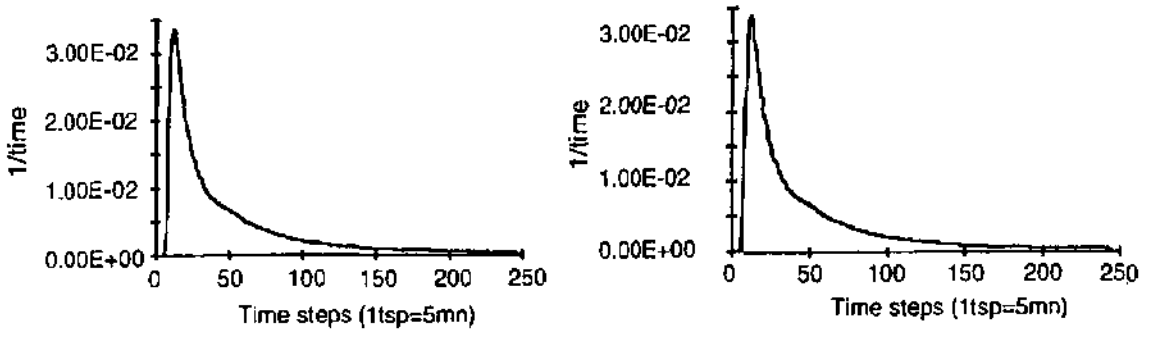

Figure 2.19.a and b: ***Grand-Hallet impulsa responsea:*** *a) with measured input function and b) with astimated triangular input.*

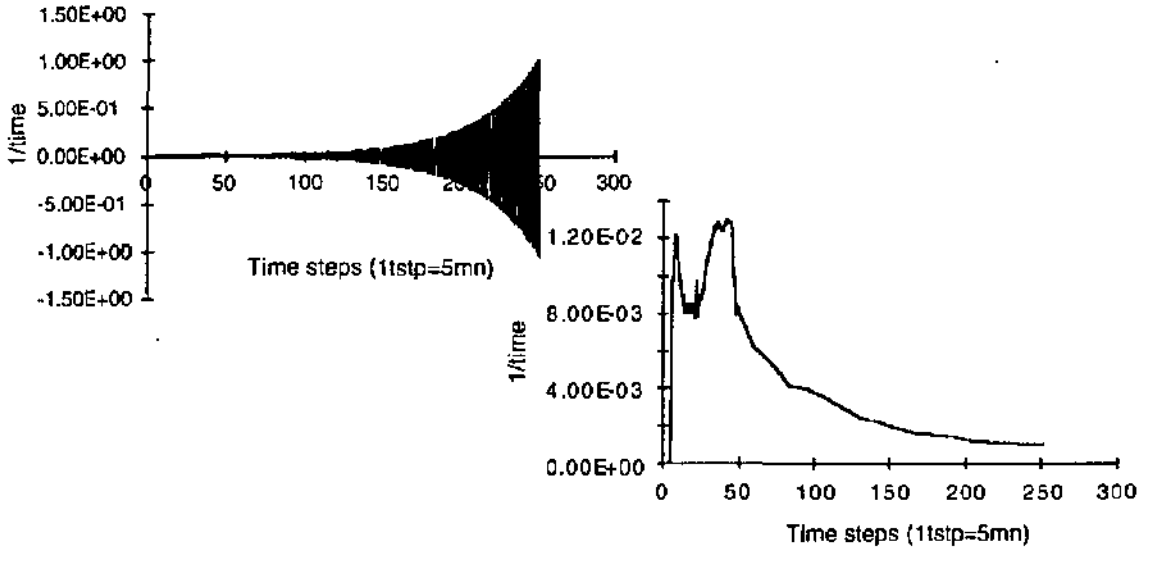

Figure 2.19.c and d: ***Jandrain impulse responses:*** *c) with estimated triangular input and d) Jandrain: with measured input.*

b.2. Deconvolution of a breakthrough curve with and without smoothing using triangular input functions (tracing test T7 amont, Bure)

The difference in the resulting impulse response is not important. The smoothing of the breakthrough curve allowed removal of some of the irregularities due principally to measurements errors, especially for the salt tracing test. The measurement of the water's electrical conductivity provided basic data that was transformed into concentration or mass flux, versus time. Irregularities on the breakthrough curve are due either to measurament errors of the probe, or to natural variations of the water's electrical conductivity in relation to the previous or present hydrodynamic changes of the tracer system.

Smoothing the output curve before deconvolution avoided an increase in the irregularities arising from the mathematical operation (Figure 2. 20).

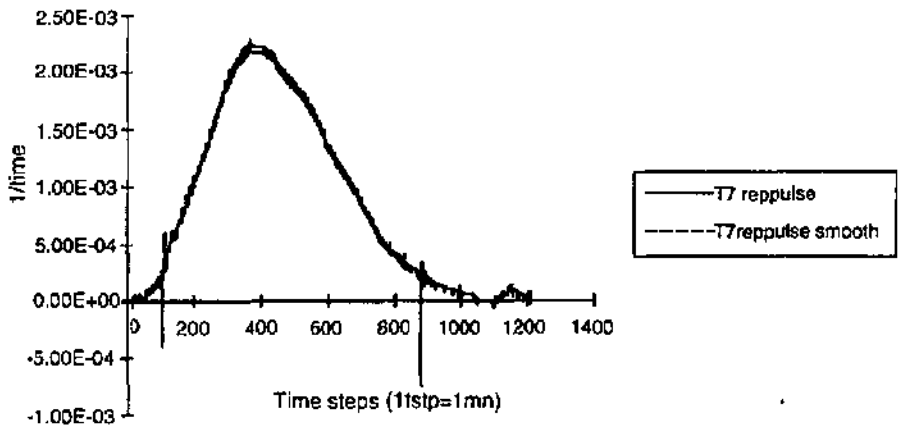

Figure 2.20.: T7 ***Transfer function****: impulse response with and without smoothing before the deconvolution process.*

b.3. Differances between an impulse response that results from deconvolution and a response such as a RTD (Resident time distribution)

As shown on figure 2.21., deconvolution with a triangular input function results in small irregularities in the impulse response, whereas there is no apparent difference with the RTD. The RTD is simply the breakthrough curve data normalized for the total recovered tracer mass at that location. In this manner it becomes a "unit function" such as the impulse response..

Figure 2.21c shows that the differences between the transfer function and the RTD are either in the location and amplitude of the concentration peak maximum or in the rising limb gradient.

There is no major difference in these cases, because the ratio of the input and recovery duration is small in the range of 1/150 to 1/200. If this ratio becomes smaller because of a higher input duration regarding the breakthrough curve duration, the difference will be more significant.

As in the process of obtaining a RTD from an output function, the input duration is not taken into consideration, RTD and transfer function are similar as long as the ratio of the input and recovering duration is small.

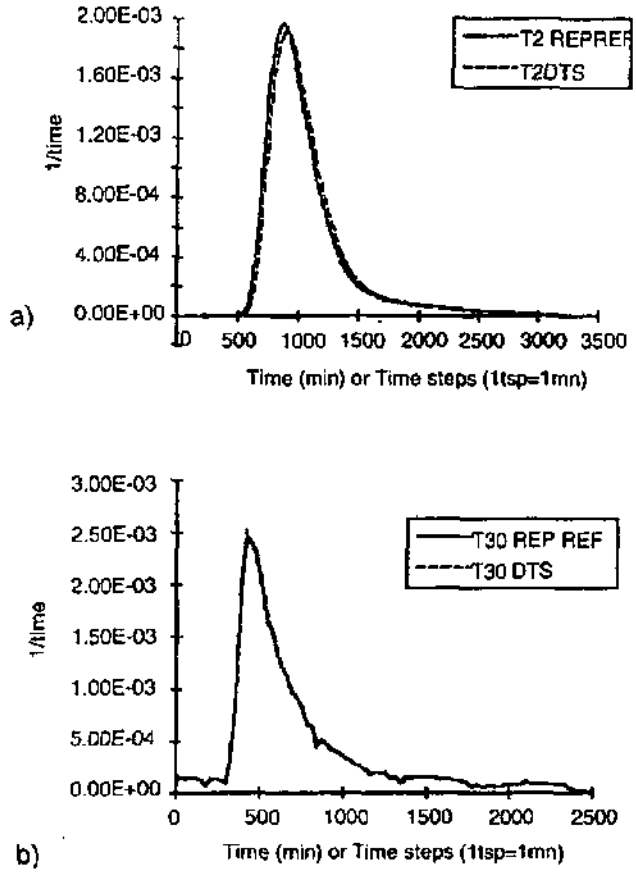

*Figure 2.21. a end b: Comparison of impulsa rasponse and **RTD functions.***

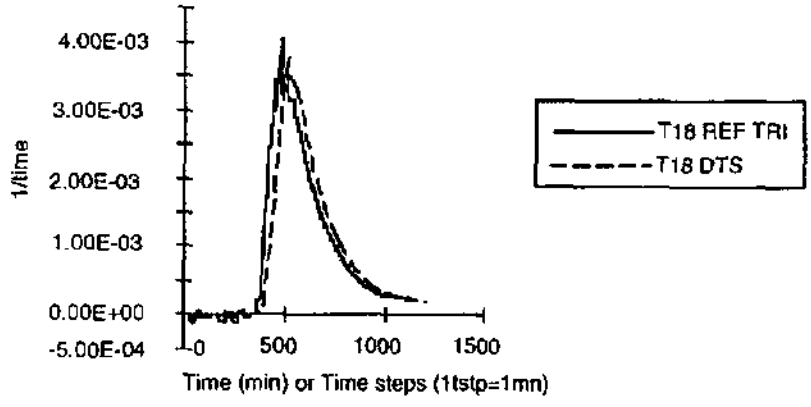

*Figure 2.21.c.: Comparison of the **Impulse response** and the **RTD functions***

b.4. Influence of the discretized time step in the deconvolution process on the indicial response

During the T2 amont test, three different time steps were used to discretise the deconvolution. The difference in times steps resulted in important predictions in the resulting indiciel response (Figure 2.22.). As the discretisation time step increased, the amplitude of the response decreased. In order to compare the effect on the impulse and indicial responses that results from non-similar time step discretisation, it was necessary to be sure initially that the impulse response was a unit function. If not and there is a difference of more than 10 to 15%, the response needs to be normalized and the comparison of the responses is pertinent.

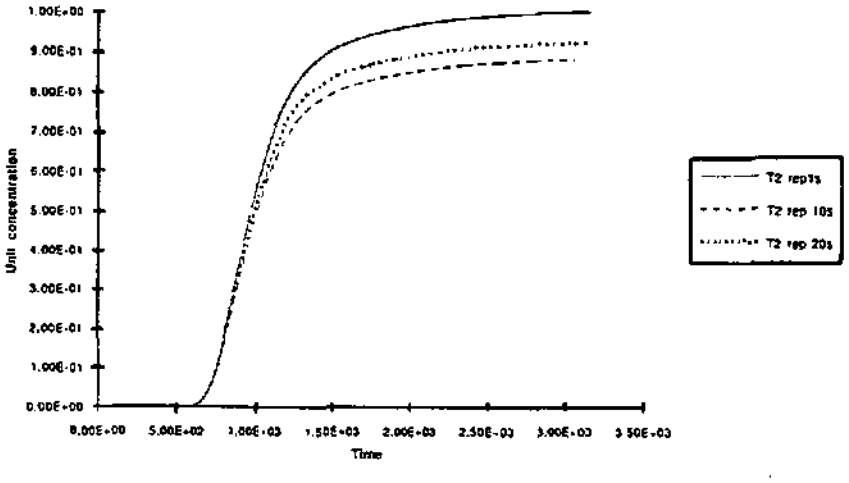

Figure 2.22.: Comparison of transfer functions - indicial responses - resulting from different discretisation increments during the deconvolution process.

Summary

The definition of an impulse response - system response to an instantaneous impulse (a Dirac) is clear. However the type of impulse conditions are not obvious when undertaking tracer injection experiments. Therefore, it is likely impossible to accomplish an theoretical impulse injection in reality.

The deconvolution operation is sensitive; the deconvolution of a breakthrough curve with irregularities gives a perturbed response. The perturbations are worse if the real input conditions do not meet the instantaneous impulse requirements. The shape of the input function contributes strongly to the occurrence of these perturbations. With a few tests, it appears that triangular input functions with duration similar to those experienced during real injection tests gives less oscillation.

Input conditions are not easily measured in the field. For this reason, all deconvolution was accomplished using a simple right-angled triangle as the input function shape. The input function is normally close to a decreasing exponential function as determined by Porel (1988). On the basis of several measured input functions, the following equation:

$C = Co\ t^{-0.485}$ is suggested as an effective on to use as the input function.

Compared to a RTD, the impulse response is not very different. The results are not influenced except when the ratio input duration to output duration is high.

Therefore, by deconvolution, all impulse responses are comparable whatever the tracer injection duration of their tracer experiment is. The input duration regarding the output duration , with the deconvolution procedure, is meaningless.

It is clear from seeing the irregularities and perturbations that develop from deconvolution, that it is important to get a breakthrough curve using with the smallest possible sampling step and to be able to smooth the breakthrough curve before any other deconvolution process. With these examples, it is clear that in reality, the input conditions are not well documented (duration, real shape) and that they rarely meet Dirac-type requirements.

2.1.1.4 Deconvolution - Convolution procedure of tracing tests with the code DYEBOX

After calculating the recovery percentage of the tracer, interpretation of tracing experiments using the numerical code DYEBOX was done as follows procedure,:

1. Smooth the output function - the tracer breakthrough curve - if needed. The output function is determined either in mass flux units versus time, or in concentration units versus time.
2. Discretise, using the smallest possible constant time step, (1, 2, 5 ,10 or 20 step units) with the code KINTER (Chyn). The choice of the time step is determined by the DYEBOX code, as the impulse response file cannot exceed 9800 rows.
3. Calculate the input function in relation to the recovered tracer mass and the injection duration measured or estimated in the field, according a simple right triangle shape. The input function is given in the similar unit as the output function.
4. Deconvoluta with the code DYEBOX using time steps of 1, 2, 5 or 10 time units: to determine the **impulse response**.
5. If needed, according to the quality of the obtained impulse response, conduct additional smoothing of the response or redraft it to remove or reduce irregularities.
6. Verify the area under the impulse response (should be a unit function). If it is not, (difference less than 10 to 15%), normalize the impulse response.
7. Convolute the impulse response with a step function unit to obtain an the **indicial response**.
8. Characterize the normalized response using gradient values at the defined and specific percentiles of 0.2, 0.5 and 0.8.
9. Interpret the variability of the transfer function.

Comments:

The indicial response is the most convenient one to use to compare one transfer function with another. Instead of defining the shape parameters of the impulse response such as skewness and symmetry (Pearson coefficient, Fisher coefficient), it is adequate to calculate the gradient at different percentiles of the indicial response.

The chosen percentiles are 0.2, 0.5 and 0.8. The gradient at percentile 0.5 is related to the statistical dispersivity of the impulse response; the corresponding time is the time at which the amplitude of the impulse response is maximum. The percentiles 0.2 and 0.8 were chosen more arbitrarily; using their gradient and corresponding time to characterize the symmetry of the impulse response. If the interval of time $t_{0.2}$ - $t_{0.5}$ is equivalent to $t_{0.5}$ - $t_{0.8}$ and the gradient at these different times are similar, the impulse response is symmetric. If the interval of time $t_{0.2}$ - $t_{0.5}$ is higher than the $t_{0.5}$ - $t_{0.8}$, consequently the gradient at $t_{0.2}$ is lower than at t_{05}, and the impulse response is asymmetric. An impulse response with inverse asymmetry occurs if the time interval $t_{0.2}$ - $t_{0.5}$ is smaller than the $t_{0.5}$ - $t_{0.8}$, consequently the gradient at $t_{0.2}$ is higher than at $t_{0.5}$.

As impulse responses do not satisfy a normal Gaussian distribution, the specific percentiles do not correspond to the characteristic percentile related to time t, plus(+) or minus(-) the standard deviation around the median of the distribution ($t_{0.5}$).

2.1.2. The CONVOX model - non steady flow system

Real tracer or karst systems are seldom invariant due to the hydrodynamic conditions variations (different constant flow rates or variable flow rates).

The numerical code CONVOX was devaloped by Dzikowski and Delay (1992) to allow simulation of a mass transfer response regardless of the input and hydrodynamic conditions. The information that is important is knowing the conditions associated with a reference tracer experiment and its pertinent reference hydrologic conditions. Repeated tracing experiments had been carried out at the same injaction point in Bure (point 1,

borehole MIL7 and borehole MIL3) and in Areuse and Noiraigue water catchments. The experimental data from these sites has allowed us to test the reproducibility (linearity and stationarity of the system) of tha systam response under similar hydrological conditions. This was done to achieve more than simply compare transfer functions. Results of the transformation methods of system responses permitted us to determine the conservation of the tracing system under various hydrodynamic conditions. Indirect information about the karst system (build up with many potential tracing subsystems) can be obtained. The results of transformation of transfer functions of repeated experimental tracer tests at three test sites are presented in Chapter 5, Part II.

The concept of tha impulse responses transformation method is based on tha assumption that a mass injected into a system has the same distribution in space at a given distance whatever the hydrodynamic conditions. For a conservative mass transfer without exchange processes such as sorption and without diffusion phenomena, the geometrical shape of the tracer cloud does not depend on the flow rate through the system but only on the space occupied by the tracer (Guizerix and Margrita, 1976).

It is necessary to possess one or two experimental sets of data to simulate a response corresponding to different hydrodynamic conditions. One of tha experimental curves transformed in RTD or using a transfer function by deconvolution is used to create an RTT (Reference Tracer Test), to calculate the tracer curve STT (simulated tracer test) as a function of the new hydrodynamic conditions. It is possible to simulate responses out of from either assumed instantaneous or step function inputs. A dilution effect that occurs externally, can also be taken into consideration.

The principle of convolution of the numerical code is based on the following integral defined by Dzikowski (1992):

$$Cs_j(t)\, dil_j(t) = \int_{-\infty}^{t} \frac{Cref_j(\tau')}{Mref} dil_j(\tau')\, Ce_i(\tau)\, Qe_i(\tau)\, d\tau$$

with

Cs_j (t) : concentration at tha outlet of tha system at time t

Cref j (t): concentration of the recovery of the reference tracer (injection at t=0)

Mraf : injected mass of the reference tracer

Ce_i (t) : input concentration at time t

Qe_i (t) : input discharge at time t

dil_j (t') : dilution rate defined as the ratio between the output discharge and the tracing system discharge.

dil j (t') = Q s_j (t') / Q st j (t') where Qs j (t') is the measured discharge at the system outlet and Q st j (t') is the discharge of the tracer system.

t' is determined as the water volume leaving the tracer system in the interval of time t and t. Vst j (t-t) = V raf j (t').

V raf_j (t') is the flushed water volume at the outlet of the system as a function of time from t'=0 (tracer injection time) for the reference hydrodynamic conditions, $Qraf_j$ (t).

For instantaneous injections, concentrations are assumed proportional to the injected mass whatever the discharge. In this manner, hydrodynamic conditions directly relate to the first arrival and recovery duration.

For step function type injections, hydrodynamic conditions govern maximum concentrations, tracer plume duration, and time of first arrival of the tracer.

Guizerix (1988) with the same basic hypothesis as Dzikowski (1992) approached system response transformation for variable discharges using a geometrical and graphical interpretation method.

The detailed description of the numerical code CONVOX is in an appendix of Dzikowski's thesis (1992).

2.2. Using deterministic or parametric models to assess vulnerability of karst aquifers

Intrinsic vulnerability[6] mapping is based on a conceptual model of the karst aquifer that is different than the model used to interpret tracer tests. In order to define the relevant attributes that can be mapped as required for the vulnerability method, a deterministic model[7] is necessary. In contrast to input-response or black-box models, deterministic models address explicitly spatial characteristics and use verified governing equations on simplified systems to define precise cause-and-effect relationships.

The karst aquifer has been described by Mangin (1976) as a input-response model build up of sub-boxes, with one sub-box for each attribute. For vulnerability of the karst aquifer, the following sub-boxes have been chosen: the karst network, the less permeable rock volumes, the soil and geological overlayer and the epikarst. Each sub-box is recharged by water. This model allows analysis of the global response of the complex karst system according to Mangin (1976) (cf. part I, chapter 2.1.1.1., fig. 2.2.). This model characterizes input-response relationships for karst aquifers. However, this type of model does not take into account the aquifer's spatial considerations and for this reason it is inappropriate for use related to the concept of karst environment vulnerability mapping.

Spatial considerations have to be included in such vulnerability mapping, as the goal of the karst groundwater vulnerability assessment is to supply vulnerability maps in 2-dimensions to delineate groundwater protection zones.

The spatial characteristics of a system can be modeled in a deterministic-distributed-parameter approach. According to Bear (1979), the framework for distributed parameters models includes:

- (1) one or more partial differential equations called field equations
- (2) initial and boundary conditions
- (3) solutions procedures

The conceptual karst aquifer model used as basis for vulnerability mapping refers essentially to this type of deterministic distributed parameter model. For vulnerability mapping, the differential equations used to simulate groundwater flow and transport processes, and the solutions procedures, are not considered. **The characteristics field** is retained from (1) without dealing with the equations and from (2) concerning the **initial and boundary conditions**.

The Darcy Law flow equation takes into consideration a *transient term* (the effect on the flux of a hydraulic potential varying through time; inside the saturated zone, this term is a function of the storage coefficient), a *steady-state term* (description of the water flux at a point in an aquifer; this being a function of the hydraulic conductivity) and a *source term* (quantity of water injected, removed by pumping or discharged at the point considered) (Király, 1973). The transport processes are also described with a differential equation involving three major parts: a *diffusion term* (a constant term describing constant concentration gradients and a variable term describing the flux of solute caused by time-variable concentrations), *an advective term* (tracer or contaminant molecules moving with

[6] *Intrinsic vulnerability: vulnerability defined only as a function of hydrogeological and geological attributes.*

[7] *Deterministic model: model that presumes that a system or process operates such that the occurrence of a given set of events leads to a uniquely definable outcome. The governing equations define precise cause-and-effect or input-response relationships (Russell Boulding, 1995).*

the flow of water) and a *source terms* (the hydraulic source term and the chemical source term) (Bear, 1972). Degradation processes and adsorption can also be taken into consideration in such transport equation.

As vulnerability mapping is focused only on intrinsic vulnerability the chemical, isotopic, thermic and biological characteristics are not considered.

The parameters values assigned within the characteristics field are a function of the knowledge of the internal geometry of the voids which results from the karstification processes. The distribution of the voids such as chennels and fractures directly controls or results in the permeability field. This field is directly related to geological attributas (petrography, sedimentology and tectonics). The conduit network geometry is a function of the fracture system geometry and of the stratification of the aquifer rocks layers.

The hydraulic gradient has been correlated to the sub-parallel fissures-strata intersections orientation, by determining the fissures groups, the fissures openings, their frequency and their orientation (Kirâly, 1978).

Permeability is strongly influanced by the enlarging of fractures that are under karstification. This enlarging is strongly influenced by the direction and the intensity of the water velocity vector during previous states (feed-back in the figure 2.23., (Kirâly, 1978)). The karst aquifer is thus a system in constent evolution:

« The actual state of flow systems and of the permeability's field is the result of a succession of auto-adjusting (short and long term) between the velocity vectors $\bar{q}$ field, the **physical parameters field** (K, m_e, S_s) and the « **boundary conditions** » (recharge of the aquifer, elevation of the outlet and outflow area geometry) » (Kirâly, 1978).

What are the boundary conditions and their consequencee from the point of view of the vulnerability ?

Boundary conditions are the conditions existing at the limits of a model or at each element of a gridded model. Two general sets of boundary conditions may be distinguished:

- ***conditions of known or imposed hydraulic potential***

In the field, these conditions exist related to water bodies such as lakes or rivers, which recharge to or discharge from the aquifer while maintaining a relatively constant head. The direction of flow, that is the flux in or out, may reverse depending on changes in hydrodynamic conditions.

Consequences for vulnerability:
If the flow enters into the system, then this type of boundary directly relates to the system's vulnerability. For example, a water catchment basin which has a river that infiltrates in the area, can be potentially contaminated according to land-use activities. This contaminated river, a boundary condition would then directly relate to vulnerability.

- ***conditions of known boundary flux*** (pumping, drainage, rainfall recharge,...)

For constant flux boundaries, zero flow boundaries correspond to or are similar to impermeable boundaries. Concentrated recharge (swallowholes), diffuse recharge (distributed over the surface), direct recharge (to outcrop) and indirect recharge (through a soil or detrital overlayer) are the main boundary flux components that can affect vulnerability in the following manners described.

Coneequences for vulnerability

Diffuse infiltration: the vulnerability depends on the length of the path taken by water prior to reaching the karst network.

- is there any soil, detrital cover ? if yes, how thick and permeable ? is there any epikarst?

Diffuse and localized contamination presents relatively little risk due to the possible dilution and attenuation of the contaminant in the overlayer of the aquifer.

Concentrated recharge from surface water (swallowholes): a concentrated infiltration of surface water represents a point of extreme vulnerability, as does the catchment besin of the losing stream or river.

What are the physical parameter fields and their consequences from the point of view of vulnerability ?

The physical parameter field for hydraulic conductivity, is mainly simplified as: (1) a highly permeable zones such as the cover (soil, detrital cover, rock layers), epikerst, the karst network, and (2) the low permeability rocks volume.

(1) The cover of the karst aquifer (soil, detrital or rock layers)

The vulnerability of these zones are dependent essentially on the thickness and the permeability of the overlayer.

- If, for a given degree of saturation, the detrital cover has low permeability, there will be little infiltraBon and considerable runoff. If the runoff infiltrates down into the karst network, this becomes similar to the case of concentrated infiltration. Otherwise, the area may be considered of low vulnerability.
- If, for a given degree of saturation, the cover is of medium permeability, it may absorb all the precipitaBon and associated potential contaminants and retain the water long enough to permit chemical attenuation. These zones are weakly vulnerable.
- If, for a given degree of saturation, the cover is highly permeable, it will absorb all the rainwater and potential contaminant, but fail to retain them long enough to permit effective attenuation. These zones are of medium to high vulnerability depending on their relation to the karst network.

(2) The epikarst

The epikarst is defined as an adsorption zone that is highly fissured due to the extension and pressure released of rock at the surface (Dodge, 1982). As a consequence of this intense fissuring, the surface is susceptible to extreme erosion, especially in uncovered karst areas. Such a superficial karst zone is not spatially uniform. Its thickness may range from several tens of centimeters to several metros. Mangin (1975), the author of this term, considered that the epikarst can sometimes act as a perched aquifer.

The existence of the epikarst has been also proved by some investigations, boreholes and hydraulic tests on the test-site of La Milandrine in the work associated with two diploma projects (Veiga, 1995 and Thierrin, 1996). Its identification on a covered karst will be discuss in the part III of this thesis.

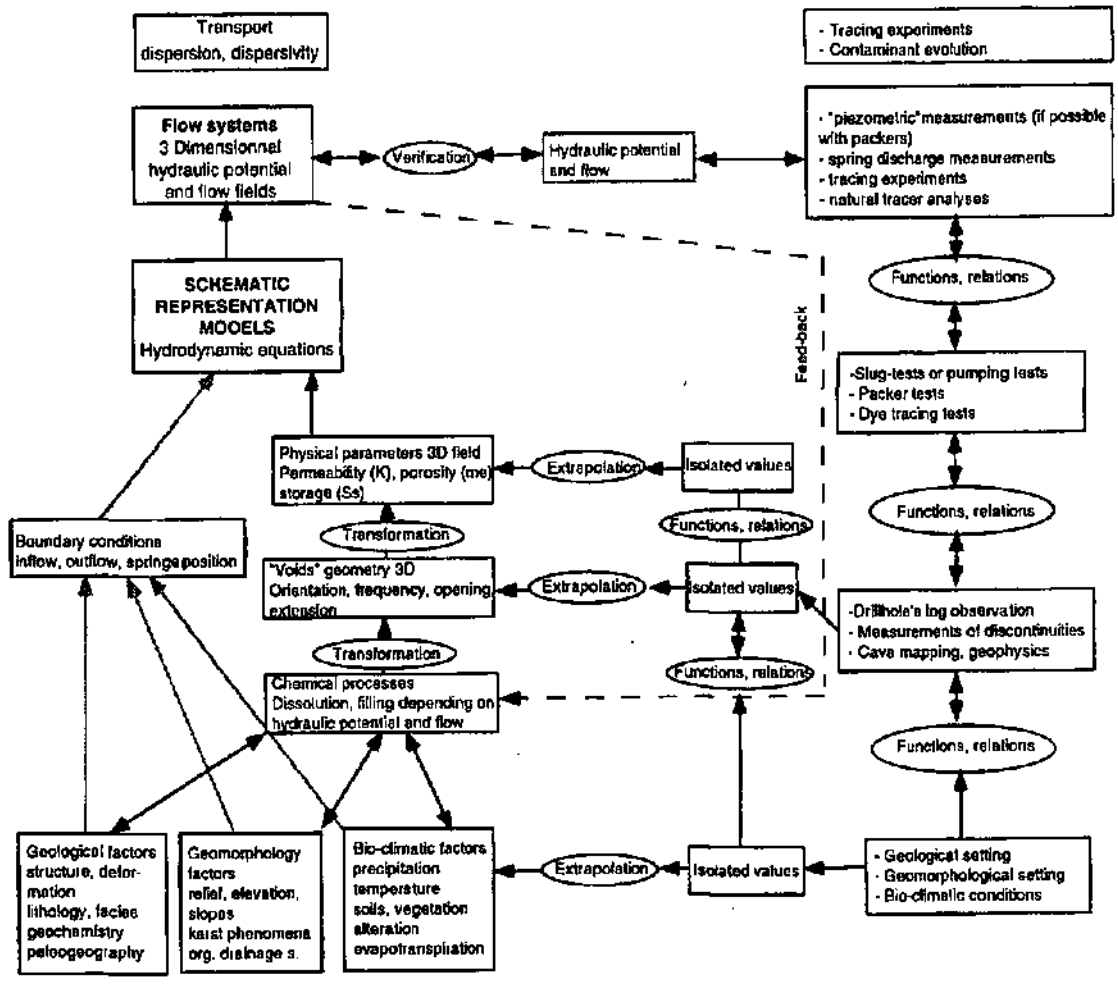

Figure 2.23.: Chart describing parameters and investigation methods of a fissured karst aquifer. Two major conditions are necessary: the « boundary conditions » of the aquifer and the physical or hydraulic characterization fields (modified after Király, 1978, in Zwahlen and Doerfliger, 1995).

On the basis of field measurements, Smart and Friedrich (1986) estimated that the epikarst zone also supplies recharge to the less permeable fissured regions of the karst during low-water periods and during minor increases in water-level (Figure 2.24.). The epikarst contributes directly to the underground conduit drainage system only during times of very high water stages.

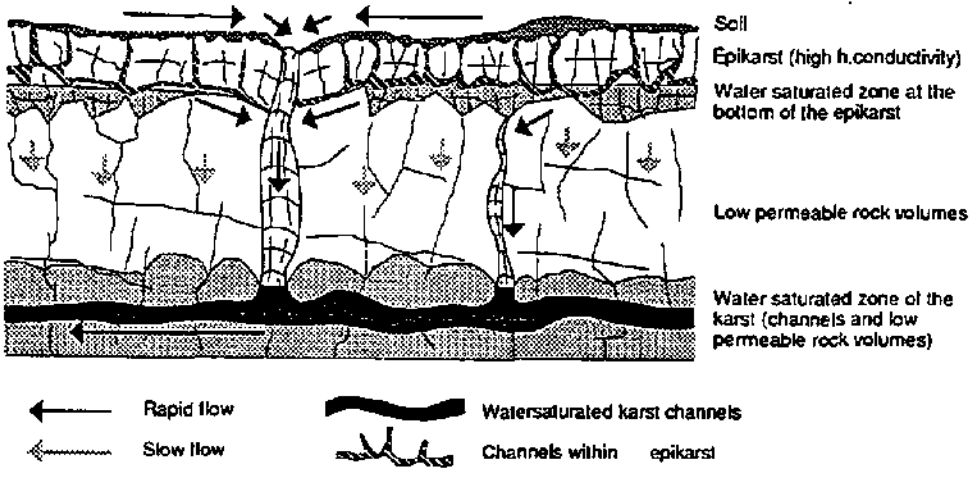

Figure 2.24.: Water recharge to « blocks » and of karst channels from the epikarst zone (Gresso & Jaannin, 1995, after Smart and Friedrich, 1986).

Karst spring response has been simulated using numerical models that have both considered and ignored the epikarst zone connected by sinkholes to the underlying karst network. Without including the epikarst, the numerical simulations do not adequately match the recorded data (Király et al. 1995).

(3) Karst network and the surrounding less permeable rocks volume

High and low permeability zones play a fundamental role in high and low degrees of vulnerability, respectively. Consequently, the existence of a karst network, its development degree, its degree of interconnectivity as well as the existence of the epikarst are important related to vulnerability for the following reasons:

- If there is a karst network and a well-developed epikarst directly connected to it, the aquifer will be highly vulnerable.
- If the epikarst is not directly connected to the karst network, theoretically the aquifer will be less vulnerable. In practice, however, to prove such a case, it is not always this clear (cf. Part III).
- If there is neither epikarst nor a karst network - the aquifer is therefore a fissured aquifer - the aquifer will then be somewhat less vulnerable.

The analysis of boundary conditions and physical parameters shows the importance of the four attributes in the assessment of vulnerability. These are depicted in the schematic representation of a karst aquifer according to a distributed paramater conceptual model (Figure 2.25.). Four major attributes exist: one for the boundary conditions and three for the physical parameter fields: the infiltration conditions, the protective cover, the epikarst zone and the karst network development.

The threa first attributes, infiltration, protective cover, and epikarst vary spatially and are relatively easy to map. In contrast, the karst network devalopmant requires the use of a

black-box type model in most cases. The input-response characterization of the karst network system reflects its vulnerability state. The karst network is a 3D attribute that is relatively difficult to map. If it is being explored by humans, a partial map of the network can commonly be obtained. If the karst channels are not accessible to humans, it is necessary to characterize it by a more global, black-box approach. Thus, the karst network development will be characterized globally for entire water catchment basins. On the block-diagram schematically representing a karst network (figure 2.25.), only one of many potential karst networks is depicted.

The conceptual model used as the basis of the vulnerability method, EPIK, is a joint model combining a black-box component for the karst network development with a distributed parameter model for the other attributes.

The question of the field identification of these attributes and their subdivision is considered in Chapter 3, Part III.

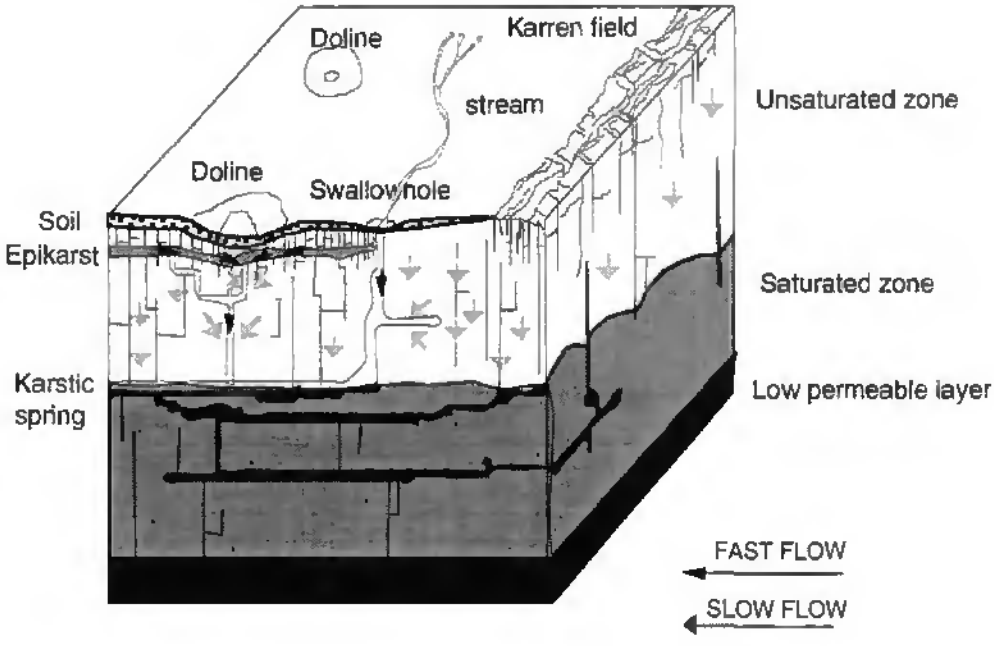

Figure 2.25.: Conceptual model of a karst aquifer used to assess the vulnerability mapping (Zwahlen & Doerfliger, 1995).

Part II

Variability in transfer functions derived from artificial tracer tests when interpreted with input-response models

Chapter 1

Theory and analysis of artificial tracer tests

1.1. Tracer test objectives

Tracer tests are commonly usad in applied karst hydrogeology. They generally give 1) qualitative information denoting the connection between the injection point and one or more outlets, or 2) quantitative relationships such as recovery rate of the tracer mass, transit time, tracer dispersivity, hydro-dispersive parameters, and transfer functions which can be derived from input-response models.

Quantitative interpretation is of importance as it provides a base of experimental data concerning the potential mechanisms of transport of various different contaminants, and parameters of the environment or the system in which the tracer is migrating. This is useful to either evaluate theories (solving problems, discovering new ones,...) or to validate transport scenarios that are typically done with one of several numerical simulation approaches.

1.2. Artificial tracers and their methods of analysis

Both chemical and microbiological artificial tracers have been used in this work. A short review of the major features of these tracers - their physical, chemical and toxicological properties is in appendices II.1. and II.2.

An ideal tracer requires the following conditions:

- absence of the tracer in the natural environment; with the smallest possible « background noise ».
- easy identification with standard analytical methods

- concentration levels of tracer easily measured with detection limits as low as possible .
- non toxicity for humans as well as fauna and flora .
- good stability related to chemical, biological and physical processes (oxidation, reduction reactions, acid-base reactions, microbiological destruction, temperature and light).
- the lowest interaction with the environment (ion exchange, adsorption).

According to many workers in the field and as recently summarized by Käss (1992), it is admittedly difficult to find ideal tracers that satisfy these requirements. The tracers that were used for the numerous experiments carried out as part of this thesis met the ideal criteria as much as possible.

Microbiological tracers such as the bacteria and viruses interact with the surrounding environment more than the major chemical fluorescent tracers. This is due to their interactions with the water which is in contact with the rocks and with colloidal particles. Some microbiological tracers are more sensitive to adsorption processes as was demonstrated in laboratory experiments by Rossi(1994).

Tracer tests were carried out in the Areuse, Noiraigue and Milandrine water catchment basins. Simultaneous injection of both bacteriophages and conventional fluorescent tracers allowed us to demonstrate that there are differences and similarities in the behavior of both of these types of tracers. The understanding of why they behave differently is a function of both the surrounding environmental and hydrodynamic conditions found in nature (see chapter 4 in the part II.).

1.3. Qualitative interpretation

Injecting an artificial tracer, whether it is chemical or biological, into an aquifer, commonly provides various types of information about the system being investigated.

First, the so called « everything or nothing » information situation (Guizerix & Margrita, 1976; Lepiller & Mondain, 1986) develops. Either the tracer reappears at the sampling point or, it is not identified in any of the water samples. A positive tracer test identifies clearly that there is a spatial relation between the injection point considered the input, and the sampling point at the spring or well considered the output. In the case of negative results, the question often arises as to the adequacy and appropriateness of the sampling points: were there enough of them?, were they in the right place and sampled at the correct time?, was there enough tracer added taking into account the natural hydrodynamic conditions?, and was the sampling duration and frequency sufficient?

According to Dzikowski (1992), the system that is identified between the injection and outlet points in a tracer test can vary over time, as a function of the change in the system hydrodynamic conditions (discharge rates, hydrodynamic state: rising and falling limb, transition, base flow or discharge influenced by a pumping action).

We immediately addressed this issue of how any changes in the environment could influence the results. The delineation of the boundaries of water catchment basins and related protection zones are commonly interpreted in light of the tracer results. Therefore, it was critical to understand how variable test results would be with fluctuations in the hydrodynamic regime.

1.4. Quantitative interpretation

1.4.1. Introduction

« The artificiel tracer test allows us to develop a bette understanding of the connection being studied and the method of migretion end transfer of the injected tracer mass.» Lepiller & Mondain, (1986) (free translation, ND).

The breakthrough curve of a dye or another type of tracer at the sampling point provides the basic result with the data that will be considered in any quantitative interpretation. This curve represents the water sample tracer plume concentration during its migration past or arrival at, a sampling point. The water sample tracer concentration is plotted against time to produce a tracer recovery curve (Figure 1.1).

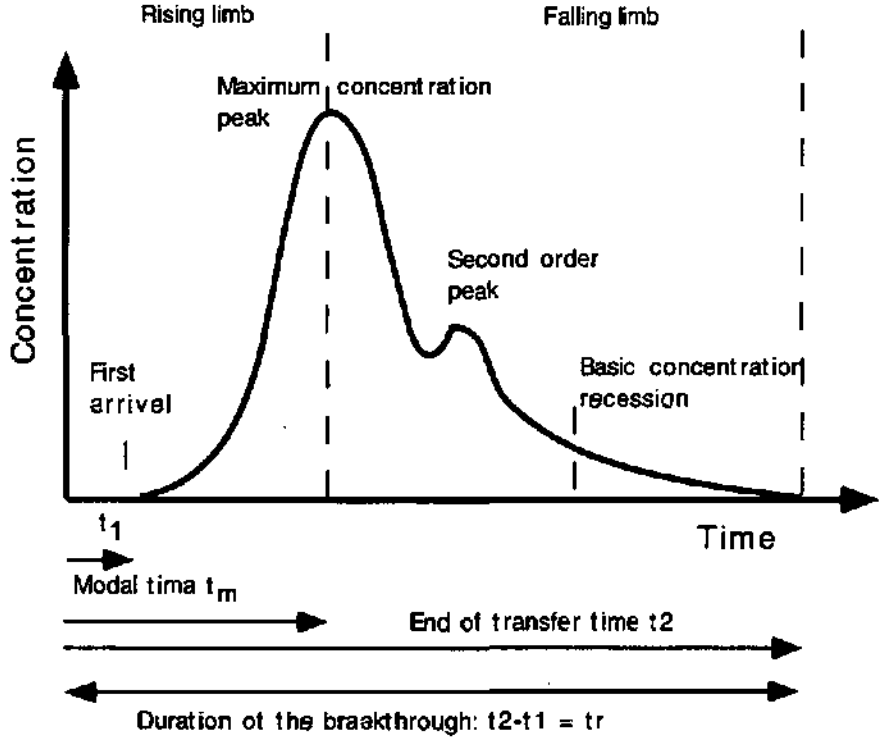

Figure 1.1: Major features of a breakthrough curve (modified after Meus, 1994).

The results of quantitative artificial tracer tests can be evaluated and the results used to determine potential contaminant transport characteristics, such as residual levels, dispersion rates, maximum concentrations (Mull et al, 1988) and also transfer functions of the flow pathways being studied.

In order to characterize the various breakthrough curve parameters, the discharge rates at the exit points have to be recorded using either manual measurements or the use of automatic discharge or water level recorders (Table 1.1).

Table 1.1.

Functions and parameters reaulting from artificial tracer breakthrough curves (modified after Lepiller & Mondain, 1986 and Maua, 1994).

Used functions	Calculated Parametera
Tracer concentration at the outlet: $C_s(t)$ · [breakthrough curve]	- Time to the leading edge t_1 .Time to the trailing edge t_2 - Recovery duration: $t_r = t_2 - t_1$ - Time to peak tracer concentration: t_m - modal velocity: $V_m = L/t_m$ - maximum velocity: $V_{max} = L/t_1$ - Maximum tracer concentration of the tracer plume: C_m
Mass flux at the outlet: $\phi(t) = Q(t) * C_s(t)$	- mass of tracer recovered: $M_r = \int \phi(t)\, dt$ - recovery rate in %: $R(\%) = \frac{M_i}{M_r}$
Residence time distribution (RTD): normalized tracer mass flux using the total recovered mass: $h(t) = \frac{\phi(t)}{M_r} = \frac{C(t)Q(t)}{\int C(t)Q(t)dt}$	- mean elapsed time : $t_{ms} = \int_0^\infty t\, h(t)\, dt = \frac{\int_0^\infty t\, C(t)Q(t)\, dt}{\int_0^\infty C(t)Q(t)\, dt} =$ time at the Center of gravity (centroid) of the recovery-tracer curve. - apparent transit velocity: $V_{app} = L / t_{ms}$ - harmonic mean $t_h = \int_0^\infty \frac{1}{t} h(t)dt = \frac{\int_0^\infty \frac{1}{t} C(t)Q(t)dt}{\int_0^\infty C(t)Q(t)dt}$ - mean transit velocity: $V = L / t_h$

Time t_1 corresponds to the time of the first arrival of the tracer. This time is dependent on the detection limit of the analysis method and the sampling frequency. When simultaneous injection of chamical and microbiological tracers has been done, small differences in t_1 are commonly observed. These differences are often due to unequal sampling frequencies and differences in the detection limit of the tracers. For example, the microbiological tracers detection limit of 0.5 phage per ml is lower than the fluorescent dye detection limit of about 10^{-11} mg/l.

The **maximum velocity, Vmax,** can also be calculated using time t_1 taking into consideration the apparent length of the tracer path (the direct distance to which it is possible to add a length l which is a, function dependent upon the unsaturated zone and the dip of the layers).

Time t_2 is effectively the end of the breakthrough curve. This time is related to the detection limit of the analysis method and the background concantration. Due to the tail that continues towards the end of the breakthrough curve, t_2 is not easily defined. The tail relates to retardation processes (sorption, exchange with stagnant water, temporary water storage conditions and remobilization).

The **modal time,** t_m is the time at the maximum concentration, or peak, of the recovery curve. It is the value that is, by convention, used to calculate the corresponding travel time velocity, Vmax and is also used to define the time after which the tracer or supposed contaminant concentration begins to decrease (Maus, 1994). If the curve has multiple peaks, whether major or minor, then the curve response is referred to as multi-modal . In this case, a velocity can be calculated for each peak. The bi- or multi- modal behavior can be accounted for if: 1) various flow paths are believed to be responsible for each peak, 2) there is en influence from recharge to the aquifer during the tracer experiment, 3) there is temporery storage of the tracer, or 4) the tracer is remobilized in the system (Atkinson et al., 1973).

The **recovered tracer mass over time (flux)** can be calculated using the outlet discharge values and the measured or extrapolated concentrations in the samples. The flux values can be plotted against the time determine the « Residence Time Distribution » (RTD).

Knowing the discharge allows calculation of the **recovered tracer mass** by integration of the multiplied concentration by the discharge from t_0 to infinity.

The **recovery rate** can be determined by considering the ratio of the recovered mass to the injected mass. Recovery rates vary considerably in karst environments: a low recovery rate is typically associated with: 1) the hypothetical existence of one or more non-measured outlets, 2) adsorption processes or 3) storage of the tracer in stagnant water. The recovery rate is also a function of the accuracy of the discharge measurements. :

By normalizing the tracer flux with the recovered trecer mass at the sampling point(s), it is possible to depict a response that characterizes the system if the tracer injection is considered to have been an impulse (Lepiller & Mondain, 1986). This response is called the residence time distribution (RTD). It has dimensions inversely proportional to time (Guizerix et al, 1970) and represents the probability that tracer molecules will be present at a given concentration in the tracer system during a time of duration dt. It is equivalent to the impulse response only if the input function is a Dirac (see Chapter 2, Part I).

The mean travel time, t_{ms}, corresponds to the time at the center of gravity (centroid) of the tracer mass and is determined from the RTD. It is dependent upon how convective the transport of the tracer is, as well as the dispersive and interactive effects that occur within the aquifer. The mean travel time is used to calculate the apparent transit time, V_{app}. This velocity is comparable to the effective flow velocity, **u**. In this particular case, the impulse response corresponds to a Gaussian distribution (explain Gaussian distribution) in space with the result that the mean travel time is equal to the pure convection time, t_c. Generally, the mean transit time is different from the purely advective[8] time, t_c. Only rarely are impulse responses with Gaussian distribution the result of dispersion[9], absorption, desorption[10] and stagnation [11].

Typically, the real length of the flow path, L_r, is greater than or equal to the apperent tracer distance length, L, and therefore, there is an degree of error in the velocity value.

It is also possible to calculate the **harmonic time,** the time weighted harmonic mean, and a corresponding velocity, the mean velocity. This velocity is generally higher than the

[8] *Advection: transport of mass following the flow; groundwater and the dissolved mass will move at the same rate (Domenico & Schwartz, 1990).*

[9] *Dispersion: effect of a variety of microscopic, macroscopic, and regional conditions that influence the spread of a solute concentration front through an aquifer: molecular diffusion and mechanical dispersion. Molecular diffusion is the mechanism of exchange between the solutes of flowing water and stagnant water that exists in some recessed water zones in the karst channels. The result of the mechanical or kinematic dispersion of a solute is a mixing that occurs as a consequence of local variations in the velocity field around some mean velocity of flow*

[10] *Sorption processes: reactions between solutes and the surfaces of solids of the aquifer (ion exchange, precipitation, transformation)*

[11] *Stagnation: in karst terrain, this effect results from diffusion of the tracer that is flowing in a conduit out of the main flow pathways into other parts of the regime where there is virtually no water flow. Stagnant water zones in a karst aquifer are commonly dead-end zones in karst channels.*

apparent velocity and lower than the modal velocity (Meus, 1994). However, harmonic times have not been calculated for the tracer tests interpreted as part of this thesis. Instead, the maximum, modal and mean transit time velocities have been used.

Chapter 2

Quantitative interpretation of artificial tracer tests - Experimental considerations

2.1. Site geography, geology and hydrogeology

Tracer tests were performed in karst aquifers in Switzerland (Figure 2.1) by the author at both the test-site in Bure (Tabular Jura) and the water catchment basin of the Areuse spring (Folded Jura), and by Geologists-Hydrogeologists Consultants as part of their work to outline groundwater protection zones and as part of other ongoing research work (Action COST65, Program SPP Noiraigue, Ph.D. thesis of Attinger (1988) in the Alpstein, and postgraduate diploma activities in hydrogeology).

The tracer experiments were done in water catchment basins of various sizes (<5km^2, 5-15km^2 and >75km^2), in karst aquifers of different thickness (50m, 200, and 500m) and in three different geological settings (Tabular Jura, Folded Jura and Alps (Helvetic zone). They were also performed under different hydrologic conditions (rising limb, falling limb and base flow conditions).

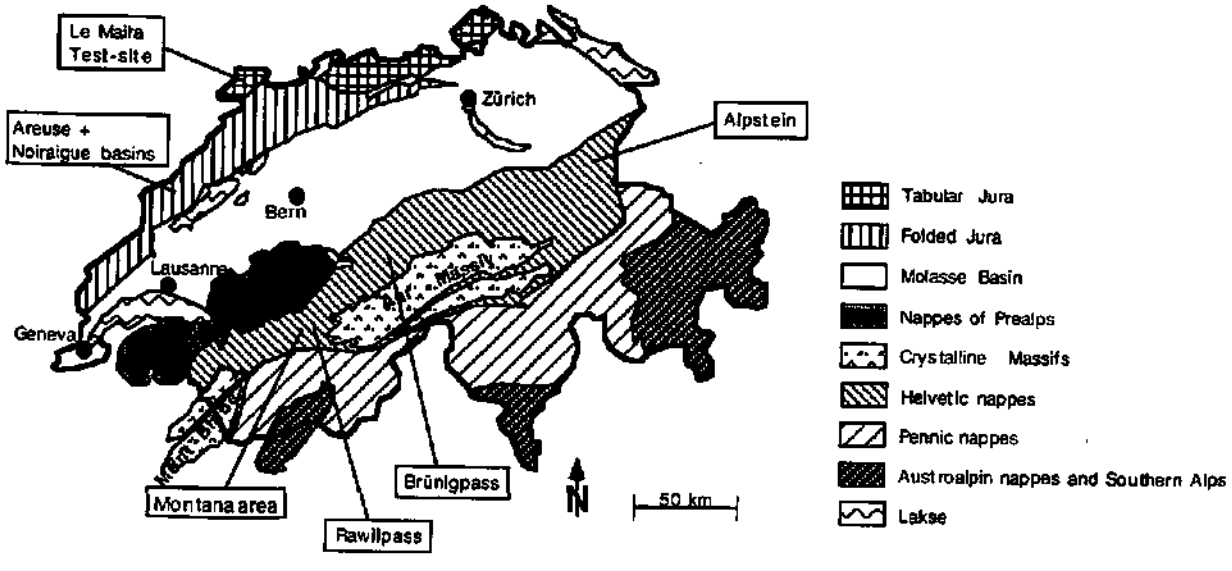

Figura 2.1.: Location of tracer test sites in Switzerland..

All tracer test data regarding injection point (nature, coordinates), sampled springs (coordinates, discharge), tracer (nature, quantity) and the calculated parameters (recovery rate, velocity, gradient) are either in database 4D (Appendix II.8) or in the tables in

appendices II.3 to II.5. Both data sources are complementary. In addition, the raw data for all recovery curves (concentration versus time) are given in full in Appendix II 7.

2.1.1. Water catchment basin of the Areuse spring

The water catchmant basin of the Areuse spring consists of two synclines, the Brévine valley and the eastern part of the Verrières valley. The Brévine valley (~1050 m. a.s.l.) consists of a large depression of about 85 km^2 and is considered to be a syncline polje (Bürger, 1959). This valley is bordered to the NW and SE by two anticlines ranges, the Grand-Taureau - Mont-Châteleu - Les Roussottes and the Crêt-du-Cervelet - Grand-Som-Martel, respectively (Figure 2.2). The Verrières valley (930 m. a.s.l.) stands between two anticlinas ranges: Les Comées - Les Fontenettes in North and the Mont-des-Verrières in South (Tripet, 1972).

The water catchment basin boundaries were defined taking into account both the geological structures and tracer test results (Bürger, 1959; Müller et Zötl., 1980).

The upper Jurassic limestone (320 to 350 m of thickness) makes up the aquifer. The Argovian marls-limestone complex, considered as relatively impervious, is a regional aquiclude and underlies the aquifer. Therefore, the lower boundary of the basin correspond to where this Argovian complex intersects with the outflow zone at the point it emerges on the topography.

The Areuse spring, also called "la Doux" spring (coord.: 534.225/195.450; ~750 m. a.s.l.) is the major outflow from the basin. It amergas in the upper Sequanian limestone at the foot of a small cliff in the NW part of the St-Sulpice cirque. The mean annual discharge of the Areuse spring is 4.68 m^3/s. Discharges are recorded by limnigraph at the federal station in St-Sulpice (NE).

Two injection points were chosan: the Moulin du Lac des Taillères swallowhole (coord.: 534.300/202.000, 1036 m. a.s.l.) located in the Brévine valley, and the Belle Perche swallowhole (coord.: 528.800/195.320; 935 m. a.s.l.) located in the eastern part of the Verrières valley. The hydraulic connection with the spring of these points is well documented.

- The Lac des Taillères swallowhole has been the object of tracer expariments since the end of last century (Desor, 1864 and Desor, 1904). This swallowhole is the single inlet to Taillères Lake (1.9km length, 200 to 300m width). Its substratum consists of clays and till terrain above molasse sediments of Cretaceous age (Tripet, 1972). The swallowhole was constructed in order to increase the storaga capacity of the lake and to regulate the base flow discharge of Areuse spring. Currently, it is out of order.
- The Belle Perche is a swallowhole where a stream disappears throughout the year draining water out of the upper peat fields. The mean annual discharge of the stream is about 25l/s.

2.1.2 Water catchment basin of Noiraigue spring

The water catchment basin of the Noiraigue spring is a 70 km^2 " Vallée des Ponts " area located in the Swiss Jura mountains at an elevation ranging from 1000 to 1300 meters (Figure 2.2.). The karst aquifer consists of a 500 meter thick Upper Jurassic and Lower Cretaceous limestone. These limestonas are folded into a single syncline pinched by two anticlines characterized by a faulty contact. The Argovian marls make up the underlying regional aquiclude.

The Noiraigue spring, the only outlet of the basin, is at an elevation of about 740 m and is directly related to a regional fault. The spring occurs in the Sequanian limestone in the Noiraigue village at a distance of about 4 km from the principal swallowhole of the area.

Three hundred meters of Molasse sandstone cover the central part of the syncline. This formation is overlain by Quatamary deposits consisting of glacial till and post-glacial marl deposits (Atteia and Kozal, 1995).

Four swallowholes have been used as tracer injection points; the Bied in Pont-de-Martel, locally referred to as « of Voisinage » (coord.: 545.700/204.880), Roche Berthoud (coord.: 543.600/202.250), Brot-Dessus (coord.:547.000/203.000) and la Combe Varin (coord:.545.200/202.500).

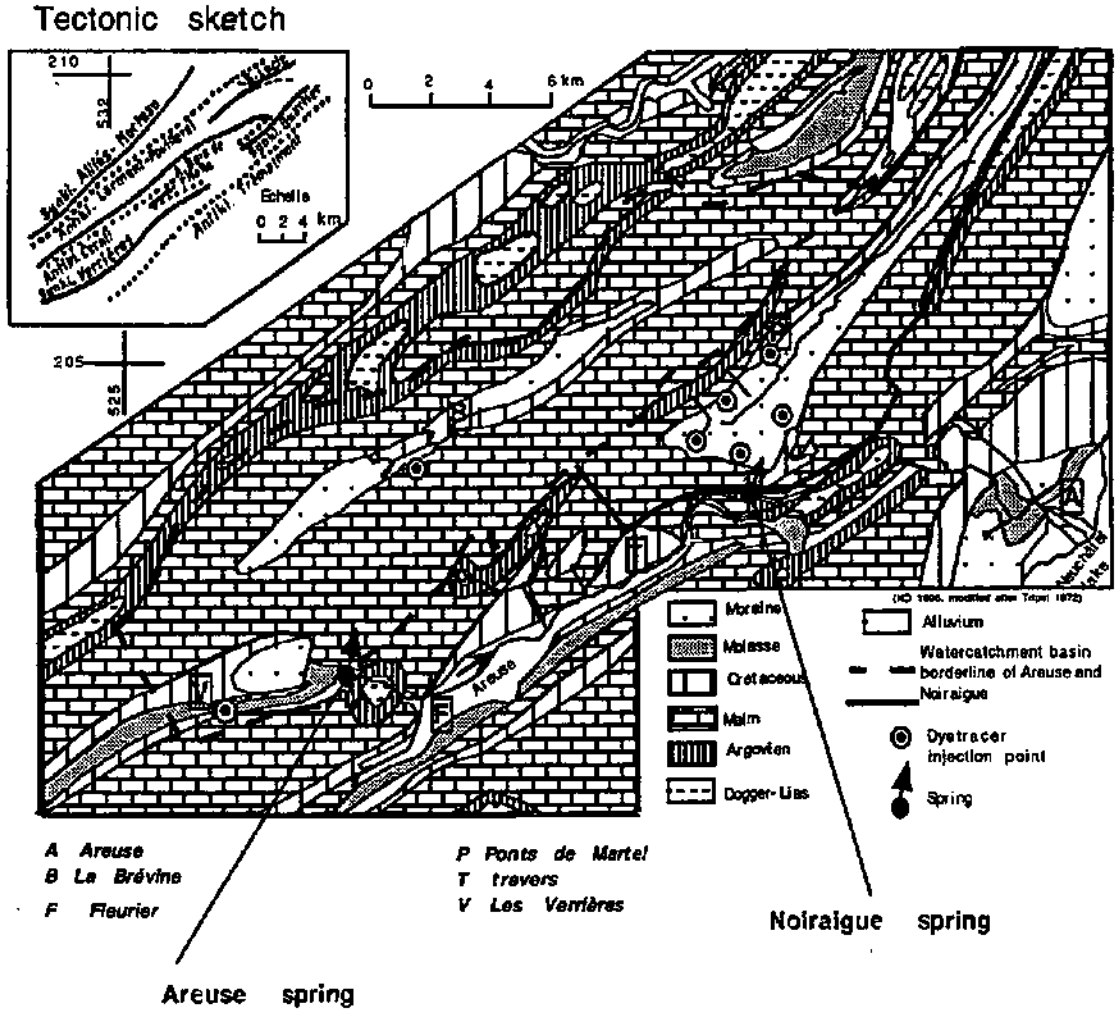

Figure 2.2.: Areuse and Noiraigue catchment map - location of injection points (modified from Tripet, 1972).

2.1.3 Water catchment basin of La Milandrine, Bâme, Saivu and La Font springs

The Bure test-site is located in Ajoie, in the northern Switzerland in the Tabular Jura. The Bure plateau belongs to the regional Ajoie plateau, an upper Jurassic sub-tabular formation, which disappears to the North under the post-Eocene terrain of the Sundgau. To the south, the Ajoie plateau is over thrust by the northern front-line of the Folded Jura.

The Bure plateau consists of sub-horizontal limestone layers of the Malm. A system of fractures and faults exist throughout the area and are related to tha Rhine graben tectonics to the northeast and the Folded Jura to the south (Figure 2.3.). The major tectonics elements are the vertical sub-meridian faults (tectonics system in « keys of keyboard »). Two other faults families are present at the plateau scale: N40 to N70° and N130 to N150° (Turberg, 1993).

The basin is oriented North-South, with a surface of about 15km^2 (Figure 2.4). Due to the « keyboards' keys » structure, the outline of the water catchment of the Saivu-Bâme-Font

springs is complex. The basin boundaries have been approximately defined taking into consideration the stratigraphy, tectonics and the tracer experiment results (Gretillat, 1992). The water catchment of these springs includes the karst network of La Milandrine, that drains the rainfall water of the Bure plateau. There is no surface drainage on the plateau. Water infiltrates through the soil to recharge the aquifer, its less permeable fissured limestone blocks and its more highly permeable network. An underground river, La Milandrine, flows in the karst network . This underground stream drains or is drained by the surrounding rock volume in accordance with the hydrological conditions.

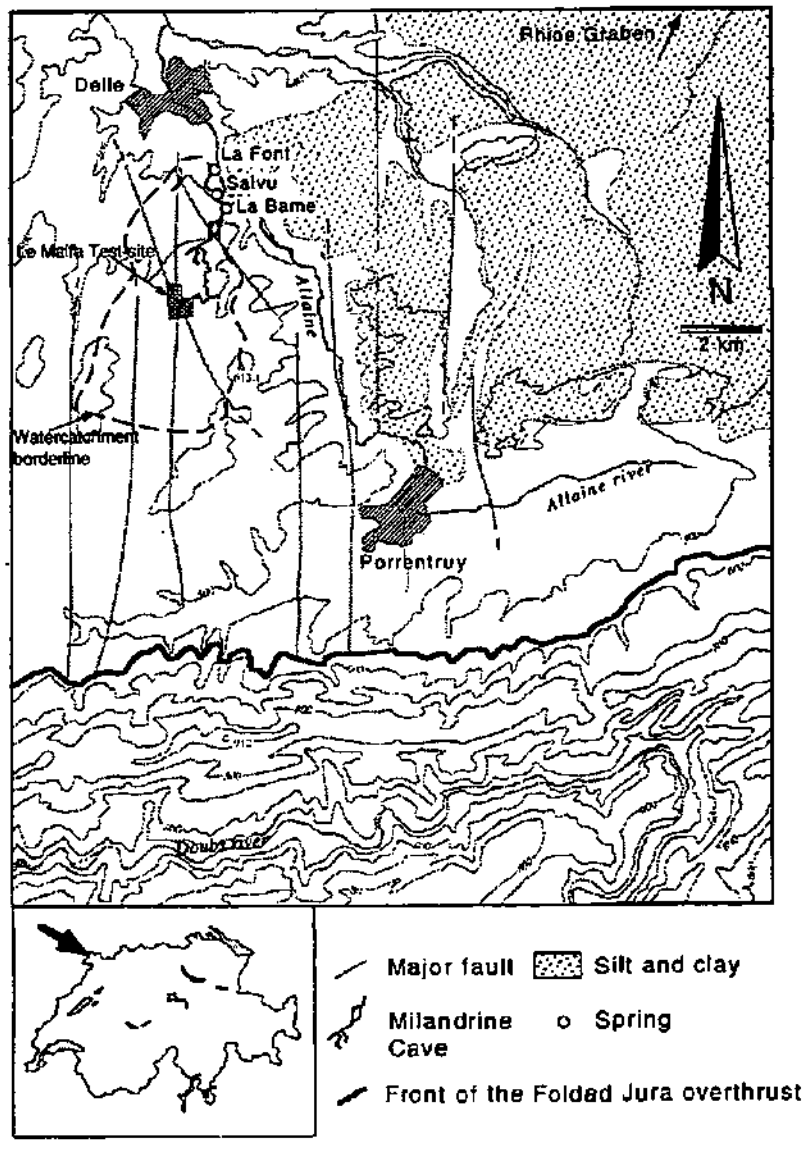

Figure 2.3: Tectonic setting of the Maira test site and of the La Font, Saivu and La Bâma catchment (after Jeannin, 1996).

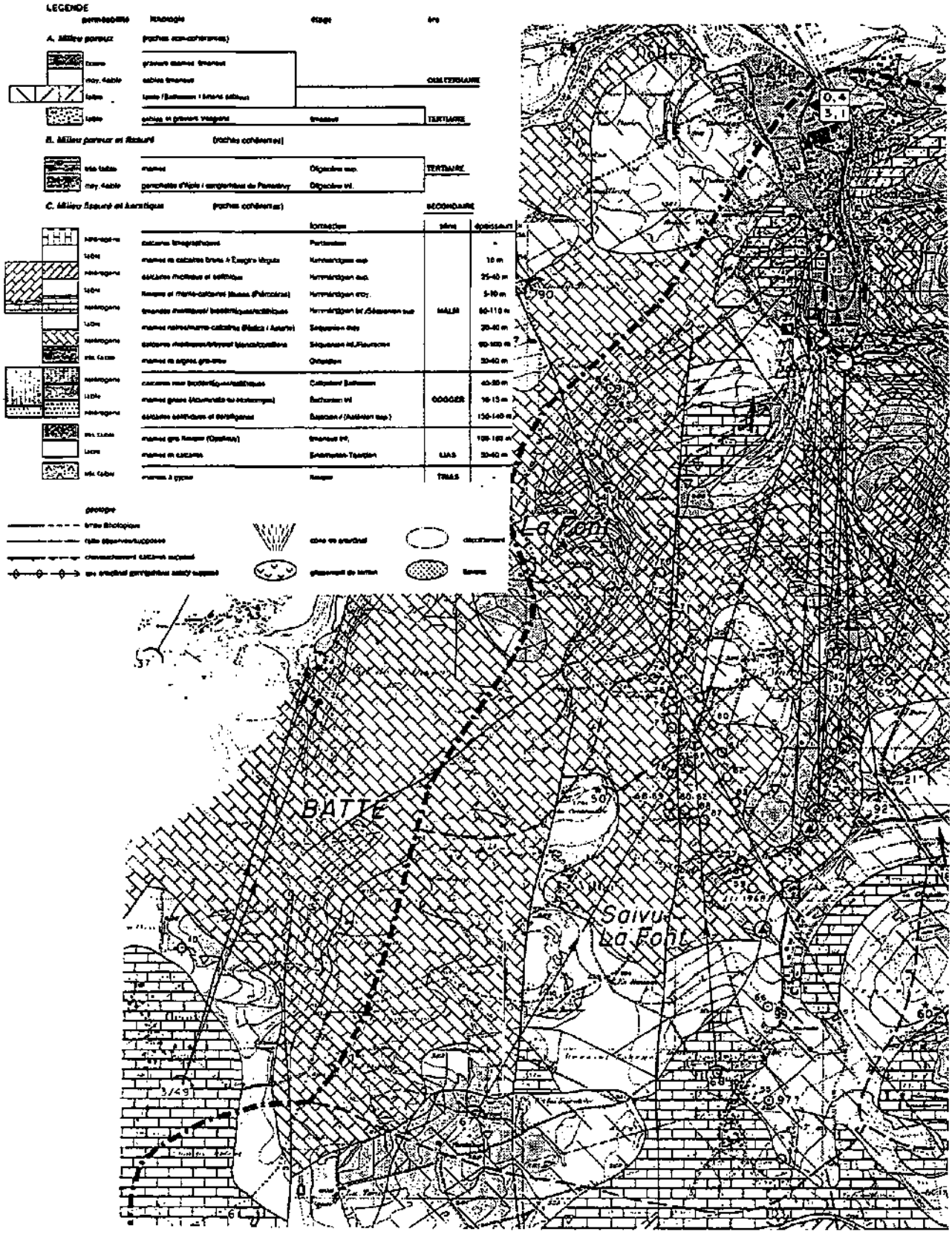

Figure 2.4.: Extract of the hydrogeological map of the Ajoie (Gretillat, 1992).

Quaternary deposits up to 20 meters thick overlie the lAssertates and Nautilus limestones of middle Sequanian age. These limestone average about 30 meters in thickness. The underlying limestones are the Lower Sequanian/Rauracian reef limestones with thickness from 60 to 80 meters. These limestone constitute the aquifer that overlies the Oxfordian marls, the underlying aquitard (Jeannin, 1995) (Figure 2.5).

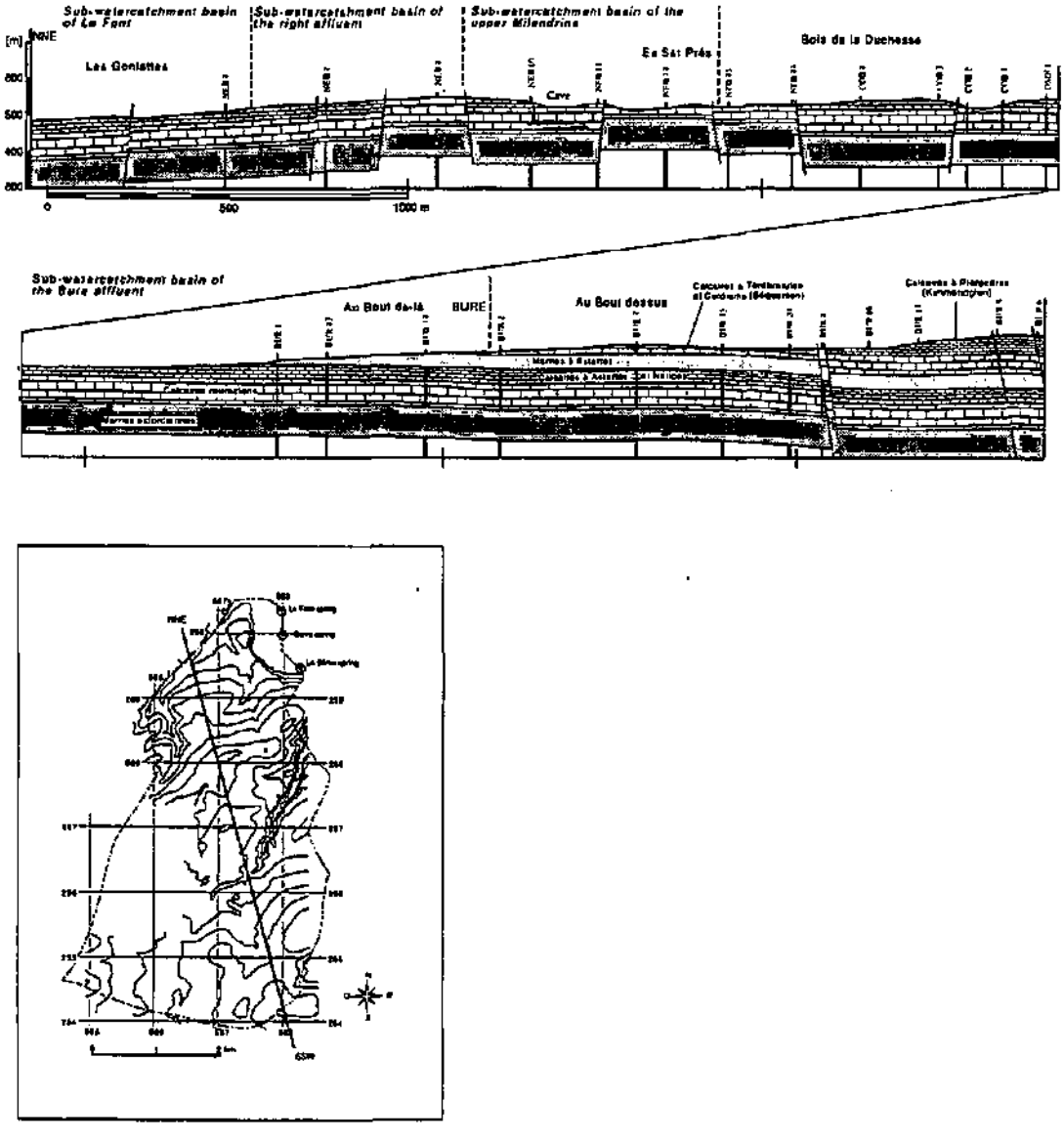

Figure 2.5: NNE-SSW geological profiles with borehole locations (after Jeannin, 1995).

The Maira site in Bure is in the upper part of the basin and is equipped with a dense borehole network. There are more than twenty boreholes in less than a square kilometer and ten boreholes are located along two W-E profiles. The mean tracer distance between profiles 1 and 2 and the sampling points in the upper part of the karst network is 400m and 180m, respectively. The tracer distance to the La Font, La Bâme and Le Saivu springs is an average of 4500m more than the previous tracer distance if the true length of the karst network is taken into consideration (Maréchal, 1994).

The unsaturated zone extends to a depth of about 40 meters where the boreholes used in the tracer network are located.

The injection point locations are all shown on Figure 2.6. The majority of the tracer experiments have been carried out in the lower part of the boreholes. Salt was diluted in 3000 to 4000 litters of water was injected and the same amount of clean water was injected to flush the tracer into the formation. The technique of injection for the bacteriophages into the boreholes was similar.

Some surface points have also been used as tracer injection points. They are at a naturally open holes in a swallowhole (pt1), at the edge of a depression with about 30 cm of overlying soils (pt6), and at an uncovered limestone in fault zones (pt 9., pt 3., pt 11).

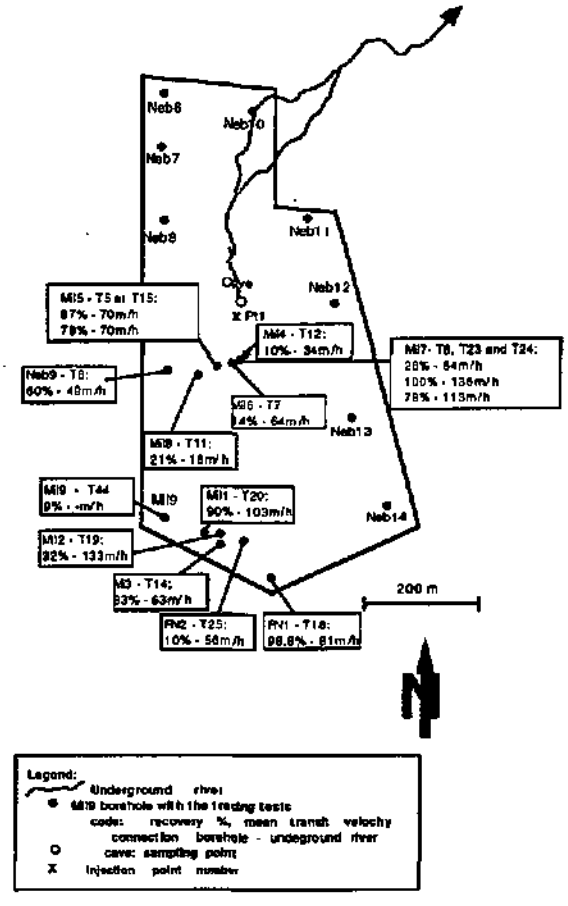

Figure 2.6.: Location of Bure site injection points (boreholes, artificial holes and surface points) and the network relationship to the upper Milendrine sampling point.

2.1.4 Various test sites in the Folded Jura and Tabular Jura

Some tracer tests had been made as part of work done by either by the Consulting Hydrogeologists MFR SA (Delémont), or by Gretillat when he designed the hydrogeological map of the Ajoie. They are listed in the hydrogeological map database (Gretillat, 1992).

Only the tracer test that was carried out in Courfaivre (JU, Folded Jura) is described here:

Courfaivre

The tracer test JU10 was done as part of the postgraduate work in hydrogeology by Alain Hohl (1992). The injection point is located in a 30 cm open fissure from which air flows are routinely observed. This point is located in the Upper Malm limestone and is the source area for the Chenal spring that was sampled.

The Chenal spring is known to be the outlet of the aquifers that occur in the Kimmeridgian limestone. The spring flows out where it is in contact with Quaternary rock debris. The aquifer is located in the Folded Jura. The spring is situated to the north of the Vellerat anticline; an anticline that is oriented east-west with a sub-horizontal axis.

2.1.5. Alps: Montana, Brünigpass and Alpstein

Montana

Tracing tests of the Montana area were made by the Geologists-Hydrogeologists F. Clavien (Sion, VS) during the spring of 1990. The objective of their work was to outline water protection zones for the water catchment basins of the Cry d'Er, Bella Lui and Petit Bonvin springs.

Springs of the Montana area are all located in the Wildhorn nappe (Helvetic Zone). All the injections took place in the Malm limestone. This karstified limestone subsides to the South. An important fold occurs in the area and the normal flank of this fold constitutes the Petit Bonvin and Plumachit. The Mont-La Chaux, Belle Lui, Tubang and Grand Bonvin mountains peaks are located on the inverse flank of the fold. The Mollens and Icogne springs were used to carry out the tracer tests in the Tsa Plateau, Plumachit and La Tsa Bonna (tracer tests ALP1, ALP2 and ALP3).

Brünigpass

The test (ALP5) was carried out as part of a hydrogeological study in the Brünigpass area (National Roads, N8) by the Geologists-Hydrogeologists consulting company, Dr. von Moos AG, Zürich (1981). This test took place in the Dogger and Malm karst aquifer, which has a complex tectonic structure. This aquifer is part of the Helevetic Wildhorn nappe.

The injection point is situated in the swallowhole of a small mountain lake, Alp Sewlisee, a part of which is located 1060m from the sampled spring Sewliwal - OW4 (Wildberger, 1982).

Alpstein

The tracer tests ALP7 to ALP20 were carried out by Attinger (1988) in the Alpstein area, in the northeast part of Switzerland, between the Rhine valley and Toggenburg. This area was studied in order to determine the water catchment limits of the major springs basins, the purpose of the Ph.D. work of Attinger.

The Alpstein geological setting is that the area is part of the Säntis nappe (Helvetic Zone) where there are strong tectonic influences. The northwest front of the Säntis fold overthrusts the sub-alpine molasse. A series of folds, overthrusts and minor faults exist naarby (Heierli, 1984) (Figure 2.7).

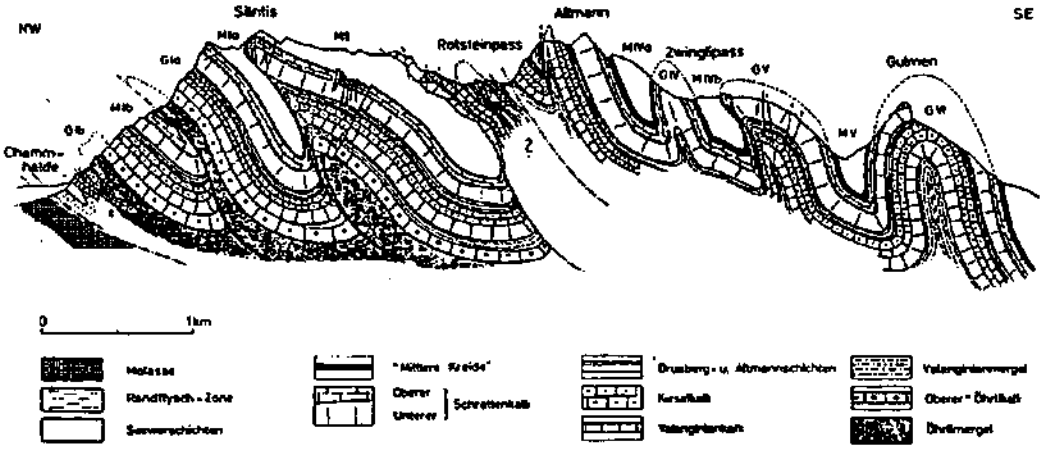

Figure 2.7. : Geological profile of the Alpstein area (Heierli, 1984).

The springs used for the tracer tests are located either in the well karstified Seewerkalk (Turonian) or Schrattenkalk limestone (Barremian-Aptian), or in the Kieserkalk (Hauterivian). Springs also come out of the highly fissured layers of the Valanginian. The above-mentioned limestones are karstified with interlayers such as the marls of the Drusberg layer (lower Barremian) and the Valanginian marls. These marl layers which are about 500 meters thick constitute relatively low permeability hydrogeological barriers.

2.2. Classical quantitative interpretation

The results of quantitative interpretation of the tracer tests using first, recovery rate and velocities, and second, the general characteristics of the transfer functions as impulse responses are presented and discussed in this section. The specific analysis of the characteristics of the transfer functions as indicial responses is presented in Chapter 3.

2.2.1 Jura Tracer tests

2.2.1.1 The Tabular Jura (appendices II.3, II.6 and II.7)

The recovery rate of these tracer tests varied between 1 % and 100% with an average of about 35%.

The average recovery rate of the tracer tests conducted using the Saivu spring was 30%. This recovery rate is believed to be lower than for the entire system. According to Jeannin and Grasso (1994), a loss of the stream at the end of the karst network may tend to reduce the Saivu discharge to about one half of the total karst system discharge. The stream is beliaved to be connected to the Alleine river.

The tracer distance was celculeted as a direct line between the injection point and the upper Milandrine sampling point. For the tracer tests that were sampled at the three major springs of the Maira water catchment basin (Font, Bâme and Saivu), the tracer distance included the true length of the karst network. As for the true distance, the tracer distances are believed to be 1.2 to 1.5 times longer than the direct straight line distance between the two points (Appendix II.3). Based on the results of the fractal dimensional analysis of karst network (Jeannin, 1992), this multiplication factor appears to be in the sama range as the fractal dimension. For several karst galleries in Switzerland, the fractal dimension is between 1.02 to 1.12. For Bure, the dimension is 1.11 (Maréchal, 1994).

The mean of all the modal velocities for the tracer tests were 102 (100)[12]m/h (true distance) and 75 m/h (64), using the estimated tracer distance. The highest value for the modal velocity was 500 m/h (250 m/h) whereas the lowest is about 15m/h.

The average of the mean transit velocity (calculated using the center of gravity (point) of the impulse response) is 96.5 m/h (72.5 m/h) with standard deviations of 88 and 58, respectively, and 117.5 m/h (86.4) for the +95% confidence interval and 75.5 m/h (58.6) for the -95% confidence interval. The lowest velocity was 2.5 m/h and the highest 350m/h.

The mean transit velocity is generally lower than the modal velocity and this certainly reflects the dispersion of the impulse response.

Some impulse responses of recovery curves that were the results from sampling at the upper part of the Milandrine in the cave (T2 to T8, T11 to T15 and T19 to T25) are presented on the Figure 2.8. These tracer tests were performed during the base flow to the end of falling limb conditions. With the exception of the impulse responses of T23, T24 and T5, all the rest of the impulse responses do not have an amplitude higher than 0.0055 [min^{-1}]. Some responses have a similar shape in that they are only shifted along the time axis. The transit time differs as a function of the diecharge values and the tracer distance.

Tracer tests T23, T24 and T5 with their recovery rates higher than 50% and their mean transit velocities greater than 70m/h characterize tracer-systems of high hydraulic conductivity (Figure 2.8).

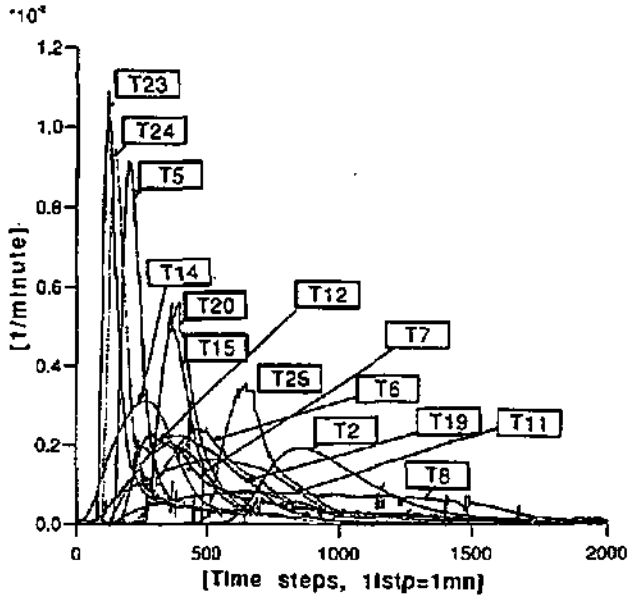

Figure 2.8: Impulse responses (transfer functions) of tracer tests done in lMaira and sampled at tha upper part of the Milandrine.

For the 14 impulse responses, three groups of impulse responses can be defined qualitatively using recovering rate and apparent hydraulic conductivity of the tracer system as two criteria:

- The first group includes the impulse responses that are very narrow and have a high intensity [1.1 10^{-2} min-1]. They result in tracer curves with a recovery rate higher than 60%.. The apparent hydraulic conductivity of the tracer systems is high [T23, T24, T5].
- In the second group, there are transfer functions with more than 60% recovery rates, but

[12] *The first number is the mean (eg. 100) and the number in brackets (eg (64)), is tha standard deviation.*

from karst systems with a medium hydraulic conductivity. The peak intensity of the impulse responses are lower than the first group and the curves are more enlarged [T14, T20, T15, T25].

- In the third group, there are the transfer functions of tracer tests with a recovery rate lower than 30% with curves that are spread out. These functions likely have to be related to low hydraulic conductivity tracer systems (Doerfliger, 1994) [T12, T7, T6, T2, T8, T19, T11].

All the times for tracer tests were noted on the hydrograph of the Bârnie, Şaivu and Font springs in order to compare impulse responses during their variable hydrological conditions. The three rising limb, falling limb and base flow recession hydrological conditions were taken into account in the analyses (Appendix II.8).

2.2.1.2. The Folded Jura (Appendices II.4 and II.6)

The recovery rate for tracer tests in this region varied from 1 to 100% at the Areuse spring with the recovery rate for conventional tracers not lower than 40%.

The recovery rates for classical tracer tests at the Noiraigue spring has been in the range of 30 to 100%.

The maximum velocity range was from 2 to 200m/h (mean 70m/h; standard deviation: 67, +95% confidence interval: 112.5; -95% confidence interval: 27.5); the modal velocities varied between 2 and 140m/h (mean 53m/h; standard deviation: 52, +95% confidence interval: 86.5; -95% confidence interval: 20). The mean transit velocity was 42 m/h (maximum 132m/h; minimum 1.5m/h and standard deviation 42.5, +95% confidence interval: 69; -95% confidence interval: 15). All of these values were calculated using an estimated tracer distance.

Intensities of the impulse responses using conventional tracers (Figures 2.9 and 2.10) were between 3.25 10^{-3} [min^{-1}] and 0.05 10^{-3} [min^{-1}]. The impulse responses with a small intensity are consistently related to tracer tests that were performed during base flow conditions where there are characteristically low transit velocities. Shifting of responses to the right along the time axis is related to the distance and the transit duration effects.

The responses of the NOIR1 tracer tests are different from the NOIR2 tracer tests. For the Areuse tracer experiments, the only tracer tests carried out in 1993 have different responses from the others showing an obvious difference of intensity.

It is difficult to determine a mean response for the Foldad Jura aquifer when using as a reference only the graphical representation of the impulse responses.

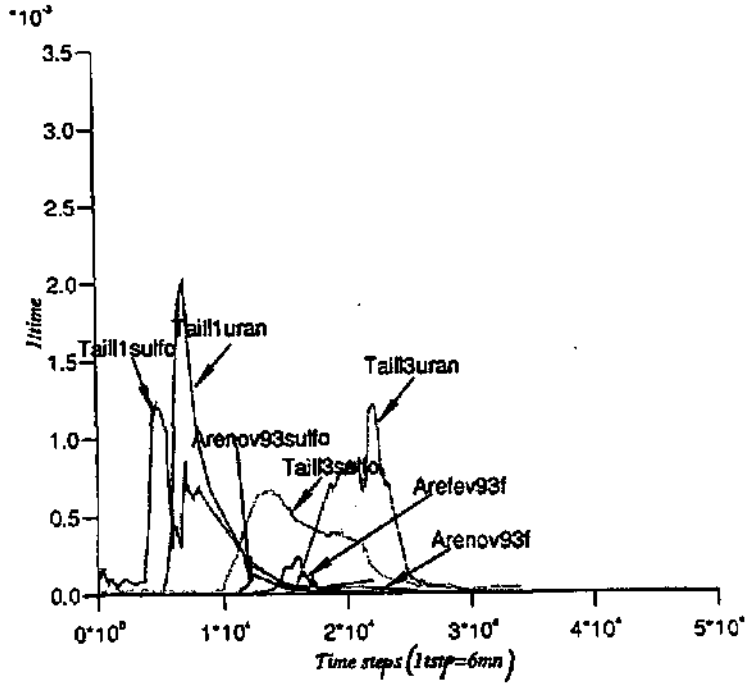

Figure 2.9.: Impulse responses of tracer tests at tha Areuse spring.

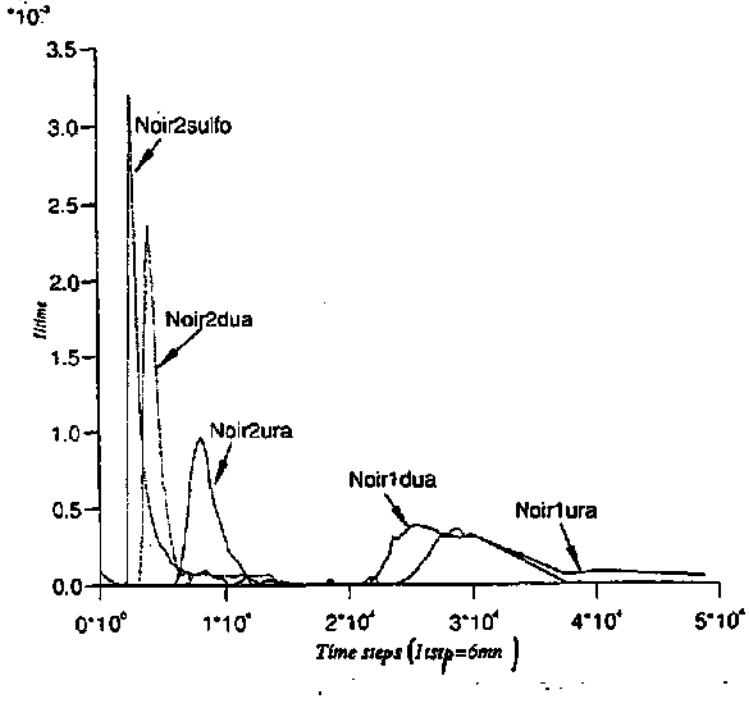

Figure 2.10: Impulse responses of tracer tests at the Noiraigue spring.

2.2.2 Alps Tracer tests (Appendices II.5 and II.6)

Results of quantitative interpretation of tracer experiments are in Appendix II.5. Recovery curves of the tracer tests of the Alpstein and the hydrograph during the tracer breakthrough are in Appendix II.9.

The mean recovery rate of these eighteen tracer tests with tracer distances of from 1000 to 7500 meters was 20%. The lowest recovery rate was about 1% and therefore has no significance. The value of the recovery rate was taken into consideration when interpreting the impulse responses (Figure 2.11).

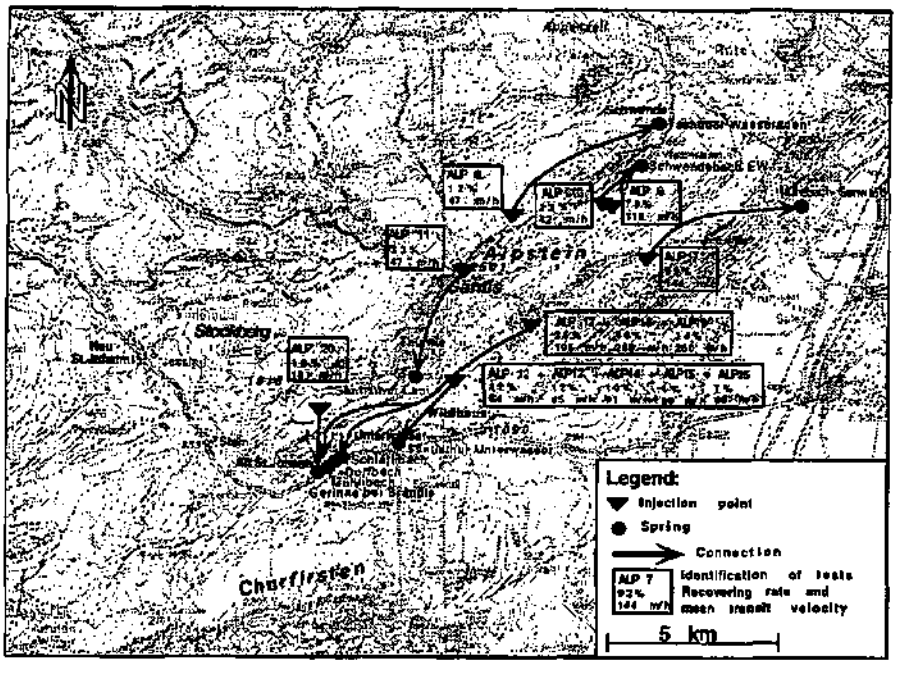

Figura 2.11.: Sitas of tracer tests performed in the Alpstein with mean transit velocity and recovery rate data.

The transit velocities (modal, mean transit and maximal) were over a relatively wide range of from 5 to 360 m/h.

Among the impulse responses (using a 1 minute deconvolution step), two groups of impulse responses with different amplitudes were able to be distinguished. When the recovery rate was higher than 70 percent, the impulse responses were narrow and their peaks had a high intensity greater than 0.0015 [min-1]. The rest of the tracer tests had a recovery rate lower than 15 percent with an essentially similar response intensity of 0.0005 [min^{-1}] (Doerfliger, 1994) (Figure 2.12).

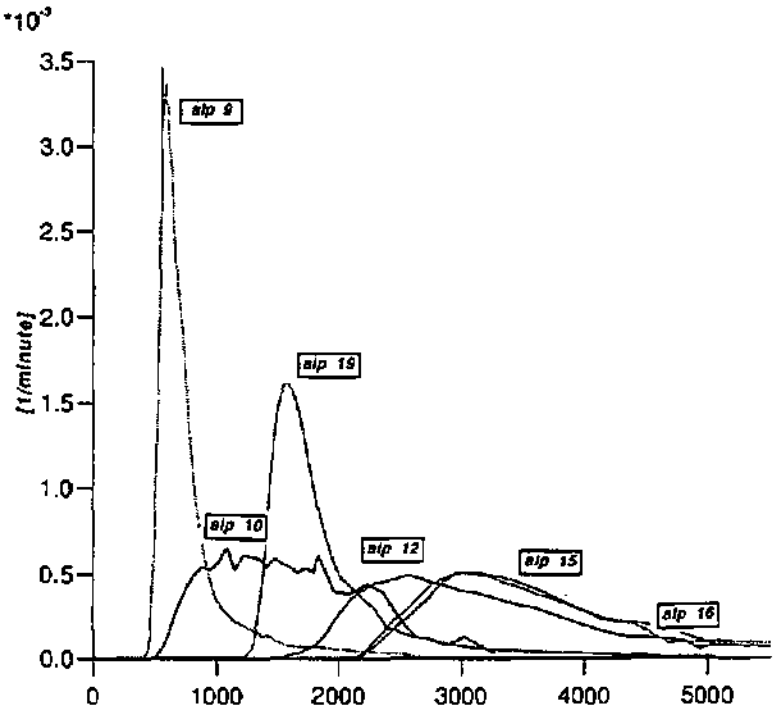

Figure 2.12.: Impulse responses of the Alpstein tracer tests using a one minute time step for deconvolution.

Chapter 3

Variability of tracer test transfer functions

3.1. Introduction

The variability of transfer functions was studied in order to characterize an environment with a statistical transfer function. This environment could be either the geological context, the water catchment basin or a typical morphological sector of a water catchment basin that is determined by the nature of the injection point.

Such a statistical transfer function could be used to simulate pollution in an environmental audit, for example, using the convolution of a mean transfer function [indicial response] with a fictitious input corresponding to a pollution point-source. The confidence interval around the mean value is considered to approach the probable error. In this manner, optimistic and pessimistic forecasting could be accomplished at lower cost in the scope of hydrogeological audits or impact studies.

Simulating or accomplishing tracer experiments in karst aquifers requires information on the discharge conditions as well as the hydrodynamic state of the sampled spring. A tracer does not commonly migrate with water at the same velocity and with the same transport parameter values and it's response also depends on the outlet discharge intensity. It is usually necessary to confirm if the hydrodynamic conditions are absolutely essential to characterize a transfer function. So the remaining question became: is it possible to distinguish a typical mean transfer function according hydrodynamic conditions for each geological context group of tracer experiments or for all tracer tests ?

To study the variability of transfer functions, the results of 96 tracer experiments have been used. 14 were done in the Swiss Alps, 12 in the Folded Jura and 70 in the Tabular Jura. Each tracer experiment had been treated with the black-box model and the data or simulated response was transformed into an impulse response and indicial response. The data related to the tracer tests (included transfer functions) are in tables in Appendixes II.3 to II.5.

Transfer function variability:

The first step was to approximate tha degree of variability that transfer functions could have. This was done by using indicial tracer test responses that had been selected as a function of their geological setting, the hydrological conditions that were in effect during the tracer test (Figure 3.1), their water catchment size (Figure 3.2) and the hydraulic conductivity of the tracer system (Figure 3.3).

The variability of the transfer function around the 0.5 percentile is quite noticeable. The transfer functions are more or less steep; the larger variability seems to be around the upper part of the curve. But, to determine if there is a significant difference between the means at the various gradient for each considered group, the interpretation of these plots are too restrictive. The transfer functions plots for each group give just a qualitative image. To distinguish the effect among groups, it is necessary to analyze the variance of chosen parameters.

Transfer functions are expressed in terms of impulse responses or indicial responses. Parameters suitable for a statistics analysis of an impulse response can be: Pearson coefficient $\beta 1$, Fisher coefficient γ (Skewness measurement), and Pearson coefficient $\beta 2$ for the flattening degree of a curve. For indicial responses, the gradients at three specific percentiles are used to distinguish the character of different responses. Responses are not

similar when they clearly have a steeper or a flatter curve in the upper, middle or lower part of it. Gradients at the percentiles are proportional, by definition, to impulse response intensity. The higher the gradient, the higher the intensity and vice-versa (Figure 3.4.).

To be practical, the gradient at three percentiles: 0.2, 0.5 and 0.8 was chosen as a simplified way to compare each condition s statistical value. Using the three percentile values provided characteristics associated with the lower, middle and upper parts of the indicial response curve. The 0.2 and 0.8 percentiles are similar to the 0.841 and 0.159 Gaussian distribution percentiles. For Gaussian distribution, the time at the 0.841 and 0.159 percentiles correspond to the time $t_{0.5}$ (median time) plus or minus the standard deviation, respectively. However, karst system transfer functions do not typically have to Gaussian distribution. Instead, they are asymmetric due mainly to various retardation factors (stagnation, adsorption).

The modal velocity, calculated with the modal time of the impulse response, was also taken into consideration in the variance analysis. Two parameters, gradient and modal velocity, were considered adequate to describe tracer test transfer function variability. However, to simulate contaminant transport, considering only the modal velocity was shown to be insufficient to determine the mean characteristics of the various tracer experimants.

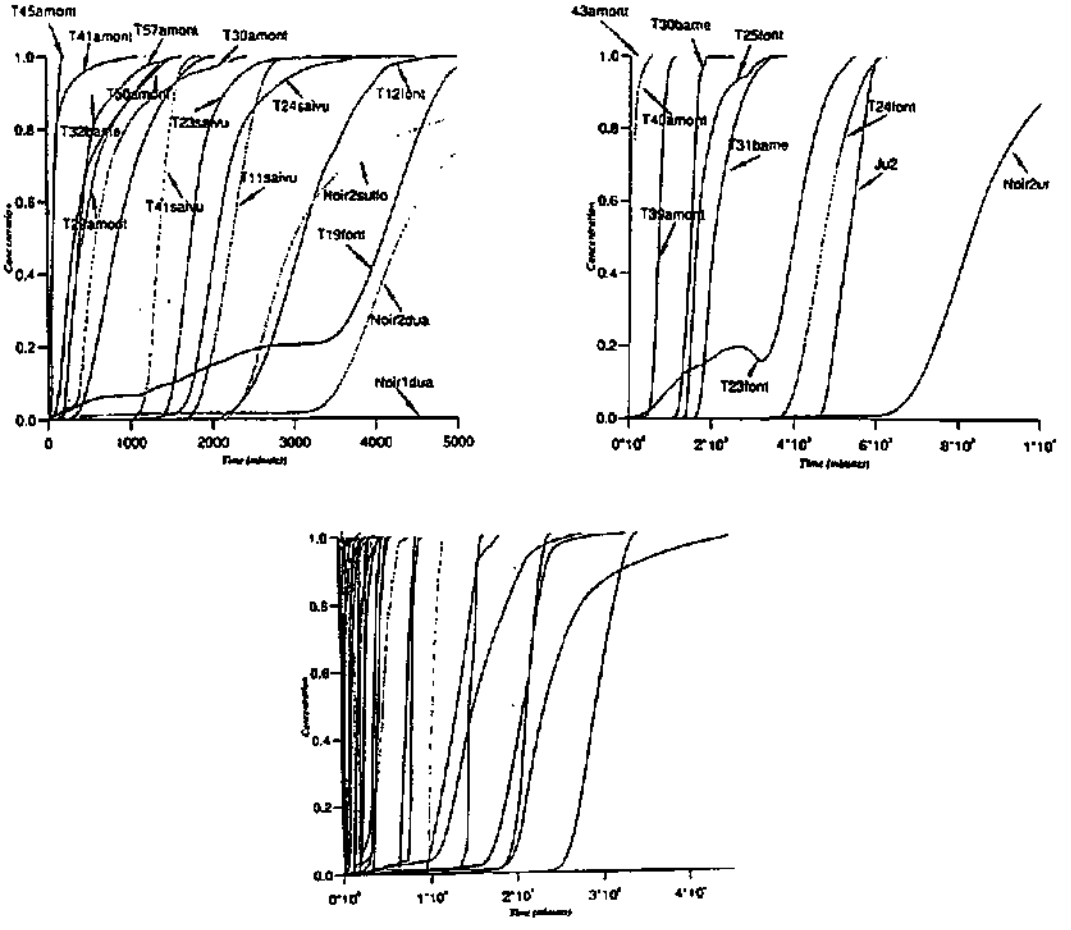

Figure 3.1a. : Transfer function variability with geological setting and hydrological conditions - (a) indicial responses of Jura tracer tests related to hydrological conditions.

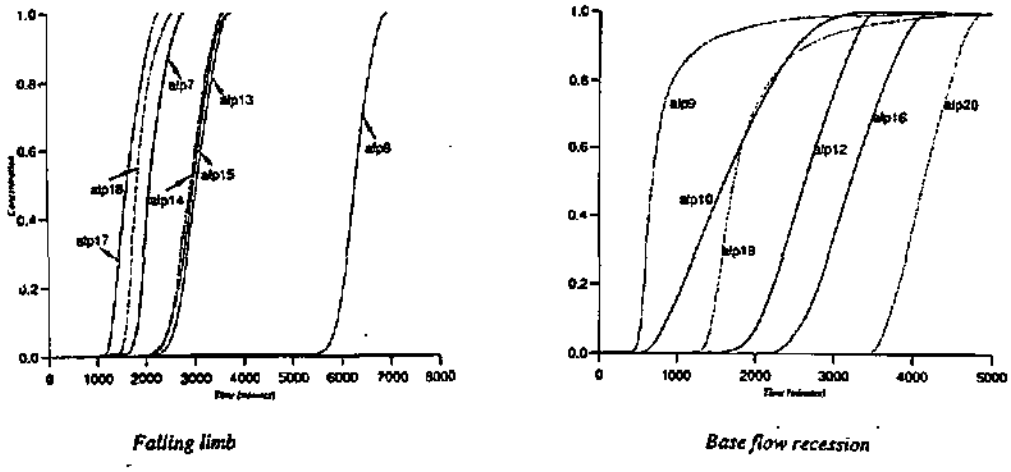

Figure .3.1b. : Transfer function variability with geological setting and hydrological conditions - (b) indicial responses of Alps tracer tests relatad to hydrological conditions.

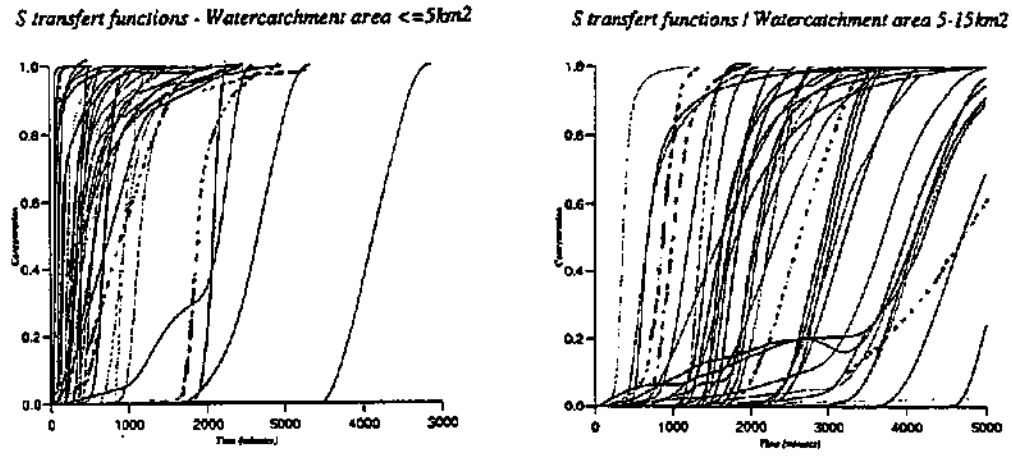

Figure 3.2. : Transfer function variability with catchment size -

(a) indicial responses in catchment sizes less than 5 km².

(b) indicial responses in catchment sizes from 5 km² to 15 km².

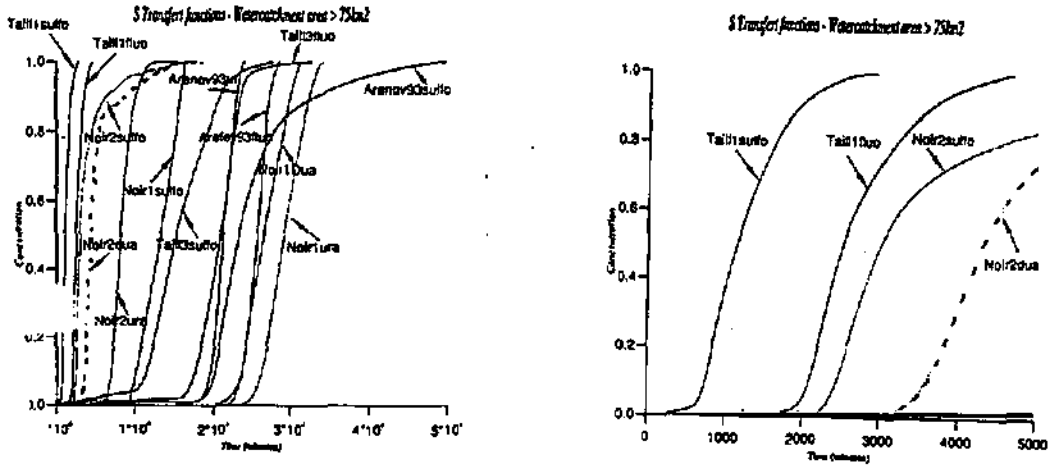

Figure 3.2c. : Transfer functions variability with catchment size - c) indiciel responses in catchment sizes greater then 75 km².

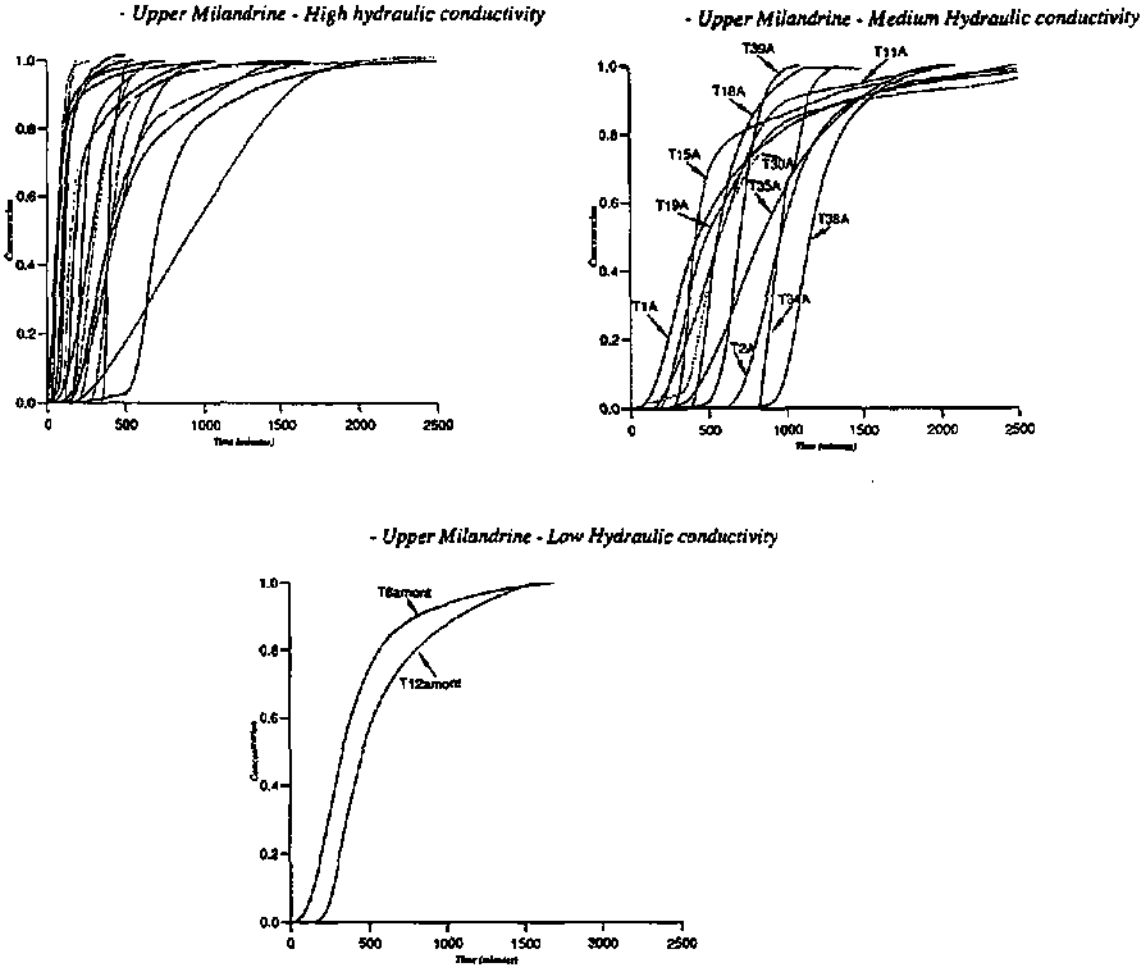

Figure 3.3.: Transfer function variability with tracer system epparent hydraulic conductivity.

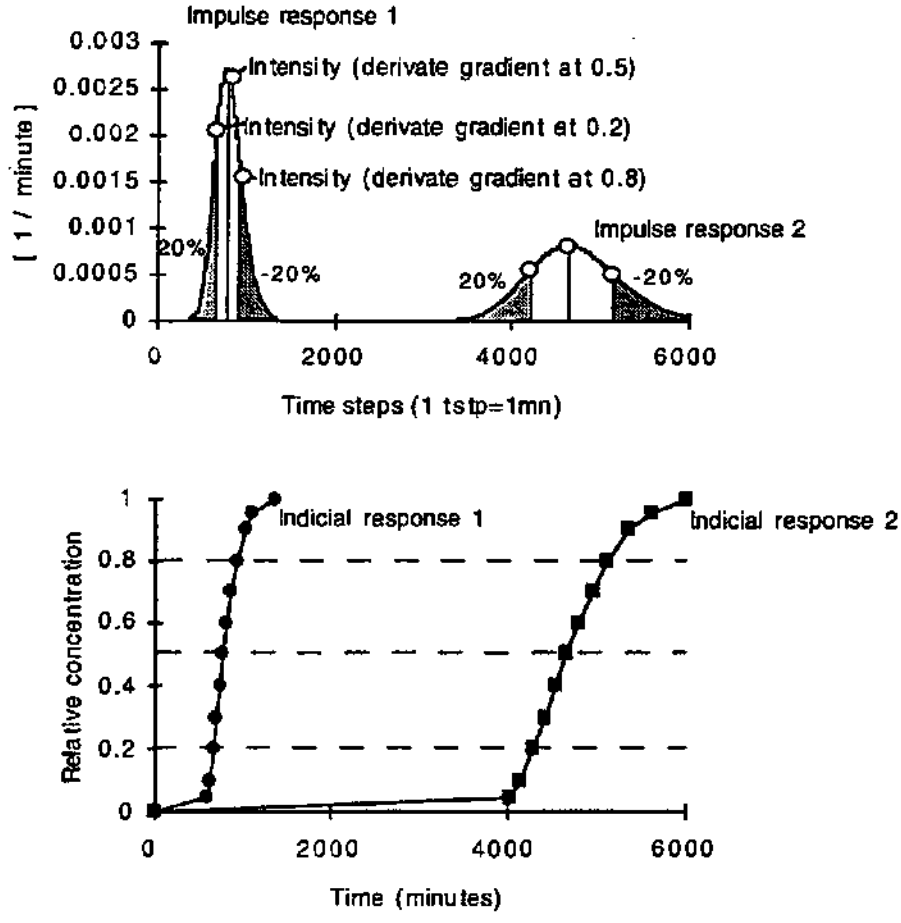

Figure 3.4.: Relation between the indicial response 0.2, 0.5 and 0.8 percentile gradients and the intensity of the corresponding impulse response for 20%, 50% and 80% of the area under the curve.

3.2. Variance analysis - transfer functions for modal velocity and gradient

A variance analysis was carried out on the modal velocity and the 0.5 percentile gradient to compare the following conditions pertinent to each tracer test: geological setting, hydrodynamic conditions, nature of injection point, catchment size, , the tracer distance and the outlet discharge. These conditions were compared to determine if their mean values (gradient at 0.5 and modal velocity) were significantly different. The question to answer was does the gradient at 0.5 and the modal velocity differ among these six test-specific conditions.

Each condition, referred to as tracer test parameters, was subdivided into various categories as following :

CONDITION	CATEGORY
1. Geological setting:	- Alps -Tabular Jura - Folded Jura
2. Hydrologic conditions:	- Base flow recession - Rising limb - Falling limb
3. Injection point nature:	- Karst network - Swallowhole - Borehole - Artificial hole (man-made pit or trench) - Surface point (sinkhole, uncovered limestone)
4. Catchment size:	- up to 5km^2 - 5 to 15 km^2 - greater than 75 km^2
5. Tracer distance:	- up to 100m - 100 to 1000 m - 1000 to 3000 m - greater than 3000 m
6. Discharge volume:	- up to 100 l/s - 100 to 500 l/s - 500 to 1000 l/s - 1000 to 5000 l/s - 5000 to 10'000 l/s - greater than 10'000 l/s

A single factor variance analysis[13] [ANOVA] was carried out on each group to determine if the categories of each condition influenced the transfer functions. The questions addressed from this perspective were, for example:

- Can we differentiate a transfer function developed for tracer tests in the Alps from those derived from tests in the Jura?
- Do hydrological conditions affect the transfer functions?

[13] *ANOVA: Single factor variance analysis is a statistical method of testing the hypothesis that a number of populations, as represented by samples, are identical. When several groups of data are compared, ANOVA is used to determine if their means are significantly different. Each group is assumed to have a normal distribution around its mean. All groups have the same variance (Helsel and Hirsch, 1992).*

Single factor varianca analysis:

Variance analysis is a parameter test that determines whether each parameter's mean is identical. This analysis was done on all data using an analysis program called JMP[14].

The variation within a condition is estimated by the within-group or square of the mean error (MSE, the error is treated as a source in the variance analysis in the JMP program), computed from the data. The variation between group means is estimated by the treatment maan square (MST, model as source in JMP).

The square of the error in the mean (MSE) is equivalent to the error or within-group sum of squares divided by the number of degrees of freedom in the error (N-k):

$$MSE = \frac{\sum_{j=1}^{k}\sum_{i=1}^{n_j}\left(y_{ij}-\bar{y}_j\right)^2}{N-k}$$

where N-k= error degrees of freedom.

The mean squares for treatment is equal to the treatment sum of squares divided by its degree of freedom (k-1):

$$MST = \frac{\sum_{j=1}^{k} n_j\left(\bar{y}_j-\bar{y}\right)^2}{k-1}$$

where k-1= treatment degrees of freedom.

The degree of freedom (DF) is the number of independent pieces of information used to calculate the statistic.

When the treatment mean square (MST or model) is larger than the error mean squared as measured by an F-test[15], the conclusion is that the group means are significantly different. (Helsel and Hirsch, 1992).

In order to quantify the relative importance of "significant difference" between several tracer test conditions, the value of Rsquare in the summary of fit is used. When Rsquare[16] is greater than or equal to 0.75, the difference is considered as highly significant. When Rsquare is greater than or equal to 0.25 and lower than 0.75, the difference is of medium significance or moderately significant. Finally, when Rsquare is greater than or equal to 0.1 and lower to 0.25, the difference is of slightly significant or of low significance.

Multiple factor analysis

Multiple factor (multi-factor) variance analysis was also carried out: in these cases, two or

---

[14] *JMP, software designed and written by John Sall, Katherine Ng and Michael Hecht, 1989-1991 - version 2.0.4.*

[15] *Test satistic F : F = MST/MSE*

Decision rule: To reject Ho: the mean of every group is identical, compared to: H1: at least one mean differs

Reject Ho if $F \geq F_{1-\alpha,k-1,N-k}$ *; the 1-α quantile [of an F distribution with k-1 and N-k degrees of freedom; otherwise do not reject Ho (Helsel and Hirsch, 1992).*

[16] *Rsquare measures the proportion of the total variation accounted for by the model. The remaining variation is attributed to random error. Rsquare is 1 if the model fits perfectly. Rsquare is 0 if the fit is no better than the mean. Using quantities from the corresponding variance analysis table, the Rsquare for any interval response fit is always calculated as the (sum of squares for model)/(sum of squares for C total) (JMP software).*

more variations in each of the test conditions, influences were simultaneously tested to determine if either cause significant differences between treated parameters means. Each parameter is assumed to hava a normal distribution around its mean; all parameters have the same variance. This analysis allows calculation of a whole-model test considering the experimental values and the predicted ones and taking into consideration influences of each considered group. The significant difference is subordinated to the results of the effect test: A probability>F equal to 0.05 or lower than 0.05; this value is the significance level α.

3.2.1. Results of the variance analysis

Results of the single factor variance analysis (with 0.2 and 0.8 percentiles shown as additional information) are summarised in Tables 3.1 and 3.2.

Rasults of the multi-factor variance analysis for the geological setting condition (Alps, Tabular Jura and Folded Jura) and the injection point, hydrological conditions, catchment size, tracer distance and discharge volume are in Sections 3.2.1.1 to 3.2.1.3.

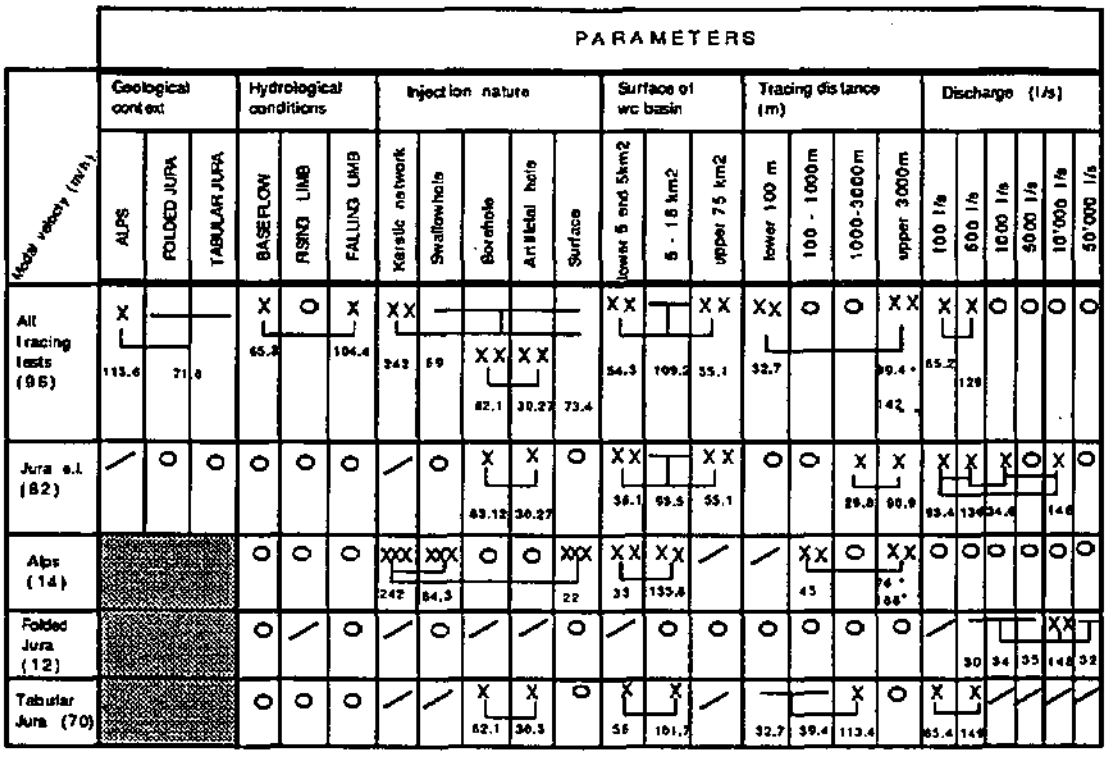

Legend: XXX significantly different, Rsquare upper or equal to 0.75
XX significantly different, Rsquare upper or equal to 0.25 and lower than 0.75
X significantly different, Rsquare equal to 0.1 and lower than 0.25
group of parameters that are different from another
difference between this and that
O no significantively difference
101.7 mean value of the modal velocity; * mean value for the distance between 3000 and 5000m
** mean value for the distance upper than 5000 m.

Table 3.1. Significant and non significant differences of modal velocity means. Modal velocity was calculated using the approximate tracer distance for all tracer tests, even if relativaly true distances ara known for the major tracer tests that were carried out in the Maira test site in the Tabular Jura.

Results in Table 3.1 illustrate that there are only a few significant differences (xxx): injection point conditions cause diffarances in the Alps setting. For these tracer tests, the mean modal velocity was higher when the injection was directly into the karst network than when it was injected into a swallowhole as shown by tha significant difference in modal velocity amplitudes.

About 50 percent of the differences are moderately significant (xx). These are the cases for the injection point, the catchment size and the tracer distance conditions considering all tracer tests.

About 50% of the differences among the varied conditions are not significant (o).

Hydrological conditions result in no significant difference for any of the geological settings. Howevar, there was a low degree of significance among all the tracar test base flow conditions and falling limb conditions.

Generally, the modal velocity, mean values, for significant class in considered groups, vary between 22 to 242 m/h.

	PARAMETERS																							
	Geological context			Hydrological conditions			Injection nature					Surface of wc basin			Tracing distance (m)				Discharge (l/s)					
Grad 0.5	ALPS	FOLDED JURA	TABULAR JURA	BASE FLOW	RISING LIMB	FALLING LIMB	Karstic network	Swallowhole	Borehole	Artificial hole	Surface	lower 5 and 5km2	5 - 15 km2	upper 75 km2	lower 100 m	100 - 1000m	1000-3000m	upper 3000m	100 l/s	500 l/s	1000 l/s	5000 l/s	10000 l/s	50000 l/s
All tracing tests (96)	X			X	X	O	O	O	O	X	X	XX		XX	XX	XX	O	XX	O	O	O	O	X	X
	76.5	82.4	80.9	81	76					76.2	69.1	63.5	76.4	83.5	88.4	82.8		78.1					82.7	79
	0.24	0.13	0.16	0.16	0.25					0.24	0.12	0.11	0.24	0.11	0.03	0.12		0.21					0.13	0.3
Jura s.l. (82)		O	O	O	O	O		X	X	X	X	XX		XX	XX	XX	O	XX	O	O	O	O	X	X
								83.5	80.7	78.2	83.8	84	76.3	83.8	88.4	82.8		77.8 *	0.2				87.5	70
								0.11	0.16	0.24	0.1	0.1	0.24	0.11	0.03	0.12		83.2**	0.12				0.04	0.4
Alps (14)				O	O	O	O	O	O	O	O	O	O			XX	O	XX	O	O	O	O	O	O
																85		76.2*	0.24					
																0.46		79.2 **	0.5					
Folded Jura (12)				O	/	O	/	XX	/	/	XX	/	X X	X X	O	O	O	O	/		XX		XX	XX
								83.5			70		70	83.5							81.7		87.5	70
								0.11			0.35		0.36	0.11							0.15		0.04	0.4
Tabular Jura (70)				O	O	O	/	/	X	X	X	X	X	/	X				O	O	/	/	/	/
									80.7	76.2	84.75	84	76.5		88.4	83.6	77.9	76.1						
									0.16	0.24	0.09	0.1	0.24		0.03	0.11	0.21	0.25						

Legend: XXX significantly different , Rsquare upper or equal to 0.75
XX significantly different , Rsquare upper or equal to 0.25 and lower than 0.75
X significantly different , Rsquare equal to 0.1 and lower than 0.25

——— group of parameters different from another

└——┘ difference between this and them

O no significant difference

83.5 mean value of the gradient α at the percentile 0.5; * mean value for 3000 to 5000 m ; ** mean value for upper 5000 m distance

8.4 mean value of the tang β when b is equal to 90° gradient α. When gradient α tends to 90 °, tang β tends to ∞ When gradient α tends to 45 °, tang β tends to 1.

/ no available data

*Table 3.2.: Significant and non significant differences of means of **gradient at 0.5 percentiles.***

Table 3.2. shows there is no highly significant difference among any of the conditions and their categories for the indicial 0.5 percentile variance analysis. For other relationships, about half of the differences are moderate and the other half of low significance. The low significance is related principally to geological setting, hydrological conditions and injection point conditions, where as moderate significence characterizes the catchment size, tracer distance and discharge rete conditions.

The hydrological conditions provoke no major difference within each class of the geological context, contrary to the low degrae difference among all the tracer tests between base flow conditions and rising limb conditions.

Generally, the gradient at 0.5 percentile which represents the mean values, for significant class of considered parameters, varies between 65 with a slope of 0.46[17] to 88.4 degrees with a slope of 0.028-.

Comments on variations in means of the 0.2 and 0.8 percentile gradients

The significant differences for the gradient at 0.5 percentile are not exactly the same for the gradient at 0.2 and at 0.8. There are essentially variations among the discharge and the nature of the injection point conditions. A significant difference does exist for the gradient at the 0.8 percentile between a discharge of less than 5000 l/s and greater than 50'000 l/s for all conditions. In addition, there is no major difference among the discharge parameters for the gradients at 0.2 considering all tracer experiments and tracers in the Jura geological setting.

Concerning tracer experiments in Jura, significant differences disappear in the injection point nature: there are no longer any more difference between borehole and artificial hole for gradients at 0.8 end no longer any more difference between swallowhole and borehole, between swellowhole / borehole and artificial hole /surface for gradients at 0.2 percentile.

Considering the tracer experiments carried out in the Tabular Jura, an additional difference appears between 100 and 500 l/s discharges for gradients at 0.8 percentile.

Considering all tracer tests, the ANOVA on the value of the gradients at 0.5 and at 0.8 provide significant results for the hydrological conditions parameter when there is no significant difference taking into account the values of the gradient at 0.2 percentile.

Generally the mean value of the gradient at 0.2 vary between 66.5 degrees- slope of 0.44 (Alps, tracer distance lower than 1000m) and 89.5 degrees - slope of 0.0088 - (all tracer tests, tracer distance lower than 100m), when the mean value of the gradient at 0.8 very between 50 - slope of 0.84 - (Folded Jura, surface as injection point) and 88 degrees - slope of 0.035 - (Jura, tracer distance lower than 100m.).

3.2.1.1. Variance analysis on all tracer tests.

Among all tracer tests (96 tracer tests), a low significant difference in the **geological context** and in the hydrological conditions parameters eppears. The mean characteristic values (modal velocity and gradients at given percentiles) of the transfer functions of tracer experiments permit to distinguish the **Alps** transfer functions from the **Jura** transfer functions. The mean transfer function of the Tabular Jura is not significantly different than for the Folded Jura (Figure 3.5).

[17] *The slope at the given percentile is calculated as the tangent of β (tanβ), where β = 90° - gradiant. [for gradient values close to 90 degrees, tan β tends to∞; for gradient values approaching 45 degrees, tan β tends to 1]*

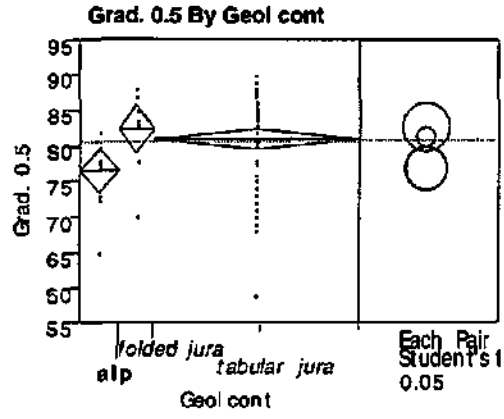

Figure 3.5: Variance analysis of the geological context 0.5 percentile gradient.

Source	*Sum of Squares*	*Mean square*	*F ratio*
Model	*279.19*	*139.6*	*3.77*
Error		*3443.74*	*37*
			Prob>F
			0.0267

For the **hydrological conditions**, the **base flow** mean transfer function differs from both the **falling limb** (gradient) or the rising limb (modal velocity). The rising limb (gradient at 0.5 percentile) respectively the falling limb (modal velocity) transfer functions are rather similar to the base flow mean transfer function (Figure 3.6.). The difference between base flow and rising limb is not significant (Prob>F higher than 0.05).

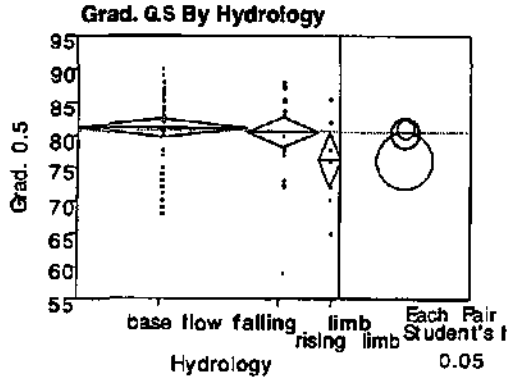

Figure 3.6: Variance analysis of the hydrological conditions 0.5 percentile gradient.

Source	*Sum of Squares*	*Mean square*	*F ratio*
Model	*177.2*	*88.6*	*2.32*
Error	*3545.74*	*38.12*	*Prob>F*
			0.1036

Moderate differences in the injection point nature, catchment size, and tracer distance occur for all tracer tests.

Injection point transfer functions differ for tracer tests where the injection occurred directly into the karst network and other injection points for mean modal velocity. A significant difference between transfer functions for boreholes and artificial holes also exists for modal velocity. Concerning the gradient, a significant difference exists between tracer tests carried out using an artificial hole and surface dispersion (including those where the tracer was injected directly into a sinkhole or doline).

Catchment size has a major difference in mean value gradients between small, large and medium size. Mean transfer functions of catchments up to 5km^2 are similar those for sizes larger than 75 km^2. The catchment size does not respond independently of its geological context. Most of the data from tracer tests carried out in the Folded Jura correspond to those in catchment sizes greater than 75 km^2. However, no tracer tests have been done in such a large catchment area in either the Alps or Tabular Jura. Consequently, the difference observed reflects mainly geological context and tracer system structure (cf. Conclusion 3).

For **tracer distance**, there is a significant difference in the transfer function for peak velocities between short and long distances (up to 100m and greater than 3000m). Mean gradient values for 1000m is different than upper 3000m. Most tracer distances larger than 3000m are found in the Folded Jura group although such distances occur also in the Alps tracer tests.

Transfer functions can differentiate **discharge rates** for the up to 100 l/s and 100 to 500 l/s using the modal velocity and for the 10'000 l/s and 50'000 l/s using gradient values...

The **multi-factor analysis** on the gradient at 0.5 gives a significant whole-model test (Prob>F=0.0000; Rsquare=0.51) with the geological context, the injection point nature and the catchment size (respectively instead of the catchment size, the discharge rate for the modal velocity) as significantly different from each other and from the tracer distance, the hydrological conditions and the discharge rate groups (Table 3.3). Considering the gradient at 0.2, the whole-model is significant with only for geological context and catchment size. For the 0.8 gradient, the whole-model is significant (Prob>F=0.0035) but without a significant group.

Table 3.3.

Multi-factor analysis for the 0.5 percentile gradient and modal velocity for all tracer tests

Totality of tracers	Gradient at 0.5		Modal velocity	
	Prob >F	*Rsquare*	*Prob >F*	*Rsquare*
Groups				
		0.51		0.47 (0.48)
injection	0.0083		0.0026 (0.0025)	
tracer path distance	0.62		0.14 (0.13)	
discharge	0.178		0.018 (0.0015)	
catchment size	0.0065		0.148 (0.0065)	
hydrological conditions	0.3841		0.3451 (0.5453)	
geological context	0.0188		0.0183 (0.009)	

A Prob>F of less than or equal to 0.05 is significant.

Values between the brackets ara for modal velocities calculated with true tracer distances.

Conclusion 1

- There is a **significant difference** between the mean **Jura** and **Alps** transfer functions. This difference results from the geological structure of the aquifer and its karstification degree. The Alps karst aquifers are mainly located in complex structural areas. In contrast, the Tabular Jura karst aquifers are horizontal layers where fault systems have developed (normal and inverse faults). In the Folded Jura, karst aquifers are formad within limestone layers that have anticline and synclinal structures. In addition, the Alps and parts of the Tabular Jura were covered by ice during the Quaternary and this influanced tha degree of karstification. Karstification degree is not only due to the geological structure and to the ice Age, but also to the nature of the limestone (percent pure calcite, grain size, heterogeneous or homogeneous texture), the type of water and various tectonics phases. Karst networks mostly unexplored or at best partially known. The analysis to date has not been able to explain the observed differences by taking into consideration the other conditions relatad to the karst systems. Therefore, it is difficult to be more precise to explain the difference between the mean transfer functions. Nevertheless, the differences in response in the two setting should be taken into consideration when forecasting potential pollution. For example, the mean modal velocity is 113 m/h in the Alps, about 50 percent higher than the value of 72 m/h for the Jura range and such differences reflecting travel time distances are important resource protection-related characteristic.
- According to karst hydraulic behavior (cf. Part I, chap.1.), tha water flow velocity of base flow conditions is lower than during rising or falling limb conditions. Exceptions can occur if rising or falling limbs are of minor amplitude compared to the karst system base flow. Consequently there is a significant difference between base flow transfer functions and those for rising or falling limbs and this is substantiated by the analysis. Since base flow and rising limbs discharges may be similar in various aquifers, their transfer functions may also have similar appearances and cannot be distinguished. Even with data from 96 tracer tests that had these two hydrologic conditiona, the was no meaningful difference in transfer function.
- According to the results of the MANOVA, transfer functions of tracer tests can be differentiated principally by their geological context, their catchment size (reflecting the ratio of unsaturated zone and transfer in partially saturated open channels) and the injaction point.

3.2.1.2. Variance analyaia on Alps tracer tests

As discussed above, hydrological conditions cannot be distinguished for their modal velocity percentile gradient values. In the Alps, however, this lack of distinction is more likely related to the larger number of tracer tests done during rising or falling limbs (12) compared to only two during base flow.

In the Alps, the **injection point, catchment size** and **tracer dietance** conditions result in high to medium significant differences. Only the tracer distance shows a gradient value of significant difference.

The **injection point** differentiates tracer tests started directly in the karst network or at swallowholes from those beginning at the surface in dolines or sinkholes (Figure 3.7).

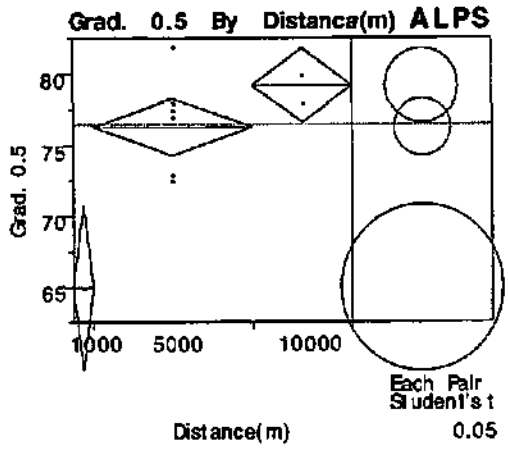

Figure 3.7. : Variance analysis of the 0.5 gradient for tracer distance in the Alps.

Source	Sum of Squares	Mean square	F ratio
Model	169.2	84.6	11.8
Error	78.8	7.16	Prob>F
			0.0018

Using the modal velocity, tracer tests in catchment sizes up 5km^2 can be distinguished from tracer tests in medium size catchments (5 to 15 km^2).

The tracer path length has distinguishing transfer functions for both the modal velocity and the 0.2, 0.5 and 0.8 gradient percentiles. The mean transfer function for the 100 to 1000m length is significantly different than for a length greater than 3000m (Figure 3.8).

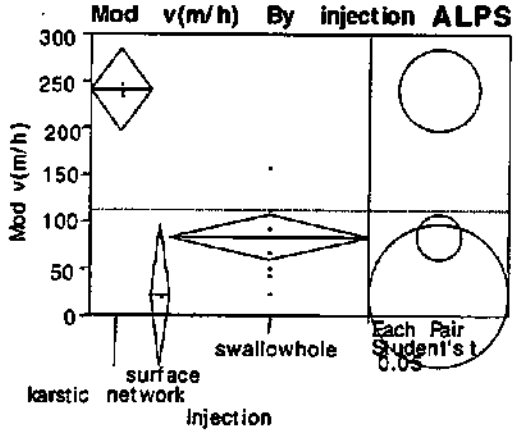

Figure 3.8.: Variance analysis of modal velocity for injection points in the Alps.

Source	Sum of Squares	Mean square	F ratio
Model	66435.1	33217.6	27.04
Error	13514.1	1228.6	Prob>F
			0.0001

Multi-factor analysis results for the 0.5 gradient and modal velocity, taking into account the injection point, tracer distance, discharge, catchment size and hydrological conditions are in Table 3.4.

Table 3.4

Multi-factor analysis of the 0.5 gradient and modal velocity for tracer tests in the Alps

ALPS	**Gradient at 0.5**		**Modal velocity**	
	Prob >F	*Rsquare*	*Prob >F*	*Rsquare*
Groups				
		0.91		0.995
injection	0.23		0.0008	
tracer distance	0.0047		0.0007	
discharge	0.1803		0.105	
catchment size	0.087		0.0003	
hydrological conditions	0.1775		0.05	

Prob >F lower or equal to 0.05 is significant

Tracer distance is the single condition with significance for the 0.5 gradient, . For the modal velocity, the tracer distance, injection point, catchment size and hydrological conditions are significantly different.

Conclusion 2

In the Alps:

- **Tracer distance** characterizes transfer functions. Other conditions are important to classify the characteristic modal velocity of tracer tests. Major differences result from changes of injection point.
- The injection point, tracer distance and catchment size are the only conditions whose classes cause differences in transfer function characteristics.

3.2.1.3. Jura tracer test variance analysis results

The significant differences of tracer tests carried out in the Jura are in Tables 3.1 and 3.2. These differences result from adding the differences of tracer experiments in the Tabular Jura to those in the Folded Jura and therefore, no analysis is pertinent. Comments are oriented to both the Folded Jura and the Tabular Jura settings.

In the Tabular and Folded Jura, as in the Alps, there is no significant difference as for the various hydrological conditions. In Folded Jura tracer tests, three of 12 were done under falling limb conditions. The catchment size is also critical and can induce an insignificant difference. But in the Tabular Jura, even with a reasonable number of tests in each hydrological condition category (base flow, falling and rising limbs), no significant difference appears. A reason for this is discussed in Section 3.2.1.3.b.

a) Folded Jura

Within the three conditions, injection point nature, water catchment basin surface and discharge groups, some mean value differences at the 0.2, 0.5 and 0.8 gradient percentiles are significant. On the contrary, there are only moderate differences for discharge using the modal velocity.

For the **injection point** condition, the transfer function is different if it is a sinkhole or a surface point (Figure.3.9.).

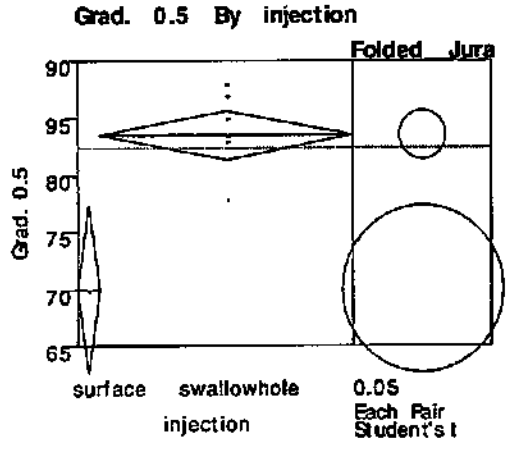

Figure 3.9.: Injection point variance enalysis for the 0.5 gradient.

Source	*Sum of Squares*	*Mean square*	*F ratio*
Model	*167.06*	*167.06*	*15.39*
Error	*108.5*	*10.85*	*Prob> 0.0028*

Only one tracer test was carried out in a water catchment basin smaller than 10 km^2. Transfer functions for sizes greater than 75km^2 are different than the above mentioned tracer test.

Finally, for **discharge rates**, thare are significant difference between transfer functions resulting from tracer tests carried out with discharges of 1000 l/s and 10'000 l/s at tha spring. In addition, there is a difference between tracer tests with a discharges less than 1'000 l/s and greater than 50'000 l/s.

The multi-factor analysis points out the significant importance of the injaction point and the discharge to differentiate transfer functions. The whole-model test for the gradient at the 0.2 percentile (Prob>F=0.039) is significant; the injection point (Prob>F=0.013) and the discharge (Prob>F=0.0178) are significantly different from other conditions (Table 3.5.).

Table 3.5.

Multi-factor variance analysis of the 0.5 gradient and modal velocity in the Folded Jura

Folded Jura	**Gradient at 0.5**		**Modal velocity**	
	Prob >F	*Rsquare*	*Prob >F*	*Rsquare*
Groups				
		0.877		0.87
injection	0.012		0.018	
tracer distance	0.62		0.18	
discharge	0.024		0.0075	
water catchment size	0.21		0.93	
hydrological conditions	0.59		0.5878	

Prob > F lower or equal to 0.05 is significant

b) Tabular Jura

There are only low degrees of difference for the injection point, catchment size, tracer distance and discharge.

Transfer functions for tests beginning with the **injection point** directly into a borehole or artificial hole are different from those with a sprinkled release onto the surface (Figure 3.10).

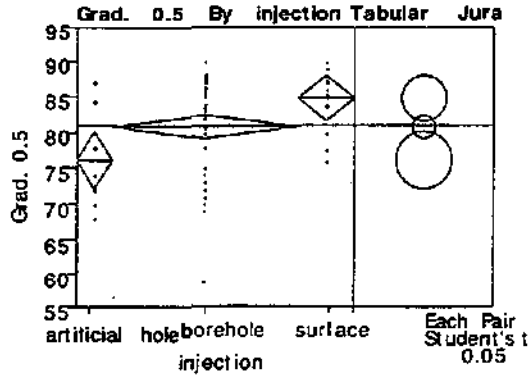

Figure 3.10. : Variance analysis of the 0.5 gradient for injection points.

Source	*Sum of Squares*	*Mean square*	*F ratio*
Model	*410.8*	*205.4*	*5.5*
Error	*2509.37*	*37.4*	*Prob>F*
			0.006

For the injection point condition modal velocity, tests initiated in boreholes have different mean values than those in artificial holes.

The injection points in the Tabular Jura are either sinkholes or natural collapse holes (sinkhole point 1 in Bure), the edge of a depression with about 30 to 50 cm of brown soil in a fault zone (point 6 in Bure), the edge of a fractured limestone outcrop (point 3 in Bure), direct on uncovered limestone (less then 10cm of soil) in a fault zone (point 8 and point

11 in Bure) or uncovered limestone where no major faults occur (point 9 in Bure). If we compare tracer data from tests at point 1 (natural hole in the sinkhole located South of the artificial entrance of the cave system, 20 m apart) to those in the Tabular Jura, surface points appears to be significantly different only to those started in artificial holes. The transfer function 0.5 percentile gradient mean value is 76 for artificial holes and 83 for the surface tests. There is no difference between the transfer functions for surface points and boreholes. The modal velocity differs batween boraholes (82 m/h) and artificial holes (30m/h). Surface points are generally located in fault zones and the soil with some 50cm of thickness in a fault context does not modify the transfer function shape. The effect of soil and importance of the unsaturated zone is illustrated by a significant difference between artificial hole and borehole transfer functions.

Tracer tests can be differentiated relative to **catchment size**. There is a significant difference between tests catchment sizes less than or equal to 5km^2 and those of middle size from 5 to 15 km^2. However, this size effect may be artificial as the majority of Tabular Jura tests were in the same aquifer on the Bure Plateau in Ajoie. The tracer systems to the upper Milandrine sampling point in the cave has a size of 5km^2 and is mainly an unsaturated subsystem (soil and more or less intensely fractured limestone) and a saturated subsystem with drains. The tracer systems of 15km^2 size (La Bâme, Le Saivu and La Font springs) consist of an unsaturated subsystem and a consequent saturated system with some 5 km of channels. Thus, the major difference is due to the variations in the ratio of the unsaturated to saturated subsystem in the tracer systems. The systems with a size of 5km^2 and 15km^2 are characterized by ratios of 1 to >1, and <1, respectively. Therefore, the saturated subsystem is dominant (Figure 3.11).

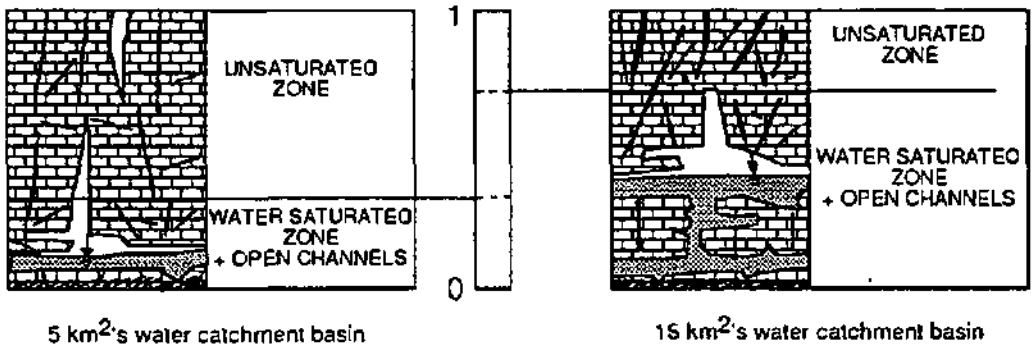

Figure 3.11.: Relative ratio of saturated (channels) and unsaturated subsystems at a 5km^2 and of 15 km^2 tracer systems in Bure.

The outlet **diacharges** of up to 100 l/s and 100 to 500 l/s have differences in both a mean modal velocity and 0.8 percentile mean gradient. For the 0.2 and 0.5 percentiles, there is no difference.

For the **tracer distance** condition, the transfer functions for lengths less than 100 m are able to be distinguished from those of between 100 to over 3000m. Results of tracer tests injected in the open hole in the doline - sinkhole (about 25 m. from the sampling point in the upper part of the cave) (Figure 3.12.) are different from the others. The injection point conditions seem to be dominant in this case and therefore has an important potential impact on vulnerability assessment.

Figure 3.12: Photograph of point 1 at the doline south of the artificial pit used to access the La Milandrine karst network.

The **multi-factor** variance **analysis** indicates: for the 0.5 gradient, the whole-model test is significant and there are significant differences for injection point, discharge and the catchment size conditions (Prob>F=0.0015, 0.0018, and 0.012 respectively). Taking into consideration the modal velocity, the whole-model test is also validated (MST=14125; MSE=2963, Rsquare=0.477), when no groups are significantly different (Table 3.6.).

Table 3.6.

Tabular Jura tracer test multi-factor analysis of the 0.5 gradient and modal velocity

Tabular Jura	Gradient at 0.5		Modal velocity	
	Prob >F	*Rsquare*	*Prob >F*	*Rsquare*
Groups				
		0.53		0.477 (0.574)
injection	0.015		0.06 (0.019)	
tracer distance	0.916		0.4 (0.178)	
discharge	0.0018		0	
catchment size	0.012		0.07 (0.65)	
hydrological conditions	0.95		0.68 (0.89)	

Prob>F less than or equal to 0.05 is significant.

Values between brackets correspond to modal velocity calculated with true distance.

Conclusion 3

- The injection point plays an important role in characterizing transfer functions. In the Folded Jura, surface tracer test transfer functions are different from those in swallowholes. In the Tabular Jura, the main difference is between tracer tests carried out into boreholes and artificial holes and those with a direct sprinkling onto the surface. An important aspect related to groundwater protection is that there is a difference in response between artificial hole and surface dispersion tests where there is no more than 50 cm of soil and with mainly faulted areas (cf. General conclusions, Chapter 1).
- Transfer functions are influenced by the catchment size in the Tabular Jura. This influence is directly linked to the compounds of the tracer system and mainly to the rabo of the unsaturated to saturated subsystem.
- Tracer distance is significant in the Tabular Jura and can be also related to the tracer system composition.
- Discharge is significant for tracer tests in both the Folded and Tabular Jura when there is no major difference in hydrological condition. The same range of discharge can correspond to either base flow, or rising limb or falling limb conditions. In addition, for the same hydrological conditions and different discharge at the spring, the tracer-system varies.

3.2.1.4. Apparent hydraulic conductivity variance analysis

The apparent K for the tracer system in the upper part of La Milandrine at the Bure test site has been estimated using borehole logs. Three groups have high, medium and low hydraulic conductivity. Unfortunately, only two tracer tests were done in low K systems.

Boreholes MIL1, MIL7, MIL3, MIL6, FN2 and some surface releases (uncovered fractured limestone, natural hole in doline) are at the entrance of a high K tracer system. Borehole MIL1 had a fracture zone with open fissures at 30 m below ground surface (bgs). In borehole MIL3, water flows from an open fracture at 35m bgs. Borehole MIL7 intersects a cavity. Borehole FN2 is relatively fissured in the lower part at depths between 30m and 40m bgs.

Boreholes MIL2, MIL5, MIL8, FN1, some surface points and artificial holes are at the entrance of a medium K system. Borehole MIL2 has a zone of open fractures at 10 meters in the epikarst. When performing tests, the tracer was injected at the bottom of the borehole. The tracer mixture consisted of 3000 liters of water with from 100 to 500 kg of NaCl and the system was subsequently flushed with 3000 liters of borehole water) . This

borehole is considered to be of medium hydraulic conductivity since below a depth of 10m there is no intensively developed fracturing. Fractures are present almost all along the borehole. In borehole FN1, except opposite the more karstified sections considered epikarst in the upper part of the borehole from 6m to 25m), there are few open fissures in the borehole.

Boreholes NEB 9 and MIL4 are of low permeability. They do not intersect important fractures. In MIL4, there are three fracture zones; one at less than 10 meters, a second between 10m and 15m and a third in the lower part near the contact between Rauracian limestone and Liesberg layers.

Carrying out tracer tests in less permeable blocks with classical tracers is difficult. During high water levels, hydraulic gradients can be reversed. The tracer then can get trapped in the low permeability blocks and it is subsequently released during the next low water level when the block water drains into the karst network. Therefore, it is important to take samples during a long period of time, generally over 6 weeks. In these situations, if the tracer peak concentration on the breakthrough curve is low; it is difficult to perform successful tracer tests. Tracer concentrations of the water samples is close to the detection limit of the analysis method. A tracer test was done in borehole MIL9 which has low permeability. A long injection time was used to avoid an overflow of the tracer out the borehole (6 hours). Unfortunately the sulfurhodamine G and the bacteriophages were not detected over the next six weeks.

The variance analysis points out that there is a relatively significant (percentile 0.5) to a true significant difference (percentile 0.8) between the tracer of the medium and high hydraulic conductivity classes at the 0.5 and 0.8 percentile gradients (Prob >F=0.07, 0.028). The difference is not significant for the 0.2 percentile gradient.

3.3. Mean transfer functions

As long as groups (conditions + categories) have significant differences in transfer functions, a mean transfer function and a corresponding « 95% confidence intervals » can be determined.

- For all tracer tests, mean transfer functions for tests in the Alps setting, the Tabular and Folded Jura (Figure 3.13.), the base flow and falling limb conditions (Figure 3.14.) can be calculated using the time value at each percentile of the curve (0.05, 0.1, 0.2 to 0.9, 0.95 and 1).
- If the mean transfer functions of the Alps and Jura tracer tests are dissimilar, their 95% confidence intervals overlap. The time error[18] of the Jura mean transfer function (+ or - 1500 minutes) is approximately twice that of the Alps (+ or - 700 minutes). The upper part of the Alps transfer function is less curved than that for the Jura (Figure 3.13.).
- Rising and falling limb mean transfer functions are similar and there is no significant difference. The base flow mean transfer function is delayed along the time axis and its upper part is more curved than those of the rising or falling limb. The mean transit time is longer during base flow conditions and consequently the rising and falling limb mean transfer functions appear in priority along the time axis. The time error of the base flow mean transfer function is about 1750 minutes.

[18] *Time Error corresponds to the time intervall between the time at 50% percentile of the mean transfer function and the time at 50% percentile of the « + or - 95% condidence intervals » functions.*

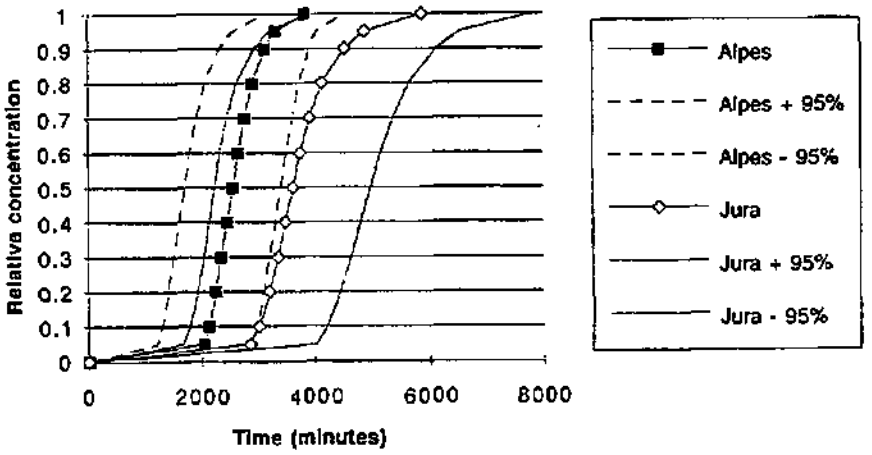

Figure 3.13. : Alps and Jura tracer test mean transfer functions.

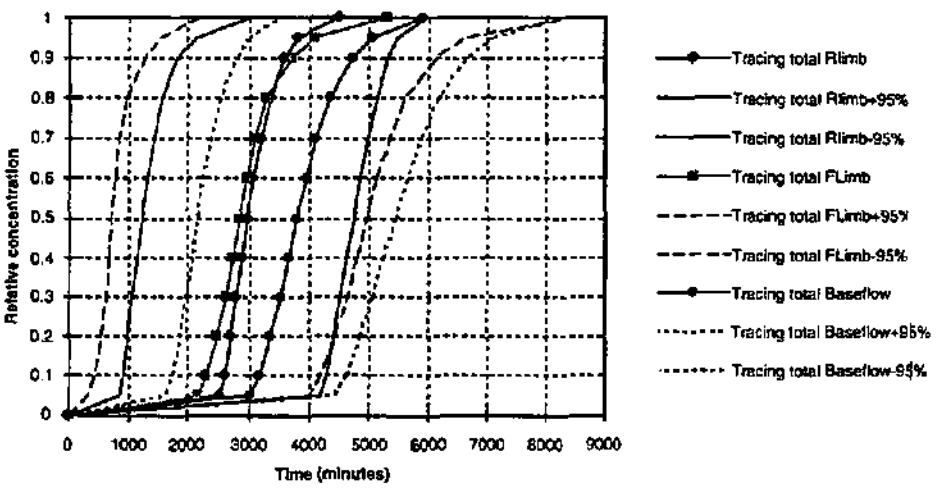

Figura 3.14. :Tracer test mean transfer functions under base flow, falling and rising limb conditions.

- Within the Alps context, the tracar distance has only low significance. A mean transfer function can be calculated for 5000m and 10'000m tracer systems. The low significance is illustrated on Figure 3.15. The main difference is in the 95% confidence intervals; due to the stronger standard deviation around the mean and the large time duration for the 10'000m tests, the time errors are twice the 5'000 m time error around the means (3'000 minutes instead of 1'500 minutes).

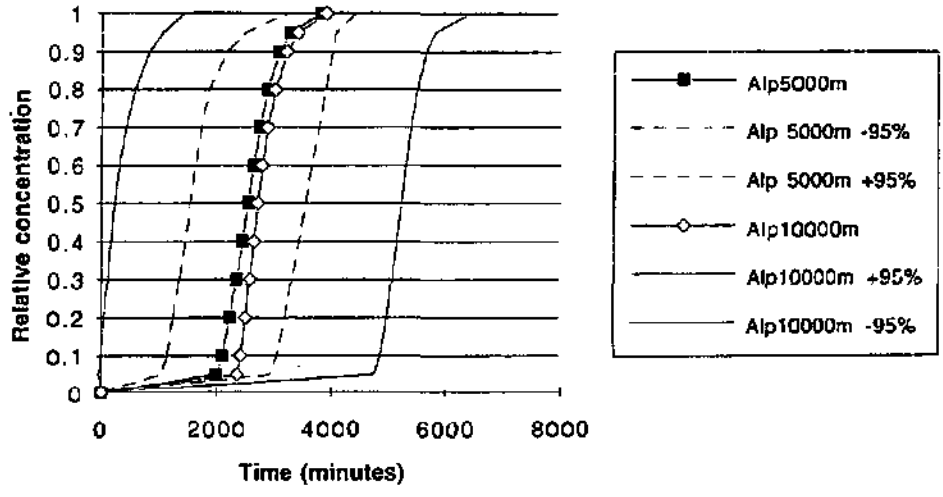

Figure 3.15.: Alps tracer tests mean transfer functions for tracer system of 5000m and 10000m.

- In the Folded Jura, the differences among groups have low significance. However, these results may be skewed as they are dependent upon the comparison of one tracer test done with injection at the surface in a 10 km^2 basin, with other tests done using swallowholes as injection points in basins larger than 75km^2. In this case, it is not appropriate to try to define differences in mean transfer functions for injection point conditions.
- In the Tabular Jura, mean transfer functions can be identified for the injection point, catchment size and tracer system K.

  Figure 3.16 shows that the mean transfer function is displaced along the time axis for different types of injection points. The surface injection point mean transfer function has a relatively staep curve that appears first with a average time errors of about 500 minutes. Second, the borehole mean transfer function has a 500 minute time error but is more curved in the upper part than those on the surface. Arfificial hole mean transfer functions have large time errors of about 2600 minutes. Except for the position of the surface mean transfer function, the time sequencing makes sense. As mentioned above, surface points used for tracer experiments have a fast response and are all located in a high tectonics zone. In addition, they do not typically have a soil layer through which to travel prior to entering the system. They are not representative of surface points in karst aquifers. The structural setting of these points explains why there is a fast response and a steep transfer function. They reflect direct connection to the karst network, as for example, a doline connected by a vertical shaft to the network.

  The large time errors of the artificial hole mean transfer functions reflect the how variable these tracer systems can be. Tracer transit time can be affected by migration through the soil and the unsaturated zone to the saturated zone.

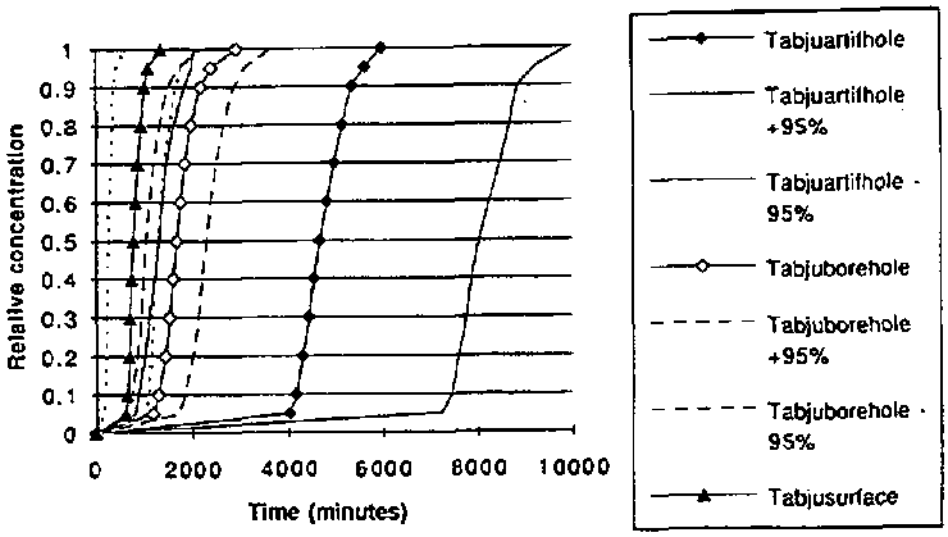

Figure 3.16.: Tabular Jura injection point mean transfer functions.

The effect of the catchment size on mean transfer functions is in figure 3.17. The 5km^2 transfer function is asymmetrical, steeper in the lower than the upper part and the upper part is more curved. The time error is relatively small (100 minutes) compared with that of the 15km^2 size (1000 minutes). The 15km^2 mean transfer function is essentially symmetrical. Its 0.5 percentile gradient is closer to 60 than to 80 degrees, the value for the 5km^2 size. This major difference in the shape of the curve, independent of the time axis shift, is explained as above with the compounds of the tracer systems. The 15km^2 transfer function is influenced by a long migration through the saturated subsystem of the tracer system. The tracer travels in open channels of varying widths including through underground lakes and inflows from connected and completely submerged drains. The dispersion and retardation that occur influence the transfer function due to adsorption on clays in the aquifer and the effect of stagnant water zones...Transfer functions which result from the black-box model do not give direct information as to which of these parameters are the most significant.

The explanation of transfer function asymmetry in this context was presented in Maréchal (1994). He did an analysis of dispersion at the la Milandrine test site calculating it using the analytical solution of a one-dimensional model from Sauty and Kinzelbach, (1988). Tracer breakthrough curves at the upper Milandrine sampling point have a distinct tailing effect. This effect is weak or completely absent on the tracer recovery curves at the system springs. The network variation and the influx, causing dilution, are identified as the mechanisms responsible for the shape of the breakthrough curve along the Milandrine underground river.

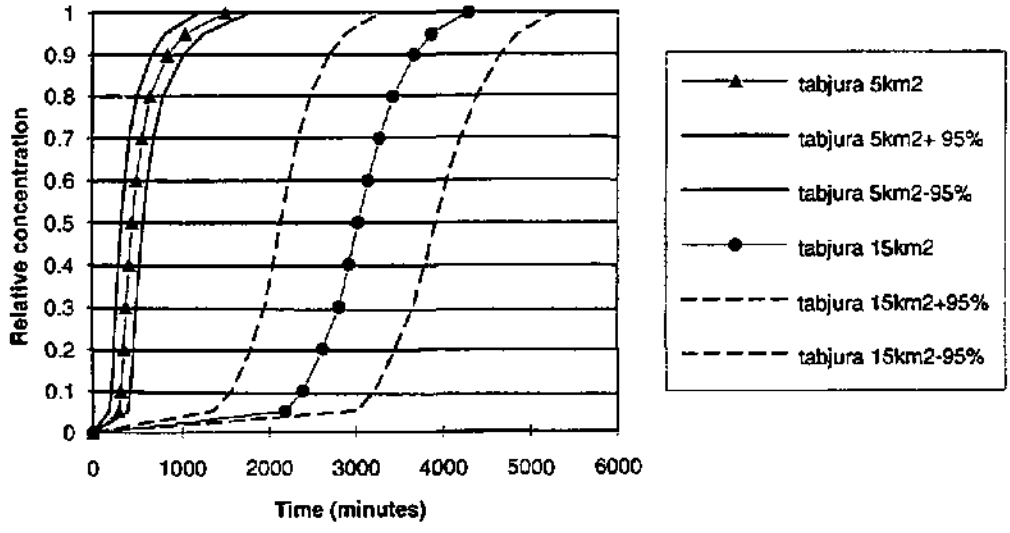

Figure 3.17.: Tabular Jura mean transfer functions for 5 and 15km² catchment sizes.

For the tracer system K, Figure 3.18 illustrates the changes along the time axis for the two distinct mean transfer function in the Tabular Jura, more specifically in the upper part of the Milandrine aquifer. They are similar time errors of 160 minutes but the high K mean transfer function is steeper around the 0.5 percentile and less curved in the upper part than the medium K mean transfer function.

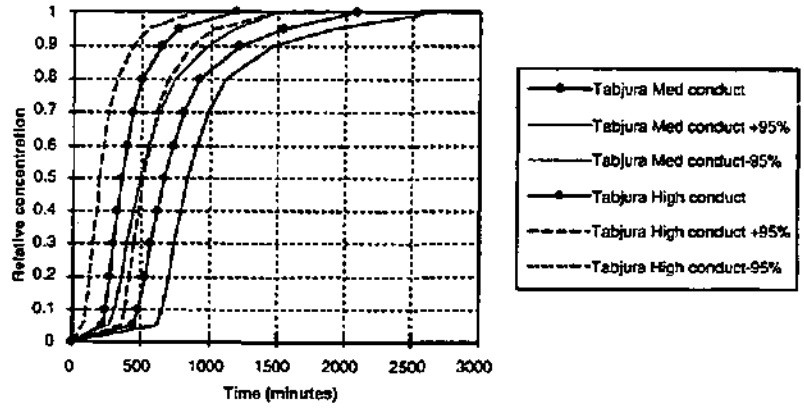

Figure 3.18.: Medium and high hydraulic conductivity mean transfer functions in the catchment basin of the upper Milandrine.

3.4. Conclusions

Variations in transfer functions can be distinct and characteristic for tracer tests in karst aquifers. Significant differences between characteristic conditions and categories classes appear in the transfer functions.

Each type of injection point is characteristic with a mean modal velocity associated with each mean transfer function:

- artificial holes: 34 m/h (30 m/h)[19], [+95%: 58m/h ; -95%: 9.5m/h]

- boreholes: 110 m/h (82 m/h) , [+95%: 139m/h ; -95%: 80m/h]

- surface: 117 (60 m/h) ; [+95%: 184 m/h : - 95%: 50m/h]

Tracer system K values have variable mean transfer functions. Their difference is relatively small but occurs specifically in the curvature of the upper part. Less dispersion and retardation occurs in moderate compared to high K systems due to the tracer being more trapped in fissures during its migration. Their related mean modal velocities are different:

- medium K: 35 m/h [+95%: 48: -95%: 22m/h]

- high K: 72 m/h [+95%: 93; -95%: 52 m/h]

Only among the geological context and hydrological conditions is there a low significant difference. No model characterizes either condition. Alps and Tabular Jura mean transfer functions under base flow or falling limb conditions, respectively, cannot be estimated. An Alps mean transfer function was determined with a 95% confidence interval and this relative steep function has a mean modal velocity of 114 m/h (160 m/h for +95%, 68 m/h for -95%). The Jura mean transfer function has a modal velocity is of 72 m/h (86m/h for +95% and 58 for -95%). The mean transfer function for the Jura includes a large variation of transfer function shapes similar to those for the Alps. The effect of the injection point and tracer system K are able to be distinguished.

For most conditions, significant differences occurred for the 0.5 and 0.8 percentile gradients, whereas there was no difference for gradients at the 0.2 percentile. This points out the effect of tailing in tracer experiments caused due to retardation factors in heterogeneous environments (decay, adsorption, immobile water) (Biver & Meus, 1992).
The hydrological condition is not as significant in determining the mean transfer function for given geological conditions. Distinguishing among the different geological contexts has to be related to, first, the number of tests in each geological context and, second, to the existence of other parameters such as the karst network development (length, connectivity), the unsaturated zone (especially for surface or doline injection points). Unfortunately, these parameters are difficult to determine.

The catchment size is significant for all tracer tests independent of their geological setting or just for the Tabular Jura tracer experiments. This size effect is influenced by the compounds of the tracer system. This reflects the difference in ratio of unsaturated and saturated conditions in the tracer subsystem.

There is no similar statistical behavior of modal velocity and gradient. This is due to various impulse responses having the same modal time. The slope of the corresponding indicial responses varies according to tracer distance (from 20m to 6000m).

[19] *The value between the brackets is calculated with the true and measured tracing distance.*

Chapter 4

Comparing breakthrough curves and transfer functions for microbiological (bacteriophages) and conventional tracers

Tracer tests were conducted simultaneously with microbiological (bacteriophages) and chemical (fluorescent dyes or salt) tracers. They were repeated several times at three test sites in the Tabular and Folded Jura.

The objective of using microbiological tracers was to be able to interpret their response in terms of transfer functions using the model, DYEBOX. The classical tracer results were considered as the standard for comparing the transfer functions.

About 20 tracer tests were completed in the following test sites: the Maira test site (11 simple or multi-tracer tests, repeated), the catchment of the Areuse spring (3 repeated multi-tracer tests) and the catchment of the Noiraigue spring (2 simple repeated tracer tests).

Seven bacteriophages (Appendix II.10) were used for these tracer tests. Swallowholes, dolines or boreholes with high to medium hydraulic conductivity conditions were chosen as injection points.

4.1 Tests with fluorescent, salt and bacteriophage tracers

4.1.1. Tracer tests in the Maira test-site

Two injection points were used in addition to MIL9 borehole where the tracer test was negative.

The first injection point was a naturally occurring open hole at the flat bottom of a doline located in the upper part of the explored karst network. It is about 20 meters from the sampling point in the cave. Borehole MIL3 at a distance of 450m from the sampling point was the second injection point. Chemical tracers and bacteriophages were injected simultaneously several times (Figure 4.1.)

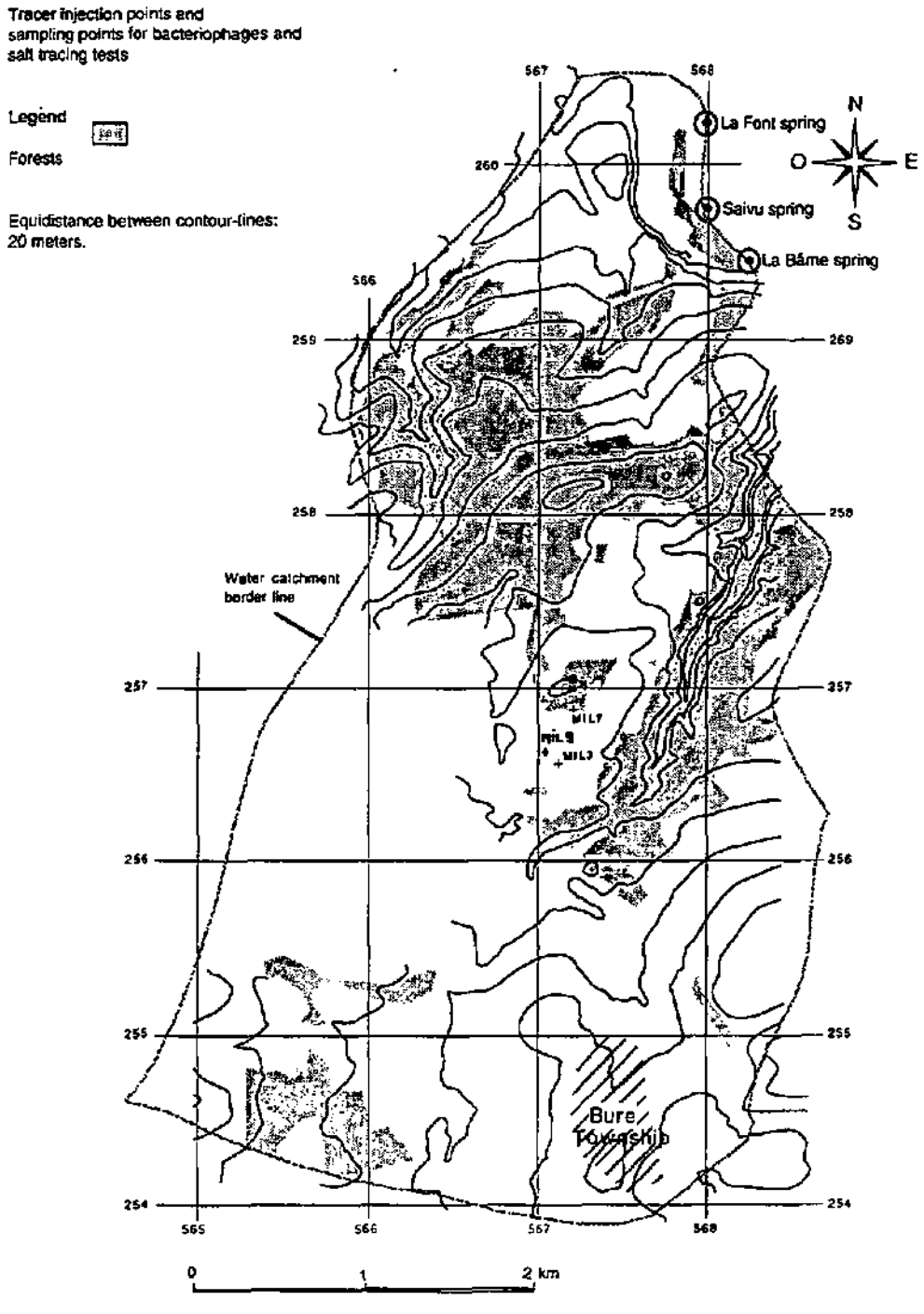

Figure 4.1: Maira test site injection and sampling points.

Borehole MIL9 is located in a block of low permeability. The hydraulic gradient can reverse at high water level stages such as occurred during the tracer test attempt. This reversal could explain why the tracer was never observed at the sampling points during the following six weeks. In addition, the tracer did not show up during sampling in the subsequent 7 days when base flow conditions developed. Either the tracer never reached the sampling point or its concentration was so low it was not able to be detected.

Table 4.1

Tracer tests at the Maira test aite

Designation	Injection point	Tracer	Quantity (kg or ptu)	Recovery rate	Discharge (l/min)
T43 2.11.94	doline pt1	H40/1 NaCl	7.2E+10 pfu 150 kg	13% 31%	3900
T44 12.12.94	borehole MIL9	Napthionate H6/1	2 kg 6.27E+08 pfu	0% 0%	3900
T45 12.12.94	doline pt1	H40/1 NaCl	4.03E+10 pfu 250 kg	9% 30%	15210
T47 18.1.95	borehole MIL3	H40/1 H6/1 NaCl	5.93E+11 pfu 1.45E+12 pfu 250 kg	40% 6% 70%	4065
T50 4.4.95	borehole MIL3	H40/1 H6/1 NaCl	7.26E+12 pfu 4.41E+12 pfu 300 kg	100% 23% 96%	5237
T51 4.5.95	borehole MIL3	H6/1 H4/4 H40/1 NaCl	5.43E+12 pfu 3.63E+11 pfu 1.57E+13 pfu 250 kg	3% 6% 40% 65%	1796
T53 21.6.95	borehole MIL3	H2/1 T7 H4/4	2.01E+12 pfu 6.35E+13 pfu 5.04E+13 kg	0% 2% 23%	2700
T54 21.6.95	doline pt1	Psf2 H40/1	1.27E+12 pfu 3.31E+13 pfu	5% 18%	2700
T55 21.8.95	borehole MIL3	H40/1 T7	9.3E+12 pfu 5.11E+13 pfu	60% 0.5%	973
T56 21.8.95	doline pt1	f1 Psf2	4.26E+13 pfu 3.32E+12 pfu	0.75% 21%	973
T57 21.9.95	borehole MIL3	f1 T7 H6/1 H40/1 uranine	6.5E+12 pfu 3.86E+13 pfu 4.1E+12 pfu 9.96E+12 pfu 0.15 kg	0.5% 1.3% 15% 74% 94%	4000

All tracer tests were done during base flow recession to end of falling limb periods under relative similar hydrological conditions(Figure 4.2.).

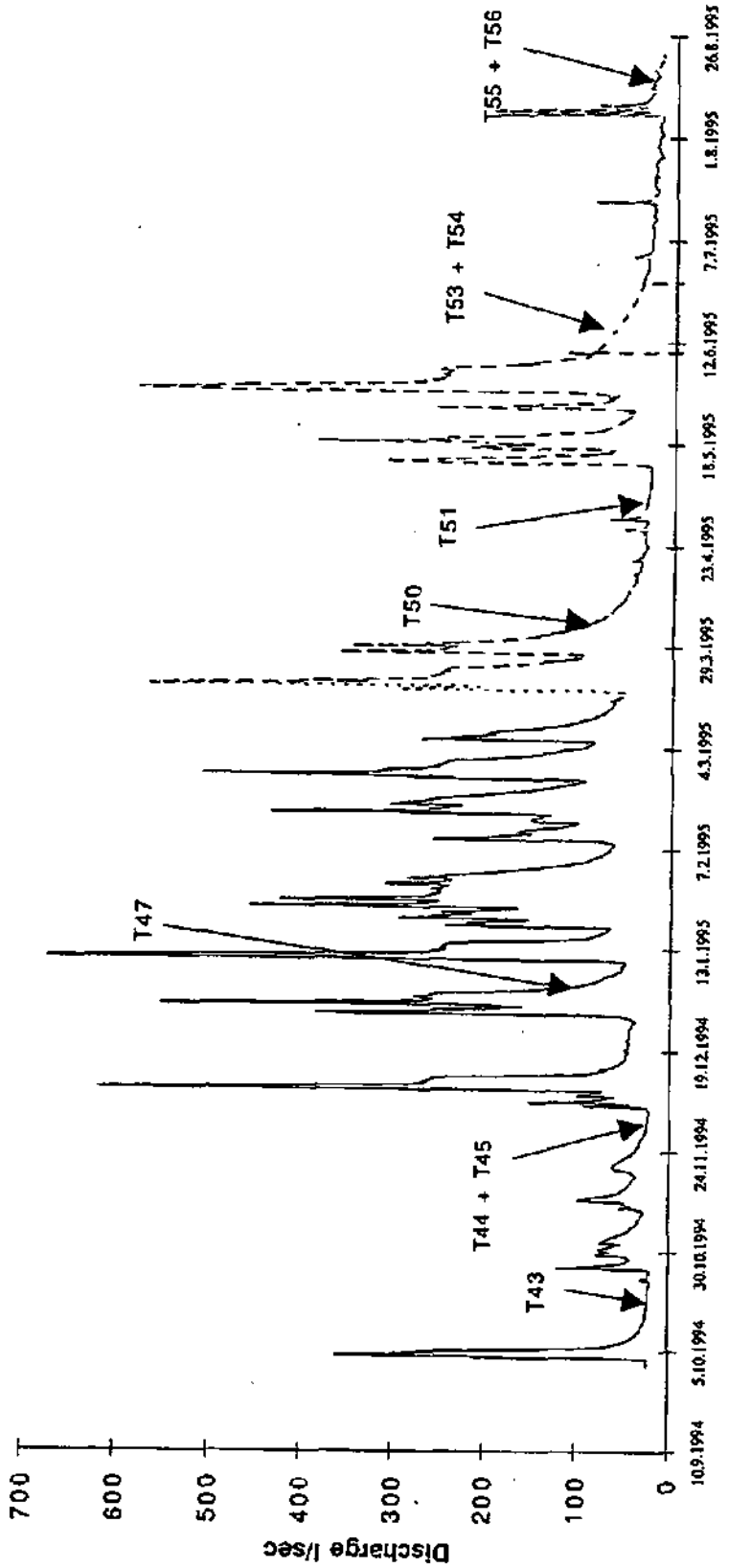

Figure 4.2.: Hydrograph of the Milandrine (upper part of the underground karstic network) showing tracer test activities.

4.1.2. Tracer tests in the Areuse catchment

Four multi-tracer tests were done (Table 4.2). Samples were taken from the Areuse spring in all cases. The two injection points used were the swallowhole of the Moulin du Lac, Lac des Taillères, in the La Brévine valley (direct distance to the spring: 6.15km) and the swallowhole of the Belle Perche in les Verrières (3.6 km away from the spring). The last swallowhole is recharged by a small stream, le Bied, draining water from a peat zone (Figure 4.3).

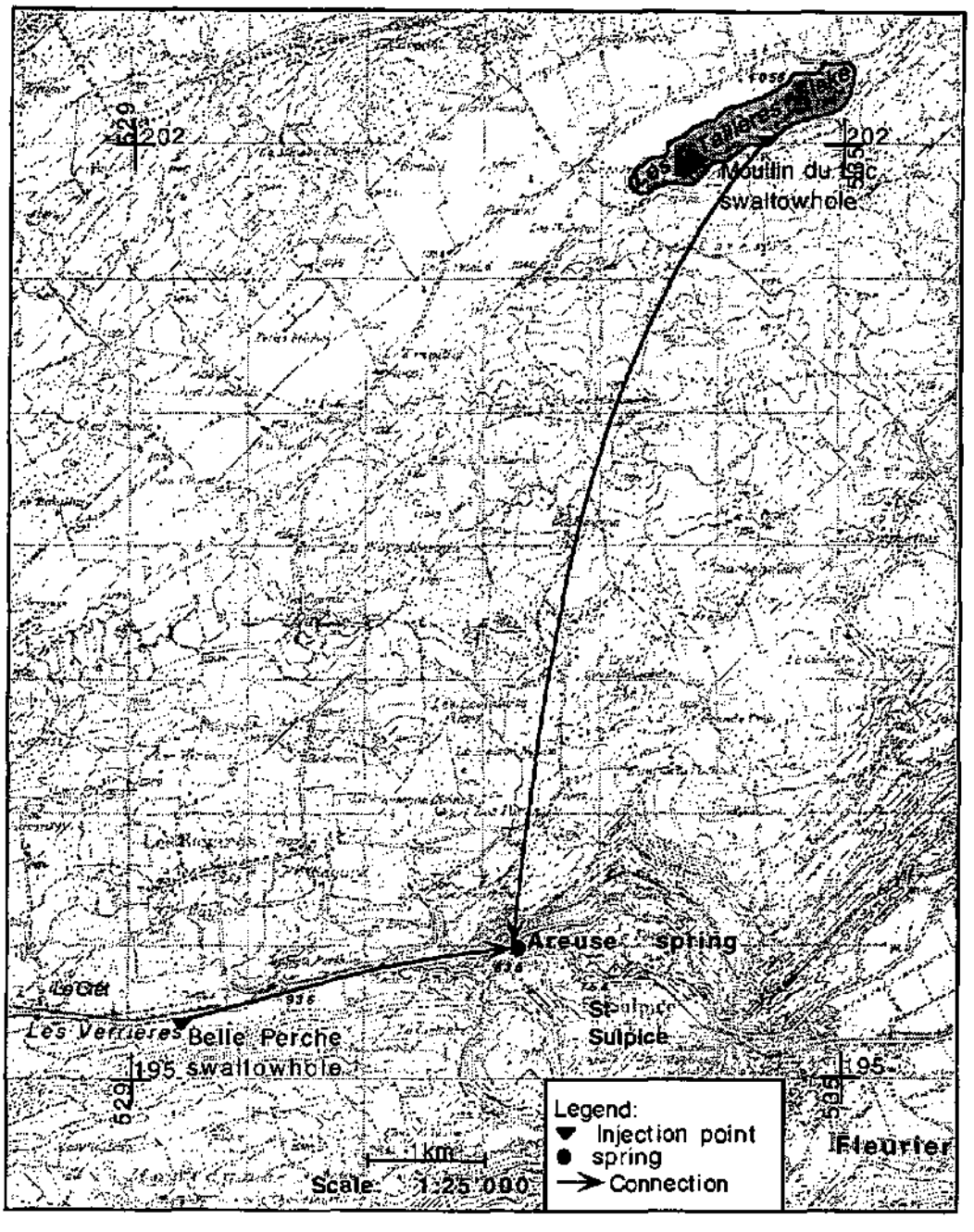

Figure 4.3: Map of the injection points and Areuse spring.

Three of the four tracer tests were done during low water conditions. The fourth, "Areuse 2", occurred during a series of rising limbs (Figure 4.4.). In addition, the breakthrough curves of this tracer test possess several irregularities. Consequently, this tracer test was deemed inappropriate to be interpreted by deconvolution. Adsorption and variations in discharge rate can cause irregular conditions because:

- the tracer is trapped either in the epikarst or in the unsaturated zone and becomes remobilized after rainfall when infiltration from the rain reaches the aquifer.

- the tracer is adsorbed on colloids or aquifer materials.

- water level variations in a perched aquifer occurs at the level of the epikarst and could remobilize the trapped tracer in the unsaturated zone.

The bacteriophage f1 breakthrough curve (Areuse0) was not interpreted in terms of transfer functions because its recovery rate was less than 1%. The few phages per ml (maximum 6) increased oscillations resulting in a "low number effect". The error in phage concentration is probably on the order of the background noise of 1 to 2 coliphages per ml., as the host bacteria of f1 is an *Escherichia coli*, bacteria that can be in the natural environment due to agriculture activities in the catchment.

Table 4.2.

Tracer tests in the Areuse basin

Designation	Injection point	Tracer	Quantity (kg or pfu)	Recovery rate	Discharge (l/min)
Areuse 0	Lac des Taillères swallowhole	Uranine	5kg	40%	70'800
3 11. 1993		Sulfo G extra	8.550 kg	80%	
(Rossi , 1994)		H6/1	1.49E+15 pfu	1%	
		H40/1	9.18E+15 pfu	21%	
		f1	2.15E+15 pfu	0.15%	
Areuse 1	Lac des Taillères swallowhole	Uranine	5kg	56%	600'000
21.2.1995		H40/1	1.683E+14 pfu	51%	
		Psf2	1.174E+13 pfu	10%	
		H6/1	5.714E+13 pfu	25%	
	Belle Perche swallowhole	Sulfo. G extra	8kg	50%	
		H2/1	2.597E+13 pfu	4.5%	
		H4/4	4.477E+14 pfu	10%	
Areuse 2	Lac des Taillères swallowhole	Uranine	5kg	100%	900'000
31.7.1995		H6/1	3.32E+13 pfu	11.5%	
		H4/4	8.45E+13 pfu	2.5%	
	Belle Perche swallowhole	Sulfo G. extra	7.920kg	12%	
		H40/1	5.92E+14 pfu	1%	
Areuse 3	Lac des Teillères swallowhole	Uranine	5kg	99%	60'000
30.10.1995		H6/1	3.09E+13 pfu	16%	
		H4/4	3.25E+14 pfu	10%	
	Belle Perche swallowhole	Sulfo G extra	7.920kg	37%	
		H40/1	3.86E+14 pfu	13%	

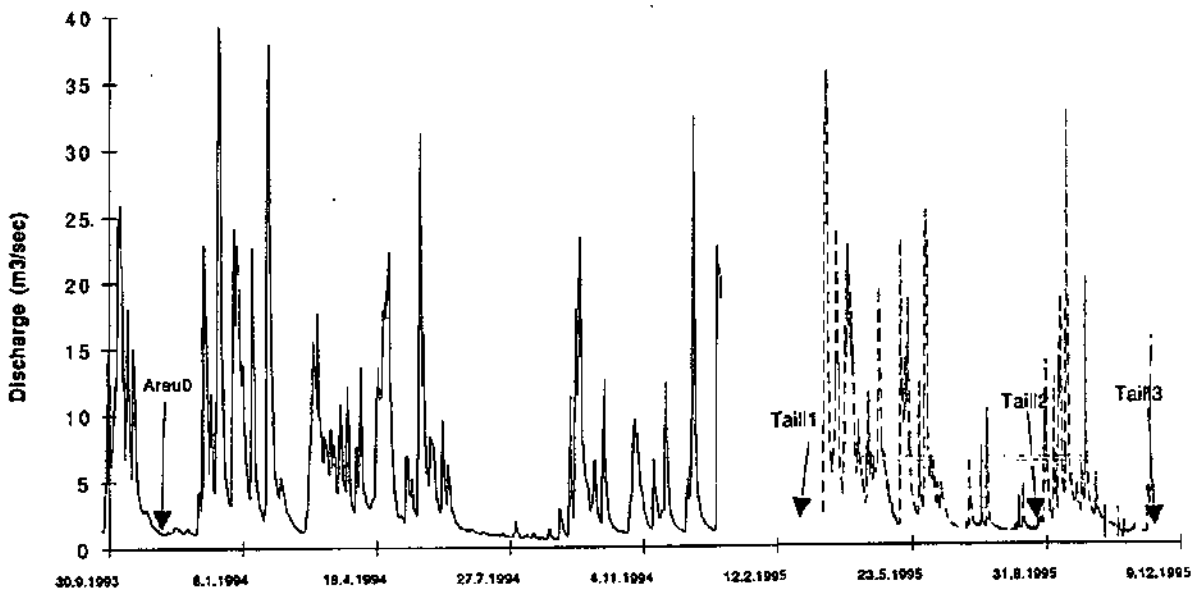

Figure 4.4.: Areuse spring tracer tests and hydrograph

4.1.3. Tracer tests in the Noiraigue basin

Two tracer experiments using bacteriophages and duasyn were carried out in the summer and fall 1995 as part of Module 2 of the SPP Environment program (Atteia et al., 1996). The injection point was a swallowhole located about 0.7 km from the Noiraigue spring (Figure 4.5.).

Table 4.3.

Tracer tests in the Noiraigue spring basin

Designation	Injection point	Tracer	Quantity (kg or pfu)	Recovery rate	Mean diecherge (l/min)
NOIR1 28.7.1995 (Gogniat, 1995)	Swallowhole Brot Dessus	Duasyn H4/4	2.8kg 3.68E+13 pfu	85% 51%	60'000
NOIR2 20.9.1995 (Gogniat, 1995)	Swallowhole Brot Dessus	Duasyn H4/4	3kg 1.65E+14 pfu	98% 34%	84'000

Tracer tests were carried out in low water conditions. The tracers were recovered during falling limb conditions or sometimes at the end of the tracer migration in small rising limbs. For this reason, the mean discharge had be used to interpret the tests in terms of transfer functions. The recovery rates, besides, are calculated integrating the total discharge curve.

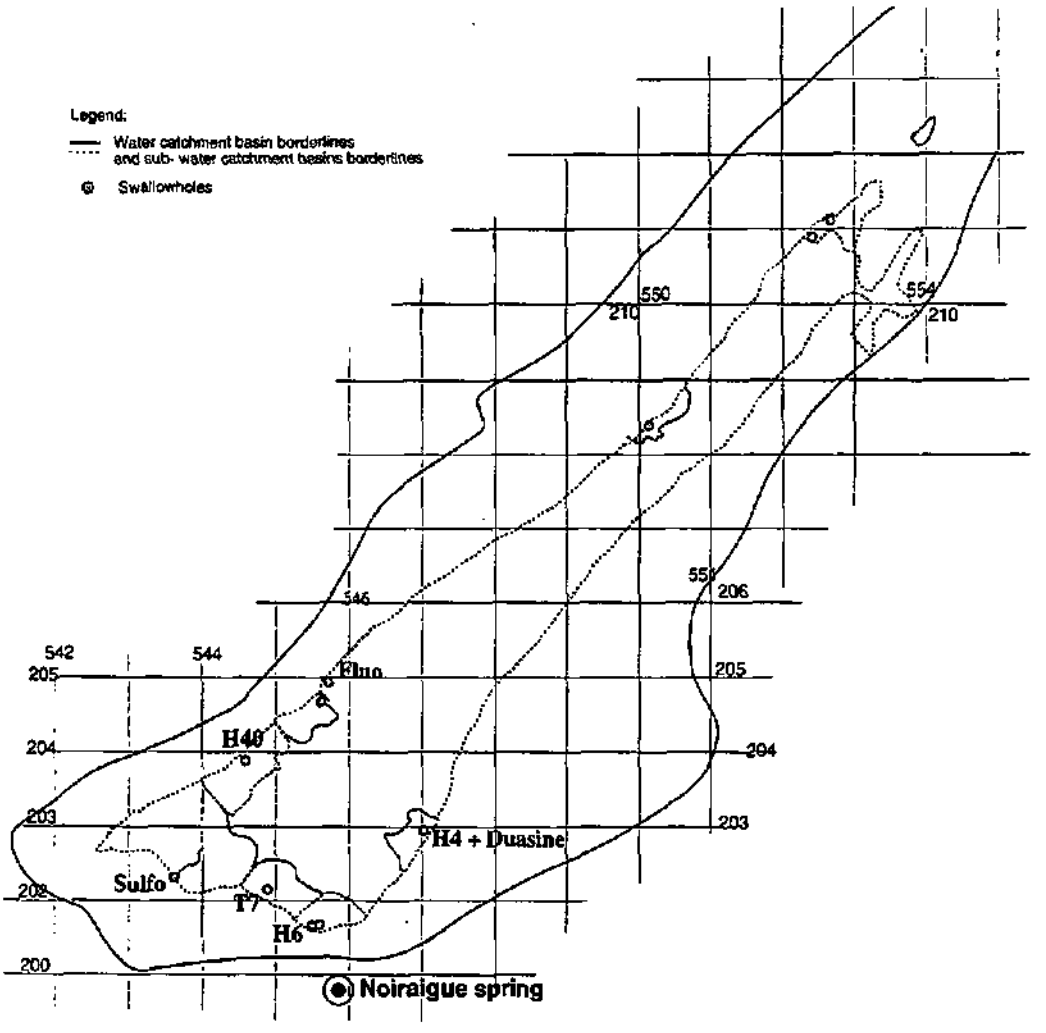

Figure 4.5.: Map of the Noiraigue spring basin with its injection points(Atteia et al., 1996).

4.2. Quantitative interpretation

4.2.1. Classical quantitative interpretation

Recovery rates and both maximum and mean velocities were calculated from the breakthrough curves and the discharge data (Appendix II.11). These results are summarised in Appendix II.10.

4.2.1.1. Tracer recovery rate

The **recovery rate** shows variations for different tracers during the same test. The microbiological tracers (phages) have systematically lower recovery rates than chemical tracers. This is due to the adsorption processes that are different for phages than for chemical tracers. The recovery rates also differ among the phages themselves: H40/1 and H4/4 have higher recovery rates than H6/1, H2/1, Psf2, f1 and T7. Each phage, as a function of its structure, has a specific adsorption behavior that has been determined in the laboratory (Rossi, 1994):

- H6/1 has a type QEA (Quasi-Equilibrium-Adsorption) behavior regarding the adsorption (Grant et al., 1993); the specific conditions (nature of particles in suspension that can provoke the adsorption) are described in Appendix II.2. The H6/1 phage behaves generally the same as H40/1 and H4/4. Therefore,

the percentage of active and virulent H6/1 phages after 180 minutes (bacteriophages in a water solution with Ca-Montmorillonite and separately with Attapulgite) is less than 10% than for H40/1.

- Psf2, T7 and f1 have principally QEARI (Quasi-equilibrium - adsorption and reduced inactivation) and QEASS (Quasi-equilibrium - adsorption and surface sink) (f1 with the Attapulgite) when in contact with some colloids. The percentage of phages (Psf2 and f1) that are still virulent after 180 minutes is lowered to 20%, whereas it is about 70% for T7.
- This phage adsorption behavior for colloids is certainly different in situ in the karst tracer system. The suspended particles in the water are numerous and the contact time is commonly longer than 180 minutes. The transit time of the tracer tests varied from one hour to tens of days.
- The recovery rates also depend on the discharge conditions during the tracer experiment. In function of the hydrological conditions, divergence or trapping of the tracer can be affective. Recovery rates during "Areuse1" were in general, lower (including the fluorescent dyes) than Areuse2 where the discharge was 1.5 times higher. Consequently the transit times were longer for the "Areuse 1 " test. Recovery started after 3 to 4 days and 11 days for the Areuse 1 and Areuse 2 tests, respectively.

Recovery rates of tests done simultaneously using phages and salt (Maira test site) were not affected. Tracer tests T45 and T54 have a difference of up to two in their recovery rates (with and without salt). However, since the discharge conditions differed, it is not a conclusive result. Some consistent tests could document with certainty the influence of the salt on phage recovery rates. Marine phages, when they are injected simultaneously with salt, are centrifuged in order to avoid any further phage production with the host bacteria. These bacteria in some salty water could remain active longer.

4.2.1.2. Characteristic velocities

Maximum and **maan tranait velocities** are similar for the microbiological and chemical tracers. The difference of less than 15 percent is principally due to 1) the sampling frequency difference (every 5 to 15 minutes for the electrical conductivity of the water (NaCl) and typically every 30 to 45 minutes for the phages, 60 minutes at the Maira test site) and 2) the extrapolation between measurements (in Appendix II.12). The difference is greater if the mean transit velocity, calculated at the impulse response center of gravity, is used. This difference reflects variability in dispersion for the chemical and microbiological tracers. In general, the mean velocity of salt and fluorescent tracers is lower than for phages. The bacteriophage dispersion is less due to that the smaller size of the bacteriophages (in Appendix II.12).

4.2.2. Transfer functions

Phages and chemical tracer tests are interpreted in terms of transfer functions. Both impulse and indicial response are analyzed by deconvolution as described in Part I.

Certain phage breakthrough curves appear to have oscillations. The H6/1 breakthrough curve in the Areuse 3 test is a good example (Appendix II.11). This oscillating effect was observed to be stronger for the H6/1 than the H4/1 phages when they were injected simultaneously in the Lac des Taillères swallowhole. The H6/1 phage maximum concentration at the outlet was lower than for the H4/4 phage (14 vs. 90 per ml). No oscillations were observed on the uranine breakthrough curve injected simultaneously with the H6/1 and H4/4 phages. The oscillations on the phage breakthrough curves increase due to the low number effect and therefore may be artificial. The phage low recovery rate is directly related to phage inactivation by adsorption or mechanical effects (turbulent flows). In the case above, the oscillations cannot relate to the hydraulic phenomena such as divergence within the karst network, or water level variations in the epikarst. If these hydraulic phenomena occur, oscillations would also occur in fluorescent tracer breakthrough curve and this was not the case.

Due to the oscillating effect it is necessary to proceed to some curve fitting before to execute the deconvolution operation.

4.2.2.1. Impulse responses

Impulse responses sometimes have irregular breakthrough curves and in these cases the deconvolution process increases them. Before conducting a deconvolution of the impulse response breakthrough curve, a fitting takes place (mobile mean or in the majority of the case, manual redraw). The phage impulse response and the chemical tracers transfer functions are not similar. These differences are shown on figures 4.6 and 4.8.

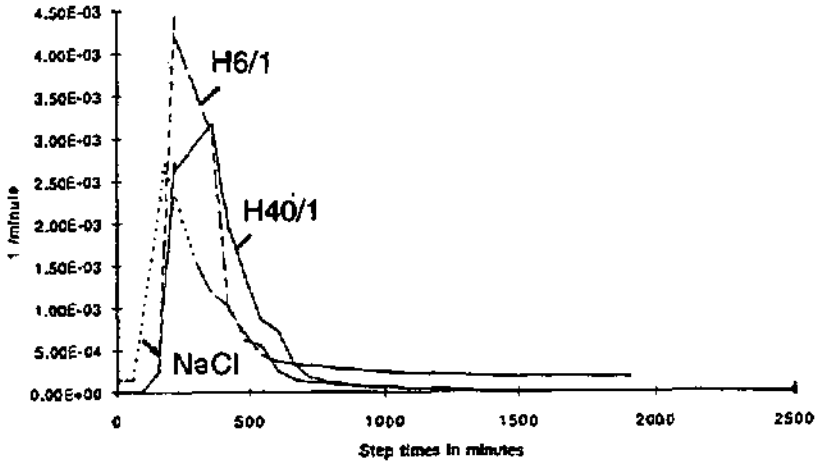

Figure 4.6.: Impulse responsas of the T50 tracer test in the MIL3 borehole at Le Maira (JU) with marine phages H40/1, H6/1 and NaCl salt.

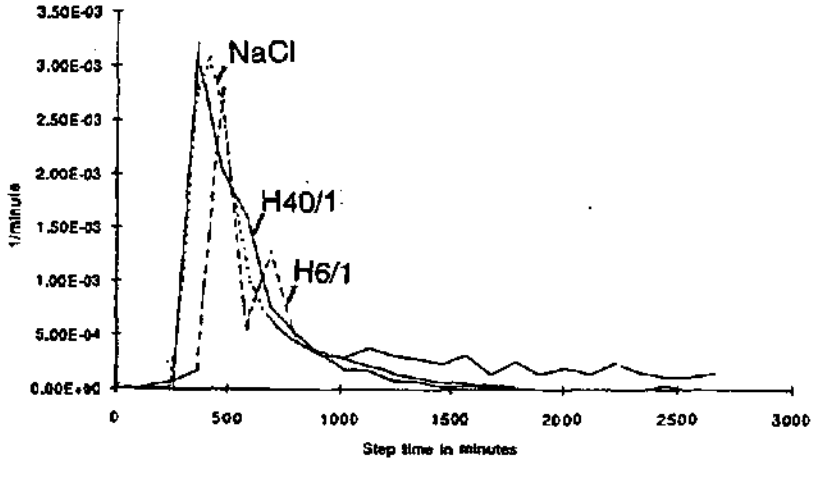

Figure 4.7.: Impulse responses of the T51 tracer test in the MIL3 borehole at Le Maira (JU) with marine phages H40/1 and H6/1, and NaCl salt.

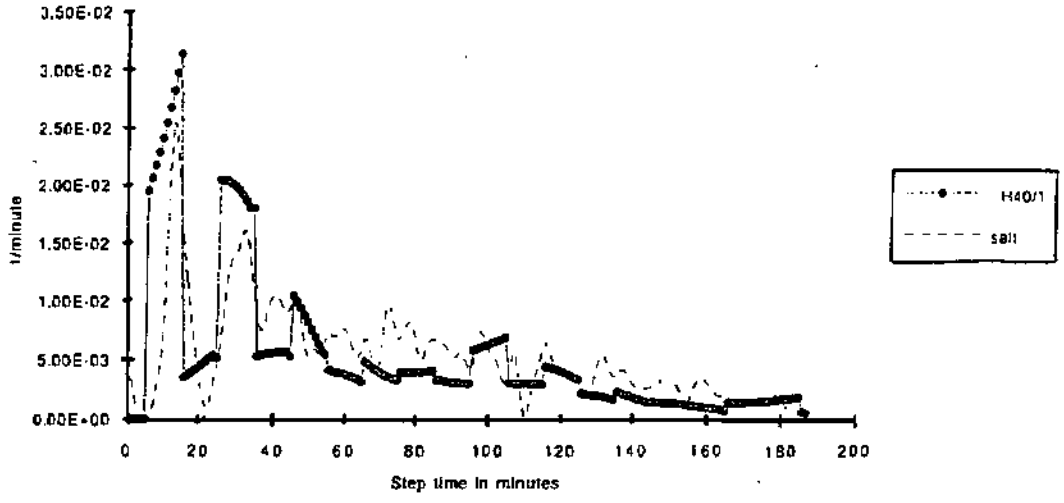

Figure 4.8.: Impulse responsas of tha T45 double tracer test at Le Maira (JU) using the marine phage H40/1 and NaCl salt.

There are differences in the beginning of the rising limb of the impulse response, in the intensity. The difference in the beginning of the impulse response is caused principally by unequal tracer sampling frequencies. Sampling with a too large time interval gives curves which do not have adequate data, in the case of rapid transit, to get more than one maasured point before the maximum concentration is observed. The T47 test at Bure (borehole MIL3) is a good example in that the sampling for the phage was done with a 45 to 90 minute frequency, whereas the electrical conductivity of the water was recorded every 15 minutes (Figure 4.9.).

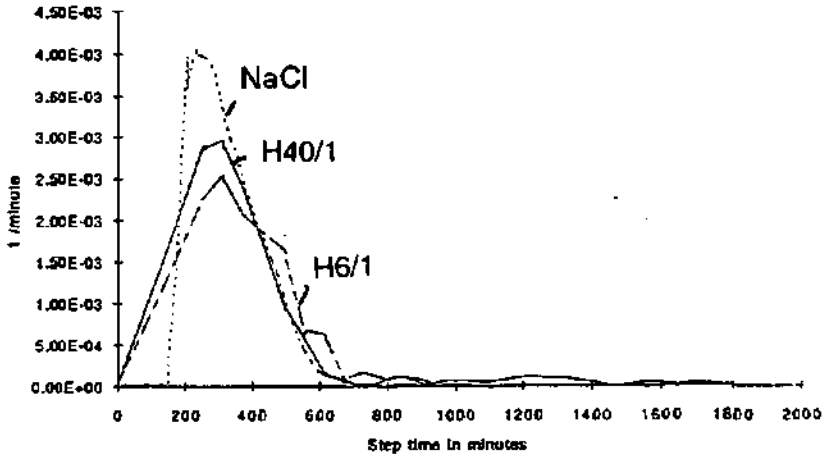

Figure 4.9.: Impulse responses of the T47 tracer tests at Le Maira (JU) with marine phages H40/1 and H6/1 and NaCl salt.

Due to this sampling frequency difference, the phage impulse response begins almost directly from the start, whereas the salt response appears to be delayed by 170 minutes. The early phage detection modifies the intensity and increases the duration of the phage impulse response. A similar effect can be observed with test T51 which was performed in the same borehole as for test T47. The maximum concentration peak is not the same. The H6/1 phage impulse response shape is bi-modal, whereas both the H40/1 and the salt impulse responses have one peak.

4.2.2.2. Indicial responses

Tracer test indicial responses of in Figures 4.10 to 4.12. They are plotted as a function of their test site and for the Maira test site, as a function of their injection point (MIL3 borehole and point 1).

The 0.2, 0.5 and 0.8 percentiles gradients were calculated and they are relative values without any explicit physical meaning. They are principally dependent on dispersion, adsorption and stagnant water effect in the tracer system.

- At **Maira**, in general, the mean gradient at the 0.2, 0.5 and 0.8 percentiles are 86, 85.5 and 72.4, respectively. The phage and salt difference at the given percentiles averages only 0 to 5 percent, with exceptions of 25 to 37 percent for the T43, T50 and T51 tests at the 0.2 and 0.8 percentiles.
- At **Areuse**, in general, the mean gradient at 0.2, 0.5 and 0.8 percentiles are 86[20] (86.5)[21], 84 (85), and 78 (79), respectively. The percentile gradients do not differ by more than 10 percent for the phages and fluorescent dyes. The largest differences occur in the 0.8 percentile gradient. A difference also exists among the fluorescent dyes. The injection conditions may influence this difference. The injection duration is not always the same for the dyes and phages.

  The **Areuse** indicial responses are generally similar for all tracers. At this site, the sampling frequency was identical for the tracers in all cases. In addition, both tracers had similar analytical accuracy.
- At **Noiraigue**, for the NOIR1 and NOIR2 tests, the difference among the percentile gradients is less than 5%. One exception was that the duasyn 0.8 percentile gradient for NOIR2 was lower than for the phages. As at Areuse, the sampling frequency was similar and therefore cannot be used to explain the difference in gradient. The difference may be due to higher dispersion of the other fluorescent dye compared to duasyn.

4.3. Perspectives and comments

It is possible to interpret phage responses in a similar way to classical fluorescent dyes, in terms of transfer functions, even if they have recovery rates consistently 30 to 50 percent less than chemical tracers.

Phages, due to their size and structure, behave like a vertebrate pathogenic virus and bacteria. The transfer functions derived from phage responses have the same error as contaminants.

[20] *Areuse - Lac des Taillères swallowhole*

[21] *Areuse - Belle Perche swallowhole*

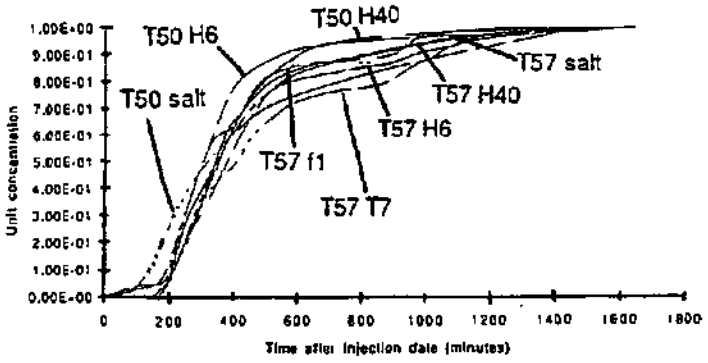

[a]

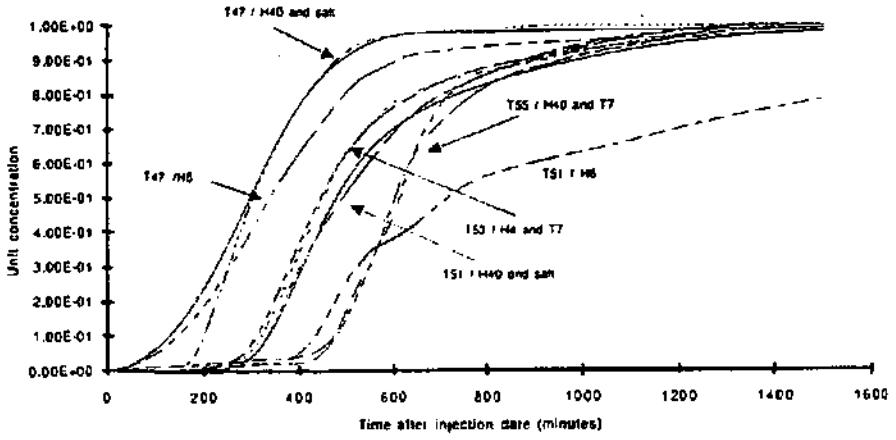

[b]

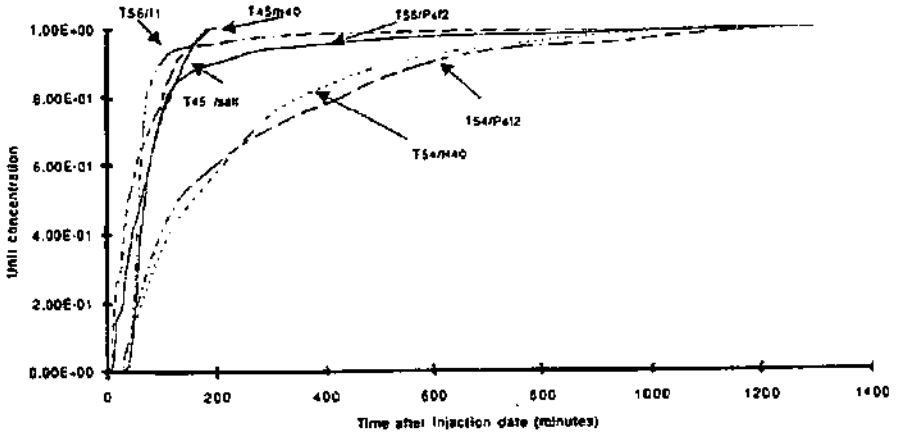

[c]

Figures 4.10.: Indicial responses for tracer tests performed [a] from the MIL3 borehole during falling limb period, [b] from the MIL3 borehole in a base flow recession, and [c] from Point 1 injection.

[a]

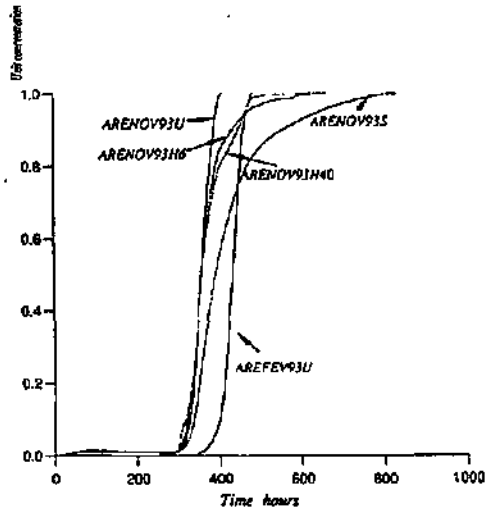

[b]

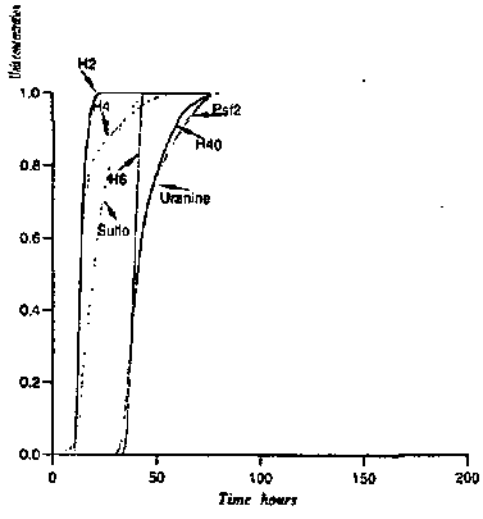

[c]

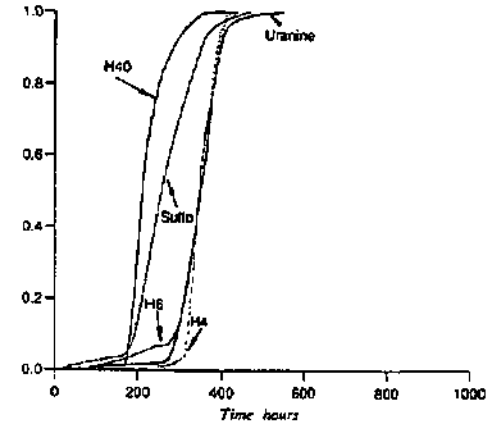

Figure 4.11.: Indicial responses for Areuse (Folded Jura) tracer tests during base flow recession : [a] test 1993 (February and November), [b] Taill 1 test and [c] Taill3 test.

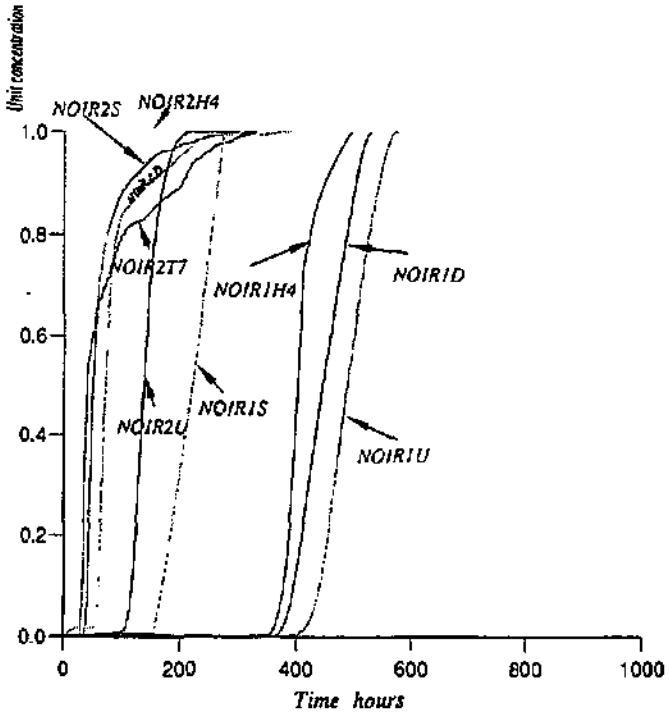

Figure 4.12.: Indicial responses for Noiraigue (Folded Jura) tracer tests during in falling limb conditions.

The major difference between phage and classical dyes transfer functions concerns principally the 0.8 percentile gradients. This is due to 1) the concentration error on the recovery curve, and 2) differences in specific adsorption processes and dispersion. Phages, because of their size, have lower dispersion during transport than fluorescent dyes or salt.

Phage recovery curve irregularities resulting from number and adsorption effects can be adjusted manually by digitizing or automatically by mobile mean. In this way, important oscillations can be avoided after the deconvolution operation.

According to laboratory inactivation tests (phage solutions in contact with clays, agitation), more than 90% of phages are inactivated after three hours (Rossi, 1994). Recovery rates after several hours to several days of underground transit in water prove that in the natural environment phages are more resistant to this type of inactivation. Some phages, when adsorbed on colloids, become temporarily protected and consequently retain their virulence. This effect may be due to the flow regimes in karst aquifers which occur under both laminar and turbulent conditions.

Marine bacteriophages are good potential tracers in karst environments. The problem of retained background levels of moderate biological activity is avoided. These background levels can distort microbiological tracer recovery curves for phages such as T7 and f1, *Escherichia coli* virions, particularly when T7 and f1 have low concentrations.

Chapter 5.

Interpretation of repeated tracer tests with the CONVOX model

5.1. Introduction

« *The transfer of water, on one hand, and the transport of tracer on the other hand, are connected by reletions thet are neither simple nor necessarily unique when the discharge fluctuates* » Guizerix, Margrite, Molinari et al., 1970 (free translation).

In order to test tracer system invariance, repeated tracer tests are performed under various discharges.

Five different tracer-systems were considered: three of them are located in the Maira test site [point 1 (natural hole in a sinkhole (doline)), boreholes MIL3 and MIL7] and two in the Areuse catchment [Lac des Taillères swallowhole and Belle Perche swallowhole]. Tracer tests were thus made from 3 to 8 times in the same injection point either in the Maira test site or in the Areuse catchment.

The veriance analysis of 0.2, 0.5 and 0.8 percentile gradients of the indicial responses allows study of the variability of the tracer tests done several times with the same injection point. This answers the question: Are the gradients significantly different from one test to another considering the discharge of the sampling point ?

Certain of these repeated tracer experiments were interpreted with the CONVOX model of Dzikowski (cf. chapter 2., Part I). Simulating the transfer function (impulse function or RTD) of a tracer test for given conditions (discharge, mass flux) from a reference test allow us to obtain information about the tracer system by comparing the result of the simulation and an experimental transfer function. In order to fit the simulated response to the experimental response, the concept of a dilution rate is introduced. Comparing the simulated and experimental curves shows that variance can exist in the tracer-system for different discharges. This is important to know to answer the following two questions: Is the tracer-system always the same under various hydrological conditions, under various discharges? and, Does the system possess a constant water volume or a variable water volume when it is carrying the tracer ?

5.2. Statistical analysis on repeated tracer tests

The gradient was calculated at the 0.2, 0.5 and 0.8 percentiles of the transfer functions for the repeated tracer tests. A classical statistical analysis on these values was carried out. The results are in the following table 5.1.

Teble 5.1.

Statistics of the 0.2, 0.5 and 0.8 percentile gradients for the repeated test transfer functions

Maira Pt1		minimum	maximum	mean	etd. Deviation
	gradient at 0.2	88 - *0.035*	90 - *0*	89.25 - *0.013*	0.96
	gradient at 0.5	87 - *0.052*	90 - *0*	88.4 - *0.028*	1.37
	gradient at 0.8	86 - *0.07*	90 - *0*	87.8 - *0.038*	1.7
Maira MIL3					
	gradient at 0.2	81 - *0.16*	87 - *0.052*	85.2 - *0.084*	1.8
	gradient at 0.5	80 - *0.17*	87 - *0.052*	83.7 - *0.11*	2.3
	gradient at 0.8	68 - *0.4*	82 - *0.14*	77.1 - *0.23*	5.4
Maira MIL7					
	gradient at 0.2	82 - *0.14*	89 - *0.017*	87.5 - *0.04*	2.8
	gradient at 0.5	85.5 - *0.08*	88 - *0.035*	87.1 - *0.05*	0.9
	gradient at 0.8	74 - *0.28*	88 - *0.035*	82.7 - *0.13*	5.2
Belle Perche swallowhole					
	gradient at 0.2	80 - *0.17*	86 - *0.035*	84 - *0.10*	5
	gradient at 0.5	78 - *0.21*	88 - *0.035*	83 - *0.12*	7
	gradient at 0.8	70 - *0.36*	85 - *0.087*	87.5 -*0.044*	10.6
Lac Taillères swallowhole					
	gradient at 0.2	82 - *0.14*	89 - *0.017*	86 -*0.07*	3.6
	gradient at 0.5	83 - *0.12*	87 - *0.052*	85 - *0.086*	2
	gradient at 0.8	80 - *0.17*	82 - *0.14*	81.3 - *0.15*	1.2

0.017 value of the slope calculated from the tang α where a is equal to 90^0 - gradient value.

The transfer functions on Figure 5.1 shows that there was good reproducibility among the tests in surface point 1, borehole MIL3 and borehole MIL7 in the Maira test site that were repeated several times. The standard deviation values show the greatest variability at the 0.8 percentile gradient.

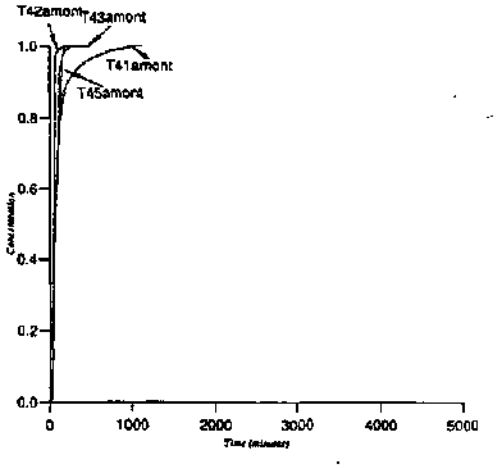

Figure 5.1 (a): Transfer functions - indicial responses - of repeated tracer tests in three different tracer-systems in the Maira test site: surface point 1.

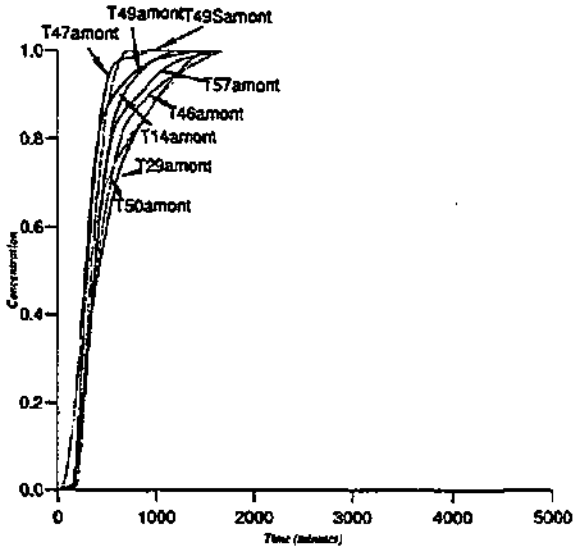

Figure 5.1 [b].: Transfar functions - indicial rasponses - of repeated tracer tests in three different tracer-systems in the Maira test site : borehole MIL3.

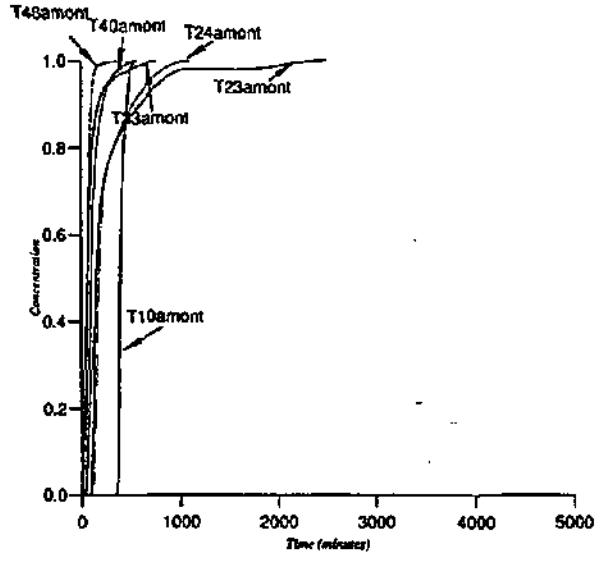

Figure 5.1.[c]: Transfer functions - indicial responses - of repeated tracer tests in three different tracer-systems in the Maira test site: borahole MIL7.

The repeated tracer tests were performed under similar base flow recession hydrological conditions. The only factor able to influence the variability of the gradient is the discharge. There was no significant difference among the gradient values over the discharge range that appeared as a result of the variance analysis.

Systematic study of repeated tracer tests (24 times) had been carried out in the Mendip Hills, Somerset by Stanton & Smart (1981). They showed that time is inversely proportional to the mean discharge of the spring. The higher the discharge, the shorter the time, as implicitly expected.

Figures 5.2 and 5.3 shows that for the repeated tests in the MIL3 and MIL7 borehole there is a dramatically decreasing modal time when discharge increases. When the discharge is higher than 50 l/s, the modal time is in the same range of values. For the repeated tracer tests in the Areuse catchment or from surface point 1 in Le Maira test site, the number of repeated tracer test is too small to definitively establish this relationship (less than 5 repeated tests).

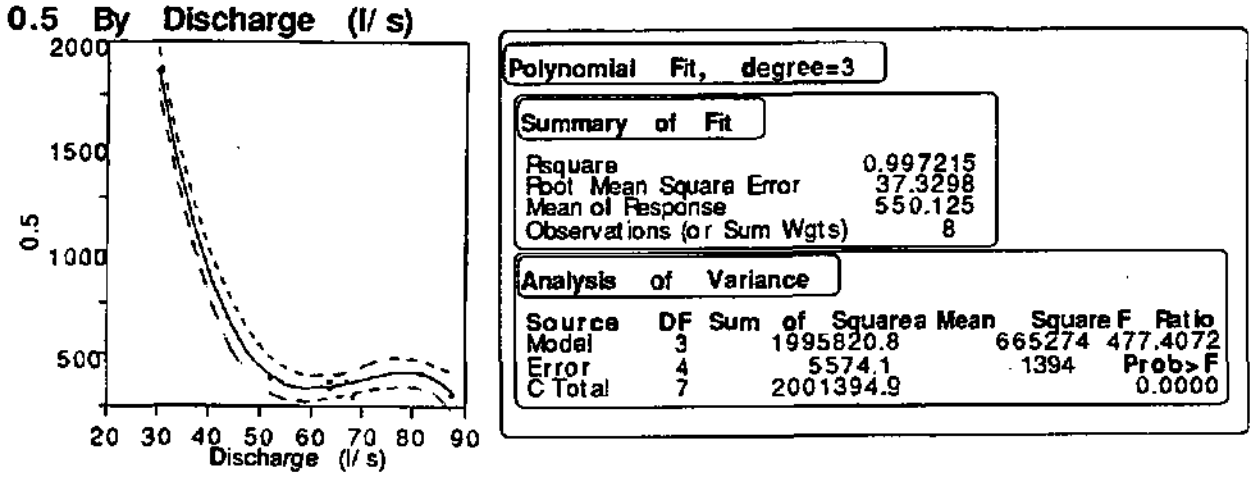

Figure 5.2: Relation between modal time and discharge rate for repeated tests in borehole MIL3.

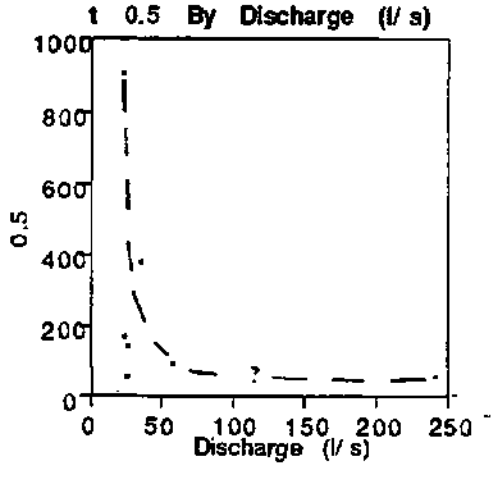

Figure 5.3: Relation between modal time and discharge rate for repeated tests in borehole MIL7.

The relation between the discharge rate at the spring and the gradient of the transfer function at the given percentiles is not very obvious. It appears that the gradient at 0.5 percentile is proportional to the discharge. The higher the gradient, the higher the discharge. In other words, the higher the discharge, the higher the maximal intensity of the impulse response, the lower the dispersion (Figures 5.4, 5.5). For the other repeated tests, the variation of the discharge is too small to definitively establish this relationship (Figure 5.6). For the repeated tracer test in both the borehole MIL3 and the surface point 1, the discharge range is from 20 to 90 l/s, when for the repeated tests in the borehole MIL7 the discharge range is from 20 to 250 l/s.

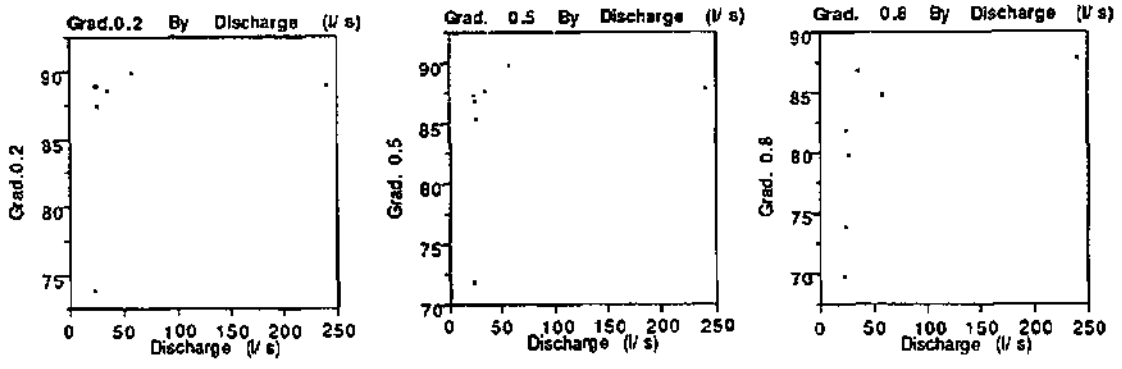

Figure 5.4. : Plot gradient values at 0.2, 0.5 and 0.8 percentile versus discharge for the repeated tracer tests performed in the borehole MIL7 in the Maira test-site.

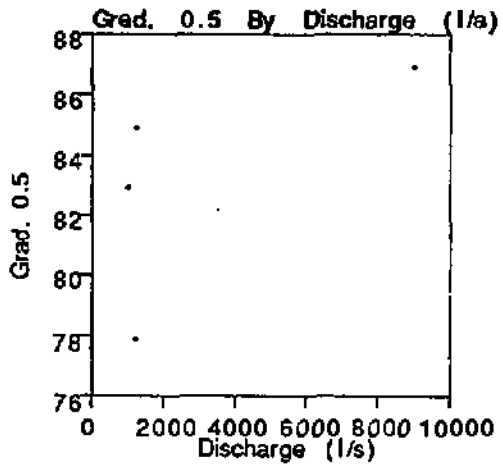

Figure 5.5. : Plot gradient values at 0.5 percentile versus discharge for the repeated tracer tests performed in the Lac des Taillères swallowhole.

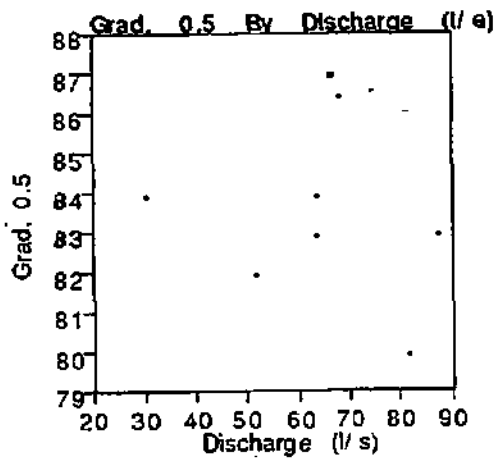

Figure 5.6. : Plot gradient values at 0.5 percentile versus discharge for the repeated tracer tests performed in the borehole MIL3 in the Maira test-site

5.3. Interpretation of the repeated tracer tests with CONVOX

5.3.1. Results

(a) Areuse water catchment - Lac des Taillères swallowhole

The uranine test in the tracer-system Lac des Taillères swallowhole - Areuse spring was carried out in February and November 1993 under different discharge levels. The impulse response of the November 1993 test was simulated, using as reference, the February 1993 results.

In order to have an optimal simulation of the transfer function, following data related to the dilution rate are considered:

Qs/Qreal = 0.88 (a) or 0.8 (b) for the reference test.

Qs/Qreal = 0.96 (a): constant discharge (mean value of the discharge) for the simulated response.

0.7 (b): variable discharge versus time (discharge hydrograph) for the simulated response.

The data of the simulation are in the following table 5.2.:

Table 5.2.

Data for the reference test and simulated response

	Injected mass	Discharge	Dilution rate
Reference test Arefev93fluo	3.8 kg (recovered mass)	51'000 l/min	0.88 (a) 0.8 (b)
Simulated test (experimental response: Arenov93fluo)	2 kg (recovered mass) as instantaneous injection	70'800 l/min (a) history of discharge during the recovery duration (b)	0.96 (a) 0.7 (b)

Figure 5.7 shows the difference between the two simulated curves (a) and (b) and the experimental response. The experimental curve shows an abrupt falling limb after the peak, resulting in an interruption of sampling due to freezing. But, the second peak of the experimental curve and the consequently longer tailing effect are not present on the simulated curves.

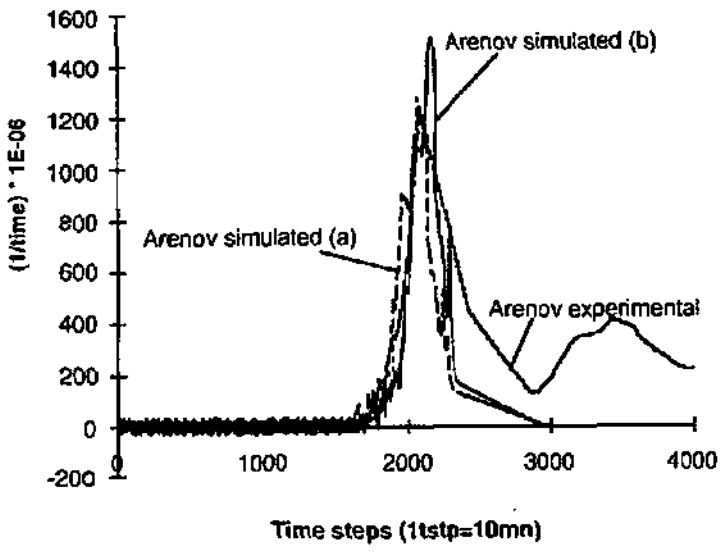

Figure 5.7.: Simulated (a and b) and experimental curves of the Arenov93fluo tracer test using as reference test Arefev93fluo - Areuse spring.

(b) Maira test site

b.1. Borehole MIL3 as entrance of the tracer system MIL3-upper Milandrine

Three tests T47, T50 and T51 are considered using test T47 as reference test. The responses corresponding to the initial conditions of tracer tests T50 and T51 were simulated. The data of the optimal simulations are in the table 5.3.:

Table 5.3.

Data for the MIL3 borehola tracer test aimulations

	Mass injected	Discharge	Dilution rate
Reference test T47 amont	173 kg	4065 l/min	1
Simulated test (experimantal test T50)	288kg during 10 minutes in 3 successive injections	5238 l/min	1
Reference test T47 amont	173 kg	4065 l/min	a) 0.85 b) 0.95 c) 1
Simulated test (experimental test T51)	163 kg during 2 minutes in 2 injections.	1796 l/min	a) 0.55 b)0.8 c)0.85 with a mass of 90kg during 2min.

Figures 5.8 and 5.9 show a difference essentially in the falling limb of the curves. The simulated curve has either a too abrupt falling limb or the smallest gradient in comparison to the experimental curve. The amplitude of the simulated curves is in the same range of the experimental one.

For a discharge rate in the same range as the reference test, no extra dilution is required in order to simulate the T50 tracer test. The tracer-system appears to be invariant under this condition. But for smaller discharges on the order of one-half of the reference discharge, it is necessary to take into consideration a dilution rate in order to fit the simulated curve to the T51 experimental curve.

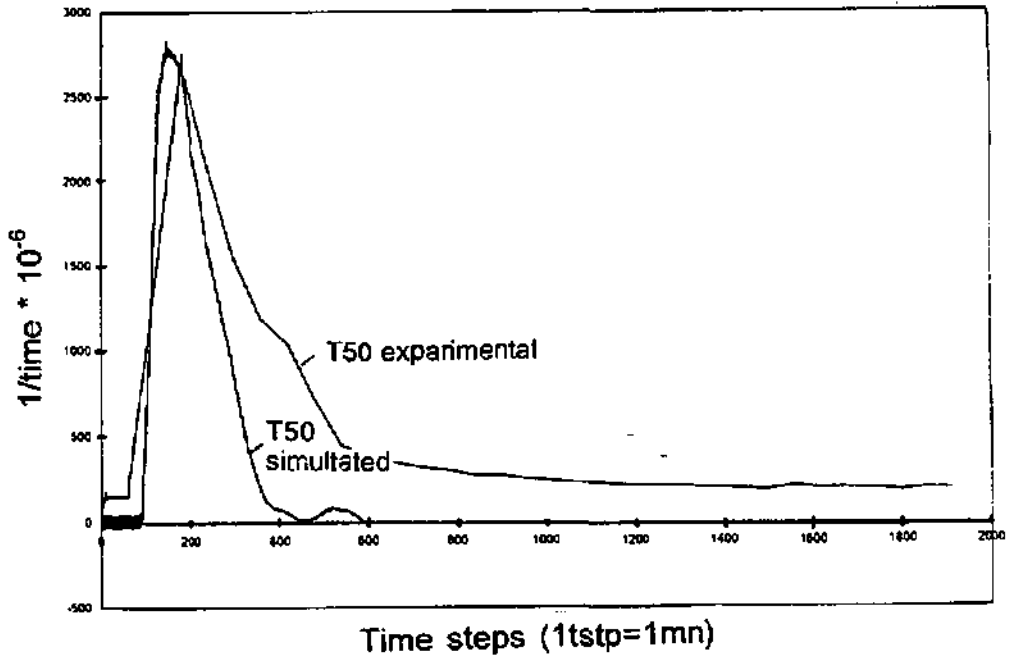

Figure 5.8.: Simulated and experimental impulse response of the T50 tracer test using T47 as a reference.

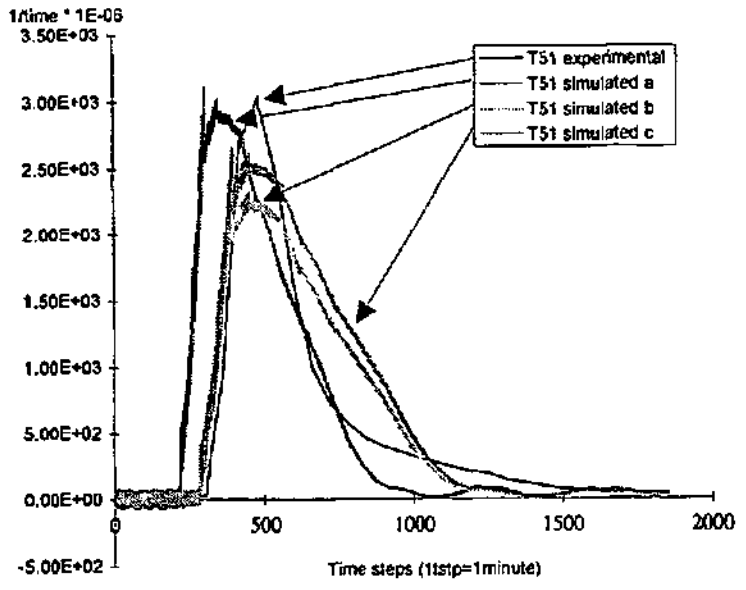

Figure 5.9.: Simulated and experimental impulse response of the T51 tracer test using T47 as a reference.

b.2. Borehole MIL7 as entrance of the tracer system MIL7-upper Milandrine

Three tests T24, T23 and T40 were simulated using the T40 test as a reference. The data of the optimal simulations are in Table 5.4.

Table 5.4.

Data for the MIL7 borehole tracer test simulations

	Mass injected	Discharge	Dilution rate
Reference test T48 amont	495 kg	14'408 l/min	1
Simulated test (experimantal test T23)	50 kg during 5 minutes	1518 l/min	0.2
Reference test T48 amont	485 kg	14'408 l/min	a) 0.85 b) 0.95 c) 1
Simulated test (experimental test T24)	30 kg during 50 minutes (instead of 39.5kg)	1380 l/min	0.28
Reference test T48 amont	485 kg	14'408 l/min	1
Simulated test (experimental test T40)	54 kg during three injections of 3 minutes (instead of 80 kg)	1512 l/min	0.05

Figures 5.10, 5.11 and 5.12 show that if the amplitude of the curves are simulated well, the tail effect and the less abrupt end of the falling limb of the experimental curves differ only slightly from the simulated one. The derivation is more different in the case of the simulation of the T40 test.

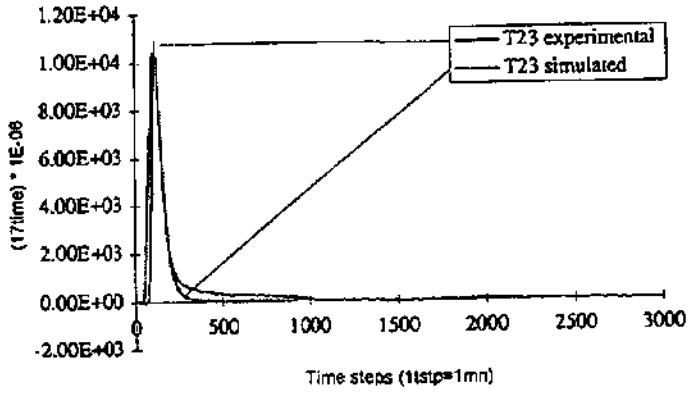

Figure 5.10.: Simulated and experimental impulse response of the T23 tracer test using T48 as a reference.

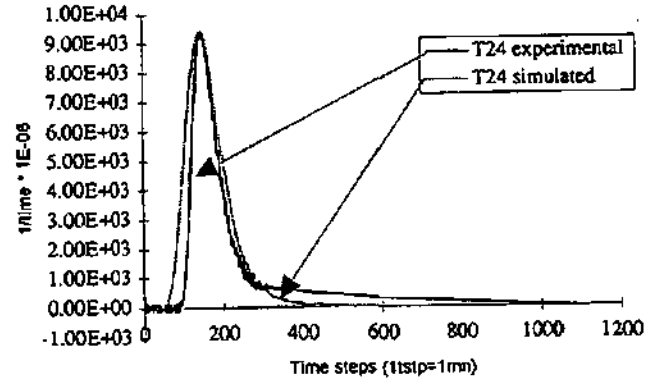

Figure 5.11.: Simulated and experimental impulse response of the T24 tracer test T24 using T48 as a reference.

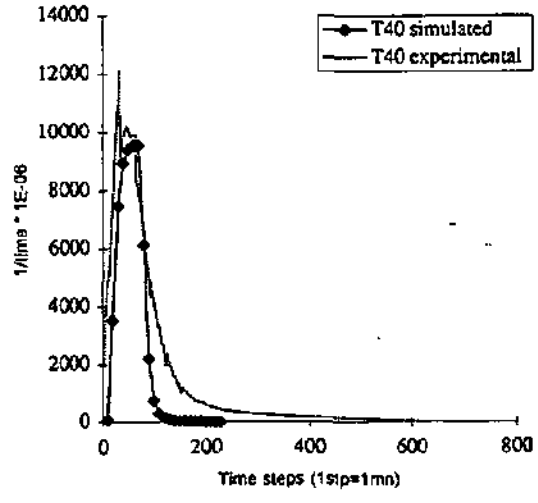

Figure 5.12.: Simulated and experimental impulse response of the T40 tracer test using T48 as a reference.

If the T23 experimental test is simulated correctly with a dilution rate of 0.2, for a similar discharge range, it is necessary to use a dilution rate of 0.05 and to lower the value of the recovered mass in order to simulate the T40 tracer test.

b.3. Surface point 1 aa entrance of tha tracer system point 1-upper Milandrine

The tracer experiment T45amont was simulated using the tracer test T43amont as the reference test. The data of the best simulation are in Table 5.5.

Table 5.5.

Data for the Surface Point 1 tracer test simulation

	Mass injected	Discharge	Dilution rate
Reference test T43amont	46.5 kg	3900 l/min	1
Simulated test (exparimental test T45)	34 kg during 20minutes with a 2 minutes time step (instaad of 30 kg)	14130 l/min	1

Figure 5.13 shows the difficulty associated with attempting to simulate a multi-peaked curve. The long tail of the T45amont experimental curve T45 amont was not able to be matched. The two major peaks were taken into account with the simulated curve.

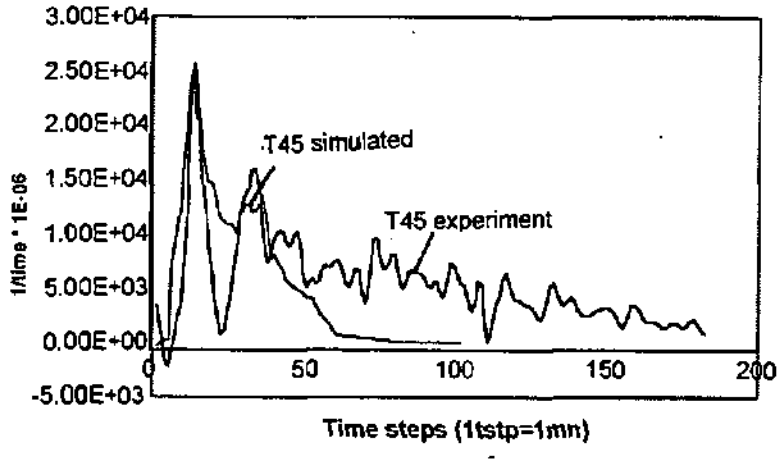

Figure 5.13.: Simulated and experimental impulse response of the T45 tracer tast using T43 as a refarence.

5.3.2. Comments

With these transfer function simulation examples of various discharge conditions, it is apparent that the water volume is rarely constant. The tracer-system is not invariant under various discharges at the outlet. For the simulated curve to match the experimental one, it is necessary to introduce a dilution rate.

Under different hydrological conditions, the tracer system can be the same or it can vary. The variation can be related to volume. However, changes in volume do not necessarily represent a different or new tracer system, particularly if the system has an unsaturated component as part of the karst network (Figure 5.14.).

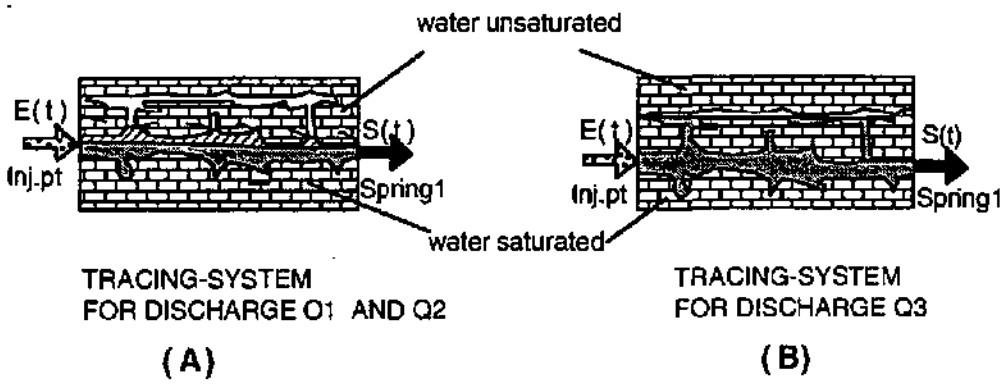

Figure 5.14: The variance of a tracer-system as a result of various discharges. (Qi): schematic illustration of the real tracer-system.

In order to have a satisfying simulation, an input function that was often different from an impulse had to be considered.

In some cases, simulation required considering additional dilution rates and modifying the amount of mass injected.

In the four various tracer-systems considered, it appears clear that it is difficult to fit all the curve. The tail, according to the reference curve, is usually under estimated or non existent. The double peaked nature of the curve is simulated using a double peaked input function. Generally, we assume that a double peaked curve is due to either variable discharge during the recovery period or to the structure of the tracer-system. For the structural reason, one path is considered more or less sinuous and there is one or more connections in the high permeable volume of the tracer-system.

5.4. Conclusions

If repeated tracer tests demonstrate variability, it is characterized by a low to insignificant degree especially for the 0.2 and 0.5 gradients. The variability of the 0.8 gradient is directly linked to the difficulty of fitting the tail of the impulse response with the CONVOX model. This reflects the variance of the tracer system. The injection procedures were identical for all tracer tests as wera the variation of the tracer dispersion and retardation factors.

The CONVOX model of the reference response allows transforming the reference response using experimental data from at least two tracer tests.

It was assumed that the tracer system does not depend upon the hydrodynamic conditions. For variable or constant water volume, the tracer system is considered to be the same. Based on the above results, we conclude that the tracer system is not the same under various discharge rate. Moreover, when taking into account a dilution rate that accounts for the variable water volume of the system, it appears necessary to add a dilution effect on the injected mass. This reflects the variance of the tracer-system. Under various

discharge rates, the flow systems are modified and the tracer-system is different. This was verified using simulation tests of tracer tests from the Areuse and the Milandrine catchments.

The tracer system of an experiment done under given discharges is far from being unique. It is necessary to conduct a number of repeated tracer tests in order to determine over which discharge ranges the tracer system is not changeable.

The use of this kind of model for pollutant simulation is therefore limited or requires an adequate number of tracer tests to determine the discharge range for which the simulations are realistic.

Chapter 6

Summary of the results

1. Comparing transfer functions from tracer tests performed in various karst aquifers has been done for the first time. A variability in transfer functions indeed exists. This variability principally reflects the two- and three-dimensional heterogeneity of physical parameters inherent in karst aquifers.
2. Mean transfer functions from the Alps from the Jura can be distinguished without considering hydrological conditions. In these cases, the transfer functions are dependent upon the 1) injection point, and 2) structure, i.e. ratio of unsaturated to saturated conditions. Therefore, transfer functions for typical injection conditions can be used to evaluate vulnerability zones or delineate realistic groundwater protection areas.
3. Although hydrological conditions are not significant, it is still important to identify at what point on the hydrograph, the tracer recovery period occurs. Tracer test data for all geological settings were available for the most part for tests done during base flow recession.

It is possible to interpret bacteriophages in terms of transfer functions. This is true despite the fact that their recovery rates are consistently lower than those of classical tracers. The major difference between phage and classical tracer transfer functions is the degree of dispersion and the adsorption. The adsorption of the phages on particles in the aquifer and the dispersion of phages are lower than for classical dyes, due to their size.

5. Transfer functions determined for tracer tests that were repeated under essentially the same conditions show only a small variability for the 0.8 percentile gradient. This variability is linked to the difficulty to fit the entire, particularly the tail of the curve using the CONVOX model. Those differences reflect the variance within the tracer system. The system influenced during a tracer test under a given discharge can change from one test to another. It is still necessery to repeat tracer tests to determine in which discharge range the tracer-system is invariant.

6. There is legal requirement to determine protection zones. The typical way of doing this relies heevily on tracer test breakthrough curves. However, due to limited funding, there are rarely an adequate number of tests to adequately perform this evaluation. Therefore, there is typically a large error in the interpretation. This error is consequently related to transfer functions. In order to increase the feasibility of effective use of transfer functions, we recommend the use of a field fluorometer or conductivity meter for salt tracers. Two preliminary comparison tests of the manually sampled recovery curve and recovery curves that result from a continuous record of fluorescence are very promising. The difference in the amplitude of the maximum concentration peak is less than 5% compared to laboratory analysis. We used a prototype fluorometer developed by Schnegg and Costa of the Institute of Geology, University of Neuchâtel.

Part III

Intrinsic vulnerability mapping of karst aquifers based on a multiattribute approach - the EPIK method -

Chapter 1

Swiss water protection law

Water quality problems from agriculture and to a lesser extent industrial contaminants occur too frequently during the year, in karst watercatchment. A new approach of outlining the protection zones in karst areas has been developed to improve this situation, and to assist enforcing the new Water Protection Law. The approach was developed with cooparation among tha Swiss National Hydrological and Geological Survay (SNHGS) of the Federal Office of the Environment, Forests and Landscape (FOEFL), another unit of the FOEFL and Hydrogeology Center of the University of Neuchâtel. This approach, an overlay index mathod which takes into account the particular hydrogeological behavior of karst aquifers, is the result of this thesis research work. This new approach, specifically dedicated to catchmants in karst environments, is explained in Part III.

1.1. Water protection

The new federal law on protection of water came into effect in November, 1992. The basis for surface and subsurface water protection in this law (Leaux, 814.20) gives more emphasis to the quantitative protection of natural waters than the previous law. Preventive measures are particularly preferred for quality issues.

Protecting subsurface water for quality purposes requires, in particular, outlining groundwater protection zones. Guidelines for dalineation of protection zones for groundwater in different hydrogeological settings (porous media, fissured aquifers and karst aquifers) were defined in the seventies, and revised in the eighties. New guidelines and regulations to implement the new law are still in progress. The multiattribute overlay method « EPIK » has been developed to apply this new law in karst environments.

1.2. Definition of protection zones in karst terrain

1.2.1. Introduction

In Europe, many karst areas provide water supply resources which play an important role for the development of large regions. About 35 percent of Europe is made up of carbonate rock outcrops.

In Switzerland, karst areas correspond mainly to: Jura (Tabular and Folded Jura, from Geneva to Basel), northern slopes of the Alps including the Prealps and, some areas in the south-eastern part of Switzerland (Austroalpine domain) (Tripet et al., 1995). These regions commonly have agricultural and forestry activities and are centers of important tourism and industrial development. Most of their water supplies are provided by karst subsurface water in the form of springs and capture structures such as wells or water galleries. About 15 percent of groundwater used for water supply is provided from karst areas in Switzerland.

Karst waters represent an important natural resource which needs protection. Protection zones are defined to reach certain qualitative protection goals.

1.2.2. Protection zones: definition and restrictions

According to the Water Protection Law and related regulations, three different zones have to be outlined in the water catchment of a water supply:

- **Zone S1**: This zone has to 1) protect the supply source against damage and 2) prevent any direct pollutant penetration into the subsurface water flowing to the source. For this reason, supply sources such as wells or springs and distances of from 5m to 10m around the source and infiltration points (swallowholes, fissured zones) are defined as zone S1.

- **Zone S2**: This zone has to 1) provide a sufficient protection against microbiological (bacteria, viruses) and non-degradable contaminants and 2) allow enough time for emergency action in the case of an accidental spill.

  In accordance with 1982 guidelines for outlining protection zones, all areas of a water catchment where rapid surface water infiltration could reach the supply source in a short period of time (few days) are to be considered as zone S2.

- **Zone S3**: This zone should provide additional safety. It could in many cases, correspond to the rest of the catchment not covered by zones S1 and S2. This is a buffer zone between zones S1, S2 and the adjacent so-called protection sectors or perimeters. Generally, the S3 zones corresponds to the rest of the catchment.

If, under present regulations, protection of the whole catchment area is not required, in many cases the whole catchment is associated with zones S1, S2 and S3. In the case where there is a protective cover of low permeability and considerable thickness, such areas could be under less land use restriction as persistent and mobile contaminants may not reach the source as easily, for example, runoff and loss into a swallowhole. This question is currently under discussion.

Particuler lend use restrictions are assigned to the three zones. In S1, no activity is allowed except the growth of natural grass without fertilizers. The S1 zone is physically delineated with fences end is commonly the property of the water supply egency. In S2, construction activities, among others, are not allowed and there are restrictions regarding agricultural and forestry such as the limited use of fertilizers and other chemicals. In S3, industrial plants are subject to restrictions. Quarrying end waste disposal are not allowed in any of the three zones (Tripet et al, 1995; Doerfliger & Zwahlen, 1995).

To date, protection zones for all Swiss karst areas heve been defined eccording to the existing guidelines. Despite this important step, these current protection zones provide incomplete protection due partly to the inadequate hydrogeological foundation upon which they were defined. In general, S1 and S2 zones usually do not encompass a wide enough area whereas the S3 zone is commonly too extensive (almost over all the catchment) (Doerfliger & Zwahlen, 1995). To develop a new approach to outline realistic and effective groundwater protection zones in a karst

environment, economic considerations also needed to be taken into account. The multi-attribute approach has to be able to be used cost-effectively by consulting geologists under contract to local communities or the state. Relatively straightforward methods are required for them to be able to determine the attributes in the field and within a reasonable time according the catchment size.

Chapter 2

The vulnerability mapping concept

2.1. Vulnerability definition

The term vulnerability was used in the sixties in France, introduced as a scientific term in hydrogeological literature by Margat and Albinet (1971). In the seventies, several vulnerability maps were established in various European countries.

Vulnerability has been used as certain zones were more sensitive than other to the contaminant intiltration to the subsurface waters. In technical literature, several definitions of vulnerebility exist. In the framework of this thesis, the vulnerability term is defined, distinguishing the intrinsic and the specific vulnerability, as following:

Intrinsic vulnerability reprasents the inherent hydrogeological and geological characteristics which determine the sensitivity of groundwater to contamination by human activities.

This definition is in agreement with the definition of Foster (1987) and Daly et al. (1994), as reported in the COST action 65 final report (1995). A definition of aquifer vulnerability is proposed by Foster and Hirata (1988) and Adams and Foster (1992) as in Robins et al., (1994):

" Aquifer vulnerability is a function of the intrinsic properties of the overlying soil and rock column or unsaturated zone of the aquifer, with the risk of groundwater pollution dependent on the interaction of the "natural" aquifer vulnerability and the subsurface contaminant load imposed by human activity. "

The contaminant' load imposed by human activity can be due to localized releases from sources such as hazardous waste disposal sites, municipal landfills, underground storage tanks, gas and oil pipelines [*point-source*] and to substances released at or near the soil surface in a dispersed manner such as fertilizers and pesticides [*non-point sources*].

Intrinsic (also called general or natural) vulnerability refers essentially to risks associated with non-point sources. Point-sources can be put on a potential pollution risk map, and combining such a map with a vulnerability map of a catchment provides an excellent tool for the groundwater manager and water protection officials.

Intrinsic vulnerability, as opposed to specific vulnerability, considers all kind of contaminants. **Specific** vulnerability is defined for a given contaminant that is characterized through particular properties, that could be different from one contaminant to another. The assessment of specific vulnerability requires consideration of the characteristics of the aquifer relative to the contaminant and the contaminant itself, in addition to intrinsic hydrogeological and geological characteristics.

The approach developed in this thesis contributes to outlining protection zones in karst aquifers considering only intrinsic vulnerability. Specific vulnerability is not included. Intrinsic vulnerability to

[1] *Contaminant: All undesirable solutes not usually present in water, introduced into the hydrologic environment are referred to as contaminants regardless of whether or not the concentration is harmful to health. The term pollutant, is reserved for cases where contaminant concentration attain critical levels that are considered to be objectionable (after Freeze & Cherry, 1979).*

a contaminant in a typical pollution scenario has no precise meaning following Andersen & Gosk (1987) and Adams and Foster (1992). Instead, they suggest carrying out specific vulnerability mapping for individual contaminants.

However, the concept of intrinsic vulnerability is necessary to provide as much as possible unbiased information, the basis to proceed to protection zones outlining in karst aquifer. That is the first step needed to outline protection zones.

As vulnerability is not a physical property, it cannot be measured; it has to be assessed. The assessment of the vulnerability reflects the probability that contamination will easily occur in an aquifer. In this sense, the vulnerability assessment is a predictive statement such a weather forecast is (CTAGWA, 1993).

2.2. Vulnerability and karst fissured aquifers

Karst aquifers are characterized by dual porosity/permeability environment with a highly heterogeneous structure with higher conductivity in underground channels surrounded by lower conductivity blocks. Recharge from the surface is either diffuse or concentrated (Doerfliger & Zwahlen, 1995). Consequently, karst aquifers possass a particular hydraulic behavior generating springs with strong flood peaks of short duration followed by lower flow rate, long duration depletion curves (Tripet et al., 1995).

Consequently, the floods caused by rapid infiltration concentrated within very permeable areas are swift and violent and the filtration and auto-purification processes do not have enough time to develop as they do in the interstitial porosity aquifers (Doerfliger & Zwahlen, 1995).

There is a high range of flow velocities as determined from to dye tracer experiments in karst aquifer. Due to the hydraulic conductivity structure heterogeneity in particuler, the residence time of groundwater is not a simple function of the distance between a given point of the catchment and the spring. Variability of the transfer functions (Part II) also illustrated the important spatial heterogeneity of karst aquifers physical characteristics. Therefore, concentric protection zones used for water supplies in porous media are not appropriate to karst aquifers (Tripet et al., 1995) and an input-response or black-box model is also inappropriate to deal with this spatial heterogeneity. A single mean transfer function is not representative of an entire catchment.

Because of karst recharge and subsurface heterogeneity, parts of a catchment will be more sensitive to contaminants than others leading to variable degrees of vulnerability. Determining these degrees within one catchment is the goal of the vulnerability concept.

The vulnerability concept is therefore based on a conceptual parametric model of the karst aquifer (Part I, Section 2.2).

2.3. Overlay method : multi-attribute and index mapping

2.3.1. Overview of vulnerability mapping

Groundwater vulnerability maps are classified as interpretative groundwater protection maps (Zaporozec, 1989). As opposed to hydrogeological maps, these vulnerability maps do not show the elements of a groundwater system. They only show some specific characteristics of elements related to vulnerability in the subsurface (Vrba and Zaporozec, 1994).

Groundwater vulnerability maps are used for groundwater protection planning and decision-making.

2.3.2. Summary of overlay methods

The vulnerability assessment approach is illustrated with the four phases shown on the flow diagram in Figure 2.1.

The first phase of the assessment is to define relevant attributes corresponding to those parameters in the conceptual model that represent the hydrogeological characteristics of a given setting, in this case, karst. The second phase is to use indirect and direct methods in the field to

determine the range of attribute values and to establish representative attribute maps. In phase three, a GIS system is used to overlay and apply weighting of the attributes. The fourth phase is to validate the vulnerability maps and to translate them into groundwater protection maps.

Vulnerability maps are usually based on evaluating conditions which take into account geology, hydrology, and soil characteristics (Part 2, Figure 1).

The basic attributes that should be known to assess groundwater vulnerability of any hydrogeological aetting are subdivided in parameters according to Vrba & Zaporozec (1994) in the Table 2.1.

Table 2.1.

Attributes of groundwater intrinaic vulnerability and their parameters

Attributes / Peremeters	Primary importance			
	Racharge	Soil	Unseturated Zone	Saturated Zone
Principal	- net annual recharge - annual precipitation	- texture - structure - thickness - organic matter content - clay content - permeability	- thickness - lithology - water travel time	- lithology - thickness - efficient porosity - hydraulic conductivity - groundwater flow direction - age and residence time
Supplementary	- evapotranspiration - air temperature	- Cation exchange capacity - carbonate content	- weathering rate - permeability	- storage capacity - transmissivity

These attributes are of primary importance whereas others such as topography, underlying geological unit of aquifer, contact with surface and sea water ara ot secondary importance (Vrba and Zaporozec, 1994).

Vulnerability is assessed by overlaying the various attribute maps and using a weighting system (Part 3, Figure 2.1). such as a hierarchical system, parametric system, analog or numerical models. These above listed methods are part of the assessment:

Hierarchical systems: are established for the hydrogeological complex and to set (HCS) methods of assessing groundwater vulnerability. It is a system besed on comparing a given area to criteria representing vulnerability conditions in other areas, such as other catchments or aquifer systems. This method is used commonly to evaluate vulnerability of various hydrogeological settings at a medium to large scale, covering canton or national territories. This method results in a relatively qualitative assessment (Civita, 1990b).

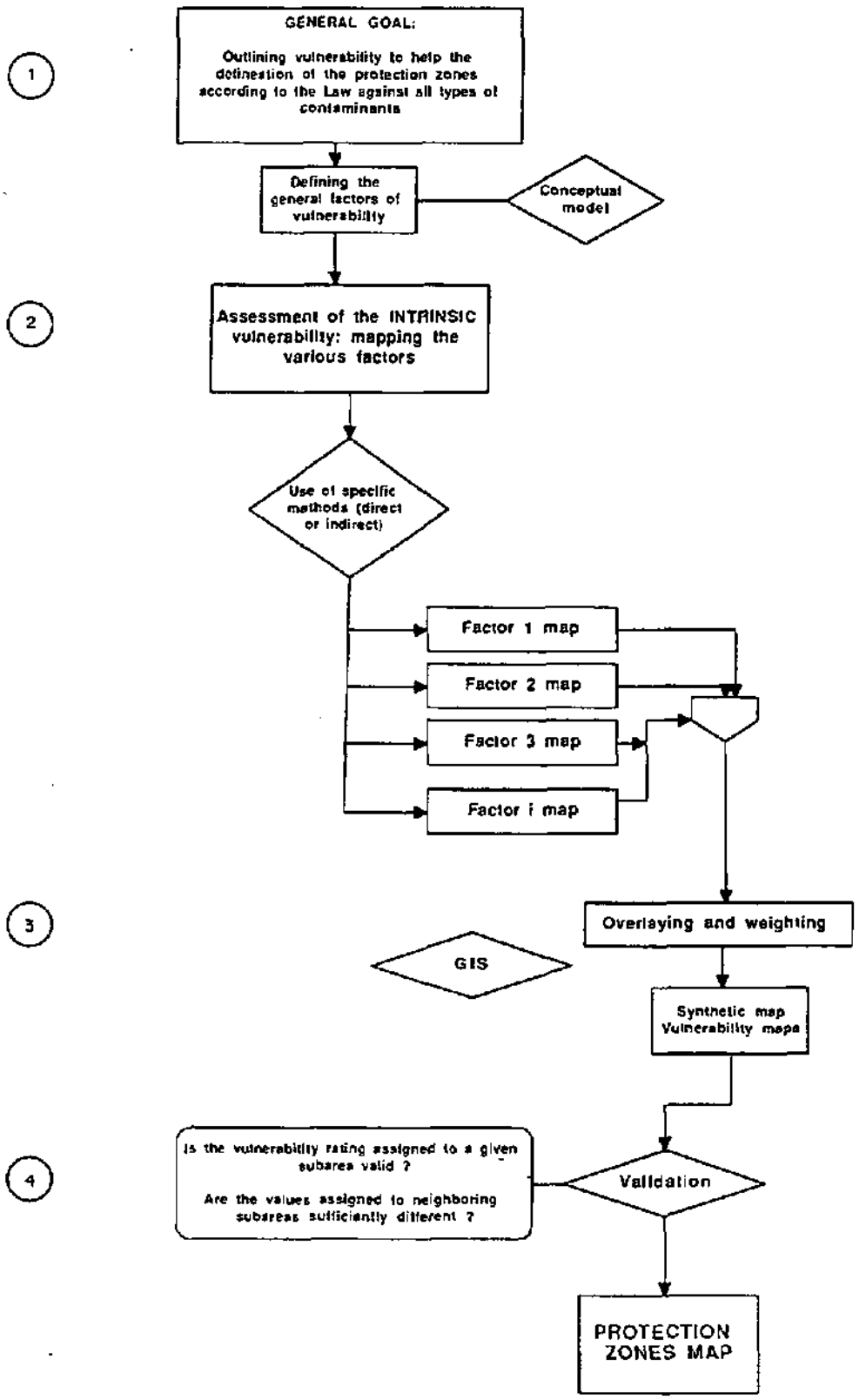

Figure 2.1. : General flow diagram describing the vulnerability assessment procedure using an overlay method

The parametric system method includes (Vrba and Zaporozec, 1994) :

- the **matrix system**: this system uses at least two categories of attributes subdivided in a certain number of parameters. The two attributes and their parameters are the two compounds Xn, Ym of a matrix NxM. N is the number of parameters of X, M the number of Y, respectively. The combination of X_n and Y_m provide a relative degree of vulnerability (from extreme to low through high and moderate, for example).
- the **rating system**: this system is derived from the 'Le Grand system' (Le Grand, 1964 and 1983). A range is attributed to any parameter judged adequate to take into account in the vulnerability assessment. The range is divided, according to the variation interval of each parameter. From any point of the assessed area, the rating points are totaled. The final score is subdivided into segments from a minimum value to a maximum one, expressing a reletive degree of vulnerability.
- the **point count system models**: these models are also called " parameter weighting and rating methods ". They differ from the rating system in that, in addition to a rating, a multiplier reflecting a relative importance weight, is assigned to each parameter. The ratings for each class or interval of given attribute are multiplied by the weight related to the attribute and then the products are added up to arrive at a final score. The higher or lower the score, the greater the vulnerability of the area is, depending of the sense of the weighting and rating systems. At the end, the final numerical score range is assigned to classes of different degrees of vulnerability (extreme, high, moderate, low, for example). One of the first point count system models called DRASTIC was developed by Aller et al., (1987) for the US Environmental Protection Agency. This acronym takes its initials from seven parameters. Each parameter is given a double rating from 1 to 10 and from 1 to 5. The first one assigns a relative weight inside the parameter set. For this purpose, the most significant parameters have weight of 5, the least significant, 1. The second assigns a value between 1 and 10 to each given interval of each parameter. The resulting index is made up of the sum of product ratings weighing the seven parameters. The higher the DRASTIC index, the greater the vulnerability. This method provides a ralative evaluation and as for other methods, the DRASTIC does not provide an absolute answer.

This point count system model was chosen for the EPIK method and is developed in Chapter 5 (Part III).

- Analog relations and numerical models: these techniques are based on complex or simple mathematics resulting in a vulnerability index. Complex model techniques can be used but have the problem of gathering all the data needed. As Le Grand (1983) stated, ".... mathematical approaches appear to be suited for advanced stages of contaminant studies and for long-term formal studies, but not for preliminary stages or places where data are scarce. "

2.4. Use of a geographical information system

Groundwater vulnerability maps are mainly a static representation of different parameters, reflecting a temporary situation (Barrocu et al., 1993). Vulnerability maps can be made by manually overlaying single information coverage (paper and transparent papers) and more recently by using a database tool: the Geographical Information system (GIS). GIS has been demonstrated as an effective method for a wide variety of mapping, planning and management needs. It is a powerful tool that integrates data and analysis of data.

Any data can be digitized and stored in the computer. Data can be put into vector format (polygons) manually, semi-automatically using a digitizing tablet, and automatically with a scanning system incorporating line-following software (Vrba and Zaporozec, 1994).

Vector format can be transformed into raster format. In raster format, a value or a code can be assigned at each pixel belonging to each polygon. The size of the pixel is defined in relation to the scale of the map and with the accuracy of the availability of data. The use of a too small pixel size can induce a false accuracy of the data whereas information can disappear if the pixel size is too large. If the adequate pixel size is too large for certain morphological features characterizing a given parameter, a second overlaid grid with smaller pixel size can be displayed for such data.

GIS allows integrating data from different sources such as remote sensing images and numerical topographical models. It easily allows vulnerability map updating and combining various weights, thereby comparing different scenarios of vulnerability maps. GIS is without doubt a useful tool to outline protection zones from vulnerability maps although it requires development time to use it.

In this thesis, IDRISI for Windows (Idrisi, 1987-1995, J.R. Eastman, Clerk University) on Personal Computer was used. This geographic information and image processing software system was developed by the Graduate School of Geography at Clark University (USA).

The selection of scale is an important point. The scale has to be 10'000 to 5'000 to use groundwater vulnerability maps as the basic information to outline protection zones in catchments of spring or wells. In Switzerland, the protection zones are presented on 1:5'000 land parcel maps.

As scale defines the accuracy of available data requirements, the minimum and maximum size of the pixels used in GIS is pertinent. A 20m to 50m pixel size seems reasonable.

2.5. The EPIK method - an overlay index multi-attribute method

The new method proposed to assess vulnerability of the springs or water catchments is a multi-attribute method called EPIK. The acronym EPIK is for the four attributes taken into consideration: **E**pikarst, **P**rotective cover, **I**nfiltration conditions and **K**arst network (Doerfliger & Zwahlen, 1995).

These attributes correspond to four specific karst system characteristics related to the parametric conceptual model (Section 2.2, Part I). With this method, the sensitivity of the underground water in karst areas can be evaluated in a comprehensive yet objective manner. Determining the various parameters of each attribute is performed with the help of several methods - direct or indirect, local or global - such as tracer tests, geophysics, geomorphologic studies, hydrograph analysis, auguring or back hoe pits, and air photo interpretation.

First, the limits of the water supply source catchment area are determined. Then, the four following steps are done: (1) epikarst mapping, (2) protective cover mapping, (3), infiltration condition mapping, (4) characterization of the karst network development and calculating an attribute which is representative of the entire catchment.

Using GIS, the weighting of the various layers can be performed easily (Chapter 4). A validation operation is undertaken to avoid errors or inappropriate vulnerability degrees. To validate the weighting system, detailed geophysics or tracer experiments for example, may be done. This is a complex process that can be based on experimental assumptions. The assumptions may be related to use of a characteristic transfer functions in different settings.

Two examples in the St-Imier (BE) test site and Maira-Bure (JU) illustrate the EPIK method with its limits, advantages and disadvantages (chapter 5).

The last operation consists of establishing a relationship between the vulnerability degree and the defined protection zones (Chapter 6).

Chapter 3

Which attributes and parameters ?

3.1. Attributes related to the karst conceptual model

According to the conceptual parameter model defined in the Part I, four attributes have been selected to assess the sensitivity to contaminants of the karst catchment. Epikarst, Protective cover, Infiltration conditions, and karst network development (EPIK). They reflect the relatively rapid transit and the possible reduction of the contaminant that occurs in the aquifer. Their definition, assessment methods and the further development required to improve evaluation or definition of each attribute are presented in this chapter.

3.2. Attribute E: Epikarst

a)definition and categories

The epikarst, also called the 'subcutaneous' zone, is a subsurface water adsorption zone which is highly fissured due to the extension and pressure release of rock at the surface. This zone is subject to extreme weathering (Dodge, 1982), has an average depth from 0.5 to 2m (Bonacci, 1987) but can extend to 10 m (Photo 3.1.). Boreholes in the epikarst in two sections at Maira (Tabular Jura) have 2m to 6m of epikarst (Veiga, 1995).

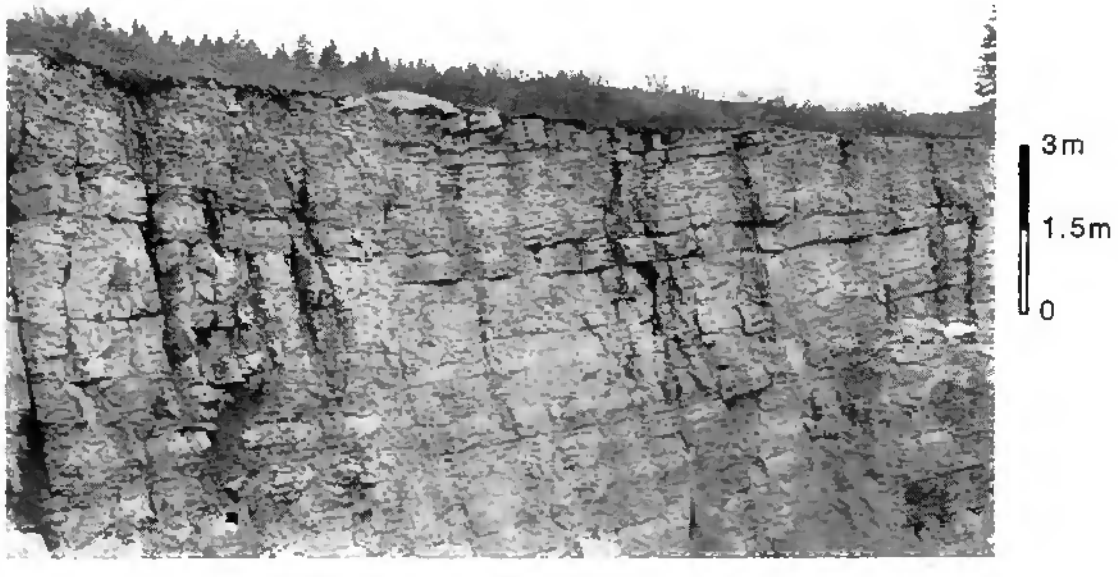

Photos 3.1 a : Les Breuleux Quarry, Portlandien limestone (Folded Jura) (Petit-Crêt, coord. 568.200 / 228.600)

Photos 3.1 b and c : Les Breuleux Quarry, Portlandien limestone (Folded Jura) (Petit-Crêt, coord. 568.200 / 228.600)

The epikarst, due to the pecularities of the hydraulic conductivity structure at the top of a karst massif is characterized by two major features: water storage and flow concentration (Klimchouk, 1995). The karst aquifer has essentially continuous layers whose initial high hydraulic conductivity decreases rapidly with depth (Drogue, 1992). Therefore, beneath the epikarst, the rock mass has lower permeability so that its infiltration is easier than its drainage. After heavy rainfalls, this zone often resembles a large reservoir where the water is temporarily stored (Williams, 1983). Mangin (1973,1975) defined it as e possible temporary perched aquifer with a base that is a leaky capillary barrier. It has slow percolation into tight fissures and rapid drainage via connected pipes according to Ford & Williams (1989). On the basis of field measurements, the epikarst recherges the less permeable fissured regions of the karst aquifer during low water periods and during minor water level rises. The epikarst only contributes directly to the underground conduit drainage system during times of high water (Smart & Friedrich, 1986).

Water flow within the epikarst has a lateral component moving through fracturas towerds vertical pipes and a vertical component with slow percolation into small fissures and rapid drainage through vertical pipes (Ford & Williams, 1989).

The epikarst exists in bare and covered karst regions but is not necessarily a continuous "layer" according to the above authors.

Does the epikarst exist in all kerst aquifers ?

Epikarst underlies unconsolidated soils. Absent this soil, epikarst morphological features are essentially "Karrenfields" (German) or "lapié" (French).

Epikarst results from major fracturing and extreme weathering. The development of an epikerst is certainly related to the presence of a soil cover which supplies needed CO_2. The importance of the soil has already been demonstrated relative to increased subsurface weathering (Aubert, 1969, Nicod, 1990).

According to Williams, (1985), epikarst mechanisms (water storage and flow concentration) are responsible for initiating closed depressions at the surface. Spatial variability of fractures and their associated hydraulic conductivity develop from tectonic and lithology influences. Weter in the epikarst drains to preferential vertical pipes connected to the karst aquifer network. Preferential weathering occurs around these vertical pipes due to the drawdown cone in the epikarst water table. As the water surface is lowered, the drawdown cone tends to distort the topographic expression and solution dolines develop (Klimchouk, 1995) (Photo 3.2, Figure 3.2 a+b).

The presence of an epikarst zone under a unconsolidated soil may be associated with uneven landscape commonly depicted by a succession of disordered bumps and hollows such as sinkhole [dolines] fields, or aligned dolines. Sinkholes, however, are not always synonymous with epikarst. Sinkholes may also result from subsidence or collapse processes unrelated to epikerst mechanisms.

To understand solution doline development, we could assume that the epikarst may be present under soil even if no typical morphological features are present (in a tabular zone for example) (Figure.3.2.a Williams, 1983). If the soil controls the infiltration rate of water recharging the epikarst, the nature and thickness of the soil should permit determining if the epikarst is present. Soil thickness is regulated by how fissured the limestone is. Thin soils have high fissuring, the karst has rapid flow and extreme weathering occurs. Thick soils heve low fissuring where the karst has low flow and moderate weathering occurs (Gaiffe & Buckert, 1990). In addition, the physical condition of the limestone banks relates to the type of soil (Gaiffe & Schmitt, 1980).

- highly fractured and crushed limestones induce black and rocky soil, (humo-calcic: thin soil, low water content).
- flag limestones favor development of brown soil.
- karrenfields are covered partially with organic detritus (litho-calcic soils).

Photo 3.2: The epikarst zone and an old vertical pipe connected to it (Quarry of Buix, coord.: 569.600 / 259.800).

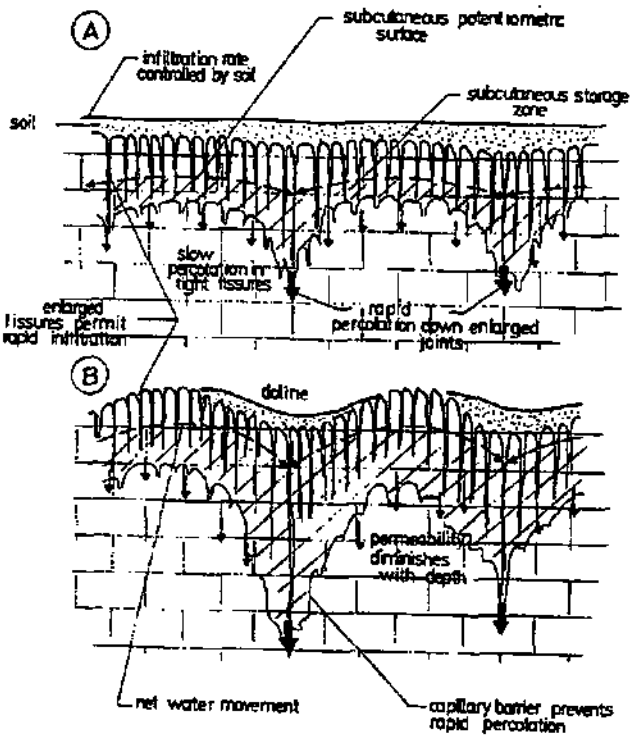

Figure 3.2.: A: Subcutaneous storage, lateral subsurface flow to zones of high permeability . B: the evolution of solution dolines (Williams, 1983).

Therefore, in covered tabular karst aquifers, the soil nature and thickness may be a clue to determine if an epikarst exists.

If, according to the above authors, the epikarst is not uniform at the top of karst aquifers, it may be difficult to categorize the epikarst zone if it is:

- well developed and connected to the karst network,
- developed but not connected to the network by a vertical pipe
- absent.

To distinguish between the first and the second parameters may require tracer tests. First, this is not an easy method to map this category and it is costly. Second, it may still be difficult to determine, even based on research, a set of typical reference transfer functions and associated parameters to uniquely characterize it.

For this reason and to address these difficulties, we subdivided the epikarst into three classes by indirectly classifying related types of geomorphologic features which are easy to map:

E_1 - Swallowholes and closed depressions where a stream disappears:
- Sinkholes or dolines (from all kinds of genesis)
- Shafts
- Karrenfields
- Cuestas
- Outcrops with high fracturing (along roads or railways/artificial outcrops in quarries)

E_2 - Intermediary zones in the alignment of dolines
- Dry valleys

E_3 - The rest of the catchment

Comments:

Dry valleys in karst are elongated valleys at the bottom of which there may be dolines, shafts and caves. In such valleys, there are no permanent watercourses and rarely intermittant rivers because the karstification process has been stronger and faster than the valley formation process (Bonacci, 1987). The dry valleys are related to a high karstification zone as the water is directly lost from the stream. According to various authors (Bonacci, 1987, Ford and Williams, 1989, Bögli, 1980) however, the dry valley is not definitely related to the epikarst.

As there is no more watercourse in a dry valley, the water flow disappears into the karst underground due to a highly karstified substructure. Does this zone uniformly match the valley form? It is rather difficult to answer this question. Consequently we assume dry valleys should be classified as E_2.

b) assessment methods:

Mapping the three classes E1 to E3 is equivalent to mapping the individual geomorphologic features of interest. In order to do this, we first used topographic maps (1:25'000, 1:10'000 or 1:5'000) to identify and outline these features. Interpretation of aerial photographs allowed us to confirm and delineate the observed objects directly on topographic maps. Observed intersections of lineaments from aerial photographs or from remote sensing analysis (Landsat photo analyzed with GIS) may correspond to highly fractured sectors. If no typical geomorphologic features are associated to these sectors, they could be mapped as E_2 rather than E_3. These methods are used to evaluate the epikarst attribute and its classes and are supplemented by field verification.

c) perspectives

Mapping the geomorphologic features associated with the epikarst is a simplification of epikarst mapping. Some parts of the watershed (parts) that do not have these particular morphological features could also be associated with epikarst. If any of these parts have a litho-calcic soil less than 10cm, they should be classified as E_2 or when in doubt as E_3.

If the RMT-R[2] geophysical method permits defining the conductive zones, it is necessary to associate this information with specific soil investigations to identify if the epikarst is present when its typical morphological features are absent (Veiga, 1995). These detailed surveys including geophysics and soil profiles cannot be performed over large areas or the whole catchment for practical reasons (time, cost).

Another geophysical method such as the radar[3] should be tested at different test sites in further work to determine the image of the thickness of the soil and of the extent of fissure development in the first 5m of the top limestone layer.

Geophysical methods are focused methods that could be used to confirm or discount the presence of an epikarst.

---

[2] *RMT-R geophysical method: a radiomagnetotelluric method to determine the apparent resistivity using very low frequency (12 to 240 Hz). The electrical field Ex and the magnetic field Hy are measured using a set of two electrodes and an antenna to receive an emitted frequency. The measured apparent resistivity corresponds to the mean resistivity of a sector of the terrain whose thickness depends of the used frequency (F) [P(m) = 503 (pa/F)$^{-1/2}$] and of the true resistivity of the terrain. The phase, a measure of the difference between the electricel and magnetic compounds of the signal gives information about the anisotropy of the environment. If the value is equal to 45 degrees, there is no anisotropy; if the value is lower than 45 degrees, a conductive layer is at the surface of a double layer model and if the value is higher than 45 degrees, a resistant layer is at the surface (Turberg, 1993).*

[3] *Georadar: the radar signal of 80 to 1000 Mhz penetrates into the ground and is reflected. It permits, using the same principle as the seismic method, obtaining a reflection image of the subsoil and ground (Huggenberger P., 1992).*

3.3. Attribute P: Protective cover

a)definition and classes

For this attribute, we include both the soil and other geological overburden such as quaternary deposits (glacial till, silt, loess, rocks debris,....), and other non-karst layers, for example, clay and sandstone.

The upper unconsolideted overburden of the equifer is commonly regarded as one of the most important attributes when assessing groundwater vulnerability. The soil and other geological layers have attenuation capacity (Zaporozec, 1985) due to specific parameters such as texture/structure, thickness, content of organic matter and clay minerals, degree of water saturation and hydraulic conductivity. These soil parameters are related to physical, chemical and biological properties that allow attenuation (natural protective filter, reterdation, degradation of contaminants).

The content of the organic matter and clay minerals of a soil is regrouped under the parameter Cation exchange capacity (CEC). This capacity is important for ion contaminants, especially heavy metals. CEC reflects the soils ability to be retard contaminant migration to the water table (Sueis et al., 1990). The CEC value is characteristic of the amount of clays, silts and organic matter in a soil. The organic matter is important in contaminant retardation.

The hydraulic conductivity of a soil is also an important parameter. It changes with the degree of water saturation of a soil. It correlated to the ability of the soil to be penetrated by water and/or a contaminent under a hydraulic gradient.

Intuitively, the thickness of a soil is an important property when assessing groundwater vulnerability. The thinner the soil, the greater the vulnerability.

Soils are classified according to pedologic standards (AFES/INRA; 1992). More than thirty different types of soil have been differentiated. In temperate climates, for simplicity, we consider 9 major soil types that occur in the karst aquifers of the Jura, Prealps and Alps.

These soils range from high stone content to high clay/silts to organic matter. They are the following:

PEYROSOL: mineral soil with stone (soil particles larger than 2mm in diameter or longest dimension: Xp horizon[4]) layers (stone content greater than 40 percent of the total), or with small stones layers (stone content less than 40 percent: Xc horizon).

LITHOSOL: litho-calcic soil with humus on the karrenfields (A or O, S < 10cm, R).

RENDISOL and RENDOSOL: calcic and carbonate soils, without S horizon (mineral horizon = rock weathering horizon) or other layers under the A horizon (organo-mineral horizon) [evt. O, A, then C or M or R].

CALCOSOL: calcareous brown soil (A horizon above Asca transition, Sca compact, silt-clay, homogeneous, brown or light brown, no stones, C).

[4] *Brief review of the terminology of soil horizons (AFES,INRA, 1992):*

Holorganic horizons: *H peat / O surface organic horizon other than peat.*

Orgeno-mineral horizons: *A organo-mineral topsoil: Aca A calcareous, Aci A non calcareous, Ado A dolomitic, Ah A rich in organic matter (>8 percent C organic), An Anmoor (hydromorph conditions).*

Mineral horizons: *S: rock weathering horizon, on the bottom of the horizon A, but with a different structure. E: Eluvial horizon (material removed), hell,poor in clay content and/or in organic matter and/or in metal oxides. B:illuvial horizon or weathered subsoil (material washed in). G:gley horizon with hydromorphic traces. X: horizon with a content of soil particles higher than 2cm, higher than 60 percent of the total.*

Substratum: *C: deep mineral horizon, with important fragmentation or geochemical alteration. M: soft geological material. R: hard geological material.*

CALCISOL: calcic (non calcareous) brown soil (A horizon with o.m., aggregates structure, dark brown, silt, no stones, S polyhedral structure, light brown to ocher, C or M or R).

BRUNISOL: brown soil (A horizon, dark brown, aggregate structure, roots zone, S horizon: light brown, polyhedral structure, silty).

NEOLUVISOL: brown washed out soil (A dark brown, aggregate structure, roots, E light color, poor in o.m. or clay, light ochre, B rich in clays , darker ochre, C altered limastone ancompassed in some clay).

REDUCTISOL: organic soil with gley with silt and clays and Fe-reduction. Hydromorphy (A brown, aggregate structure with spots of Fe-reduction, temporary hydromorph zone, roots; Go oxidized horizon with rust spots, silt-clay; Gr grey-green clay horizon, permanent water level).

HISTOSOL: (undrained organic matter that has remained wet within at least 20 cm of the surfaca) - organic hydromorph soil such as peat (soil that overlays not diractly the limastone).

This classification is not related to organic matter content, taxture or hydraulic conductivity. Consequently, two "Brunisols", for example, do not necessarily have the same hydraulic conductivity or the same CEC value.

First, the parameters such as CEC and hydraulic conductivity are often related to each other. If a soil is rich in clay content, its CEC is high end its hydraulic conductivity is low. In addition, this kind of soil is commonly deposited in areas with great thickness.

Second, if the soil usually forms a continuous layer, its parameters such as thickness, CEC, and hydraulic conductivity vary spatially. Determining the CEC value even experimentally and the value of hydraulic conductivity require identity of the soil categories. If no data are available on the catchment being studied, this necessitates considerable work with three parameter values needing to be estimated (CEC, Hydraulic conductivity and thickness). These represent three potential sources of error.

Third, it has to be understood that a complete pedological study with soils and related parameters maps is not common in Switzerland. In order to get such CEC or hydraulic conductivity maps based on even an extrapolation of experimental values for reference soils, it is necessary to map the various soil categories. This requires considerable time and a cost investmant that is commonly not possible as part of the typical scope of outlining groundwater protection zones.

For these reasons, we consider only the thickness of the soil as the basic parameter available at a reasonable cost to assess the intrinsic vulnerability of a karst catchment.

We differentiate two cases, both according to the presence of geological layers overlying the limestone and their hydraulic conductivity. To be conservative, we consider three classes with the boundary range of 20cm, 100cm and higher, instead of tha 10cm and 50cm and higher values described previously (Tâche et al., 1996).

A. Soil lying directly on limestone or on large detritus layers that have a high hydraulic conductivity. (e.g. rocks debris, lateral gleciel till)

P_1 - 0 - 20 cm of soil
P_2 - 20 - 100 cm of soil
P_3 - > 100 cm of soil

B. Low permeability geologic overlying layers with or without soil (E.g. lake silts, clays)

P_3 - > 100 cm of soil and/or overlying geological layers with low permeability.
P_4 - > 100 cm of soil with a thick ovarlying geologic layer of low permeability (necessary to check, with for example boreholes, holes with hand or motor auger)

b) sssessment methods:

From published materials (geological maps, geological and regional studies), we can outline the sactor with and without soil, and the sectors with or without overlying geological layers. Aerial photographs and satellite imagery are helpful to evaluate soil presence, and probably the thickness (scele of sizes) if supplemented with field verification.

With a hand auger, the thickness is measured directly in the field. If the catchment is not large, it may be possible to perform auger holes on a regular grid. If the catchment is large, the mesh size has to be bigger and it may be necessary to assume similar attributes for similar morphology. This would mean that for a measured thicknass at one point, the same thickness is given inside a square of 100m if the point is surrounded by the same morphology.

c) perspectives:

For further method development, it would be useful to perform geostatistical methods such as kriging on the attribute P data.

3.4. Attribute I: Infiltration conditions

a)definition and classes

Infiltration conditions concern the type of recharge to the karst aquifer. They do not include the recharge in term of quantity (annual mean recharge, efficient precipitation) or in terms of spatial variability. As described in Part I, diffuse and concentrated recharge have specific consequences in term of groundwater vulnerability. Thus we differentiate classes from diffuse to concentrated infiltration conditions, and an intermediate case where runoff may be imporiant.

The runoff coefficient depends on the slope and its vegetation. According to various runoff coefficient values from Sautier (1984)(Table 3.2.), we consider intuitive theoretical runoff coefficient boundary limits of 0.22 end 0.34 for meadows and pastures, and cultivated fields, respectively. This limit corresponds to a boundary slope of 25 and 10 percant for the meadows and pastures, and cultivated fields, respectively (with cultivation in the slope direction). We have no scientific argument for this limit.

Table 3.2.
Runoff coefficient values for representative Swiaa caaes. Runoff coefficient is a function of slope and vegetativa cover (Sautier, 1984).

Slope %	Forest	Meadows -Pastures	Cultivated fields in the slope direction.
0.5	0.01	0.005	0.12
1	0.01	0.020	0.13
2	0.02	0.040	0.14
4	0.04	0.070	0.23
6	0.05	0.090	0.27
8	0.06	0.110	0.31
10	0.07	0.130	0.34
15	0.08	0.170	0.40
20	0.10	0.190	0.45
25	0.12	0.220	0.50
30	0.13	0.250	0.55
35	0.14	0.270	0.59
40	0.15	0.290	0.62
45	0.16	0.310	0.65
50	0.17	0.330	0.69

We differentiata four classes from I_1 to I_4, from higher to lower vulnerability, and two cases A and B, representing the location of the swallowhole in a stream being either inside (A) or outside (B) the water catchment area.

A. Inside the catchment of a stream that has a swallowhole (Figure 3.3.)

I_1 - Perennial or temporary loss streams
- Bed and banks of stream
- Perennial and temporary stream feeding a swallowhole or a sinkhole (doline)
- Infiltrating stream
- Artificially drained sectors of the water catchment area.

I_2 - Naturally drained sectors of the catchment whose slope is higher than 10 percent for cultivated areas, 25 percent for meadows and pastures.

I_3 - Undrained sectors of the catchment whose slope is lower than 10 percent for cultivated zones, 25 percent for meadows and pastures.

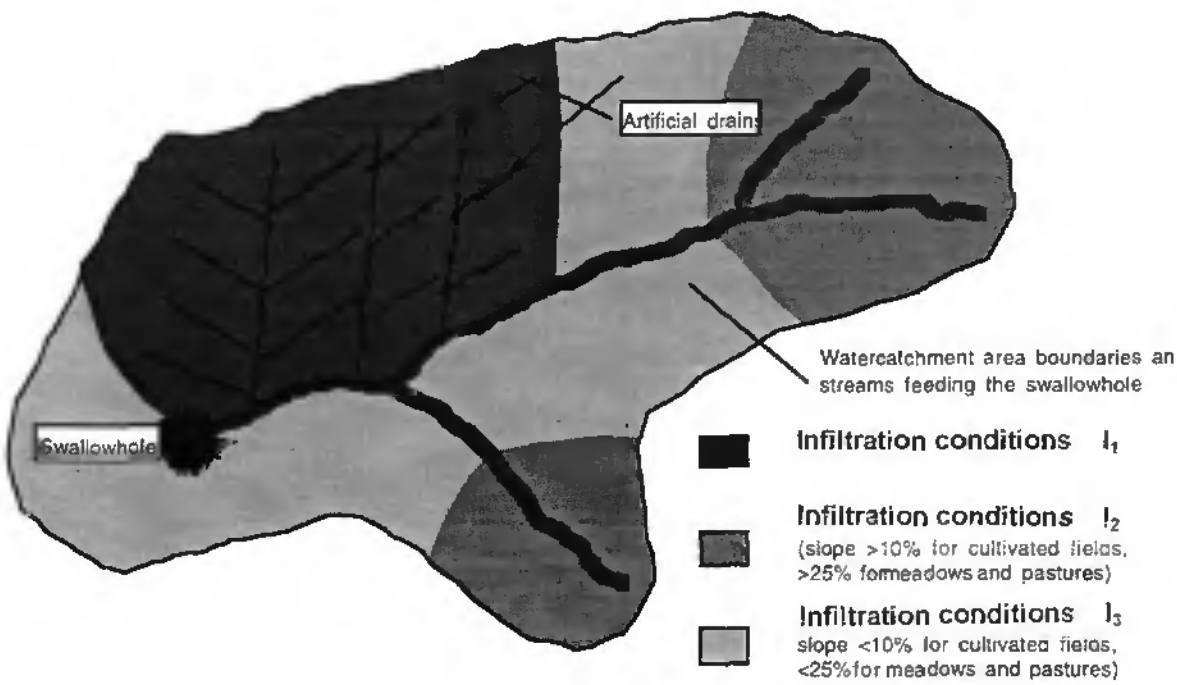

Figure 3.3: Infiltration conditions in a water catchment area of a losing stream (Tâche et al., 1996).

B. Outside the catchment of losing streams - in the rest of the catchment (Figure 3.4).

I_3- Low lying areas[5] which collect runoff and the slopes which generate this runoff (slopes greater than 10 percent for cultivated zones and 25 percent for meadows and pastures).

I_4- The rest of the catchment.

[5] *Area of I_3: 50m to 100m to either side from the area where the slope changes abruptly.*

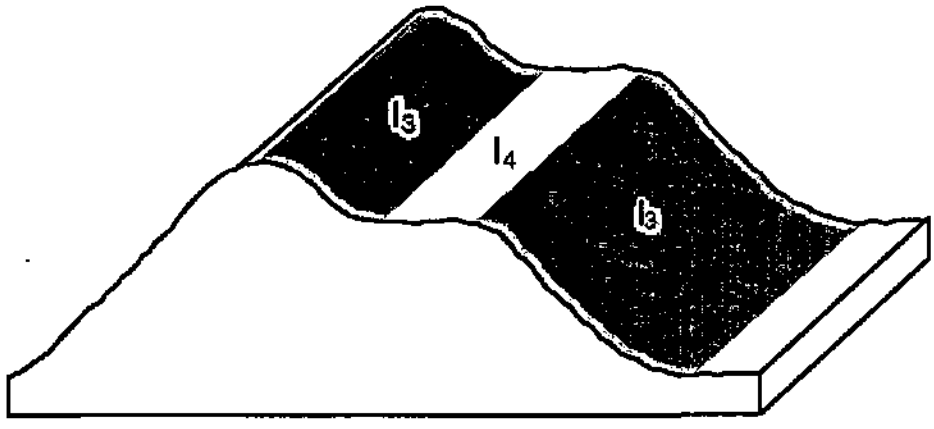

Figure 3.4 :Infiltration conditions for terrain with high runoff from the slopes into low lying area. (Tâche et al., 1996).

b) assessment methods

Obtaining the data to classify each sector of the catchment requires studying topographic maps and is technically demanding in comparison to date for classifying the epikarst or soil thickness. The use of a geographic information system (GIS) is necessary to determine the critical slope and low topography zones.

c) perspectives

To assess groundwater vulnerability of karst resources, it may be important to consider the recharge, particularly if vulnerability to drought in addition to contaminants is to be evaluated. Therefore, recharge may be judged on the basis of field measurements derived from the water balence equation.

Spatial variability of precipitation could be considered, affecting an additional coefficient in the weighting system, according to maximum and minimum precipitation intensities and corresponding infiltration points (diffuse, intermediate or concentrated). To determine statistical values, contour maps of long term precipitation data would be useful.

3.5. Attribute K: Karst network development

a)definition and classes

A karst network or cave system is a network of solution openings greater than 5mm to 15mm in diameter or width. This size is the effective minimum aperture for turbulent flow although that will not necessarily occur as soon as the minimum value is attained. A cave, according to the International Speleological Union is a natural underground opening in rock that is large enough for human entry. Solution cave systems are complex landforms. They occur in a great variety of three-dimensional patterns in rock blocks. They are affected by hydrochemical factors dependent upon lithologic, tectonic, climatic, biologic end pedologic conditions and by external water base level controls (Ford & Williams, 1989). They are more or less developed and connected.

In order to appreciate the contrast between the cave system and the surrounded less permeable blocks, we consider the karst network development or nature and extent of connectivity of karst aquifers. There is a relation between the degree of the karst network development and the number of outlets of the studied karst system. A system with a well developed karst network may possess one and only one spring, whereas a system with a poorly developed network may often heve several outlets. This is not e general law and is based on the assumption of the hierarchy of the karst network (Mangin, 1975).

We differentiate three classes:

K_1 - Presence of a well developed karst network (network with decimeter to meter size channels that are rarely filled but well connected).

K_2 - Presence of a poorly developed karst network (drain network, or poorly connected or filled network, or network with decimeter or smaller sized openings).

K_3 - Presence of a joint karst spring (outlet of a karst aquifer in porous terrain with a possible filter effect). Non karst fissured aquifer.

b) ssessment methods:

Features such as vertical shafts or open cavities leading to a speleological maze are not always found at the surface in all karst catchments. In this case, indirect methods related to analysis of hydrograph data could be used to assess network connectivity.

We can determine the reaction time of the aquifer based on the total flood hydrograph when a minimum of two floods events have been recorded continuously and the precipitation and the spatial variability of the catchment are known. If we observe a rapid response - rising limb of high intensity (at least twice the base discharge), we may suppose that there is a karst network. As rapid response, we understand, for example, a response in a time interval of from 6 to 12 hours (according the size of the catchment), after a high precipitation intensity (> 15mm). For season, climate and elevation reasons, this intensity can not be take into consideration for the precipitation occurring in July, August and September for the sites located between 300 and 1700m (a.s.l) and in December till March for the sites located between 1700 and 3000m. (a.s.l.).

Bakalowicz & Mangin (1980) point out that karst aquifers appear heterogeneous, but the heterogeneity is not the result of a random juxtaposition of different types of voids. It stems from the distribution of voids around a drainage axis, according to a certain hierarchy. Considering the karst drainage system as characterized by an impulse function that transforms the input - precipitation - to hydrograph responses at springs, they claim that by analysis of this function we can identify the connectivity of the network: analysis of flood and base flow recession. Mangin (1982b) defined different types of karst systems using spectral and correlation analysis (Figure 3.5).

KARSTIC SYSTEM TYPES	MEMORY EFFECT ($r = 0.1$-0.2)	SPECTRAL RANGE (truncation frequency)	REGULATION TIME	UNIT HYDROGRAPH
ALIOU (Well Drained)	POOR (5 d)	VERY WIDE (0.30)	10-15 d	
BAGET	SMALL (10-15 d)	WIDE (0.20)	20-30 d	
FONTESTORBES	LARGE (50-60 d)	NARROW (0.10)	50 d	
TORCAL (Poorly Drained)	EXTENSIVE (70 d)	VERY NARROW (0.05)	70 d	

Figura 3.5 : Classification of karst systems from the results of correlation and spectral analysis of four karst systems, studied in detail and used as references (Mangin, 1982b).

Well drained aquifers react rapidly and their response to an infiltration event dissipates quickly leaving little inertial capacity internally. Because the response reactions are complete in relatively short periods of time, there is virtually no lasting 'memory effect'. The shape of the impulse response is very sharp and not spread out. By contrast, poorly drained systems retain inertia and can have memory effects from previous event. In this case; the shape of the impulse response is rounded and spread out (Mangin, 1994).

A classification of karst systems from the results of recession curves analysis was built by Mangin (1975) using two variables k and I, with k the ratio between the maximum dynamic volume obtained during the longest event period and the annual average volume releted to the event duration.

$$K = \frac{V_d}{V_t}$$

where Vd = dynamic volume (event volume), Vt= annual flow volume normalized to the event duration.

I corresponds to the value of the following function:

$$y = \frac{1-\eta t}{1+\varepsilon t}, \; for \; t = 2day$$ after the maximum of the rising limb.

Based on the study of 60 different systems, five principal karst systems were differentiated (Figure 3.6):

I : k < 0.1, i < 0.25, well karstified downstream system, well developed speleological network

II : 0.1 < k <0.5, i < 0.25, well karstified upstream system laading downstream to a large flooded karst (case of systems which have evolved).

III: k <0.5, 0.25 < i < 0.5, system more karstified upstream than downstream with a delay in its input

IV: k < 0.5, i > 0.5, zone of complex systems (composites)

V: k > 0.5, non-karst systems.

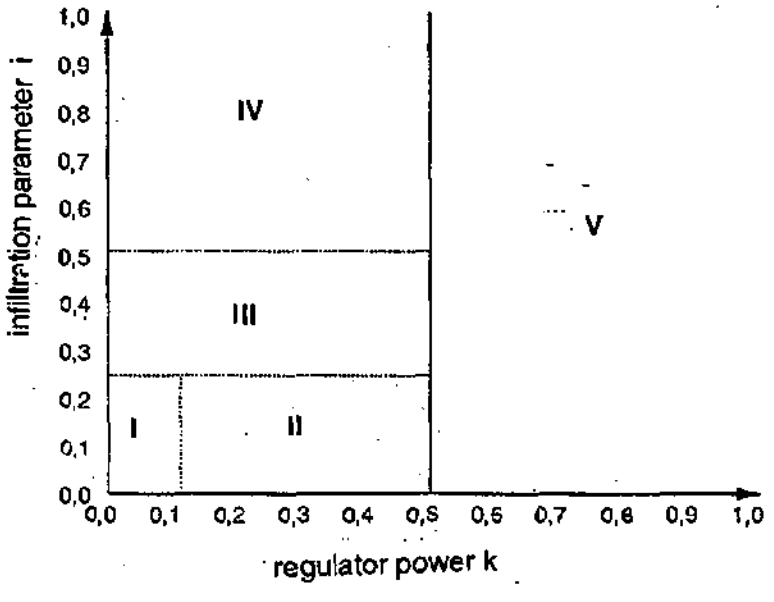

Figure 3.6 : Classification of karst systems basad on the results of recession curves analysis (Mangin, 1975).

Class K_1 may be related to cases I, II and III, class K_2 to case IV and class K_3 to case V.

Comments: this method requires a long duration hydrograph of at least one entire cycle. The classification of karst systems based on the results of recession curves analysis may vary for the same aquifer, as for various recession curves, according to Grasso & Jeannin (1994), the parameter i may vary considerably. The decreasing limb is influenced by variation in precipitation, degree of aquifer saturation before the rising limb and catchment size.

Artificial tracer tests may provide useful information about the existence of a karst network. The transit velocity is calculated from the first arrival or modal times, according to the hydrodynamic conditions. From a swallowhole connected to the karst network, the mean transit velocity is in the range of 15m/h and greater for low water and 75 to 100m/h and greater for high water. These velocities imply the existence of a karst network. Consequently, with tracer test techniques, it is possible to ditterentiate between K_1, K_2 and K_3.

The weter quality variation after heavy rains (after snow melt or heavy storms in summer) may also give information identifying the presence of e karst network. If the water quality or chemical content varies rapidly after precipitation, it may imply a cavity system (K_1 or K_2). But, in contrast, if the water quality is stable, we cannot conclude that there is no karst network.

Speleological data may also be localized within e catchment. Therefore, it is necessary to differentiate between the active and inactive cave system parts on cave system map.

However, it is not as easy to differentiate class K1 from class K2 using the same assessment method.

Remarks

The role of the four attributes is clear. However, how to assign the attributes to the given indices it less clear perticularly for the epikarst.

The epikarst is a signiticant attribute in term of vulnerability assessment in a karst environment. It may temporarily collect contaminants and release them either directly in e vertical pipe connected to the karst network or slowly through cracks of the low permeability blocks. Unfortunately, at this time, it is not possible with the existing technology in epikarst or geophysics to differentiete the presence or absence of an epikarst in a tabular zone. To simplify characterizing the epikarst using geomorphologic features, it is easy and feasible to carry out epikarst mapping in a karst catchment. In addition, zones without the distinctively characteristic morphology should be examined on the basis of aerial or Landsat photographs analysis. The zone where lineaments intersect should probably be mapped in E2. Further developments on epikarst investigation methods should be carried out.

The protective cover is an important attribute characterized only by its thickness. Mapping the CEC and hydraulic conductivity parameters even if it requires more time, commonly results in a more pertinent protection factor in a part with the same cover thickness. Further scientific research should be conducted, independent of economic reasons, to determine the importance of these parameters to vulnerability assessment and to guarantee better groundwater protection. To date, mapping the thickness of the protective cover is feasible and without major problems.

For infiltration conditions, they are determined relatively easily from topographical maps and numerical elevation models using a GIS. The present weekness of this attribute could be the arbitrary slope percent differentiating I_3 from I_4. If available precipitation data allows e large spetiel variability in the concerned catchment to be determined, it may be possible to use this parameter attributing less weight in I_1 end I_2 sectors as opposed to the I_4 sector.

The karst network development reflects the general sensitivity of the karst catchment. The classification of a karst aquifer from its hydrograph appears critical. It is rather difficult to differentiate K_1 from K_2 and may not be achievable .

The four attributes do not specifically take into account the depth of the water table. However, the depth does not seem relevant to karst aquifers because fast and direct recharge from runoff may be highly localized through sinkholes or swallowholes which have no effective filtration capacity (Ray et al., 1993).

Summary of the EPIK approach attributes (Figure 3.7 and Table 3.3)

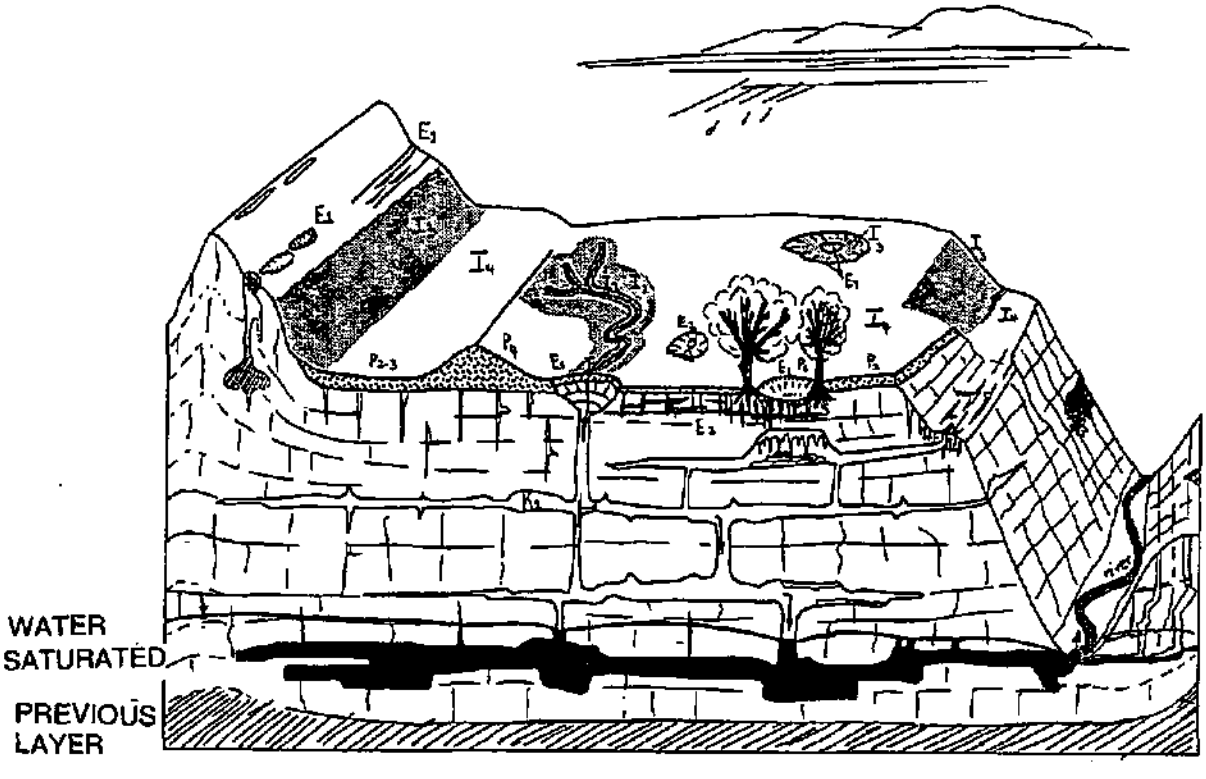

Figure 3.7 :The karst aquifer model with its various attributes.

Table 3.3.

Attribute characteristics summary.

Karst morphology related to epikarst.	E_1	Swallowholes - sinkholes or dolines - Karrenfields - cuestas -	
	E_2	Intermediate zones between the aligned dolines - dry valleys.	
Absence of a karst morphology.	E_3	The rest of the catchment.	
		A. Soil lying directly on the aquifer limestone layers or on some high permeability grob detritus layers *	B. Soil lying on low permeability geological layers **
Absence of protective cover	P_1	0 - 20 cm of soil	0 - 20 cm of soil on layers that have a thickness smaller than 1m.
	P_2	20 - 100 cm of soil	20 - 100 cm of soil on layers that have a thickness smaller than 1m.
	P_3	> 100 cm of soil	> 100 cm of soil or presence of low permeability overlying geological layers.
Major protective cover	P_4	–	> 100 cm of soil and thick detritus layers of very low hydraulic conductivity (point-information needs to be checked).
Concentrated infiltration	I_1	Perennial or temporary loss streams - Perennial or temporary stream feeding a swallowhole or a sinkhole (doline) - infiltrating surface stream - water catchment areas of the above mentioned streams (including the artificial drainage system).	
	I_2	Water catchment areas of the stream, mentioned under I_1 (without artificial drainage system) whose slope is higher than 10 percent for cultivated areas and 25 percent for meadows and pastures.	
	I_3	Water catchment areas of the stream, mentioned under I_1 (without artificial drainage system) whose slope is lower than 10 percent for cultivated areas and 25 percent for meadows and pastures -low topographic zones collecting the runoff water and slopes feeding those low areas (slope higher than 10 percent for cultivated sectors and than 25 percent for meadows and pastures).	
Diffuse infiltration	I_4	The rest of the catchment.	

High developed karst network	K_1	Karst network with meter to decimeter sized conduits that are weakly plugged and well connected.
Low developed karst network	K_2	Karst network with drains or conduits that are badly connected or even partially plugged up, or also with a size in the decimeter range or even less.
Joint karst network	K_3	Outlet in porous media with a possible filter effect - non karst but fissured aquifer.

* *Examples :rock debris, lateral glacial tills.* ** *Examples : lake silt , clays.*

Chapter 4

Evaluation of the protection factor

In order to quantitatively evaluate the vulnerability degree or the protection factor of each cell or pixel at a site, a numerical rating based on points has been set up using the EPIK attributes. The system contains two major parts: weighting and rating.

The protection factor is calculated with the following basic formula and the values are added:

$$F_p = (\alpha \cdot E_i) + (\beta \cdot P_j) + (\gamma \cdot I_k) + (\delta \cdot K_l)$$

To assign a weighting value to α, β, γ, δ and to rate i-j-k-l, we carried out several tests despite the inherent difficulties of precisely validating the assigned weighting.

What is an adequate value for each given attribute?

Intuitively, according the definition of the attributes, a swallowhole, uncovered karst and concentrated infiltration are the worst vulnerability cases.

We also took into consideration the following:

- A sinkhole covered with thick soil (E_1-P_3) is more vulnerable than flag limestone with a thin overlying soil cover (E_3-P_1)
- A stream sinking into a swallowhole (I_1) has a high degree of vulnerability, independent of the protective cover.
- A dry valley (E_2) is as vulnerable as a low topographical point where runoff collects.

The goal of testing different weighting and rating approaches was to find a convenient system. Preference was given to establishing a linear weighting which would more clearly identify each attributes contribution to the resulting protection factor.

First, we considered a simple additive model with all attributes assigned the same weight. In this case, the index value of each attribute corresponds to the assigned weight. The lower the value of the index, the higher the contaminent potential (Table 4.1). In this first test, we do not take into consideration the influence of the K attribute.

Table 4.1.
Results of adding linear weights using $F_p = E_i + P_j + I_k + K_l$

	I_1=1			I_2=2			I_3=3			I_4=4		
	E_1=1	E_2=2	E_3=3	E_1=1	E_2=2	E_3=3	E_1=1	E_2=2	E_3=3	E_1=1	E_2=2	E_3=3
P_1=1	3	4	5	4	5	6	5	6	7	6	7	8
P_2=2	4	5	6	5	6	7	6	7	8	7	8	9
P_3=3	5	6	7	6	7	8	7	8	9	8	9	10
P_4=4	6	7	8	7	8	9	8	9	10	9	10	11

The lower the protection factor (F_p), the lower the groundwater protection. The groundwater vulnerability maps prepared for part of St-Imier and for the entire Bure site using this approach, we note the following:

- The stream banks that feed the two swallowholes at St-Imier (Figure 4.1) have a protection factor of 7 (values ranging from 1 to 10), but these zones are particularly vulnerable.
- At St-Imier, the slopes higher than 10 or 25 percent, according their vegetation cover, that develop runoff into streams, have a value of 8.
- At Bure, the major dolines have the same protection factor as dry valleys (Figure 4.2.)

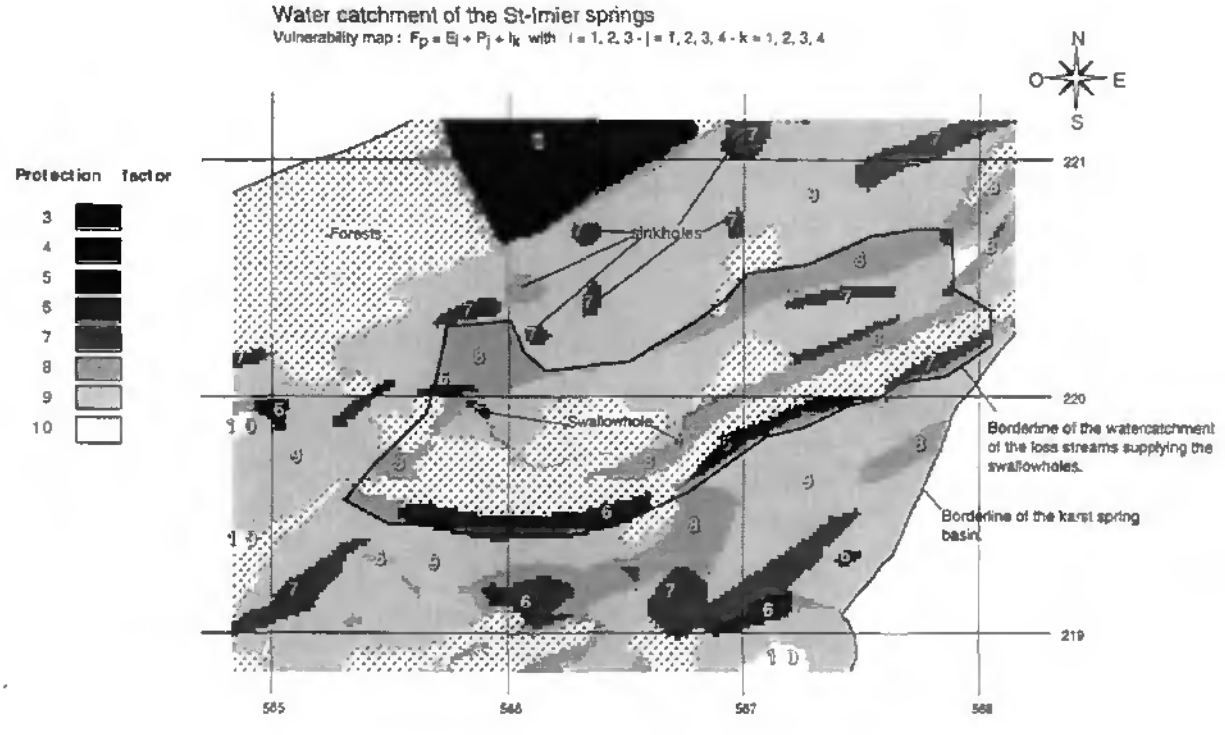

Figure 4.1.: Extract of the St-Imier vulnerability map with a simple linear weighting system : Fp= Ei + Pj + Ik, where i= 1, 2, 3, j= 1, 2, 3,4 and k=1, 2,3,4. (modified after Tâche et al., 1996).

This first test shows that it is more realistic to assign a relative weight to the attribute with respect to their significance to the vulnerability. When comparing E, P and I, the relative weight of the attribute has to be higher if the attribute contributes more significantly to vulnerability. By assigning lower relative values to more significance (E=1,I=1 and P=3, for example), we obtained a vulnerability map with a result that was not logical: dry valleys and some areas without karst features (E_3) were more vulnerable than dolines (Figure 4.3.).

Each attribute was assigned a relative weight (α, β, γ and δ) ranging from 1 (most significance) to 3 (least significance). The epikarst (E) and infiltration conditions (I) were considered to have the same relative significance to the resulting vulnerability. Therefore, they were assigned the same relative weight, 3. We believe that the protective cover (P) makes a greater contribution to groundwater protection in karst environments than E or I. The attribute K plays an intermediate role and got for this reason the relative weight of 2. By being more significant, P was assigned a value of 1. In addition, we modified the E attribute values as follows: E_1=1, E_2=3 instead of 2, and E_3=4 instead of 3. This was done to emphasize the sensitivity of the sinkholes and to moderate the vulnerability of the attributes E_2 and E_3 in comparison to I_2.

At the present stage of development of the EPIK approach, the following values of relative weight and ratings have been used as follow to produce the vulnerability map of the two sites in the Jura (Chapter 5).

Table 4.2.
Ratings for attributes E, P, I and K.

E_1	E_2	E_3	P_1	P_2	P_3	P_4	I_1	I_2	I_3	I_4	K_1	K_2	K_3
1	3	4	1	2	3	4	1	2	3	4	1	2	3

Note: The lower the weighting value, the higher the vulnerability.

The relative weight ranges from 1 to 3 (Table 4.3.).

Table 4.3.
Assigned relative weights for EPIK attributes

α	β	γ	δ
3	1	3	2

The results of calculating Fp for the various possible combinations are in Table 4.4.

Table 4.4
Calculation of Fp where Fp = (Ej · 3) + (Pj · 1) + (Ik · 3) + (K_l · 2)

K_1=1	I_1=1			I_2=2			I_3=3			I_4=4		
	E_1=1	E_2=3	E_3=4	E_1=1	E_2=3	E_3=4	E_1=1	E_2=3	E_3=4	E_1=1	E_2=3	E_3=4
P_1=1	9	15	18	12	18	21	15	21	24	18	24	27
P_2=2	10	16	19	13	19	22	16	22	25	19	25	28
P_3=3		17	20	14	20	23	17	23	26	20	26	29
P_4=4		18	21	15	21	24	18	24	27	21	27	30

K_1=2	I_1=1			I_2=2			I_3=3			I_4=4		
	E_1=1	E_2=3	E_3=4	E_1=1	E_2=3	E_3=4	E_1=1	E_2=3	E_3=4	E_1=1	E_2=3	E_3=4
P_1=1	11	17	20	14	20	23	17	23	26	20	26	29
P_2=2	12	18	21	15	21	24	18	24	27	21	27	30
P_3=3		19	22	16	22	25	19	25	28	22	28	31
P_4=4		20	23	17	23	26	20	26	29	23	29	32

K_1=3	I_1=1			I_2=2			I_3=3			I_4=4		
	E_1=1	E_2=3	E_3=4	E_1=1	E_2=3	E_3=4	E_1=1	E_2=3	E_3=4	E_1=1	E_2=3	E_3=4
P_1=1			22		22	25		25	28	22	28	31
P_2=2		20	23		23	26	20	26	29	23	29	32
P_3=3		21	24		24	27	21	27	30	24	30	33
P_4=4		22	25		25	28	22	28	31	25	31	34

incompatibilities

Remarks:

- specific conditions regarding the groundwater protection zones: the sectors mapped I_1 have to be designated S_1, the sectors mapped E1 have to be designated as S_1 or S_2.

- Incompatibilities: E_1 and I_1 conditions cannot exist with P3 or P4.

The attribute K can be considered as a global attribute, but according to the geological and hydrogeological setting of a watercatchment may be differentiated and regionalized.

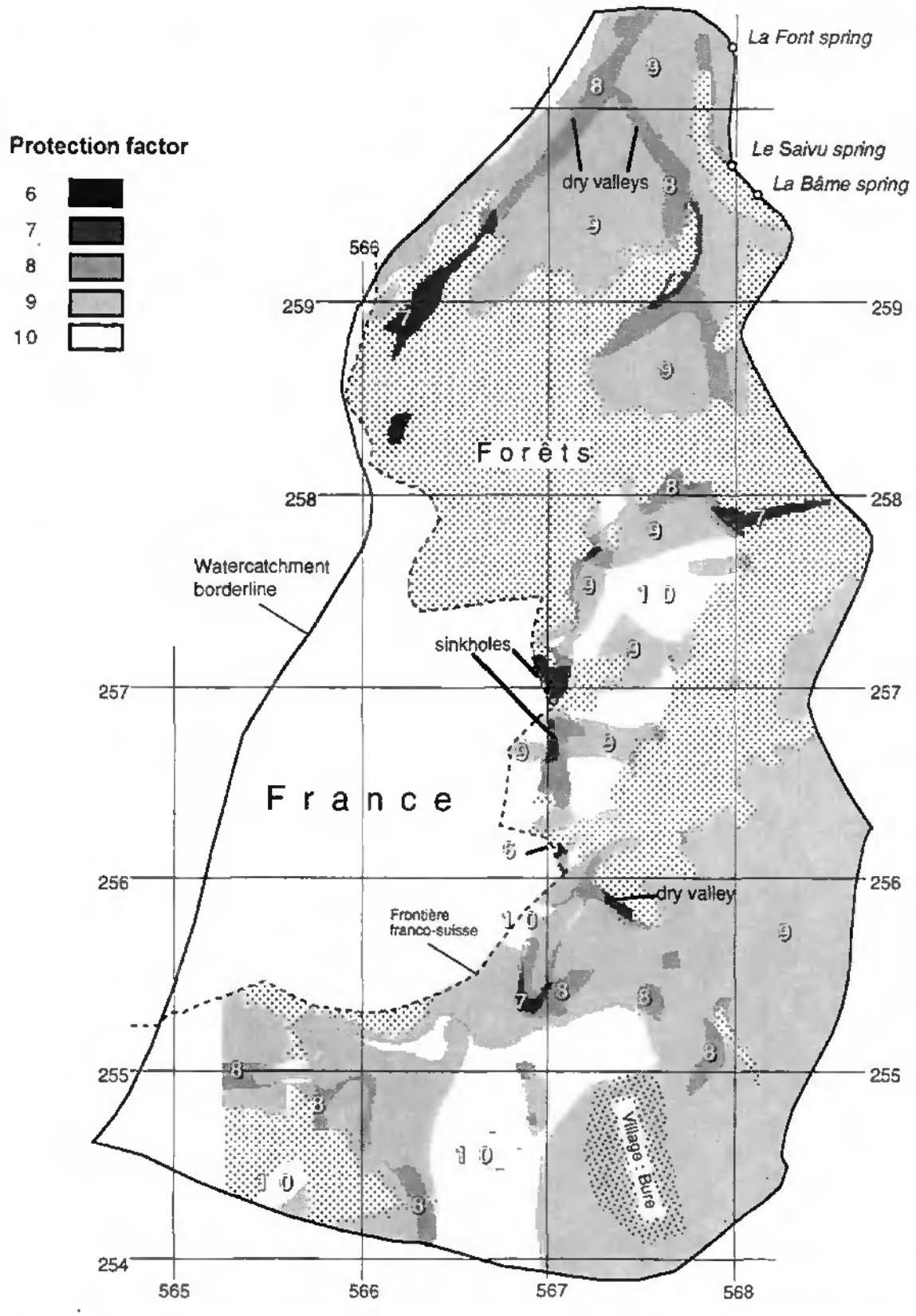

Figure 4.2.: Vulnerability map of the Font, Saivu and Bâme catchment with a simple weighting system : Fp= Ei + Pj + Ik, where i= 1, 2, 3, j= 1, 2, 3,4 and k=1, 2,3,4. (modified after Tâche et al., 1996).

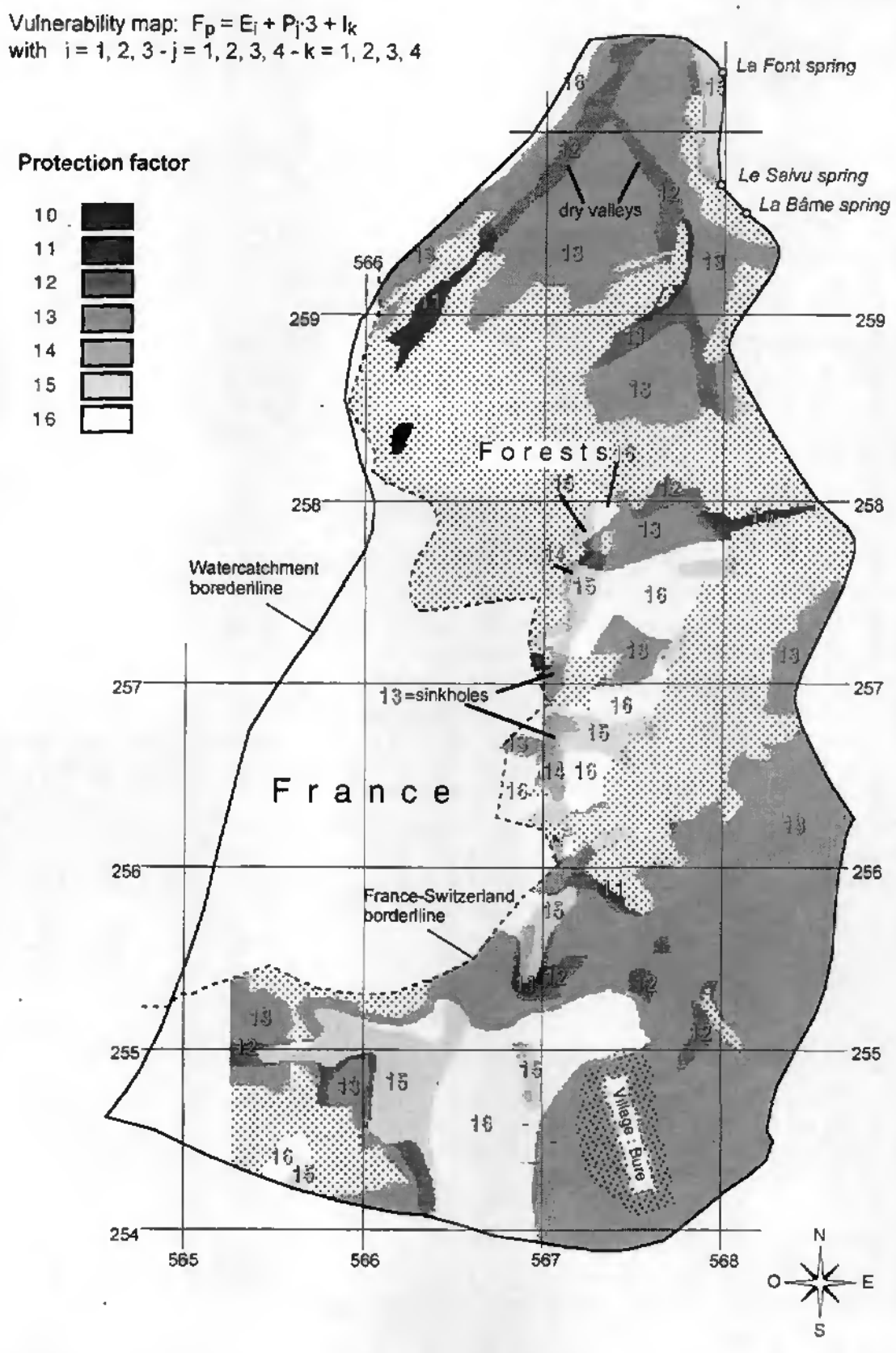

*Figure 4.3.: Vulnerability map of the Font, Saivu and Bâme catchment with the following formula: Fp = Ei + Pj *3 + Ik , where i = 1, 2, 3; j= 1, 2,3,4; k=1,2,3,4. (modified after Tâche et al., 1996).*

Chapter 5

Vulnerability mapping at two Swiss Jura sites

For both sites, we purposely did not map the forested areas. We decided that forests can be directly assigned to groundwater protection zone S2 as no thick protective cover is present in these areas. However, this may not be true in all cases.

5.1. Catchment of the springs of St-Imier

The springs used by the small town of St-Imier (Jura Bernois, Switzerland) provides a typical example, that occurs all too frequently, of how inappropriate it is to delineate groundwater protection zones in karst environments according to the actual practical guidelines (FOEFL, 1977).

5.1.1. Geography, geology and hydrogeology

The catchment of the springs of La Raissette, La Grande Dou and Le Torrent has an area of about 140 km^2 and is located in the western part of Switzerland in cantons Bern and Neuchâtel. The springs are used to supply water to different townships including St-Imier.

Geologically, the area is part of the folded Jura (Figures 5.1, 5.2). The aquifer is in Sequanian to Portlandian age (Malm) limestones which range in thickness from 200m to 400m. The underlying aquiclude is Argovian marl. Structurelly, the spring catchment extends from the northern side of the Gumigel - Chasseral anticline to the southern flank of the Montagne du Droit - Mont-Soleil - Mont-Crosin anticline both of which have a SW-NE direction.

In the 1980's, protection zones were established only on the northern part of the catchment (Schindler, 1988). Their limits (Figure 5.3) were based on practical instructions prepared specifically for this purpose by the Federal Office of Environment, Forests and Landscape (FOEFL, 1977). An S3 protection zone covers essentially all the area that was considered.

However, despite establishing the protection areas, pollution from liquid manure occurs typically four times a year following snow melt and violent thunderstorms with heavy rainfall.

5.1.2. Mapping the E, P and I attributes

We used various assessment methods to map each of the three attributes (Figures 5.4. to 5.6). For each attribute, we focused on the southern part of the catchment between coordinates 565.000/219.000, 568.000/219.000 and 565.000/221.000, 568.000/221.000 (Figures 5.5, 5.7 and 5.9).

a) Comments on the Epikarst map

The epikarst attribute was mapped according to definition. Topographical maps and aerial photographs were used with field verification done in some areas.

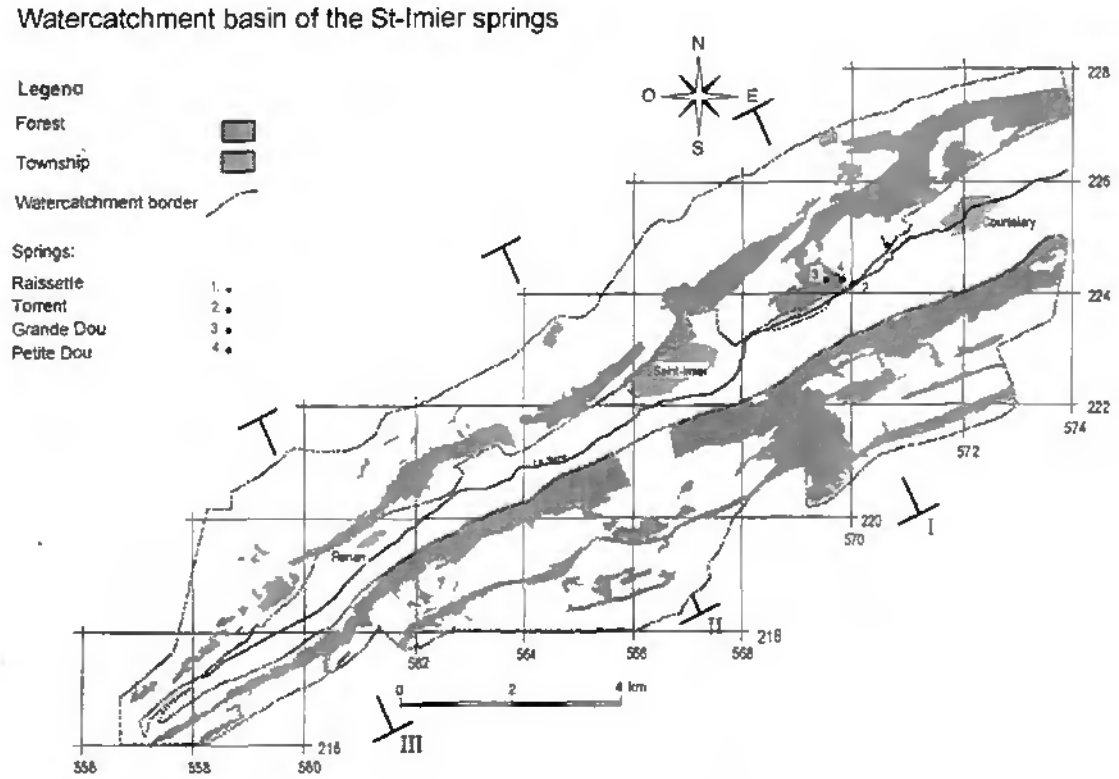

Figure 5.1. Topography of the St-Imier springs catchment showing geological cross-section locations.

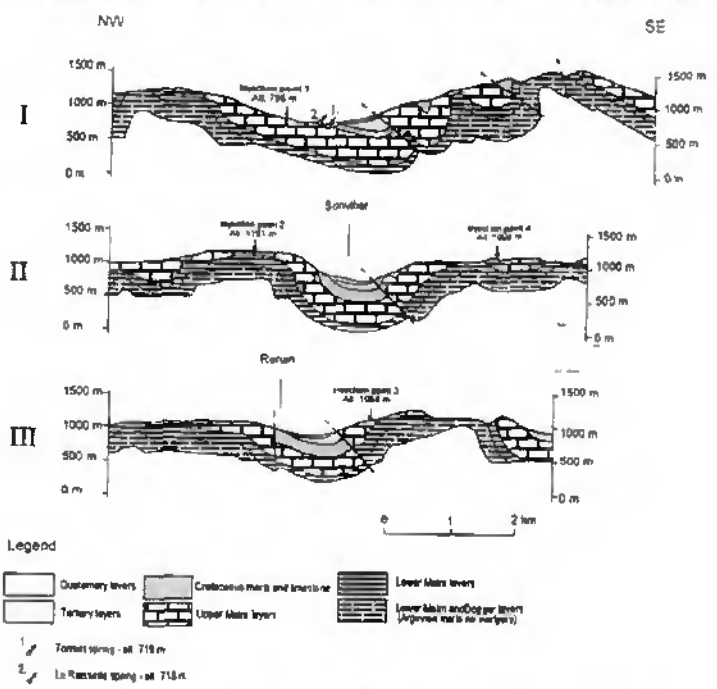

Figure 5.2.: Geological cross-sections (modified after Kempf T. & Della Valle G., 1981)

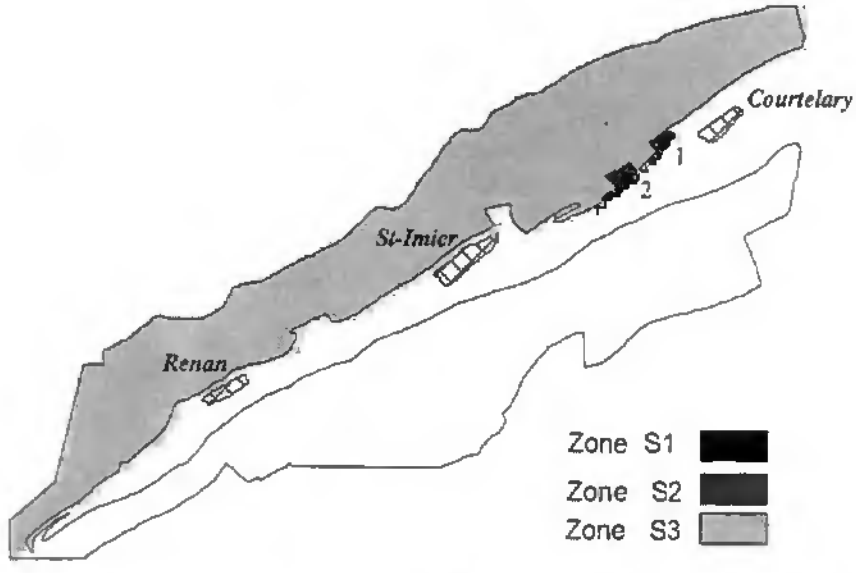

Figure 5.3.: Previous groundwater protection zones of the St-Imier springs catchment.

The largest area of E_1 is 0.5 to 0.75 km². This area is located in a forested area at the edge of the woods, where major roads intersect. It is uncovered karst with apparent open fractures. Karrenfields extend west, east and south from St-Imier township (Figure 5.4). The rest of the E_1 zone has more rapid response conditions with swallowholes (Figure 5.5) or sinkholes (dolines).

The E_2 sector occupies a larger area then E_1 sector. It has a large area of dry valleys and intermediate zones in the alignment of dolines (north of the springs and of Courtelary) (Figure 5.4). The sector above the Raissette Spring is mapped as E_2 as well as part of the sector far to the west of Torrent spring. This is not a dry valley or even an intermediate zone in a doline alignment. According to a tracer test done in this sector, it makes sense to attribute this sector to class E_2 (cf. 5.1.5.).

The rest of the catchment, representing about 70 percent of the area is defined as E_3.

b) Comments on the Protective cover map

As the St-Imier site was the first site where we tested the EPIK approach, the ranges in values of the Protective cover attribute changed during the method development. The ranges in thickness of the protective cover was at the time of mapping 0 to 10cm and 10cm to 50cm and higher instead of 0 to 20cm and 20cm to 100cm and higher[6].

In order to map this attribute, we used a hand-auger at 250 locations without a grid. We applied the morphological equivalence principle so that if the area surrounding an auger hole (square of 100 to 200 m approximately) had similar morphology, we assumed that the same range of the protective cover extended over the entire area. An error factor was determined statistically.

More than half of the mapped surface had a protective cover thicker than 0.1m and less than 0.5m. Some areas such as cuestas, slopes of closed depressions or dry valleys and forest sectors thet intercepted major roads with no protective cover (less than 0.1 m to 0m). The rest of the catchment was characterized as E_3 (Figures 5.6 and 5.7).

[6] *For future work, we recommend mapping the real thickness of the protective cover instead of mapping the class corresponding to the given range. In this manner we can use the data even if we change the thickness range in further development of the EPIK approach.*

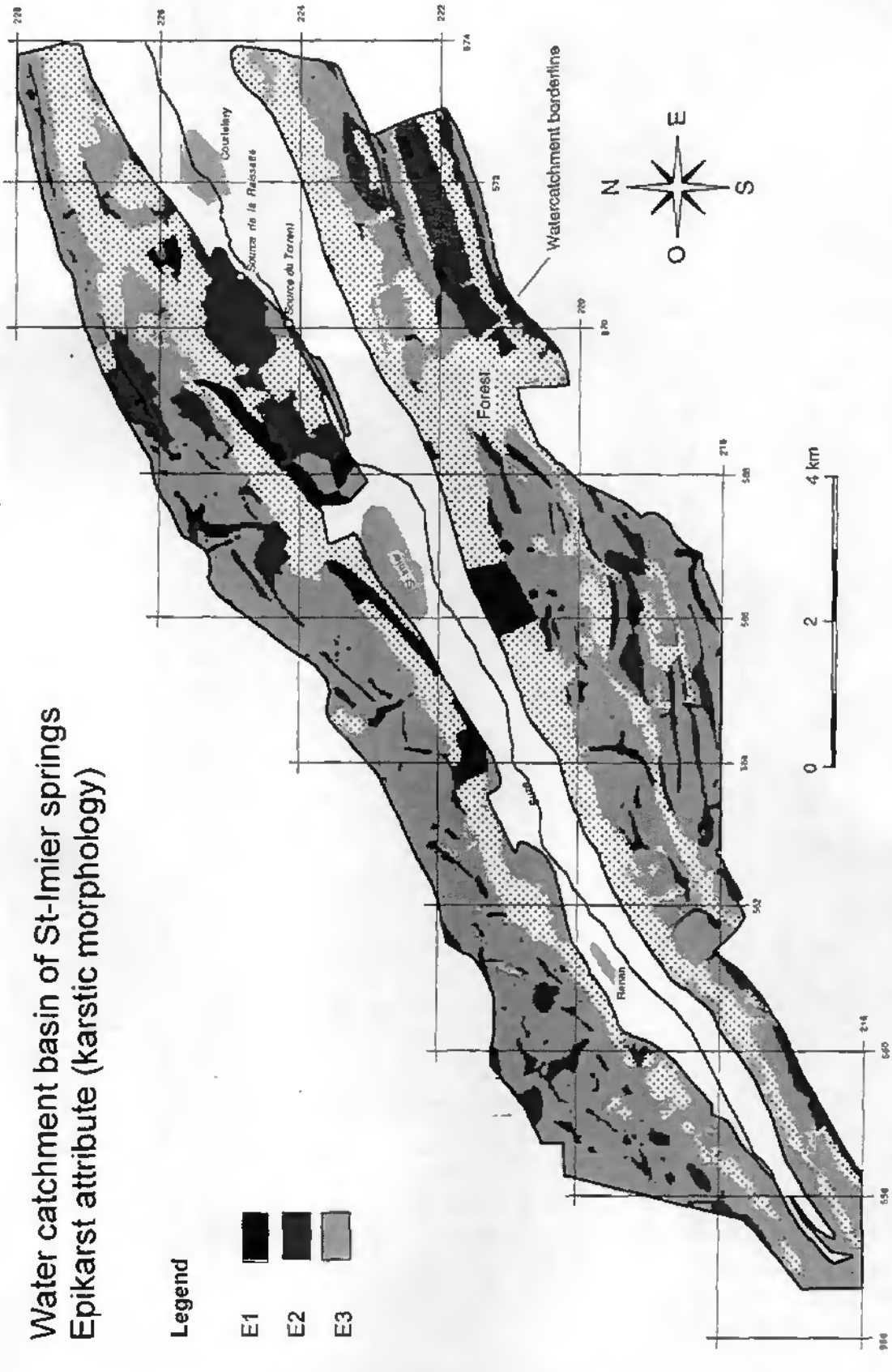

Figure 5.4.: Epikarst attribute map of St-Imier (Tâche et al., 1996).

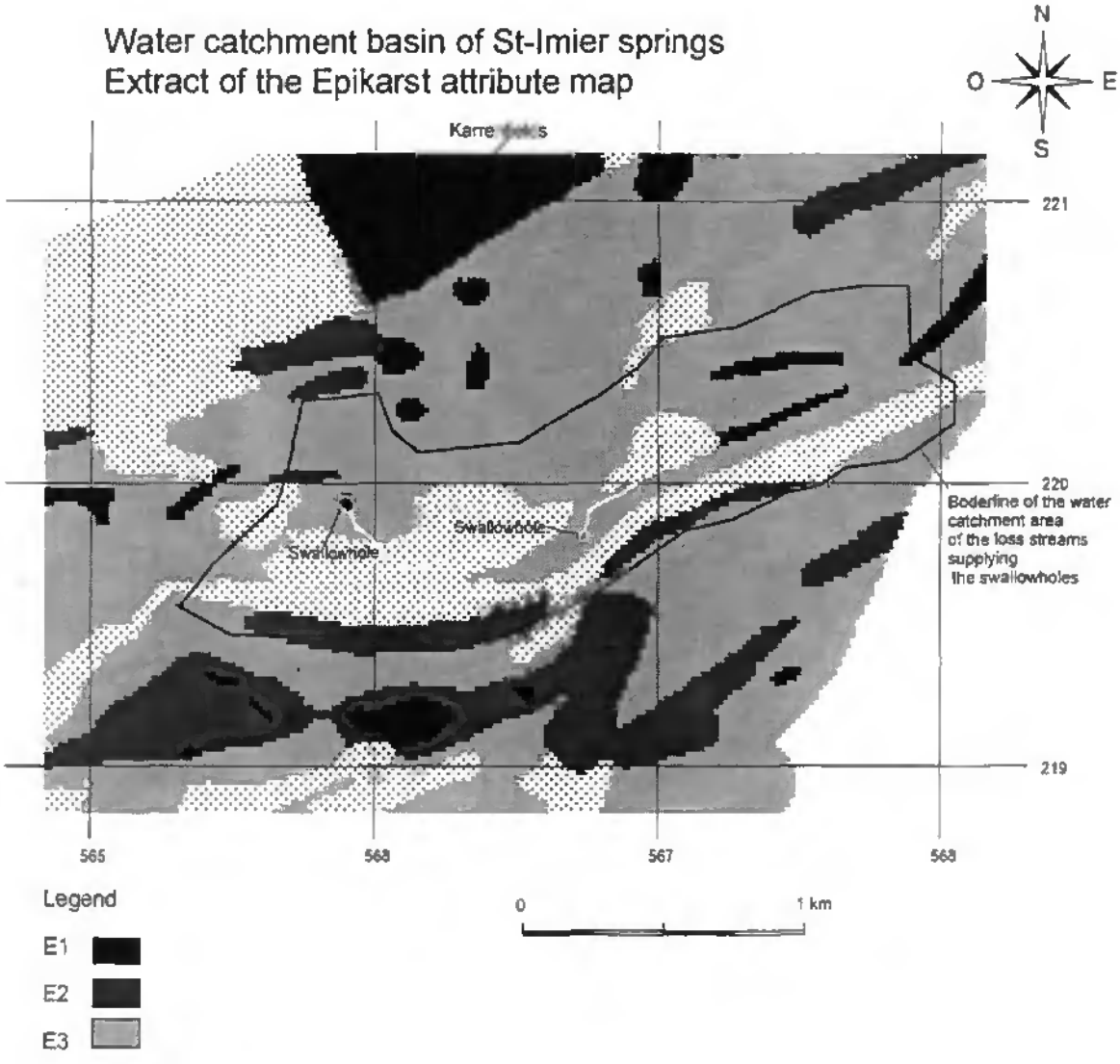

Figure 5.5.: Extract of the Epikarst attribute map of St-Imier (Tâche et al., 1996).

c) Comments on the Infiltration conditions map

According to the definition of the Infiltration conditions attribute, we mapped the two swallowholes and the banks of the losing streams in I_1. Slopes higher than 25 percent for pasture areas in the catchment of the two losing streams were designated I_2 (Figure 5.9). The extracted infiltration conditions attribute map is the only part of the entire catchment where both I_1 and I_2 are present.

In order to assign I_2 and I_3 designations in the catchment, we used the topographic elevation model and the IDRISI GIS program run on a PC. The I_3 attribute covers less than half of the entire catchment area (Figure 5.8).

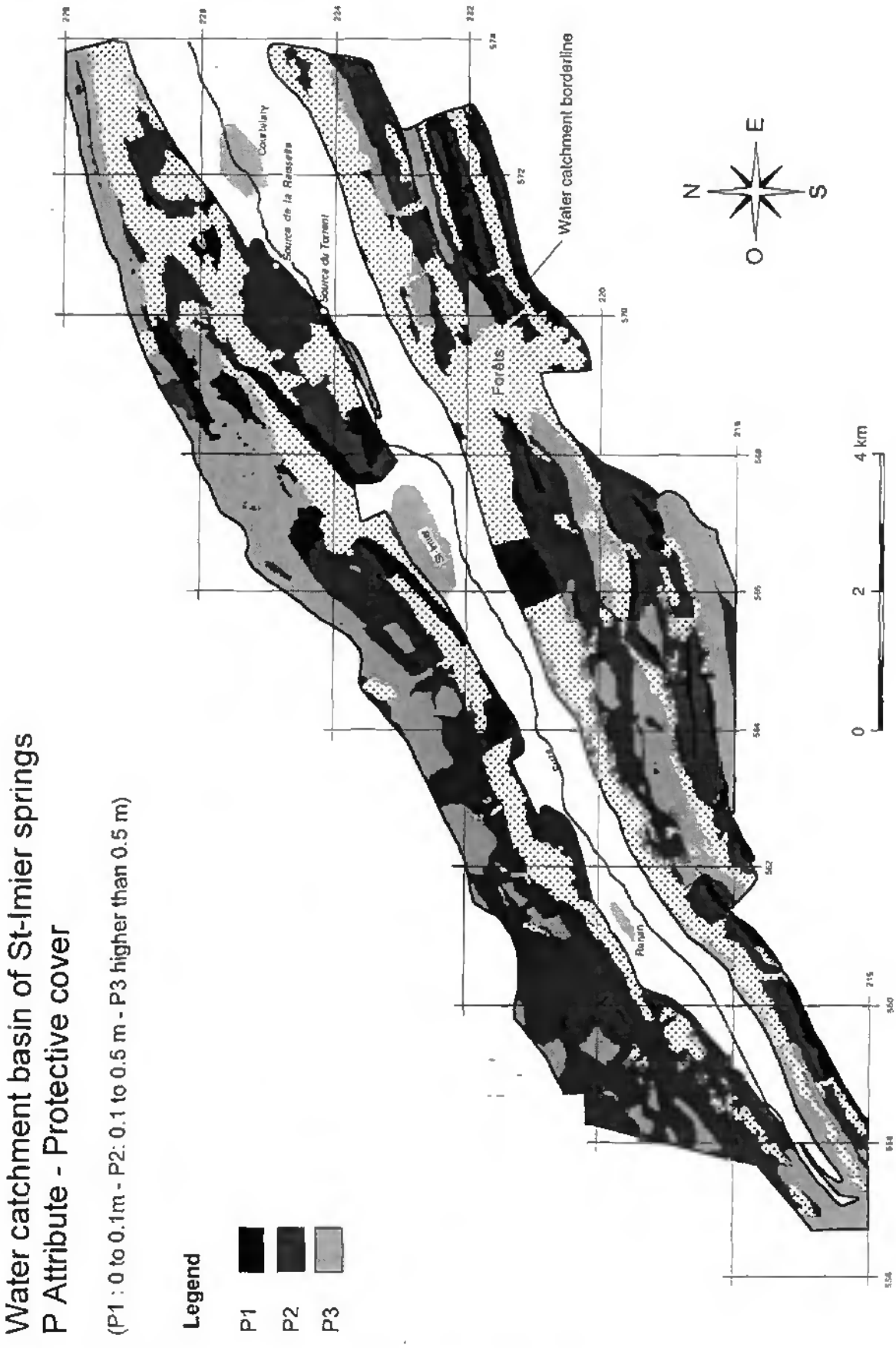

Figure 5.6.: Protective cover attribute map of St-Imier (Tâche et al., 1996).

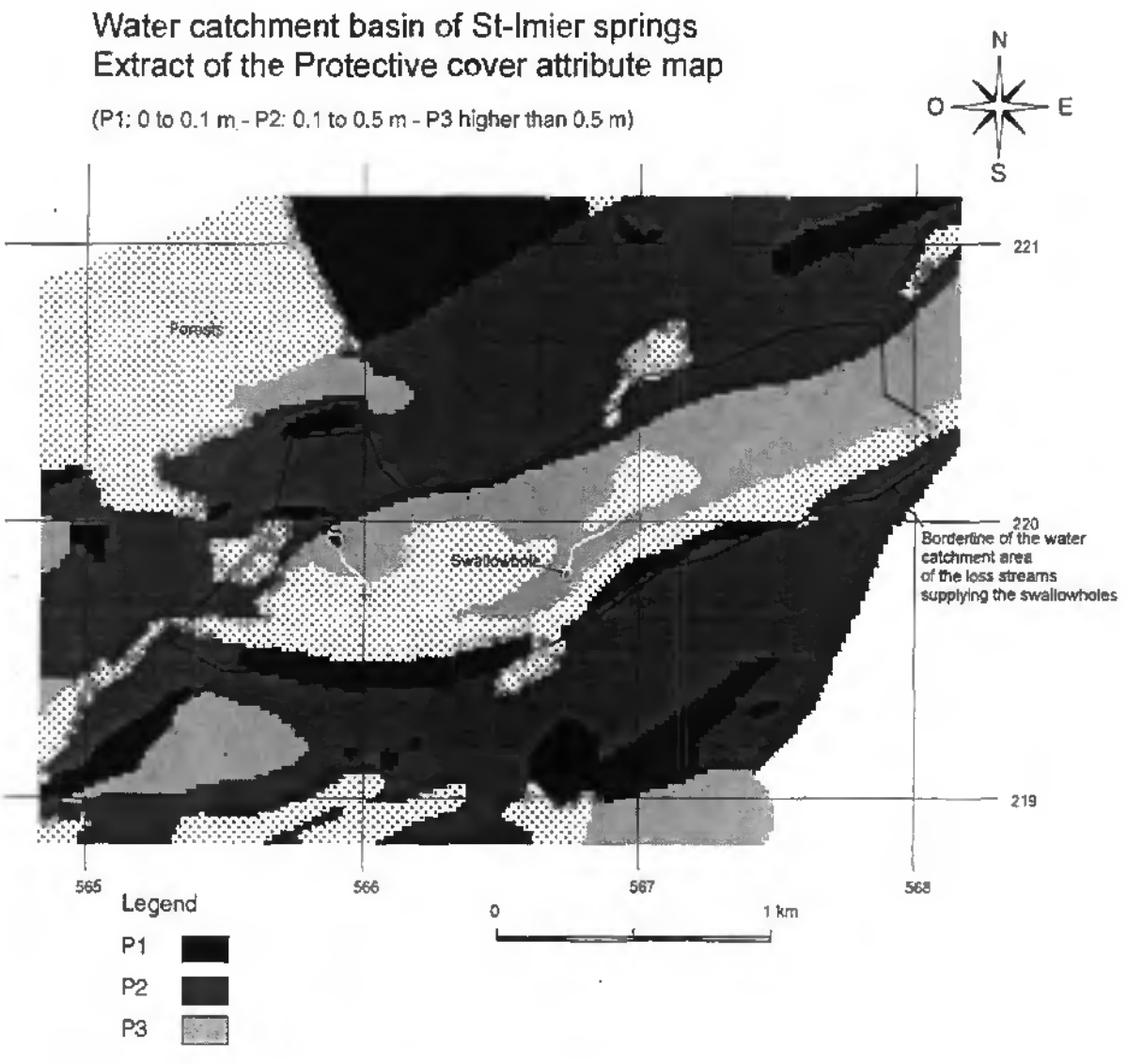

Figure 5.7.: Extract of the Protective cover attribute map of St-Imier (Tâche et al., 1996).

5.1.3. Characterization of the karst network development

No speleological network, major shaft or cave is known in the St-Imier spring catchment. One important collapse doline with perennial ice is located in the south-east part of the catchment at Creux de Glace (572.900/222.500, 1340m).

Characterizing the karst network development was done using indirect methods such as hydrograph analysis and tracer tests.

We had only the mean daily discharge values for the Raissette spring and precipitation from a single meteorological station (Mont-Soleil) for the whole catchment -. Therefore, we were not able to effectively use the Mangin methods ot spectral analysis and comparison of dynamic and runoff water volume.

By comparing the Raissette spring hydrograph with precipitation events (Figure 5.10), it was possible to conclude that the spring reacts rapidly in less than 12 hours and with very narrow peaks. The duration of the recession period may exceed 24 hours. This spring has typical karst behavior.

The Raissette spring chemical end bacteriological analysis are sparse being done only once a month, independent of hydrological conditions. Therefore, it is difficult to estimate the degree of karst development.

There have been 18 tracer tests done in the catchment but most of the data is incomplete releted to for exemple, recovery rate, hydrological conditions, and so forth. However, we were able to conclude that:

- the maximum velocities range from 17 to 76 m/h in low to medium water stage.

- although no transter functions were calculated, there is a reletively narrow breakthrough curve peak decreasing over the following 5 days.

Consequently, the St-Imier springs catchment could be either in K_1 or K_2, but definitively not K_3. Distinguishing between K_1 end K_2 is arbitrary. However, to develop a stricter groundwater policy, we assigned K_1 to the whole cetchment. This may not however, heve an influence on the resulting vulnerability map in relation to the protection factor value.

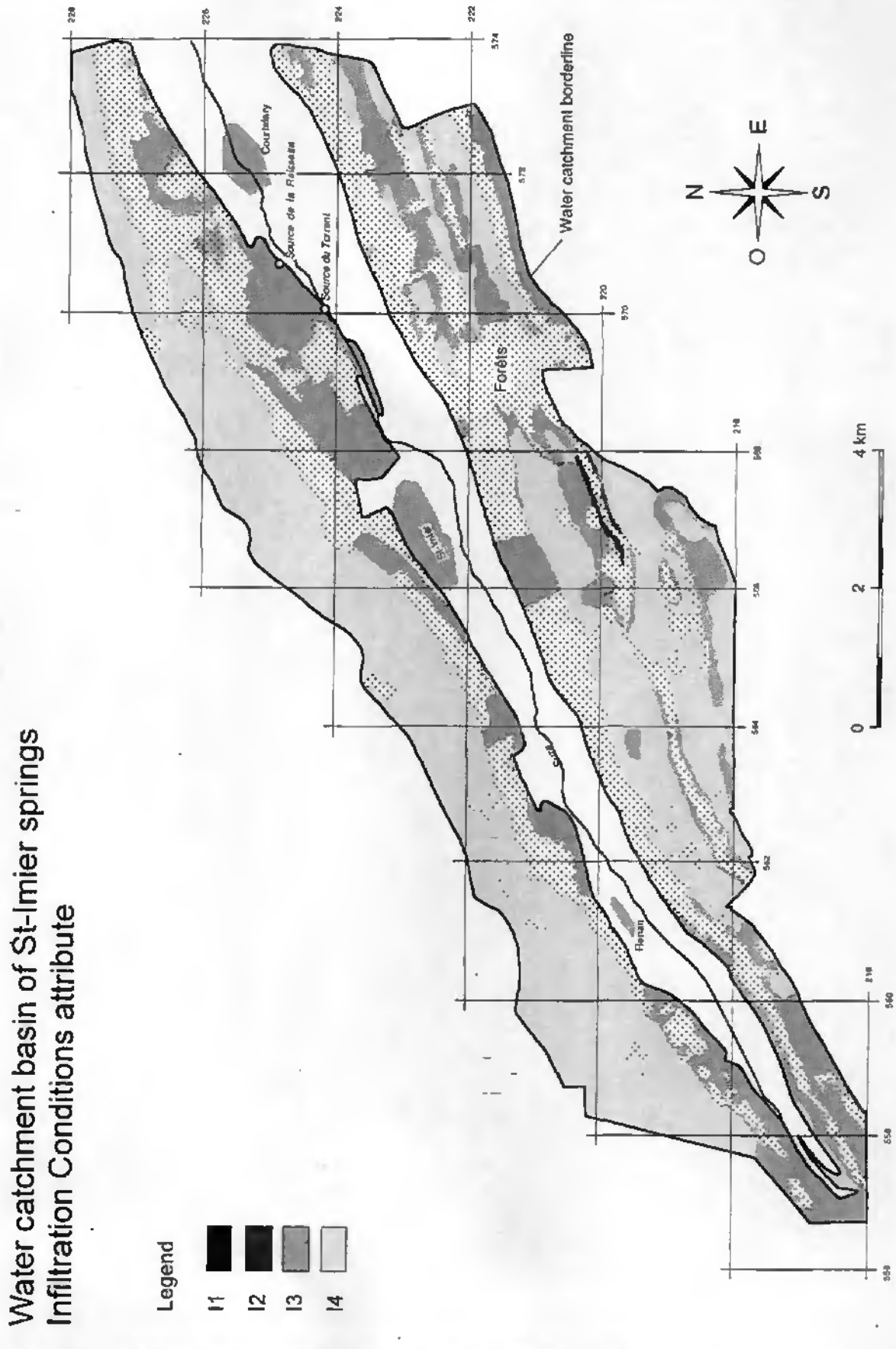

Figure 5.8: Infiltration conditions attribute map of St-Imier (Tâche et al., 1996)

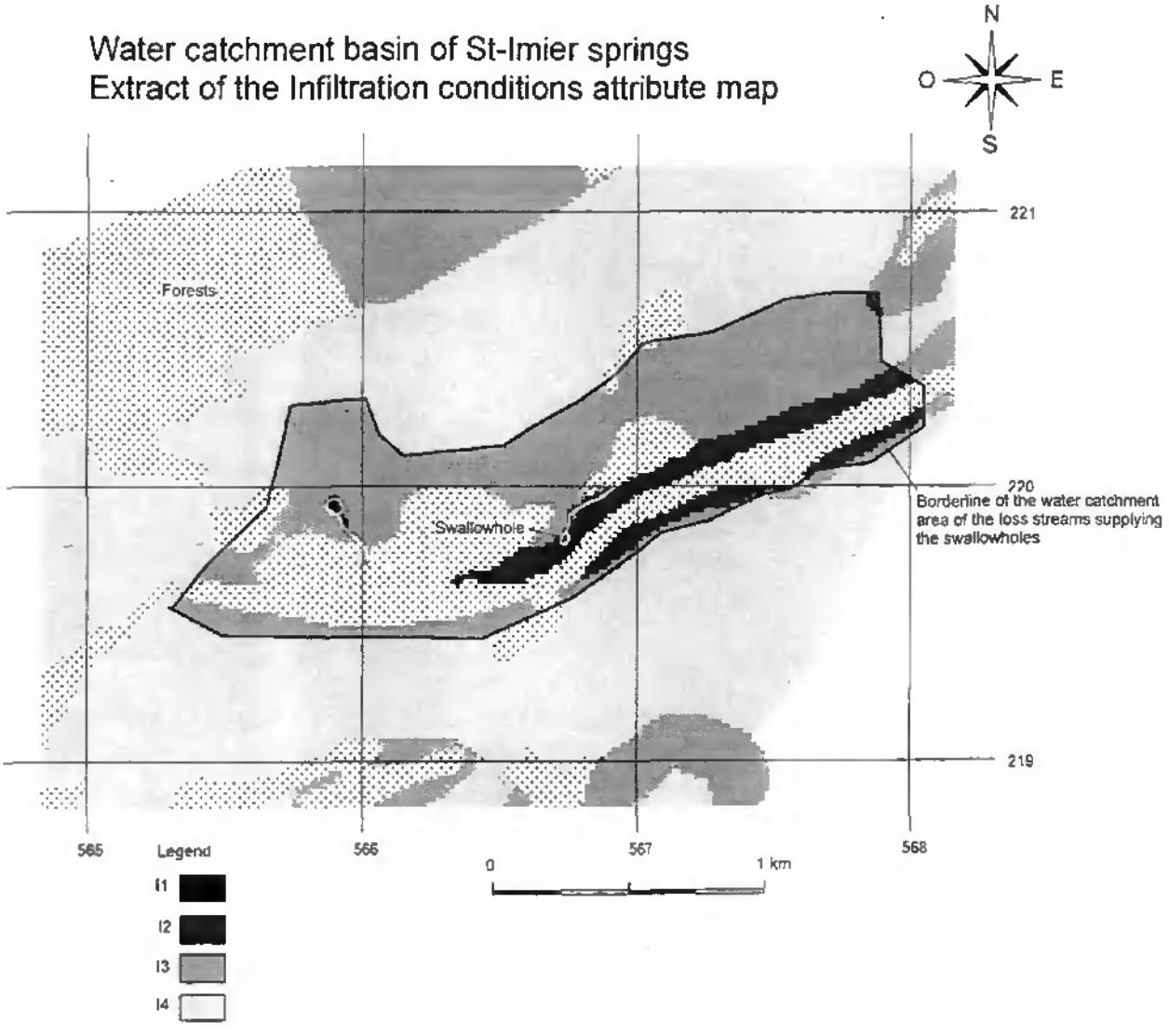

Figure 5.9.: Extract of the infiltration conditions attribute map of St-Imier (Tâche et al., 1996)

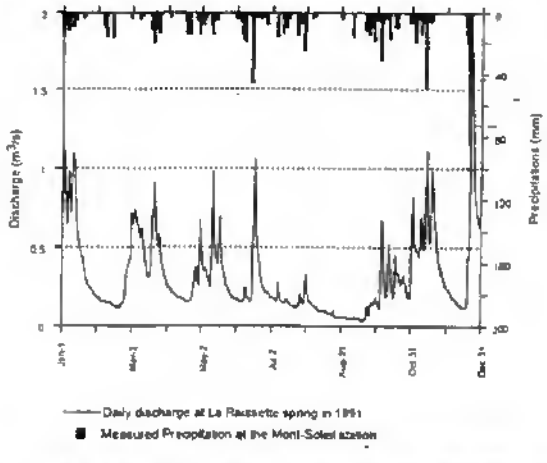

Figure 5.10.: Precipitation/discharge relationships at the Raissette spring from January 01, 1991 to January 01, 1992 (Doerfliger et al., 1995).

5.1.4. The resulting vulnerability map of St-Imier

We obtained the vulnerability map by overlaying the three attribute maps and calculating the protection factor with the equetion (chepter 4) for each catchment 'cell' (20m x 20m) (Figures 5.11 end 5.12). These maps (Tâche et al., 1996) illustrate:

- swallowholes are the points with the highest degree of vulnerability/lowest degree of protection (9/29).

- karrenfields loceted in forested areas (specifically zones next to major roads) without protective cover are also particularly vulnerable (15/29), as are sinkholes (dolines) (16/29 to 20/29).

- the dry velleys, low lying areas and slopes with runoff to these zones have a moderate vulnerability (21 to 26) and are consistently less vulnerable then sinkholes and karrenfields.

- the highest values (26 to 29) correspond to zones where no attributes have medium to high vulnerability. Some cases era borderline: E_2-P_3-I_4 (26), E_3-P_1-I_4 (27).

5.1.5. Validation of vulnerability zones at St-Imier

A multi-tracer test (2.5.1995) and geophysics were done at four sites to validate the vulnerebility results. One site had high vulnerability (Fp=17), two medium vulnerability (Fp=22 and 20) and one low vulnerability (F= 25). (Table 5.1).
We expect similer normalized response from the two injections in areas of medium vulnerability with a relatively ebrupt 0.5 percentile gradient. For injection in high vulnerability areas, the normalized response should be more abrupt at the 0.5 percentile then for the medium case. Finally, the response in low vulnerability zones should have a slope at the 0.5 percentile that tends to 1 (0 is vertical) (cf. Part II, Chapter 3).
Geophysics should provide information about fracture intensity end the nature and extent of the epikarst.

Table 5.1.
Validation test data at four aites at St-Imier

Sector	Coord.xy z	Protection factor	Main features of the site	Infiltration test	Tracer (type and quantity)	Geophysical investigation
Comoret (1)	570.400/ 225.000; 796	20/27	artificial hole(1m) into the limestone	$1.5\ 10^{-5}$m/s (Porchet) 3 m^3 of water 1 m^3 in 3 hours	H4/4 bacteriophages $2.84\ 10^{14}$ pfu	yes: VLF-R
L'Assesseur (2)	562.900/ 222.00; 1191	18/27	sinkhole (diam. 10m., depth 2m)	6m^3 in 40 minutes	H40/1 bacteriophages $4.32\ 10^{14}$ pfu	no: high voltage line in vicinity
La Juillarde l'Embossu (3)	560.525/ 217.550; 1088	23/27	artificial hole (diam. 1m, depth 0.8m): soil , limestone rock	3 m^3 1 m^3 in 3 hours	Uranine 10kg	no: because of buried water and electrical conduits.
Creux-Joly (4)	560.200/ 219.200; 1099	15/27	collapse sinkhole (diam 20m, depth 10m) bottom covered partially with snow ,wood debris and other garbage)	5 m^3 in 15 minutes	Duasyn 10kg	yes: VLF-R multi-directional

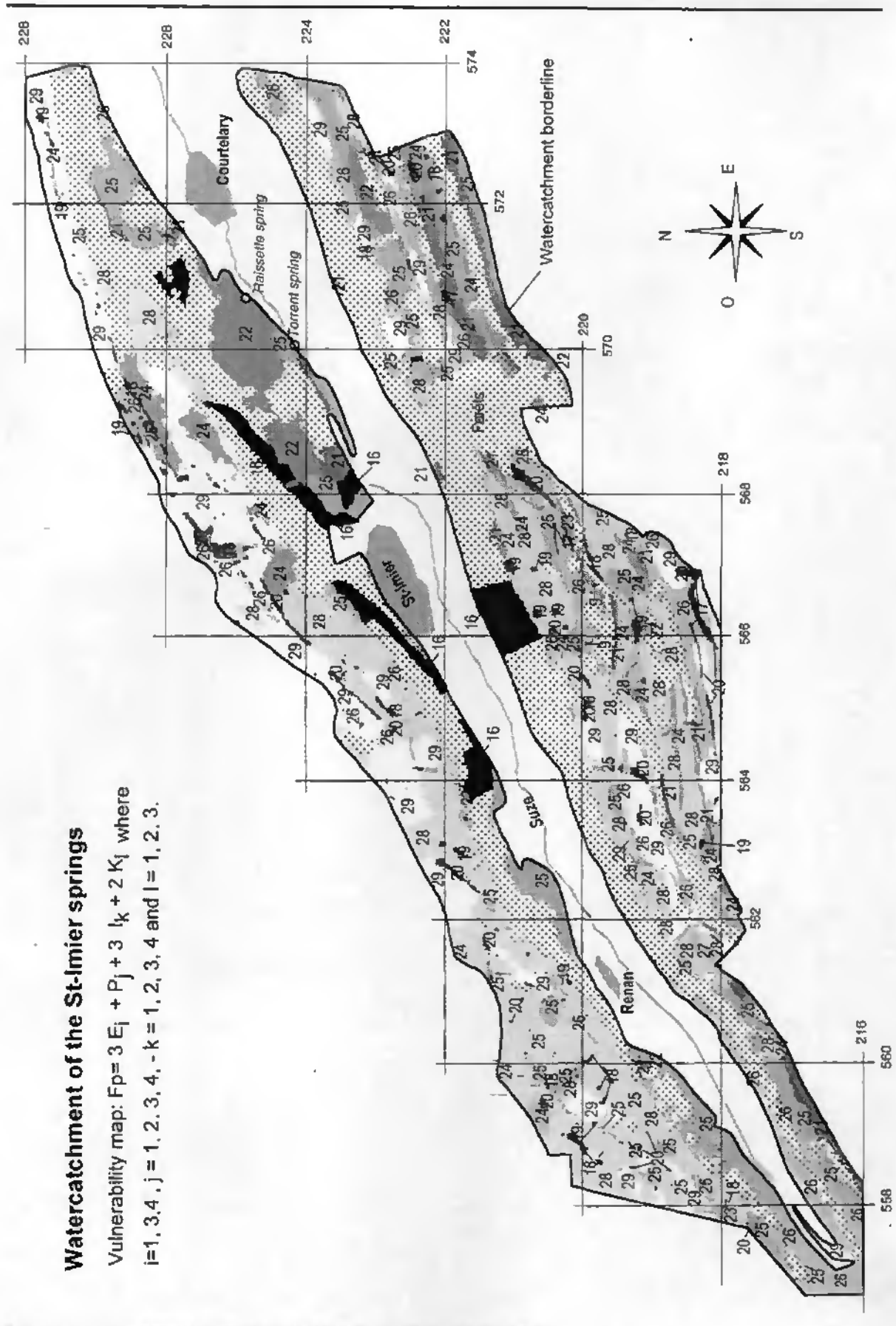

Figure 5.11.: Vulnerability map of St-Imier springs (Tâche et al., 1996). .

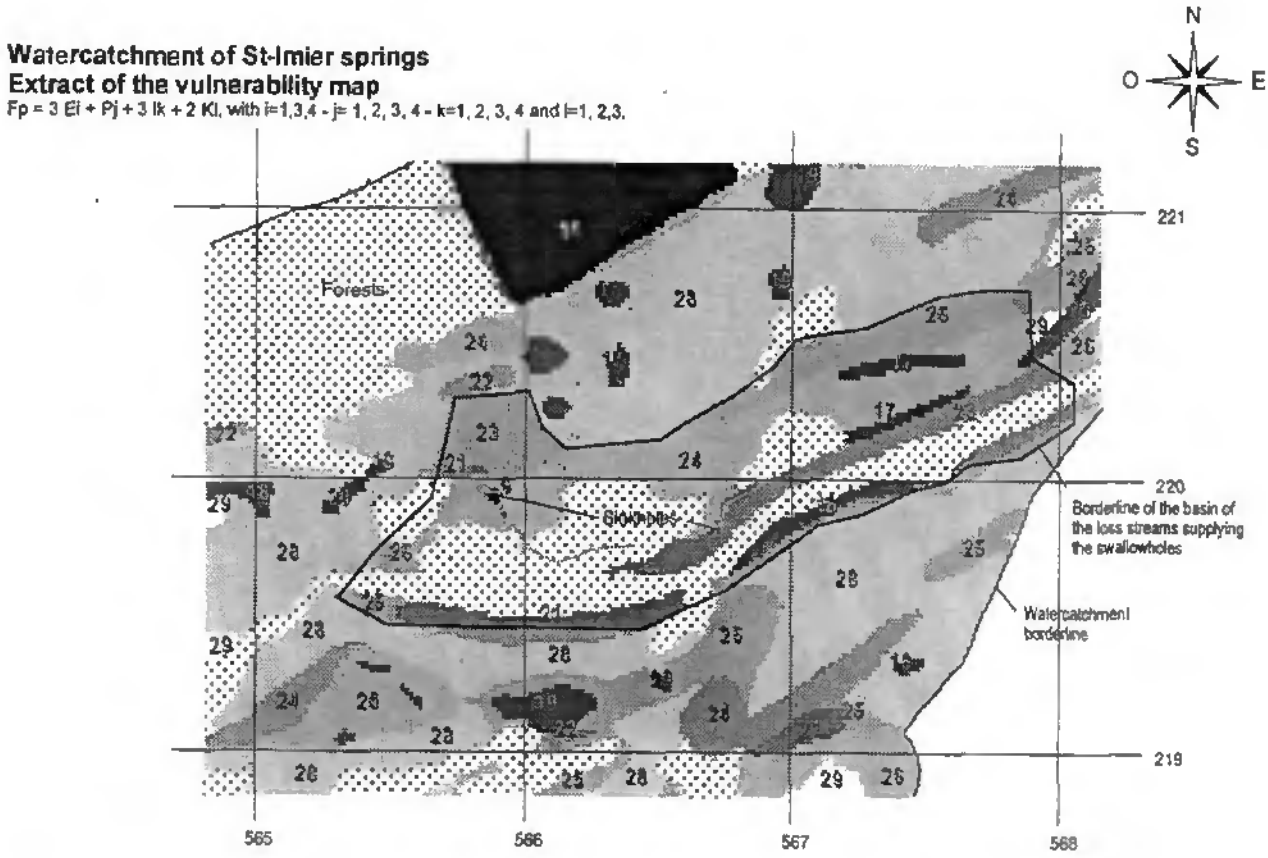

Figure 5.12.: Extract of the vulnerability map of St-Imier springs (Tâche et al., 1996).

a) multi-tracer tests with bacteriophages and fluorescent dyes:

Four tracer tests were done on in May 1995 during a low to medium water level stage. The major springs were sampled with an automatic sampler (4 to 6 times a day) and by hand at least two times a day as cited in the Table 5.2. The results are in Table 5.3:

Table 5.2.
Sampled springs

Sampled springs	Coordinates and elevation (m)	Comments
Raissette	570.720/224.850; 718	captured spring: water supply of St-Imier
Torrent	570.080/224.145; 719	captured spring: water association of Franches Montagnes
Grande Dou	569.5800/224.230; 750	non captured spring
Petite Dou	569.860/224.180; 730	non captured spring
Borcairde	571.015/225.045; 705	non captured spring
Courtelary (s. Helbling)	571.890/225.400; 715	captured spring: "water fontaines" network.

Table 5.3.
Tracer test results

Tracar /injection site	Springs	Maximum velocity (m/h)	Modal velocity (m/h)	Recovery rate %
(1) Cormoret - H4/4 phages	La Raissette La Borcairde	16m/h (22h)	11m/h (33h)	30 percent
(2) L'Assesseur - H40/1 phages	Torrent Petite & Granda Dou	22 m/h (325h)	19m/h (380h)	0.5 percant higher concentration - RR not calculated
(3) La Juillarde - uranine	-	-	-	-
(4) Craux-Joly - duasyn	-	-	-	-

Two of the four tracer tests were positive: H4/4 and H40/1. The tracers experiments with uranine in la Juillarde and with duasyn in le Creux-Joly were both negative as neither dye was detected at the springs.

The bacteriophage H4/4 eppeared at Raissette spring after about 22 hours with a maximum concentration peak after 33 hours (Figure 5.13). It was found in some of the Borcairde spring samples after less than 48 hours but with lower concentrations. The recovery rate was lower then 50 percent possible due to tracer retention in the unsaturated zone or the existence of outlets that were not sampled (for example: outlets into Tertiery layers in the valley). This rapid reaction of the La Raissette spring to the tracer injection suggests good connectivity in the karst network and a connection between a hypothetical epikarst end this network. Therefore, it was appropriate to assign E_2 for the epikarst in this area.

The bacteriophege H40/1 eppeared at Torrent spring after about 324 hours, with a maximum peak around 380 hours (Figure 5.14). It was detected in higher concentration at both the Petite and Grande Dou springs but since the sampling was done only twice e day it was not possible to draw e recovery curve. The bacteriophages did not emerge at the Raissette spring. The tracer system may vary with the water level and hydrologicel conditions so,tracers injected in the south-west part of the catchment may arrive at the Raissette spring.

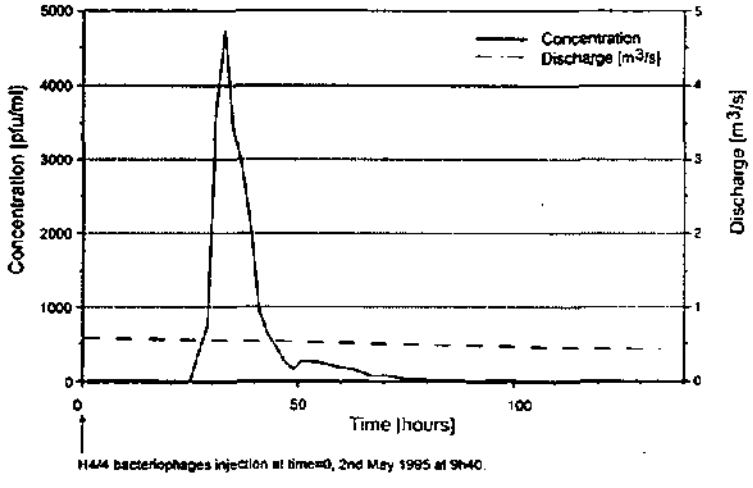

Figure 5.13: Bacteriophage H4/4 recovery curve at the Raissette spring (Doerfliger et al., 1995)

The recovery rate of the H40/1 bacteriophage at the Torrent spring was less then 1 percent. Such a low recovery rate may be the result of the following conditions:

1. A large tracer amount was recovered at the Petite and Grande Dou springs, but since the discharge level was not measured, an accurate recovery rate was not able to be calculated.

2. A relatively long transit time and the relatively high ambient temperature at the Raissette spring may effect the virulence of the bacteriophages.

3. A large amount of the tracer may have been trapped in the unsaturated zone which extends to thickness of 100m.

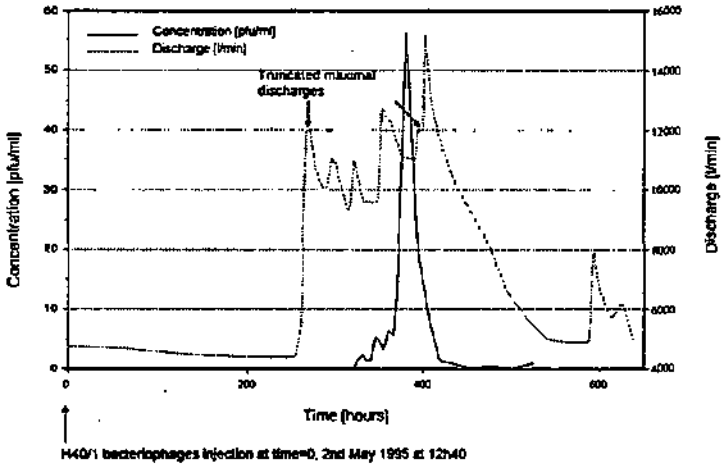

Figure 5.14: Bacteriophage H40/1 recovery curve at tha Torrent spring (Doerfliger at al., 1995).

No uranine was detected in the samplers at the various springs. This tracer was injected with only $3m^3$ in a low permeability artificial hole. The tracer may have been trapped in the unsaturated zone. Its recovery appears to have been diffused over a long time period with low concentrations. This injection point is located above an overthrust fault that may modify the flow system into the Tertiary layers. Finally, aluminum sulfate is added daily to the water at the Raissatte and this may heva masked the uranine concentration. This negative result does not modify assigning low vulnerability to this area. In order to disprove or confirm such hypothesis, additional tracer tests in high water level conditions with sufficient flushing water should be done.

Several reasons exist for the negative tracer test with duasyn in the collapsed sinkhole (Creux-Joly):

1. The quantity of duasyn (10kg) was insufficient and therefore the major concentration at the springs was below the detection level.

2. The injection point is located in an area where the water catchment limit is unconfirmed. It may be connected to the water catchment of the Seyon in Canton Neuchâtel .

3. The trecer was trapped in the unsaturated or saturated zones.

It is difficult to clearly understand what occurred based solely on the tests done to date. This apparently vulnerable catchment should be the object of additional work. A tracer test should be done during high water level conditions and with a more appropriate tracer amount.

b) geophysical investigations

The radio-magnetotelluric (VLF-R) method was used at the same two areas.

On the Creux-Joly site, multi-directional measurements spaced at 10m intervals were done in profiles about 15m apart (Appendix III.5).

A north-south structure is clear from the resistivity map (Figure 5.15), specifically in the southern part of the area. This structure is perpendicular to the Pontins anticline axis. A preferential N-S fracture direction corresponds to the direction of the maximum resistivity.

In the high resistivity zone, the preferential fracture orientation tends to be E-W. This orientation is related to a secondary E-W fracturing that affects the filling material of the major tectonic activity.

The major N-S tectonic activity was also visible on the resistivity profiles whatever the emitter direction or the frequency (Figure 5.16.). A conductive zone centered on measurement station 11 was surrounded by resistant zones, typical of a fractured zone. The sinkhole was located next to this tectonic activity and is certainly associated with it.

In Cormoret, the result of the geophysical measurements was completely different. No preferential direction of fractures was noticeable as the apparent resistivity and the phase were relatively homogeneous. Their variations were not significant (Figure 5.17) (Doetliger et al., 1995).

c) conclusions

The two bacteriophage tracer tests had the expected results with their relatively high maximum and modal velocities. Assigning the hydrological conditions a medium vulnerability is justified.

Figure 5.18 shows the impulse responses of these two trecer experiments. The H4/4 tracer test has a more abrupt peak than the H40/1 one and is less affected by dispersion (qualitatively) as the tracer distance was different.

Figure 5.19 shows the normalized responses of the same tests. The two responses had a steep gradient at the 0.5 percentiles. They are relatively similar and representative of consistent vulnerability as it is the case according to the vulnerability mapping.

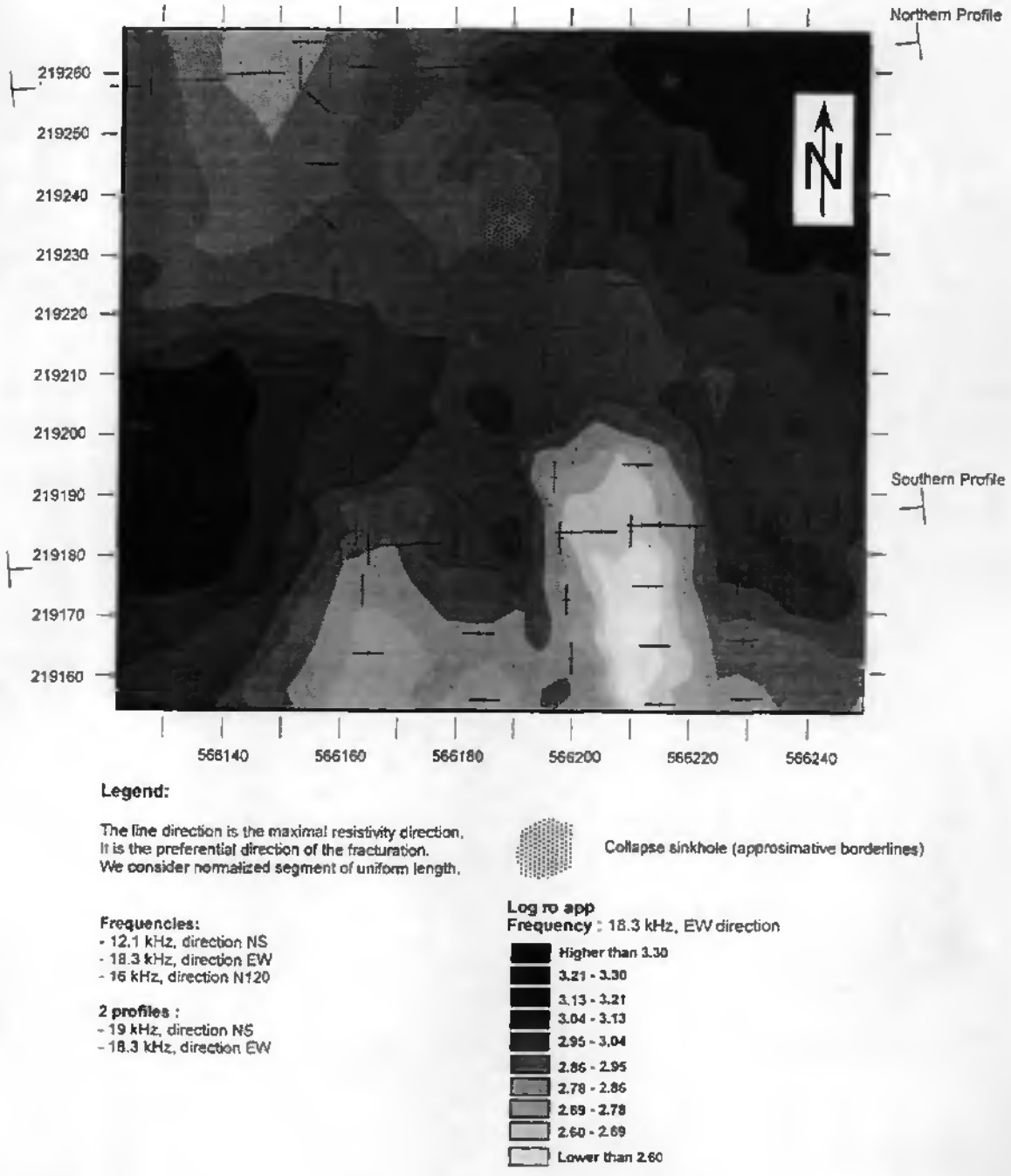

Figure 5.15: Map of apparent resistivity and the direction of the maximum normalized resistivity at Creux-Joly (after Doerfliger et al., 1995).

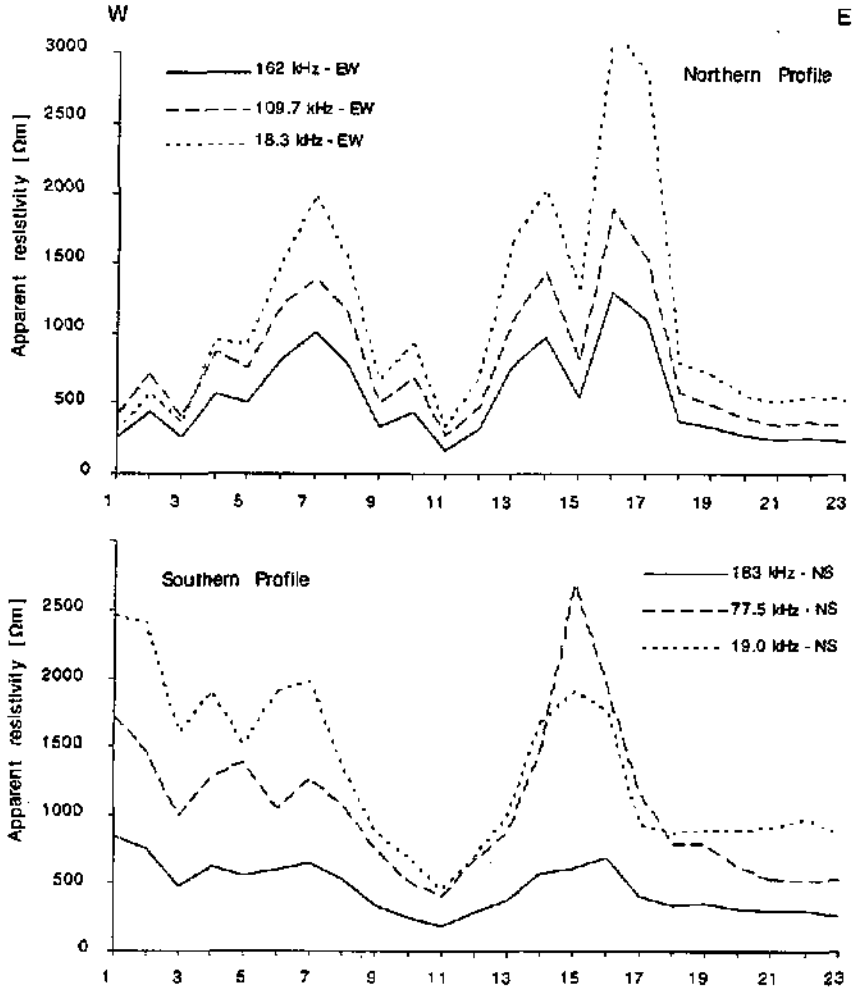

Figure 5.16: N and S apparent resistivity profiles at Creux-Joly (Doerfliger et al., 1995).

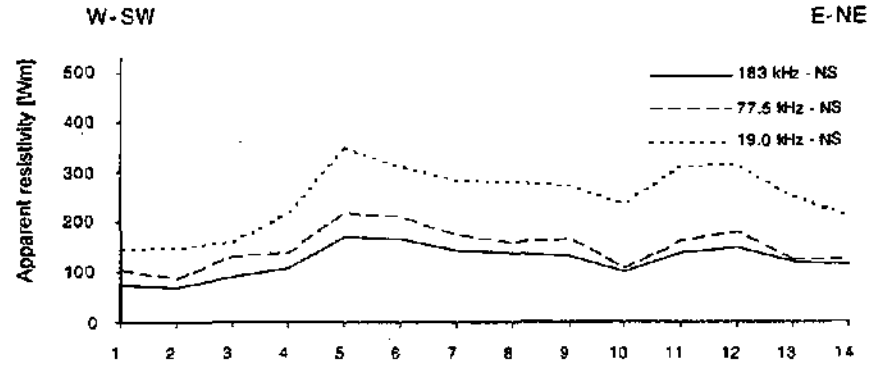

Figure 5.17: Profile WSW-ENE at Cormoret (coordinates cf. injection point): apparent resistivities measured in the NS direction.

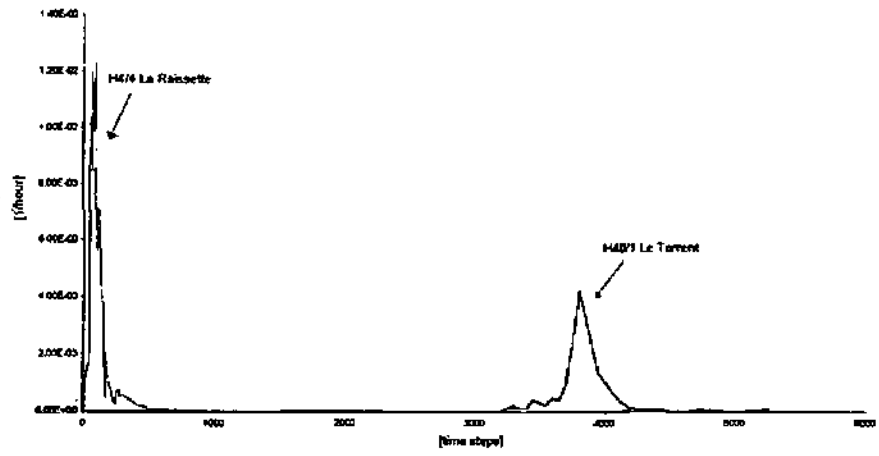

Figure 5.18: Impulse responses of the H4/4 and H40/1 tracer experiment (Doerfliger et al., 1995).

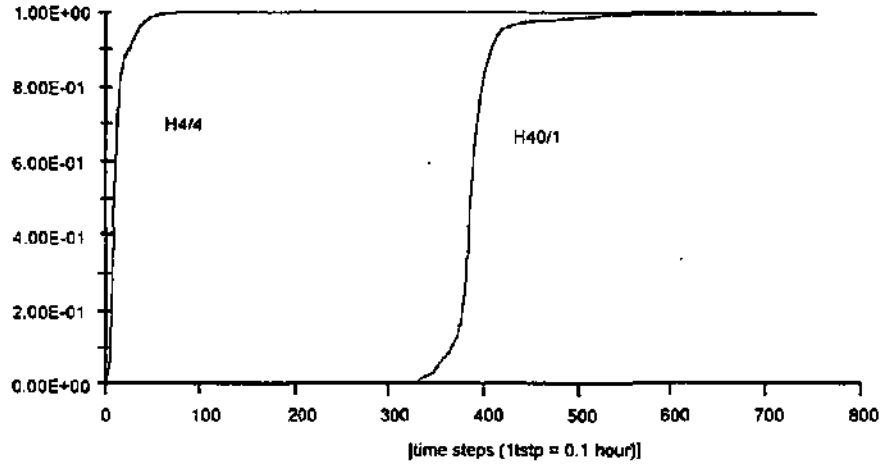

Figure 5.19: Normalized responses of the H4/4 and H40/1 tracer experiments (Doerfliger et al., 1995).

The situation that occurred where two other tracers were not recovered at the springs is symptomatic of the difficulty mapping the catchment boundaries in karst environments.

The geophysical investigations allowed us to demonstrate fractured zones when these zones are characterized by an readily recognizable resistivity contrast with the surrounding layers. This is the case at Creux-Joly with a 20/27 protection factor where the resistant limestone layers are located next to a conductive fractured zone.

On the other hand, being conclusive is difficult when the geophysical measurements do not have sufficient resistivity contrast. Such a situation does not mean, however, that there is no fracturing or no epikarst. Geophysics may be "blind" to secondary fracturing in some cases as was demonstrated at Cormoret. In spite of an injection point located in an homogenous zone of apparent resistivity, the tracer rapidly reached the spring. We had previously suspected that a connection existed between fractures and epikarst and the karst network that feeds the Raissette spring (Doerfliger et al., 1995).

From these findings, the following major conclusions mey be drawn:

1. A result from only one method at a site is not sufficient to confirm the attributes of this site in order to define the degree of vulnerability. A negative tracer test in a high vulnerability zone may not modify its attributes but requires further tracer tests in high water conditions.
2. Tracer tests permit improved delineation of the catchment (e.g. Cormoret) but a negative result should not result in the exclusion of this point from the catchment. However, a sinkhole will always remain a particularly vulnerable point for karst groundwater.
3. Even if areas of major tectonic activity are well investigated by geophysics methods such as VLF-R, it is difficult to conclusively distinguish varying degrees of fracture intensity from, or the presence of, en epikarst (Doerfliger et al., 1995).
4. It is difficult to calibrate the vulnerability weighting system. However, the results of calibration using four sites should be adequate when these sites are representative of the rest of the catchment.

5.2. La Font, Le Saivu and La Bâma catchment

The geography, geology and hydrogeology of this catchment was presented in Chapter 2.1.3. of Part II. The waters of La Font and La Saivu are used partially as artificial recharge to the alluvial aquifer of L'Allaine. Major pollution sources ere the agriculture natural or artificial fertilizers, two dump sites in the township of Bure and oil spills from eccidents.

Part of the catchment is located in France and as we did not have access to a topographic map of this part, we concentrated our effort on the part within Switzerland.

As for vulnerability mapping at St-Imier, the forested areas are directly assigned to the S2 groundwater protection category.

5.2.1. E, P and I attributes of La Font, Le Saivu and La Bâme catchment

a) Comments on the Epikarst map

The sinkholes and karrenfields have been assigned to E_1, dry valleys to E_2. The rest of the catchment is assigned E_3 (Figure 5.20).

Seven boreholes were performed as part of the COST 65 Action in the upper part of the karst aquifer (5 to 15 m). Based on this data, the epikarst appears to have a thickness from 2 to 9m. Its thickness varies from 2 to 9m between two boreholes 5m apart. Three of these boreholes are located north of the sinkhole near coordinate 257.000/567.000 next to the artificial shaft used to access to the karst network of La Milandrine. The others are situated in the zone between the two major aligned sinkholes near coordinates 256.800/567.100.

Using logs of boreholes drilled along the future N16 expressway, it appeers that there is an epparent epikarst as the upper part is variably fissured. But it is difficult to quantify the intensity of epikarst development and the kind of connections that may exist with the karst network. At the present time, the morphological approach to the epikarst does not contradict the information from the boreholes. Boreholes in the zones of the major dolines have a high degree of fracturing in their upper parts. Some boreholes in the forested areas north of the major sinkholes (around 258.000/567.000) have a high fractured upper zone as epikarst. This is in spite of the fact that they are not associated with specific morphologicel features such as sinkholes or dry velleys (NEB 18, NEB 19, NEB 17 tor example, Figure 5.21 and Table 5.4.). But, they ere situated on a surface manifestation of a major regional tault, in the extension of the alignment of two major sinkholes.

Table 5.4.
Epikarst characteristica uaing boreholes log

Borehole code	coord. X	coord. y	elevation (m. a.s.l)	epikarst comments
VGC4	566609	259272	411.2	extremely fractured limestone to 6.6m
VGC5	566672	259124	444.7	highly fractures rock to 4m with silt-gravel matrix
VGC6	566734	259032	455.2	medium fractured rock
NEB15	566823	258784	471.6	medium fractured rock
NEB16	566905	258590	486.2	medium to highly fractured rock, with marls from a karst filling
NEB17	566955	258377	490.1	medium fractured rock
NEB18	567015	258068	519.1	highly fractured rock with vertical fractures to 6 m.
NEB19	567064	257893	529.1	highly fractured rock, sub horizontal to oblique fractures
NEB20	567084	257685	540.7	weathering evidence to 2.4m
NEB21	567101	257505	518.4	highly weathered chalky limestone to 2.15m, then extremely fractured rock
NEB22	567152	257404	513.5	to 510.10, highly weathered limestone
NEB6	566984	257366	534.8	medium fractured rock
NEB10	567141	257332	515.7	medium fractured rock
NEB7	566975	257258	517.3	medium to highly fractured rock
NEB11	567251	257151	521.7	medium to highly fractured rock to 4m, karst features at -6m.
NEB8	566985	257149	529.3	medium to highly fractured rock
NEB23	567215	257015	529.9	highly to extreme fractured rock
NEB12	567300	256986	538.7	medium fractured rock
MIL4	567078	256870	523.7	fissured limestone (without other information)
NEB9	566971	256850	523.0	medium fractured rock
MIL9	566954	256635	530.7	fissured limestone (without other information)
MIL2	567056	256586	521.0	fissured limestone (without other information)
MIL3	567056	256583	520.9	fissured limestone (without other information)
FN2	567102	256578	523.7	fissured limestone to 10m, then limestone with soil-filled fissures
FN1	567178	256538	526.5	medium fractured rock
COB4	567457	256520	530.4	no observation regarding the fissuring
COB5	567496	256300	535.4	medium fractured rock
DMF1	567589	256016	540.4	clay limestone
DMF2	567646	255777	542.9	highly fractured rock to 12m.

b) Comments on the Protective cover map

Some 90 holes drilled with a hand-auger were done to evaluate the thickness of the protective cover, including soil and quaternary layers such as loess.

The quaternary layers ware not differentiated from soil as they are essentially loess. No area was mapped as P4 although local loess layers can be up to 10m thick based on borehole logs. Extrapolating from these data had ambiguous results (Table 5.5.)

It appears that there is a large variability in the thickness and it is necessary to be aware that there are limits associated with extrapolating the data from the hand-auger holes. The resulting map ot the protective cover attribute has inaccurate limits between aach class.

A single area if the northarn part of tha catchmant is classifiad as P1 and more than half of the catchment is classitied as P2 (Figure 5.22).

Table 5.5.
Protective cover and ita thicknesa derived from boreholes.

Borehole code	coord. X	coord. y	elevation (m. a.s.l)	Thick. soil (m)	Other layer	Thickness (m)	Lithology
VGC4	566609	259272	411.2	1.6		1.6	dirt and loess
VGC5	566672	259124	444.7	0.5		0.5	dirt and loess
VGC6	566734	259032	455.2	0.9		0.9	dirt and loess
NEB15	566823	258764	471.6	1.00		1.00	dirt and loess
NEB16	566905	258590	486.2	0.7		0.7	dirt and clay silt
NEB17	566955	258377	490.1	2.1		2.1	dirt and clay silt (loess)
NEB18	567015	258088	519.1	0.30	3.50	3.8	dirt above calcareous gravel from the Rauracian
NEB19	567064	257893	529.1	0.40	1.50	1.9	dirt above calcareous gravel (weathering zone)
NEB20	567084	257685	540.7	0.3		0.3	dirt with calcareous gravel
NEB21	567101	257505	518.4	0.6	1.00	1.6	dirt and loess and calc. gravel.
NEB22	567152	257404	513.5	0.9		0.9	dirt and calc. gravel. in silt matter.
NEB6	566984	257366	534.8	2.5		2.5	dirt and clay silt
NEB10	567141	257332	515.7	1.3		1.3	dirt and clay silt
NEB7	566975	257258	517.3	5.75		5.75	dirt and clay silt
NEB11	567251	257151	521.7	1.5		1.5	dirt and clay silt
NEB8	566985	257149	529.3	0.4		0.4	dirt
NEB23	567215	257015	529.9	0.7		0.7	dirt and clay silt
NEB12	567300	256986	538.7	0.6		0.6	dirt and clay silt
MIL4	567078	256870	523.7	0.3		0.3	clay dirt
NEB9	566971	256850	523.0	1.6		1.6	dirt and clay silt
MIL9	566954	256635	530.7	0.2		0.2	dirt
MIL2	567056	256586	521.0	2.5		2.5	dirt
MIL3	567056	256583	520.9	3.2		3.2	clay dirt
FN2	567102	256578	523.7	0.25	2.00	2.25	dirt on biodetridal limestone in silt matrix
FN1	567178	256538	526.5	5.5		5.5	dirt and clay silt
COB4	567457	256520	530.4	1.3		1.3	dirt and clay silt
COB5	567496	256300	535.4	0.7		0.7	loess
DMF1	567589	256016	540.4	1.4		1.4	dirt and clay silt (loess)
DMF2	567646	255777	542.9	6.9	3.4	10.3	dirt on loess to 6.9m,then silt gravel.

c) Comments on the Infiltration conditions map

As there is no stream nor losing stream in the catchment, the only difference to be made was between araas of I_3 and I_4. With e numerical elevation model and aerial photographs (1:10'000 and 1:25'000), the I_3 and I_4 classes of the infiltration conditions were mapped taking into eccount the slope intensity higher than 10 percent as major fields are potentially cultivatad (Figure 5.23).

5.2.2. Characterization of the Milandrine aquifer karst network development

The karst network of the Milandrine aquifer or of the catchment of the La Font, Le Saivu and La Bâme springs exist with 9km of cavities mapped by the Jura Speleological club (Figure 5.24). According to Maréchal (1994) the fractal dimension of the Milandrine karst network is lower than 2, corresponding to low complaxity and density. The total cross sectional area of all network conduits rangas from 0.04 to 126 m^2. The highest value corresponds to a large room with a ceiling collapse. Commonly, the sizes are from 2 to 4 m^2. Normally it would be tha sections between 2 and 0.05 m^2 that are rather difficult to measure as well as to explore. Plotting the sections and the sum of the length of the galleries whose sections are higher than the various measured sections on log-log paper allows extrapolation of the real extension of the karst network (Curl, 1986, Maréchal, 1994). This leads to 43 km total length for the galleries. The explored part of the karst network has a tree-like structure that is not well developed. From this viewpoint, the karst network development is assigned to K_1.

Comparing the hydrograph of the upper Milandrine in the karst network and the precipitation during the same hydrological cycle allows monitoring the rapid and abrupt responses of the spring following rains (less than 12 hours) (Figure 5.25). Using hydrological cycles of the upper Milandrine (18.4 to 1.6.1990/ 5.7 to 22.9.1990/ 16.5 to 5.10.1991/ 21.7 to 29.8.1992 / 22.6 to 20.8.1993) Grasso & Jeannin (1994) classified the unexplored karst system according to the Mangin method (1975) with the characteristic K and i parameters in classes II and III. The upper part of the network has higher connectivity compared to the lower part closer to the spring where it is more saturated. From the hydrograph as well as the cave system information, the karst network development of the Milandrine aquifer is assigned to K_1.

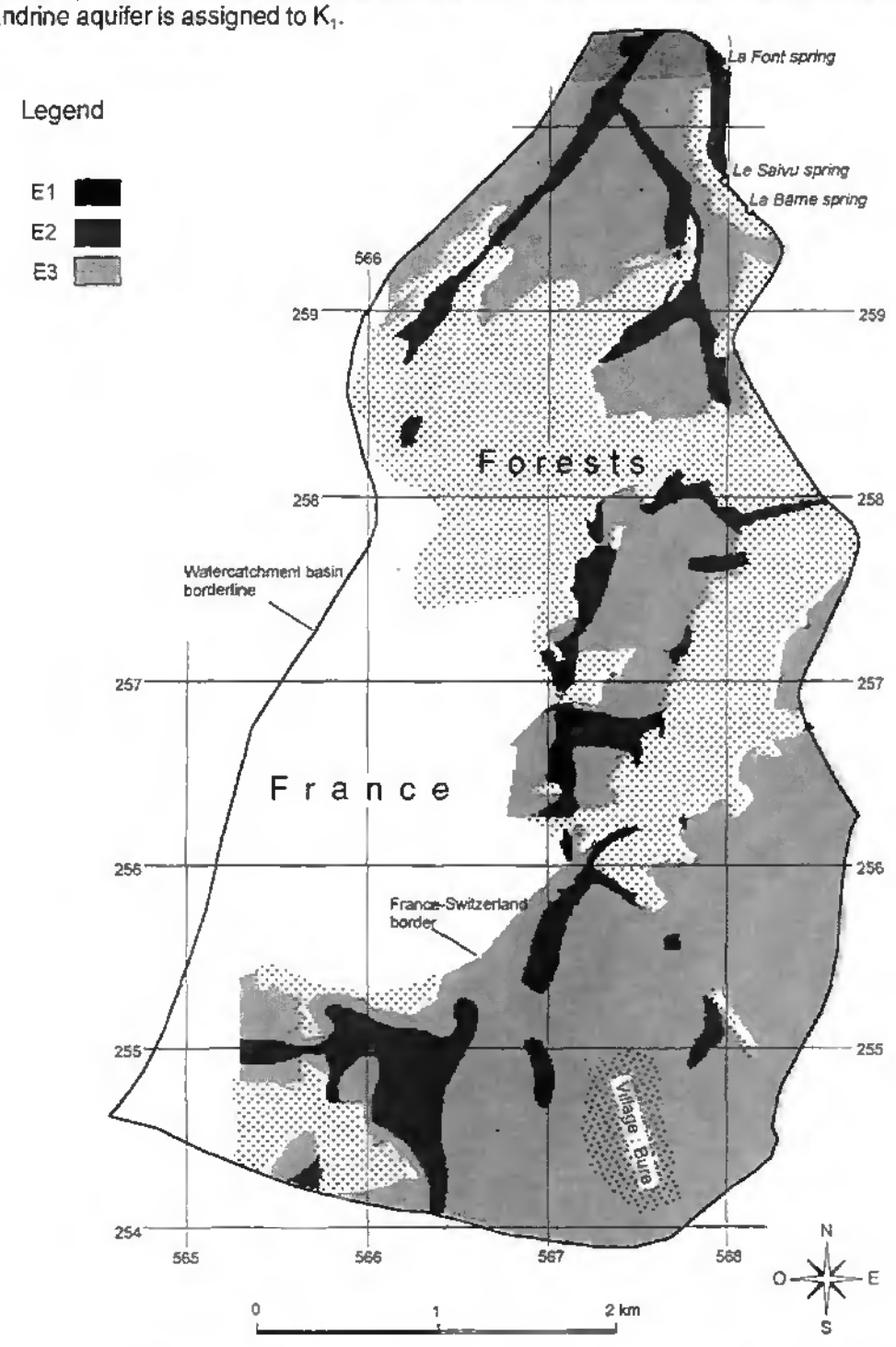

Figure 5.20: Epikarst attribute map of La Font, Le Saivu and La Bâme catchment (modified after Tâche et al., 1996)

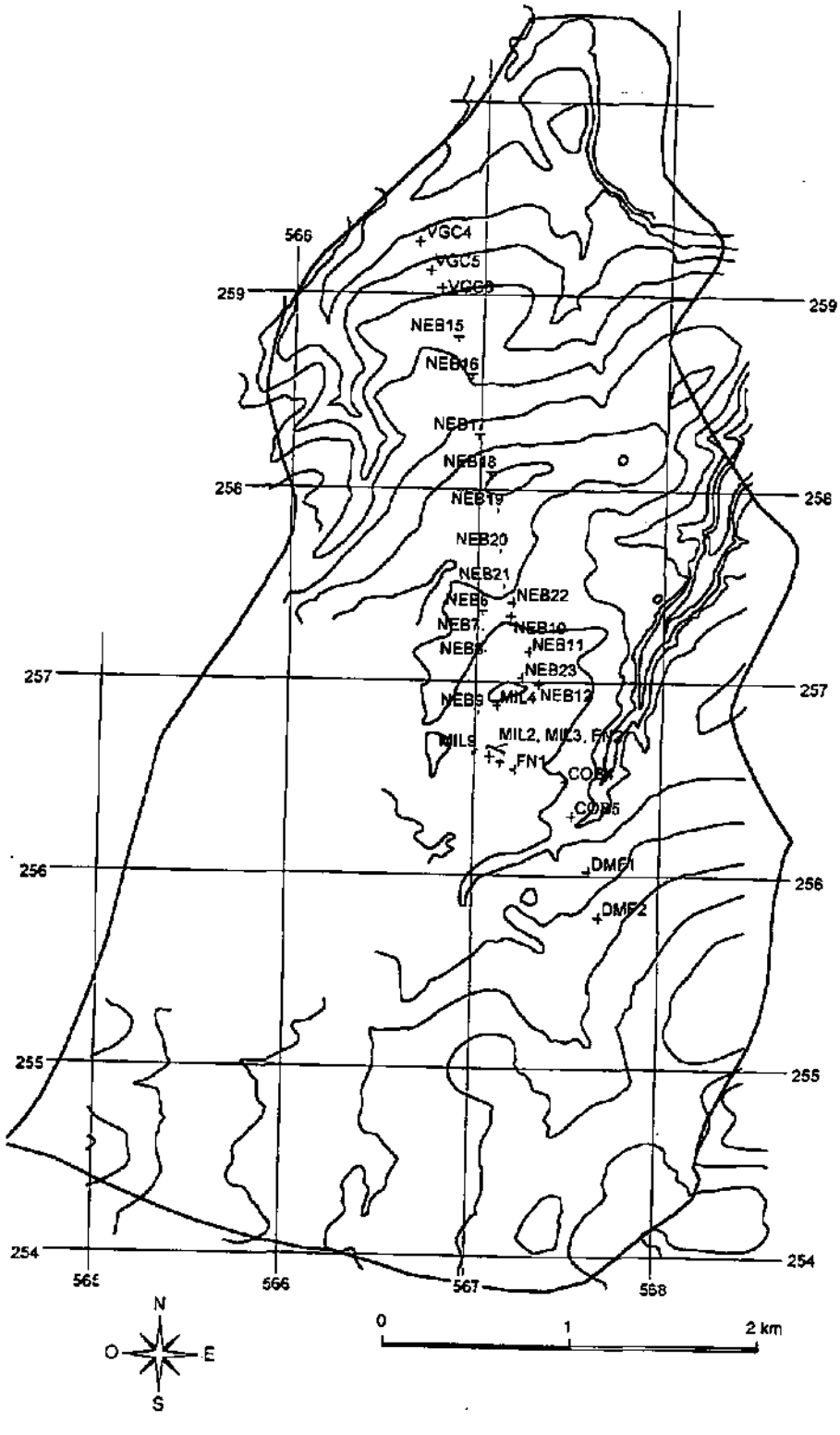

Figure 5.21.: Location of major boreholes in La Font, Le Saivu and La Bâme catchment (Doerfliger et al., 1995).

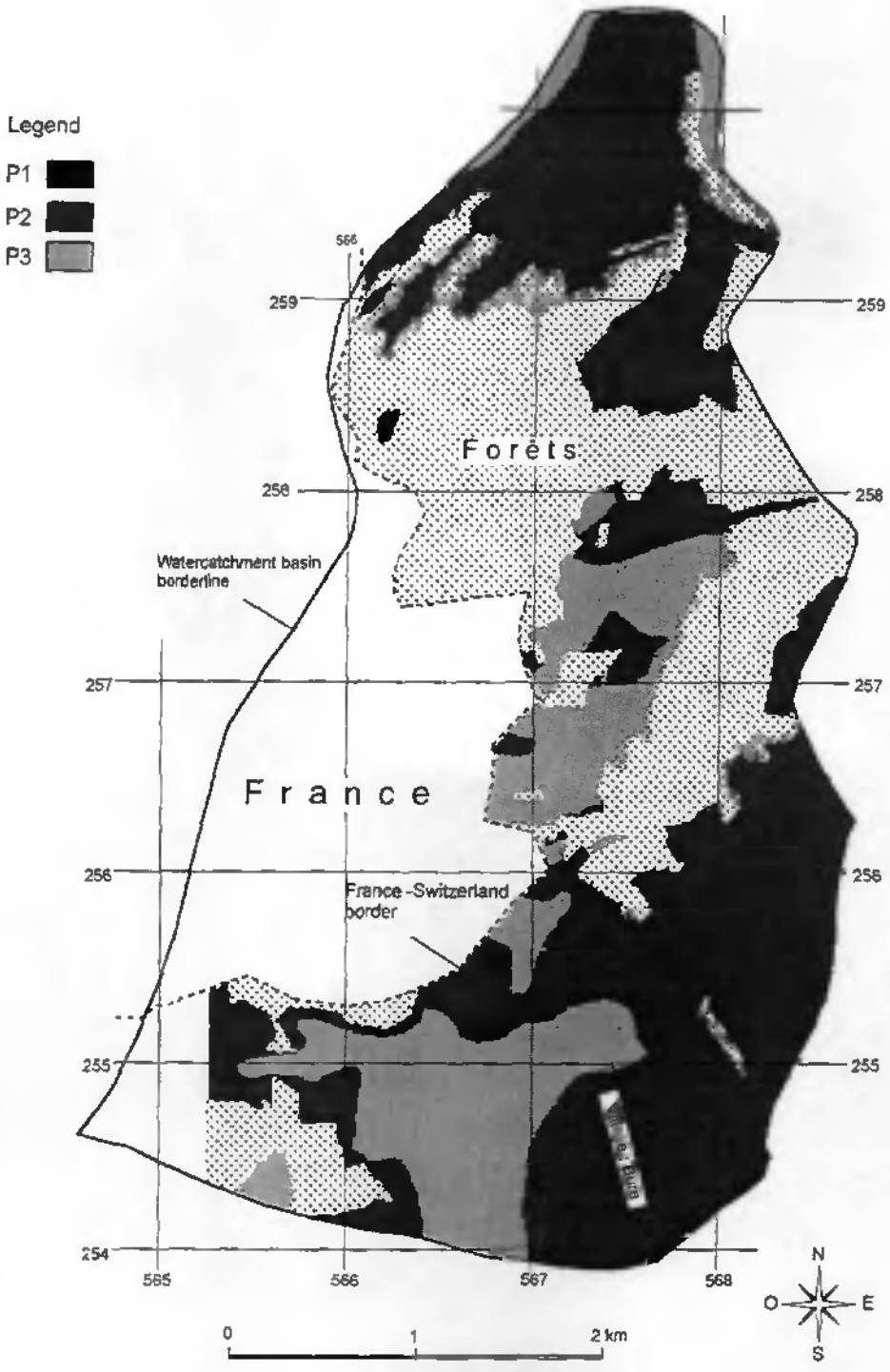

Figure 5.22.: Protective cover attribute map of La Font, Le Saivu and La Bâme catchment (modified after Tâche et al., 1996).

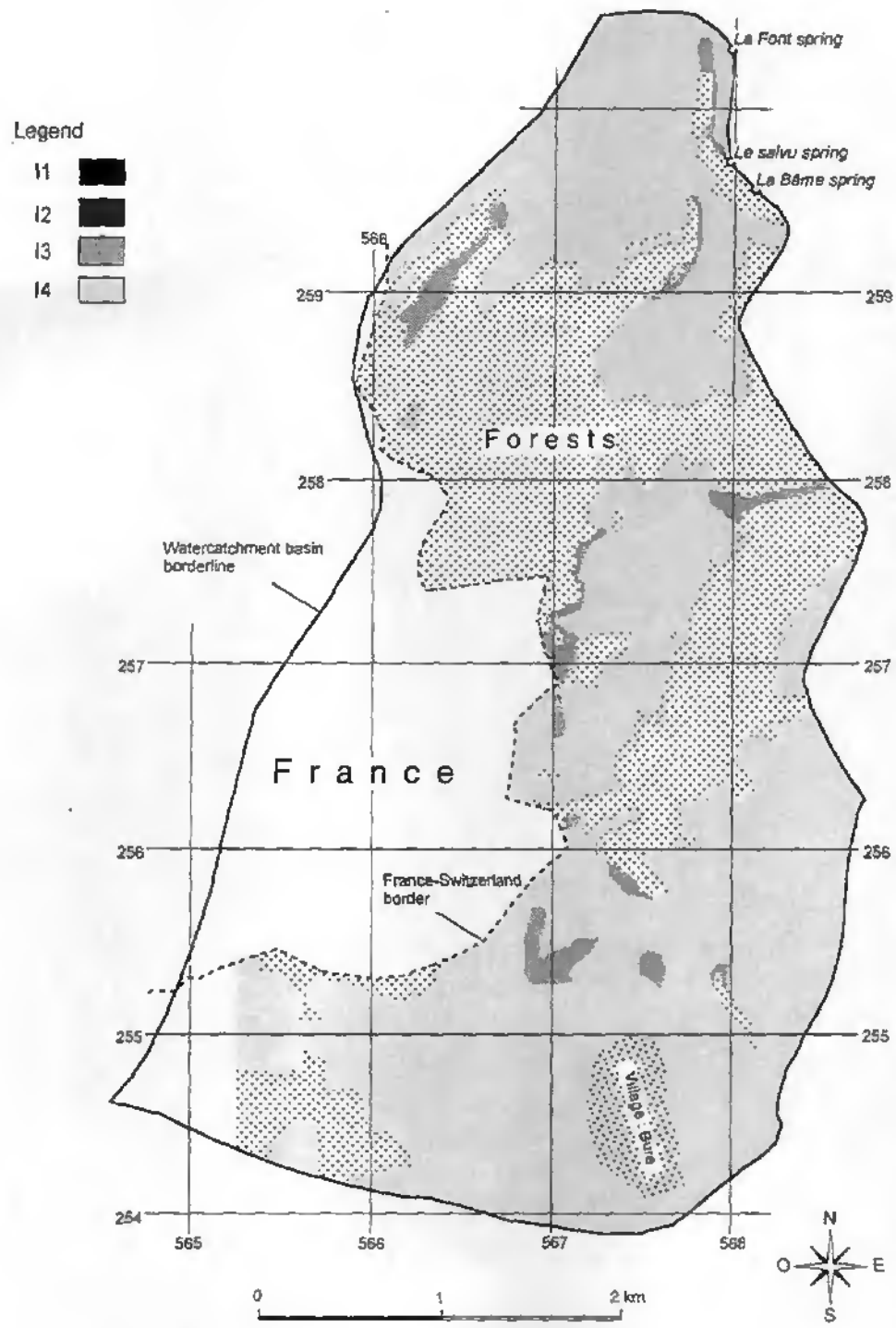

Figure 5.23.: Infiltration conditions attribute map of La Font, Le Saivu and La Bâme catchment (modified after Tâche et al., 1996).

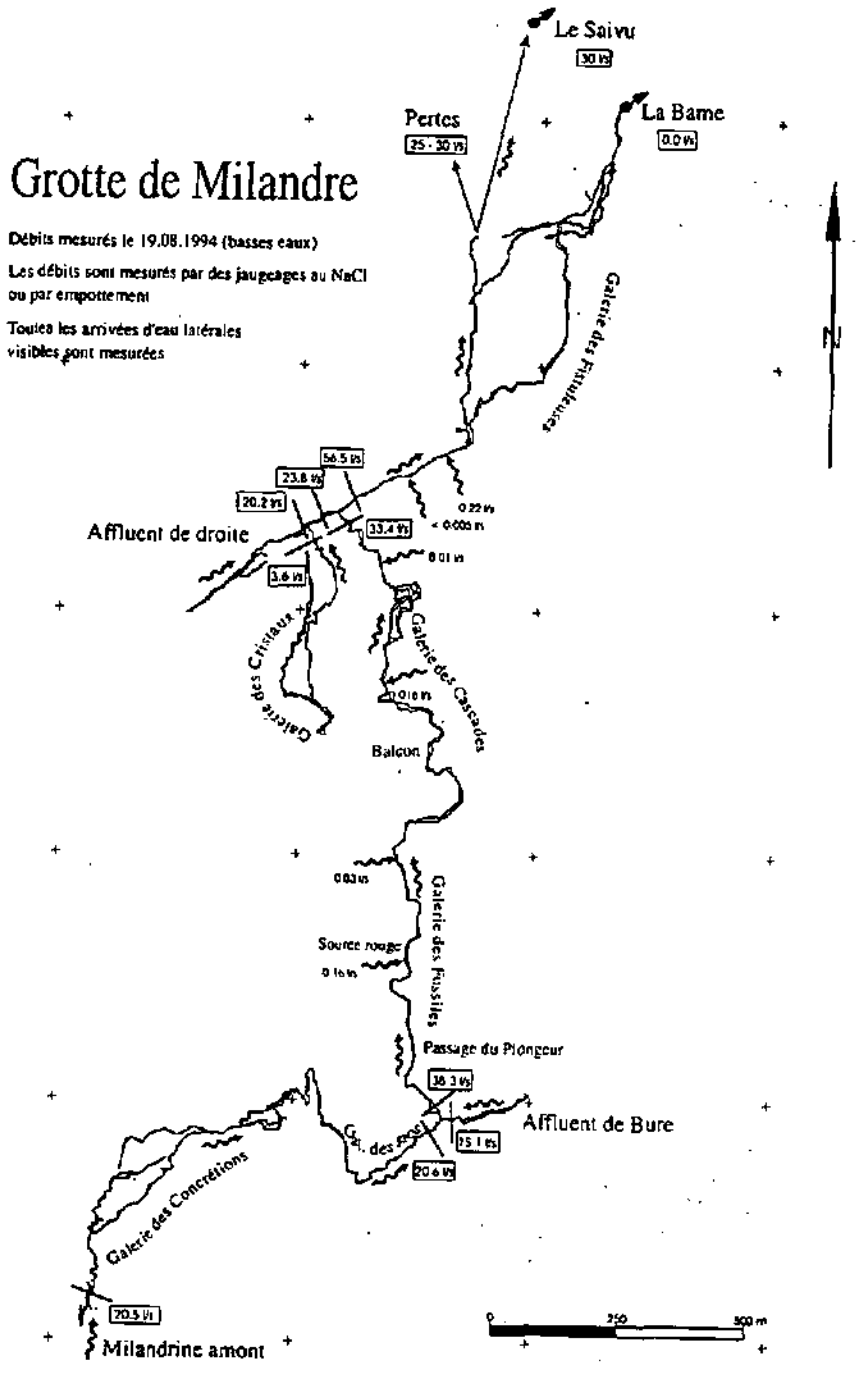

Figure 5.24.: Karst network of La Milandrine - plan map (Grasso & Jeannin, 1994).

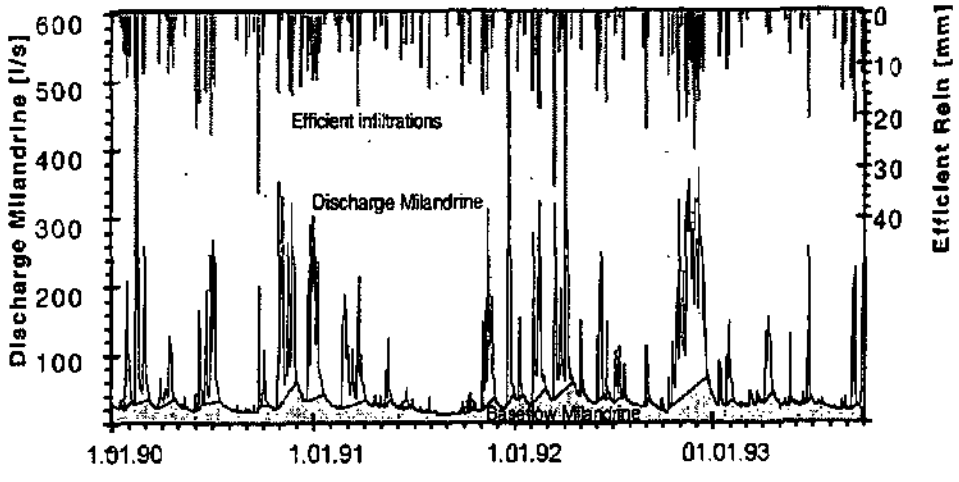

Figure 5.25.: Relation Efficient precipitation and discharge of the upper Milandrine (Grasso & Jeannin, 1995).

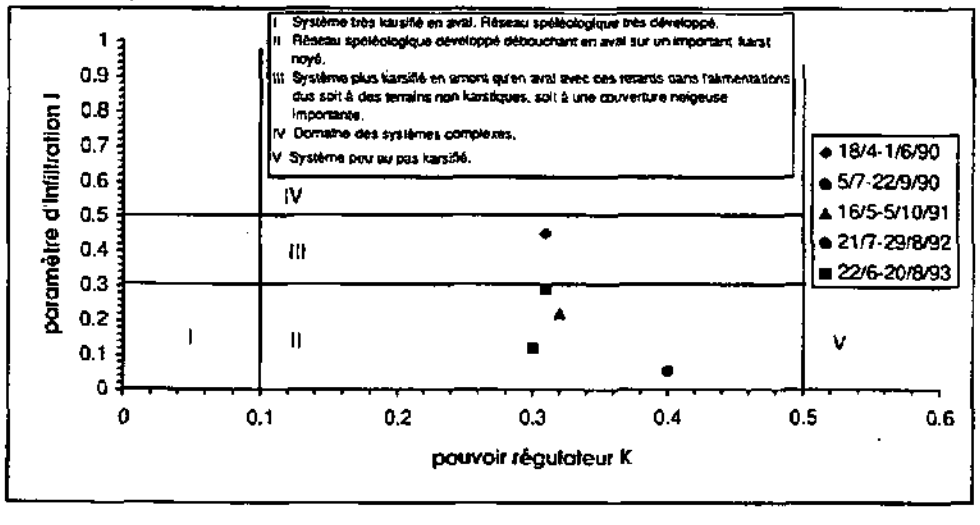

Figure 5.26.: Classification of the upper part of the La Milandrine hydrograph for different cycles (after Mangin (1975) (in Grasso and Jeannin, 1994)).

5.2.3. Vulnerability map for La Font, Le Saivu and La Bâme catchment

As there are no swallowholes or surface streams in the catchment, the sinkholes are the least protected points. Their protection factor ranges from 17/29 for the dolines located at the foot of steep slopes to 20/29 for those with low relief. Although there is a major protective cover with more than 1m of soil (P_3), the sinkhole that is directly connected to the karst network (567.000/257.000) has low protection. It is apparently one of the most vulnerable points in the whole catchment.

The dry valleys that are both clearly evident on topographic maps (22/29) and have thick protective cover (26/279 have medium vulnerability.

Finally the zones with a protection factor that is higher than 26 (27 to 29) correspond to the less vulnerable areas (E_3 - P_3 - I_4) for example (Figure 5.27) (Tâche et al., 1996).

5.2.4. Validation tests on vulnerability zones in the La Font, Le Saivu and La Bâme catchment.

Carrying out validetion tests on zones of varying vulnerability in this catchment refers to the use of available data from tracer tests (Part II) and from geophysical investigations (Turberg, 1993, Veiga,1995). Transfer functions are useful in such tests.
Concerning tracer tests, we considered only those done from the surface, as tracer tests in boreholes only partially reflect groundwater vulnerability. Transfer to the unsaturated zone is very often subtracted.
The applicable tracing tests are: T1amont (artificial hole), T2amont (artificial hole), T30amont, T34amont, T35amont, T39amont and T41amont (Figure 5.28). They are located in the preferentially high vulnerability zones with values of protection factor ranging from 17 to 20. The tracer tests T39amont and T34amont are located in zones protection factors of 27. Tracer test T35 was in a border zone between a 25 sector and a 17 sector. For these tests, we expect to have steep normalized responses, except for the T39amont and T34amont. They are situated in fault zones or on the border of such a tectonics accident zone according to the geological model resulting of radio-magnetotelluric investigations carried out by Turberg ,1993. Tracer tests T1 and T2 are situated side by side in a conductive zone corresponding to a major North-South fault.
The highest vulnerability zone (protection value 15) are validated with very steep normalized responses as shown in figure 5.28 (T41). This corresponds to an injection in the still active sinkhole (regular hole opening by collapsing of the soil) near the artificial entrance to the Milandrine underground network. The normalized responses of the T1 and T2 tests have a gradient at 0.5 percentile that tends more to 60 degrees than 90 degrees as test T41 does. This reflects transit through the fault zone characterized with karst clay providing a good contrast of resistivity. The same phenomena probably influences the normalized responses of test T35 and T30, whose injection points are located along the same N-S fault zone. These results do not contradict medium vulnerability designation.

The normalized responses of the tests T34 and T39, injected in low vulnerability zones (using the EPIK approach), should have a slope at 0.5 percentile that tends more to 60 degrees (1) than 90 degrees (0). However, the opposite was observed as shown on Figure 5.28. Near this major fault zone, the epikarst is certainly developed even if no specific morphological features are evident. A zone of 100 to 200m to each side of this zone should be assigned E_2 or E_1 for the Epikarst attribute.

Only one tracing test was done into a surface point in a low vulnerability area (29); this area is characterized with red clay soil thicker than 1m. Unfortunately, there was no tracer recovery at the upper Milandrine measurement point.

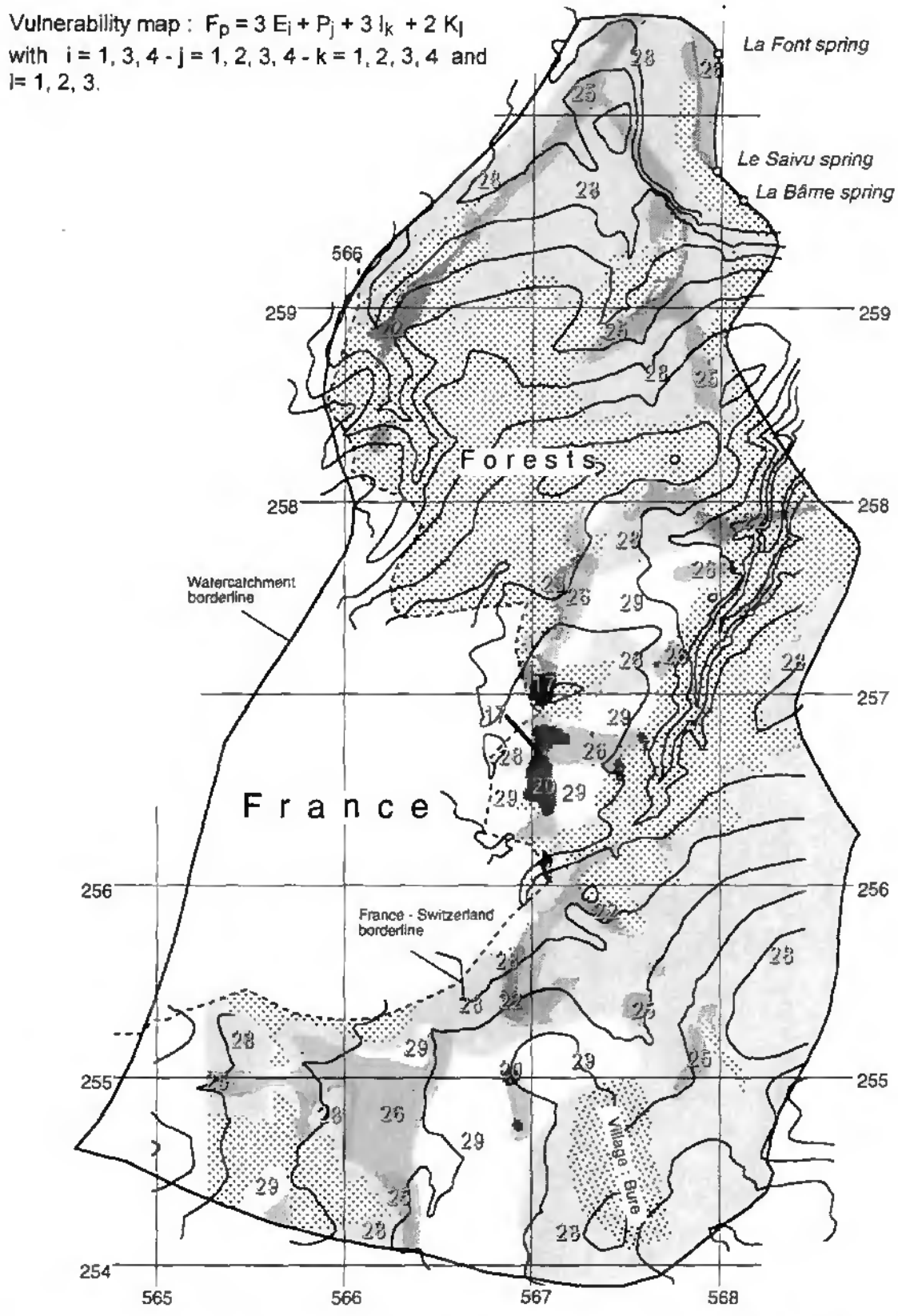

Figure 5.27: Vulnerability map of La Font, Le Saivu and La Bâme catchment (modified after Tâche et al., 1996).

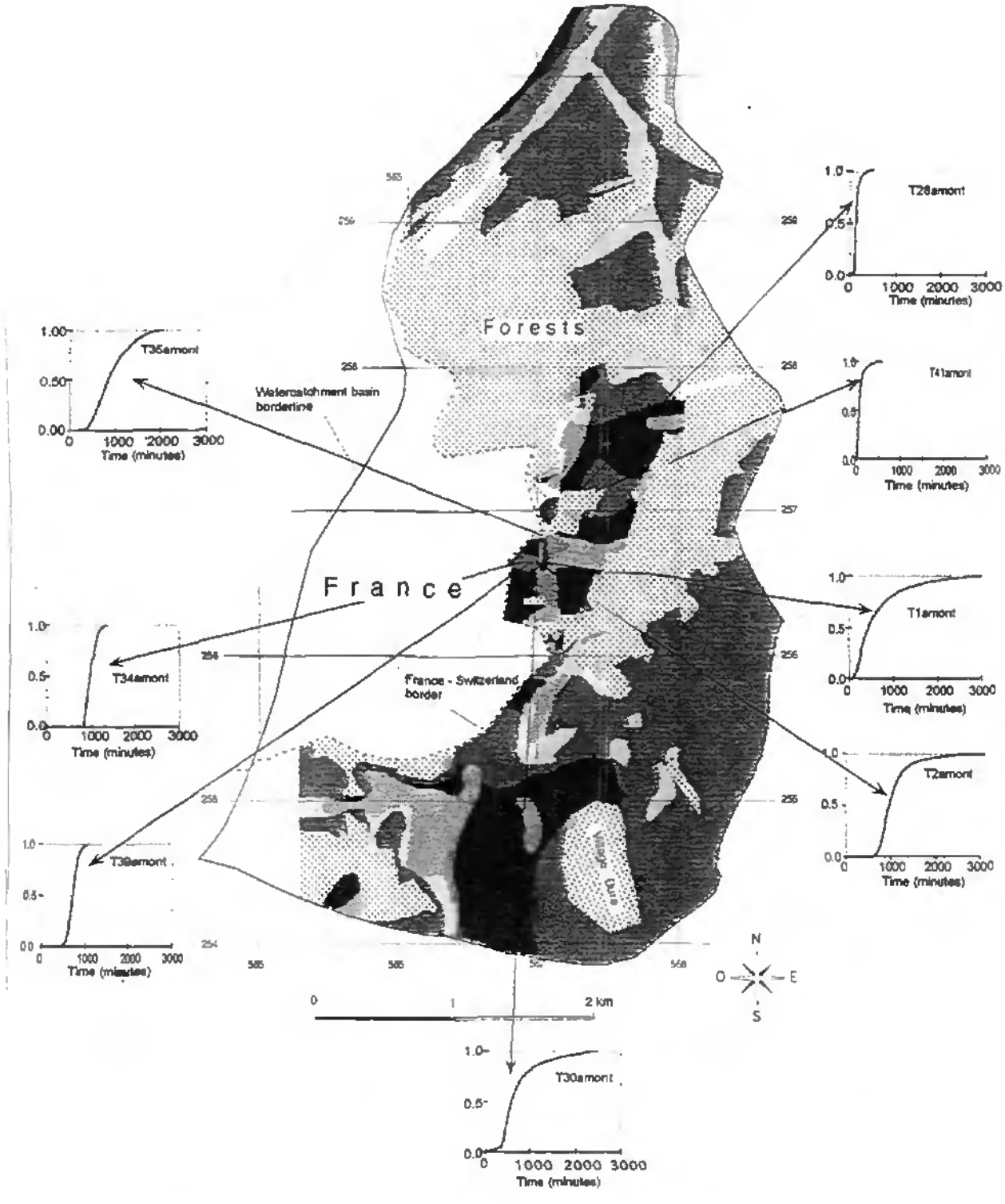

Figure 5.28: Locations of surface injection tracing tests and corresponding normalized responses in the La Font, Le Saivu and La Bâme springs catchment.

Chapter 6

From vulnerability maps to protection zones maps

6.1. Introduction

A vulnerability map is used to outline the groundwater protection zones according to their definition. Taking into account the degree of the karst network development, for each case we can suggest possible equivalents between the vulnerability values and groundwater protection zones.

6.2. Groundwater protection maps of St-Imier and Le Maira-Bure

6.2.1. Groundwater protection at St-Imier (Tâche et al., 1996).

The following relationships have been developed between the attributes end groundwater protection zones:

- swallowholes and losing streams supplying them have to be designated S1 (protection factor from 9 and 20).

- groundweter protection areas S1 or S2 are attributed to sinkholes, karrenfields and cuestas (protection factor from 15 to 20).

- zones with E2 or I3 heve to be essigned groundwater protection S2 (protection factor from 18 to 27).

Teking into consideration that the karst network development is well developed (K1), we suggest assigning the following protection factors to the protection zones:

S1= protection factors between 9 end 19

S2= protection factors between 20 and 25

S3= protection factors between 26 and 29

We also considered some additional restrictions such es the sectors in I1 heve to be attributed to S1 independently of their protection factor higher than 19 (e.g. Losing stream and its banks, protection factor of 20).

Figure 6.1 shows the great majority ot sinkholes, karrenfields and cuestas ere in S1 zone and the most sectors in E2 or I3 are in S2 zone. The low vulnerability areas are generally characterized by a thick protective cover end are located away from concentrated intiltration zones or strong karst features. They are logically in S3.

Figure 6.1 makes it possible to visualize the proposed limits of the protection zones S1 through S3 of the catchment. The comparison between the previous protection zones end the present ones show that the EPIK-derived protection zones S1 and S2 are clearly more abundant at the scale of the besin in comparison to Figure 5.3. This should ellow implementing more effective restrictions with regard to the land use.

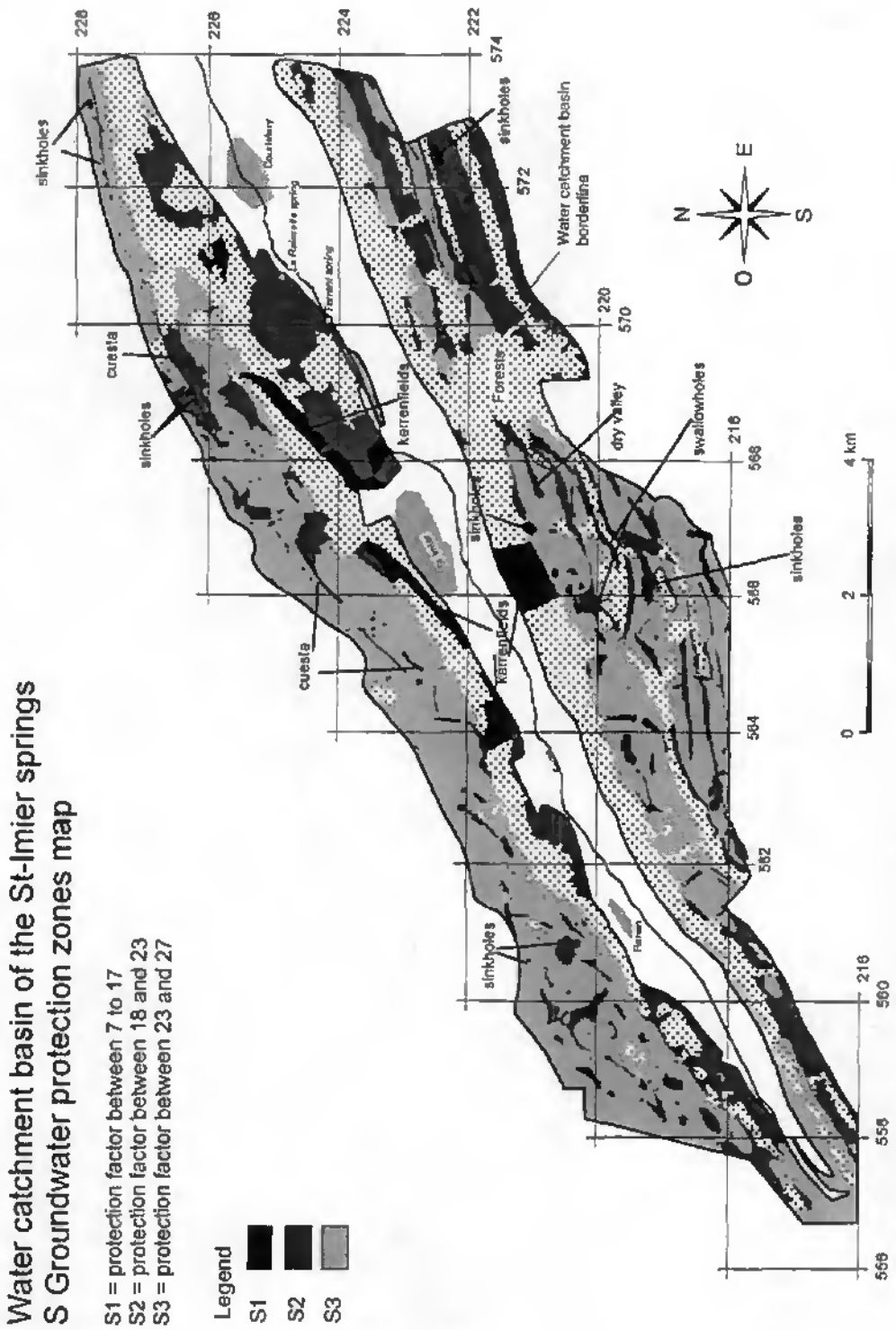

Figure 6.1.: Groundwater protection zones at St-Imier (modified after Tâche et al., 1996).

6.2.2. Groundwater protection of Le Saivu, La Font and Bâme catchment (Tâche et al., 1996).

As the karst network is well developed (K1), the major sinkhole connected to the Milandrina (protection factor of 17) has to be listed as a S1 groundwater protection zone.

The dry valleys that are generally connected to the low topographical zones and the slopes whose runoff water is supplied to them (protaction factor between 22 and 26) have to be listed as S2.

The sectors with a protection factor higher than 26 should be listed as S3.

According to thasa observations, tha equivalance groundwater protection zones - vulnerability classes are listed as following (Figure 6.2):

S1 = protection factor equal to 19

S2 = protection factor between 20 and 28

S3 = protection factor between 28 and 31.

6.3. Conclusions

From vulnerability maps, it is possibla to outline groundwater protection zones taking into account statements regarding the goals of the groundwater protection zone to be attained. The statemants are the following:

S1 at least swallowholes and losing streams.

S1 or S2 : sinkholes, karrenfields and cuestas

S2 preferred to S3 for areas with E2 or I3

AS for protection valuas higher than 28, assuming the presence of P4.

According to the two above examples of groundwater protection maps established from EPIK vulnerability maps, thera is no automatic correlation between protaction factors and S protection zones. The protection factors assigned to each S zone do not differ markedly in the two examplas. The difference refers to natural conditions in that particular karst anvironment (loosing streams) that influences the protection factor (low and high limit of the range). At present, using the above rasults, the correlation is:

S1 = protection factor lowar than 18 $\pm$2

S2 = protection factor between 19 $\pm$2 and 24 $\pm$2

S3 = protaction factor between 25 $\pm$2 and 29

AS = protection factor higher than 29

Furthermore, there is a distinct advantage in not having an automated approach to correlate the protection factors and zones. Using site-specitic fiald verification results in a more meaningful , valldity in the vulnerability of aach catchment part.

Finally the Karst network development degree attribute may also influence this equivalence. This was the case in the two above examples where the K attribute was K1. However, further tests on other karst hydrogeological settings will justify the need for this attribute.

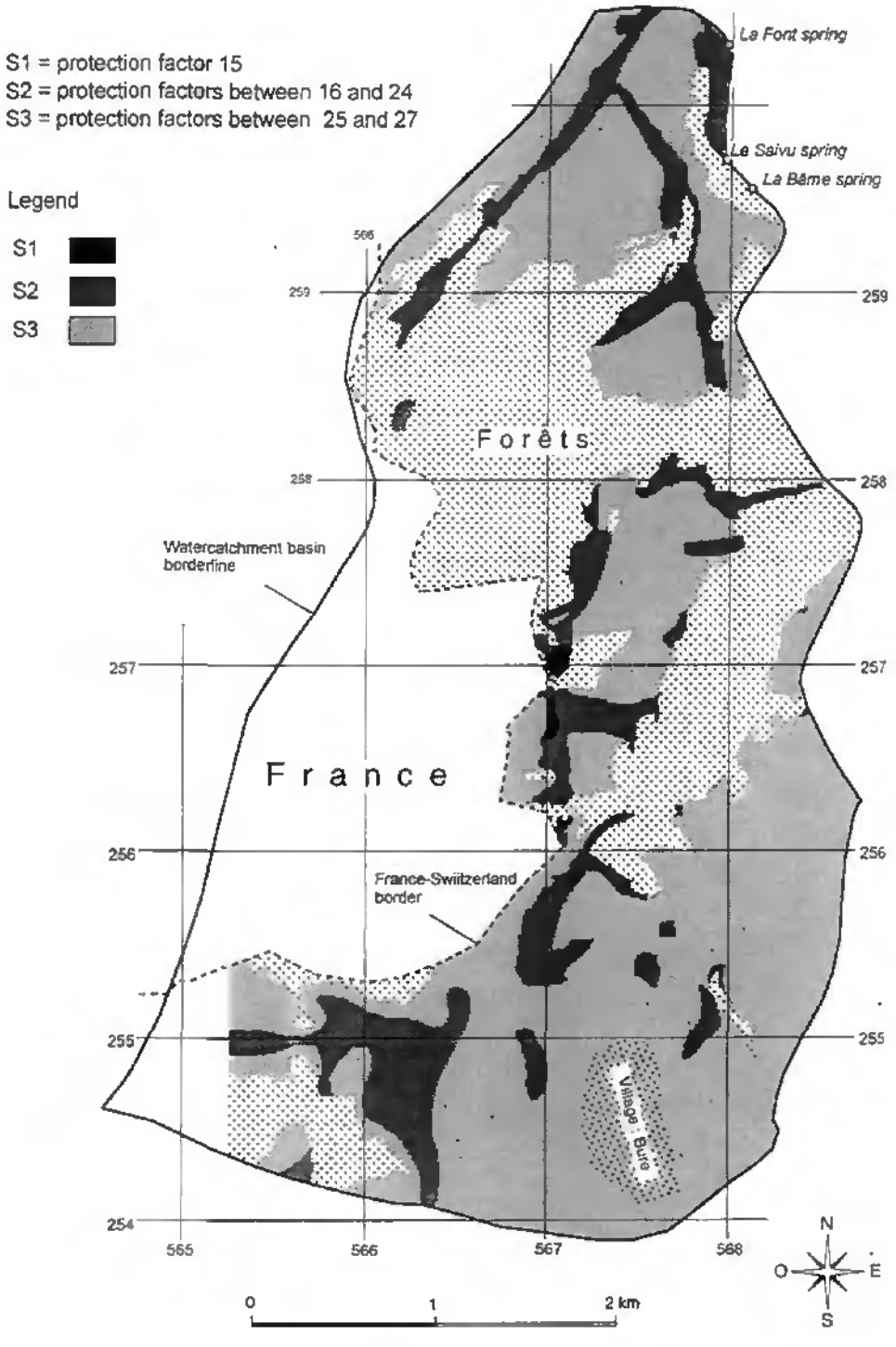

Figure 6.2. Groundwater protection zones of La Font, Le Saivu and La Bâme springs catchment (modified after Tâche et al., 1996).

Chapter 7

Comments and conclusion

The use of attributes that taka into account how a karst aquifer functions, such as the epikarst through its morphological features, the protective cover, the infiltration conditions and the development of the karst network, makas it possible to obtain maps that represent the vulnerability ot karst catchment (Doerfliger & Zwahlen, 1995). The EPIK method allows outlining protection zonas that are consistent with the hydrogaological behavior of karst aquifers. If proves that it is teasible to contribute to a better protection of karst groundwater.

Nevertheless, although tha concept underlying these new vulnerability maps is becoming clearer today, further developments are still needed to fully appreciate its pertinence, specifically regarding the epikarst and the protective cover attributes. The epikarst is still tha mathod's weak point.

The usa of a geographic intormation systam (GIS) for the examples of St-Imier and Bure has also made it possible to test the sensitivity of the various weighting systems and to simplify synthesis of vulnerability maps.

Validating vulnerability zones remains difficult. For future research, in order to evaluate the sensitivity of the weighting systems, specific distribution curves for each attribute by class should be established and also generally applied to the catchment. This may indicate if it is appliceble to the overall spatial heteroganeity and ba a means to validate the weighting system. The validation require further improvements and a more scientific basis.

Vulnerability mapping combined with potential hazard mapping of a catchment will provide appropriate tools to outline tha protection zones and astablish appropriate corrasponding regulations.

General conclusions

Karst aquifers are characterized by a highly heterogeneous structure with diffuse or concentrated surface recharge. Therefore, contaminants may be released as point-sources or diffusely into the karst aquifer with various consequences that affect aquifer water quality.

Tharafore, karst aquifers requires a specific groundwater protection stratagy. The results of this study contribute to the development of this strategy and are presented in this section.

Further parspectives ara also suggested for interpreting artificial tracer tests and vulnerability mapping in karst environment.

The contribution of tracer test input-response interpretation to karst groundwater protection :

Can we forecast the effects of point-source contamination using transfer functions?

Preliminary remarks: only artificial tracers considered as ideal tracers were used to determine the transfer functions. In karst aquifers, uranine and sulfurhodamine G extra are relatively ideal. Bacteriophages behave differently according to their different structures and can be adsorbed. Thus, the transfer functions also reflect tha processes of advection and dispersion which can be applicable to contaminants such as hydrocarbons and pesticides. Heavy metals are sensitive to the sorption and to degradation. Therefore, transfar functions follow the worst case scenario of point-source contamination in karst aquifers. Our study of transfer function variability is not exhaustive. Tracer tests are not adequate enough to allow a good statistical distribution. However, within the scope of hydrogeological impact assessments, the statistical sample size and distribution are often much worse due to lack of funding to develop good hydrogeological information.

- From an economic viewpoint, we would like to determine the characteristic mean transfer functions for a catchment identified by soma dafined paramaters such as size, mean transit distance, degree of karst system development, aquifer thickness, nature of the injection site and hydrological conditions. But, such functions do not exist! No significant differences betwean these parameters exist. Nevertheless, mean transfer functions from tracer tests which correspond to geological contexts or injection point types can be ditterentiated. Karst aquifers in the Jura and in the Alps have different historical development (Jeannin, 1996), and their is a significant difference evident in their transfer functions.

  From experimental tracer tests, mean transfer functions with 95 percent confidence intervals were calculated for the Alps, the Jura, various injection points in the Tabular Jura and for different hydraulic conductivity. The mean transfer function were treated as normalized responses to obtain their corresponding impulse responses.

  Transfer functions are principally influenced by type of injection site. The Alps and Jura geological context mean transfer functions do not have a representative and meaningful breekthrough curves for e given input function for all possible locations and aquifers. We established limitations in the use of these mean transfer functions for contaminant simulations based on a mathematical convolution operation.

For the Alps mean transfer function, it can be manipulated by convolution to simulate a forecast only for the effect of an accidental injection from a swallowhole. In this case, the spring is on average 5000 meters away from the injection point in well karstified aquifers of about 500m in thickness. The mean discharge of the spring is 300'000 l/min. The hydrological conditions are in base flow's recession. Based on the experimental results, this mean transfer function does not allow input-response transport simulation in tracer system when the release occurs from a borehole or sinkhole. For smaller distances, we also cannot recommend the application of a mean transfer function. The results of the simulation of an input equal to a mass of 750kg injected during 15 minutes (right triangle as input shape) are in Figure 1.

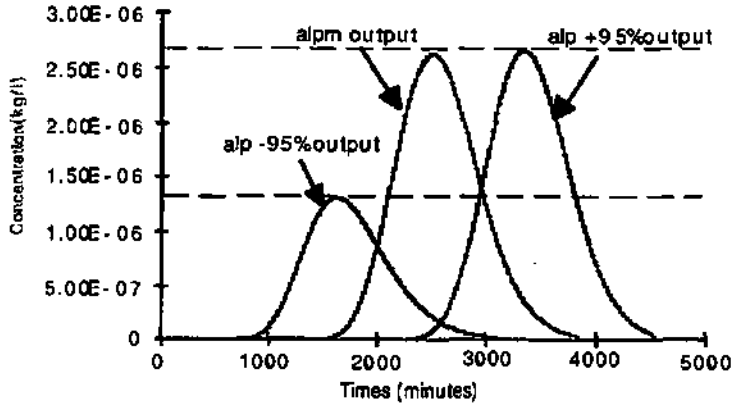

Figure 1.: Simulated breakthrough curves obtained by convolution of the Alps mean impulse response with the input function. (alpmoutput: recovery curve with mean impulse response; alp+-95%output recovery curve with the +or-95% confidence interval impulse response).

Figure 1. shows that from a pessimistic viewpoint, it is necessary to double the peak concentration. The three curves give their maximum time and modal time, the time to react to a contaminant release and if necessary, immediately turn off the water supply.

For the Jura, the mean transfer is calculated with a large number of experimental transfer functions. The simulated recovery curve for the same mass injected as was the case in the Alps has an error of 10%. This is considered to represent the response of a contaminant injected in an artificial hole or borehole in the Tabular Jura (60m thickness, well karstified aquifer) with a tracer distance of less than 3000m and a discharge rate about 3600 l/min (Figure 2). But these resulting curves for an equivalent discharge are not the same as from tracer tests performed in a swallowhole with a distance of more than 5000m from the spring done in either the Tabular or Folded Jura. The peak concentration, the maximum time and the modal time can be completely different.

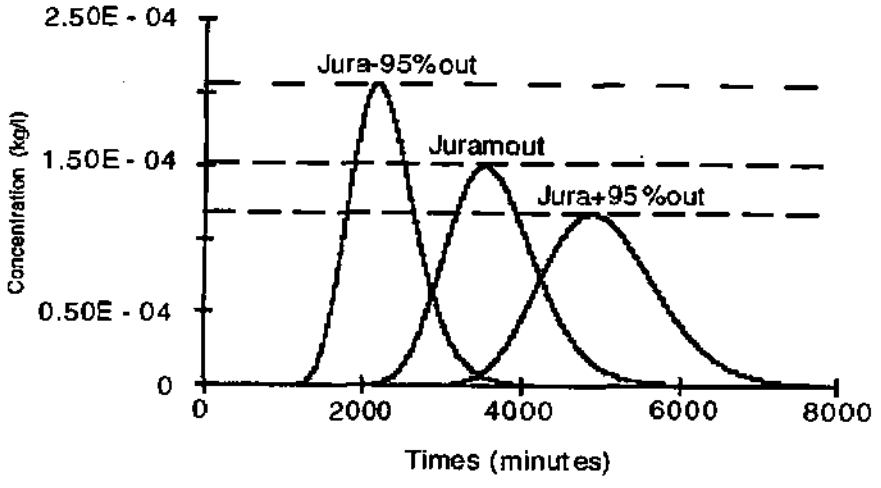

Figure 2.: Simulated breakthrough curves obtained by convolution of Jura mean impulse response with the input function. (juramout: recovery curve with mean impulse response; jura+-95%output recovery curve with +or-95% confidence interval impulse response).

The results of simulation of a mass of 750kg injected during 15 minutes into a borehole of medium to high hydraulic conductivity or into an artificial hole with a mean discharge of 3600 l/min and mean tracer distance of 1000m are in Figures 3 and 4. Based on the experimental results of tracer tests using surface injection points, it appears inappropriate to simulate injection from such a surface point. The experimental surface points are very specific to a local context such as at Bure which lies directly in connection to a major regional fault system.

The simulations provide results for various confidence intervals of the mean gradient values at each 0.1 percentile that may be interpreted as a potential recovery curve with the above conditions. As a safety factor for water protection, we suggest considering the -95% recovery curve with the highest concentration peak as the case suitable for prediction.

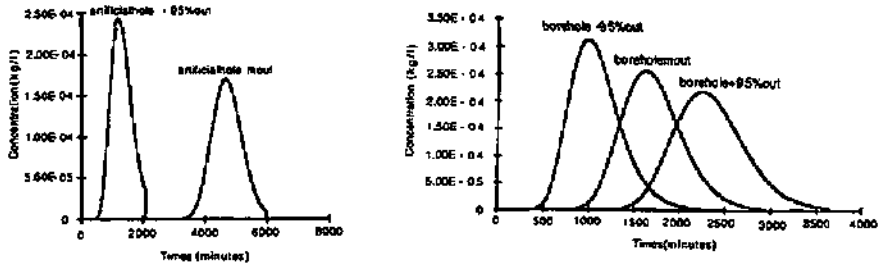

Figure 3.: Simulated breakthrough curves obtained by convolution of the artificial hole and borehole mean impulse response with an input function. (artificialhole mout and borehole mout: recovery curve with the mean impulse response; artificial hole or borehole +-95%output recovery curve with the +or-95% confidence interval impulse response).

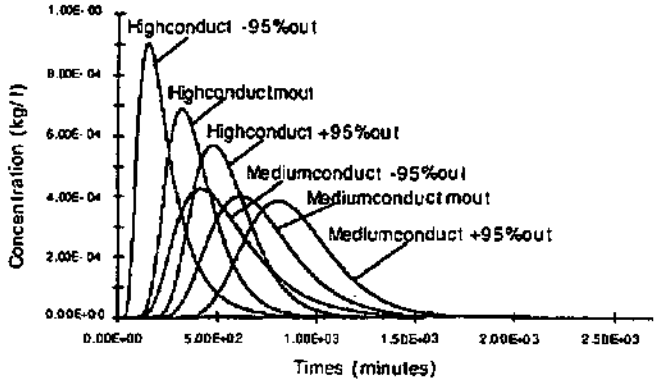

Figure 4.: Simulated breakthrough curves obtained by convolution of tha High and medium hydreulic conductivity mean impulse response with an input function in the Tabular Jura. (Highconductivitymout or Mediumconductivitymout: recovery curve with the mean impulse response; High or mediumconductivity +and -95%output recovery curves with the +or-95% confidence intervals impulse response).

- Transfer function variability within a catchment is important and depends principally on the injection site, thet is, the proximity of the injection point to the karst network. This refers also to the degree of development of the karst network.
- The vulnerability mapping of karst catchments based on a multi-attribute approach - the EPIK method - provides protection areas of variable vulnerability degree. Besed on the experimental transfer functions, characteristic transfer functions may be associated with each area. Theoretically, we assume that a low vulnerability area corresponds to a lower slope in the normalized responses of a tracer test (= low peak concentration and long recovery period). In contrast, higher vulnerability degrees have steeper normalized responses (=high peak concentration and short recovery period). Based on the experimental transfer functions, typical transfer functions resulting from various injection points may be drawn to characterize a vulnerability range area (Figure 5). The mean transfer functions of tracer tests that were done using artificial holes and in medium hydraulic conductivity result in a good simulation of what should be seen for the normalized response of tracer tests in medium vulnerability zones. The typical transfer functions of high vulnerability zones are for transfer functions of a tracer injected into a surface point that is directly connected to the karst network or to e high hydraulic conductivity environment from a borehole. This knowledge, even if intuitively predictable, may benefit qualitatively predicting the recovery curve of planned tracer test done as part of vulnerability area validation.

  Validation of a low vulnerability areas with a tracer experiments appears difficult and may not be possible. Injection of a tracer by spraying onto the surface requires similar equipment used by Flury et al, 1993 to study the pesticide transport through unsaturated field soils, namely air-lifted sprinklers in a square of 1m x 1m surrounded on three sites by wood partitions. The expected recovery response may have a low peak concentration and a long low duration. It is difficult in this situation to determine the right injection conditions (tracer quantity, water dilution volume for flushing, injection duration) to obtain a concentration above the detection limit.

The link between normalized responses and vulnerability zone may also be used as a instructive tool to explain the vulnerability of some hydrogeological settings in a karst environment to planners and decision makers.

- It is not necessary to carry out numerous tracer tests in the same karst aquifer in order to perform statistical tests. At the scale of a karst catchments, tracer tests are not the single tool used to protect groundwater. A multi-attribute approach such as the suggested EPIK method must be applied to karst aquifer vulnerability studies to define an adequate protection zone consistent with its physical parameters spatial heterogeneity. For critical areas, tracer tests should likely be performed. However, in as part of hydrogeological impact assessments, it remains useful to carry out at least three repetitive tracer tests under various and widely contrasting hydrological conditions to define characteristic transfer functions which can be used to establish realistic and effective contaminent predictions.

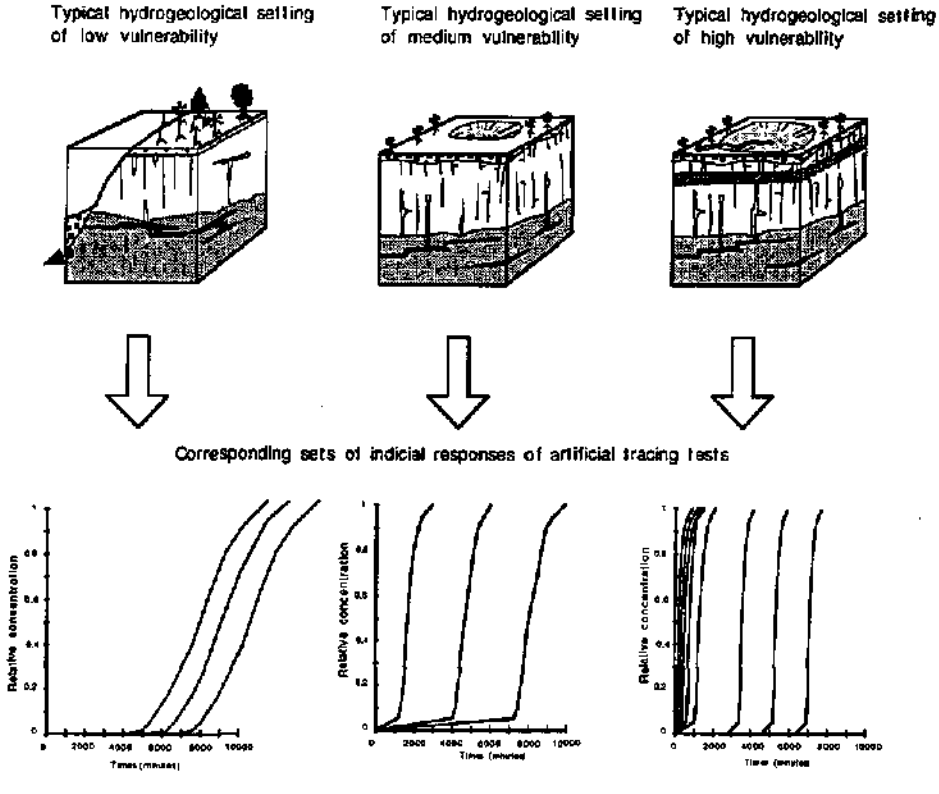

Figure 5.: Possible relationships between typical hydrogeological settings of various vulnerability degrees and the normalized responses of artificial tracer tests.

Contribution to defining karst groundwater protection zones from a multi-attribute vulnerability approach:

Is it possible to prepare vulnerability maps, within a realistic timeframe and for reasonable cost, that define groundwater protection zones with complex karst atructures?

Preliminary remarks:

- Saverel cases of karst catchment protection zone mapping show that the classical manner of proceeding based on outlining different potential contaminant travel timelines is not appropriate to karst environments.

- It is difficult, perhaps not even feasible, to verify a groundwater protection zone as it includes enforcement of ragulations by the designated authority and public awareness of karst groundwater.

- Outlining karst groundwater protection zones using as a tool the multi-attribute approach of vulnarability mapping is feasible within a reasonable tima. The rasulting maps of groundwater protection zones are more substantial than maps based on equal travel time lines used typically for porous media aquifers.
- Vulnerability maps can be made that reflect the specific hydrogeological behavior of karst (duality: hydraulic conductivity and recharge) and take into consideration attributes such as the epikarst, the protective cover, the infiltration conditions and tha karst network development. Howaver, characterization of these affributes requires improvement. The method is limited by first, the lack of appropriate instrumantation or methods needed to adequately investigate some of the parameters (epikarst, protective cover and karst network) and second, the difficulty in validating a weighting system.

  -The epikarst needs further development work from geophysics, satellite imagery to identify and map the apikarst and also more detailed hydrodynamic data.

  -EPIK stresses the protective role of the cover (overlying soil or geological layers) assuming that tha cover has a considarable protection against all kinds of contaminant transfer to the groundwater. In future, managers of karst groundwater catchments will more and more have to face the contaminant problems and it will be necessary in further focus the research on the role of the cover regarding various types of contaminants such as heavy metals, organic chemicals, fertilizers, pesticides, bacteria and viruses and the adsorption-desorption, advection, diffusion processes which occur and vary according to contaminant type and soil nature.

  -The quantitativa aspect of recharga from the Infiltration conditions affribute could possibly be treated taking into consideration the spatial variability in addition to its different categories.

- GIS is a useful tool to use for multi-attribute mapping. However additional tests are naeded to determine a more appropriate weighting system and to accomplish vulnerability mapping on the two catchments in Swiss Jura. Assessing infiltration conditions mapping as a function of slope is an essential contribution that needs to b done.
- Weighting and integrating indices of key attributes into a protection factor represents a logical procedure. It may, however, result in a simplistic index that is less distinctive than desired (Bengtsson and Rossen, 1995). Validation of vulnerability zones is not obvious and remains as the weakness of tha method. Tha indax should at least take into account an error factor.
- Distribution curves of vulnerability zones could ba established and compared to a reference curve based on catchment map vulnerability zones. This could lead to a general understanding of the importance of high vulnerability zones in the whole catchment.

- The probability of a specific contaminant effecting groundwater quality above an existing compliance levels (required level for drinking water) could be assessed taking into account the characteristics of the contaminants, the cover, the presence of the epikarst and the general karst network development. Such an approach, using the Bayesian statistic has already been carried out in porous media taking into consideration retention time (Bengtsson & Rossen, 1995).
- From vulnerability maps, it is possible to outline groundwater protection zones taking into consideration the goals to be obteined with such zones, as required in the state water law. No automatic correlation of groundwater protection zones is suggested from the vulnerability map. However, the ranges of protection factor assigned to each S groundwater protection zones are not too different for the two examples. Developing a correlation between protection factor and zones by field validation allows a better estimation of vulnerability degree assigned to each part of the catchment.
- The EPIK method can result in objective vulnerability maps that define groundwater protection zones in karst catchments. However, their acceptance and the regulatory restrictions associated with each protection zones will not be effective without increased public awareness. Educational programs are needed that explain the value of water and how karst aquifers behave. The public tergeted for these educational programs may be broad-based, but in particuler should include planners and decision makers in water management.

Benefits of this study to the knowledge of the karst Hydrogeology

- The interpretation of tracer tests in terms of transfer functions based on an input-response model supports deterministic approach to karst aquifers. Transfer function variability and the related transit velocity shows that the velocity within the network conduits is less variable than the velocity between low permeable blocks and the network. For borehole injection points, hydraulic conductivity is the major parameter that affects the transfer function.
- Typical transfer functions of artificial tracer experiments depend upon the injection conditions including the nature of the injection point. If the hydraulic conductivity of the tracer-system and the ratio of the unsaturated:saturated zones influence the transfer function, it seems complex and difficult to determine with a general law these parameters from the transfer functions. At the scale of the La Font, Le Saivu and La Bâme catchment, we were able to distinguish characteristic mean transfer functions for a high hydraulic conductivity tracer system, medium hydraulic conductivity tracer system, artificial hole's injection point, borehole injection point and surface injection point. In general, we considered that the hydrogeological conditions may also have influenced these typical transfer functions. But due to lack of data, we cannot prove it. There is no established relationship between the structure of the karst aquifer and the response of tracer experiments.
- The transfer functions studied as part of this thesis are in some cases close to a theoretical curve of 1-D transport equation. With further development, it would likely be possible to define from experimental curves, a "velocity" and "dispersion" that would be interpreted specifically to the karst environment. By knowing reasonable values of velocity and dispersion of a tracer transported in a karst network, it may be possible to calculate a value for transport in the network.
    - A 1D numerical transport analytical solution (appendix GC 1) was used to simulate mass transport in water for various sets of velocity, dispersivity and tracer distance. This illustrated the effect of these parameters on the transfer functions. For a given tracer distance and dispersivity, the higher the velocity, the steeper the transfer function or sigmoidal curve. The effect of the dispersivity is stronger on the sigmoidal curve when the velocity is small. For a given velocity, increasing dispersivity independently of the tracer distance results in a

decreased slope mainly around the 0.5 and 0.8 percentiles of the sigmoidal curve. If dispersivity and velocity both influence the shape of the curve, the tracer distance is also affected. For curves simulated with the same velocity and dispersivity, the greater the tracer distance, the more the sigmoidal curve moves away from vertical. A simple 1D transport analytical solution shows the multiple effect of three basic parameters on the tracer recovery curves and their transfer functions.

This kind of simulation illustrates that the complexity of transport in a karst tracer system needs to include the processes of exchange (adsorption, immobile water effect, dilution by additional water sources).

- Transfer function simulations of repeated karst Jura tracer tests using CONVOX (Dzikowski, 1992) showed that invariance of tracer systems is relatively sensitive to variation of discharge and to variation of general hydrological conditions.
- All results emphasize the importance of hydrodynamic and particularly transport relationships between surface injection site and karst network. This relation depends on the degree of connectivity and development of the network. This has been demonstrated from a hydraulic point of view (Jeannin, 1996). This assumption should also be integrated in the EPIK approach in future developments as the transfer functions already corroborate it.

Further developments in karst hydrogeology may be necessary to work on the evolution of pertinent groundwater protection strategy:

-Interpretation of tracer tests in karst aquifers in terms of aquifer structure. With a tracer test performed in a sinkhole for example, we could determine what tracer system structure exists: the degree of karst network development (density, connectivity), ratio of karst network to low permeability blocks. The use of numerical transport simulation models may contribute as a first step. The second step would integrate the experimental data of tracer tests (comparison to experimental recovery curves and transfer functions). Simulations may be computerized from two kinds of models: a double porosity reservoir model (The double reservoir model had been developed for hydraulic purpose by Király (in Bürger, 1983)) and a 2D or 3D deterministic[1] model with finite elements of a theoretical karst aquifer encompassing a 1D karst network. Different sets of tracer simulations with various injection points (sinkhole, swallowhole, karst network), various karst network geometry, density, connectivity and hydraulic conductivity may be computerized. Resulting recovery curves may be interpreted into transfer functions by deconvolution. As the simulated transfer functions would be related to known parameters, they could be ranked into classes related to the various simulation sets. Comparing the theoretical transfer functions with the experimental functions, tracer tests may be interpreted in terms of karst aquifer structure and hydrological conditions. Such an approach has already been performed to understand the hydraulic transfer function of karst aquifer (Eisenlohr, 1994). It was also used to show the effect of dilution on tracer tests by simulation of tracer tests in a theoretic karst aquifer (FE) by Rossier and Király, 1992.

[1] *Considering a theoretical 2D deterministic numeric model (FE) with an 1D karst network allows simulating tracer tests with the knowledge of the physical parameters fields (hydraulic conductivity field, storage coefficient field), the geometry of the karst network (density, connectivity degree) and the boundary conditions (hydraulic potential, impervious boundary). Hydraulic conductivity is attributed to the karst network (two different conductivities may be given considering the developing of the network: higher hydraulic conductivity to the major channels and lower conductivity for the minor channels) and to the low permeability blocks.*

- theory of the genesis of the karst network (chemical and physical processes, statistic approach) continuing the major works of Ford (1965, 1968, 1971), Ewers (1982), Mandelbrot (1983),Curl (1986), Ford & Williams (1986) and Jaquet & Jeannin (1994).

- development and hydrodynamics functioning of the epikarst continuing after Williams (1983), Smart & Friedrich (1986), Drogue (1974).

- correspondence of the mean trensfer functions to specific conteminents based on field or laboratory experiments of contaminant transfer in various conditions related to the real environment.

Literature references

ACKERMANN, H.-W., DUBOW, M.S. 1987. Virus of procaryotes, vol.I: General properties of bacteriopheges. CRC Press, Boca Reton, Florida, 202 pp.

ACKERMANN, H.-W., DUBOW, M.S. 1987. Virus of procaryotes, vol. II: Natural groups of bacteriopheges. CRC Press, Boca Raton, Florida, 242 pp.

ADAMS B., FOSTER S.S.D., 1992: Land-surface zoning for groundwater protection. Journ. Institution of Water and Environmental Management, No 6., p. 312-320.

AFEWS /INRA 1992: Référentiel pédologique - principaux sols d'Europe, INRA Edit. Techniques et Pratiques, pp. 219.

ALBINET M., MARGAT J.,1970: Cartographie de la vulnérabilité à la pollution des nappes d'eau souterraine . Orléans, France, Bull. BRGM., 2éme série, section 3, No4, p-13-22.

ALLEMAN R., MDAGHRI ALAOUI A. 1991: Evaluation comparative de différents traceurs artificiels en hydrogéologie et méthodologie d'analyse. Bulletin du Centre d'hydrogéologie de l'Université de Neuchâtel, No 10 (1991). pp1-10.

ALLER L., BENNET T., LEHR J.H.-, PETTY RT.J., AND HACKETT G., 1987: DRASTIC: a standardized system for evaluating ground water pollution potential using hydrogeologic settings. U:S. Environmental Protection Agency, Ada, OK, EPA /600/2-878-036, 455p.

ANDERSDEN L.J. & GOSK E., 1987: Applicability of vulnerability maps. In Vulnerability of soil and groundwater to pollutants (W. van duijvenbooden and H.G. van Waegeningh, eds), TNO Committee on Hydrological Research, The Hague, Proceedings and Information No. 38, p.321-332; also printed in Environmental Geology and Water Sciences, 1989, 13/1, p.39-43.

ATKINSON T.C., 1977 : Diffuse flow and conduit flow in limestone terrane in the Mendip Hills, Somerset, Great Britain. Journal of hydrology, v. 35, p. 93-110.

ATTEIA O., KOZEL R., 1995: Colloid transport in the Noiraigue karstic aquifer (NW Switzerland), 5p., Solutions 95, IAH-AIH, Int. Congress XXVI, Edmonton, 4-10 June 1995.

ATTINGER R., 1988: Tracerhydrologische Untersuchungen im Alpstein, Methodik des kombinierten Tracereinsatzes für die hydrologische Grundlagenerarbeitung in einem Karstgebiet. Thèse de doctorat, Univ. Berne, 170 pp.

AUBERT D.,1969: Phénomènes et formes du kart jurassien. Eclogae geol. Helv. 62(2), 325-399.

BAKALOWICZ M., MANGIN A.,1980: L'aquifère karstique. Sa définition, ses caractéristiques et son identification. Mem. L.sr.Soc. geol. France 11, 71-79.

BARROCU G., BIALLO G.,1993: Application of GIS for equifer vulnerability evaluation. HydroGIS 93: Application of Geographic Information Systems in Hydrology and Water Resources, Proceedings of the Vienna Conference, April 1993, IAHS Publ. No 211, 1993, p.571-579.

BEAR J., 1979: Hydraulics of Groundwater: New York, McGraw-Hill.

BEAR, J. 1972: Dynamics of Fluids in Porous Media.New York, American Elsevier, 764p.

BEAUDOINGG., ASTRUC J.G., BARADAT J.M., BOUZIGES M., CHARENTUS T., COUSTOU J.C., GETTO D., MOUYON P., RICARD J., SAUTY J.P., TARRISSE A., VICENTE A., 1989: Traçages et protection des captages dans le karst: détermination des paramètres de transfert et prévision de la propagation des pollutions dans le réseau karstique de l'Ouysse, Causse de Gramat (Lot, France) - Hydrogéologie, 4, 1989, pp. 279-292.

BENOIT-GUYOD J-L., J. ROCHAT, ALARY J., ANDRE C AND TAILLANDIER G.,1979: Correlations between physiochemical properties and eco toxicity of fluorescent xanthenic water tracers. - Toxicol. Eur. Res., 2 (5): pp 241à246, Paris.

BÖGLI A.,1980: Karst hydrology and physical speleology. Springer, Berlin Heidelberg New York.

BONACCI O., 1887: Karst Hydrology, with special reference to the Dinaric Karst, Springer-Verlag, Berlin, Heidelberg, New York, 184 p.

BOX G.E.P. AND JENKINS G.M., 1976: Time Series Analysis: Forecasting and Control. Editor: Holden Day. 575p.

BÜRGER A., 1959: Hydrogéologie du bassin de l'Areuse - Univ. de Neuchâtel, Fac. des Sciences, thèse, 304 p.

CASTAGNY, G. & MARGAT, J., 1977: Dictionnaire français d'hydrogéologie, BRGM, 249 p.

CIVITA M., 1990b, Legenda unificata per le carte delle vulnerabilità all'inquinamento dei corpi idrici sotterranei /Unified legend for the aquifer pollution vulnerability maps (in Italain and English) G.N.D.C.I. - C.N.R., PUbl.. n276, Pitagora Editrice Bologna, 13 p.

CTAGWA 1993: Groundwater vulnerability assessment. Predicting relative contamination potential under conditions of uncertainty. National Research council. National academy press, Washington, D.C., 204 p.

CURL R.L, 1986: Fractal dimensions and geometries of caves. Math. Geol. 18(8), pp. 765-783.

DALY D. & WARREN W.P,.1994: Vulnerability mapping - Geol. Survey of Ireland, Newsletter No. 25, Dublin.

DESOR E. 1864: Expériences sur la durée du parcours souterrain des eaux de la Noiraigue. B.S.N. 9: 37 pp.

DIETRICH C.R., NEWSAM G.N., ANDERSSEN R.S., GHASSEMI F. & JAKEMAN A.J., 1889: A practical account of instabilities in identification problems in groundwater systems. BMR., Journal of Australian Geology & Geophysics, 11, pp 273-284. Reprinted from BMR Journal Vol. 11 No 243.

DODGE M. , 1982: Structure, fonctionnement hydrodynamique et vulnérabilité des aquifères karstiques. in: Journée d'étude sur la protection des eaux karstiques, Bruxelles, 29 nov. 1982. - Soc. nationales des distributions d'eau et comm. de protection des sites spéléologiques, pp. 42-46.

DOERFLIGER N., 1994 : Réflexion sur la variabilité des fonctions de transfert obtenues par traçage en milieu karstique (Jura tabulaire et Alpes du domeine helvétique). Bulletin d'Hydrogéologie, No13, Publié par le Centre d'Hydrogéologie, Université de Neuchâtel, Peter Lang (Ed.) pp. 69-86.

DOERFLIGER N. & ZWHALEN F., 1995: EPIK: a new method for outlining of protection areas in karstic environment. Antalya, nov. 1995; International symposium on karst groundwater.

DOMENICO P.A. & SCHWARTZ F.W., 1990: Physical and chemical hydrogeology. John Wiley & Sons, New York, Toronto, Singapore, 824p.

DOOGE JC. 1973: Linear theory of hydrologic systems. U.S. Dept. Agric., Washington D.C. Tech. Bull No 1468, 327p.

DREISS S.J., 1982: Linear Kernels for Karst aquifers. Water Ress. Res., Vol. 18, No 4, pp. 865-876.

DROGUE C.,1974: Structure de certains equifères karstiques d'après les résultats de travaux de forage.Compte rendus de l'Académie des Sciences, Série III, Paris, 278, p- 2621-2624.

DROGUE C.,1992: Hydrodynamics of karstic aquifers: experimental sites in the Mediterranean karst, Southern Frence. In Back, W., (Ed-in-chief) Hydrogeology of Selected Karst Regions. Hannover, Heise, 133-149.

DZIKOWSKI M., 1992: L'analyse des systèmes-traçages à débit variable et volume constant. Possibilités d'application en milieu karstique. Thèse, Université des Sciences et technologies de Lille, février 1992.

DZIKOWSKI M.AND DELAY F., 1992: Simulation algorithm of time-dependent tracer test systems in hydrogeology. Computers & Geosciences. Vol. 18, No 6, pp 697-705

EISENLOHR L., 1994: Variabilité des réponses naturelles des aquifères karstiques. De l'identification de la réponse globale vers la connaissance de la structure de l'aquifère. Thèse université de Neuchâtel.

EWERS R.O., 1982: An analysis of solution cavern development in the dimentions of length and breadth, PhD Thesis Geography, McMaster University, Hamilton, Ontarion, pp 398.

FLURY M., LEUEN8ERGER J., STUDER B., FLÜHLER H., JURY W.A., ROTH K., 1993: Pesticide Transport through Unsaturated Field Soils: Preferential Flow, pp 293.

FORD T.D., 1965: The origin of limestone caverns: a model from the central Mendip Hills, England, National Speleology Society American Bulletin, 27, pp. 109.

FORD T.D., 1968: Features of cavern development in central Mendip., Trans., Cave Res.Gp. G.B., 10, pp 11-25.

FORD T.D., 1971: Characteristics of limestone solution in the southern Rocky Mountains and Selkirk Mountains, Alberta and British Columbia. Can. J. Earth Sci. 8 (6), pp. 585-609.

FORD T.D. & WILLIAMS, 1989: Karst geomorphology and hydrology, Unwin Hyman, London, Boston, Sydney, Weelington, 601pp.

FOSTER S.S.D. 1987: Fundamental concepts in aquifer vulnerability, pollution risk and protection strategy. In Vulnerability of soil and groundwater to pollutants (W. van Duijvenbooden edn H.G. van Waegeningh, eds) TNO Committee on Hydrological Research, The Hague, Proceedings and INformation, No 38, p. 69-86.

FREEZE R.A. & CHERRY A.J., 1979: Groundwater. Prenctice-Hall, Inc. Englewood Cliffs, pp 604.

GAIFFE M.& BUCKERT S.,1990: Origine paléoécologique de l'aptitude des calcaires jurassiques à la fracturation. Conséquences tectoniques, pédogénétiques et écologiques. Bull. Soc. Neuchâtel. Sci. nat. 113, 1990, pp. 191-206.

GRANT S.B., LIST E.J., LINDSTROM M.E., 1993: Kinetic analysis of virus adsorption and inactivation in batch experiments. Water Res. Research 29, pp. 2067-2085.

GRASSO A.D.& JEANNIN P-Y., 1994: Estimation des pertes dans la partie avale du réseau karstique de la Milandrine: bilan hydrique au sein d'un aquifère karstique. Bulletin d'hydrogéologie, No13, 1994, Publié par le Centre d'Hydrogéologie, Université de Neuchâtel, Peter Lang (Ed.), 115-128.

GRETILLAT P-A., 1992: Carte hydrogéologique de l'Ajoie, Canton du Jura - Suisse. Eléments pour la gestion et la protection des eaux, 1:25'000 Rép. et Canton du Jura, OEPN, St-Ursanne.

GUIZERIX J. & MARGRITA R., 1976: Méthodologie d'étude par traceur des transferts de masses. La Houille Blanche. No 3/4. 1976. Tech. des traceurs en hydrologie et en hydraulique. pp. 187-196.

GUIZERIX J., 1988: A geometrical interpretation of tracer experiments in non steady (flow, volume) systems. 4th conference on Radioisotope Application and Radiation Processing in Industry. Leipzig-G.D.R. Sept. 1988.

GUIZERIX J., MARGRITA R., MOLINARI J., GAILLARD B., CALMELS P. & COROMPT P., 1970: Contribution à la mesure des débits en régime variable par une méthode de dilution de traceurs radioactifs, International Atomic Energy Agency, Vienne, Vol 2, pp 377-403.

HEIERLI H.,1984:Die Ostschweizer Alpen und ihr Vorland. Säntismassiv, Churfirsten, Mattstock, Alviergruppe, Appenzeller Molasse. Sammlung Geol. Führer, Bd. 75, Gebr. Borntträger,Berlin, Stuttgart.

HELSEL D.R & HIRSCH R.M., 1992: Statistical methods in Water Resources, Studies in Env. Sc., 49, Elsevier 1992, pp.522.

HOHL A., 1992: Etude hydrogéologique de la région de Courleivre (JU): détermination du bassin versant de la source communale du Chenal. Dipl. 3ème cycle CHYN, pp. 190.

JAQUET O, JEANNIN P-Y., 1994: Modelling the karstic medium: a geostatistical approach. In: Geostatistical simulations. M. Armstrong & P. A. Dowd (eds), Kluwer Acad. Publ., London, pp. 185-195.

JEANNIN P-Y, 1995: Action COST 65 - Projets Bure et Hölloch (Suisse): cadre théorique, position des problèmes et présentation des sites étudiées et des données disponibles. Bulletin d'Hydrogéologie, No14, pp 53-81, Ed. Peter Lang.

JEANNIN P-Y., 1996: Structure et comportement hydraulique des aquifères karstiques. Thèse, Université de Neuchâtel, 260 pp.

JEANNIN P-Y. & GRASSO A.D., 1994: Etude critique des méthodes d'analyse de la réponse globale des systèmes karstiques. Application au site de Bure (JU, Suisse). Bulletin d'hydrogéologie No13 (1994), pp. 87-113.

JEANNIN P-Y. & GRASSO A.D., 1995: Recharge respective des volumes de roche peu perméable et des conduits karstiques, rôle de l'épikarst. Bullatin d'hydrogéologie, No 14., pp. 95-111.

Jeannin P-Y., Kiràly L., Doertliger N., 1993: Développaments possibles dans le domaine de la détermination des zones de protection. Concept de vulnérabilité des aquifères karstiques. Rapport de la première phase, rapport interne du Chyn pour l'OFEFP, Service hydrologique et géologique national. 15pp. 10fig.

KÀSS W., (Ed) 1992: In: Geohydrologische Markierungstechnik, Gebrüder Bomträger, Berlin.

KEMPF T., DELLA VALLE G., 1981: In Données pour la protection et la gestion de l'eau souterraine du canton de Berne. Hydrogéologie du Vallon de St-Imier par le burea Jäckli. OEHE rapport, 1981.

KINTER (Chyn) informatic code

KIRALY L., 1973 : Notice explicative de la carte hydrogéologique du canton de Neuchâtel. Supplément du Bulletin de la Société neuchâteloise des Sciences naturelles, t. 96.

KIRALY L. ET ROSSIER Y., 1992: Interprétation quantitative des essais de traçage dans les aquifères karstiques. Rapport interne du Centre d'hydrogèologie pour le Service Hydrologique et géologique national, Berne. p.

KIRALY L., 1975: Rapport sur l'étact actuel des connaissances dans le domaine des caractères physiques des roches karstiques. Dans Hydrogeology of Karstic Terrains. Internat. Union of Geol. Sciencas, Series B, No 3, p. 53-67.

KIRALY L., 1978: La notion d'unité hydrogéologique. Essai de définition. Bull. du Centre d'hydrogéologie, Neuchâtel, 2, p. 83-216, 30 figures.

KIRALY L., PERROCHET P., & ROSSIER Y., 1995: Effect of the epikarst on the hydrograph of karst springs: a numerical approach. Bulletin d'hydrogéologie, No 14, pp. 199-220.

KLIMCHOUCK A., 1995 : Karst morphogenesis in the epikarstic zone. Cave and Karst science Vol. 21, No 2, March 1995. Transactions of the British Cave Research Association. p45-50.

LE GRAND H.E, 1964: System for evaluating the contamination potential of some waste sites. Journ. Amer. Water Works Assoc., 56/8, p. 959-974.

LE GRAND H.E., 1983: A standardized system for evaluating waste-disposal sites. National Water Well Assoc., Dublin, OH, 49p.

Leaux, 1993: Loi fédérale sur la protection des aaux, Confédération suisse.(814.20).

LEPILLER M. AND MONDAIN P-H., 1986: Les traçages artificiels en hydrogéologie karstique. Mise en oeuvre et interprétation. Hydrogéologie, No 1, 1986, pp. 33-53.

LIPSON, S.L., STOTZKY, G. 1983. Adsorption of reovirus to clay minerals : effects of cation-exchange capacity, cation saturation, and surface area. Appl. Environ. Microbiol. 46: 673-682

LUTTY G.A., 1978: The acute intravenous toxicity of biological stains, dyes and othar fluorescent substances.- Toxikol. and Appl. Pharamacol., 44: pp 225-249, New YOrk - London (Academic Prass).

LUTZ TH & PARRIAUX A., 1988: The identification of uranine in natural water by high performance liquide chromatography (HPLC). - Steir. Beitr. z. Hydrogeologie, 39, 141 - 147, Graz.

MANGIN A.,1973: Sur la dynamique des transferts en aquifère karstique. Proc. 6 Internat. Congr. Speleo., Olomouc 6, 157-162.

MANGIN A., 1975: Contribution à l'étude hydrodynamique des aquifères karstiques, Thèse de Doctorat d'Etat. Dijon, 124p. (Ann. Speleo., 1974 19(3), 283-332; 29(4) 495-601; 30(1) 21-124).

MANGIN A., 1976 : Les systèmes karstiques et leur méthodologie d'investigation - Ann. Sci. Univ. Besançon. 2ème Colloque d'Hydrologie en Pays Calcaire, Géologie, fasc. 25, 3ème série, pp. 263-273.

MANGIN A., 19B1: Apports des anlayses correletoires et spectrales croisées dans la connaissance des systèmes hydrologiques. C.R. Acad. Sc. Paris 293 (II), 1011-1014.

MANGIN A., 1986: Réflexion sur l'approche et la modèlisation des aquifères karstiques. Jomadas sobre etl karst en Euskadi, fév. 1986, 2, pp 11-30.

MANGIN A., 1994: Structure and functioning of karst aquifers. Consequences on karst management and protection. In Basic and applied hydrogeological reseerch in french karstic areas. Cost 65 Action, Hydrogeological aspects of Groundwater Protection in Karstic Areas. Montpellier-Millau Workshop, May 5-8, 1994., pp. 11-24. Crampon N & Bakalowicz M., Edifors. European Commission, Directorate-General Science, Research and Development.

MANGIN A., MOLINARI J., PALOC H., 1976: Les traceurs en hydrogéologie karstique. Leur apport à la connaissance des réservoirs aquifères calcaires. La Houille Blanche. No 3/4. 1976 Tech. des traceurs en hydrologie et en hydraulique. pp 261-267.

MARECHAL J-CH., 1994: Etude et modélisation de l'hydraulique et du transport dans les drains karstiques. Travail de diplôme de spécialisation en hydrogéologie, Université de Neuchâtel, inédit.

MARKING L.L.,1969: Toxicity of Rhodamine B and fluorescein sodium to fish and their compatibility with Antimycin A. - Prog. Fish-Culturist, 31: pp 139-142, Washington D.C.

MARSILY G.,de 1978: De l'identification des systèmes hydrologiques. Thèse de Doctorat d'Etat. Univ. Pierre et Marie Curie. Paris VI.

MOAGHRI ALAOUI A., 1992: Traceurs artificiels en Hydrogéologie: limites d'application et critiques des méthodes d'analyses. Colloque international, " Hydrogéologie des milieux discontinus sous climats arides ", Marrakech - Maroc, 22-25 avril 1992, 4p., 2 fig,. 2 tabl.

MERMOUD A, 1982: Contribution á l'étude des transferts simultanés d'eau et de solutés en milieu poreux. Thèse EPFL, No 432.

MEUS, PH, 1994: Hydrogéologie d'un aquifère karstique dans les calcaires carbonifères (Néblon-Anthisnes, Belgique). Apport des traçages à la connaissance des milieux fissurés et karstiques. Thèse, Université de Liège, 323p.

MOEBUS, K. 1980: A method for the detection of bacteriophages from ocean water. Helgoländer. Meersunters. 34: pp. 1-14.

MOEBUS K., HERMANN F., 1987: An electron microscopic study of bacteria from marine waters. Helgoländer, Meersunters., 34, pp. 375 - 385.

MOEBUS, K., NATTKEMPER, H. 1989. Bacteriophages sensitivity patterns among bacteria isolated from marine waters. Helgoländer. Meersunters. 34: 375-385

MOEBUS, K. 1992. Laboratory investigations on the survival of marine bacteriophages in raw and treated seawater. Helgol_nder. Meersunters. 46: 251-273

MOLINARI J., 1976: Interactions avec le milieu et développements récents dans l'emploi des traceurs artificiels. La Houille Blanche, No 3 /4, p. 197-204.

MOREL-SEYTOUX H.J., 1981: Optimisation methods in Rainfall-Runoff Modeling in Rainfell-Runoff Relationship. pp. 487-506. Proceedings of the International Symposium on Rainfall-Runoff modeling. May 18-21. Mississipi State University. U.S.A.

[MÜLLER I ET AL.]. - BAUER F., BENISCHKE F., BUB P., BURGER A., DOMBROWSKI H., GOSPODARIC R., HÖTZL H., HRIBABAR F., KÄSS W., KIRALY L., LEIBUNDGUT CH., LEDITZKY H.P., MAURIN V., MÜLLER I., PELEGA H., RAMSPACHER P., SCHOTTERER U., SIEGENTHALER U., ZOJER H., ZÖTL J., ZUPAN M., 1980: Karsthydrologische Untersuchungen mit natürlichen und künstlichen Tracern im Neueunburger Jura (Schweiz), Steir. Beitr.z. Hyrögeologie 32/pp. 5-100, Graz 1980.

NEUMANN S.P.AND DE MARSILY G., 1976: Identification ot Linear Systems Response by Parametric Programming. Water Res. Research., Vol 12, No 2, pp. 253-262.

NICOD J., 1990: Le karst jurassien: modèle géomorphologique spécifique. Bull. Soc. neuch. Sci. nat., No 113, Neuchâtel, pp. 13-25.

OFEFP 1977: Instructions pratiques pour la délimitation des secteurs de protection des eaux, des zones et des périmètres de protection des eaux souterraines.révisée en 1982.

PALOC H. , 1975: Glosseire d'hydrogéologie du karst. Hydrogeology of karstic terranes, Mem. No3, série B, UGGI &AIH, Paris.

PAYMENT P, MORIN E., TRUDEL M., 1988: Coliphages and enteric viruses in the particulate phase of river water. Can. J. Microbiol. 34 : pp. 807-910.

POREL G., 1988: Transfert de soluté en aquitère crayeux. Causes de modifications des résultats de traçages. Thèse de Doctorat en Géologie Appliquée de l'Université de Lille-Flandres-Artois.

QUINLAN J.F., 1989: Ground-water monitoring in karst terranes: recommended protocol and implicit assumption. U.S. Environ. Protec. Agency, Las Vegas, EPA 600/x-89/050, 80pp.

RAY J.A., O'DELL P.W., 1993: DIVERSITY: A new method for evaluating sensitivity of groundwater to contamination. Environmental Geology (1993): 22: pp 345-352.

RAVEN ET K.G., NOVASKOWSKI K.S.AND LAPCEVIC P.A., 1988: Interpretation of tield tests of a single fracture using a tansient solute storage model. Water Resources Research 24, No 12: pp. 2019 - 2032.

ROBINS N., ADAMS B., FOSTER S., PALMER R., 1994: Groundwater vulnerability mapping: the British perspective. Hydrogéologie, No3, 1994, pp. 35-42, 5fig., 3 tabl.

RODRIGUEZ-HERNANDEZ J.Y., 1989: Modélisation Pluie-Débit par la méthode DPFT: Développement de la méthode initiale et extension à des cas bi-entrées. These de Doctorat. Institut Nationale Polytechnique de Grenoble. 280p.

ROSSI P, 1994: Advances in biological tracer techniques for hydrology and hydrogeology using bacteriophages. Optimization ot the methods and investigation of the behaviour of the bacterial viruses in surface waters and in porous and fractured aquifers. Thesis, University Neuchâtel, 197p.

RUSSEL BOULDING J., 1995: Practical Handbook of soil, vadose zone, and groundwater contamination. Assessment, prevention and remediation. Lewis Publishers, 848 p.

SALL JOHN, NG KATHERINE AND HECHT MICHAEL, 1989-1981: JMP, software, version 2.0.4.

SAUTY J-P., 1988: Contribution à l'identification des paramètres de dispersion dans les equifères par interprétation des expériences de traçage.

SAUTY J-P., KINZELBACH, W.,1988: Computer Aided - Tracer tests interpretation. L'interprétation des traçages assistée par ordinateur. Mode d'emploi de CATTI - version 2.0 Mai 1988, Rapport BRGM, 89 SGN 217 EEE, 72 p.

SCHÄFERCLAUS W, 1954: Fischkrankheiten - 3. Aufl., 708 p., Berlin.

SCHINDLER B.,1988: Etude hydrogéologique de la zone S des captages sis à Cornoret et Villeret, 2 ème partie, rapport inédit.

SHERMAN, L.K, 1932: Stream flow rainfall by the unit Hydrograph method. Eng. News. Res. No108, pp 501-505.

SINGH K.P., BANIJKEEWIZIC A. AND RAM R.S.,1981: Some Empirical Methods of determining the Unit Hydrograph. in Rainfall-Runoff Relationship. pp 67-90. Proceedings of the International Symposium on Rainfall-Runoff Modeling. May 18-21. Mississipi State University. U.S.A.

SMART P.L., 1982: A review of the toxicity of twelve fluorescent dyes used for water tracing: National Speleological Society Bulletin, v. 46, No2, pp. 21-33.

SMART P.L. AND FRIEDRICH H., 1986: Water movement and storage in the unsaturated zone of a maturely karstified carbonate aquifer, Mendip Hills, England. pp 59-87.

SMOOT J.L., MULL D.S., LIEBERMANN T.D., 1987: Quantitative dye tracing techniques for describing the solute transport characteristics of groundwater flow in karst terrane, in Proceedings of the 2nd Multidisciplinary Conference on Sinkholes and the Environmental Impacts of Karst, Orlando, Florida, February 9-11,1987, pp. 269-275.

STANTON W.I. AND SMART P.L., 1981: Repeated dye tracers of underground streams in the Mendip Hills, Somerset. Proc. Univ. Bristol Spelaeol. Soc., 1981, 16(1), pp 47-58.

SUAIS W.I, VINATIER J-M., BARAT A., 1990: Vulnérabilité des aquifères. Recherche de critères cartographiques pertinents. Essai de cartographie automatique sur la plaine alluviale entre Rhône et Ain (01). R. 30890.RHA.4S.90 - Mai 1990 . Rapport BRGM, DRIR Rhône-Alpes.

TACHE E., DOERFLIGER N.,AND ZWAHLEN F., 1996: Vulnérabilité des eaux dans les régions karstiques et délimitation des zones de protection - Méthodologie EPIK, rapport de la phase 3b (1995-1996). Rapport inédit, 24pp., 23 fig. in appendixes.

THIERRIN, R. 1996: Etude du fonctionnement hydraulique de l'épikarst sur le site de Bure. Travail de diplôme d'ingénieur génie rural, EPFL, Lausanne.

TRIPET J-P., 1972: Etude hydrogéologique du bassin de la source de l'Areuse, Thèse de l'Université de Neuchâtel, 183p.

TRIPET J-P., DOERFLIGER N., ZWAHLEN F., 1995: Vulnerability mapping and its uses in Switzerland. Symposium of the Geological Survey of Ireland, oct. 1995.

TURBERG P., 1993: Apport de la cartographie radiomagnetotellurique à l'hydrogéologie des milieux FRACTURES. THESE, UNIVERSITE DE NEUCHATEL, P132.

VEIGA M. 1995: Caractérisation de l'épikarst et des sols sur le plateau de Bure (Jura Suisse) - étude géophysique et implantation de forages - Travail de diplôme du cycle postgrade interuniversitaire, EPFL- UNI-Ne en hydrologie et hydrogéologie, spécialisation en hydrogéologie. inédit.

VRSA J., ZAPOROSEC A., 1994: Guidebook on Mapping groundwater Vulnerability, IAH, International Contributions to hydrogeology founded by G.Castany, E.Groba and E.Romin., Vol. 16, 1994, Velrang H.Heise, 131p.

WALLISER B., 1977: Sytèmes et modèles. Introduction critique à l'analyse des systèmes. Ed. du Seuil, 248p.

WILDBERGER A., 1982: Zur Hydrogeologie des Karstes im Rawil - Gebiet. Beiträge zur Geologie der Schweiz-Hydrologie. Nr 27, pp. 175.

WILLIAMS P.W. , 1983: The role of subcutaneous zone in karst hydrology. J. Hydrol 61:45-67.

WILLIAMS P. W., 1985: Subcutaneous hydrology end the development of doline and cockpit karst. Z.Geomorph. 29(4), 463-482.

WIMPENNY, J.W.T., COTTON, N., STATHAM, M. 1972. Microbes as tracers of water movement. Water Res. 6: 731-739

ZAPOROZEC A. 1985: Groundwater pollution potential of Barron County, Wisconsin. Wis. Geological and Natural History Survey, Madison, WI, Map 87-2i, scale 1:100'000.

ZWAHLEN F. AND DOERFLIGER N., 1995 : Swiss report, COST 65 Action, Hydrogeological Aspects of Groundwater Protection in Karstic Areas. In Final report of the COST 65 Action. European Commission, Directorate-General Science, Research and Development. pp.

APPENDIX I.1

DYEBOX numerical code - Fortran 77

```
      PROGRAM  DYEBOX
C
      INTEGER A
      PARAMETER(A=9600)
      REAL*8 TEMPS(A),REST(A),TIME(A),ENTREE(A),TT(A),RESTDI(A)
      REAL*8 TITI(A),ENTREEDI(A),RESTNO(A),ENTREENO(A)
      REAL*8 H(A),PAS(A),INPUT(A),TINPUT(A)
      REAL*8 INPUTDI(A),TINPUTDI(A),VALEUR(A),TVALEUR(A)
      REAL*8 INCREMENT,DT
      INTEGER VAL,MAX,VALMAX,MAXMAX,VALH,VALINPUT,VALINPUTMAX
      INTEGER CHOIX,MAXVALEUR
C
C     CHOIX DU TYPE DE PROBLEME A TRAITER
C
      WRITE(',111)CHAR(27),'[1J'
111   FORMAT(1X,A,A)
      WRITE(*,*)'*************************************************'
            WRITE(*,*)'      CHOIX POSSIBLE          '
      WRITE(*,*)'  CALCULER LA REPONSE IMPULSIONNELLE   (1)       '
      WRITE(*,*)'  CONVOLUTION        (2)       '
      WRITE(*,*)'  CALCULER LA REPONSE IMPULSIONNELLE   '
      WRITE(*,*)'      ET CONVOLUTION          (3)       '
      WRITE(*,*)'*************************************************'
            READ(*,*)CHOIX
      WRITE(',111)CHAR(27),'[1J'
C
C     ++++++++++++++++++++++++++++++++
C     RECHERCHE DE LA REPONSE INDICIELLE
C     ++++++++++++++++++++++++++++++++
C
      IF(CHOIX.EQ.1.OR.CHOIX.EQ.3)THEN
C
      WRITE(*,*)'FICHIER CONTENANT LA COURBE DE RESTITUTION (MN)'
            CALL APPEL_FICHIER(TEMPS,REST,VAL)
C
      WRITE(*,*)'FICHIER CONTENANT LA FONCTION D'ENTREE (G/L)'
            CALL APPEL_FICHIER(TIME,ENTREE,MAX)
C
C ***************
C 1.DISCRETISATION
C ***************
C
C     DISCRETISATION DE LA COURBE DE RESTITUTION
C     --> VECTEUR DE SORTIE OU ON A DES VALEURS PAR PAS DE TEMPS
C     --> LA VALEUR AU PAS EST CELLE A LA FIN DU PAS DE TEMPS
C
      WRITE(*,*)'TAILLE DU PAS DE TEMPS (MN)'
      READ(*,*),DT
      WRITE(',111)CHAR(27),'[1J'
            CALL DISCRETOS(TEMPS,REST,VAL,TT,RESTDI,VALMAX,DT)
C
C     DISCRETISATION DE LA FONCTION D'ENTREE
C     --> VECTEUR DE SORTIE OU ON A DES VALEURS PAR PAS DE TEMPS
C
            CALL DISCRET(TIME,ENTREE,MAX,TITI,ENTREEDI,MAXMAX,DT)
C
C ***************
C 3.DECONVOLUTION
C ***************
C
            CALL DECONVOLE(ENTREEDI,TITI,MAXMAX,RESTDI,TT,VALMAX,H,PAS,
     +      VALH,DT)
C
C     SAUVETAGE DE LA REPONSE IMPULSIONNELLE POUR UN PAS DE TEMPS DT
C
            WRITE(*,*)'FICHIER CONTENANT LA REPONSE IMPULSIONNELLE (1/MN)'
            CALL SORTIE_FICHIER2(PAS,H,VALH,DT)
C
C ***************************************************
C FIN DE LA RECHERCHE DE LA REPONSE IMPULSIONNELLE
C ***************************************************

      END IF
C
C     ++++++++++++
C     CONVOLUTION
C     ++++++++++++
C
      IF(CHOIX.EQ.2.OR.CHOIX.EQ.3)THEN
C
      IF(CHOIX.EQ.2)THEN
            WRITE(*,*)'FICHIER CONTENANT LA REPONSE IMPULSIONNELLE (1/MN)'
      CALL APPEL_FICHIER2(PAS,H,VALH,INCREMENT)
            END IF
C
C     APPEL DE L'INPUT A CONVOLUER
C
            WRITE(*,*)'FICHIER DE L'INPUT A CONVOLUER (G/L)'
            CALL APPEL_FICHIER(TINPUT,INPUT,VALINPUT)
C
C     DISCRETISATION DE L'INPUT
C     -->VECTEUR DE SORTIE OU ON A DES VALEURS PAR PAS DE TEMPS
C
      CALL DISCRET(TINPUT,INPUT,VALINPUT,TINPUTDI,INPUTDI,VALINPUTMAX,
     &      INCREMENT)
C
C     CONVOLUTION DE L'INPUT DISCRETISE PAR LA REPONSE IMPULSIONNELLE
C     CES DEUX FONCTIONS SONT DISCRETISEE A DT
C
      CALL CONVOLE(TINPUTDI,INPUTDI,VALINPUTMAX,PAS,H,VALH,
     +      TVALEUR,VALEUR,MAXVALEUR,INCREMENT)
C
C     SAUVETAGE DANS UN FICHIER PAR PAS DE TEMPS
C
      WRITE(*,*)'FICHIER DE SORTIE CONVOLUE (G/L)'
      CALL SORTIE_FICHIER(TVALEUR,VALEUR,MAXVALEUR)
C
C
      END IF
      WRITE(',111)CHAR(27),'[1J'
C
C     FIN
C
      END

      SUBROUTINE APPEL_FICHIER(X,Y,MAXVALEUR)
C
C     LE FICHIER APPELE CONTIENT
C     - LIGNE 1: NOMBRE DE VALEURS CONTENUES DANS LE FICHIER
C     - LIGNES SUIVANTES
C     COLONNE 1: ORDRE
C     COLONNE 2: TEMPS
C     COLONNE 3: CONCENTRATION
C
      CHARACTER*80 FICIN
      REAL*8 X(9600),Y(9600)
      INTEGER IN,MAXVALEUR,I
      PARAMETER(IN=10)
C
10    FORMAT(A)
      TYPE *,'NOM DU FICHIER'
      ACCEPT 10,FICIN
      OPEN(UNIT=IN,FILE=FICIN,STATUS='OLD')
      READ(IN,*)MAXVALEUR
      DO 100,I=1,MAXVALEUR
            READ(IN,*)ORDRE,X(ORDRE),Y(ORDRE)
100   CONTINUE
```

```
              I=I+1
          INT=INT+TINC
              XX(I)=INT
          ELSE
              ECART=X(J)-X(J-1)
              INTER=IDNNT(ECART/TINC)
              DEBUT=Y(J-1)
              FIN=Y(J)
              PENTE=(FIN-DEBUT)/(ECART)
              DO 90,K=1,INTER
              YY(I)=(PENTE*(TINC*K))+DEBUT
              I=I+1
              INT=INT+TINC
              XX(I)=INT
90            CONTINUE
          END IF
100       CONTINUE
          NEWVAL=I-1
C
          PAS=1
          DO 200,J=1,(NEWVAL-1)
           Z(PAS)=(YY(J)+YY(J+1))/2.
           REPAS(PAS)=PAS
           PAS=PAS+1
200       CONTINUE
          VALPAS=PAS-1
C
          END

          SUBROUTINE SORTIE_FICHIER2(A,B,MAX,PAS)
C
C         LE FICHIER SAUVE A LA STRUCTURE SUIVANTE
C         LIGNE 1: NOMBRE DE VALEURS CONTENUS DANS LE FICHIER
C         LIGNE 2: VALEUR OU PAS DE TEMPS
C         LIGNES SUIVANTES:
C         COLONNE 1: ORDRE
C         COLONNE 2: NUMERO DU PAS DE TEMPS
C         COLONNE 3: CONCENTRATION AU PAS DE TEMPS
C
          REAL*8 A(9600),B(9600),PAS
          INTEGER MAX,OUT
          CHARACTER*80 FICOUT
          PARAMETER(OUT=20)
C
10        FORMAT(A)
          TYPE *,'NOM DU FICHIER'
          ACCEPT 10,FICOUT
          OPEN(UNIT=OUT,FILE=FICOUT,STATUS='NEW')
          WRITE(OUT,*)MAX
          WRITE(OUT,*)PAS
          DO 100,I=1,MAX
              WRITE(OUT,*)I,A(I),B(I)
100       CONTINUE
C
          CLOSE(UNIT=OUT)
          END

          SUBROUTINE DECONVOLE(E,X,MAXENTREE,S,XX,MAXSORTIE,N,PAS,MAX,DT)
C
          REAL*8 X(9600),XX(9600),E(9600),S(9600),PAS(9600)
          REAL*8 SOMME,N(9600),DT
          INTEGER MAXENTREE,MAXSORTIE,MAX,INDICE
C
C         LE PAS DE TEMPS EST DE DT
C
          MAX=MAXSORTIE-MAXENTREE+1
          DO 100,I=1,MAX
           SOMME=0.E+0
           IF(I.NE.1)THEN
              DO 90,J=1,(I-1)
          CLOSE(UNIT=IN)
          END

          SUBROUTINE DISCRETOS(X,Y,VALMAX,REPAS,Z,VALPAS,TINC)
C
C         DISCRETISATION A CHAQUE PAS DE TEMPS ET
C         ATTRIBUTION DE CETTE VALEUR          AU PAS DE TEMPS EN ENTIER
C
          REAL*8 X(9600),Y(9600),Z(9600),REPAS(9600)
          REAL*8 XX(9600),YY(9600),TINC,INT
          REAL*8 ECART,DEBUT,FIN,PENTE
          INTEGER VALMAX,NEWVAL,VALPAS,INTER
C
          I=1
          INT=0.D+0
C         TINC=15.D+0
C
          DO 100,J=1,VALMAX
           IF(J.EQ.1)THEN
           YY(1)=Y(J)
              XX(1)=INT
              I=I+1
           INT=INT+TINC
              XX(I)=INT
           ELSE
              ECART=X(J)-X(J-1)
              INTER=IDNNT(ECART/TINC)
              DEBUT=Y(J-1)
              FIN=Y(J)
              PENTE=(FIN-DEBUT)/(ECART)
              DO 90,K=1,INTER
              YY(I)=(PENTE*(TINC*K))+DEBUT
              I=I+1
              INT=INT+TINC
              XX(I)=INT
90            CONTINUE
           END IF
100       CONTINUE
          NEWVAL=I-1
C
          PAS=1
          DO 200,J=2,(NEWVAL)
           Z(PAS)=YY(J)
           REPAS(PAS)=PAS
           PAS=PAS+1
200       CONTINUE
          VALPAS=PAS-1
C
          END

          SUBROUTINE DISCRET(X,Y,VALMAX,REPAS,Z,VALPAS,TINC)
C
C         DISCRETISATION A CHAQUE INTERVALLE DE TEMPS
C         A PARTIR DE LA VALEUR A CHAQUE INTERVALLE
C         LA VALEUR AU PAS DE TEMPS CORRESPOND A
C         LA MOYENNE ENTRE LES DEUX VALEURS BORNANT L'INTERVALLE
C
          REAL*8 X(9600),Y(9600),Z(9600),REPAS(9600)
          REAL*8 XX(9600),YY(9600),TINC,INT
          REAL*8 ECART,DEBUT,FIN,PENTE
          INTEGER VALMAX,NEWVAL,VALPAS,INTER
C
          I=1
          INT=0.D+0
C         TINC=15.D+0
C
          DO 100,J=1,VALMAX
           IF(J.EQ.1)THEN
           YY(I)=Y(J)
              XX(I)=INT
```

```
                INDICE=I+1-J
                SOMME=SOMME+H(J)*(E(INDICE)*DT)
 90             CONTINUE
        END IF
        H(I)=(S(I)-SOMME)/(E(1)*DT)
        PAS(I)=I
 100    CONTINUE
C
        END

        SUBROUTINE APPEL_FICHIER2(X,Y,MAXVALEUR,PAS)
C
C       LE FICHIER APPELE A LA STRUCTURE SUIVANTE
C       LIGNE 1: NOMBRE DE VALEURS CONTENUS DANS LE FICHIER
C       LIGNE 2: VALEUR DU PAS DE TEMPS
C       LIGNES SUIVANTES:
C       COLONNE 1: ORDRE
C       COLONNE 2: NUMERO DU PAS DE TEMPS
C       COLONNE 3: CONCENTRATION AU PAS DE TEMPS
C
        CHARACTER*80 FICIN
        REAL*8 X(9600),Y(9600),MAX
        INTEGER IN,MAXVALEUR,I
        PARAMETER(IN=10)
C
 10     FORMAT(A)
        TYPE *,'NOM DU FICHIER'
        ACCEPT 10,FICIN
        OPEN(UNIT=IN,FILE=FICIN,STATUS='OLD')
        READ(IN,*)MAXVALEUR
        READ(IN,*)PAS
        DO 100,I=1,MAXVALEUR
                READ(IN,*)ORDRE,X(ORDRE),Y(ORDRE)
 100    CONTINUE
        CLOSE(UNIT=IN)
        END

        SUBROUTINE CONVOLE(X,E,NOMBREX,TT,Y,NOMBREY,QQ,Z,NOMBREZ,INC)
C
C.....IL EFFECTUE LA CONVOLUTION ENTRE UN FICHIER D'ENTREE
C.....ET UNE REPONSE IMPULSIONNELLE
C       LA CONVOLUTION FOURNIT UNE VALEUR A LA FIN DU PAS DE TEMPS
C       CETTE VALEUR EST AFFECTEE SUR TOUT LE PAS DE TEMPS
C       CAR LA CONVOLUTION D'UNE VALEUR MOYENNE SUR UN PAS PAR
C       UNE VALEUR MOYENNE SUR UN PAS FOURNIT
C       UNE VALEUR A LA FIN DU PAS DE TEMPS
C
        REAL*8 X(9600),Y(9600),Z(9600)
        REAL*8 TT(9600),E(9600),QQ(9600),INC
        INTEGER NOMBREX,NOMBREY,NOMBREZ,PAS
C
C
        NOMBREZ=NOMBREX+NOMBREY
C
C       A CAUSE DE L'AJOUT D'UNE VALEUR 0, SINON
C       NOMBREX+NOMBREZ-1
C
C       L'INCREMENT DE TEMPS EST DE DT (INC)
C
C       INC=15.D+0
        I=1
        Z(I)=0.D+0
        QQ(I)=0.D+0
        DO WHILE(I.LE.NOMBREX)
                PAS=I+1
                J=1
        DO WHILE(J.LE.NOMBREY)
        Z(PAS)=Z(PAS)+(E(I)*INC)*Y(J)
                QQ(PAS)=(PAS-1)*INC
                PAS=I+1+J
                J=J+1
                END DO
        I=I+1
        END DO
C
C.....FIN
C
        END

        SUBROUTINE SORTIE_FICHIER(A,B,MAX)
C
C       LE FICHIER SAUVE CONTIENT
C       - LIGNE 1: NOMBRE DE VALEURS CONTENUES DANS LE FICHIER
C       - LIGNES SUIVANTES
C       COLONNE 1: ORDRE
C       COLONNE 2: TEMPS
C       COLONNE 3: CONCENTRATION
C
        REAL*8 A(9600),B(9600)
        INTEGER MAX,OUT
        CHARACTER*80 FICOUT
        PARAMETER(OUT=20)
C
 10     FORMAT(A)
        TYPE *,'NOM DU FICHIER'
        ACCEPT 10,FICOUT
        OPEN(UNIT=OUT,FILE=FICOUT,STATUS='NEW')
        WRITE(OUT,*)MAX
        DO 100,I=1,MAX
                WRITE(OUT,*)I,A(I),B(I)
 100    CONTINUE
C
        CLOSE(UNIT=OUT)
        END
```

APPENDIX II.1

Chemical tracers

Appendix II.1. : Chemical tracers (fluorescent dyes, salt)

a) type and characteristics of used trecers

The fluorescent tracers

These tracers are subdivided in two groups: the Xanthenes group (green to red fluorescent dye) within the uranine, the duasine, the eosine and the rhodamines and the group of other fluorescent dye compounds with blue to green dominant colour, with, for exemple, the sodium napthionate.

These chamical substances, organic molecules, are made of simple-double co-ordinate bonds. Once they are in a solute, they can adsorb the energy as light and emit another by molecular excitation. The emitted light by fluorescence has a larger well length than the excitted one. Each substance or tracer is characterised by some specific spectrum of emission end adsorption (Allemann et al., 1991).

Major characteristics

URANINE

Technical designation: Acid Yellow 73
Synonym: sodium fluoresceine
Chemical name: dinatric spiro [isobenzofuran - 1(3H),9' è [9H] xanthen] - 3- one, 3',6' - dihydroxy] salt.
Chemical formula: $C_{20}H_{10}O_5Na_2$
Molar mass: 376. 28
Excitation frequency: 491 nm
Emission frequency: 512 nm
Fluorescence (uranine as reference): 100%

Comments: The term of fluorescein sensu strictum is very often abusively used, and principally in the american litterature as it is mentioned by Quinlan (1989). The fluorescein s.s. has not the same chemical formula; the ion Na is absent in benefit to 2 H.

The uranine when it is concentrated is of the unfluorescent dark red colour. After a strong dilution, a decreasing of the fluorescence progressively appears beceuse of the ion Na dissociation of the " uranine " ions group.

In accord with Käss, 1994, the various colours of the uranine correspond to the following concentration ranges:

1E-1 mg/l	red
1E-2 mg/l	red green
1 E-3 mg/l	yellow green
1E-4 to 1E-5 mg/l	green
1E-5 to 1E-8 mg/l	faint green
1E-8 mg/l	eye visible detection limit

Toxicity : LD50 (mg/kg): 6271 for rats (Smart, 1982)
4740 for mice (Lutty ,1979)
LC50 (mg/l) 1372 (96h) for Rainbow trults (Marking, 1969)
2269 (96h) for " cat fish " (Marking, 1969)
> 752 (24h) for the carps (Benoît-Guyod, 1979)
non carcinogenic and non mutagen (Smart, 1982)

Recovering rate: very good in karstic environment

EOSIN
Technical designation: Acid Red 87
Synonym:Yellow eosine, Eosine G, Eosine YS, ...
Chemical name: spiro [isobenzofuran - 1(3H),9' à [9H] xenthen] - 3- one,2',4',5',7' - tetrabromo - 3',6' - dihydroxy - dinetrium salt.
Chemical formula: $C_{20}H_6O_5\ Br_4Na_2$
Molar mass: 691.88
Excitation frequency: 516 nm
Emission frequency: 538 nm
Fluorescence (uranine as reference): 18%
Toxicity : LD_{50} (mg/kg): > 1000 for rats (Smart, 1982)
> 550 for mice (Lutty ,1978)
LC_{50} (mg/l) > 138 (24h) for carps (Benoît-Guyod, 1979)
uncertain carcinogenic property and not to exclude the mutagen property
Recovering rate: good in karstic and porous media environment

Comments: The eosine is a little bit more absorbed than the uranine; its fluorescence is less function of the pH value than the uranine. As very sensitive to the light, the eosine is not used as surface water tracer.

AMIDORHODAMINE G
Technical designation: Acid Red 50
Synonym: sulforhodamine G extra (Hoechst), Amidorhodamine
Chemical name: Xanthylium, 9 - (2, 4-disulfophenyl) -3,6 - bis (ethylanmino) - 2,7 - dimethyl-Natrium.
Chemical formula: $C_{25}H_3O_7\ N_2S_2Na$
Molar mass: 552.59
Excitetion frequency: 530 nm
Emission frequency: 551 nm
Fluorescence (uranine as reference): 14%
Toxicity : LD_{50} (mg/kg): > 10000 for rats (Smart, 1982)
LC_{50} (mg/l) > 88 (24h) for carps (Benoît-Guyod, 1979)
no available data concerning the mutagen and carcinogenic properties.
Recovering rate: good in karstic environment; bad in porous media environment; high interaction with clays and humus.

Comments: This substence is relatively easy to distinguish from the uranine by spectrofluometry in comparison to the eosine. It is also characterized by a good stability to light and pH.

DUASYN
Technical designation:Acid yellow 245 (liquid)
Synonym:duasyn-fluorescenzgelb T flüssig
Chemical name: -
Chemical formula: -
Molar mass: -
Excitation frequency: 446 nm
Emission frequency: 480 nm
Fluorescence (uranine as reference): -
Toxicity : LD_{50} (mg/kg): > 2000 for rats
no available data concerning the mutagen and carcinogenic properties.
Recovering rate: good in karstic and porous media environment

SODIUM NAPHTIONATE
Technical designation: Sodium napthionate
Synonym: naphtosodium acid
Chemical name: 4 - Aminonaphtalin - 1- sulfonacid, Natrium salt.
Chemical formula: $C_{10}H_8O_73NSNa$
Molar mass: 245.23
Excitation frequency: 320 nm
Emission frequency: 430 nm
Fluorescence (uranine as reference): 8%
Toxicity : . LD_{50} (mg/kg): no available data in specific litterature
no available data concerning the mutagen and carcinogenic properties.
Recovering rate: good in karstic environment; but prudence is necessary in dealing with high organic matter content water: the natural fluorescence of high organic matter water is similar to napthionate.

Comments: The napthionate is a grey pink powder; its intensity is 14 time less than the uranine. It is necessary to inject generally 20 times the uranine quantity for a given experiment. One major incovenient is the interference of the emission frequency of the organic matter, naturally in water. Consequently, the napthionate peak can be masked; without a density spectrum at the corresponding frequency interval, oragnic matter can be identified as naphtionate.

General comments for the fluorescent tracers

Under the used concentrations for the tracing tests (more often less than 10mg/l), the fluorescent tracers do not induce some toxicity proofs or mutagen or teratogen properties. Meanwhile, it is necessary in handling the tracers to protect hands and breath paths (nose and mouth) as the substances are generally powder conditioning; this powder is extremly volatile. It is also necesaary to undertake the psycological effect of a red or green colour of the water on the people, even if it is not dangerous.

The salts

On the test site of La Milandrine - Bure, livestock salt has been used; it is pink coloured NaCl salt. It provides good results in the tracer experiments and is determined by measuring the electrical conductivity of water. It is a easy and relatively accured mean.

In karstic environment, the natural electrical conductivity changes with the discharge variations, the hydrodynamic state of the aquifer. It is necessary to keep in mind the existence of this natural process before any interpretation of salt breakthrough curves. When the conductivity background is not steady, but is affected by high variations, it is uselesa to interprete such a response. It is necessary to accomplish such salt tracer experiments when the hydrodynamic conditions are as stable as far as possible.

Another disadvantage is the quantity of salt to be injected; to provoke an significant increase of the elecrical conductivity of the water, it is necessary to use a large quantity. In the test-site of Bure, we used 100 to 500 kg per tracer tests for mean discharge of 35l/s and small distances (less than 500 metres for the upstream point in the cave and less than 5000 metres for the downstream point at the springs).

Injection of salt induces an increasing of water density; a matter of avoiding that the salt solution get stratified in the lowest part of the aquifer, the salt is diluted in large quantities of water (several cubic metres) and just after the salt injection, a water flush is accomplished.

Some characteristics of the Sodium chlorine:

NaCl: sodium chlorine
Molar mass: 58.44
The solubility varies in function of the temperature:
- 356 g/l for 0^oC
- 356.6 g/l for 5^oC
- 357 g/l for 10^oC

Toxicity: LD_{50} for rats (oral): 3000 mg/kg
For fisches and fish eggs: till 10'000 mg/l (Schäperclaus, 1954).

APPENDIX II.2

Analytical principles for fluorescent and chemical tracers

Appendix II.2.:Analytical principles for fluorescent and chemical tracers

The fluorescent tracers are analysed either by spectrometry or by liquid chromatography (HPLC). Under this appendix, only the principle of the spectrometry will be briefly developed. For more details concerning the principles, the limits and advantages and disadvantages of the methods, many references such as Käss (1994), Mdaghri Alaoui A., (1992), Behrens H. (1988) and Lutz et al., (1988) are available.

Principles of the spectrometer

The principles of the spectrometer used in the CHYN laboratory to determine the water samples concentration are the following:

a light source, a xenon tube, characterised with a large well lengths renge spectrum, is filtered in order that only the light whose well length corresponds to the excitation well length of the given fluorescent tracer get through it. The so filtered light gets through a small tank containing the water sample with the supposed tracer. The water solution emits by fluorescence a light characterised by its higher well length. This light is directed to the photoelectrical cell. The resulting photoelectric energy is measured after amplification, by a galvanometer (Alleman and Mdaghri Alaoui, 1991).

The spectrometer LS-5P-PE (Perkin Elmer) used in the Centre of Hydrogeology Laboratory allows to measure light intensities for all the spectrum in function of the well length. This is accomplished by simple or double scanning. A simple scanning consists in doing either an excitation spectrum or an emission spectrum. In the first case, the emission well length stays constant, when in the second case, the excitation of the sample is carried out with a given well length.

In the case of the double scanning, the well length interval between the excitation and the emission remains fixed when one accomplishes a spectrum scanning. The resulting peak has a maximal intensity and corresponds to the well length of the analysed tracer.

The scanning permits to identify the concentration background and to ensure that the induced fluorescence by the organic matter does not correspond to the tracer. The organic matter in the water induces some fluorescent peaks in the UV and particularly masks the presence of naphtionate. In the cases of high concentration of organic matter in the water, the use of napthionate as tracer is strongly inadvisable.

Detection limits for different tracers:

uranine: 0.01 to 0.001 ppb

sulforhodamine G extra: 0.02 ppb

naphtionate : 0.1ppb

eosine: 0.25 ppb

Interference between tracers (Alleman & Mdaghri Alaoui A., 1991):

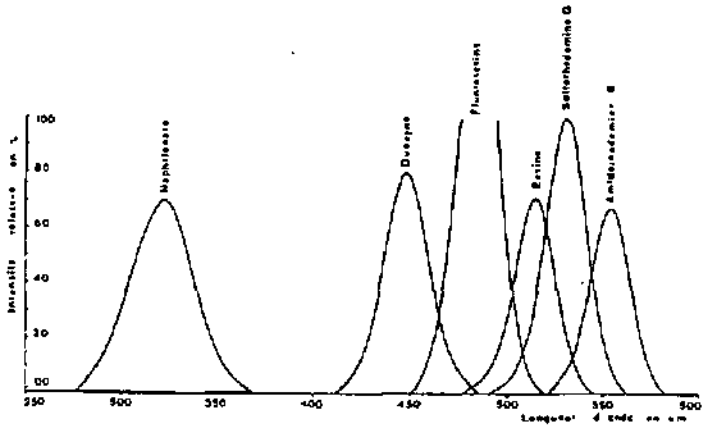

Figure 1.: Spectre of major fluorescent dyes used in hydrogeology

The eosin can interfered with the uranine signal; for this reason it is necessary to saparate the two signals modifying the pH or using the HPLC.

The sulforhodamine G extra does not interfered with the uranine. Therefora if there is high concentration of uranine in comparison to sulforhodamine G, its response can be modifiad.

Limits of the methods:

The spectrometer permits to obtain good results whose reproducibility is less than those ot the liquid chromatography (HPLC). The interference questions can be solved due to the modification of the pH (acidification); the presence ot uranine in higher concentration than a second one whose well langth is close to, induces difficulties to distinguish specific spectrum. It is obvious that a clear separation of the various tracer is produced by HPLC. This method shows more advantages, as on the other hand it allows a lower detection limit than the spectrometer doas. Therafore, it is necessary to be critical to the very low concentration around the datection limits and their significance. If the spectrometer is in some way disadvantageous, it has an unegligible advantage: analyses costs are obviously lower than those of the HPLC.

Field conductivimeter

The tracing tests carried out with sodium chlorine as tracer had been measured simply with the use of an electrical conductivity / temperature probe connected to a data taker; the frequency of value recording can be set in function of the tracing tests. The translation of the measures in electrical conductivity, corrected at 20 or 25°C in salt concentration is done on the basis of a calibration accomplished on various samplas by Jeannin. In function of the instruments, on uses tha correlation factor of 1.57 or 1.72, empirically datarminad in situ.

According to the tests, tha measurement tima staps are set on 5, 15 to 30 minutas, till exceptionally 60 minutes.

APPENDIX II.3

Table of tracer tests data performed in Tabular Jura

Tracing tests carried out on the Bure Plateau (Ajoie, Swiss Jura)

Quantitative interpretation using a global approach - Black box model -

Bajocian - Upper Hauterivian (karstic network)

injection date	Code	Concentration	Geological context	TRACER	Mass (kg or l)	Recovery %	Flowrate (l/s)	Injection duration	Injection site	Surface of WCB	Position on hydrograph	Tracing distance (m)
13.8.1991	11outlament.dat	Bure	Tabular Jura	NaCl	200	31	18	Irlang. 05'	artificial hole	5 km2	Base flow recession	395
20.8.1991	12outlament.dat	Bure	Tabular Jura	NaCl	200	32	14	Irlang. 45'	artificial hole	5 km2	Base flow recession	410
8.12.1991	13outlament.dat	Bure	Tabular Jura	NaCl	50	67	23	Irlang.15'	borehole MIL5	5 km2	Base flow recession	183
6.12.1991	14outlament.dat	Bure	Tabular Jura	NaCl	50	60	23	Irlang. 70'	borehole NEB 9	5 km2	Base flow recession	295
9.12.1991	17outlament.dat	Bure	Tabular Jura	NaCl	500	14	23	Irlang.12'	borehole MIL6	5 km2	Base flow recession	174
10.12.1991	18outlament.dat	Bure	Tabular Jura	NaCl	500	28	23	Irlang.12'	borehole MIL 7	5 km2	Base flow recession	178
16.12.1991	116outlament.dat	Bure	Tabular Jura	NaCl	18	21	36	Irlang. 15'	borehole MIL 7	5 km2	Base flow recession	177
19.5.1992	191outlament.dat	Bure	Tabular Jura	NaCl	100	21	32	Irlang. 12'	borehole MIL 6	5 km2	Base flow recession	195
26.5.1992	192outlament.dat	Bure	Tabular Jura	NaCl	100	18	30	Irlang. 12'	borehole MIL 4	5 km2	Base flow recession	180
8.9.1992	114outlament.dat	Bure	Tabular Jura	NaCl	150	83	21	Irlang.10'	borehole MIL 5	5 km2	Base flow recession	452
10.9.1992	115outlament.dat	Bure	Tabular Jura	NaCl	50	78	19	Irlang. 4'	borehole MIL 5	5 km2	Base flow recession	178
2.12.1992	116outlament.dat	Bure	Tabular Jura	NaCl	950	98.6	150	Irlang. 02'	borehole PN 1	5 km2	Falling limb	513
15.12.1992	119outlament.dat	Bure	Tabular Jura	NaCl	200	32	48	Irlang. 12'	borehole MIL 2	5 km2	Falling limb / Base flow recession	452
2.4.1993	120outlament.dat	Bure	Tabular Jura	NaCl	250	90	30	Irlang. 31'	borehole MIL 1	5 km2	Falling limb / Base flow recession	484
22.9.1993	121outlament.dat	Bure	Tabular Jura	NaCl	50	100	25.3	Irlang.11'	borehole MIL 7	5 km2	Falling limb	172
6.9.1993	124outlament.dat	Bure	Tabular Jura	NaCl	50	79	24	Irlang.11'	borehole MIL 7	5 km2	Falling limb / Base flow recession	172
9.9.1993	125outlament.dat	Bure	Tabular Jura	NaCl	500	48	33	Irlang. 35'	borehole FM 2	5 km2	Base flow recession	458
12.4.1994	126outlament.dat	Bure	Tabular Jura	NaCl	300	7	56.7	Irlang. 15'	surface point 8	5 km2	Base flow recession	126
3.2.1994	129outlament.dat	Bure	Tabular Jura	NaCl	350	109	51.4	Irlang.11'	borehole MIL5	5 km2	Base flow recession / Base flow recession	452
23.3.1994	130outlament.dat	Bure	Tabular Jura	NaCl	300	47.5	56.9	Irlang. 12'	surface point 11	5 km2	Karstified limb / Base flow recession	533
25.3.1994	131outlament.dat	Bure	Tabular Jura	NaCl	500	63.5	53	Irlang. 20'	borehole MIL7	5km2	Base flow recession	172
15.5.1994	132outlament.dat	Bure	Tabular Jura	NaCl	350	9	40	Irlang.15'	surface point 8	5 km2	Base flow recession	434
5.7.1994	135outlament.dat	Bure	Tabular Jura	NaCl	300	2.5	30	Irlang20'	surface point 3	5 km2	Base flow recession	265
30.8.1994	136outlament.dat	Bure	Tabular Jura	NaCl	250	14.5	22	Irlang.20'	karst borehole FM1	5 km2	Base flow recession	513
9.9.1994	139outlament.dat	Bure	Tabular Jura	NaCl	200	2	22	Irlang.30'	surface point 8	5 km2	Base flow recession /Falling limb	172
13.9.1994	140outlament.dat	Bure	Tabular Jura	NaCl	100	80	25.2	Irlang. 20'	borehole MIL7	5 km2	Falling limb recession /Falling limb	172
26.9.1994	141outlament.dat	Bure	Tabular Jura	NaCl	150	03	48	Irlang. 13'	surface point	5 km2	Falling limb / Base flow recession	20
19.10.1994	142outlament.dat	Bure	Tabular Jura	NaCl	150	100	23	Irlang.13'	surface point 1	5 km2	Base flow recession	20
2.11.1994	143outlament.dat	Bure	Tabular Jura	NaCl	150	31	65	Irlang. 13'	surface point 1	5 km2	Falling limb / Falling limb	20
7.11.1994	1431outlament.dat	Bure	Tabular Jura	H401	2.70E+10	13	65	Irlang. 13'	surface point 1	5 km2	Falling limb	20
12.12.1994	144outlament.dat	Bure	Tabular Jura	naphtionate	0.00	0%	65		borehole MIL9	5 km2	Falling limb / Falling limb	425
12.12.1994	1448outlament.dat	Bure	Tabular Jura	H401	0.72E+08	0%	65		borehole MIL9	5 km2	Falling limb / Falling limb	425
12.12.1994	145outlament.dat	Bure	Tabular Jura	NaCl	100	29.8	235.5	Irlang. 19'	surface point 1	5 km2	Falling limb	20
12.12.1994	1459outlament.dat	Bure	Tabular Jura	H4011	4.03E+10	9	233.0	Irlang. 19'	surface point 1	5 km2	Falling limb	20
19.12.1994	146outlament.dat	Bure	Tabular Jura	NaCl	250	60	51.6	Irlang. 16'	borehole MIL5	5 km2	Base flow recession	452
18.1.1995	147outlament.dat	Bure	Tabular Jura	NaCl	250	69	67.75	Irlang. 15'	borehole MIL5	5 km2	Base flow recession	452
18.1.1995	1471B1outlament.d	Bure	Tabular Jura	H401	1.45E+12	8	67.75	Irlang. 15'	borehole MIL5	5 km2	Base flow recession	452
18.1.1995	1471B2outlament.d	Bure	Tabular Jura	H4011	5.93E+11	29	67.75	Irlang. 15'	borehole MIL5	5 km2	Base flow recession	452
30.1.1995	148outlament.dat	Bure	Tabular Jura	NaCl	500	91	240.13	Irlang. 13'	borehole MIL2	5 km2	Karstified limb / Base flow recession	172
8.2.1995	149outlament.dat	Bure	Tabular Jura	NaCl	150	58	83.4	Irlang. 17'	borehole MIL3	5 km2	Base flow recession	452
6.9.1995	145uranine.dat	Bure	Tabular Jura	uranine	0.15	49	83.4	Irlang. 17'	borehole MIL3	5 km2	Base flow recession	452
4.4.1995	150outlament.dat	Bure	Tabular Jura	NaCl	300	96	81.3	Irlang. 10'	borehole MIL3	5 km2	Falling limb	452
4.4.1995	1501B1outlament.d	Bure	Tabular Jura	H401	1.41E+12	23	87.3	Irlang. 10'	borehole MIL3	5 km2	Falling limb	452
4.4.1995	1501B2outlament.d	Bure	Tabular Jura	H4011	2.26E+12	100	87.3	Irlang. 10'	borehole MIL3	5 km2	Falling limb	452
8.5.1995	151B1outlament.d	Bure	Tabular Jura	H401	5.43E+12	3	29.93	Irlang. 14'	borehole MIL3	5 km2	Base flow recession	452
8.5.1995	151B2outlament.d	Bure	Tabular Jura	H4011	2.63E+11	0	29.93	Irlang. 14'	borehole MIL3	5 km2	Base flow recession	452
8.5.1995	151B3outlament.d	Bure	Tabular Jura	H4011	1.57E+13	48	29.93	Irlang. 14'	borehole MIL3	5 km2	Base flow recession	452
8.5.1995	151outlament.dat	Bure	Tabular Jura	NaCl	250	65	29.93	Irlang. 14'	borehole MIL3	5 km2	Base flow recession	452
21.6.1995	153B1outlament.d	Bure	Tabular Jura	T7	6.25E+12	2	65	Irlang. 13'	borehole MIL3	5 km2	Base flow recession	452
21.6.1995	153B2outlament.d	Bure	Tabular Jura	H311	9.01E+12	8	65	Irlang. 15'	borehole MIL3	5 km2	Base flow recession	452
21.6.1995	153B3outlament.d	Bure	Tabular Jura	H414	5.84E+12	23	65	Irlang. 13'	borehole MIL3	5 km2	Base flow recession	452
21.6.1995	1531outlament.dat	Bure	Tabular Jura	Pyr2	1.27E+12	5	65	Irlang. 9'	surface point 8	5 km2	Base flow recession	20
21.6.1995	154B2outlament.d	Bure	Tabular Jura	H4011	3.31E+13	18	45	Irlang. 9'	surface point 8	5 km2	Base flow recession	20
21.6.1995	155B1outlament.d	Bure	Tabular Jura	H4011	9.30E+12	69	16.21	Irlang. 34'	borehole MIL3	5 km2	Base flow recession	452
21.6.1995	155B2outlament.d	Bure	Tabular Jura	T7	9.11E+13	9.5	16.21	Irlang. 34'	borehole MIL3	5 km2	Base flow recession	452
21.6.1995	156B1outlament.d	Bure	Tabular Jura	T1	4.28E+13	0.25	16.21	Irlang. 13'	surface point 1	5 km2	Base flow recession	20
21.6.1995	156B2outlament.d	Bure	Tabular Jura	Pyr2	3.32E+11	21	16.21	Irlang. 13'	surface point 1	5 km2	Base flow recession	20
22.9.1995	157B1outlament.d	Bure	Tabular Jura	T1	6.50E+12	0.5	50.667	Irlang. 13'	borehole MIL3	5 km2	Falling limb	452
22.9.1995	157B2outlament.d	Bure	Tabular Jura	T7	3.88E+13	1.3	50.667	Irlang. 13'	borehole MIL3	5 km2	Falling limb	452
22.9.1995	157B3outlament.d	Bure	Tabular Jura	H311	4.16E+12	15	06.67	Irlang. 15'	borehole MIL3	5 km2	Falling limb	452
22.9.1995	157B4outlament.d	Bure	Tabular Jura	H4011	9.98E+12	73.5	06.67	Irlang. 13'	borehole MIL3	5 km2	Falling limb	452
22.9.1995	157uranine.dat	Bure	Tabular Jura	uranine	0.15	94	66.67	Irlang. 13'	borehole MIL3	5 km2	Falling limb	452
22.9.1995	157uranine.dat	Bure	Tabular Jura	uranine	0.15	90	66.67	Irlang. 13'	borehole MIL3	5 km2	Falling limb	452

Fort - spring

21.5.1992	112outlant.dat	Bure	Tabular Jura	NaCl	100	3.8	35.6	Irlang. 12'	borehole MIL4	45 km2	Base flow recession	5793 (3410)
9.9.1992	114outlant.dat	Bure	Tabular Jura	NaCl	150	12.3	13.9	Irlang. 30'	borehole MIL3	45 km2	Base flow recession	6085 (3580)
16.9.1992	115outlant.dat	Bure	Tabular Jura	NaCl	50	6.2	10	Irlang. 4'	borehole MIL5	45 km2	Base flow recession	6811 (3580)
23.12.1992	119outlant.dat	Bure	Tabular Jura	NaCl	200	5.8	27.8	Irlang. 12'	borehole MIL2	45 km2	Falling limb / Base flow recession	6085 (3720)
2.4.1993	120outlant.dat	Bure	Tabular Jura	NaCl	250	19	35.4	Irlang. 31'	borehole MIL1	45 km2	Base flow recession	6077 (3720)
22.9.1993	123outlant.dat	Bure	Tabular Jura	NaCl	50	23.4	21.03	Irlang. 11'	borehole MIL7	45 km2	Falling limb / Karstified limb	5805 (3423)
6.9.1993	124outlant.dat	Bure	Tabular Jura	NaCl	50	19.3	25	Irlang. 11'	borehole MIL7	45 km2	Falling limb	5805 (3423)
9.9.1993	125outlant.dat	Bure	Tabular Jura	NaCl	500	32.2	29.5	Irlang. 35'	borehole FM2	45 km2	Falling limb	6089 (3763)

Sahro spring

12.8.1991	T1eautsahru.dat		Bure	Tabular Jura	NaCl	260	11.5	28.88	triang. 95°	artificial hole	15 km2	Base flow recession	8523 (3150)
20.8.1991	T2eautsahru.dat		Bure	Tabular Jura	NaCl	200	9	24.8	triang. 45°	artificial hole	15 km2	Base flow recession	8543 (3150)
16.8.1992	T1beautsahru.dat		Bure	Tabular Jura	NaCl	170	13.5	20	triang. 12°	borehole MS 8	15 km2	Base flow recession	8328 (3065)
21.5.1992	T12eautsahru.dat		Bure	Tabular Jura	NaCl	100	6.5	73	triang.18°	borehole MS 4	15 km2	Rad falling limb/base flow recession	5293 (2935)
7.10.1992	T17eautsahru.dat		Bure	Tabular Jura	NaCl	250	13	33	triang. 3°	borehole MS 7	15 km2	Falling limb	5305 (3000)
7.1.1993	T20eautsahru.dat		Bure	Tabular Jura	NaCl	50	95.75	66	triang. 31°	borehole MS 1	15 km2	Rad falling limb/base flow recession	5577 (3700)
27.1.1993	T23eautsahru.dat		Bure	Tabular Jura	NaCl	50	74.3	66.7	triang. 11°	borehole MS 7	15 km2	Rad falling limb/base flow recession	5385 (3006)
6.5.1993	T2Beautsahru.dat		Bure	Tabular Jura	NaCl	50	85.7	60.75	triang.11°	borehole MS 7	15 km2	Falling limb	5305 (3000)
9.8.1993	T25eautsahru.dat		Bure	Tabular Jura	NaCl	300	7.6	19	triang. 35°	borehole FN2	15 km2	Rad falling limb/base flow recession	5589 (3336)
11.3.1994	T30eautsahru.dat		Bure	Tabular Jura	NaCl	300	15	91	triang. 42°	surface point 11	15 km2	Base flow recession	5464 (3140)
17.9.1994	T32eautsahru.dat		Bure	Tabular Jura	NaCl	500	19.8	91.8	triang. 232°	borehole NEB13	15 km2	Base flow recession	4633 (3000)
20.9.1994	T34eautsahru.dat		Bure	Tabular Jura	NaCl	150	8.33	56.5	triang.°	surface point 1	15 km2	Rad falling limb	5153 (3153)

Bärm spring

7.1.1993	T26eautbärme.dat		Bure	Tabular Jura	NaCl	50	5.9	65	triang.31°	borehole MS 1	15 km2	Base flow recession	5077 (3315)
6.5.1993	T24eautbärme.dat		Bure	Tabular Jura	NaCl	50	6	8	triang. 11°	borehole MS 7	15 km2	Base flow recession	9805 (4808)
12.1.1994	T29eautbärme.dat		Bure	Tabular Jura	NaCl	300	9	150	triang. 15°	surface point 8	15 km2	Base flow recession	4761 (2385)
2.2.1994	T27eautbärme.dat		Bure	Tabular Jura	NaCl	308	45	193	triang. 11°	borehole MS 7	15 km2	Falling limb	5085 (3100)
11.3.1994	T30eautbärme.dat		Bure	Tabular Jura	NaCl	308	9	186	triang. 121°	surface point 11	15 km2	Rising limb	5188 (3085)
31.3.1994	T31eautbärme.dat		Bure	Tabular Jura	NaCl	300	28	99	triang. 60°	natural hole near NEB13	15 km2	Rising limb	4133 (2370)
19.4.1995	T31eautbärme.dat		Bure	Tabular Jura	NaCl	500	35	244	triang. 232°	borehole NEB13	15 km2	Falling limb	4133 (2635)

Various tracer tests

JU1	Boécourt	Tabular Jura	Lixiviat	1	7.2	26.5	triang.240°	artificial hole	3 km2	Base flow recession	1800
JU2	Boécourt	Tabular Jura	Suite Q. petite	5	23	31	triang.60°	artificial hole	12 km2	Rising and falling limbs	1550
JU3	Bocourt	Tabular Jura	Lixiviat	5	15	150	triang.5°	artificial hole	0 km2	base flow recession	3750
JU4	Mormont	Tabular Jura	Nephélinite	50	60	37	triang. 60°	artificial hole	5 km2	Base flow recession	2100
JU5	Courcelles	Tabular Jura	Lixiviat	1	95	80	triang. 5°	artificial hole	5 km2	Base flow recession	1875
JU10	Courtelevre	Folded Jura	NaCl	9300	2.5	60000	triang. 30°	tracavre	6 km2	Base flow recession	900

* : approximative direct distance till the upper part of the karstic network, added to the true measured distance of the underground network

( ) : approximative direct tracing distance

injection date :	Code	Time steps of the Gravity center	MAX (t/MM)	Max. step time nombre	Time step	MODE	Gradient at 0.2	Gradient at 0.5	Gradient at 0.8	Mean transit velocity (m/h)	Modal velocity (m/h)	Max. velocity (m/h)
		Transfert functions - Kernel function					S transfert functions					
12.8.1991	T1eautjament.dat	1123	1.50E-03	5250	7	unimodal	63	88	54.5	20	23.11	30
29.8.1991	T2eautjament.dat	1056	1.50E-03	3100	1	unimodal	84	84.5	73.5	33	27.3	49.5
5.12.1991	T5eautjament.dat	280	9.30E-03	608	1	unimodal	90	88	85	70	45	65.5
9.12.1991	T6eautjament.dat	623	2.40E-03	1400	1	unimodal	80.5	84	76	49	22.7	50
9.12.1991	T7eautjament.dat	456	2.30E-03	1200	1	unimodal	84	83.5	80	38	17.5	41
10.12.1991	T8eautjament.dat	954	8.00E-04	3350	1	unimodal	74	72	70	69	19.9	60
18.12.1991	T10eautjament.dat	466	2.40E-03	1800	1	unimodal	69.75	67.5	67	30	25	31
19.5.1992	T11eautjament.dat	657	1.50E-03	2100	1	unimodal	80.5	68	73.5	14	11	18
21.5.1992	T12eautjament.dat	643	2.30E-03	2350	1	unimodal	83.5	66	62	54	31.5	28.5
9.9.1992	T14eautjament.dat	337	1.70E-03	1850	1	unimodal	85.5	84	81	63	37.5	66.5
15.9.1992	T15eautjament.dat	595	5.00E-03	2460	1	unimodal	82	85	56	70	39.6	93
7.12.1992	T16eautjament.dat	602	4.70E-03	1350	1	plurimodal	67	63.5	79	81	56.5	84
23.12.1992	T19eautjament.dat	715	2.20E-03	4000	1	bimodal	87.5	90	60	133	60.5	152
7.1.1993	T20eautjament.dat	446	5.70E-03	2100	1	unimodal	88.5	87	79	103	52.5	110
27.4.1993	T23eautjament.dat	279	1.10E-02	2000	1	unimodal	87.5	85.5	60	130	93	172
6.5.1993	T24eautjament.dat	254	9.50E-03	1100	1	unimodal	83	87.5	74	113	91	110.5
9.8.1993	T25eautjament.dat	616	3.60E-03	2400	1	unimodal	87	86	70	56	39	87.5
12.1.1994	T28eautjament.dat	133	1.75E-02	309	1	unimodal	90	90	65	90	73.5	108
2.2.1994	T29eautjament.dat	370	2.40E-03	1615	1	unimodal	84	80	60	75	104	247
11.3.1994	T30eautjament.dat	721	2.50E-03	2448	1	unimodal	83	80	60	49	78	107
3.5.1994	T33eautjament.dat	127	1.05E-02	735	1	unimodal	90	90	65	81	109	295
15.8.1994	T34eautjament.dat	907	3.30E-03	1385	1	unimodal	87.5	85.5	82.5	28	28	33
5.7.1994	T35eautjament.dat	905	1.35E-03	2033	1	unimodal	79	77.5	67	14	17	49
30.8.1994	T38eautjament.dat	1713	2.75E-03	2030	1	unimodal	74	83	86	28	28	38.5
7.9.1994	T39eautjament.dat	714	4.00E-03	1102	1	unimodal	82	86	82.5	15	15	21.5
13.9.1994	T40eautjament.dat	99	1.21E-02	675	1	unimodal	89	87	87	229	227	656
28.9.1994	T41eautjament.dat	410	2.75E-03	1085	1	unimodal	90	90	90	10	21	52.5
19.10.1994	T42eautjament.dat	466	3.50E-03	702	1	unimodal	90	89	89	3	24	60
7.11.1994	T43eautjament.dat	72	1.77E-03	276	1	unimodal	89	87	87	17	20.5	50
2.11.1994	T43Beautjament.dat	69	2.20E-03	335	1	bimodal	87.5	87	78	18	27.3	34.5
12.12.1994	T44eautjament.dat	-	-	-	-	-	-	-	-	-	-	-
12.12.1994	T44Beautjament.dat	-	-	-	-	-	-	-	-	-	-	-
12.12.1994	T45eautjament.dat	121	7.57E-03	103	1	unimodal	80	87.5	86	18	63.5	216
12.12.1994	T45Beautjament.dat	37	3.13E-03	387	1	unimodal	90	87.5	87.5	33	12	710
19.12.1994	T46eautjament.dat	541	3.13E-03	1351	1	unimodal	85.5	82	78	96	98	163
10.1.1995	T47eautjament.dat	219	4.60E-03	942	1	unimodal	88.5	86.5	82	124	115	183
10.1.1995	T47Beautjament.dat	389	2.94E-03	1002	1	unimodal	85	84	82	79	86	181
10.1.1995	T47B2eautjament.dat	318	2.93E-03	1002	1	unimodal	85.5	86.5	82	85	86	181
30.1.1995	T48eautjament.dat	70	2.04E-02	404	1	unimodal	83	86	88	147	153	372
8.2.1995	T49eautjament.dat	362	3.52E-03	709	1	unimodal	87	84	82	75	94	139
8.2.1995	T49eautjament.dat	421	3.22E-03	1295	1	unimodal	88	83	77	65	93	158
4.4.1995	T50Beautjament.dat	359	2.20E-03	2296	1	unimodal	84	86	50	74	151	271
4.4.1995	T50B2eautjament.dat	329	4.16E-03	1935	1	unimodal	91	85	60	69	176	271
4.4.1995	T50eautjament.dat	552	3.12E-03	1911	1	unimodal	85	83	79	50	94	271
8.5.1995	T51B1eautjament.dat	989	2.70E-03	2052	1	bimodal	85	80	65	28	37	76
8.5.1995	T51B2eautjament.dat	702	3.00E-03	2552	1	bimodal	87	87	69	39	74	98
8.5.1995	T51B3eautjament.dat	673	3.00E-03	2052	1	unimodal	85	84	72	47	74	108

4.8.1995	T51coulement.dat	833	3.00E-03	1790	1	unimodal	88.5	84	80.5	43	65	108
21.8.1995	T52Bcoulement.dat	528	3.00E-03	1332	1	unimodal	87	85	70	62	70	123
27.8.1995	T52B2coulement.dat	-	-	-	1	-	-	-	-	-	-	-
21.8.1995	T53Bcoulement.dat	617	3.34E-03	1332	1	unimodal	87	85	70	53	70	123
21.8.1995	T54Bcoulement.dat	244	6.48E-03	1224	1	bimodal	85	85	71	5	34	73
21.8.1995	T5 coulement.dat	229	5.55E-03	1194	1	bimodal	80	80	75	6	34	80
21.8.1995	T55Bcoulement.dat	629	4.35E-03	1370	1	unimodal	86.5	85	78	42	46	89
21.8.1995	T55B2coulement.dat	655	4.70E-03	1320	1	unimodal	86.5	85	75	41	43	86
21.8.1995	T56Bcoulement.dat	78	4.56E-01	1265	1	unimodal	90	90	88	15	18	36
21.8.1995	T56B2coulement.dat	112	2.80E-03	1265	1	unimodal	90	90	87	13	18	36
22.9.1995	T57Bcoulement.dat	398	3.60E-03	1654	1	bimodal	87	88.5	80	48	102	271
22.9.1995	T57B2coulement.dat	521	3.44E-03	1659	1	bimodal	85	83.5	72	62	68	271
22.9.1995	T57B3coulement.dat	443	3.34E-03	1659	1	bimodal	85	87	78	53	104	244
22.9.1995	T57B4coulement.dat	423	6.64E-03	1659	1	bimodal	80	83	73	64	184	244
22.9.1995	T57ur3coulement.dat	423	3.10E-03	1704	1	bimodal	86	87	78	60	74	250
22.9.1995	T57ur2coulement.dat	423	3.10E-03	1704	1	bimodal	86	87	78	60	74	250

Fern spring

21.5.1992	T12coulfern.dat	3982	7.50E-04	4781	1	unimodal	72	74	68	117 (70)	1154 (98)	172.5 (101)
8.9.1992	T14coulfern.dat	4193	5.50E-04	6735	1	unimodal	69	71	64	87.5 (53)	91.5 (55.5)	124.5 (75)
16.9.1992	T15coulfern.dat	1823	8.50E-04	4133	1	unimodal	69	87	67	191.6 (114)	180.5 (90)	302 (180)
23.12.1993	T19coulfern.dat	3727	0.80E-04	5817	1	unimodal	67	72	70	90.5 (55)	87 (53)	143.5 (70)
7.1.1993	T20coulfern.dat	4864	7.50E-04	6163	1	unimodal	69	73	63.5	90 (55)	91.5 (56)	130.5 (80)
27.4.1993	T23coulfern.dat	4895	5.80E-04	6177	1	unimodal	61	73	60	81.5 (48)	87.5 (51.5)	143.5 (87)
6.5.1993	T24coulfern.dat	4735	7.00E-04	6050	1	unimodal	71	75	62	73 (43)	77 (43.5)	100 (59)
9.6.1993	T25coulfern.dat	1733	1.93E-03	3478	1	unimodal	85	80	60	210.5 (128)	210.5 (123.5)	328 (198)

Sahra spring

12.8.1991	T1coulsahra.dat	2869	1.13E-03	4599	1	unimodal	72	70	55	98 (56)	81 (40)	140.5 (83)
20.8.1991	T2coulsahra.dat	4251	7.40E-04	5476	1	bimodal	65	77	60	77.5 (44)	76 (43)	113 (65)
18.5.1992	T11coulsahra.dat	2141	1.91E-03	3401	1	unimodal	60	60.5	60	149.5 (86)	142.5 (87)	203.5 (117)
21.5.1992	T12coulsahra.dat	3344	3.00E-03	5547	1	unimodal	67	75	58	140.5 (78)	160 (93)	201 (111)
7.10.1992	T17coulsahra.dat	3432	7.00E-04	5450	1	unimodal	58	59	53	87 (49)	85 (48)	266.5 (151)
7.1.1993	T20coulsahra.dat	4749	3.50E-04	6600	1	unimodal	82	83	78	71.5 (42)	79 (41)	107.5 (59)
27.4.1993	T23coulsahra.dat	1869	1.91E-03	4183	1	unimodal	83	84	75	177 (100)	191 (108)	233.5 (132)
6.5.1993	T24coulsahra.dat	2048	1.40E-03	4751	1	unimodal	83	78	60	180 (88)	159 (90)	286 (150)
9.6.1993	T25coulsahra.dat	1210	1.59E-03	1815	1	unimodal	82	80	78	277 (165)	287 (167)	478 (275)
11.3.1994	T30coulsahra.dat	2150	2.00E-03	2050	1	unimodal	84	83.5	78	158 (96)	243 (142)	340 (206)
19.4.1994	T32coulsahra.dat	713	2.49E-03	2629	1	unimodal	83.5	82	84.5	227 (350.5)	414 (768)	710 (460)
28.9.1994	T41coulsahra.dat	1394	3.40E-03	1898	1	unimodal	85	85	83	230 (131)	246 (140.5)	316 (180)

Bâme spring

7.1.1993	T20coulbâme.dat	5289	1.30E-03	16869	1	unimodal	88	78	60	37.5 (21)	34 (24)	48.5 (28)
6.5.1993	T24coulbâme.dat	5203	6.75E-04	6370	1	unimodal	85	74	56	50 (33)	57 (33.5)	77.5 (45)
17.1.1994	T28coulbâme.dat	1611	2.50E-03	7000	1	unimodal	82.5	84	81	178 (104)	309.5 (184)	520 (304)
7.2.1994	T29coulbâme.dat	1945	2.47E-03	7376	1	unimodal	86	85.5	85	292 (178)	292 (176)	542 (331)
11.3.1994	T30coulbâme.dat	1414	3.30E-03	1970	1	unimodal	84	85.5	84	249 (430)	324.5 (192.5)	474 (281)
31.3.1994	T31coulbâme.dat	2174	4.90E-03	3681	1	unimodal	82	76	60	115 (77)	176 (118)	246 (165)
19.4.1994	T32coulbâme.dat	505	4.00E-03	1549	1	unimodal	87	88	80	491 (337)	807 (318)	1000 (686)

Various tracer tests

AR1	1592	2.20E-05	4180	15	bimodal	76	74	76	2.5	3	5
AR2	901	3.40E-04	5250	10	unimodal	73	72	71	10.3	18.5	21
AR3	1884	4.10E-04	8100	5	unimodal	85	80	70	24	22.5	30
AR4	585	9.50E-04	3800	5	unimodal	75	78	74	44	58	60
AR5	665	2.00E-03	6600	5	unimodal	86.5	81	86	34	55	67
AR10	2053	8.70E-04	5400	1	unimodal	75	70	50	26	37	60

( ) : velocities calculated with approximative direct distance

APPENDIX II.4

Table of tracer tests data performed in the Folded Jura

Tracing tests carried out on the Areuse watercatchment basin (Swiss Jura)

	Injection date	Code	TRACER	Mass [KG OU PFU]	Recovery %	Discharge (l/min)	Injection duration	Injection site	Surface of WCB	Position on hydrograph	Tracing distance (m)
AREUSE 0	3.11.1993	Arenov93ur	Uranine	5.00E+00	40%	70800	45min	Lac Taillères swallowhole	127 km2	Base flow recession	6150
	3.11.1993	Arenov93sulfo	Sulforhodamine G extra	8.55E+00	50%	70800	10min	Lac Taillères swallowhole	127 km2	Base flow recession	6150
	3.11.1993	Arenov93H6/1	Bacteriophages H6/1	1.49E+16	1%	70800	5min	Lac Taillères swallowhole	127 km2	Base flow recession	6150
	3.11.1993	Arenov93H40/1	Bacteriophages H40/1	9.18E+15	21%	70800	5min	Lac Taillères swallowhole	127 km2	Base flow recession	6150
	3.11.1993	Arenov93fl	Bacteriophages f1	2.15E+16	0.15	70800	5min	Lac Taillères swallowhole	127 km2	Base flow recession	6160
AREUSE 1	21.2.1995	Taill1uranine	Uranine	5.00E+00	58%	540000	30min	Lac Taillères swallowhole	127 km2	Base flow recession	6150
	21.2.1995	Taill1H40/1	H40/1	1.88E+14	51%	540000	30min	Lac Taillères swallowhole	127 km2	Base flow recession	6150
	21.2.1995	Taill1Pst2	Pst2	1.17E+13	19%	540000	30min	Lac Taillères swallowhole	127 km2	Base flow recession	6160
	21.2.1995	Taill1H6/1	H6/1	5.71E+113	25%	540000	30min	Lac Taillères swallowhole	127 km2	Base flow recession	6150
	21.2.1995	Taill1sulfoG	Sulfo G extra	6.00E+00	30%	540000	60min	Belle Perche swallowhole	127 km2	Base flow recession	3600
	21.2.1995	Taill1H2/1	H2/1	2.50E+13	5%	540000	60min	Belle Perche swallowhole	127 km2	Base flow recession	3600
	21.2.1995	Taill1H4/4	H4/4	4.48E+14	10%	540000	60min	Belle Perche swallowhole	127 km2	Base flow recession	3600
AREUSE 2	31.7.1995	Taill2Uranine	Uranine	5.00E+00	100%	180000	15min	Lac Taillères swallowhole	127 km2	Successive rising limbs	6150
	31.7.1995	Taill2H6/1	H6/1	3.32E+13	12%	180000	15min	Lac Taillères swallowhole	127 km2	Successive rising limbs	6150
	31.7.1995	Taill2H4/4	H4/4	8.45E+13	3%	180000	15min	Lac Taillères swallowhole	127 km2	Successive rising limbs	6150
	31.7.1995	Taill2sulfo	Sulfo G extra	7.92E+00	12%	180000	15min	Belle Perche swallowhole	127 km2	Successive rising limbs	3600
	31.7.1995	Taill2H40/1	H40/1	5.92E+14	1%	180000	15min	Belle Perche swallowhole	127 km2	Successive rising limbs	3600
AREUSE 3	30.10.1995	Taill3Uranine	Uranine	5.00E+00	80%	60000	20min	Lac Taillères swallowhole	127 km2	Base flow recession	6150
	30.10.1995	Taill3H6/1	H6/1	3.09E+13	18%	60000	15min	Lac Taillères swallowhole	127 km2	Base flow recession	6150
	30.10.1995	Taill2H4/4	H4/4	3.25E+14	10%	60000	15min	Lac Taillères swallowhole	127 km2	Base flow recession	6150
	30.10.1995	Taillesulfo	Sulfo G extra	7.92E+00	37%	60000	90min	Sulfo Perche swallowhole	127 km2	Base flow recession	3600
	30.10.1995	Taill3H40/1	H40/1	3.88E+14	15%	60000	10min	Belle Perche swallowhole	127 km2	Base flow recession	3600

			Transfert functions - Kernel function				S transfert functions		
Code	Step time at the Gravity center	MAX (t/hour) ex (l/min)	Max. step time numbers	Step time	MODE	Gradient at 0.2	Gradient at 0.5	Gradient at 0.8
Arenov93ur	2868.5	0.0000991 (l/min)	5000	10 min	unimodal	87	85	82
Arenov93sulfo	2816.16	0.0001265 (l/min)	5000	10 min	unimodal	81.5	78	59
Arenov93H6/1	2211	0.00017 (l/min)	5000	10 min	unimodal	87	82	76
Arenov93H40/1	2213.36	0.00017 (l/min)	5000	10 min	bimodal	87	81	70
Arenov93fl	-	0.0001009 (l/min)	5000	10 min	plusimodal	-	-	-
Taill1uranine	2791	0.00108 (l/min)	3000	2 min	unimodal	89	87	82
Taill1H40/1	2718	0.0011 (l/min)	3600	2 min	unimodal	89	87	82
Taill1Pst2	2346.3	0.0024 (l/min)	1400	2 min	unimodal	89	87	82
Taill1H6/1	2617.74	0.00135 (l/min)	3700	2 min	unimodal	89	86	89.5
Taill1sulfoG	2680	0.00053 (l/min)	3000	2 min	bimodal	89	86	85
Taill1H2/1	1831	0.0018 (l/min)	1500	2 min	unimodal	89.5	87.5	86
Taill1H4/4	2156	0.00193 (l/min)	3700	2 min	unimodal	89.5	87.5	80
Taill2Uranine	-	-	-	-	-	-	-	-
Taill2H6/1	-	-	-	-	-	-	-	-
Taill2H4/4	-	-	-	-	-	-	-	-
Taill2sulfo	-	-	-	-	-	-	-	-
Taill2H40/1	-	-	-	-	-	-	-	-
Taill3Uranine	3474.1	1.21E-03 (l/h)	5657	0.1h	bimodal	82	83	80
Taill3H6/1	3401.8	1.16E-03 (l/h)	5179	0.1h	bimodal - pluri	82	83	80
Taill3H4/4	3492.5	1.49E-03 (l/h)	5658	0.1h	bimodal - pluri	85.5	83	80
Taillesulfo	2750.45	8.725E-04 (l/h)	5636	0.1h	bimodal	80	78	70
Taill3H40/1	2221.36	1.65E-03 (l/h)	4418	0.1h	bimodal	85	83	72

Tracing tests carried out on the Areuse watercatchment basin (Swiss Jura)

Velocities

Code	*Mean transit velocity (m/h)*	*Modal velocity (m/h)*	*Max. velocity (m/h)*
Arenov93ur	13.80	16.20	22.73
Arenov93sulfo	13.10	16.20	22.73
Arenov93H6/1	16.70	18.30	23.50
Arenov93H40/1	16.67	18.30	23.15
Arenov93I1	-	18.30	25.00
Tall1uranine	132.00		
Tall1H40/1	136.00	160.50	220.00
Tall1Pst2	157.00	160.50	180.00
Tall1H6/1	131.00	160.50	220.00
Tall1sulfoG	81.09	136.50	181.75
Tall1H2/1	132.50	136.50	181.75
Tall1H4/4	100.20	143.00	201.00
Tall2Uranine	-	16.00	22.50
Tall2H6/1	-	17.00	21.00
Tall2H4/4	-	14.00	21.00
Tall2sulfo	-	14.00	17.70
Tall2H40/1	-	15.00	17.00
Tall3Uranine	17.70	18.50	24.00
Tall3H6/1	18.00	18.00	23.50
Tall3H4/4	17.60	18.00	23.50
Tall3sulfo	13.00	18.00	21.60
Tall3H40/1	16.20	17.50	21.50

APPENDIX II.5

Table of tracer tests data performed in the Alps

Tracing tests carried out in the ALPS (Helvetic domain,Switzeriand)

Quantitative interpretation using a global approach - Black box model -

Amont = Upper Milandrine (karstic network)

Code	Denomination	Geologic context	TRACER	Mass (KG)	Recovery %	Discharge (l/s)	Injection duration	Injection site	Surface of WCB	Position on hydrograph	Tracing distance (m)
ALP1	La Tsa - Mollens	Helvetic	Eosine	15	1.2	15000	triang. 15'	Laplaz	5*m2	falling limb - base flow recession	3280
ALP2	Plumachit	Helvetic	Naphtionate	18	?	15000	triang. 60'	limestone hollow	5*m2	falling limb - base flow recession	1230
ALP3	Tsa Bonna ICO13	Helvetic	Uranine	10	6	8560	triang. 15'	swallowhole	1-2km2	falling limb - base flow recession	1350
ALP5	Brünigpass	Helvetic	Amido. G. extra	20	0.5	3600	triang. 60'	swallowhole - aee	1-2km2	base flow recession (?)	1060
ALP7	Fälensee - M.	Helvetic	Rhodamine	8	82	633	triang. 30'	swallowhole	10km2	falling limb	3500
ALP8	Oehrligrubb - T.	Helvetic	Uranine	15	10	100	triang. 0'	swallowhole	8*m2	falling limb	3500
ALP9	Reclen - S.	Helvetic	Naphtionate	20	78.5	154	triang. 15'	swallowhole	12km2	falling limb	1200
ALP10	Seealpsee - B.	Helvetic	Rhodamine	0.02	12	220	triang. 1'	swallowhole	16km2	falling limb	1000
ALP11	Säntisgipfel - S.	Helvetic	Rhodamine	10	35	2890	triang. 30'	swallowhole	16km2	falling limb	4000
ALP12	Stein - Säntish.	Helvetic	Naphtionate	30	12	3500	triang. 15'	swallowhole	10km2	falling limb	3000
ALP13	Stein - Mühbach	Helvetic	Naphtionate	30	12	1100	triang. 15'	swallowhole	7km2	falling limb	1750
ALP14	Stein - Dorfbach	Helvetic	Naphtionate	30	11	1100	triang. 15'	swallowhole	10km2	falling limb	1750
ALP15	Stein - Schlatt.	Helvetic	Naphtionate	30	1.5	1100	triang. 15'	swallowhole	10km2	falling limb	1750
ALP16	Stein - G.	Helvetic	Naphtionate	30	?	1100	triang. 15'	swallowhole	14km2	falling limb	5000
ALP17	Zwinglipass - S	Helvetic	Uranine	5	25.5	4600	triang. 2'	in the karstic network	7km2	falling limb	6000
ALP18	Zwinglipass - D.	Helvetic	Uranine	5	16	960	triang.2'	in the karstic network	10km2	falling limb	7500
ALP19	Zwinglipass - M.	Helvetic	Uranine	5	14.5	1130	triang. 2'	in the karstic network	7km2	falling limb	7500
ALP20	Risi - Alt. St. J.	Helvetic	Eosine	1	10	690	triang. 1Z	swallowhole	3km2	base flow recession	1750

		Transfert functions - Kernel function				S transfert functions					
Code	Time steps at the Gravity center	MAX (t/MH)	Max. step time numbers	Time step	MODE	Gradient at 0.2	Gradient at 0.5	Gradient at 0.8	Mean transit velocity (m/h)	Model velocity (m/h)	Max. velocity (m/h)
ALP1	856	5.20E-07	8250	15	unimodal	-	-	-	169	84	-
ALP2	831	1.50E-07	8400	10	unimodal	74	73	70	50	22	160
ALP3	2827	6.50E-11	5250	10	bimodal	-	-	-	7	6	39
ALP5	857	8.20E-05	4500	15	unimodal	-	-	-	25	25	67
ALP7	1462	2.20E-03	2600	5	unimodal	82	80	70	144	150	199
ALP8	508	1.20E-03	7000	2	unimodal	77	78	70	47	52	69
ALP9	3160	3.30E-03	4600	1	unimodal	85	82	85	110	115	169
ALP10	1021	8.50E-04	3250	1	plurimodal	66	66	58	42	45	120
ALP11	2835	2.30E-05	9250	30	plurimodal	-	-	-	47	16	44
ALP12	3307	5.00E-04	7500	1	unimodal	73.5	73	70	54	59	119
ALP13	895	4.70E-04	7000	5	unimodal	77	77	70	85	83	148
ALP14	2162	5.70E-04	7250	2	plurimodal	77	78	70	91	95	160
ALP15	3554	5.10E-04	7000	1	unimodal	76	77.5	70	80	95	154
ALP16	3012	5.30E-04	7600	1	unimodal	73	72.5	66	80	94	150
ALP17	1111	8.50E-04	7100	2	unimodal	60	78	70	105	240	360
ALP18	1161	1.45E-05	7200	2	unimodal	62.5	80	74	260	236	338
ALP19	1027	1.05E-05	8050	1	unimodal	62	80	56	260	250	368
ALP20	2714	4.20E-04	7200	2	plurimodal	77.5	72	72	16	25	31

APPENDIX II.6

Database files of tracer tests

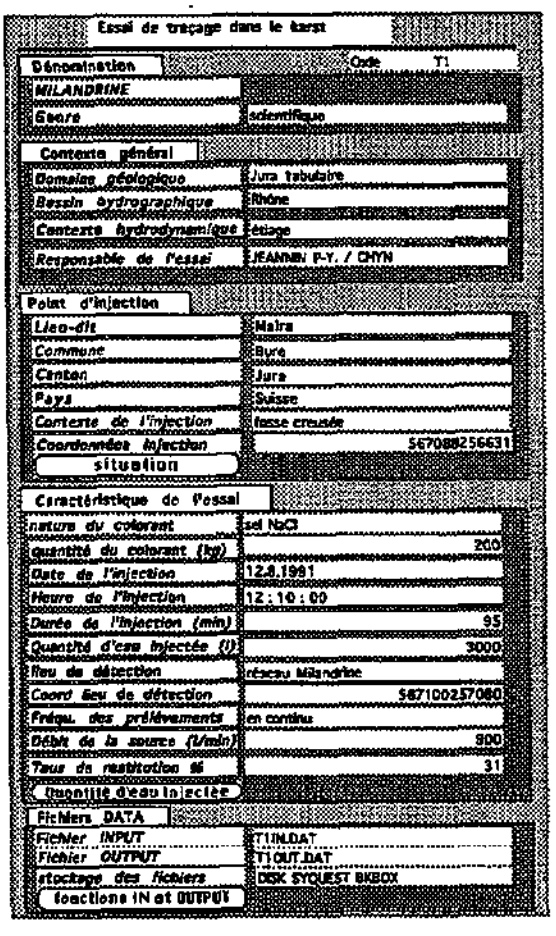
Essai de traçage dans le karst
Dénomination
Code T1
MILANDRINE
Genre scientifique
Contexte général
Domaine géologique Jura tabulaire
Bassin hydrographique Rhône
Contexte hydrodynamique étiage
Responsable de l'essai JEANNIN P-Y. / CHYN
Point d'injection
Lieu-dit Maira
Commune Bure
Canton Jura
Pays Suisse
Contexte de l'injection fosse creusée
Coordonnées injection 5670882566311
situation
Caractéristique de l'essai
nature du colorant sel NaCl
quantité du colorant (kg) 200
Date de l'injection 12.8.1991
Heure de l'injection 12 : 10 : 00
Durée de l'injection (min) 95
Quantité d'eau injectée (l) 3000
lieu de détection réseau Milandrine
Coord lieu de détection 567100257080
Fréqu. des prélèvements en continu
Débit de la source (l/min) 900
Taux de restitution % 31
Quantité d'eau injectée
Fichiers DATA
Fichier INPUT T1IN.DAT
Fichier OUTPUT T1OUT.DAT
stockage des fichiers DISK SYQUEST 88BOX
fonctions IN et OUTPUT

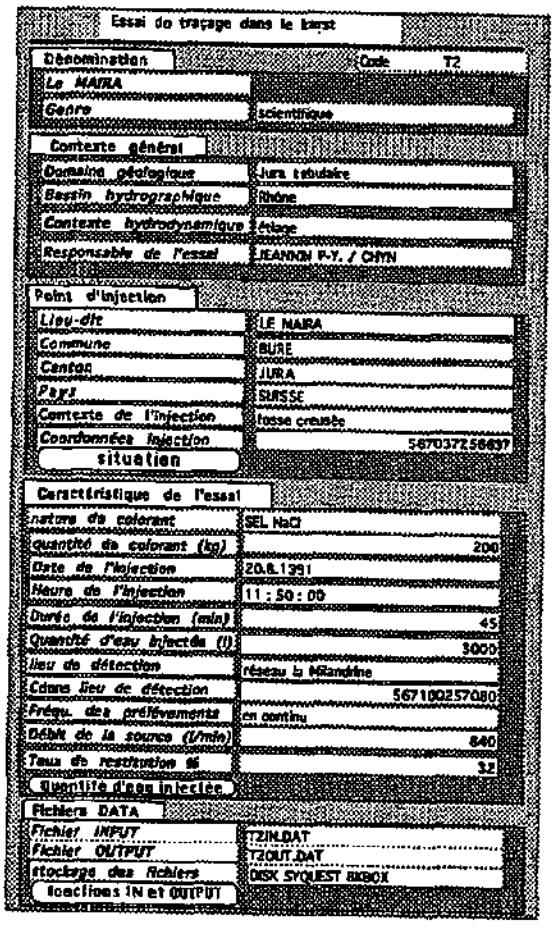
Essai de traçage dans le karst
Dénomination
Code T2
Le MAIRA
Genre scientifique
Contexte général
Domaine géologique Jura tabulaire
Bassin hydrographique Rhône
Contexte hydrodynamique Etiage
Responsable de l'essai JEANNIN P-Y. / CHYN
Point d'injection
Lieu-dit LE MAIRA
Commune BURE
Canton JURA
Pays SUISSE
Contexte de l'injection fosse creusée
Coordonnées injection 5670372566837
situation
Caractéristique de l'essai
nature du colorant SEL NaCl
quantité du colorant (kg) 200
Date de l'injection 20.8.1991
Heure de l'injection 11 : 50 : 00
Durée de l'injection (min) 45
Quantité d'eau injectée (l) 3000
lieu de détection réseau la Milandrine
Coord lieu de détection 567100257080
Fréqu. des prélèvements en continu
Débit de la source (l/min) 840
Taux de restitution % 32
Quantité d'eau injectée
Fichiers DATA
Fichier INPUT T2IN.DAT
Fichier OUTPUT T2OUT.DAT
stockage des fichiers DISK SYQUEST 88BOX
fonctions IN et OUTPUT

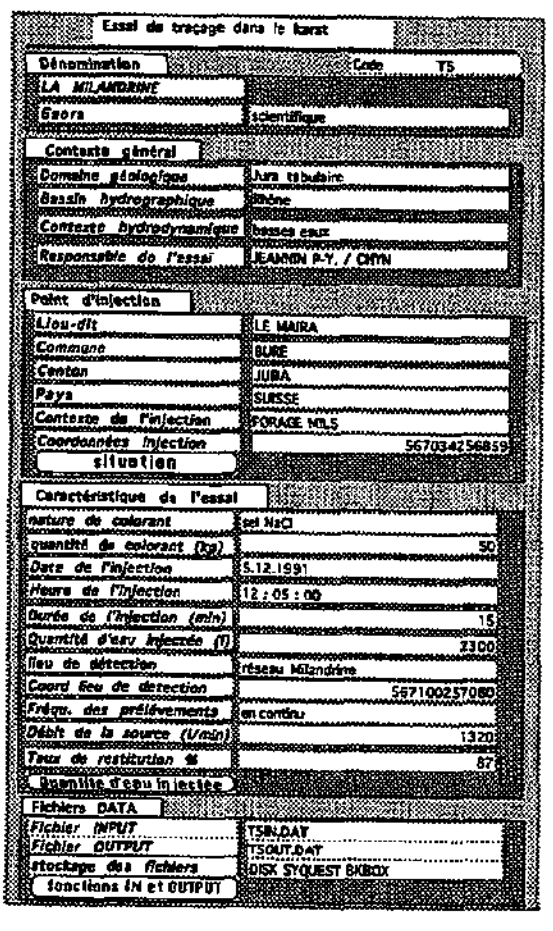
Essai de traçage dans le karst
Dénomination
Code T5
LA MILANDRINE
Genre scientifique
Contexte général
Domaine géologique Jura tabulaire
Bassin hydrographique Rhône
Contexte hydrodynamique basses eaux
Responsable de l'essai JEANNIN P-Y. / CHYN
Point d'injection
Lieu-dit LE MAIRA
Commune BURE
Canton JURA
Pays SUISSE
Contexte de l'injection FORAGE MIL5
Coordonnées injection 567034256859
situation
Caractéristique de l'essai
nature de colorant sel NaCl
quantité de colorant (kg) 50
Date de l'injection 5.12.1991
Heure de l'injection 12 : 05 : 00
Durée de l'injection (min) 15
Quantité d'eau injectée (l) 2300
lieu de détection réseau Milandrine
Coord lieu de détection 567100257080
Fréqu. des prélèvements en continu
Débit de la source (l/min) 1320
Taux de restitution % 87
Quantité d'eau injectée
Fichiers DATA
Fichier INPUT T5IN.DAT
Fichier OUTPUT T5OUT.DAT
stockage des fichiers DISK SYQUEST 88BOX
fonctions IN et OUTPUT

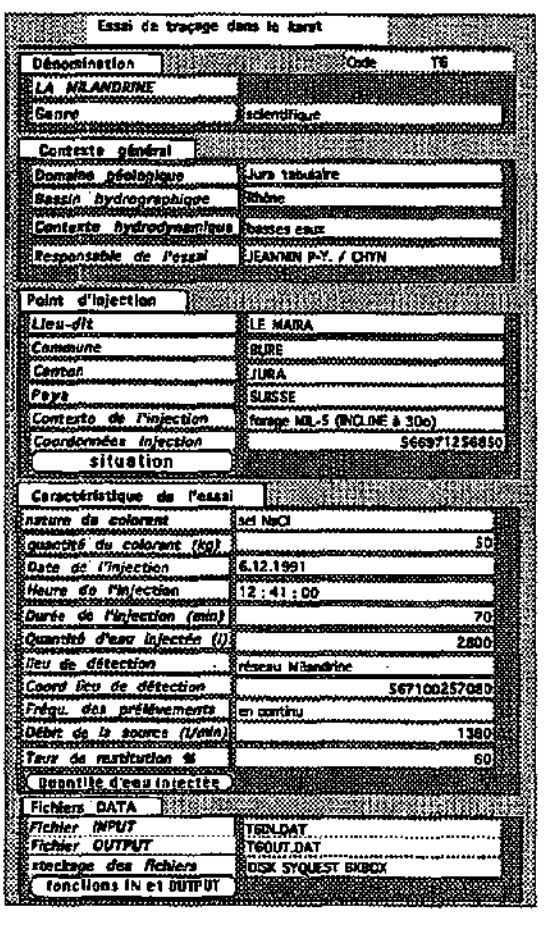
Essai de traçage dans le karst
Dénomination
Code T6
LA MILANDRINE
Genre scientifique
Contexte général
Domaine géologique Jura tabulaire
Bassin hydrographique Rhône
Contexte hydrodynamique basses eaux
Responsable de l'essai JEANNIN P-Y. / CHYN
Point d'injection
Lieu-dit LE MAIRA
Commune BURE
Canton JURA
Pays SUISSE
Contexte de l'injection forage MIL-5 (INCLINE à 30o)
Coordonnées injection 566971256850
situation
Caractéristique de l'essai
nature de colorant sel NaCl
quantité du colorant (kg) 50
Date de l'injection 6.12.1991
Heure de l'injection 12 : 41 : 00
Durée de l'injection (min) 70
Quantité d'eau injectée (l) 2800
lieu de détection réseau Milandrine
Coord lieu de détection 567100257080
Fréqu. des prélèvements en continu
Débit de la source (l/min) 1380
Taux de restitution % 60
Quantité d'eau injectée
Fichiers DATA
Fichier INPUT T6IN.DAT
Fichier OUTPUT T6OUT.DAT
stockage des fichiers DISK SYQUEST 88BOX
fonctions IN et OUTPUT

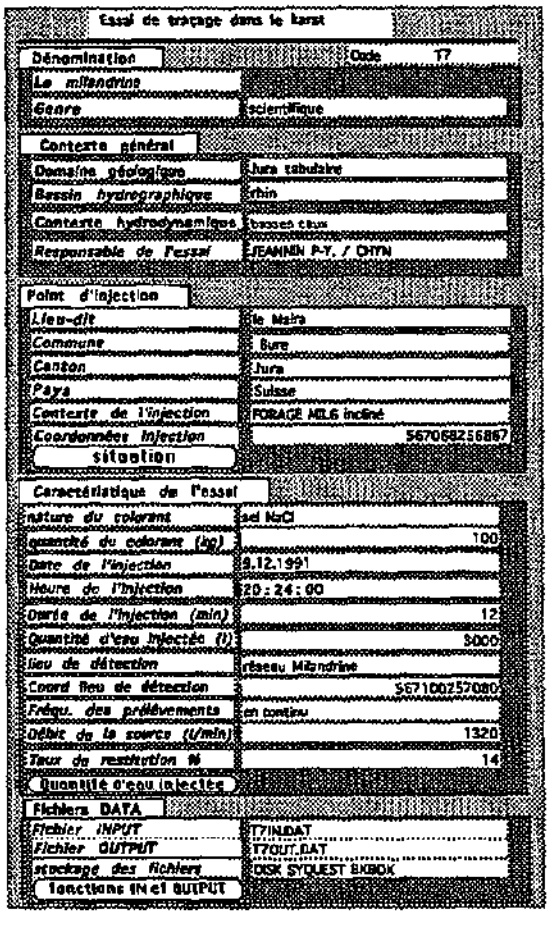
Essai de traçage dans le karst
Dénomination
Code T7
La Milandrine
Genre
scientifique
Contexte général
Domaine géologique
Jura tabulaire
Bassin hydrographique
Rhin
Contexte hydrodynamique
basses eaux
Responsable de l'essai
JEANNIN P-Y. / CHYN
Point d'injection
Lieu-dit
le Maira
Commune
Bure
Canton
Jura
Pays
Suisse
Contexte de l'injection
FORAGE MIL6 incliné
Coordonnées injection
567068256867
situation
Caractéristique de l'essai
nature du colorant
sel NaCl
quantité du colorant (kg)
100
Date de l'injection
9.12.1991
Heure de l'injection
20:24:00
Durée de l'injection (min)
12
Quantité d'eau injectée (l)
3000
lieu de détection
réseau Milandrine
Coord lieu de détection
567100257080
Fréqu. des prélèvements
en continu
Débit de la source (l/min)
1320
Taux de restitution %
14
Quantité d'eau injectée
Fichiers DATA
Fichier INPUT
T7IN.DAT
Fichier OUTPUT
T7OUT.DAT
stockage des fichiers
DISK SYQUEST 8XBOX
fonctions IN et OUTPUT

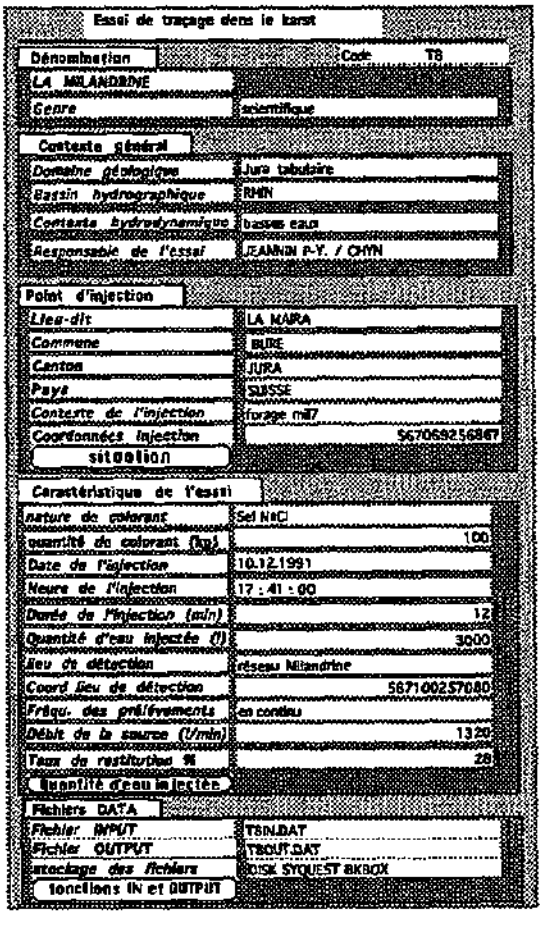
Essai de traçage dans le karst
Dénomination
Code T8
LA MILANDRINE
Genre
scientifique
Contexte général
Domaine géologique
Jura tabulaire
Bassin hydrographique
RHIN
Contexte hydrodynamique
basses eaux
Responsable de l'essai
JEANNIN P-Y. / CHYN
Point d'injection
Lieu-dit
LA MAIRA
Commune
BURE
Canton
JURA
Pays
SUISSE
Contexte de l'injection
forage mil7
Coordonnées injection
567069256867
situation
Caractéristique de l'essai
nature du colorant
Sel NaCl
quantité du colorant (kg)
100
Date de l'injection
10.12.1991
Heure de l'injection
17 : 41 : 00
Durée de l'injection (min)
12
Quantité d'eau injectée (l)
3000
lieu de détection
réseau Milandrine
Coord lieu de détection
567100257080
Fréqu. des prélèvements
en continu
Débit de la source (l/min)
1320
Taux de restitution %
28
Quantité d'eau injectée
Fichiers DATA
Fichier INPUT
T8IN.DAT
Fichier OUTPUT
T8OUT.DAT
stockage des fichiers
DISK SYQUEST 8XBOX
fonctions IN et OUTPUT

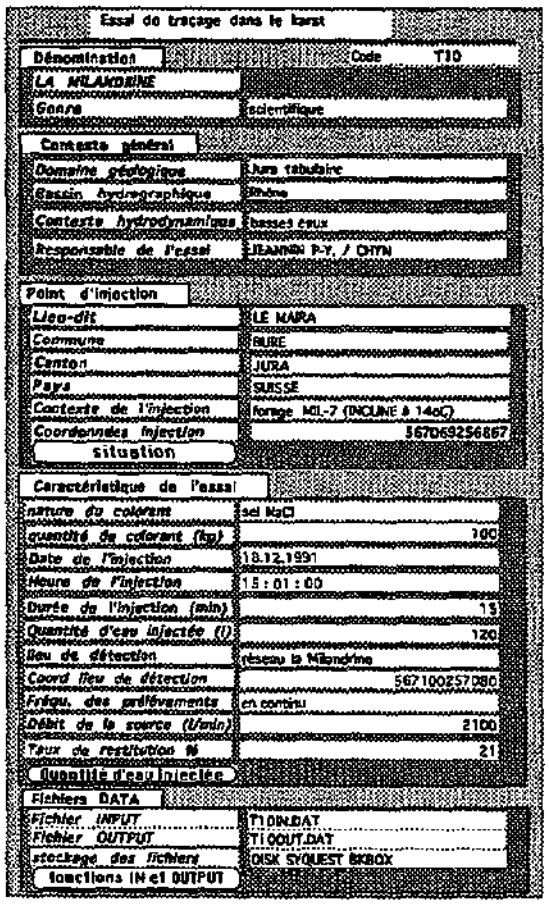
Essai de traçage dans le karst
Dénomination
Code T10
LA MILANDRINE
Genre
scientifique
Contexte général
Domaine géologique
Jura tabulaire
Bassin hydrographique
Rhône
Contexte hydrodynamique
basses eaux
Responsable de l'essai
JEANNIN P-Y. / CHYN
Point d'injection
Lieu-dit
LE MAIRA
Commune
BURE
Canton
JURA
Pays
SUISSE
Contexte de l'injection
forage MIL-7 (INCLINE à 14oC)
Coordonnées injection
567069256867
situation
Caractéristique de l'essai
nature du colorant
sel NaCl
quantité de colorant (kg)
100
Date de l'injection
18.12.1991
Heure de l'injection
15 : 01 : 00
Durée de l'injection (min)
13
Quantité d'eau injectée (l)
120
lieu de détection
réseau la Milandrine
Coord lieu de détection
567100257080
Fréqu. des prélèvements
en continu
Débit de la source (l/min)
2100
Taux de restitution %
21
Quantité d'eau injectée
Fichiers DATA
Fichier INPUT
T10IN.DAT
Fichier OUTPUT
T10OUT.DAT
stockage des fichiers
DISK SYQUEST 8XBOX
fonctions IN et OUTPUT

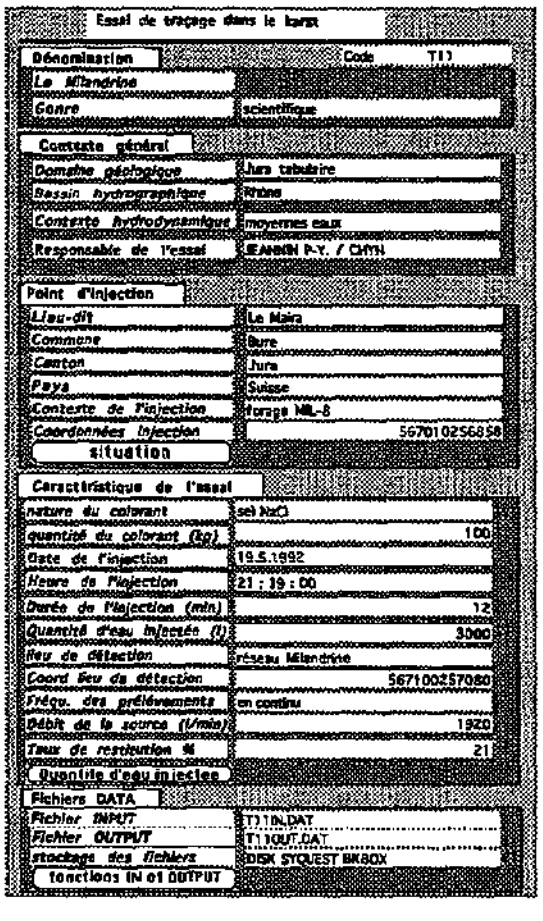
Essai de traçage dans le karst
Dénomination
Code T11
La Milandrine
Genre
scientifique
Contexte général
Domaine géologique
Jura tabulaire
Bassin hydrographique
Rhône
Contexte hydrodynamique
moyennes eaux
Responsable de l'essai
JEANNIN P-Y. / CHYN
Point d'injection
Lieu-dit
Le Maira
Commune
Bure
Canton
Jura
Pays
Suisse
Contexte de l'injection
forage MIL-8
Coordonnées injection
567010256858
situation
Caractéristique de l'essai
nature du colorant
sel NaCl
quantité du colorant (kg)
100
Date de l'injection
19.5.1992
Heure de l'injection
21 : 39 : 00
Durée de l'injection (min)
12
Quantité d'eau injectée (l)
3000
lieu de détection
réseau Milandrine
Coord lieu de détection
567100257080
Fréqu. des prélèvements
en continu
Débit de la source (l/min)
1920
Taux de restitution %
21
Quantité d'eau injectée
Fichiers DATA
Fichier INPUT
T11IN.DAT
Fichier OUTPUT
T11OUT.DAT
stockage des fichiers
DISK SYQUEST 8XBOX
fonctions IN et OUTPUT

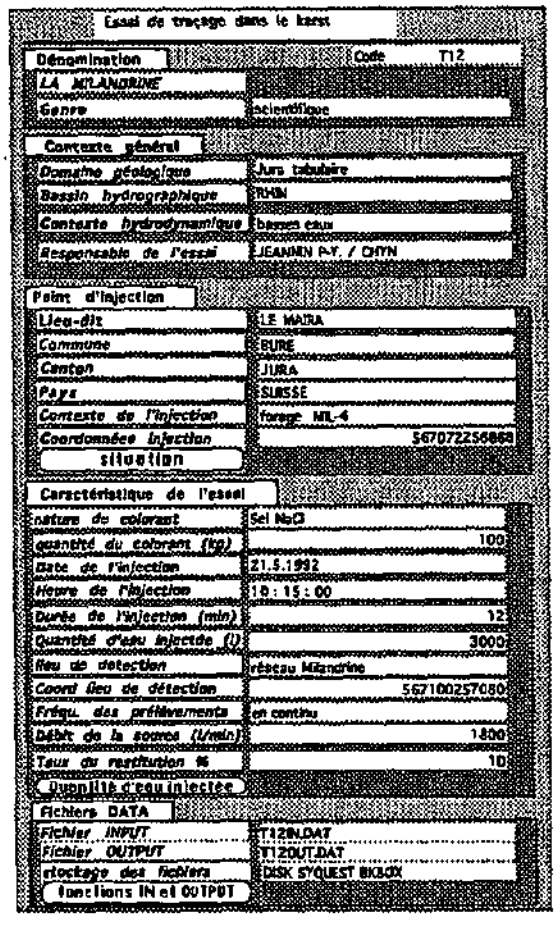
Essai de traçage dans le karst
Dénomination
Code T12
LA MILANDRINE
Genre
scientifique
Contexte général
Domaine géologique
Jura tabulaire
Bassin hydrographique
RHIN
Contexte hydrodynamique
basses eaux
Responsable de l'essai
JEANNIN P-Y. / CHYN
Point d'injection
Lieu-dit
LE MAIRA
Commune
BURE
Canton
JURA
Pays
SUISSE
Contexte de l'injection
forage MIL-4
Coordonnées injection
567072256862
situation
Caractéristique de l'essai
nature du colorant
Sel NaCl
quantité du colorant (kg)
100
Date de l'injection
21.5.1992
Heure de l'injection
10 : 15 : 00
Durée de l'injection (min)
12
Quantité d'eau injectée (l)
3000
lieu de détection
réseau Milandrine
Coord lieu de détection
567100257080
Fréqu. des prélèvements
en continu
Débit de la source (l/min)
1800
Taux de restitution %
10
Quantité d'eau injectée
Fichiers DATA
Fichier INPUT
T12IN.DAT
Fichier OUTPUT
T12OUT.DAT
stockage des fichiers
DISK SYQUEST 88BOX
fonctions IN et OUTPUT

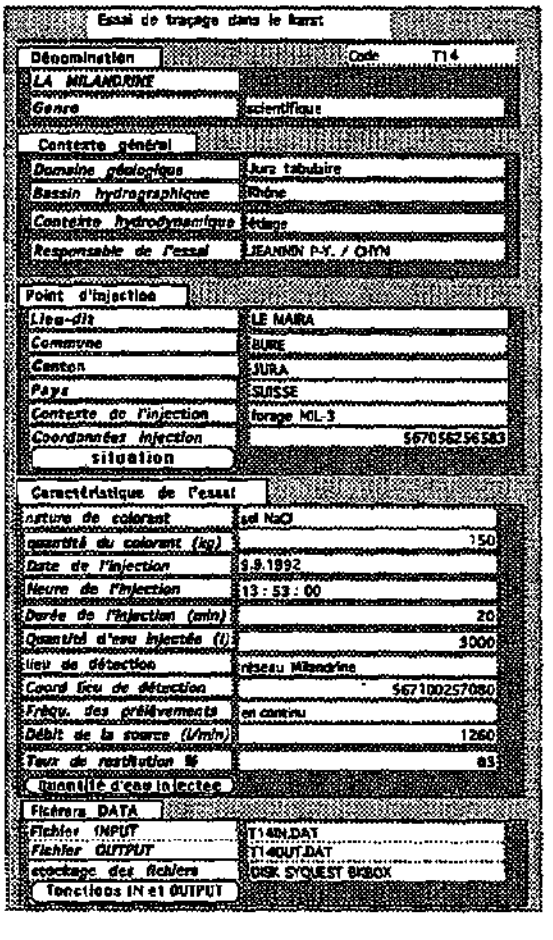
Essai de traçage dans le karst
Dénomination
Code T14
LA MILANDRINE
Genre
scientifique
Contexte général
Domaine géologique
Jura tabulaire
Bassin hydrographique
Rhône
Contexte hydrodynamique
étiage
Responsable de l'essai
JEANNIN P-Y. / CHYN
Point d'injection
Lieu-dit
LE MAIRA
Commune
BURE
Canton
JURA
Pays
SUISSE
Contexte de l'injection
forage MIL-3
Coordonnées injection
567056256583
situation
Caractéristique de l'essai
nature de colorant
sel NaCl
quantité du colorant (kg)
150
Date de l'injection
9.9.1992
Heure de l'injection
13 : 53 : 00
Durée de l'injection (min)
20
Quantité d'eau injectée (l)
3000
lieu de détection
réseau Milandrine
Coord lieu de détection
567100257080
Fréqu. des prélèvements
en continu
Débit de la source (l/min)
1260
Taux de restitution %
83
Quantité d'eau injectée
Fichiers DATA
Fichier INPUT
T14IN.DAT
Fichier OUTPUT
T14OUT.DAT
stockage des fichiers
DISK SYQUEST 88BOX
fonctions IN et OUTPUT

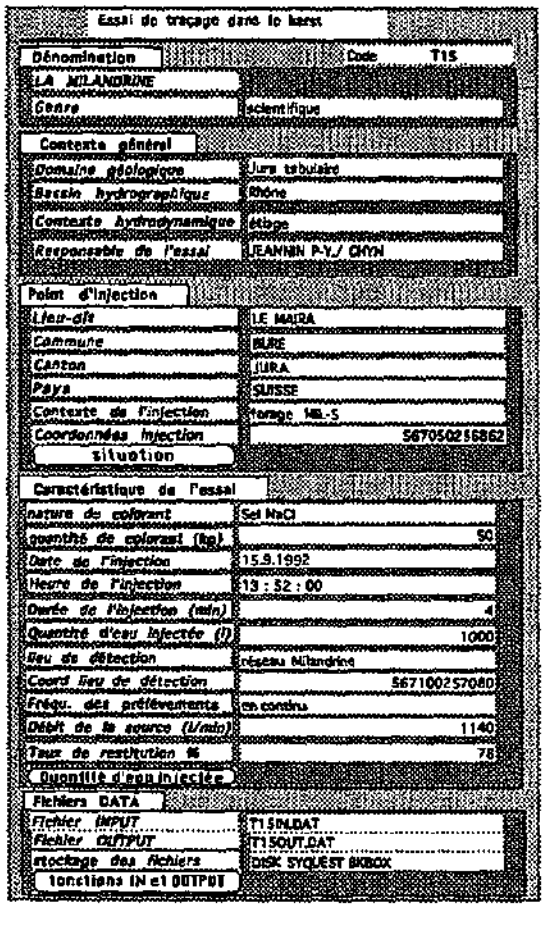
Essai de traçage dans le karst
Dénomination
Code T15
LA MILANDRINE
Genre
scientifique
Contexte général
Domaine géologique
Jura tabulaire
Bassin hydrographique
Rhône
Contexte hydrodynamique
étiage
Responsable de l'essai
JEANNIN P-Y./ CHYN
Point d'injection
Lieu-dit
LE MAIRA
Commune
BURE
Canton
JURA
Pays
SUISSE
Contexte de l'injection
forage MIL-5
Coordonnées injection
567050256862
situation
Caractéristique de l'essai
nature du colorant
Sel NaCl
quantité de colorant (kg)
50
Date de l'injection
15.9.1992
Heure de l'injection
13 : 52 : 00
Durée de l'injection (min)
4
Quantité d'eau injectée (l)
1000
lieu de détection
réseau Milandrine
Coord lieu de détection
567100257080
Fréqu. des prélèvements
en continu
Débit de la source (l/min)
1140
Taux de restitution %
78
Quantité d'eau injectée
Fichiers DATA
Fichier INPUT
T15IN.DAT
Fichier OUTPUT
T15OUT.DAT
stockage des fichiers
DISK SYQUEST 88BOX
fonctions IN et OUTPUT

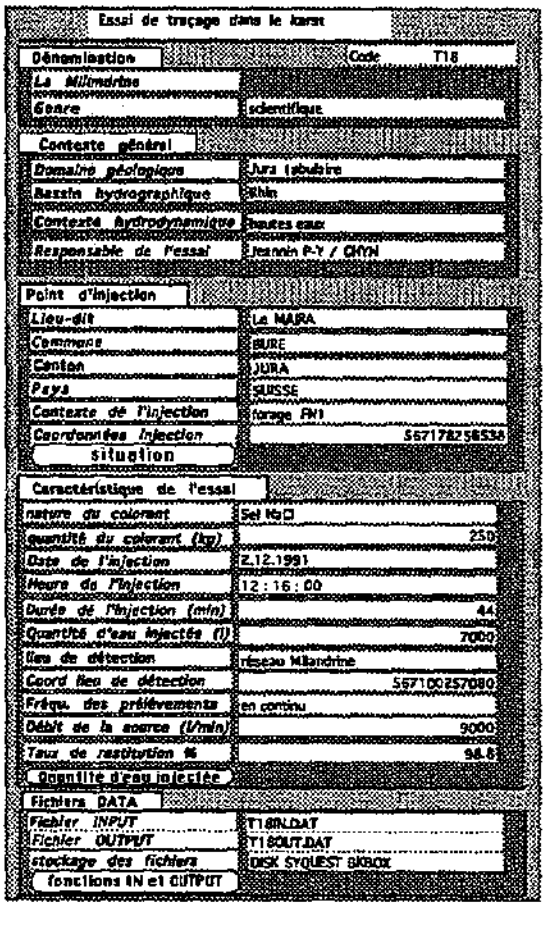
Essai de traçage dans le karst
Dénomination
Code T18
La Milandrine
Genre
scientifique
Contexte général
Domaine géologique
Jura tabulaire
Bassin hydrographique
Rhin
Contexte hydrodynamique
hautes eaux
Responsable de l'essai
Jeannin P-Y / CHYN
Point d'injection
Lieu-dit
La MAIRA
Commune
BURE
Canton
JURA
Pays
SUISSE
Contexte de l'injection
forage PH1
Coordonnées injection
567178256534
situation
Caractéristique de l'essai
nature du colorant
Sel NaCl
quantité du colorant (kg)
250
Date de l'injection
2.12.1991
Heure de l'injection
12 : 16 : 00
Durée de l'injection (min)
44
Quantité d'eau injectée (l)
7000
lieu de détection
réseau Milandrine
Coord lieu de détection
567100257080
Fréqu. des prélèvements
en continu
Débit de la source (l/min)
9000
Taux de restitution %
98.8
Quantité d'eau injectée
Fichiers DATA
Fichier INPUT
T18IN.DAT
Fichier OUTPUT
T18OUT.DAT
stockage des fichiers
DISK SYQUEST 88BOX
fonctions IN et OUTPUT

Essai de traçage dans le karst

Dénomination		Code T19
La milandrine		
Genre	scientifique	

Contexte général	
Domaine géologique	Jura tabulaire
Bassin hydrographique	Rhône
Contexte hydrodynamique	hautes eaux
Responsable de l'essai	JEANNIN P-Y. /CHYN

Point d'injection	
Lieu-dit	LE MAIRA
Commune	BURE
Canton	JURA
Pays	SUISSE
Contexte de l'injection	forage MIL-2
Coordonnées injection	567056256588
situation	

Caractéristique de l'essai	
nature du colorant	SEL NaCl
quantité du colorant (kg)	200
Date de l'injection	23.12.1992
Heure de l'injection	11 : 24 : 00
Durée de l'injection (min)	12
Quantité d'eau injectée (l)	3000
lieu de détection	réseau La Milandrine
Coord lieu de détection	567100257080
Fréqu. des prélèvements	en continu
Débit de la source (l/min)	2880
Taux de restitution %	32
Quantité d'eau injectée	

Fichiers DATA	
Fichier INPUT	T19IN.DAT
Fichier OUTPUT	T19OUT.DAT
stockage des fichiers	DISK SYQUEST 88KBOX
fonctions IN et OUTPUT	

Essai de traçage dans le karst

Dénomination		Code T20
LA MILANDRINE		
Genre	scientifique	

Contexte général	
Domaine géologique	Jura tabulaire
Bassin hydrographique	Rhône
Contexte hydrodynamique	décrue
Responsable de l'essai	JEANNIN P-Y. / CHYN

Point d'injection	
Lieu-dit	LE MAIRA
Commune	BURE
Canton	JURA
Pays	SUISSE
Contexte de l'injection	forage MIL-1
Coordonnées injection	567049256588
situation	

Caractéristique de l'essai	
nature du colorant	sel NaCl
quantité du colorant (kg)	250
Date de l'injection	7.1.1993
Heure de l'injection	14 : 58 : 00
Durée de l'injection (min)	11
Quantité d'eau injectée (l)	5000
lieu de détection	réseau La Milandrine
Coord lieu de détection	567100257080
Fréqu. des prélèvements	en continu
Débit de la source (l/min)	1800
Taux de restitution %	90
Quantité d'eau injectée	

Fichiers DATA	
Fichier INPUT	T20IN.DAT
Fichier OUTPUT	T20OUT.DAT
stockage des fichiers	DISK SYQUEST 88KBOX
fonctions IN et OUTPUT	

Essai de traçage dans le karst

Dénomination		Code T23
La Milandrine		
Genre	scientifique	

Contexte général	
Domaine géologique	Jura tabulaire
Bassin hydrographique	Rhône
Contexte hydrodynamique	basses eaux
Responsable de l'essai	JEANNIN P-Y /CHYN

Point d'injection	
Lieu-dit	Le Maira
Commune	Bure
Canton	Jura
Pays	SUISSE
Contexte de l'injection	forage MIL-7
Coordonnées injection	567069256867
situation	

Caractéristique de l'essai	
nature du colorant	NaCl
quantité du colorant (kg)	50
Date de l'injection	27.4.1993
Heure de l'injection	14 : 55 : 00
Durée de l'injection (min)	11
Quantité d'eau injectée (l)	7500
lieu de détection	Réseau La Milandrine
Coord lieu de détection	567100257080
Fréqu. des prélèvements	en continu
Débit de la source (l/min)	1518
Taux de restitution %	100
Quantité d'eau injectée	

Fichiers DATA	
Fichier INPUT	T23IN.DAT
Fichier OUTPUT	T23OUT.DAT
stockage des fichiers	DISK SYQUEST 88KBOX
fonctions IN et OUTPUT	

Essai de traçage dans le karst

Dénomination		Code T24
La Milandrine		
Genre	scientifique	

Contexte général	
Domaine géologique	Jura tabulaire
Bassin hydrographique	Rhône
Contexte hydrodynamique	basses eaux
Responsable de l'essai	JEANNIN P-Y / CHYN

Point d'injection	
Lieu-dit	LE MAIRA
Commune	BURES
Canton	JURA
Pays	SUISSE
Contexte de l'injection	forage MIL7
Coordonnées injection	567069256867
situation	

Caractéristique de l'essai	
nature du colorant	NaCl
quantité du colorant (kg)	50
Date de l'injection	6.5.1993
Heure de l'injection	12 : 37 : 00
Durée de l'injection (min)	11
Quantité d'eau injectée (l)	5700
lieu de détection	Réseau Milandrine
Coord lieu de détection	567100257080
Fréqu. des prélèvements	en continu
Débit de la source (l/min)	1440
Taux de restitution %	79
Quantité d'eau injectée	

Fichiers DATA	
Fichier INPUT	T24IN.DAT
Fichier OUTPUT	T24OUT.DAT
stockage des fichiers	DISK SYQUEST 88KBOX
fonctions IN et OUTPUT	

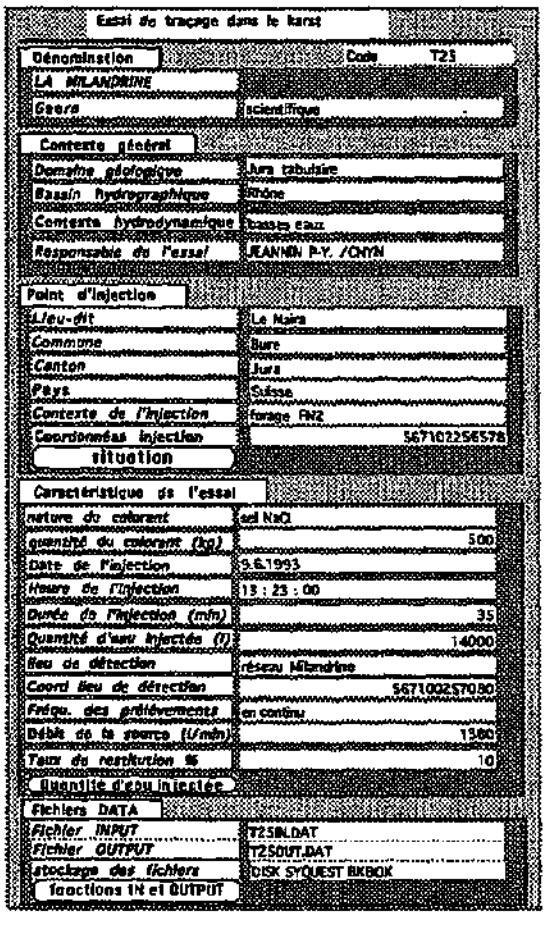
Essai de traçage dans le karst
Dénomination
Code T23
LA MILANDRINE
Genre scientifique
Contexte général
Domaine géologique Jura tabulaire
Bassin hydrographique Rhône
Contexte hydrodynamique basses eaux
Responsable de l'essai JEANNIN P-Y. /CHYN
Point d'injection
Lieu-dit Le Naira
Commune Bure
Canton Jura
Pays Suisse
Contexte de l'injection forage RN2
Coordonnées injection 567102256578
situation
Caractéristique de l'essai
nature du colorant sel NaCl
quantité du colorant (kg) 500
Date de l'injection 9.6.1993
Heure de l'injection 13 : 23 : 00
Durée de l'injection (mn) 35
Quantité d'eau injectée (l) 14000
lieu de détection réseau Milandrine
Coord lieu de détection 567100257080
Frégu. des prélèvements en continu
Débit de la source (l/mn) 1360
Taux de restitution % 10
Quantité d'eau injectée
Fichiers DATA
Fichier INPUT T23IN.DAT
Fichier OUTPUT T23OUT.DAT
stockage des fichiers DISK SYQUEST RKBOK
fonctions IN et OUTPUT

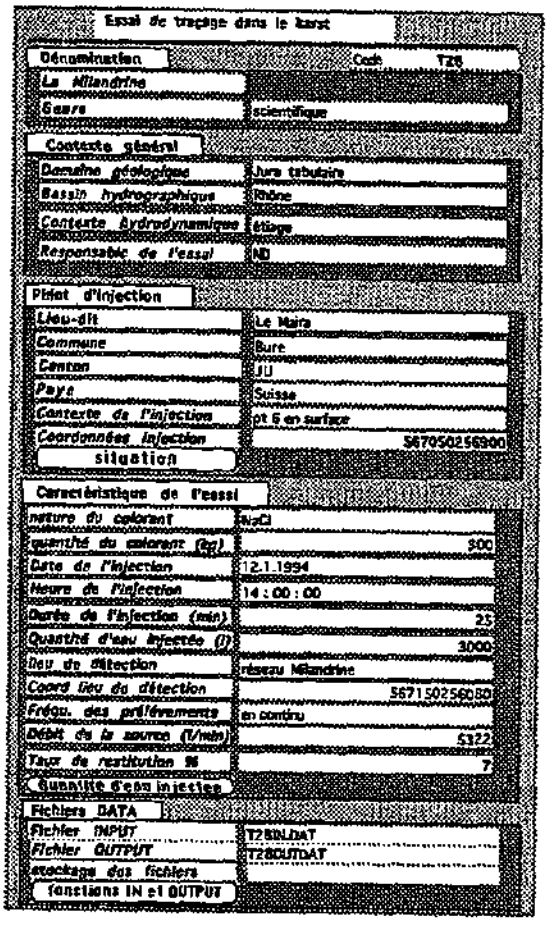
Essai de traçage dans le karst
Dénomination
Code T28
La Milandrine
Genre scientifique
Contexte général
Domaine géologique Jura tabulaire
Bassin hydrographique Rhône
Contexte hydrodynamique étiage
Responsable de l'essai ND
Point d'injection
Lieu-dit Le Naira
Commune Bure
Canton JU
Pays Suisse
Contexte de l'injection pt 6 en surface
Coordonnées injection 567050256900
situation
Caractéristique de l'essai
nature du colorant NaCl
quantité du colorant (kg) 300
Date de l'injection 12.1.1994
Heure de l'injection 14 : 00 : 00
Durée de l'injection (min) 25
Quantité d'eau injectée (l) 3000
lieu de détection réseau Milandrine
Coord lieu de détection 567150256080
Frégu. des prélèvements en continu
Débit de la source (l/mn) 5122
Taux de restitution % 7
Quantité d'eau injectée
Fichiers DATA
Fichier INPUT T28IN.DAT
Fichier OUTPUT T28OUT.DAT
stockage des fichiers
fonctions IN et OUTPUT

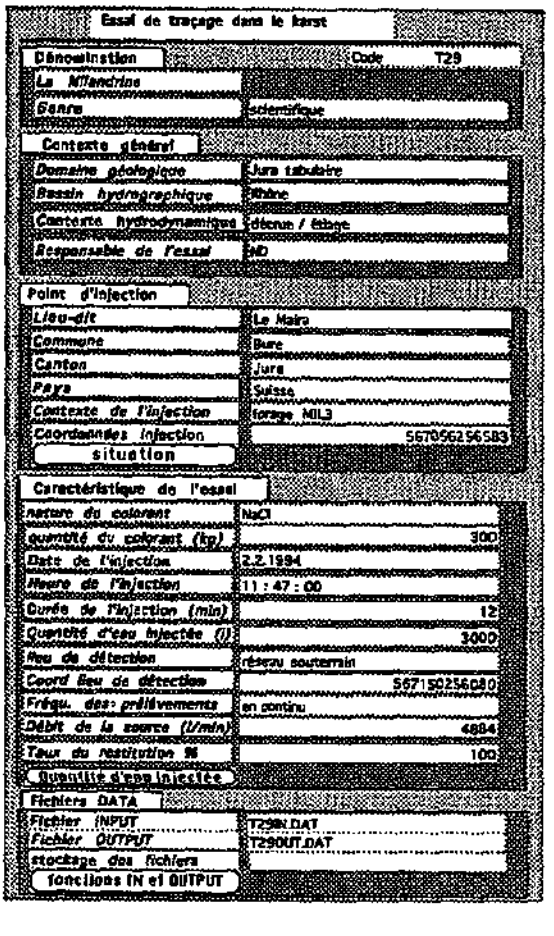
Essai de traçage dans le karst
Dénomination
Code T29
La Milandrine
Genre scientifique
Contexte général
Domaine géologique Jura tabulaire
Bassin hydrographique Rhône
Contexte hydrodynamique décrue / étiage
Responsable de l'essai ND
Point d'injection
Lieu-dit Le Naira
Commune Bure
Canton Jura
Pays Suisse
Contexte de l'injection forage MIL3
Coordonnées injection 567056256583
situation
Caractéristique de l'essai
nature du colorant NaCl
quantité du colorant (kg) 300
Date de l'injection 2.2.1994
Heure de l'injection 11 : 47 : 00
Durée de l'injection (min) 12
Quantité d'eau injectée (l) 3000
lieu de détection réseau souterrain
Coord lieu de détection 567150256080
Frégu. des prélèvements en continu
Débit de la source (l/mn) 4884
Taux de restitution % 100
Quantité d'eau injectée
Fichiers DATA
Fichier INPUT T29IN.DAT
Fichier OUTPUT T29OUT.DAT
stockage des fichiers
fonctions IN et OUTPUT

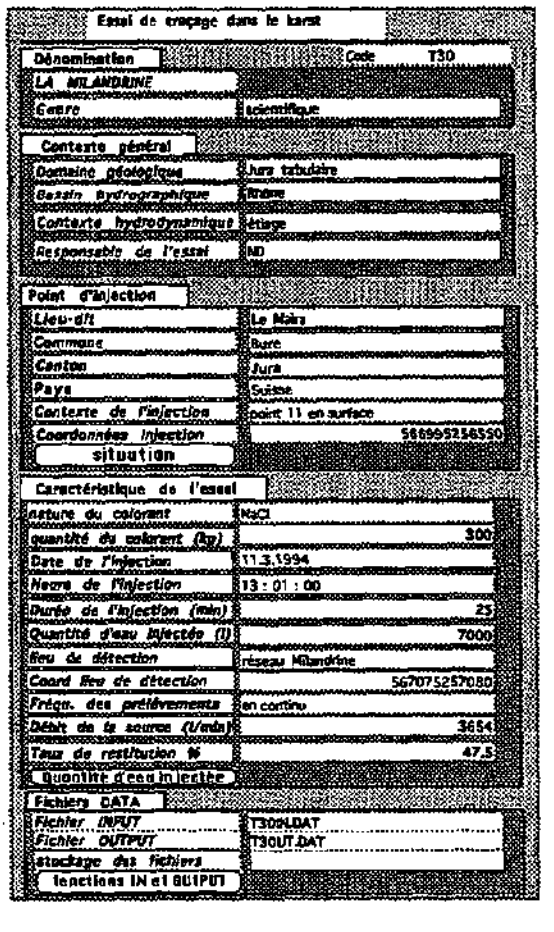
Essai de traçage dans le karst
Dénomination
Code T30
LA MILANDRINE
Genre scientifique
Contexte général
Domaine géologique Jura tabulaire
Bassin hydrographique Rhône
Contexte hydrodynamique étiage
Responsable de l'essai ND
Point d'injection
Lieu-dit Le Naira
Commune Bure
Canton Jura
Pays Suisse
Contexte de l'injection point 11 en surface
Coordonnées injection 566995256550
situation
Caractéristique de l'essai
nature du colorant NaCl
quantité du colorant (kg) 300
Date de l'injection 11.3.1994
Heure de l'injection 13 : 01 : 00
Durée de l'injection (min) 23
Quantité d'eau injectée (l) 7000
lieu de détection réseau Milandrine
Coord lieu de détection 567075257080
Frégu. des prélèvements en continu
Débit de la source (l/mn) 3654
Taux de restitution % 47,5
Quantité d'eau injectée
Fichiers DATA
Fichier INPUT T30IN.DAT
Fichier OUTPUT T30OUT.DAT
stockage des fichiers
fonctions IN et OUTPUT

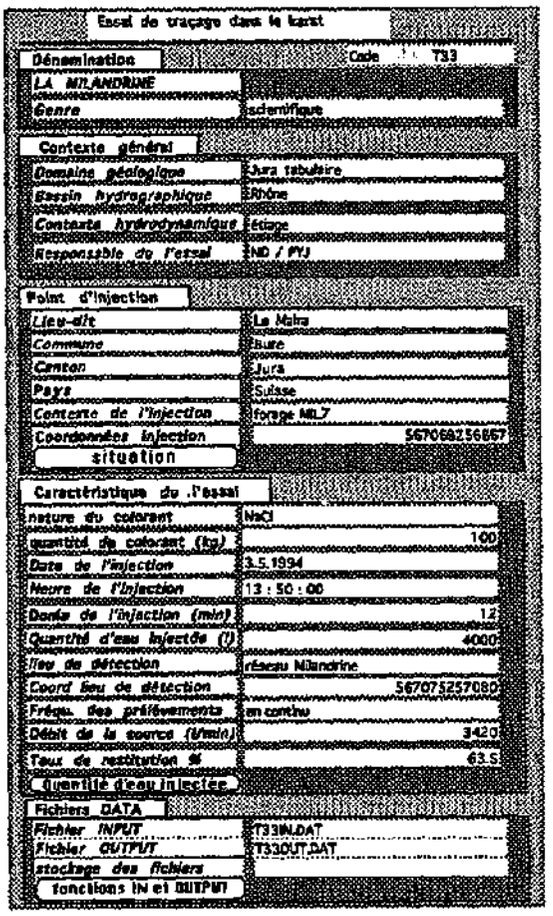
Essai de traçage dans le karst
Dénomination
Code T33
LA MILANDRINE
Genre scientifique
Contexte général
Domaine géologique Jura tabulaire
Bassin hydrographique Rhône
Contexte hydrodynamique étiage
Responsable de l'essai ND / PYJ
Point d'injection
Lieu-dit La Maira
Commune Bure
Canton Jura
Pays Suisse
Contexte de l'injection forage MLJ
Coordonnées injection 567068256867
situation
Caractéristique de l'essai
nature du colorant NaCl
quantité de colorant (kg) 100
Date de l'injection 3.5.1994
Heure de l'injection 13 : 50 : 00
Durée de l'injection (min) 12
Quantité d'eau injectée (l) 4000
lieu de détection réseau Milandrine
Coord lieu de détection 567075257080
Fréqu. des prélèvements en continu
Débit de la source (l/min) 3420
Taux de restitution % 63.5
Quantité d'eau injectée
Fichiers DATA
Fichier INPUT T33IN.DAT
Fichier OUTPUT T33OUT.DAT
stockage des fichiers
fonctions IN et OUTPUT

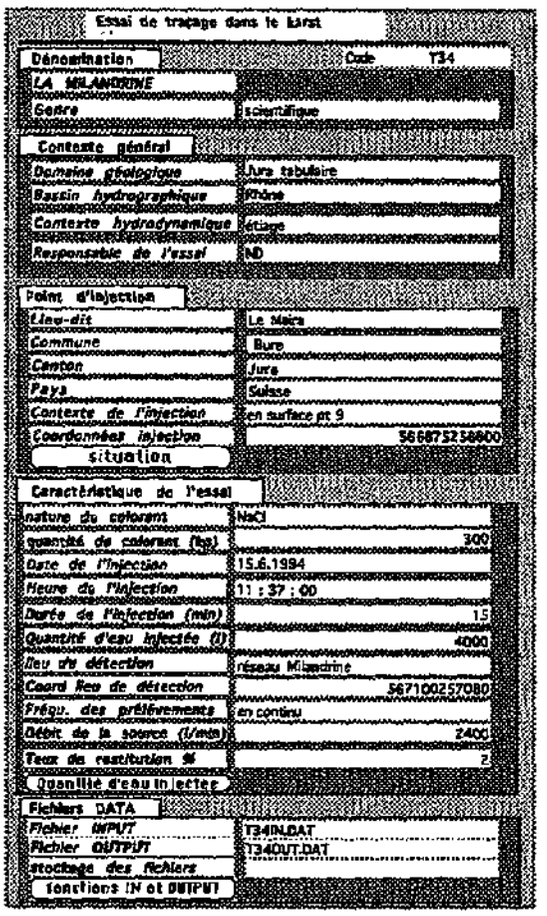
Essai de traçage dans le karst
Dénomination
Code T34
LA MILANDRINE
Genre scientifique
Contexte général
Domaine géologique Jura tabulaire
Bassin hydrographique Rhône
Contexte hydrodynamique étiage
Responsable de l'essai ND
Point d'injection
Lieu-dit Le Maira
Commune Bure
Canton Jura
Pays Suisse
Contexte de l'injection en surface pt 9
Coordonnées injection 566875258600
situation
Caractéristique de l'essai
nature du colorant NaCl
quantité de colorant (kg) 300
Date de l'injection 15.6.1994
Heure de l'injection 11 : 37 : 00
Durée de l'injection (min) 15
Quantité d'eau injectée (l) 4000
lieu de détection réseau Milandrine
Coord lieu de détection 567100257080
Fréqu. des prélèvements en continu
Débit de la source (l/min) 2400
Taux de restitution % 2
Quantité d'eau injectée
Fichiers DATA
Fichier INPUT T34IN.DAT
Fichier OUTPUT T34OUT.DAT
stockage des fichiers
fonctions IN et OUTPUT

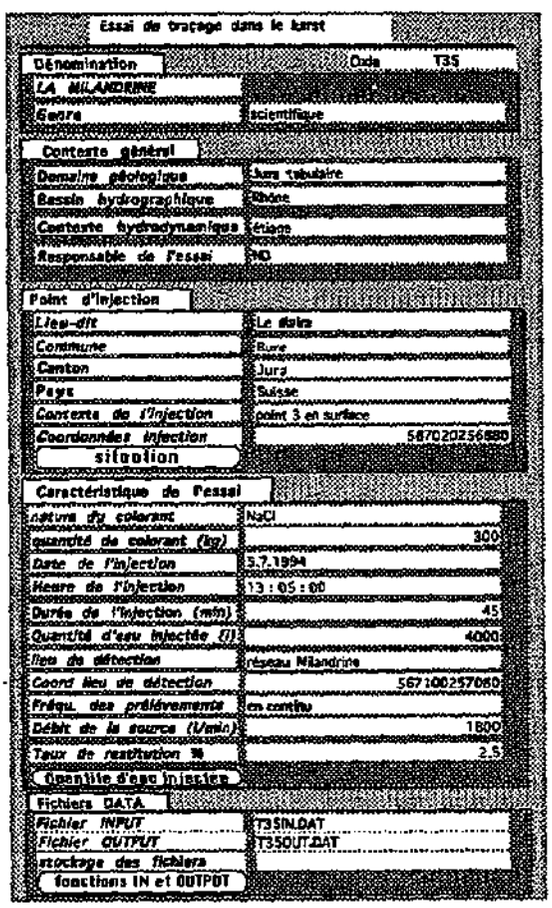
Essai de traçage dans le karst
Dénomination
Code T35
LA MILANDRINE
Genre scientifique
Contexte général
Domaine géologique Jura tabulaire
Bassin hydrographique Rhône
Contexte hydrodynamique étiage
Responsable de l'essai ND
Point d'injection
Lieu-dit Le Maira
Commune Bure
Canton Jura
Pays Suisse
Contexte de l'injection point 3 en surface
Coordonnées injection 5670202566B0
situation
Caractéristique de l'essai
nature du colorant NaCl
quantité de colorant (kg) 300
Date de l'injection 5.7.1994
Heure de l'injection 13 : 05 : 00
Durée de l'injection (min) 45
Quantité d'eau injectée (l) 4000
lieu de détection réseau Milandrine
Coord lieu de détection 567100257080
Fréqu. des prélèvements en continu
Débit de la source (l/min) 1800
Taux de restitution % 2.5
Quantité d'eau injectée
Fichiers DATA
Fichier INPUT T35IN.DAT
Fichier OUTPUT T35OUT.DAT
stockage des fichiers
fonctions IN et OUTPUT

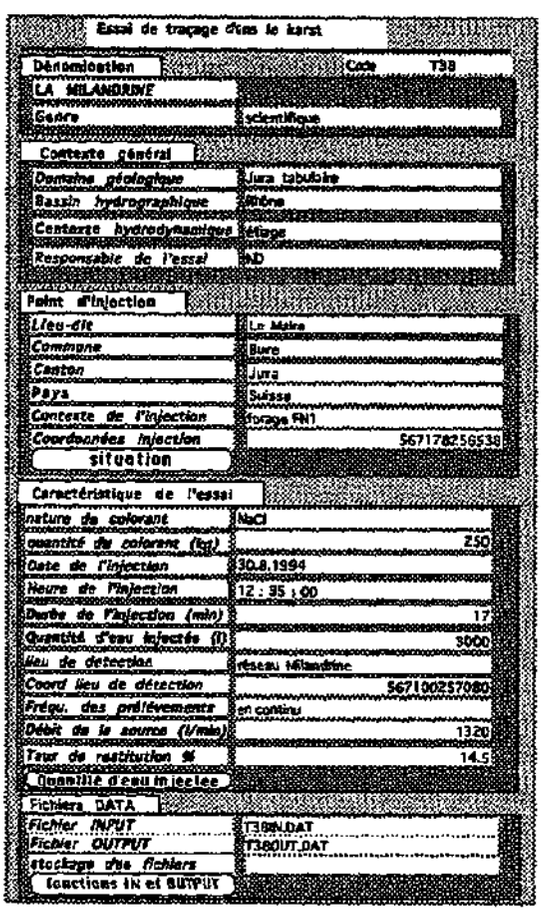
Essai de traçage dans le karst
Dénomination
Code T38
LA MILANDRINE
Genre scientifique
Contexte général
Domaine géologique Jura tabulaire
Bassin hydrographique Rhône
Contexte hydrodynamique étiage
Responsable de l'essai ND
Point d'injection
Lieu-dit La Maira
Commune Bure
Canton Jura
Pays Suisse
Contexte de l'injection forage FN1
Coordonnées injection 567178256538
situation
Caractéristique de l'essai
nature du colorant NaCl
quantité de colorant (kg) 250
Date de l'injection 30.8.1994
Heure de l'injection 12 : 35 : 00
Durée de l'injection (min) 17
Quantité d'eau injectée (l) 3000
lieu de détection réseau Milandrine
Coord lieu de détection 567100257080
Fréqu. des prélèvements en continu
Débit de la source (l/min) 1320
Taux de restitution % 14.5
Quantité d'eau injectée
Fichiers DATA
Fichier INPUT T38IN.DAT
Fichier OUTPUT T38OUT.DAT
stockage des fichiers
fonctions IN et OUTPUT

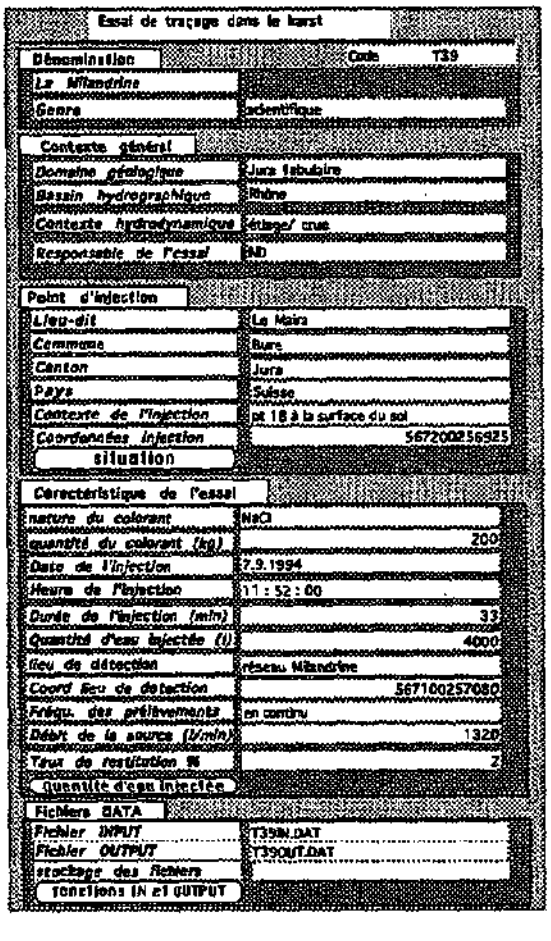
Essai de traçage dans le karst
Dénomination
Code T39
La Milandrine
Genre scientifique
Contexte général
Domaine géologique Jura tabulaire
Bassin hydrographique Rhône
Contexte hydrodynamique étiage/ crue
Responsable de l'essai ND
Point d'injection
Lieu-dit Le Maira
Commune Bure
Canton Jura
Pays Suisse
Contexte de l'injection pt 18 à la surface du sol
Coordonnées injection 567200256525
situation
Caractéristique de l'essai
nature du colorant NaCl
quantité du colorant (kg) 200
Date de l'injection 7.9.1994
Heure de l'injection 11 : 52 : 00
Durée de l'injection (min) 33
Quantité d'eau injectée (l) 4000
lieu de détection réseau Milandrève
Coord lieu de détection 567100257080
Fréqu. des prélèvements en continu
Débit de la source (l/min) 1320
Taux de restitution % Z
Quantité d'eau injectée
Fichiers DATA
Fichier INPUT T39IN.DAT
Fichier OUTPUT T39OUT.DAT
stockage des fichiers
fonctions IN et OUTPUT

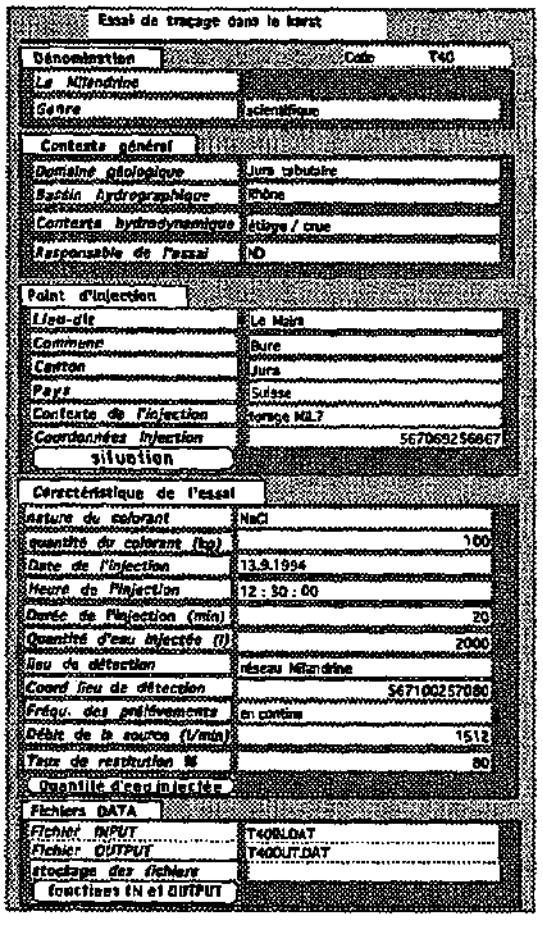
Essai de traçage dans le karst
Dénomination
Code T40
La Milandrine
Genre scientifique
Contexte général
Domaine géologique Jura tabulaire
Bassin hydrographique Rhône
Contexte hydrodynamique étiage / crue
Responsable de l'essai ND
Point d'injection
Lieu-dit Le Maira
Commune Bure
Canton Jura
Pays Suisse
Contexte de l'injection forage MI.7
Coordonnées injection 567069256867
situation
Caractéristique de l'essai
nature du colorant NaCl
quantité du colorant (kg) 100
Date de l'injection 13.9.1994
Heure de l'injection 12 : 50 : 00
Durée de l'injection (min) 20
Quantité d'eau injectée (l) 2000
lieu de détection réseau Milandrine
Coord lieu de détection 567100257080
Fréqu. des prélèvements en continu
Débit de la source (l/min) 1512
Taux de restitution % 80
Quantité d'eau injectée
Fichiers DATA
Fichier INPUT T40IN.DAT
Fichier OUTPUT T40OUT.DAT
stockage des fichiers
fonctions IN et OUTPUT

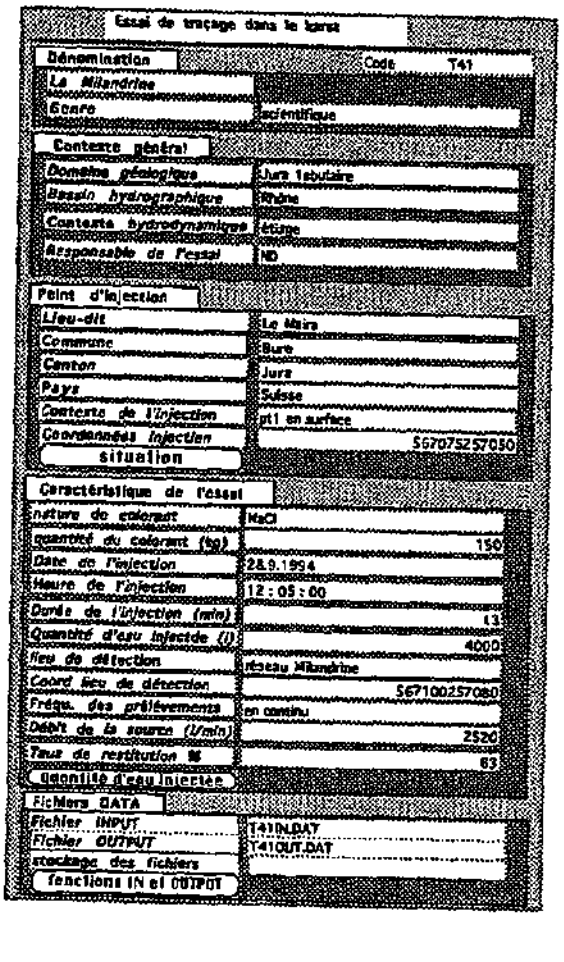
Essai de traçage dans le karst
Dénomination
Code T41
La Milandrine
Genre scientifique
Contexte général
Domaine géologique Jura tabulaire
Bassin hydrographique Rhône
Contexte hydrodynamique étiage
Responsable de l'essai ND
Point d'injection
Lieu-dit Le Maira
Commune Bure
Canton Jura
Pays Suisse
Contexte de l'injection pt1 en surface
Coordonnées injection 567075257050
situation
Caractéristique de l'essai
nature du colorant NaCl
quantité du colorant (kg) 150
Date de l'injection 28.9.1994
Heure de l'injection 12 : 05 : 00
Durée de l'injection (min) 13
Quantité d'eau injectée (l) 4000
lieu de détection réseau Milandrine
Coord lieu de détection 567100257080
Fréqu. des prélèvements en continu
Débit de la source (l/min) 2520
Taux de restitution % 63
Quantité d'eau injectée
Fichiers DATA
Fichier INPUT T41IN.DAT
Fichier OUTPUT T41OUT.DAT
stockage des fichiers
fonctions IN et OUTPUT

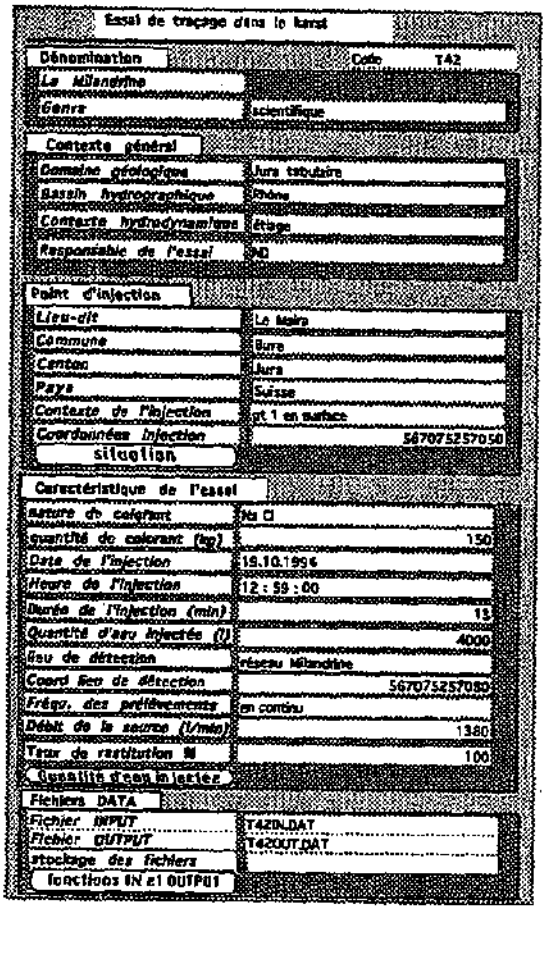
Essai de traçage dans le karst
Dénomination
Code T42
La Milandrine
Genre scientifique
Contexte général
Domaine géologique Jura tabulaire
Bassin hydrographique Rhône
Contexte hydrodynamique Etiage
Responsable de l'essai ND
Point d'injection
Lieu-dit Le Maira
Commune Bure
Canton Jura
Pays Suisse
Contexte de l'injection pt 1 en surface
Coordonnées injection 567075257050
situation
Caractéristique de l'essai
nature du colorant Na Cl
Quantité du colorant (kg) 150
Date de l'injection 19.10.1994
Heure de l'injection 12 : 59 : 00
Durée de l'injection (min) 13
Quantité d'eau injectée (l) 4000
lieu de détection réseau Milandrine
Coord lieu de détection 567075257080
Fréqu. des prélèvements en continu
Débit de la source (l/min) 1380
Taux de restitution % 100
Quantité d'eau injectée
Fichiers DATA
Fichier INPUT T42IN.DAT
Fichier OUTPUT T42OUT.DAT
stockage des fichiers
fonctions IN et OUTPUT

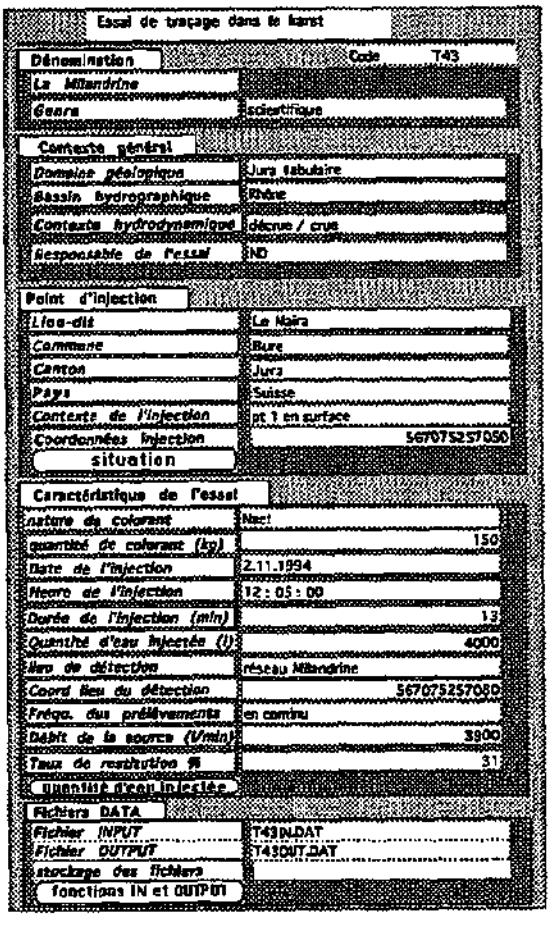
Essai de traçage dans le karst
Dénomination
Code T43
La Milandrine
Genre
scientifique
Contexte général
Domaine géologique
Jura tabulaire
Bassin hydrographique
Rhône
Contexte hydrodynamique
décrue / crue
Responsable de l'essai
ND
Point d'injection
Lieu-dit
Le Maira
Commune
Bure
Canton
Jura
Pays
Suisse
Contexte de l'injection
pt 1 en surface
Coordonnées injection
567075257050
situation
Caractéristique de l'essai
nature du colorant
Nacl
quantité de colorant (kg)
150
Date de l'injection
2.11.1994
Heure de l'injection
12 : 05 : 00
Durée de l'injection (min)
13
Quantité d'eau injectée (l)
4000
lieu de détection
réseau Milandrine
Coord lieu de détection
567075257080
Fréqu. des prélèvements
en continu
Débit de la source (l/min)
3900
Taux de restitution %
31
Quantité d'eau injectée
Fichiers DATA
Fichier INPUT
T43IN.DAT
Fichier OUTPUT
T43OUT.DAT
stockage des fichiers
fonctions IN et OUTPUT

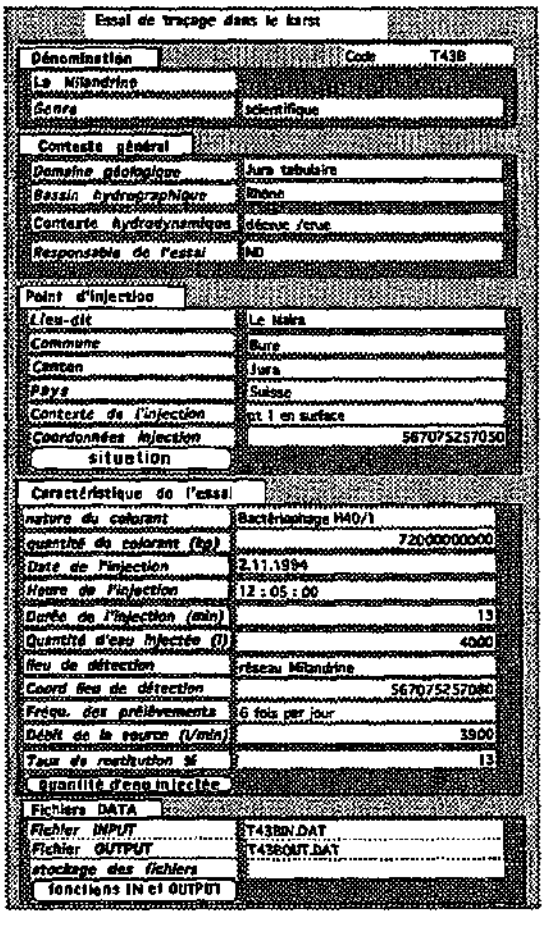
Essai de traçage dans le karst
Dénomination
Code T43B
La Milandrine
Genre
scientifique
Contexte général
Domaine géologique
Jura tabulaire
Bassin hydrographique
Rhône
Contexte hydrodynamique
décrue /crue
Responsable de l'essai
ND
Point d'injection
Lieu-dit
Le Maira
Commune
Bure
Canton
Jura
Pays
Suisse
Contexte de l'injection
pt 1 en surface
Coordonnées injection
567075257050
situation
Caractéristique de l'essai
nature du colorant
Bactériophage H40/1
quantité de colorant (kg)
720000000000
Date de l'injection
2.11.1994
Heure de l'injection
12 : 05 : 00
Durée de l'injection (min)
13
Quantité d'eau injectée (l)
4000
lieu de détection
réseau Milandrine
Coord lieu de détection
567075257080
Fréqu. des prélèvements
6 fois par jour
Débit de la source (l/min)
3900
Taux de restitution %
13
Quantité d'eau injectée
Fichiers DATA
Fichier INPUT
T43BIN.DAT
Fichier OUTPUT
T43BOUT.DAT
stockage des fichiers
fonctions IN et OUTPUT

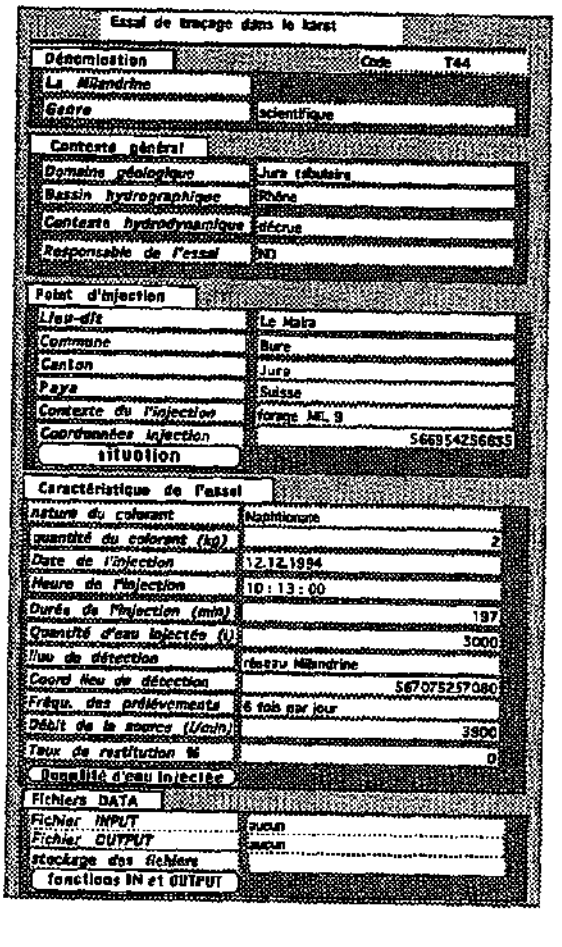
Essai de traçage dans le karst
Dénomination
Code T44
La Milandrine
Genre
scientifique
Contexte général
Domaine géologique
Jura tabulaire
Bassin hydrographique
Rhône
Contexte hydrodynamique
décrue
Responsable de l'essai
ND
Point d'injection
Lieu-dit
Le Maira
Commune
Bure
Canton
Jura
Pays
Suisse
Contexte de l'injection
forage MEL 9
Coordonnées injection
566954256635
situation
Caractéristique de l'essai
nature du colorant
Naphtionate
quantité de colorant (kg)
2
Date de l'injection
12.12.1994
Heure de l'injection
10 : 13 : 00
Durée de l'injection (min)
197
Quantité d'eau injectée (l)
3000
lieu de détection
réseau Milandrine
Coord lieu de détection
567075257080
Fréqu. des prélèvements
6 fois par jour
Débit de la source (l/min)
3900
Taux de restitution %
0
Quantité d'eau injectée
Fichiers DATA
Fichier INPUT
aucun
Fichier OUTPUT
aucun
stockage des fichiers
fonctions IN et OUTPUT

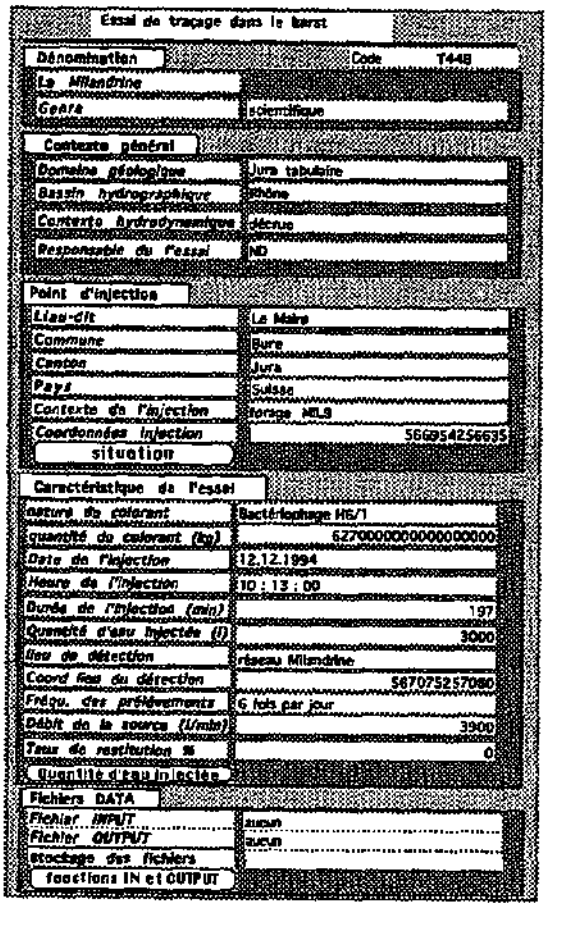
Essai de traçage dans le karst
Dénomination
Code T44B
La Milandrine
Genre
scientifique
Contexte général
Domaine géologique
Jura tabulaire
Bassin hydrographique
Rhône
Contexte hydrodynamique
décrue
Responsable de l'essai
ND
Point d'injection
Lieu-dit
Le Maira
Commune
Bure
Canton
Jura
Pays
Suisse
Contexte de l'injection
forage MEL9
Coordonnées injection
566954256635
situation
Caractéristique de l'essai
nature du colorant
Bactériophage H6/1
quantité de colorant (kg)
627000000000000000
Date de l'injection
12.12.1994
Heure de l'injection
10 : 13 : 00
Durée de l'injection (min)
197
Quantité d'eau injectée (l)
3000
lieu de détection
réseau Milandrine
Coord lieu de détection
567075257080
Fréqu. des prélèvements
6 fois par jour
Débit de la source (l/min)
3900
Taux de restitution %
0
Quantité d'eau injectée
Fichiers DATA
Fichier INPUT
aucun
Fichier OUTPUT
aucun
stockage des fichiers
fonctions IN et OUTPUT

Essai de traçage dans le karst

Dénomination — Code T45B

Genre

Contexte général

Domaine géologique

Bassin hydrographique

Contexte hydrodynamique

Responsable de l'essai

Point d'injection

Lieu-dit

Commune

Canton

Pays

Contexte de l'injection

Coordonnées injection — 0

situation

Caractéristique de l'essai

nature du colorant

quantité de colorant (kg) — 0

Date de l'injection — 00.00.00

Heure de l'injection — 00 : 00 : 00

Durée de l'injection (min) — 0

Quantité d'eau injectée (l) — 0

lieu de détection

Coord lieu de détection — 0

Fréqu. des prélèvements

Débit de la source (l/min) — 0

Taux de restitution % — 0

Quantité d'eau injectée

Fichiers DATA

Fichier INPUT

Fichier OUTPUT

stockage des fichiers

fonctions IN et OUTPUT

Essai de traçage dans le karst

Dénomination — Code T45

La Milandrine

Genre — scientifique

Contexte général

Domaine géologique — Jura tabulaire

Bassin hydrographique — Rhône

Contexte hydrodynamique — décrue

Responsable de l'essai — MD

Point d'injection

Lieu-dit — Le Maira

Commune — Bure

Canton — Jura

Pays — Suisse

Contexte de l'injection — pt 1 en surface

Coordonnées injection — 567075257050

situation

Caractéristique de l'essai

nature du colorant — NaCl

quantité de colorant (kg) — 100

Date de l'injection — 12.12.1994

Heure de l'injection — 11 : 58 : 00

Durée de l'injection (min) — 19

Quantité d'eau injectée (l) — 4000

lieu de détection — réseau Milandrine

Coord lieu de détection — 567075257080

Fréqu. des prélèvements — en continu

Débit de la source (l/min) — 14130

Taux de restitution % — 29.5

Quantité d'eau injectée

Fichiers DATA

Fichier INPUT — T45IN.DAT

Fichier OUTPUT — T45OUT.DAT

stockage des fichiers

fonctions IN et OUTPUT

Essai de traçage dans le karst

Dénomination — Code T45B

La Milandrine

Genre — scientifique

Contexte général

Domaine géologique — Jura tabulaire

Bassin hydrographique — Rhône

Contexte hydrodynamique — décrue

Responsable de l'essai — MD

Point d'injection

Lieu-dit — Le Maira

Commune — Bure

Canton — Jura

Pays — Suisse

Contexte de l'injection — pt 1 en surface

Coordonnées injection — 567075257050

situation

Caractéristique de l'essai

nature du colorant — Sactéréphage HH0/1

quantité de colorant (kg) — 40300000000

Date de l'injection — 12.12.1994

Heure de l'injection — 11 : 58 : 00

Durée de l'injection (min) — 19

Quantité d'eau injectée (l) — 4000

lieu de détection — réseau Milandrine

Coord lieu de détection — 567075257080

Fréqu. des prélèvements — 6 fois par jour

Débit de la source (l/min) — 14130

Taux de restitution % — 9

Quantité d'eau injectée

Fichiers DATA

Fichier INPUT — T45IN.DAT

Fichier OUTPUT — T45OUT.DAT

stockage des fichiers

fonctions IN et OUTPUT

Essai de traçage dans le karst

Dénomination — Code T46

La Milandrine

Genre — scientifique

Contexte général

Domaine géologique — Jura tabulaire

Bassin hydrographique — Rhône

Contexte hydrodynamique — étiage

Responsable de l'essai — MD

Point d'injection

Lieu-dit — Le Maira

Commune — Bure

Canton — Jura

Pays — Suisse

Contexte de l'injection — forage MIL3

Coordonnées injection — 567056256583

situation

Caractéristique de l'essai

nature du colorant — NaCl

quantité de colorant (kg) — 250

Date de l'injection — 19.12.1994

Heure de l'injection — 14 : 14 : 00

Durée de l'injection (min) — 18

Quantité d'eau injectée (l) — 4000

lieu de détection — réseau Milandrine

Coord lieu de détection — 567075257080

Fréqu. des prélèvements — en continu

Débit de la source (l/min) — 3036

Taux de restitution % — 86

Quantité d'eau injectée

Fichiers DATA

Fichier INPUT — T46IN.DAT

Fichier OUTPUT — T46OUT.DAT

stockage des fichiers

fonctions IN et OUTPUT

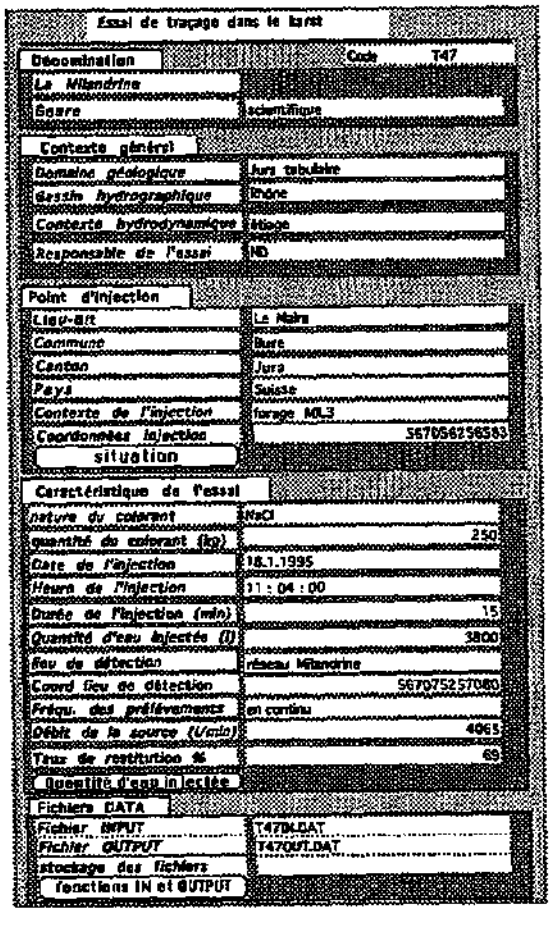
Essai de traçage dans le karst
Dénomination
Code T47
La Milandrine
Genre scientifique
Contexte général
Domaine géologique Jura tabulaire
Bassin hydrographique Rhône
Contexte hydrodynamique étiage
Responsable de l'essai ND
Point d'injection
Lieu-dit Le Maira
Commune Bure
Canton Jura
Pays Suisse
Contexte de l'injection forage MIL3
Coordonnées injection 567056256583
situation
Caractéristique de l'essai
nature du colorant NaCl
quantité de colorant (kg) 250
Date de l'injection 18.1.1995
Heure de l'injection 11 : 04 : 00
Durée de l'injection (min) 15
Quantité d'eau injectée (l) 3800
lieu de détection réseau Milandrine
Coord lieu de détection 567075257080
Fréqu. des prélèvements en continu
Débit de la source (l/min) 4065
Taux de restitution % 69
Quantité d'eau injectée
Fichiers DATA
Fichier INPUT T47IN.DAT
Fichier OUTPUT T47OUT.DAT
stockage des fichiers
fonctions IN et OUTPUT

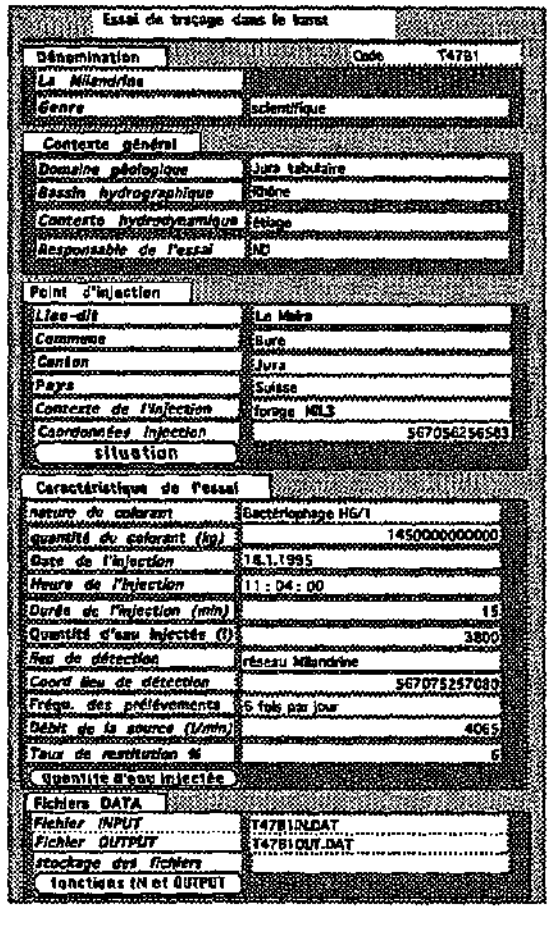
Essai de traçage dans le karst
Dénomination
Code T47B1
La Milandrine
Genre scientifique
Contexte général
Domaine géologique Jura tabulaire
Bassin hydrographique Rhône
Contexte hydrodynamique étiage
Responsable de l'essai ND
Point d'injection
Lieu-dit Le Maira
Commune Bure
Canton Jura
Pays Suisse
Contexte de l'injection forage MIL3
Coordonnées injection 567056256583
situation
Caractéristique de l'essai
nature du colorant Bactériophage MS/1
quantité de colorant (kg) 1450000000000
Date de l'injection 18.1.1995
Heure de l'injection 11 : 04 : 00
Durée de l'injection (min) 15
Quantité d'eau injectée (l) 3800
lieu de détection réseau Milandrine
Coord lieu de détection 567075257080
Fréqu. des prélèvements 6 fois par jour
Débit de la source (l/min) 4065
Taux de restitution % 6
Quantité d'eau injectée
Fichiers DATA
Fichier INPUT T47B1IN.DAT
Fichier OUTPUT T47B1OUT.DAT
stockage des fichiers
fonctions IN et OUTPUT

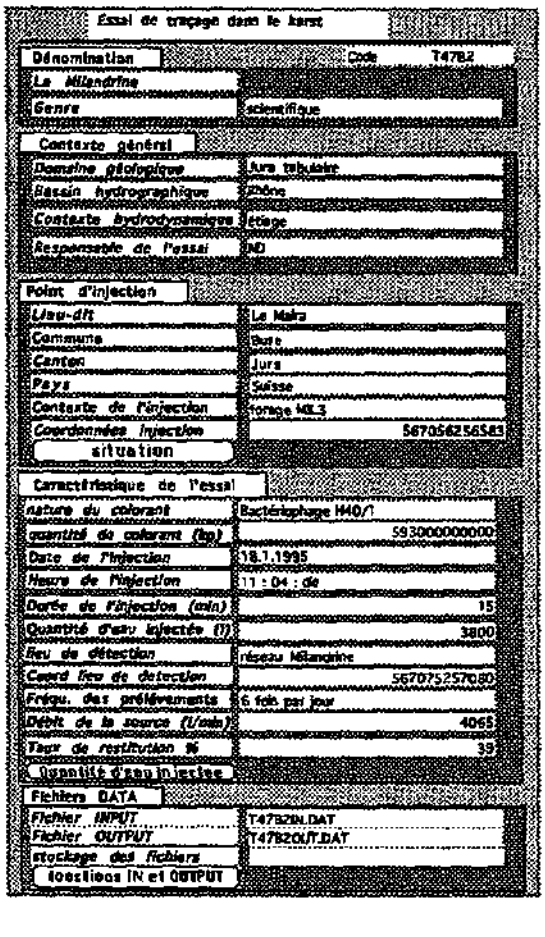
Essai de traçage dans le karst
Dénomination
Code T47B2
La Milandrine
Genre scientifique
Contexte général
Domaine géologique Jura tabulaire
Bassin hydrographique Rhône
Contexte hydrodynamique étiage
Responsable de l'essai ND
Point d'injection
Lieu-dit Le Maira
Commune Bure
Canton Jura
Pays Suisse
Contexte de l'injection forage MIL3
Coordonnées injection 567056256583
situation
Caractéristique de l'essai
nature du colorant Bactériophage MS/1
quantité de colorant (kg) 593000000000
Date de l'injection 18.1.1995
Heure de l'injection 11 : 04 : de
Durée de l'injection (min) 15
Quantité d'eau injectée (l) 3800
lieu de détection réseau Milandrine
Coord lieu de détection 567075257080
Fréqu. des prélèvements 6 fois par jour
Débit de la source (l/min) 4065
Taux de restitution % 39
Quantité d'eau injectée
Fichiers DATA
Fichier INPUT T47B2IN.DAT
Fichier OUTPUT T47B2OUT.DAT
stockage des fichiers
fonctions IN et OUTPUT

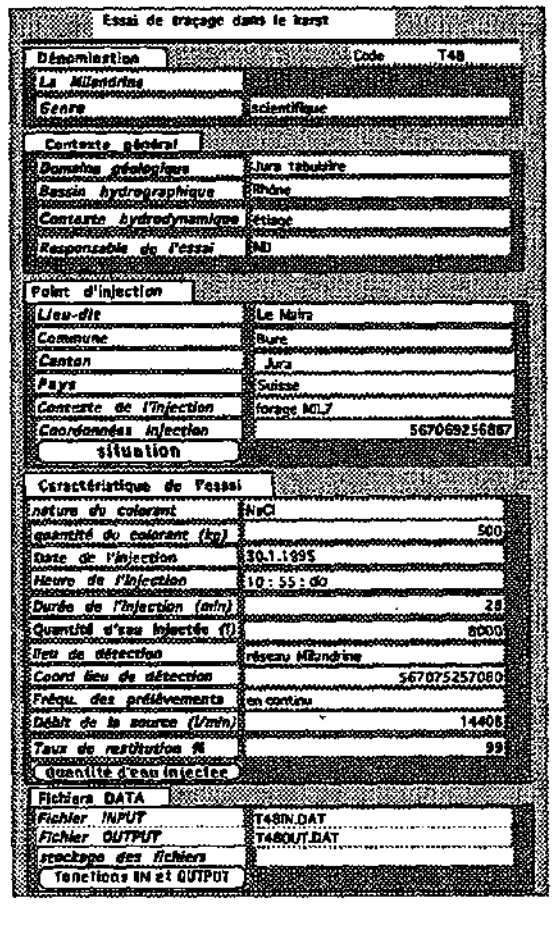
Essai de traçage dans le karst
Dénomination
Code T48
La Milandrine
Genre scientifique
Contexte général
Domaine géologique Jura tabulaire
Bassin hydrographique Rhône
Contexte hydrodynamique étiage
Responsable de l'essai ND
Point d'injection
Lieu-dit Le Maira
Commune Bure
Canton Jura
Pays Suisse
Contexte de l'injection forage MIL7
Coordonnées injection 5670692566B7
situation
Caractéristique de l'essai
nature du colorant NaCl
quantité de colorant (kg) 500
Date de l'injection 30.1.1995
Heure de l'injection 10 : 55 : do
Durée de l'injection (min) 25
Quantité d'eau injectée (l) 8000
lieu de détection réseau Milandrine
Coord lieu de détection 567075257080
Fréqu. des prélèvements en continu
Débit de la source (l/min) 14408
Taux de restitution % 99
Quantité d'eau injectée
Fichiers DATA
Fichier INPUT T48IN.DAT
Fichier OUTPUT T48OUT.DAT
stockage des fichiers
fonctions IN et OUTPUT

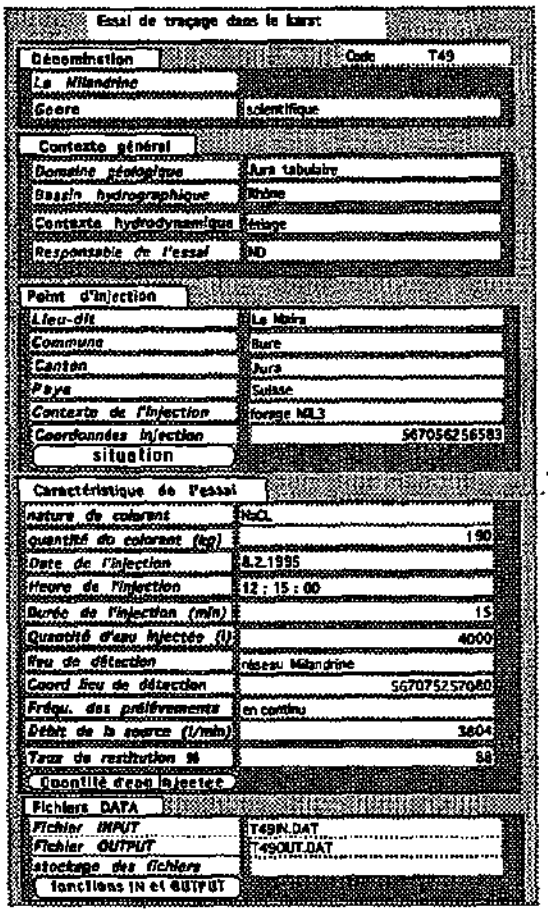
Essai de traçage dans le karst
Dénomination
Code T49
La Milandrine
Genre
scientifique
Contexte général
Domaine géologique
Jura tabulaire
Bassin hydrographique
Rhône
Contexte hydrodynamique
Etiage
Responsable de l'essai
ND
Point d'injection
Lieu-dit
Le Maira
Commune
Bure
Canton
Jura
Pays
Suisse
Contexte de l'injection
forage MIL3
Coordonnées injection
567056256583
situation
Caractéristique de l'essai
nature du colorant
NaCl
quantité du colorant (kg)
190
Date de l'injection
8.2.1995
Heure de l'injection
12 : 15 : 00
Durée de l'injection (min)
15
Quantité d'eau injectée (l)
4000
lieu de détection
réseau Milandrine
Coord lieu de détection
567075257080
Fréqu. des prélèvements
en continu
Débit de la source (l/min)
3604
Taux de restitution %
98
Quantité d'eau injectée
Fichiers DATA
Fichier INPUT
T49IN.DAT
Fichier OUTPUT
T49OUT.DAT
stockage des fichiers
fonctions IN et OUTPUT

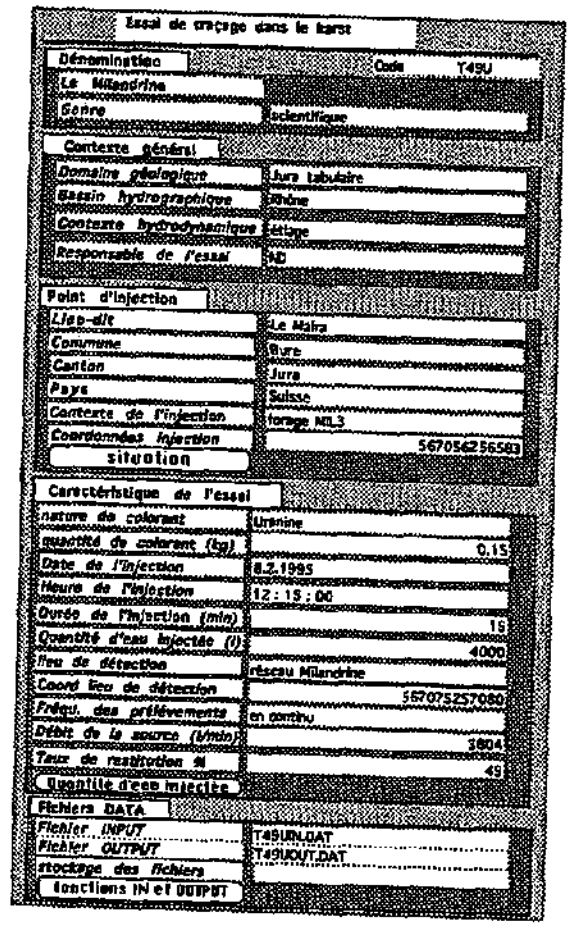
Essai de traçage dans le karst
Dénomination
Code T49U
La Milandrine
Genre
scientifique
Contexte général
Domaine géologique
Jura tabulaire
Bassin hydrographique
Rhône
Contexte hydrodynamique
Etiage
Responsable de l'essai
ND
Point d'injection
Lieu-dit
Le Maira
Commune
Bure
Canton
Jura
Pays
Suisse
Contexte de l'injection
forage MIL3
Coordonnées injection
567056256583
situation
Caractéristique de l'essai
nature du colorant
Uranine
quantité du colorant (kg)
0.15
Date de l'injection
8.2.1995
Heure de l'injection
12 : 15 : 00
Durée de l'injection (min)
15
Quantité d'eau injectée (l)
4000
lieu de détection
réseau Milandrine
Coord lieu de détection
567075257080
Fréqu. des prélèvements
en continu
Débit de la source (l/min)
3604
Taux de restitution %
49
Quantité d'eau injectée
Fichiers DATA
Fichier INPUT
T49UIN.DAT
Fichier OUTPUT
T49UOUT.DAT
stockage des fichiers
fonctions IN et OUTPUT

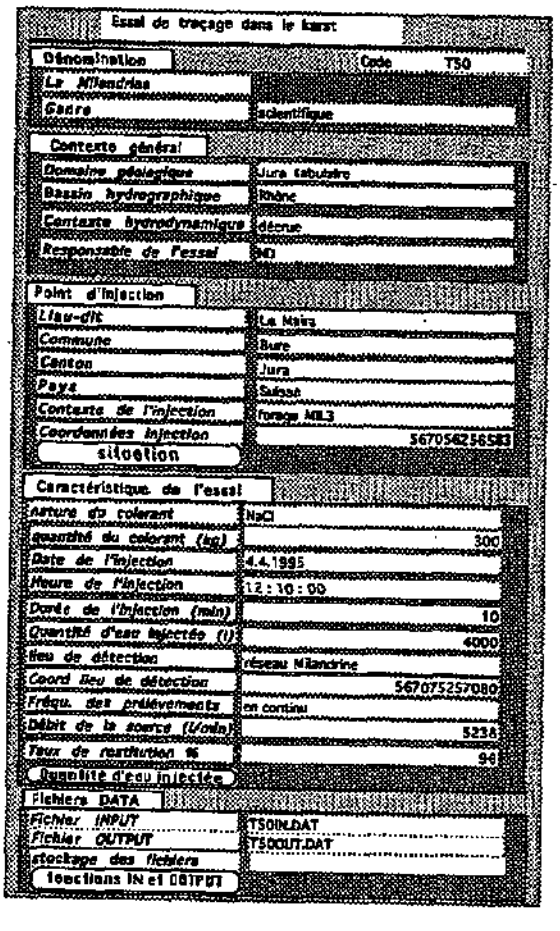
Essai de traçage dans le karst
Dénomination
Code T50
La Milandrine
Genre
scientifique
Contexte général
Domaine géologique
Jura tabulaire
Bassin hydrographique
Rhône
Contexte hydrodynamique
décrue
Responsable de l'essai
ND
Point d'injection
Lieu-dit
Le Maira
Commune
Bure
Canton
Jura
Pays
Suisse
Contexte de l'injection
forage MIL3
Coordonnées injection
567056256583
situation
Caractéristique de l'essai
nature du colorant
NaCl
quantité du colorant (kg)
300
Date de l'injection
4.4.1995
Heure de l'injection
12 : 10 : 00
Durée de l'injection (min)
10
Quantité d'eau injectée (l)
4000
lieu de détection
réseau Milandrine
Coord lieu de détection
567075257080
Fréqu. des prélèvements
en continu
Débit de la source (l/min)
5238
Taux de restitution %
94
Quantité d'eau injectée
Fichiers DATA
Fichier INPUT
T50IN.DAT
Fichier OUTPUT
T50OUT.DAT
stockage des fichiers
fonctions IN et OUTPUT

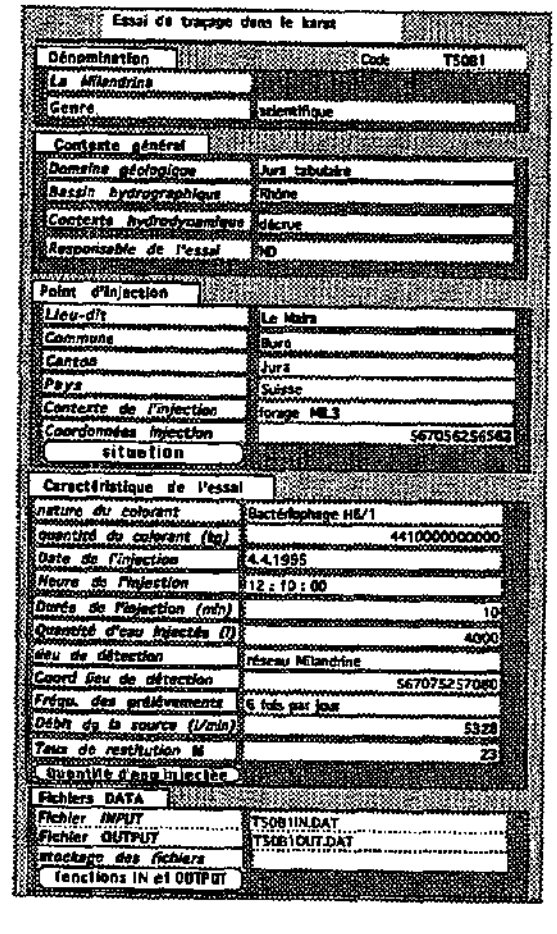
Essai de traçage dans le karst
Dénomination
Code T5081
La Milandrine
Genre
scientifique
Contexte général
Domaine géologique
Jura tabulaire
Bassin hydrographique
Rhône
Contexte hydrodynamique
décrue
Responsable de l'essai
ND
Point d'injection
Lieu-dit
Le Maira
Commune
Bure
Canton
Jura
Pays
Suisse
Contexte de l'injection
forage MIL3
Coordonnées injection
567056256583
situation
Caractéristique de l'essai
nature du colorant
Bactériophage MS/1
quantité du colorant (kg)
4410000000000
Date de l'injection
4.4.1995
Heure de l'injection
12 : 10 : 00
Durée de l'injection (min)
10
Quantité d'eau injectée (l)
4000
lieu de détection
réseau Milandrine
Coord lieu de détection
567075257080
Fréqu. des prélèvements
6 fois par jour
Débit de la source (l/min)
5328
Taux de restitution %
23
Quantité d'eau injectée
Fichiers DATA
Fichier INPUT
T5081IN.DAT
Fichier OUTPUT
T5081OUT.DAT
stockage des fichiers
fonctions IN et OUTPUT

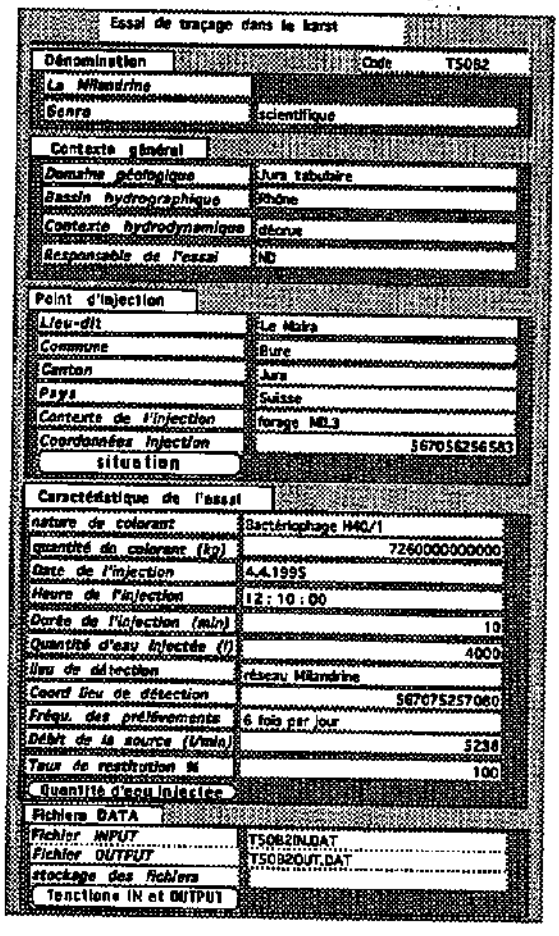
Essai de traçage dans le karst
Dénomination
Code T50B2
La Milandrine
Genre
scientifique
Contexte général
Domaine géologique
Jura tabulaire
Bassin hydrographique
Rhône
Contexte hydrodynamique
décrue
Responsable de l'essai
ND
Point d'injection
Lieu-dit
Le Maira
Commune
Bure
Canton
Jura
Pays
Suisse
Contexte de l'injection
forage MIL3
Coordonnées injection
situation
5670562565B3
Caractéristique de l'essai
nature de colorant
Bactériophage H40/1
quantité de colorant (kg)
72600000000000
Date de l'injection
4.4.1995
Heure de l'injection
12 : 10 : 00
Durée de l'injection (min)
10
Quantité d'eau injectée (l)
4000
lieu de détection
réseau Milandrine
Coord lieu de détection
567075257080
Fréqu. des prélèvements
6 fois par jour
Débit de la source (l/min)
5238
Taux de restitution %
100
Quantité d'eau injectée
Fichiers DATA
Fichier INPUT
T50B2IN.DAT
Fichier OUTPUT
T50B2OUT.DAT
stockage des fichiers
fonctions IN et OUTPUT

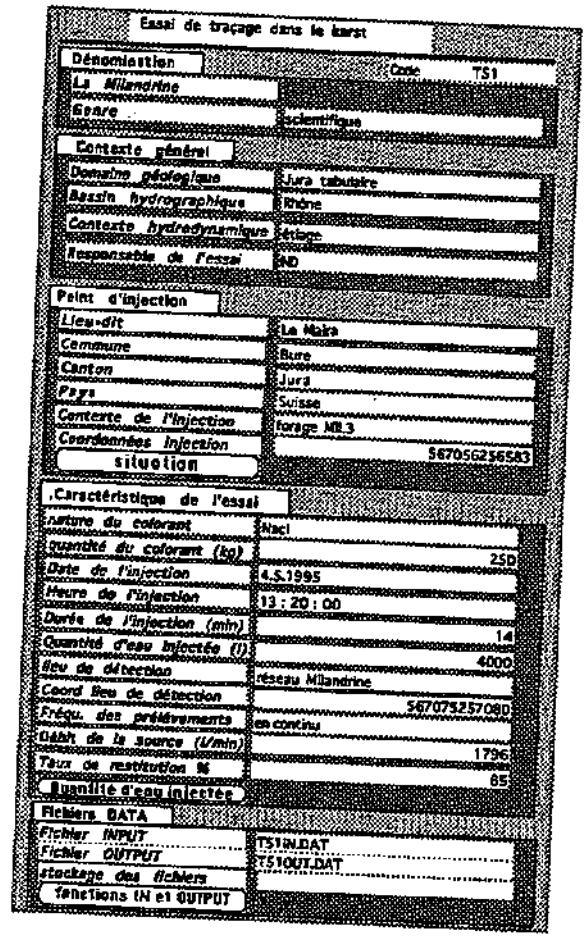
Essai de traçage dans le karst
Dénomination
Code TS1
La Milandrine
Genre
scientifique
Contexte général
Domaine géologique
Jura tabulaire
Bassin hydrographique
Rhône
Contexte hydrodynamique
étiage
Responsable de l'essai
ND
Point d'injection
Lieu-dit
Le Maira
Commune
Bure
Canton
Jura
Pays
Suisse
Contexte de l'injection
forage MIL3
Coordonnées injection
situation
5670562565B3
Caractéristique de l'essai
nature du colorant
Nacl
quantité du colorant (kg)
250
Date de l'injection
4.5.1995
Heure de l'injection
13 : 20 : 00
Durée de l'injection (min)
14
Quantité d'eau injectée (l)
4000
lieu de détection
réseau Milandrine
Coord lieu de détection
567075257080
Fréqu. des prélèvements
en continu
Débit de la source (l/min)
1796
Taux de restitution %
85
Quantité d'eau injectée
Fichiers DATA
Fichier INPUT
TS1IN.DAT
Fichier OUTPUT
TS1OUT.DAT
stockage des fichiers
fonctions IN et OUTPUT

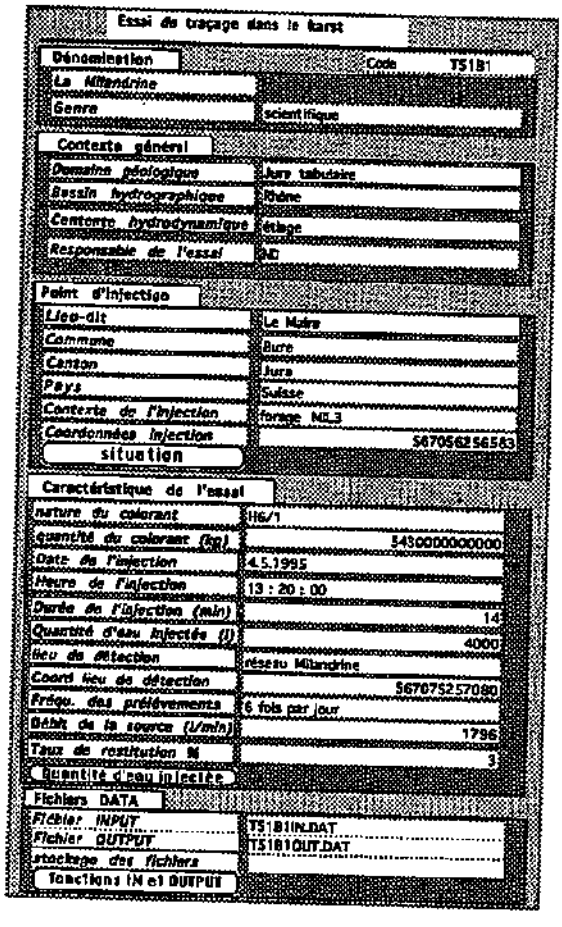
Essai de traçage dans le karst
Dénomination
Code TS1B1
La Milandrine
Genre
scientifique
Contexte général
Domaine géologique
Jura tabulaire
Bassin hydrographique
Rhône
Contexte hydrodynamique
étiage
Responsable de l'essai
ND
Point d'injection
Lieu-dit
Le Maira
Commune
Bure
Canton
Jura
Pays
Suisse
Contexte de l'injection
forage MIL3
Coordonnées injection
situation
5670562565B3
Caractéristique de l'essai
nature du colorant
H6/1
quantité du colorant (kg)
5430000000000
Date de l'injection
4.5.1995
Heure de l'injection
13 : 20 : 00
Durée de l'injection (min)
14
Quantité d'eau injectée (l)
4000
lieu de détection
réseau Milandrine
Coord lieu de détection
567075257080
Fréqu. des prélèvements
6 fois par jour
Débit de la source (l/min)
1796
Taux de restitution %
3
Quantité d'eau injectée
Fichiers DATA
Fichier INPUT
TS1B1IN.DAT
Fichier OUTPUT
TS1B1OUT.DAT
stockage des fichiers
fonctions IN et OUTPUT

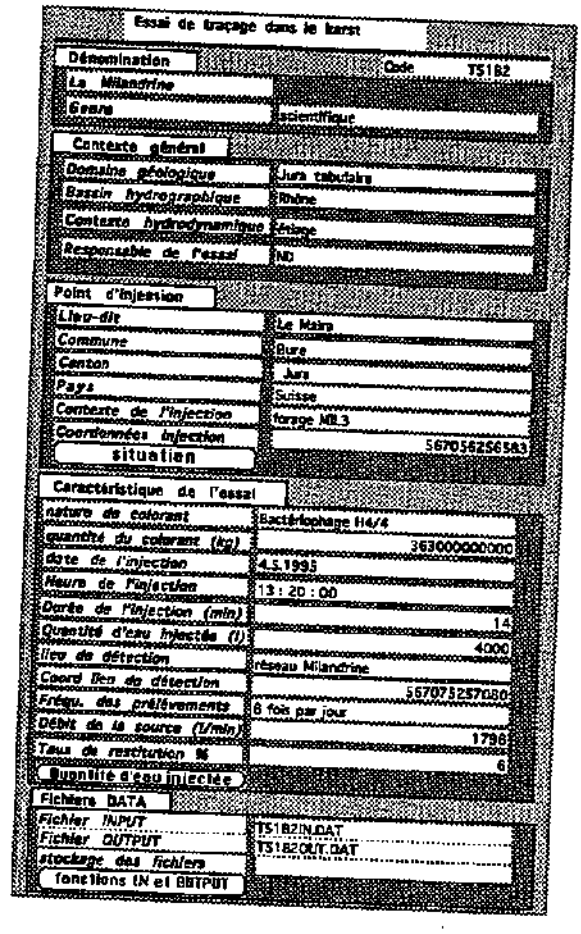
Essai de traçage dans le karst
Dénomination
Code TS1B2
La Milandrine
Genre
scientifique
Contexte général
Domaine géologique
Jura tabulaire
Bassin hydrographique
Rhône
Contexte hydrodynamique
étiage
Responsable de l'essai
ND
Point d'injection
Lieu-dit
Le Maira
Commune
Bure
Canton
Jura
Pays
Suisse
Contexte de l'injection
forage MIL3
Coordonnées injection
situation
5670562565B3
Caractéristique de l'essai
nature du colorant
Bactériophage H4/4
quantité du colorant (kg)
3630000000000
Date de l'injection
4.5.1995
Heure de l'injection
13 : 20 : 00
Durée de l'injection (min)
14
Quantité d'eau injectée (l)
4000
lieu de détection
réseau Milandrine
Coord lieu de détection
567075257080
Fréqu. des prélèvements
6 fois par jour
Débit de la source (l/min)
1796
Taux de restitution %
6
Quantité d'eau injectée
Fichiers DATA
Fichier INPUT
TS1B2IN.DAT
Fichier OUTPUT
TS1B2OUT.DAT
stockage des fichiers
fonctions IN et OUTPUT

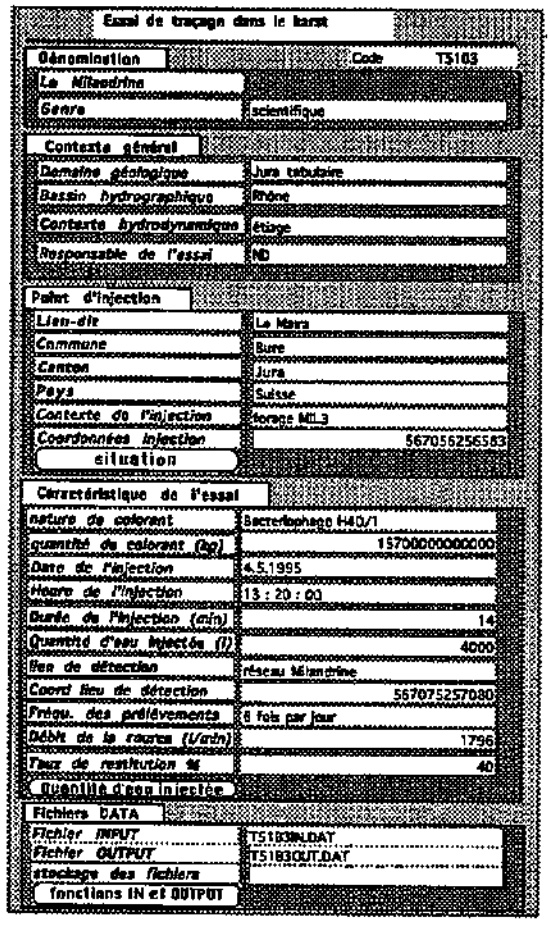
Essai de traçage dans le karst
Dénomination
Code T5183
Le Milandrine
Genre
scientifique
Contexte général
Domaine géologique
Jura tabulaire
Bassin hydrographique
Rhône
Contexte hydrodynamique
étiage
Responsable de l'essai
ND
Point d'injection
Lieu-dit
Le Maira
Commune
Bure
Canton
Jura
Pays
Suisse
Contexte de l'injection
forage MI3
Coordonnées injection
567056256583
situation
Caractéristique de l'essai
nature de colorant
Bacteriophage H40/1
quantité de colorant (kg)
15700000000000
Date de l'injection
4.5.1995
Heure de l'injection
13 : 20 : 00
Durée de l'injection (min)
14
Quantité d'eau injectée (l)
4000
lieu de détection
réseau Milandrine
Coord lieu de détection
567075257080
Frégu. des prélèvements
6 fois par jour
Débit de la source (l/min)
1796
Taux de restitution %
40
quantité d'eau injectée
Fichiers DATA
Fichier INPUT
T5183IN.DAT
Fichier OUTPUT
T5183OUT.DAT
stockage des fichiers
fonctions IN et OUTPUT

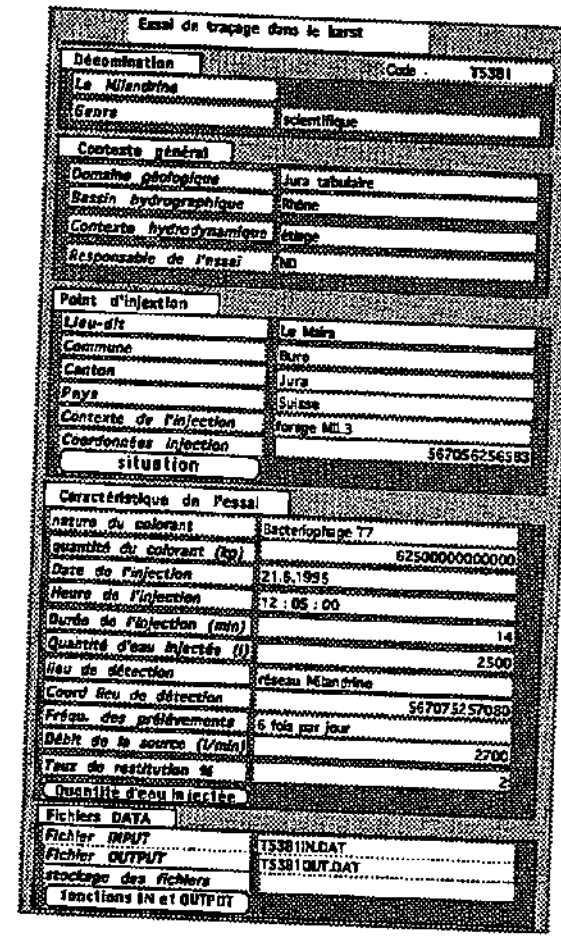
Essai de traçage dans le karst
Dénomination
Code T5381
Le Milandrine
Genre
scientifique
Contexte général
Domaine géologique
Jura tabulaire
Bassin hydrographique
Rhône
Contexte hydrodynamique
étiage
Responsable de l'essai
ND
Point d'injection
Lieu-dit
Le Maira
Commune
Bure
Canton
Jura
Pays
Suisse
Contexte de l'injection
forage MI3
Coordonnées injection
567056256583
situation
Caractéristique de l'essai
nature du colorant
Bacteriophage T7
quantité de colorant (kg)
62500000000000
Date de l'injection
21.6.1995
Heure de l'injection
12 : 05 : 00
Durée de l'injection (min)
14
Quantité d'eau injectée (l)
2500
lieu de détection
réseau Milandrine
Coord lieu de détection
567075257080
Frégu. des prélèvements
6 fois par jour
Débit de la source (l/min)
2700
Taux de restitution %
2
Quantité d'eau injectée
Fichiers DATA
Fichier INPUT
T5381IN.DAT
Fichier OUTPUT
T5381OUT.DAT
stockage des fichiers
fonctions IN et OUTPUT

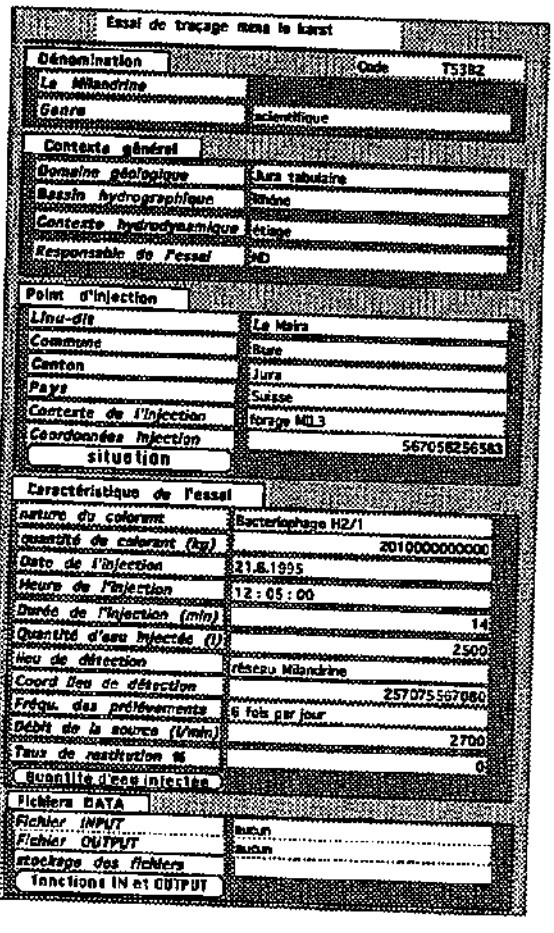
Essai de traçage dans le karst
Dénomination
Code T5382
Le Milandrine
Genre
scientifique
Contexte général
Domaine géologique
Jura tabulaire
Bassin hydrographique
Rhône
Contexte hydrodynamique
étiage
Responsable de l'essai
ND
Point d'injection
Lieu-dit
Le Maira
Commune
Bure
Canton
Jura
Pays
Suisse
Contexte de l'injection
forage MI3
Coordonnées injection
567056256583
situation
Caractéristique de l'essai
nature du colorant
Bacteriophage H2/1
quantité de colorant (kg)
20100000000000
Date de l'injection
21.6.1995
Heure de l'injection
12 : 05 : 00
Durée de l'injection (min)
14
Quantité d'eau injectée (l)
2500
lieu de détection
réseau Milandrine
Coord lieu de détection
257075567080
Frégu. des prélèvements
6 fois par jour
Débit de la source (l/min)
2700
Taux de restitution %
0
Quantité d'eau injectée
Fichiers DATA
Fichier INPUT
aucun
Fichier OUTPUT
aucun
stockage des fichiers
fonctions IN et OUTPUT

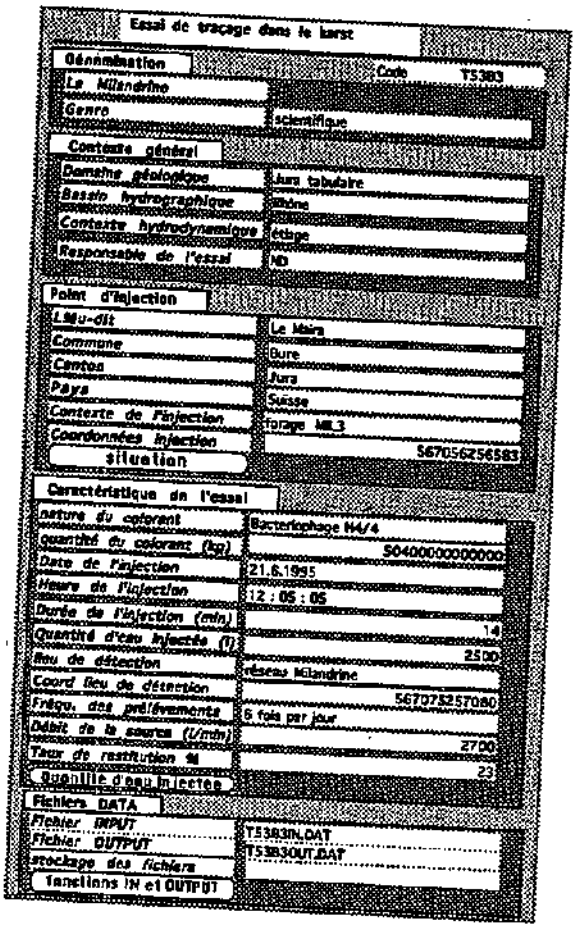
Essai de traçage dans le karst
Dénomination
Code T5383
Le Milandrine
Genre
scientifique
Contexte général
Domaine géologique
Jura tabulaire
Bassin hydrographique
Rhône
Contexte hydrodynamique
étiage
Responsable de l'essai
ND
Point d'injection
Lieu-dit
Le Maira
Commune
Bure
Canton
Jura
Pays
Suisse
Contexte de l'injection
forage MI3
Coordonnées injection
567056256583
situation
Caractéristique de l'essai
nature du colorant
Bacteriophage H4/4
quantité de colorant (kg)
50400000000000
Date de l'injection
21.6.1995
Heure de l'injection
12 : 05 : 05
Durée de l'injection (min)
14
Quantité d'eau injectée (l)
2500
lieu de détection
réseau Milandrine
Coord lieu de détection
567075257080
Frégu. des prélèvements
6 fois par jour
Débit de la source (l/min)
2700
Taux de restitution %
23
Quantité d'eau injectée
Fichiers DATA
Fichier INPUT
T5383IN.DAT
Fichier OUTPUT
T5383OUT.DAT
stockage des fichiers
fonctions IN et OUTPUT

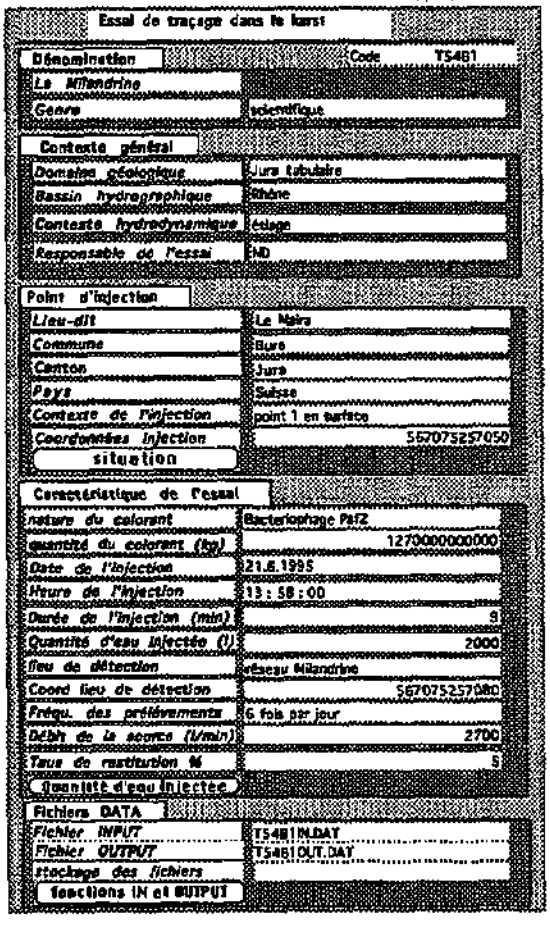
Essai de traçage dans le karst
Dénomination
Code T54B1
La Milandrine
Genre scientifique
Contexte général
Domaine géologique Jura tabulaire
Bassin hydrographique Rhône
Contexte hydrodynamique étiage
Responsable de l'essai ND
Point d'injection
Lieu-dit Le Maira
Commune Bure
Canton Jura
Pays Suisse
Contexte de l'injection point 1 en surface
Coordonnées injection 5670752570S0
situation
Caractéristique de l'essai
Nature du colorant Bacteriophage PaT2
quantité du colorant (kg) 1270000000000
Date de l'injection 21.6.1995
Heure de l'injection 13 : 58 : 00
Durée de l'injection (min) 9
Quantité d'eau injectée (l) 2000
lieu de détection réseau Milandrine
Coord lieu de détection 5670752570B0
Frégu. des prélèvements 6 fois par jour
Débit de la source (l/min) 2700
Taux de restitution % 9
Quantité d'eau injectée
Fichiers DATA
Fichier INPUT T54B1IN.DAT
Fichier OUTPUT T54B1OUT.DAT
stockage des fichiers
fonctions IN et OUTPUT

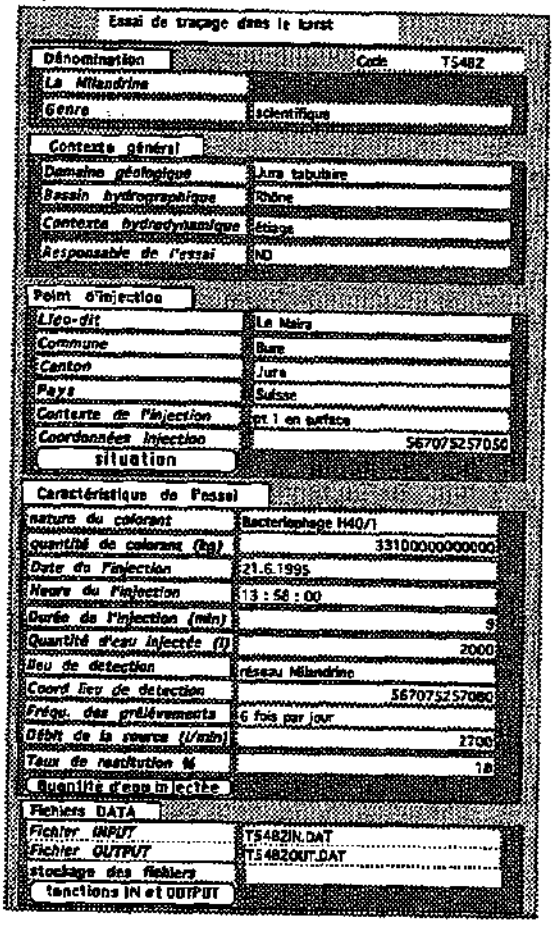
Essai de traçage dans le karst
Dénomination
Code T54B2
La Milandrine
Genre scientifique
Contexte général
Domaine géologique Jura tabulaire
Bassin hydrographique Rhône
Contexte hydrodynamique étiage
Responsable de l'essai ND
Point d'injection
Lieu-dit Le Maira
Commune Bure
Canton Jura
Pays Suisse
Contexte de l'injection pt 1 en surface
Coordonnées injection 5670752570S0
situation
Caractéristique de l'essai
Nature du colorant Bacteriophage H40/1
quantité de colorant (kg) 331000000000
Date de l'injection 21.6.1995
Heure de l'injection 13 : 58 : 00
Durée de l'injection (min) 9
Quantité d'eau injectée (l) 2000
lieu de détection réseau Milandrine
Coord lieu de détection 5670752570B0
Frégu. des prélèvements 6 fois par jour
Débit de la source (l/min) 2700
Taux de restitution % 18
Quantité d'eau injectée
Fichiers DATA
Fichier INPUT T54B2IN.DAT
Fichier OUTPUT T54B2OUT.DAT
stockage des fichiers
fonctions IN et OUTPUT

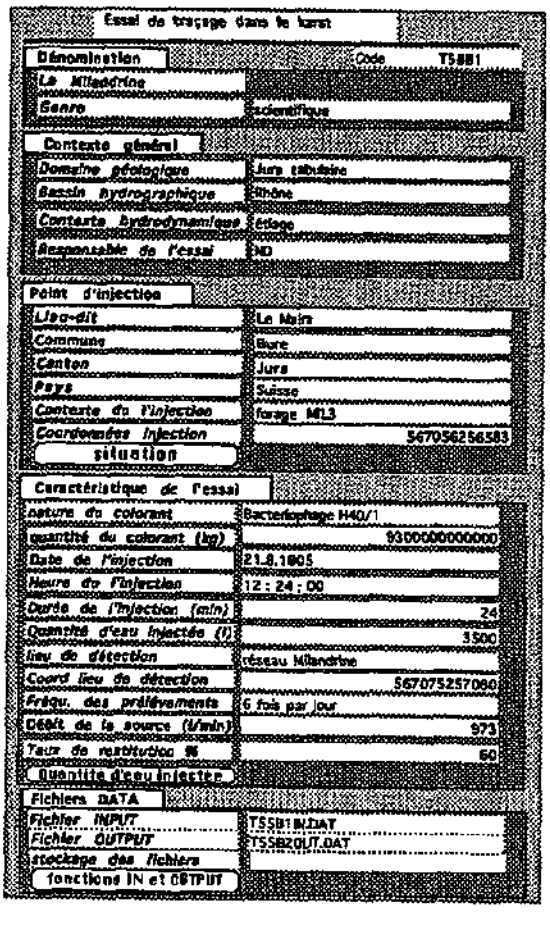
Essai de traçage dans le karst
Dénomination
Code T5SB1
La Milandrine
Genre scientifique
Contexte général
Domaine géologique Jura tabulaire
Bassin hydrographique Rhône
Contexte hydrodynamique étiage
Responsable de l'essai ND
Point d'injection
Lieu-dit Le Maira
Commune Bure
Canton Jura
Pays Suisse
Contexte de l'injection forage MI3
Coordonnées injection 5670562565B3
situation
Caractéristique de l'essai
Nature du colorant Bacteriophage H40/1
quantité de colorant (kg) 93000000000
Date de l'injection 21.8.1995
Heure de l'injection 12 : 24 : 00
Durée de l'injection (min) 24
Quantité d'eau injectée (l) 3500
lieu de détection réseau Milandrine
Coord lieu de détection 5670752570B0
Frégu. des prélèvements 6 fois par jour
Débit de la source (l/min) 973
Taux de restitution % 60
Quantité d'eau injectée
Fichiers DATA
Fichier INPUT T5SB1IN.DAT
Fichier OUTPUT T5SB2OUT.DAT
stockage des fichiers
fonctions IN et OUTPUT

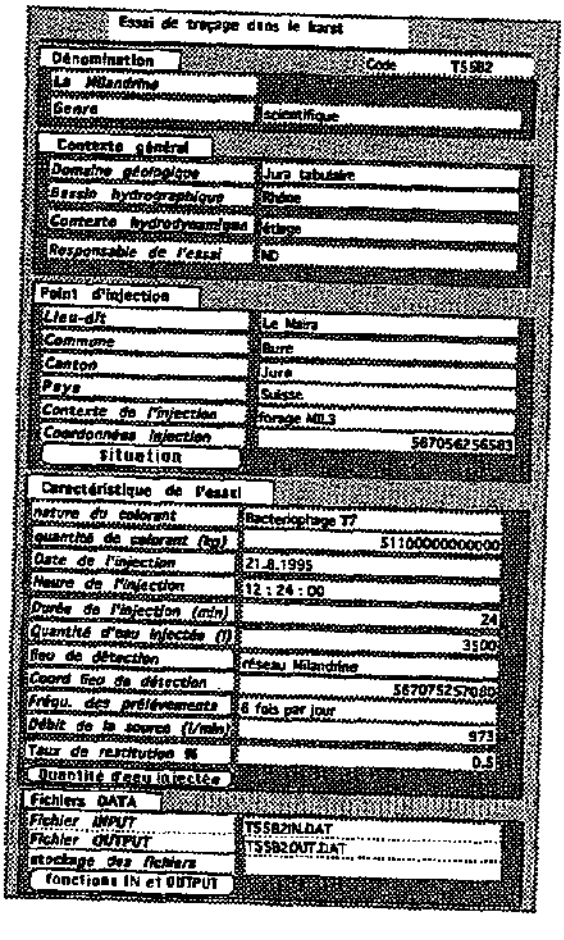
Essai de traçage dans le karst
Dénomination
Code T5SB2
La Milandrine
Genre scientifique
Contexte général
Domaine géologique Jura tabulaire
Bassin hydrographique Rhône
Contexte hydrodynamique étiage
Responsable de l'essai ND
Point d'injection
Lieu-dit Le Maira
Commune Bure
Canton Jura
Pays Suisse
Contexte de l'injection forage MI3
Coordonnées injection 5670562565B3
situation
Caractéristique de l'essai
Nature du colorant Bacteriophage T7
quantité de colorant (kg) 511000000000
Date de l'injection 21.8.1995
Heure de l'injection 12 : 24 : 00
Durée de l'injection (min) 24
Quantité d'eau injectée (l) 3500
lieu de détection réseau Milandrine
Coord lieu de détection 5670752570B0
Frégu. des prélèvements 6 fois par jour
Débit de la source (l/min) 973
Taux de restitution % 0.5
Quantité d'eau injectée
Fichiers DATA
Fichier INPUT T5SB2IN.DAT
Fichier OUTPUT T5SB2OUT.DAT
stockage des fichiers
fonctions IN et OUTPUT

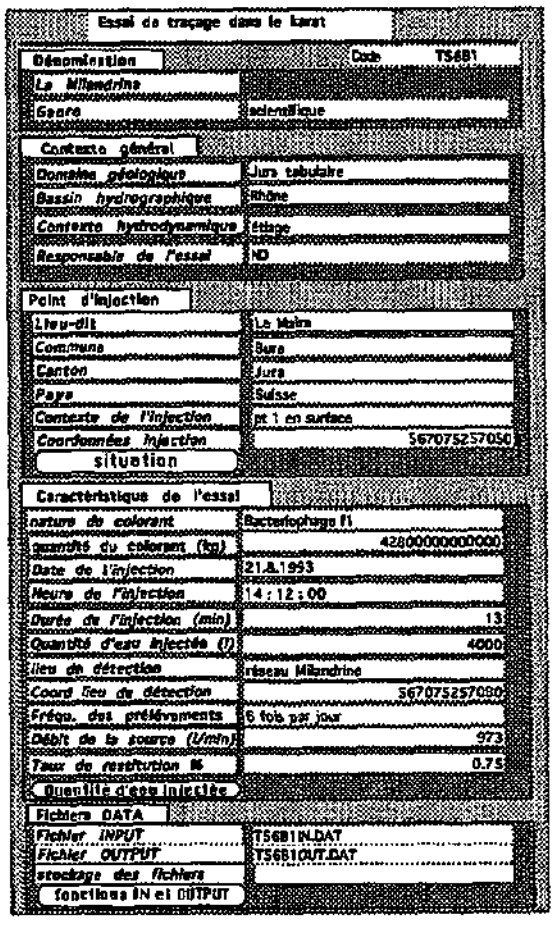
Essai de traçage dans le karst

Dénomination — Code: TS6B1

La Milandrine	
Genre	scientifique

Contexte général

Domaine géologique	Jura tabulaire
Bassin hydrographique	Rhône
Contexte hydrodynamique	étiage
Responsable de l'essai	ND

Point d'injection

Lieu-dit	La Maira
Commune	Bure
Canton	Jura
Pays	Suisse
Contexte de l'injection	pt 1 en surface
Coordonnées injection	567075257050

situation

Caractéristique de l'essai

nature du colorant	Bacteriophage f1
quantité du colorant (kg)	428000000000000
Date de l'injection	21.8.1993
Heure de l'injection	14 : 12 : 00
Durée de l'injection (min)	13
Quantité d'eau injectée (l)	4000
lieu de détection	réseau Milandrine
Coord lieu de détection	567075257080
Fréqu. des prélèvements	6 fois par jour
Débit de la source (l/min)	973
Taux de restitution %	0.75

Quantité d'eau injectée

Fichiers DATA

Fichier INPUT	T56B1IN.DAT
Fichier OUTPUT	T56B1OUT.DAT
stockage des fichiers	

fonctions IN et OUTPUT

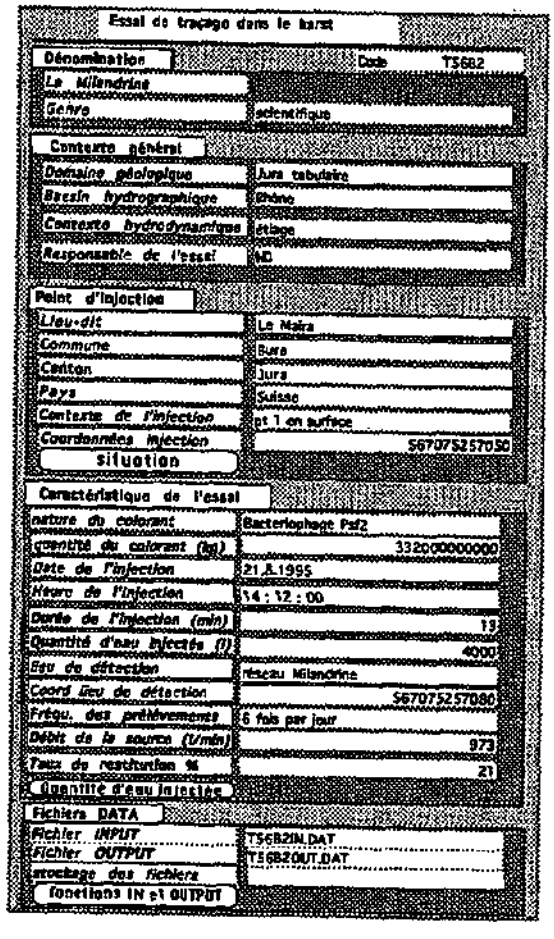
Essai de traçage dans le karst

Dénomination — Code: TS6B2

La Milandrine	
Genre	scientifique

Contexte général

Domaine géologique	Jura tabulaire
Bassin hydrographique	Rhône
Contexte hydrodynamique	étiage
Responsable de l'essai	ND

Point d'injection

Lieu-dit	La Maira
Commune	Bure
Canton	Jura
Pays	Suisse
Contexte de l'injection	pt 1 en surface
Coordonnées injection	567075257050

situation

Caractéristique de l'essai

nature du colorant	Bacteriophage Psf2
quantité du colorant (kg)	332000000000
Date de l'injection	21.8.1995
Heure de l'injection	14 : 12 : 00
Durée de l'injection (min)	13
Quantité d'eau injectée (l)	4000
lieu de détection	réseau Milandrine
Coord lieu de détection	567075257080
Fréqu. des prélèvements	6 fois par jour
Débit de la source (l/min)	973
Taux de restitution %	21

Quantité d'eau injectée

Fichiers DATA

Fichier INPUT	T56B2IN.DAT
Fichier OUTPUT	T56B2OUT.DAT
stockage des fichiers	

fonctions IN et OUTPUT

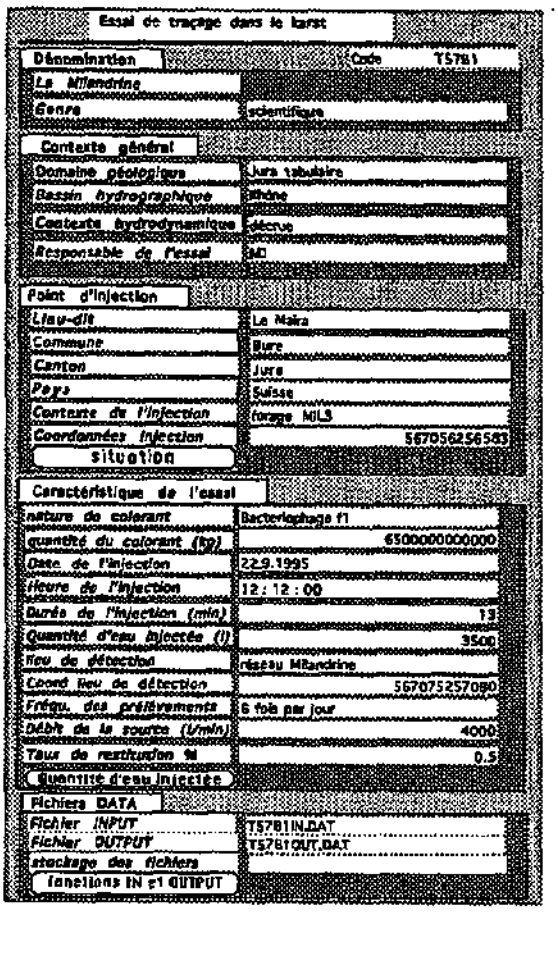
Essai de traçage dans le karst

Dénomination — Code: TS7B1

La Milandrine	
Genre	scientifique

Contexte général

Domaine géologique	Jura tabulaire
Bassin hydrographique	Rhône
Contexte hydrodynamique	décrue
Responsable de l'essai	ND

Point d'injection

Lieu-dit	La Maira
Commune	Bure
Canton	Jura
Pays	Suisse
Contexte de l'injection	forage MLS
Coordonnées injection	567056256583

situation

Caractéristique de l'essai

nature du colorant	Bacteriophage f1
quantité du colorant (kg)	6500000000000
Date de l'injection	22.9.1995
Heure de l'injection	12 : 12 : 00
Durée de l'injection (min)	13
Quantité d'eau injectée (l)	3500
lieu de détection	réseau Milandrine
Coord lieu de détection	567075257080
Fréqu. des prélèvements	6 fois par jour
Débit de la source (l/min)	4000
Taux de restitution %	0.5

Quantité d'eau injectée

Fichiers DATA

Fichier INPUT	T57B1IN.DAT
Fichier OUTPUT	T57B1OUT.DAT
stockage des fichiers	

fonctions IN et OUTPUT

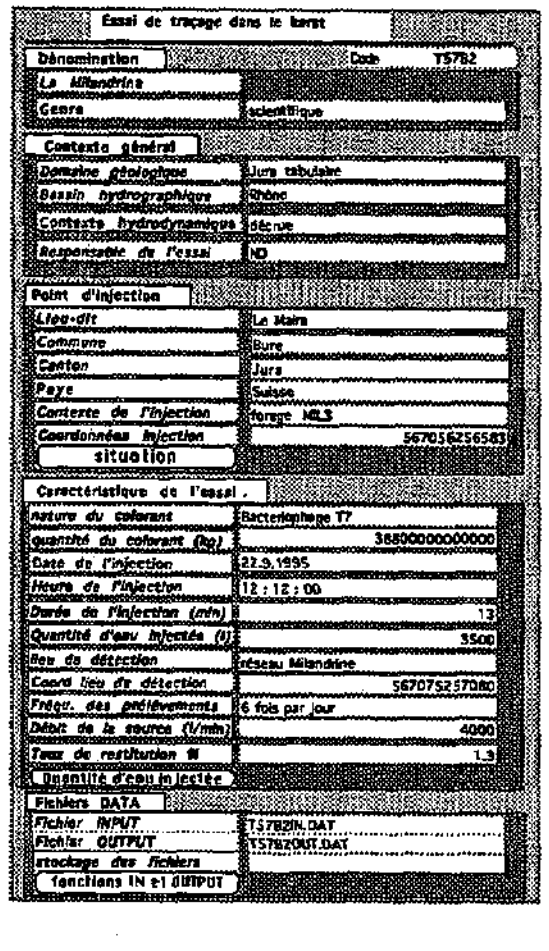
Essai de traçage dans le karst

Dénomination — Code: TS7B2

La Milandrine	
Genre	scientifique

Contexte général

Domaine géologique	Jura tabulaire
Bassin hydrographique	Rhône
Contexte hydrodynamique	décrue
Responsable de l'essai	ND

Point d'injection

Lieu-dit	La Maira
Commune	Bure
Canton	Jura
Pays	Suisse
Contexte de l'injection	forage MLS
Coordonnées injection	567056256583

situation

Caractéristique de l'essai

nature du colorant	Bacteriophage T7
quantité du colorant (kg)	36800000000000
Date de l'injection	22.9.1995
Heure de l'injection	12 : 12 : 00
Durée de l'injection (min)	13
Quantité d'eau injectée (l)	3500
lieu de détection	réseau Milandrine
Coord lieu de détection	567075257080
Fréqu. des prélèvements	6 fois par jour
Débit de la source (l/min)	4000
Taux de restitution %	1.3

Quantité d'eau injectée

Fichiers DATA

Fichier INPUT	T57B2IN.DAT
Fichier OUTPUT	T57B2OUT.DAT
stockage des fichiers	

fonctions IN et OUTPUT

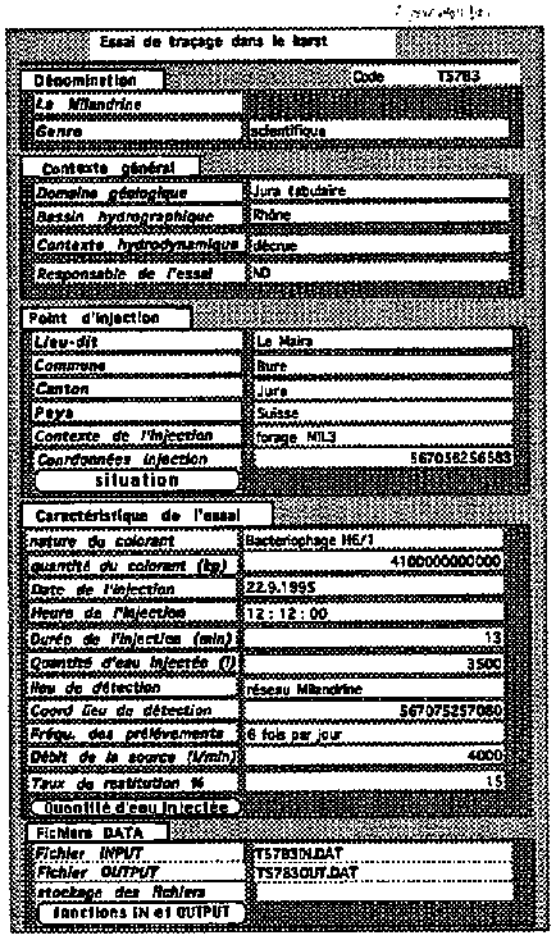
Essai de traçage dans le karst

Dénomination — Code: T57B3

Le Milandrine	
Genre	scientifique

Contexte général

Domaine géologique	Jura tabulaire
Bassin hydrographique	Rhône
Contexte hydrodynamique	décrue
Responsable de l'essai	ND

Point d'injection

Lieu-dit	Le Maira
Commune	Bure
Canton	Jura
Pays	Suisse
Contexte de l'injection	forage MIL3
Coordonnées injection	567056256583

situation

Caractéristique de l'essai

nature du colorant	Bacteriophage H6/1
quantité du colorant (kg)	4100000000000
Date de l'injection	22.9.1995
Heure de l'injection	12 : 12 : 00
Durée de l'injection (min)	13
Quantité d'eau injectée (l)	3500
lieu de détection	réseau Milandrine
Coord lieu de détection	567075257080
Fréqu. des prélèvements	6 fois par jour
Débit de la source (l/min)	4000
Taux de restitution %	15

Quantité d'eau injectée

Fichiers DATA

Fichier INPUT	T57B3IN.DAT
Fichier OUTPUT	T57B3OUT.DAT
stockage des fichiers	

fonctions IN et OUTPUT

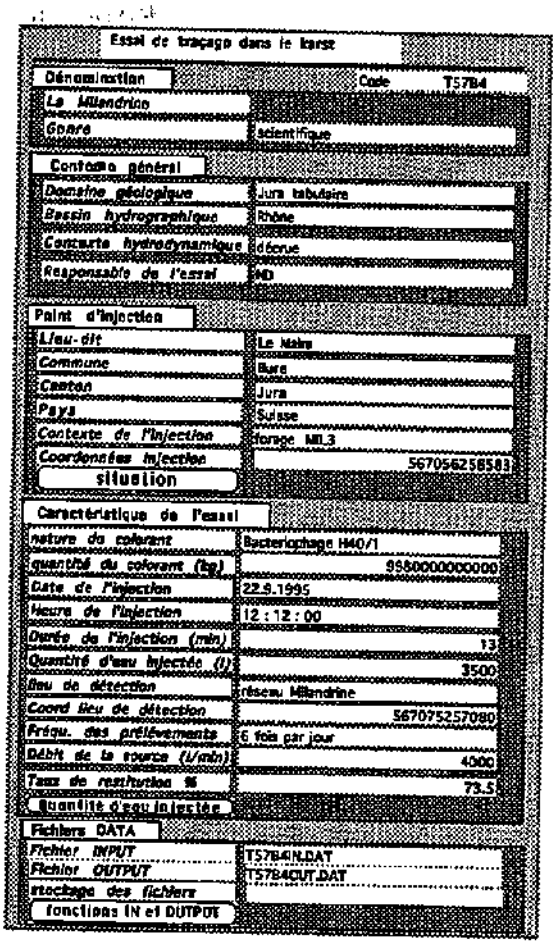
Essai de traçage dans le karst

Dénomination — Code: T57B4

Le Milandrine	
Genre	scientifique

Contexte général

Domaine géologique	Jura tabulaire
Bassin hydrographique	Rhône
Contexte hydrodynamique	décrue
Responsable de l'essai	ND

Point d'injection

Lieu-dit	Le Maira
Commune	Bure
Canton	Jura
Pays	Suisse
Contexte de l'injection	forage MIL3
Coordonnées injection	567056256583

situation

Caractéristique de l'essai

nature du colorant	Bacteriophage H40/1
quantité du colorant (kg)	9580000000000
Date de l'injection	22.9.1995
Heure de l'injection	12 : 12 : 00
Durée de l'injection (min)	13
Quantité d'eau injectée (l)	3500
lieu de détection	réseau Milandrine
Coord lieu de détection	567075257080
Fréqu. des prélèvements	6 fois par jour
Débit de la source (l/min)	4000
Taux de restitution %	73.5

Quantité d'eau injectée

Fichiers DATA

Fichier INPUT	T57B4IN.DAT
Fichier OUTPUT	T57B4OUT.DAT
stockage des fichiers	

fonctions IN et OUTPUT

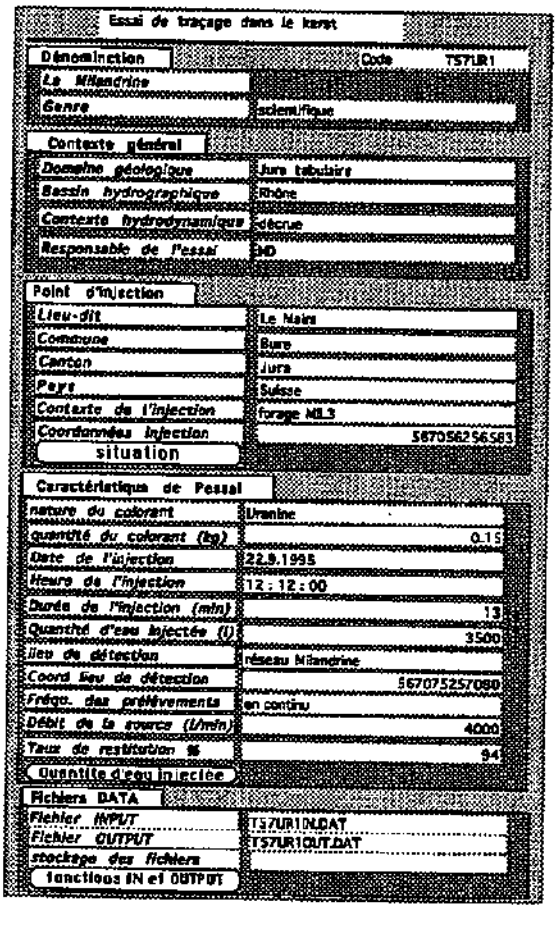
Essai de traçage dans le karst

Dénomination — Code: T57UR1

Le Milandrine	
Genre	scientifique

Contexte général

Domaine géologique	Jura tabulaire
Bassin hydrographique	Rhône
Contexte hydrodynamique	décrue
Responsable de l'essai	ND

Point d'injection

Lieu-dit	Le Maira
Commune	Bure
Canton	Jura
Pays	Suisse
Contexte de l'injection	forage MIL3
Coordonnées injection	567056256583

situation

Caractéristique de l'essai

nature du colorant	Uranine
quantité du colorant (kg)	0.15
Date de l'injection	22.9.1995
Heure de l'injection	12 : 12 : 00
Durée de l'injection (min)	13
Quantité d'eau injectée (l)	3500
lieu de détection	réseau Milandrine
Coord lieu de détection	567075257080
Fréqu. des prélèvements	en continu
Débit de la source (l/min)	4000
Taux de restitution %	94

Quantité d'eau injectée

Fichiers DATA

Fichier INPUT	T57UR1IN.DAT
Fichier OUTPUT	T57UR1OUT.DAT
stockage des fichiers	

fonctions IN et OUTPUT

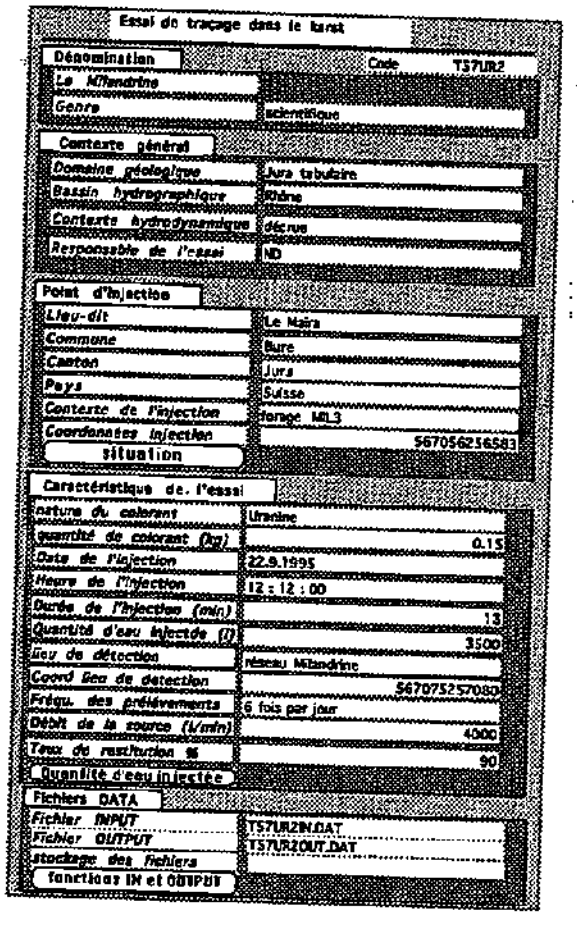
Essai de traçage dans le karst

Dénomination — Code: T57UR2

Le Milandrine	
Genre	scientifique

Contexte général

Domaine géologique	Jura tabulaire
Bassin hydrographique	Rhône
Contexte hydrodynamique	décrue
Responsable de l'essai	ND

Point d'injection

Lieu-dit	Le Maira
Commune	Bure
Canton	Jura
Pays	Suisse
Contexte de l'injection	forage MIL3
Coordonnées injection	567056256583

situation

Caractéristique de l'essai

nature du colorant	Uranine
quantité du colorant (kg)	0.15
Date de l'injection	22.9.1995
Heure de l'injection	12 : 12 : 00
Durée de l'injection (min)	13
Quantité d'eau injectée (l)	3500
lieu de détection	réseau Milandrine
Coord lieu de détection	567075257080
Fréqu. des prélèvements	6 fois par jour
Débit de la source (l/min)	4000
Taux de restitution %	90

Quantité d'eau injectée

Fichiers DATA

Fichier INPUT	T57UR2IN.DAT
Fichier OUTPUT	T57UR2OUT.DAT
stockage des fichiers	

fonctions IN et OUTPUT

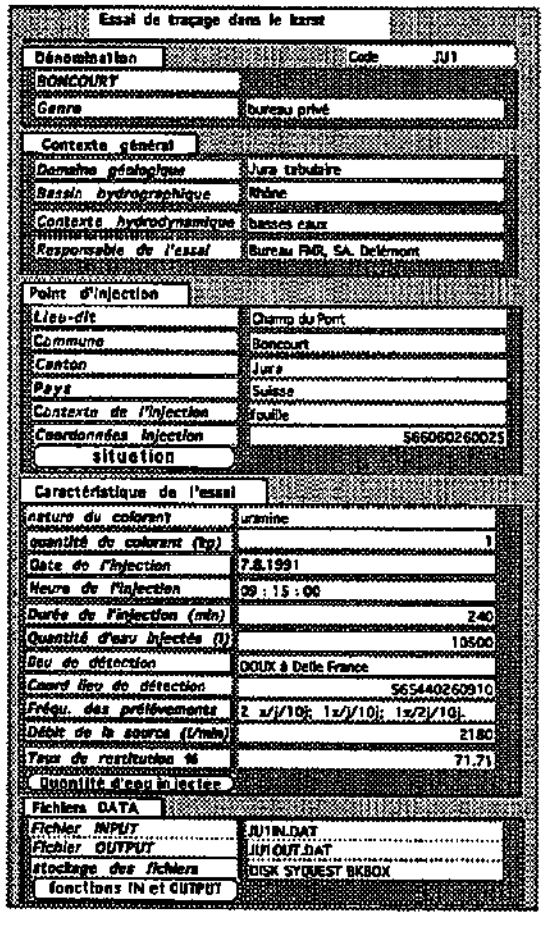
Essai de traçage dans le karst
Dénomination
Code JU1
BONCOURT
Genre
bureau privé
Contexte général
Domaine géologique
Jura tabulaire
Bassin hydrographique
Rhône
Contexte hydrodynamique
basses eaux
Responsable de l'essai
Bureau FMR, SA. Delémont
Point d'injection
Lieu-dit
Champ du Pont
Commune
Boncourt
Canton
Jura
Pays
Suisse
Contexte de l'injection
fouille
Coordonnées injection
566060260025
situation
Caractéristique de l'essai
nature du colorant
uranine
quantité du colorant (kg)
1
Date de l'injection
7.8.1991
Heure de l'injection
09 : 15 : 00
Durée de l'injection (min)
240
Quantité d'eau injectée (l)
10500
lieu de détection
DOUX à Delle France
Coord lieu de détection
565440260910
Fréqu. des prélèvements
2 x/j/10j; 1x/j/10j; 1x/2j/10j;
Débit de la source (l/min)
2180
Taux de restitution %
71.71
Quantité d'eau injectée
Fichiers DATA
Fichier INPUT
JU1IN.DAT
Fichier OUTPUT
JU1OUT.DAT
stockage des fichiers
DISK SYQUEST 88KBOX
fonctions IN et OUTPUT

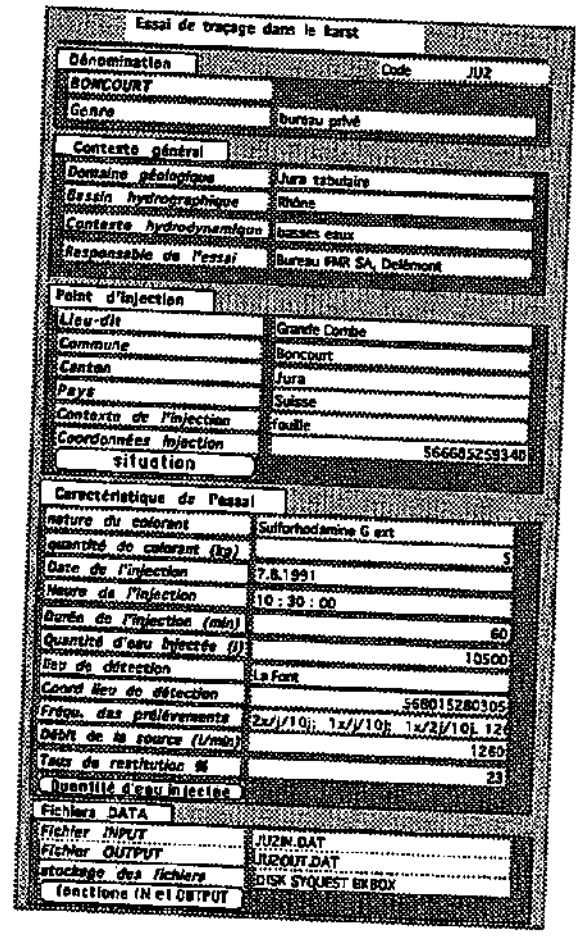
Essai de traçage dans le karst
Dénomination
Code JU2
BONCOURT
Genre
bureau privé
Contexte général
Domaine géologique
Jura tabulaire
Bassin hydrographique
Rhône
Contexte hydrodynamique
basses eaux
Responsable de l'essai
Bureau FMR SA, Delémont
Point d'injection
Lieu-dit
Grande Combe
Commune
Boncourt
Canton
Jura
Pays
Suisse
Contexte de l'injection
fouille
Coordonnées injection
566685259348
situation
Caractéristique de l'essai
nature du colorant
Sulforhodamine G ext
quantité de colorant (kg)
5
Date de l'injection
7.8.1991
Heure de l'injection
10 : 30 : 00
Durée de l'injection (min)
60
Quantité d'eau injectée (l)
10500
lieu de détection
Le Font
Coord lieu de détection
568015280305
Fréqu. des prélèvements
2x/j/10j; 1x/j/10j; 1x/2j/10j; 12
Débit de la source (l/min)
1260
Taux de restitution %
23
Quantité d'eau injectée
Fichiers DATA
Fichier INPUT
JU2IN.DAT
Fichier OUTPUT
JU2OUT.DAT
stockage des fichiers
DISK SYQUEST 88KBOX
fonctions IN et OUTPUT

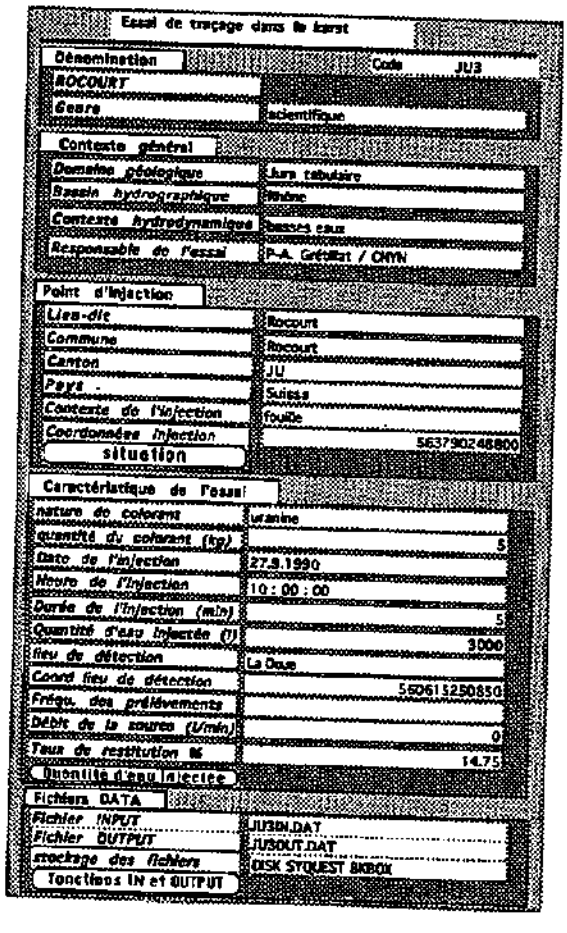
Essai de traçage dans le karst
Dénomination
Code JU3
ROCOURT
Genre
scientifique
Contexte général
Domaine géologique
Jura tabulaire
Bassin hydrographique
Rhône
Contexte hydrodynamique
basses eaux
Responsable de l'essai
P-A. Grétillat / CMYN
Point d'injection
Lieu-dit
Rocourt
Commune
Rocourt
Canton
JU
Pays
Suisse
Contexte de l'injection
fouille
Coordonnées injection
563790248800
situation
Caractéristique de l'essai
nature de colorant
uranine
quantité du colorant (kg)
5
Date de l'injection
27.9.1990
Heure de l'injection
10 : 00 : 00
Durée de l'injection (min)
5
Quantité d'eau injectée (l)
3000
lieu de détection
La Doue
Coord lieu de détection
560615250850
Fréqu. des prélèvements
Débit de la source (l/min)
0
Taux de restitution %
14.75
Quantité d'eau injectée
Fichiers DATA
Fichier INPUT
JU3IN.DAT
Fichier OUTPUT
JU3OUT.DAT
stockage des fichiers
DISK SYQUEST 88KBOX
fonctions IN et OUTPUT

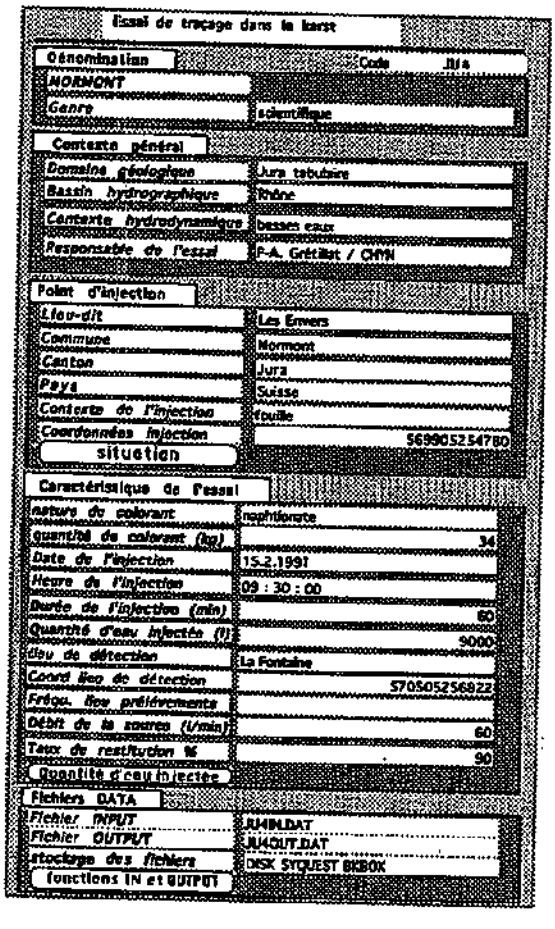
Essai de traçage dans le karst
Dénomination
Code JU4
MORMONT
Genre
scientifique
Contexte général
Domaine géologique
Jura tabulaire
Bassin hydrographique
Rhône
Contexte hydrodynamique
basses eaux
Responsable de l'essai
P-A. Grétillat / CMYN
Point d'injection
Lieu-dit
Les Emers
Commune
Mormont
Canton
Jura
Pays
Suisse
Contexte de l'injection
fouille
Coordonnées injection
569905254780
situation
Caractéristique de l'essai
nature du colorant
naphtionate
quantité du colorant (kg)
34
Date de l'injection
15.2.1991
Heure de l'injection
09 : 30 : 00
Durée de l'injection (min)
60
Quantité d'eau injectée (l)
9000
lieu de détection
La Fontaine
Coord lieu de détection
570505256922
Fréqu. des prélèvements
Débit de la source (l/min)
60
Taux de restitution %
90
Quantité d'eau injectée
Fichiers DATA
Fichier INPUT
JU4IN.DAT
Fichier OUTPUT
JU4OUT.DAT
stockage des fichiers
DISK SYQUEST 88KBOX
fonctions IN et OUTPUT

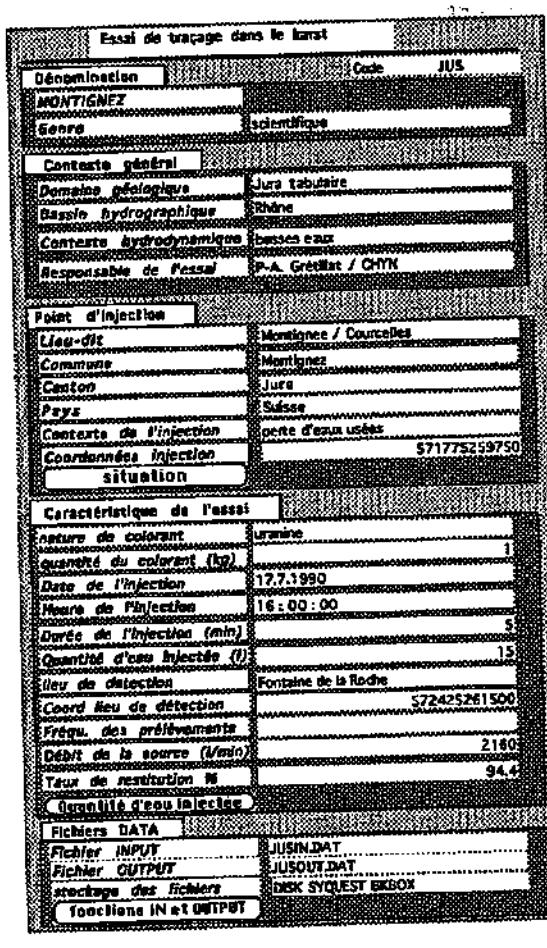

Essai de traçage dans le karst

Dénomination — Code: JUS

MONTIGNEZ

Genre: scientifique

Contexte général

Domaine géologique	Jura tabulaire
Bassin hydrographique	Rhône
Contexte hydrodynamique	basses eaux
Responsable de l'essai	P-A. Grétillat / CHYN

Point d'injection

Lieu-dit	Montignez / Courcelles
Commune	Montignez
Canton	Jura
Pays	Suisse
Contexte de l'injection	perte d'eaux usées
Coordonnées injection	571775259750

situation

Caractéristique de l'essai

nature du colorant	uranine
quantité du colorant (kg)	1
Date de l'injection	17.7.1990
Heure de l'injection	16 : 00 : 00
Durée de l'injection (min)	5
Quantité d'eau injectée (l)	15
lieu de détection	Fontaine de la Roche
Coord lieu de détection	572425261500
Fréqu. des prélèvements	
Débit de la source (l/min)	2160
Taux de restitution %	94.4

Quantité d'eau injectée

Fichiers DATA

Fichier INPUT	JUSIN.DAT
Fichier OUTPUT	JUSOUT.DAT
stockage des fichiers	DISK SYQUEST 88BOX

fonctions IN et OUTPUT

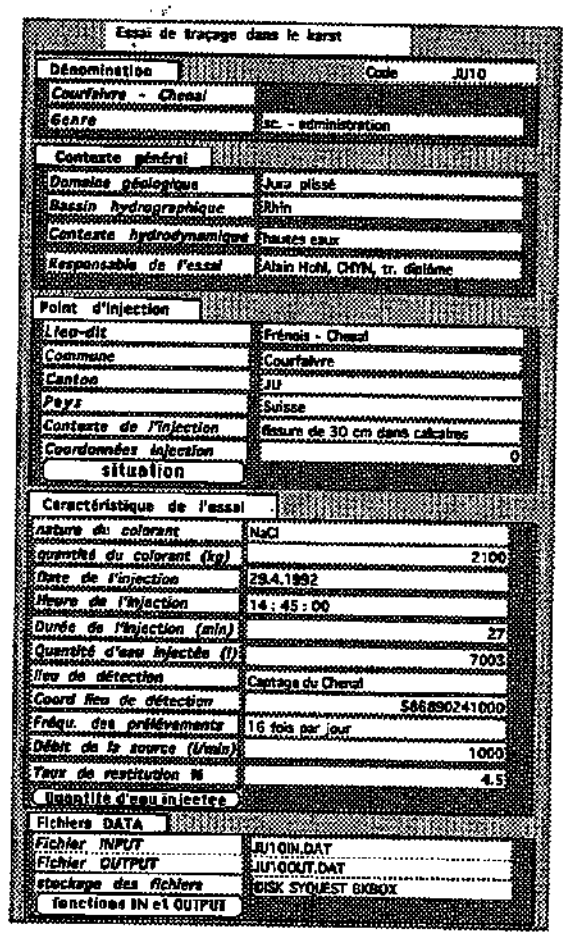

Essai de traçage dans le karst

Dénomination — Code: JU10

Courfaivre - Chenal

Genre: sc. - administration

Contexte général

Domaine géologique	Jura plissé
Bassin hydrographique	Rhin
Contexte hydrodynamique	hautes eaux
Responsable de l'essai	Alain Hohl, CHYN, tr. diplôme

Point d'injection

Lieu-dit	Frênois - Chenal
Commune	Courfaivre
Canton	JU
Pays	Suisse
Contexte de l'injection	fissure de 30 cm dans calcaires
Coordonnées injection	0

situation

Caractéristique de l'essai

nature du colorant	NaCl
quantité du colorant (kg)	2100
Date de l'injection	29.4.1992
Heure de l'injection	14 : 45 : 00
Durée de l'injection (min)	27
Quantité d'eau injectée (l)	7003
lieu de détection	Captage du Chenal
Coord lieu de détection	586890241000
Fréqu. des prélèvements	16 fois par jour
Débit de la source (l/min)	1000
Taux de restitution %	4.5

Quantité d'eau injectée

Fichiers DATA

Fichier INPUT	JU10IN.DAT
Fichier OUTPUT	JU10OUT.DAT
stockage des fichiers	DISK SYQUEST 88BOX

fonctions IN et OUTPUT

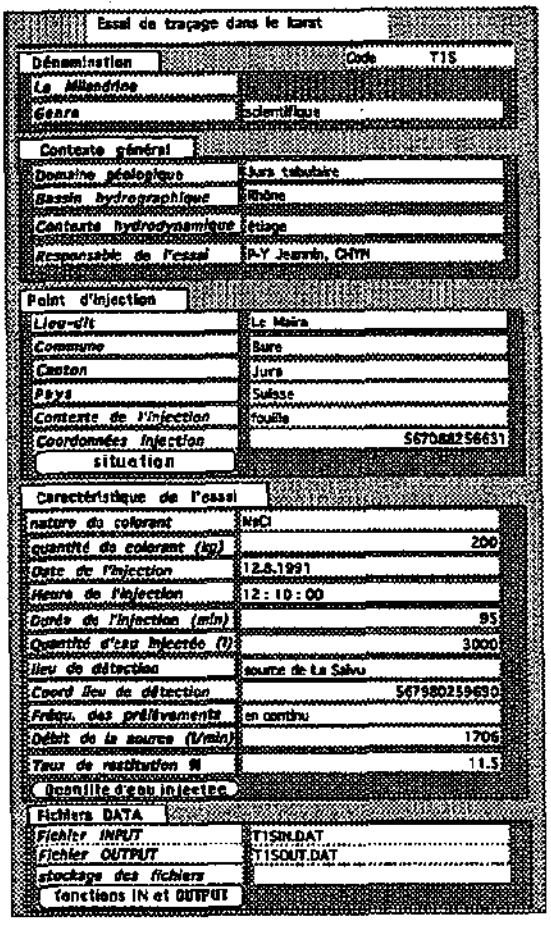
Essai de traçage dans le karst
Dénomination
Code T1S
Le Milandrine
Genre scientifique
Contexte général
Domaine géologique Jura tabulaire
Bassin hydrographique Rhône
Contexte hydrodynamique étiage
Responsable de l'essai P-Y Jeannin, CHYN
Point d'injection
Lieu-dit Le Maira
Commune Bure
Canton Jura
Pays Suisse
Contexte de l'injection fouille
Coordonnées injection 567088256631
situation
Caractéristique de l'essai
nature du colorant NaCl
quantité du colorant (kg) 200
Date de l'injection 12.8.1991
Heure de l'injection 12 : 10 : 00
Durée de l'injection (min) 95
Quantité d'eau injectée (l) 3000
lieu de détection source de la Saivu
Coord lieu de détection 567980259690
Fréqu. des prélèvements en continu
Débit de la source (l/min) 1706
Taux de restitution % 11.5
Quantité d'eau injectée
Fichiers DATA
Fichier INPUT T1SIN.DAT
Fichier OUTPUT T1SOUT.DAT
stockage des fichiers
fonctions IN et OUTPUT

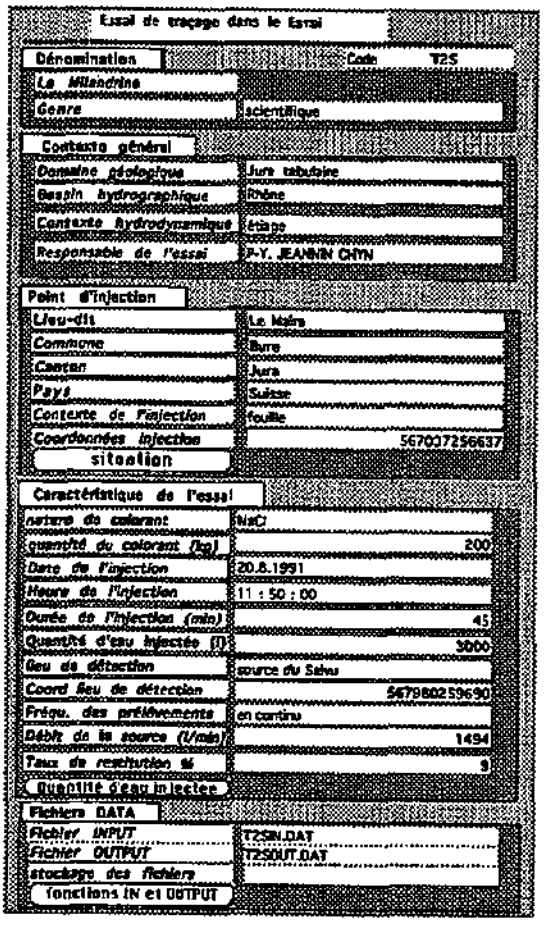
Essai de traçage dans le karst
Dénomination
Code T2S
Le Milandrine
Genre scientifique
Contexte général
Domaine géologique Jura tabulaire
Bassin hydrographique Rhône
Contexte hydrodynamique étiage
Responsable de l'essai P-Y. JEANNIN CHYN
Point d'injection
Lieu-dit Le Maira
Commune Bure
Canton Jura
Pays Suisse
Contexte de l'injection fouille
Coordonnées injection 5670072256637
situation
Caractéristique de l'essai
nature du colorant NaCl
quantité du colorant (kg) 200
Date de l'injection 20.8.1991
Heure de l'injection 11 : 50 : 00
Durée de l'injection (min) 45
Quantité d'eau injectée (l) 3000
lieu de détection source du Saivu
Coord lieu de détection 567980259690
Fréqu. des prélèvements en continu
Débit de la source (l/min) 1494
Taux de restitution % 9
Quantité d'eau injectée
Fichiers DATA
Fichier INPUT T2SIN.DAT
Fichier OUTPUT T2SOUT.DAT
stockage des fichiers
fonctions IN et OUTPUT

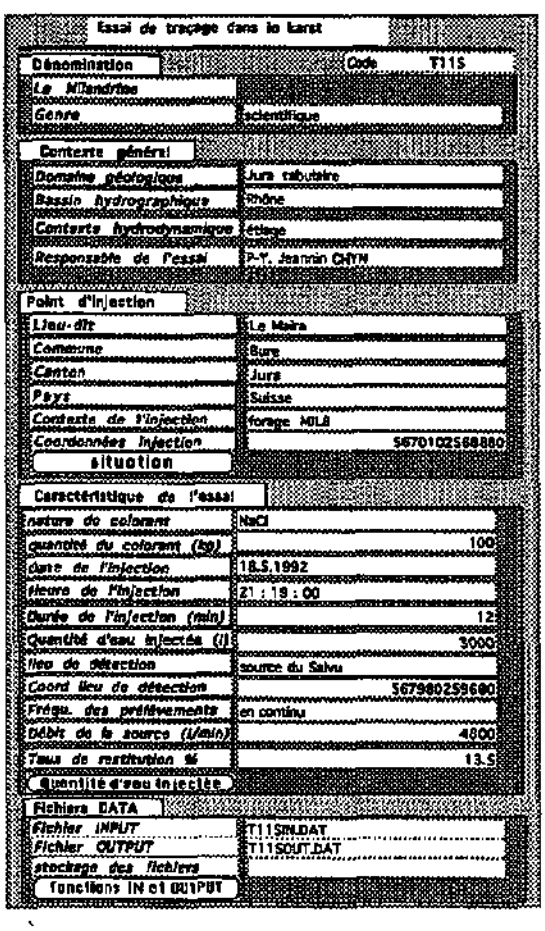
Essai de traçage dans le karst
Dénomination
Code T11S
Le Milandrine
Genre scientifique
Contexte général
Domaine géologique Jura tabulaire
Bassin hydrographique Rhône
Contexte hydrodynamique étiage
Responsable de l'essai P-Y. Jeannin CHYN
Point d'injection
Lieu-dit Le Maira
Commune Bure
Canton Jura
Pays Suisse
Contexte de l'injection forage MIL8
Coordonnées injection 567010256880
situation
Caractéristique de l'essai
nature du colorant NaCl
quantité du colorant (kg) 100
Date de l'injection 18.5.1992
Heure de l'injection 21 : 19 : 00
Durée de l'injection (min) 12
Quantité d'eau injectée (l) 3000
lieu de détection source du Saivu
Coord lieu de détection 567980259690
Fréqu. des prélèvements en continu
Débit de la source (l/min) 4800
Taux de restitution % 13.5
Quantité d'eau injectée
Fichiers DATA
Fichier INPUT T11SIN.DAT
Fichier OUTPUT T11SOUT.DAT
stockage des fichiers
fonctions IN et OUTPUT

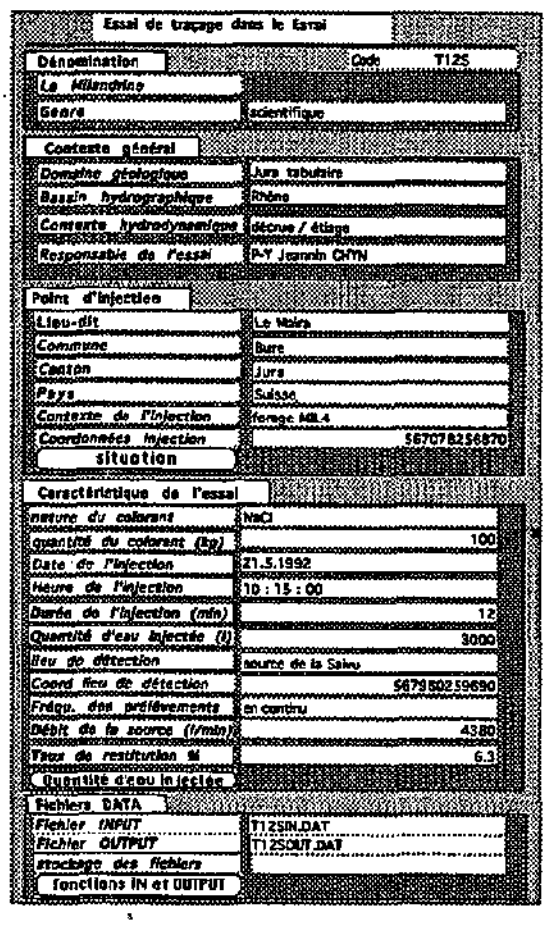
Essai de traçage dans le karst
Dénomination
Code T12S
Le Milandrine
Genre scientifique
Contexte général
Domaine géologique Jura tabulaire
Bassin hydrographique Rhône
Contexte hydrodynamique décrue / étiage
Responsable de l'essai P-Y Jeannin CHYN
Point d'injection
Lieu-dit Le Maira
Commune Bure
Canton Jura
Pays Suisse
Contexte de l'injection forage MIL4
Coordonnées injection 567078256870
situation
Caractéristique de l'essai
nature du colorant NaCl
quantité du colorant (kg) 100
Date de l'injection 21.5.1992
Heure de l'injection 10 : 15 : 00
Durée de l'injection (min) 12
Quantité d'eau injectée (l) 3000
lieu de détection source de la Saivu
Coord lieu de détection 567980259690
Fréqu. des prélèvements en continu
Débit de la source (l/min) 4380
Taux de restitution % 6.3
Quantité d'eau injectée
Fichiers DATA
Fichier INPUT T12SIN.DAT
Fichier OUTPUT T12SOUT.DAT
stockage des fichiers
fonctions IN et OUTPUT

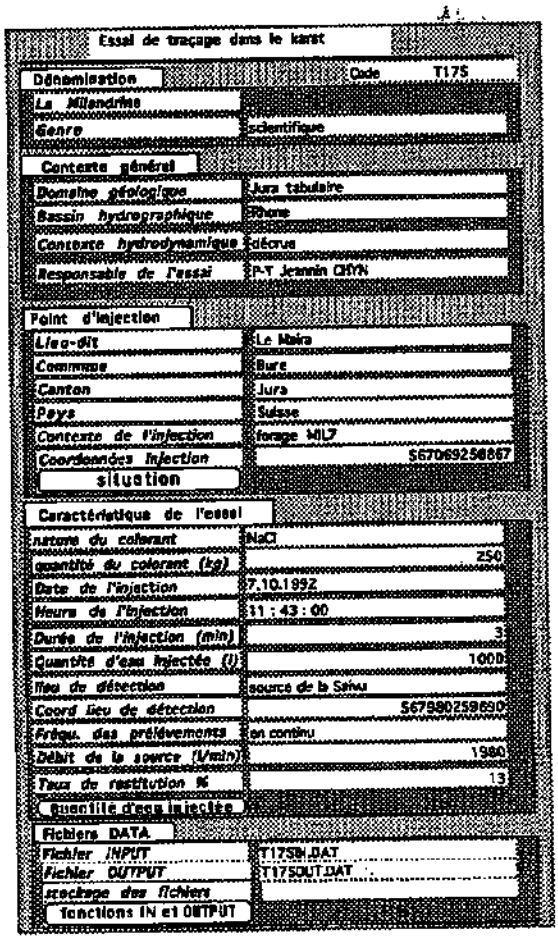
Essai de traçage dans le karst
Dénomination
Code T17S
La Milandrine
Genre scientifique
Contexte général
Domaine géologique Jura tabulaire
Bassin hydrographique Rhône
Contexte hydrodynamique décrue
Responsable de l'essai P-Y Jeannin CHYN
Point d'injection
Lieu-dit Le Maira
Commune Bure
Canton Jura
Pays Suisse
Contexte de l'injection forage MIL7
Coordonnées injection 567069256867
situation
Caractéristique de l'essai
nature du colorant NaCl
quantité du colorant (kg) 250
Date de l'injection 7.10.1992
Heure de l'injection 11 : 43 : 00
Durée de l'injection (min) 3
Quantité d'eau injectée (l) 1000
lieu de détection source de la Saivu
Coord lieu de détection 567980259690
Fréqu. des prélèvements en continu
Débit de la source (l/min) 1980
Taux de restitution % 13
Quantité d'eau injectée
Fichiers DATA
Fichier INPUT T17SIN.DAT
Fichier OUTPUT T17SOUT.DAT
stockage des fichiers
fonctions IN et OUTPUT

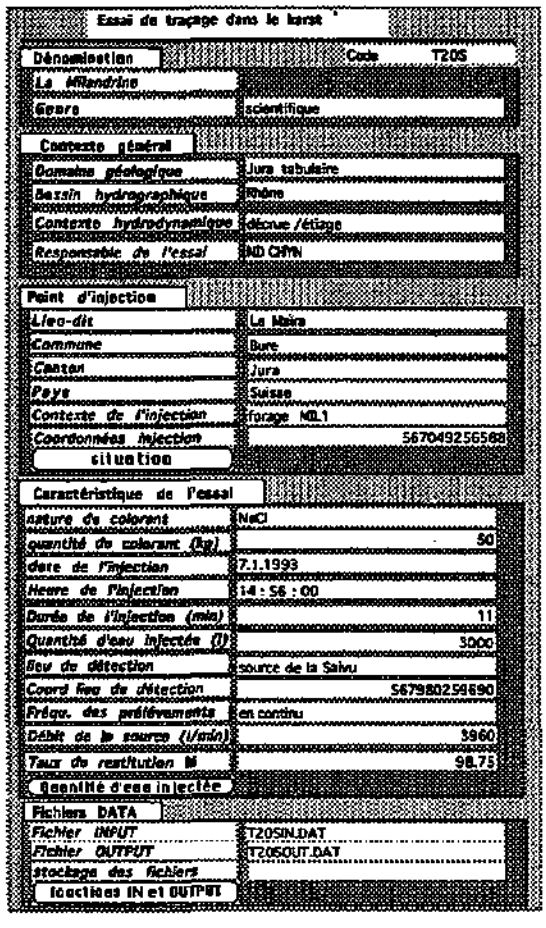
Essai de traçage dans le karst
Dénomination
Code T20S
La Milandrine
Genre scientifique
Contexte général
Domaine géologique Jura tabulaire
Bassin hydrographique Rhône
Contexte hydrodynamique décrue /étiage
Responsable de l'essai ND CHYN
Point d'injection
Lieu-dit La Maira
Commune Bure
Canton Jura
Pays Suisse
Contexte de l'injection forage MIL1
Coordonnées injection 567049256569
situation
Caractéristique de l'essai
nature du colorant NaCl
quantité du colorant (kg) 50
date de l'injection 7.1.1993
Heure de l'injection 14 : 56 : 00
Durée de l'injection (min) 11
Quantité d'eau injectée (l) 3000
lieu de détection source de la Saivu
Coord lieu de détection 567980259690
Fréqu. des prélèvements en continu
Débit de la source (l/min) 3960
Taux de restitution % 98.75
Quantité d'eau injectée
Fichiers DATA
Fichier INPUT T20SIN.DAT
Fichier OUTPUT T20SOUT.DAT
stockage des fichiers
fonctions IN et OUTPUT

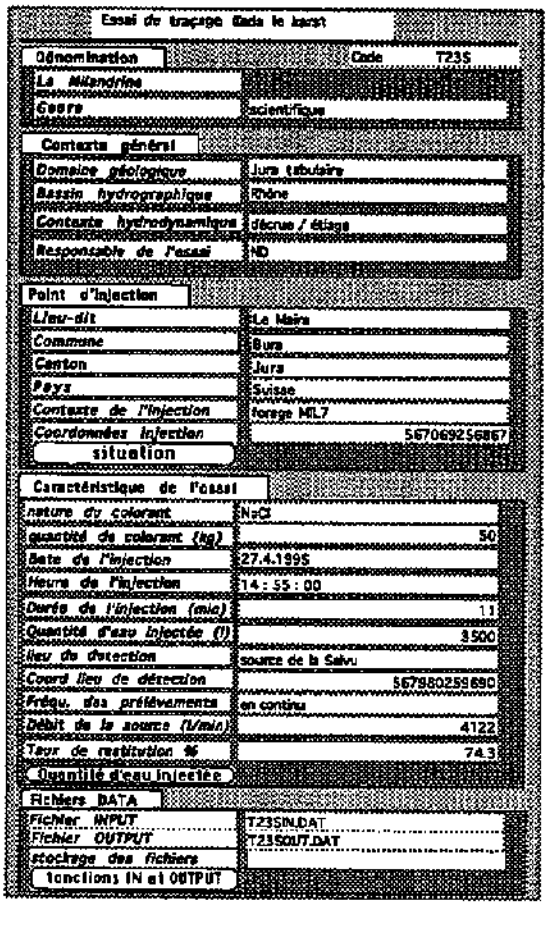
Essai de traçage dans le karst
Dénomination
Code T23S
La Milandrine
Genre scientifique
Contexte général
Domaine géologique Jura tabulaire
Bassin hydrographique Rhône
Contexte hydrodynamique décrue / étiage
Responsable de l'essai ND
Point d'injection
Lieu-dit Le Maira
Commune Bure
Canton Jura
Pays Suisse
Contexte de l'injection forage MIL7
Coordonnées injection 567069256867
situation
Caractéristique de l'essai
nature du colorant NaCl
quantité de colorant (kg) 50
Date de l'injection 27.4.1995
Heure de l'injection 14 : 55 : 00
Durée de l'injection (min) 11
Quantité d'eau injectée (l) 3500
lieu de détection source de la Saivu
Coord lieu de détection 567980259690
Fréqu. des prélèvements en continu
Débit de la source (l/min) 4122
Taux de restitution % 74.3
Quantité d'eau injectée
Fichiers DATA
Fichier INPUT T23SIN.DAT
Fichier OUTPUT T23SOUT.DAT
stockage des fichiers
fonctions IN et OUTPUT

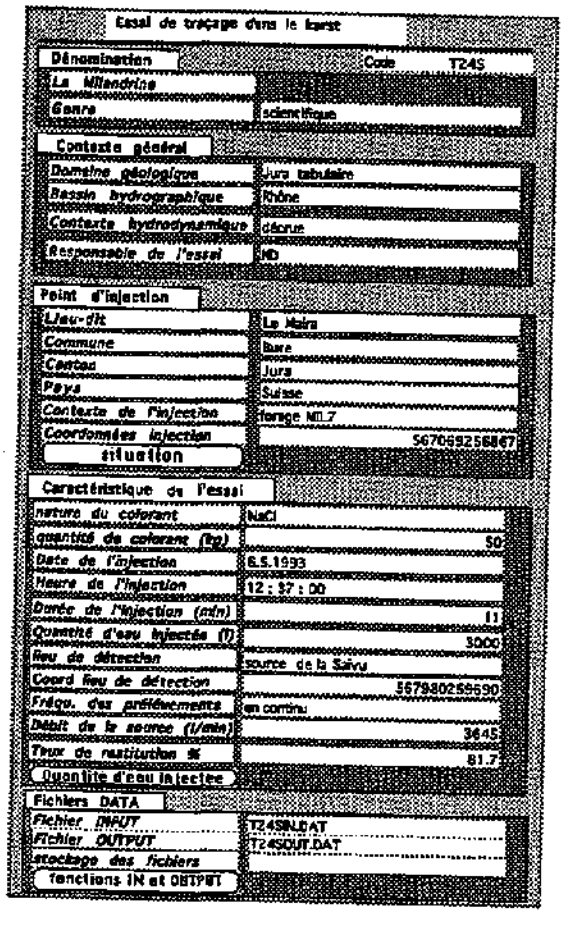
Essai de traçage dans le karst
Dénomination
Code T24S
La Milandrine
Genre scientifique
Contexte général
Domaine géologique Jura tabulaire
Bassin hydrographique Rhône
Contexte hydrodynamique décrue
Responsable de l'essai ND
Point d'injection
Lieu-dit Le Maira
Commune Bure
Canton Jura
Pays Suisse
Contexte de l'injection forage MIL7
Coordonnées injection 567069256867
situation
Caractéristique de l'essai
nature du colorant NaCl
quantité de colorant (kg) 50
Date de l'injection 6.5.1993
Heure de l'injection 12 : 37 : 00
Durée de l'injection (min) 11
Quantité d'eau injectée (l) 3000
lieu de détection source de la Saivu
Coord lieu de détection 567980259690
Fréqu. des prélèvements en continu
Débit de la source (l/min) 3645
Taux de restitution % 81.7
Quantité d'eau injectée
Fichiers DATA
Fichier INPUT T24SIN.DAT
Fichier OUTPUT T24SOUT.DAT
stockage des fichiers
fonctions IN et OUTPUT

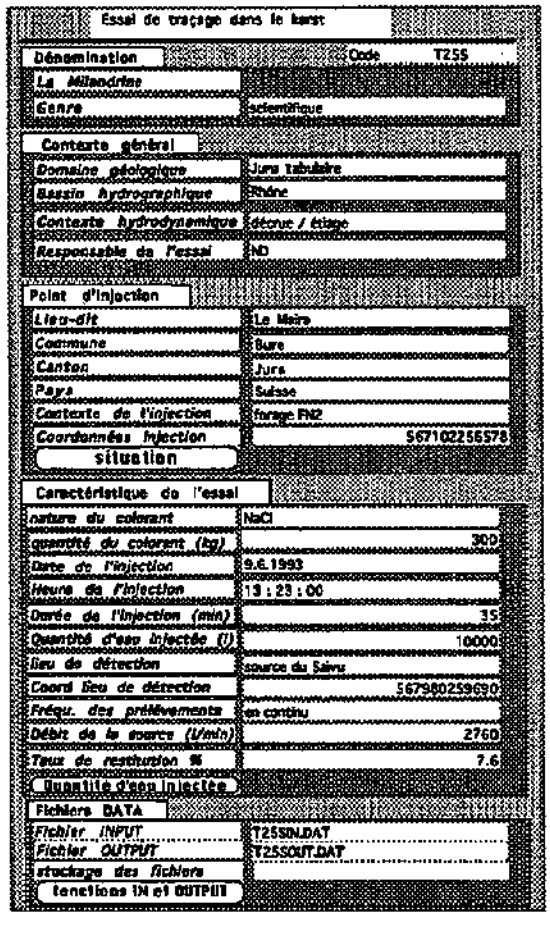
Essai de traçage dans le karst
Dénomination
Code T25S
La Milandrine
Genre scientifique
Contexte général
Domaine géologique Jura tabulaire
Bassin hydrographique Rhône
Contexte hydrodynamique décrue / étiage
Responsable de l'essai ND
Point d'injection
Lieu-dit Le Maira
Commune Bure
Canton Jura
Pays Suisse
Contexte de l'injection forage FN2
Coordonnées injection 567102256578
situation
Caractéristique de l'essai
nature du colorant NaCl
quantité du colorant (kg) 300
Date de l'injection 9.6.1993
Heure de l'injection 13 : 23 : 00
Durée de l'injection (min) 35
Quantité d'eau injectée (l) 10000
lieu de détection source du Saivu
Coord lieu de détection 567980259690
Fréqu. des prélèvements en continu
Débit de la source (l/min) 2760
Taux de restitution % 7.6
Quantité d'eau injectée
Fichiers DATA
Fichier INPUT T25SIN.DAT
Fichier OUTPUT T25SOUT.DAT
stockage des fichiers
fonctions IN et OUTPUT

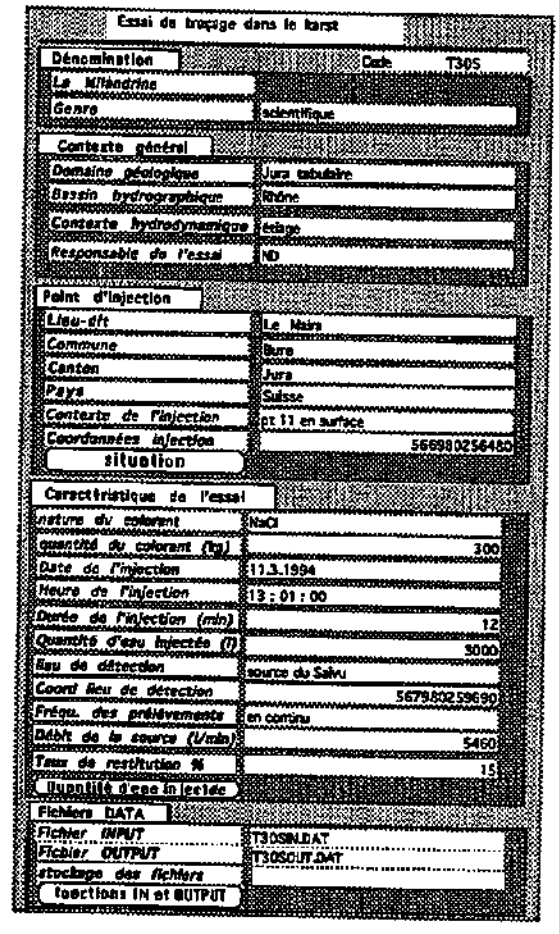
Essai de traçage dans le karst
Dénomination
Code T30S
La Milandrine
Genre scientifique
Contexte général
Domaine géologique Jura tabulaire
Bassin hydrographique Rhône
Contexte hydrodynamique étiage
Responsable de l'essai ND
Point d'injection
Lieu-dit Le Maira
Commune Bure
Canton Jura
Pays Suisse
Contexte de l'injection pt 11 en surface
Coordonnées injection 566980256480
situation
Caractéristique de l'essai
nature du colorant NaCl
quantité du colorant (kg) 300
Date de l'injection 17.3.1994
Heure de l'injection 13 : 01 : 00
Durée de l'injection (min) 12
Quantité d'eau injectée (l) 5000
lieu de détection source du Saivu
Coord lieu de détection 567980259690
Fréqu. des prélèvements en continu
Débit de la source (l/min) 5460
Taux de restitution % 15
Quantité d'eau injectée
Fichiers DATA
Fichier INPUT T30SIN.DAT
Fichier OUTPUT T30SOUT.DAT
stockage des fichiers
fonctions IN et OUTPUT

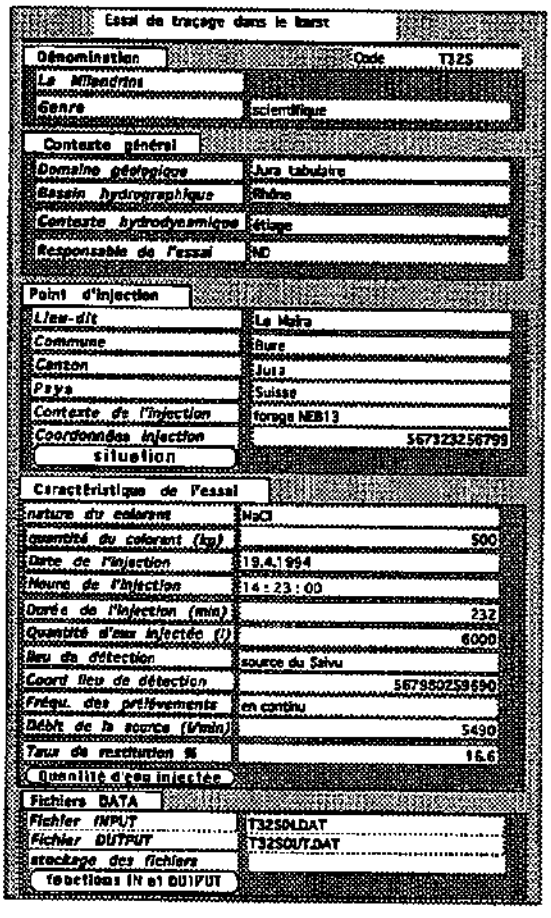
Essai de traçage dans le karst
Dénomination
Code T32S
La Milandrine
Genre scientifique
Contexte général
Domaine géologique Jura tabulaire
Bassin hydrographique Rhône
Contexte hydrodynamique étiage
Responsable de l'essai ND
Point d'injection
Lieu-dit Le Maira
Commune Bure
Canton Jura
Pays Suisse
Contexte de l'injection forage NEB13
Coordonnées injection 567323256799
situation
Caractéristique de l'essai
nature du colorant NaCl
quantité du colorant (kg) 500
Date de l'injection 19.4.1994
Heure de l'injection 14 : 23 : 00
Durée de l'injection (min) 232
Quantité d'eau injectée (l) 6000
lieu de détection source du Saivu
Coord lieu de détection 567980259690
Fréqu. des prélèvements en continu
Débit de la source (l/min) 5490
Taux de restitution % 16.6
Quantité d'eau injectée
Fichiers DATA
Fichier INPUT T32SIN.DAT
Fichier OUTPUT T32SOUT.DAT
stockage des fichiers
fonctions IN et OUTPUT

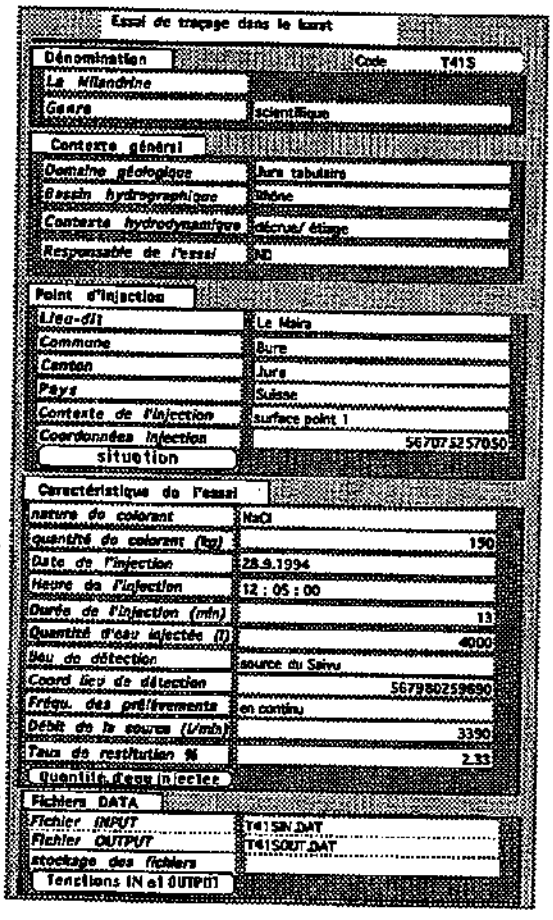
Essai de traçage dans le karst
Dénomination
Code T41S
La Milandrine
Genre scientifique
Contexte général
Domaine géologique Jura tabulaire
Bassin hydrographique Rhône
Contexte hydrodynamique décrue/ étiage
Responsable de l'essai ND
Point d'injection
Lieu-dit Le Maira
Commune Bure
Canton Jura
Pays Suisse
Contexte de l'injection surface point 1
Coordonnées injection 567075257050
situation
Caractéristique de l'essai
nature du colorant NaCl
quantité du colorant (kg) 150
Date de l'injection 28.9.1994
Heure de l'injection 12 : 05 : 00
Durée de l'injection (min) 13
Quantité d'eau injectée (l) 4000
lieu de détection source du Saivu
Coord lieu de détection 567980259690
Fréqu. des prélèvements en continu
Débit de la source (l/min) 3390
Taux de restitution % 2.33
Quantité d'eau injectée
Fichiers DATA
Fichier INPUT T41SIN.DAT
Fichier OUTPUT T41SOUT.DAT
stockage des fichiers
fonctions IN et OUTPUT

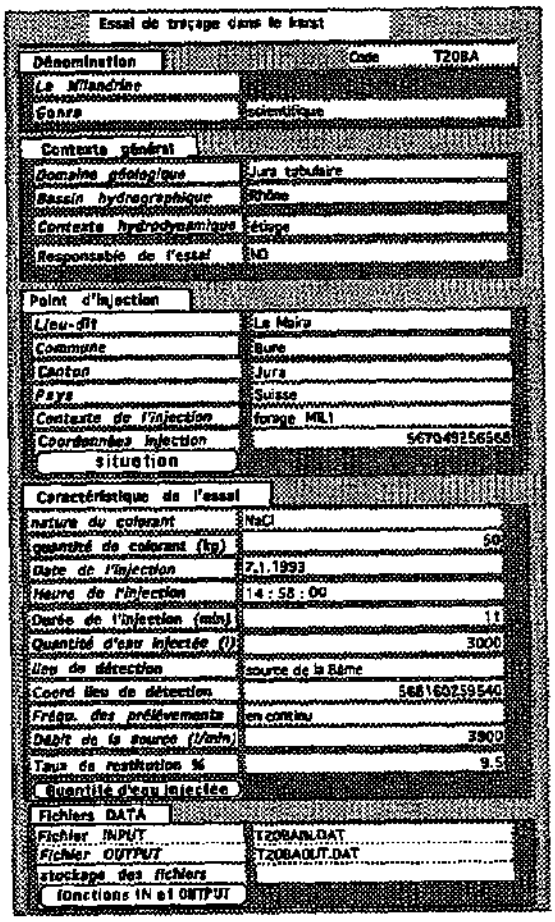

Essai de traçage dans le karst

Dénomination — Code T20BA

Le Milandrine	
Genre	scientifique

Contexte général

Domaine géologique	Jura tabulaire
Bassin hydrographique	Rhône
Contexte hydrodynamique	étiage
Responsable de l'essai	ND

Point d'injection

Lieu-dit	Le Maira
Commune	Bure
Canton	Jura
Pays	Suisse
Contexte de l'injection	forage MIL1
Coordonnées injection	567049256565

situation

Caractéristique de l'essai

nature du colorant	NaCl
quantité de colorant (kg)	50
Date de l'injection	7.1.1993
Heure de l'injection	14 : 58 : 00
Durée de l'injection (min)	11
Quantité d'eau injectée (l)	3000
lieu de détection	source de la Bâme
Coord lieu de détection	568160259540
Fréqu. des prélèvements	en continu
Débit de la source (l/min)	3900
Taux de restitution %	9.5

Quantité d'eau injectée

Fichiers DATA

Fichier INPUT	T20BAIN.DAT
Fichier OUTPUT	T20BAOUT.DAT
stockage des fichiers	

fonctions IN et OUTPUT

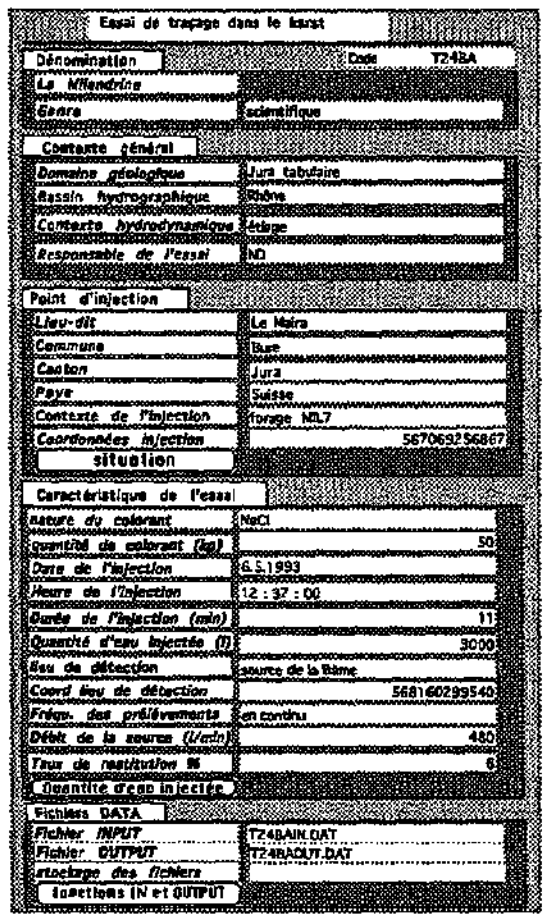

Essai de traçage dans le karst

Dénomination — Code T24BA

La Milandrine	
Genre	scientifique

Contexte général

Domaine géologique	Jura tabulaire
Bassin hydrographique	Rhône
Contexte hydrodynamique	étiage
Responsable de l'essai	ND

Point d'injection

Lieu-dit	Le Maira
Commune	Bure
Canton	Jura
Pays	Suisse
Contexte de l'injection	forage MIL7
Coordonnées injection	567069256867

situation

Caractéristique de l'essai

nature du colorant	NaCl
Quantité de colorant (kg)	50
Date de l'injection	6.5.1993
Heure de l'injection	12 : 37 : 00
Durée de l'injection (min)	11
Quantité d'eau injectée (l)	3000
lieu de détection	source de la Bâme
Coord lieu de détection	568160299540
Fréqu. des prélèvements	en continu
Débit de la source (l/min)	480
Taux de restitution %	6

Quantité d'eau injectée

Fichiers DATA

Fichier INPUT	T24BAIN.DAT
Fichier OUTPUT	T24BAOUT.DAT
stockage des fichiers	

fonctions IN et OUTPUT

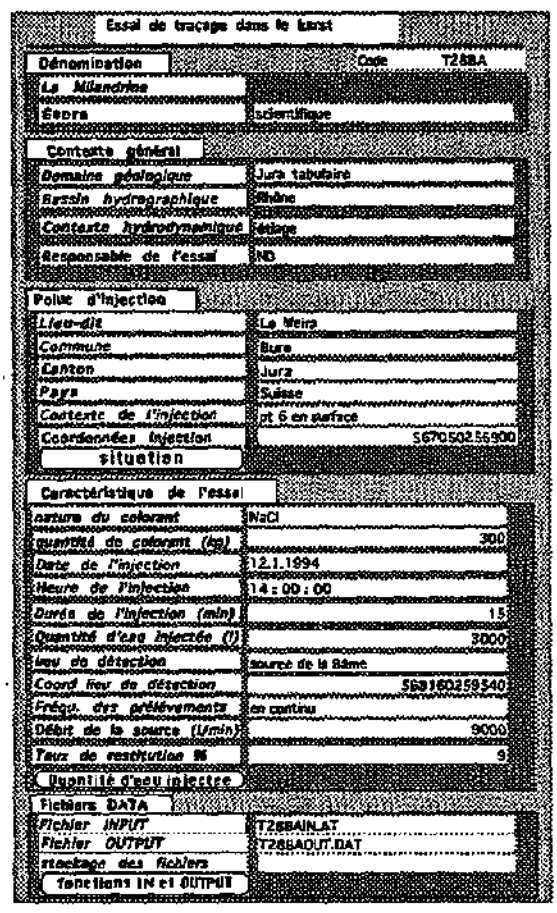

Essai de traçage dans le karst

Dénomination — Code T28BA

La Milandrine	
Genre	scientifique

Contexte général

Domaine géologique	Jura tabulaire
Bassin hydrographique	Rhône
Contexte hydrodynamique	étiage
Responsable de l'essai	ND

Point d'injection

Lieu-dit	Le Maira
Commune	Bure
Canton	Jura
Pays	Suisse
Contexte de l'injection	pt 6 en surface
Coordonnées injection	567050256900

situation

Caractéristique de l'essai

nature du colorant	NaCl
quantité de colorant (kg)	300
Date de l'injection	12.1.1994
Heure de l'injection	14 : 00 : 00
Durée de l'injection (min)	15
Quantité d'eau injectée (l)	3000
lieu de détection	source de la Bâme
Coord lieu de détection	568160259540
Fréqu. des prélèvements	en continu
Débit de la source (l/min)	9000
Taux de restitution %	9

Quantité d'eau injectée

Fichiers DATA

Fichier INPUT	T28BAIN.AT
Fichier OUTPUT	T28BAOUT.DAT
stockage des fichiers	

fonctions IN et OUTPUT

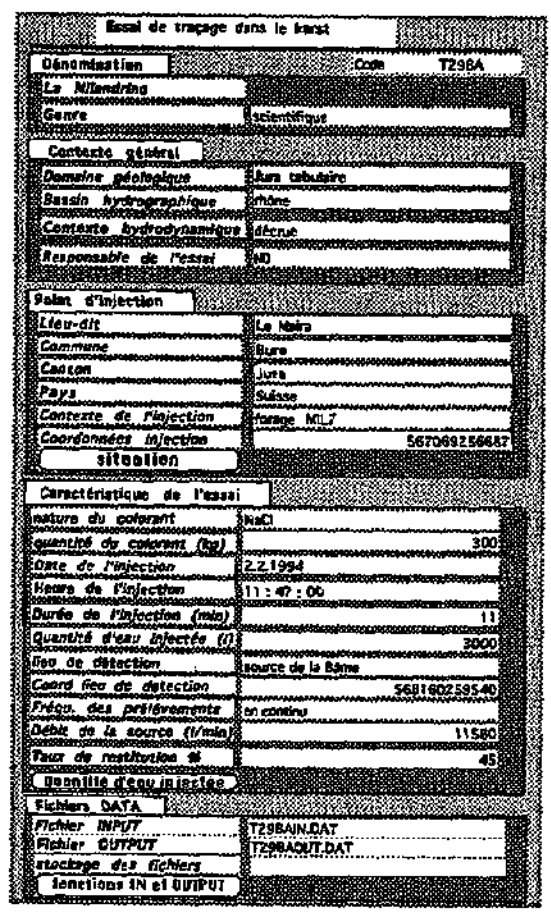

Essai de traçage dans le karst

Dénomination — Code T29BA

La Milandrine	
Genre	scientifique

Contexte général

Domaine géologique	Jura tabulaire
Bassin hydrographique	rhône
Contexte hydrodynamique	décrue
Responsable de l'essai	ND

Point d'injection

Lieu-dit	Le Maira
Commune	Bure
Canton	Jura
Pays	Suisse
Contexte de l'injection	forage MIL7
Coordonnées injection	567069256867

situation

Caractéristique de l'essai

nature du colorant	NaCl
quantité de colorant (kg)	300
Date de l'injection	2.2.1994
Heure de l'injection	11 : 47 : 00
Durée de l'injection (min)	11
Quantité d'eau injectée (l)	3000
lieu de détection	source de la Bâme
Coord lieu de détection	568160259540
Fréqu. des prélèvements	en continu
Débit de la source (l/min)	11580
Taux de restitution %	45

Quantité d'eau injectée

Fichiers DATA

Fichier INPUT	T29BAIN.DAT
Fichier OUTPUT	T29BAOUT.DAT
stockage des fichiers	

fonctions IN et OUTPUT

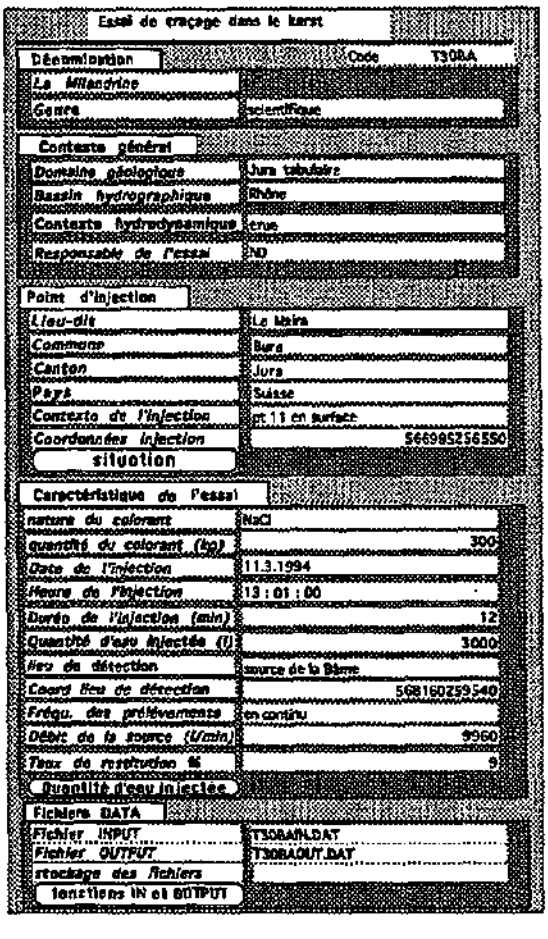
Essai de traçage dans le karst
Dénomination
Code T30BA
La Milandrine
Genre scientifique
Contexte général
Domaine géologique Jura tabulaire
Bassin hydrographique Rhône
Contexte hydrodynamique crue
Responsable de l'essai ND
Point d'injection
Lieu-dit Le Maira
Commune Bure
Canton Jura
Pays Suisse
Contexte de l'injection pt 11 en surface
Coordonnées injection 569985256550
situation
Caractéristique de l'essai
nature du colorant NaCl
quantité du colorant (kg) 300
Date de l'injection 11.3.1994
Heure de l'injection 13 : 01 : 00
Durée de l'injection (min) 12
Quantité d'eau injectée (l) 3000
lieu de détection source de la Bâme
Coord lieu de détection 568160259540
Fréqu. des prélèvements en continu
Débit de la source (l/min) 9960
Taux de restitution % 9
Quantité d'eau injectée
Fichiers DATA
Fichier INPUT T30BAIN.DAT
Fichier OUTPUT T30BAOUT.DAT
stockage des fichiers
fonctions IN et OUTPUT

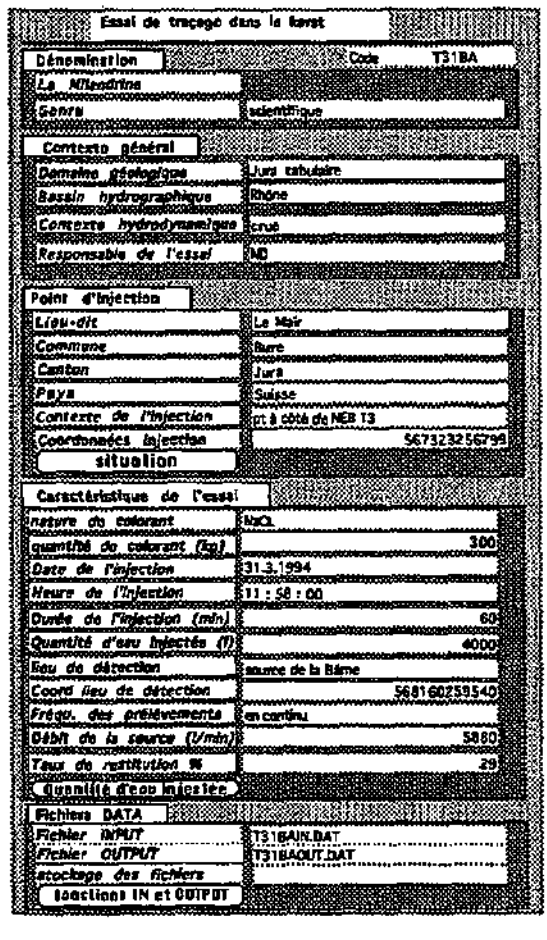
Essai de traçage dans le karst
Dénomination
Code T31BA
La Milandrine
Genre scientifique
Contexte général
Domaine géologique Jura tabulaire
Bassin hydrographique Rhône
Contexte hydrodynamique crue
Responsable de l'essai ND
Point d'injection
Lieu-dit Le Mair
Commune Bure
Canton Jura
Pays Suisse
Contexte de l'injection pt à côté de NEB T3
Coordonnées injection 567323256799
situation
Caractéristique de l'essai
nature du colorant NaCl
quantité du colorant (kg) 300
Date de l'injection 31.3.1994
Heure de l'injection 11 : 58 : 00
Durée de l'injection (min) 60
Quantité d'eau injectée (l) 4000
lieu de détection source de la Bâme
Coord lieu de détection 568160259540
Fréqu. des prélèvements en continu
Débit de la source (l/min) 5880
Taux de restitution % 29
Quantité d'eau injectée
Fichiers DATA
Fichier INPUT T31BAIN.DAT
Fichier OUTPUT T31BAOUT.DAT
stockage des fichiers
fonctions IN et OUTPUT

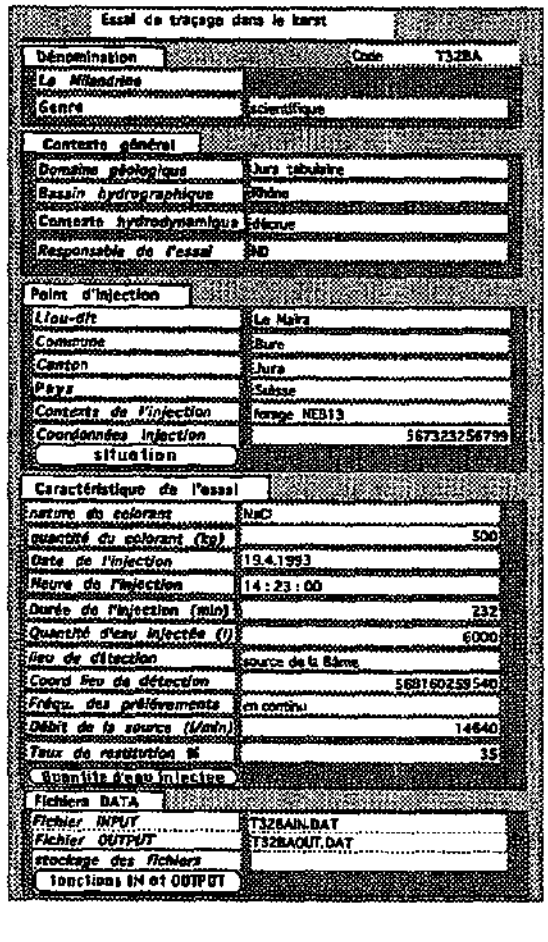
Essai de traçage dans le karst
Dénomination
Code T32BA
La Milandrine
Genre scientifique
Contexte général
Domaine géologique Jura tabulaire
Bassin hydrographique Rhône
Contexte hydrodynamique décrue
Responsable de l'essai ND
Point d'injection
Lieu-dit Le Maira
Commune Bure
Canton Jura
Pays Suisse
Contexte de l'injection forage NEB13
Coordonnées injection 567323256799
situation
Caractéristique de l'essai
nature du colorant NaCl
quantité du colorant (kg) 500
Date de l'injection 19.4.1993
Heure de l'injection 14 : 23 : 00
Durée de l'injection (min) 232
Quantité d'eau injectée (l) 6000
lieu de détection source de la Bâme
Coord lieu de détection 568160259540
Fréqu. des prélèvements en continu
Débit de la source (l/min) 14640
Taux de restitution % 35
Quantité d'eau injectée
Fichiers DATA
Fichier INPUT T32BAIN.DAT
Fichier OUTPUT T32BAOUT.DAT
stockage des fichiers
fonctions IN et OUTPUT

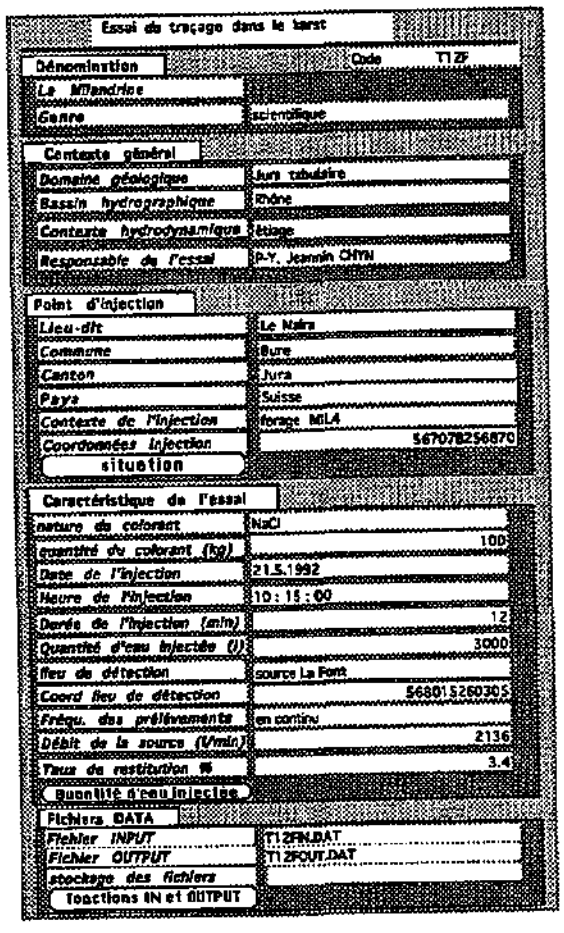
Essai de traçage dans le karst
Dénomination
Code T12F
La Milandrine
Genre scientifique
Contexte général
Domaine géologique Jura tabulaire
Bassin hydrographique Rhône
Contexte hydrodynamique Etiage
Responsable de l'essai P-Y. Jeannin CHYN
Point d'injection
Lieu-dit Le Maira
Commune Bure
Canton Jura
Pays Suisse
Contexte de l'injection forage MIL4
Coordonnées injection 567078256870
situation
Caractéristique de l'essai
nature du colorant NaCl
quantité du colorant (kg) 100
Date de l'injection 21.5.1992
Heure de l'injection 10 : 15 : 00
Durée de l'injection (min) 12
Quantité d'eau injectée (l) 3000
lieu de détection source La Font
Coord lieu de détection 568015260305
Fréqu. des prélèvements en continu
Débit de la source (l/min) 2136
Taux de restitution % 3.4
Quantité d'eau injectée
Fichiers DATA
Fichier INPUT T12FIN.DAT
Fichier OUTPUT T12FOUT.DAT
stockage des fichiers
fonctions IN et OUTPUT

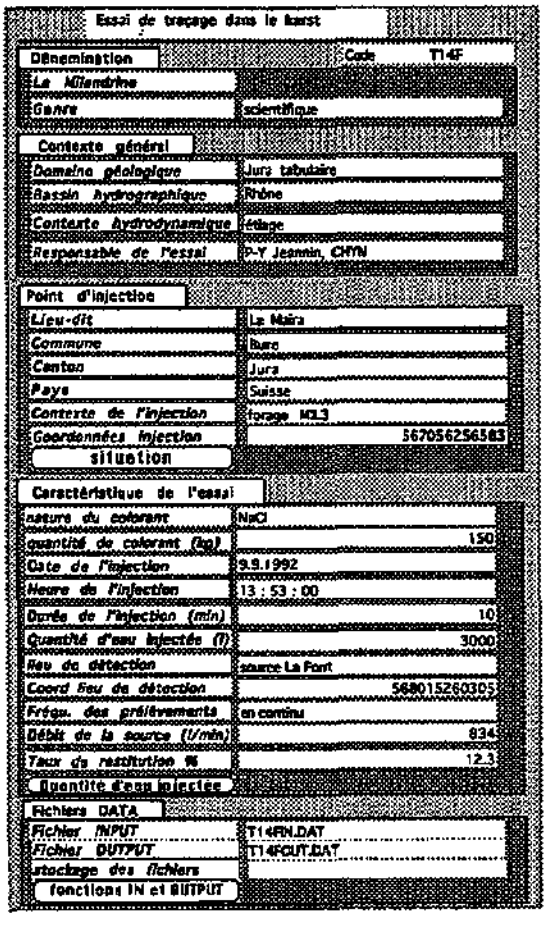
Essai de traçage dans le karst
Dénomination
Code T14F
La Milandrine
Genre scientifique
Contexte général
Domaine géologique Jura tabulaire
Bassin hydrographique Rhône
Contexte hydrodynamique Etiage
Responsable de l'essai P-Y Jeannin, CHYN
Point d'injection
Lieu-dit La Maira
Commune Bure
Canton Jura
Pays Suisse
Contexte de l'injection forage MIL3
Coordonnées injection 567056256583
situation
Caractéristique de l'essai
nature du colorant NaCl
quantité de colorant (kg) 150
Date de l'injection 9.9.1992
Heure de l'injection 13 : 53 : 00
Durée de l'injection (min) 10
Quantité d'eau injectée (l) 3000
lieu de détection source La Font
Coord lieu de détection 568015260305
Fréqu. des prélèvements en continu
Débit de la source (l/min) 834
Taux de restitution % 12.3
Quantité d'eau injectée
Fichiers DATA
Fichier INPUT T14FIN.DAT
Fichier OUTPUT T14FOUT.DAT
stockage des fichiers
fonctions IN et OUTPUT

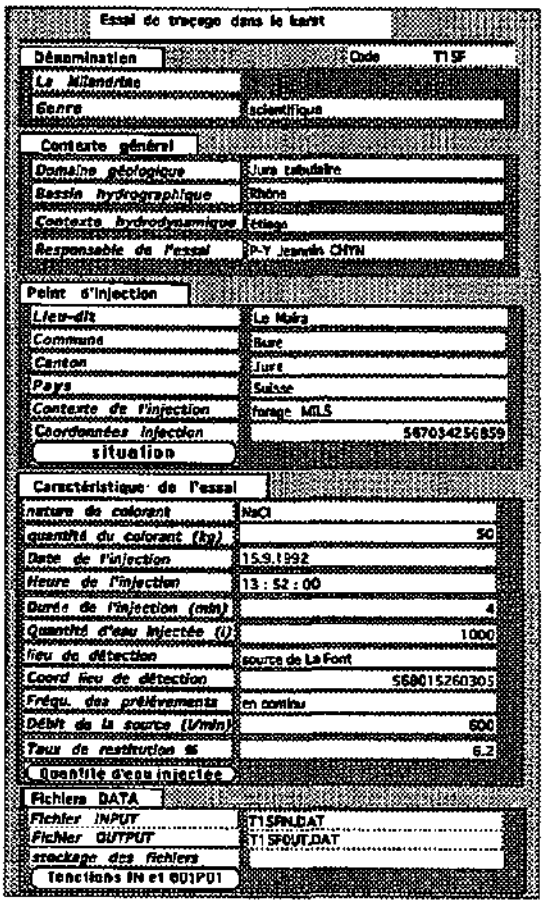
Essai de traçage dans le karst
Dénomination
Code T15F
La Milandrine
Genre scientifique
Contexte général
Domaine géologique Jura tabulaire
Bassin hydrographique Rhône
Contexte hydrodynamique Etiage
Responsable de l'essai P-Y Jeannin CHYN
Point d'injection
Lieu-dit Le Maira
Commune Bure
Canton Jura
Pays Suisse
Contexte de l'injection forage MIL5
Coordonnées injection 567034256859
situation
Caractéristique de l'essai
nature du colorant NaCl
quantité du colorant (kg) 50
Date de l'injection 15.9.1992
Heure de l'injection 13 : 52 : 00
Durée de l'injection (min) 4
Quantité d'eau injectée (l) 1000
lieu de détection source de La Font
Coord lieu de détection 568015260305
Fréqu. des prélèvements en continu
Débit de la source (l/min) 600
Taux de restitution % 6.2
Quantité d'eau injectée
Fichiers DATA
Fichier INPUT T15FIN.DAT
Fichier OUTPUT T15FOUT.DAT
stockage des fichiers
fonctions IN et OUTPUT

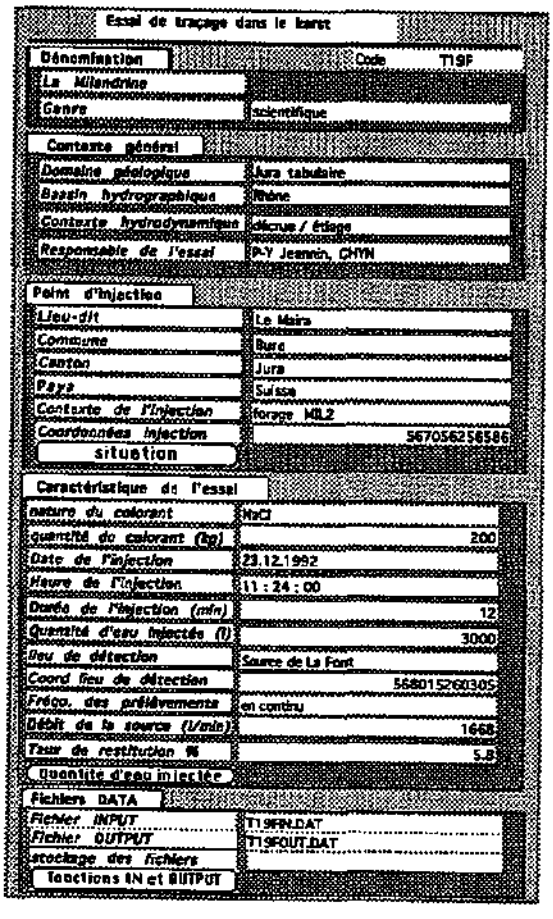
Essai de traçage dans le karst
Dénomination
Code T19F
La Milandrine
Genre scientifique
Contexte général
Domaine géologique Jura tabulaire
Bassin hydrographique Rhône
Contexte hydrodynamique décrue / étiage
Responsable de l'essai P-Y Jeannin, CHYN
Point d'injection
Lieu-dit Le Maira
Commune Bure
Canton Jura
Pays Suisse
Contexte de l'injection forage MIL2
Coordonnées injection 567056256586
situation
Caractéristique de l'essai
nature du colorant NaCl
quantité de colorant (kg) 200
Date de l'injection 23.12.1992
Heure de l'injection 11 : 24 : 00
Durée de l'injection (min) 12
Quantité d'eau injectée (l) 3000
lieu de détection Source de La Font
Coord lieu de détection 568015260305
Fréqu. des prélèvements en continu
Débit de la source (l/min) 1668
Taux de restitution % 5.8
Quantité d'eau injectée
Fichiers DATA
Fichier INPUT T19FIN.DAT
Fichier OUTPUT T19FOUT.DAT
stockage des fichiers
fonctions IN et OUTPUT

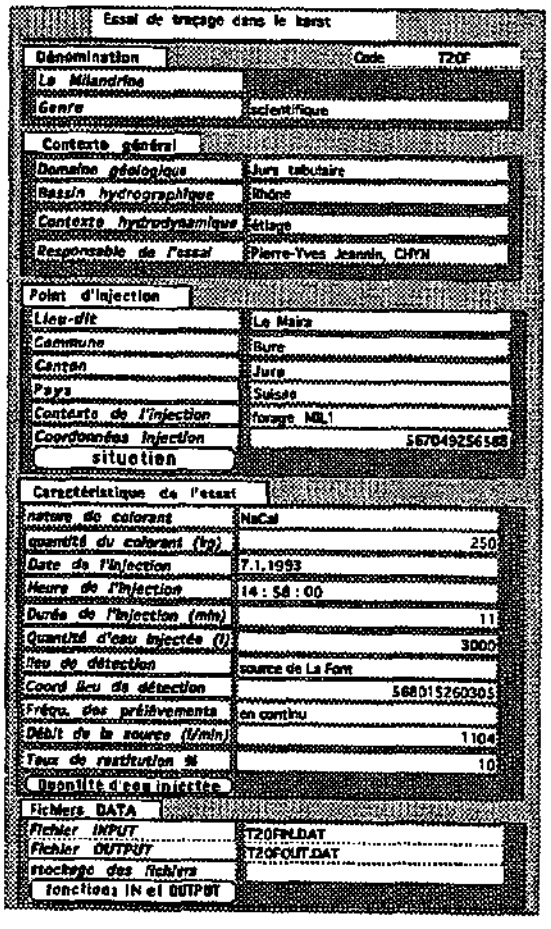
Essai de traçage dans le karst
Dénomination
Code T20F
Le Milandrine
Genre
scientifique
Contexte général
Domaine géologique
Jura tabulaire
Bassin hydrographique
Rhône
Contexte hydrodynamique
étiage
Responsable de l'essai
Pierre-Yves Jeannin, CHYN
Point d'injection
Lieu-dit
Le Maira
Commune
Bure
Canton
Jura
Pays
Suisse
Contexte de l'injection
forage MIL1
Coordonnées injection
567049256568
situation
Caractéristique de l'essai
nature du colorant
NaCal
quantité du colorant (kg)
250
Date de l'injection
7.1.1993
Heure de l'injection
14 : 58 : 00
Durée de l'injection (min)
11
Quantité d'eau injectée (l)
3000
lieu de détection
source de La Font
Coord lieu de détection
568015260305
Fréqu. des prélèvements
en continu
Débit de la source (l/min)
1104
Taux de restitution %
10
Quantité d'eau injectée
Fichiers DATA
Fichier INPUT
T20FIN.DAT
Fichier OUTPUT
T20FOUT.DAT
stockage des fichiers
fonctions IN et OUTPUT

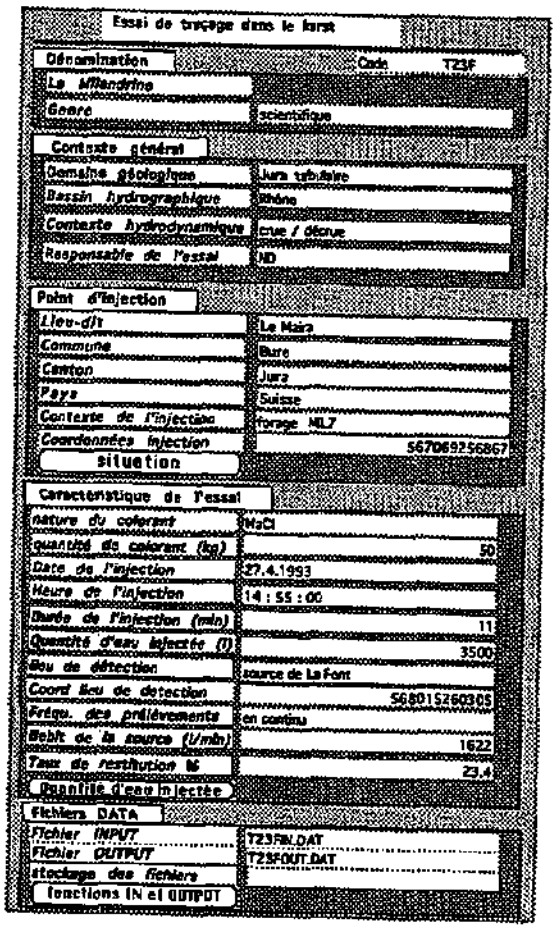
Essai de traçage dans le karst
Dénomination
Code T23F
Le Milandrine
Genre
scientifique
Contexte général
Domaine géologique
Jura tabulaire
Bassin hydrographique
Rhône
Contexte hydrodynamique
crue / décrue
Responsable de l'essai
ND
Point d'injection
Lieu-dit
Le Maira
Commune
Bure
Canton
Jura
Pays
Suisse
Contexte de l'injection
forage MIL7
Coordonnées injection
567069256867
situation
Caractéristique de l'essai
nature du colorant
NaCl
quantité de colorant (kg)
50
Date de l'injection
27.4.1993
Heure de l'injection
14 : 55 : 00
Durée de l'injection (min)
11
Quantité d'eau injectée (l)
3500
lieu de détection
source de La Font
Coord lieu de détection
568015260305
Fréqu. des prélèvements
en continu
Débit de la source (l/min)
1622
Taux de restitution %
23.4
Quantité d'eau injectée
Fichiers DATA
Fichier INPUT
T23FIN.DAT
Fichier OUTPUT
T23FOUT.DAT
stockage des fichiers
fonctions IN et OUTPUT

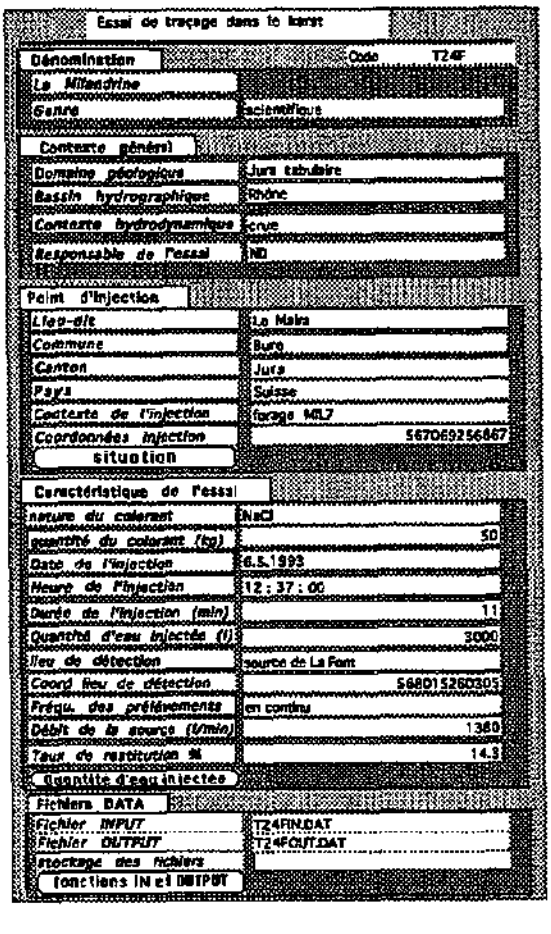
Essai de traçage dans le karst
Dénomination
Code T24F
Le Milandrine
Genre
scientifique
Contexte général
Domaine géologique
Jura tabulaire
Bassin hydrographique
Rhône
Contexte hydrodynamique
crue
Responsable de l'essai
ND
Point d'injection
Lieu-dit
Le Maira
Commune
Bure
Canton
Jura
Pays
Suisse
Contexte de l'injection
forage MIL7
Coordonnées injection
567069256867
situation
Caractéristique de l'essai
nature du colorant
NaCl
quantité du colorant (kg)
50
Date de l'injection
6.5.1993
Heure de l'injection
12 : 37 : 00
Durée de l'injection (min)
11
Quantité d'eau injectée (l)
3000
lieu de détection
source de La Font
Coord lieu de détection
568015260305
Fréqu. des prélèvements
en continu
Débit de la source (l/min)
1360
Taux de restitution %
14.3
Quantité d'eau injectée
Fichiers DATA
Fichier INPUT
T24FIN.DAT
Fichier OUTPUT
T24FOUT.DAT
stockage des fichiers
fonctions IN et OUTPUT

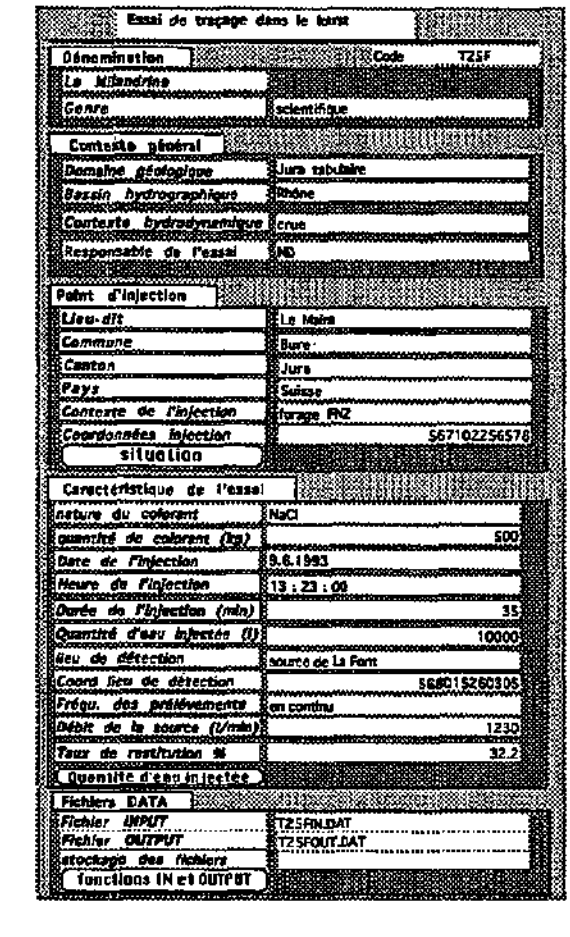
Essai de traçage dans le karst
Dénomination
Code T25F
Le Milandrine
Genre
scientifique
Contexte général
Domaine géologique
Jura tabulaire
Bassin hydrographique
Rhône
Contexte hydrodynamique
crue
Responsable de l'essai
ND
Point d'injection
Lieu-dit
Le Maira
Commune
Bure
Canton
Jura
Pays
Suisse
Contexte de l'injection
forage FN2
Coordonnées injection
567102256578
situation
Caractéristique de l'essai
nature du colorant
NaCl
quantité de colorant (kg)
500
Date de l'injection
9.6.1993
Heure de l'injection
13 : 23 : 00
Durée de l'injection (min)
35
Quantité d'eau injectée (l)
10000
lieu de détection
source de La Font
Coord lieu de détection
568015260305
Fréqu. des prélèvements
en continu
Débit de la source (l/min)
1230
Taux de restitution %
32.2
Quantité d'eau injectée
Fichiers DATA
Fichier INPUT
T25FIN.DAT
Fichier OUTPUT
T25FOUT.DAT
stockage des fichiers
fonctions IN et OUTPUT

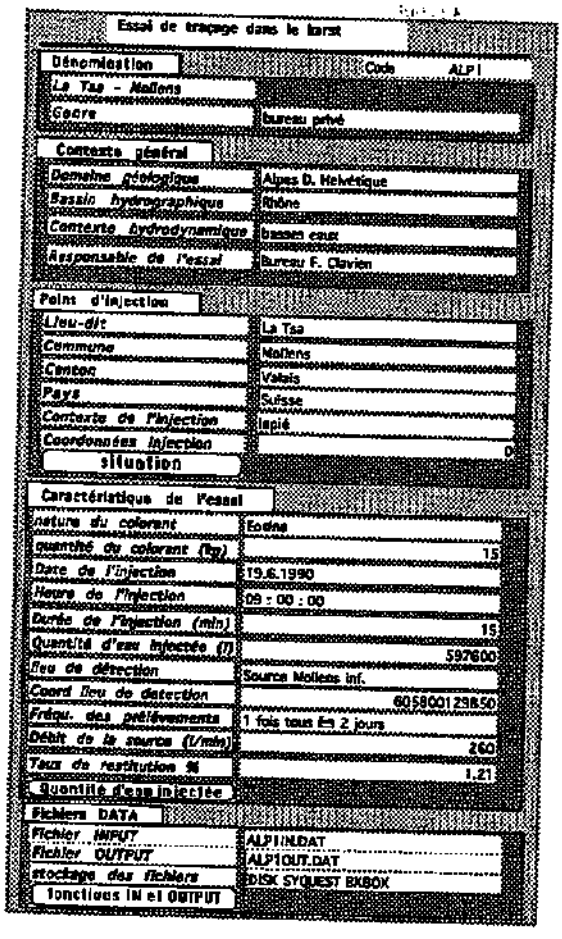
Essai de traçage dans le karst
Dénomination
Code ALP1
La Tsa - Mollens
Genre
bureau privé
Contexte général
Domaine géologique
Alpes D. Helvétique
Bassin hydrographique
Rhône
Contexte hydrodynamique
basses eaux
Responsable de l'essai
Bureau F. Clavien
Point d'injection
Lieu-dit
La Tsa
Commune
Mollens
Canton
Valais
Pays
Suisse
Contexte de l'injection
lapié
Coordonnées injection
0
situation
Caractéristique de l'essai
nature du colorant
Eosine
quantité du colorant (kg)
15
Date de l'injection
19.6.1990
Heure de l'injection
09 : 00 : 00
Durée de l'injection (min)
15
Quantité d'eau injectée (l)
597600
lieu de détection
Source Mollens inf.
Coord lieu de détection
605800129850
Fréqu. des prélèvements
1 fois tous les 2 jours
Débit de la source (l/min)
260
Taux de restitution %
1.21
Quantité d'eau injectée
Fichiers DATA
Fichier INPUT
ALP1IN.DAT
Fichier OUTPUT
ALP1OUT.DAT
stockage des fichiers
DISK SYQUEST 8X8OX
fonctions IN et OUTPUT

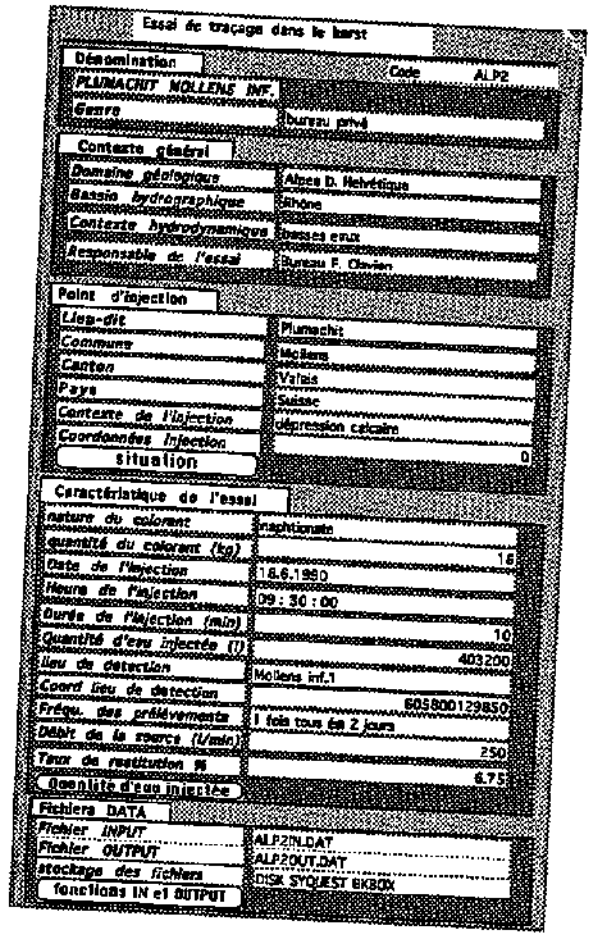
Essai de traçage dans le karst
Dénomination
Code ALP2
PLUMACHIT MOLLENS INF.
Genre
bureau privé
Contexte général
Domaine géologique
Alpes D. Helvétique
Bassin hydrographique
Rhône
Contexte hydrodynamique
basses eaux
Responsable de l'essai
Bureau F. Clavien
Point d'injection
Lieu-dit
Plumachit
Commune
Mollens
Canton
Valais
Pays
Suisse
Contexte de l'injection
dépression calcaire
Coordonnées injection
0
situation
Caractéristique de l'essai
nature du colorant
fluorescéine
quantité du colorant (kg)
16
Date de l'injection
16.6.1990
Heure de l'injection
09 : 30 : 00
Durée de l'injection (min)
10
Quantité d'eau injectée (l)
403200
lieu de détection
Mollens inf.1
Coord lieu de détection
605800129850
Fréqu. des prélèvements
1 fois tous les 2 jours
Débit de la source (l/min)
250
Taux de restitution %
6.75
Quantité d'eau injectée
Fichiers DATA
Fichier INPUT
ALP2IN.DAT
Fichier OUTPUT
ALP2OUT.DAT
stockage des fichiers
DISK SYQUEST 8X8OX
fonctions IN et OUTPUT

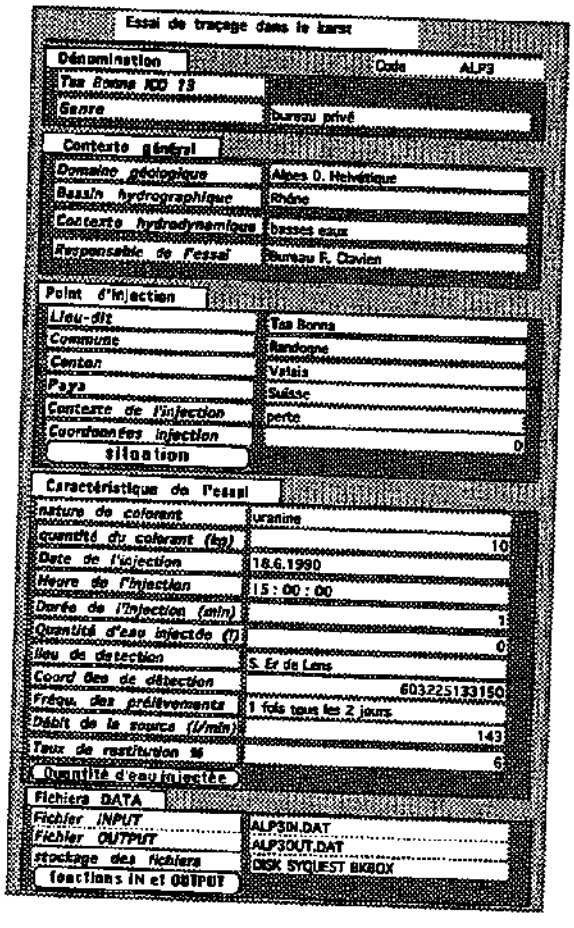
Essai de traçage dans le karst
Dénomination
Code ALP3
Tsa Borna 100 13
Genre
bureau privé
Contexte général
Domaine géologique
Alpes D. Helvétique
Bassin hydrographique
Rhône
Contexte hydrodynamique
basses eaux
Responsable de l'essai
Bureau F. Clavien
Point d'injection
Lieu-dit
Tsa Borna
Commune
Randogne
Canton
Valais
Pays
Suisse
Contexte de l'injection
perte
Coordonnées injection
0
situation
Caractéristique de l'essai
nature du colorant
uranine
quantité du colorant (kg)
10
Date de l'injection
18.6.1990
Heure de l'injection
15 : 00 : 00
Durée de l'injection (min)
1
Quantité d'eau injectée (l)
0
lieu de détection
S. Er de Lens
Coord lieu de détection
603225133150
Fréqu. des prélèvements
1 fois tous les 2 jours
Débit de la source (l/min)
143
Taux de restitution %
6
Quantité d'eau injectée
Fichiers DATA
Fichier INPUT
ALP3IN.DAT
Fichier OUTPUT
ALP3OUT.DAT
stockage des fichiers
DISK SYQUEST 8X8OX
fonctions IN et OUTPUT

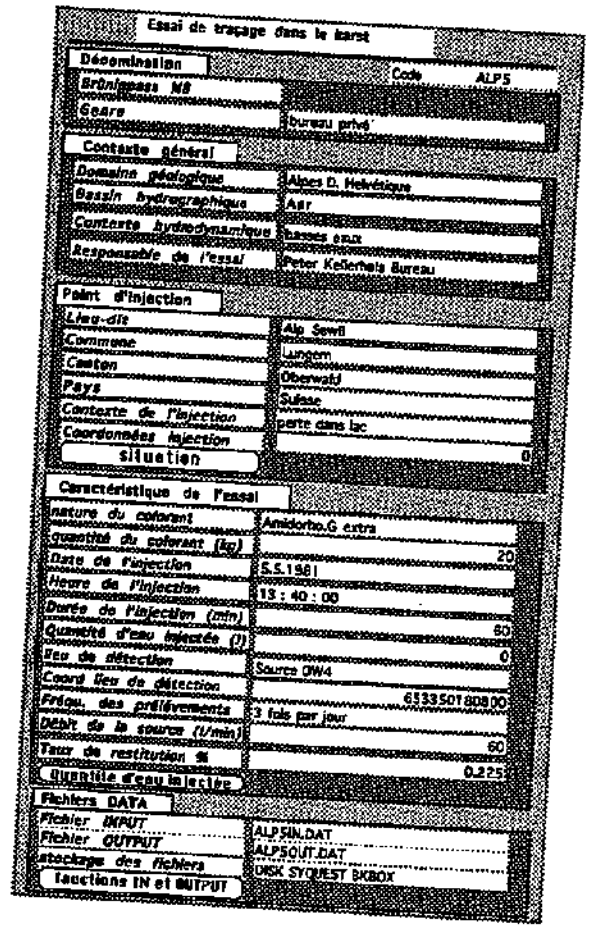
Essai de traçage dans le karst
Dénomination
Code ALP5
Brüniglass MB
Genre
bureau privé
Contexte général
Domaine géologique
Alpes D. Helvétique
Bassin hydrographique
Aar
Contexte hydrodynamique
basses eaux
Responsable de l'essai
Peter Kellenhals Bureau
Point d'injection
Lieu-dit
Alp Sewli
Commune
Lungern
Canton
Oberwald
Pays
Suisse
Contexte de l'injection
perte dans lac
Coordonnées injection
0
situation
Caractéristique de l'essai
nature du colorant
Amidorho.G extra
quantité du colorant (kg)
20
Date de l'injection
S.S.1981
Heure de l'injection
13 : 40 : 00
Durée de l'injection (min)
60
Quantité d'eau injectée (l)
0
lieu de détection
Source DW4
Coord lieu de détection
6533501808 00
Fréqu. des prélèvements
3 fois par jour
Débit de la source (l/min)
60
Taux de restitution %
0.225
Quantité d'eau injectée
Fichiers DATA
Fichier INPUT
ALP5IN.DAT
Fichier OUTPUT
ALP5OUT.DAT
stockage des fichiers
DISK SYQUEST 8X8OX
fonctions IN et OUTPUT

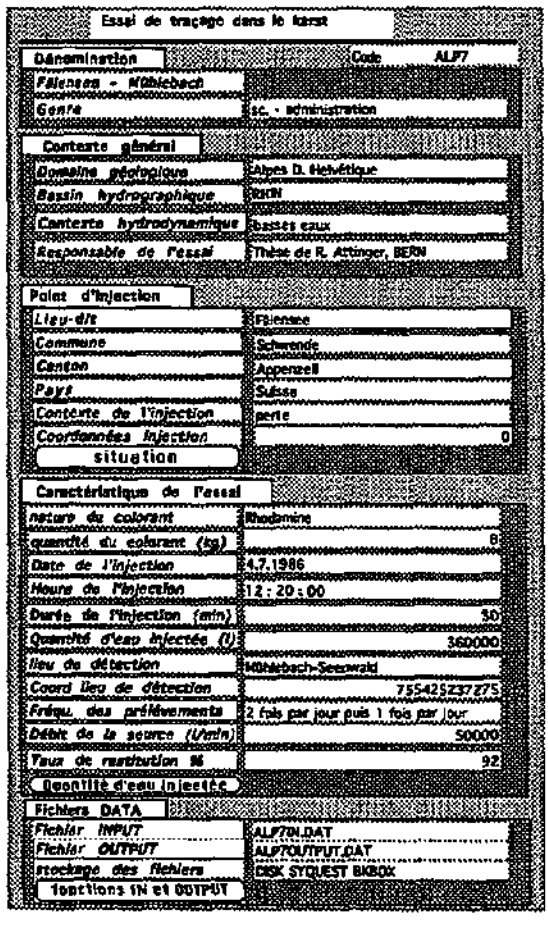
Essai de traçage dans le karst
Dénomination
Code ALP7
Fälensee - Mühlebach
Genre
sc. - administration
Contexte général
Domaine géologique
Alpes D. Helvétique
Bassin hydrographique
RHIN
Contexte hydrodynamique
basses eaux
Responsable de l'essai
Thèse de R. Attinger, BERN
Point d'injection
Lieu-dit
Fälensee
Commune
Schwende
Canton
Appenzell
Pays
Suisse
Contexte de l'injection
perte
Coordonnées injection
0
situation
Caractéristique de l'essai
nature du colorant
Rhodamine
quantité du colorant (kg)
6
Date de l'injection
4.7.1986
Heure de l'injection
12 : 20 : 00
Durée de l'injection (min)
30
Quantité d'eau injectée (l)
360000
lieu de détection
Mühlebach-Seeswald
Coord lieu de détection
755425237275
Fréqu. des prélèvements
2 fois par jour puis 1 fois par jour
Débit de la source (l/min)
50000
Taux de restitution %
92
Quantité d'eau injectée
Fichiers DATA
Fichier INPUT
ALP7IN.DAT
Fichier OUTPUT
ALP7OUTPUT.DAT
stockage des fichiers
DISK SYQUEST 88MB
fonctions IN et OUTPUT

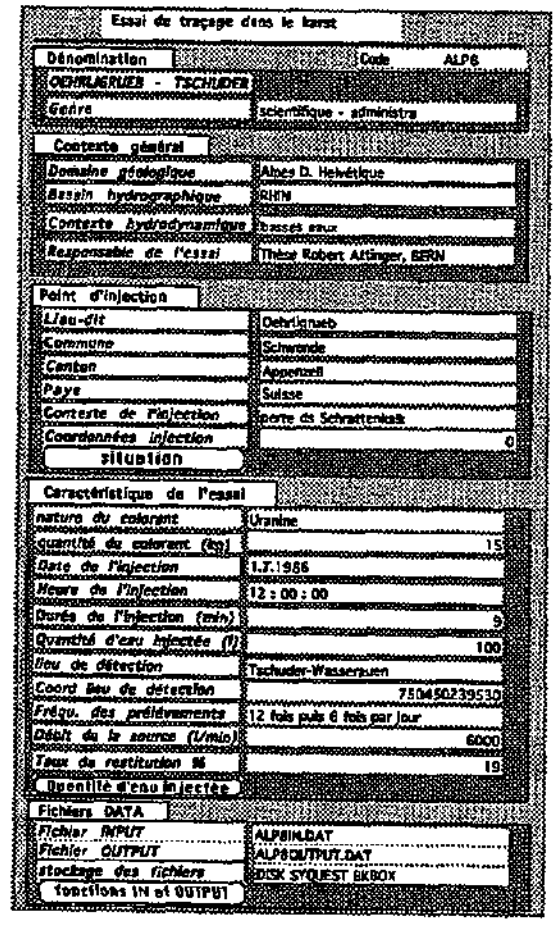
Essai de traçage dans le karst
Dénomination
Code ALP6
OEHRLIGRUEB - TSCHUDER
Genre
scientifique - administra
Contexte général
Domaine géologique
Alpes D. Helvétique
Bassin hydrographique
RHIN
Contexte hydrodynamique
basses eaux
Responsable de l'essai
Thèse Robert Attinger, BERN
Point d'injection
Lieu-dit
Oehrlignueb
Commune
Schwende
Canton
Appenzell
Pays
Suisse
Contexte de l'injection
perte ds Schrattenkalk
Coordonnées injection
0
situation
Caractéristique de l'essai
nature du colorant
Uranine
quantité du colorant (kg)
15
Date de l'injection
1.7.1986
Heure de l'injection
12 : 00 : 00
Durée de l'injection (min)
9
Quantité d'eau injectée (l)
100
lieu de détection
Tschuder-Wasserquen
Coord lieu de détection
750450239530
Fréqu. des prélèvements
12 fois puis 6 fois par jour
Débit de la source (l/min)
6000
Taux de restitution %
19
Quantité d'eau injectée
Fichiers DATA
Fichier INPUT
ALP6IN.DAT
Fichier OUTPUT
ALP6OUTPUT.DAT
stockage des fichiers
DISK SYQUEST 88MB
fonctions IN et OUTPUT

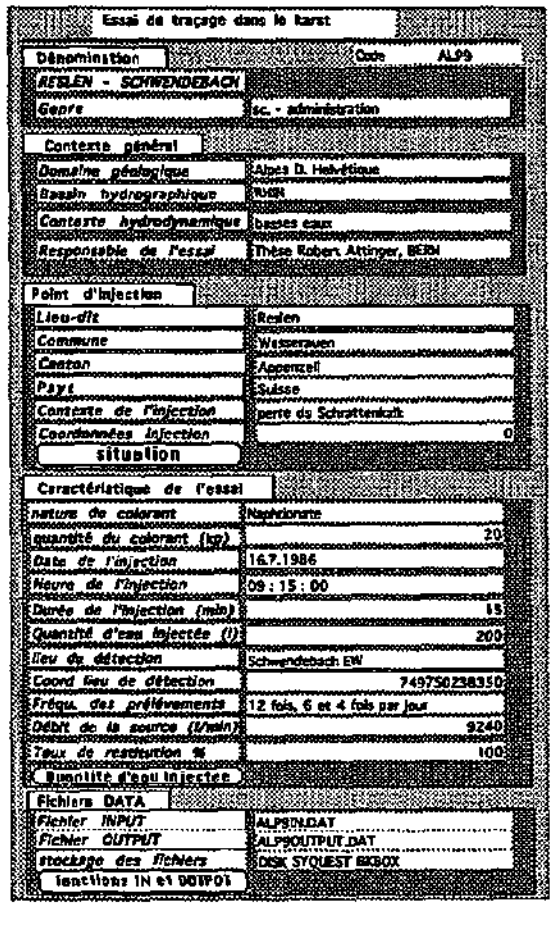
Essai de traçage dans le karst
Dénomination
Code ALP9
RESLEN - SCHWENDEBACH
Genre
sc. - administration
Contexte général
Domaine géologique
Alpes D. Helvétique
Bassin hydrographique
RHEIN
Contexte hydrodynamique
basses eaux
Responsable de l'essai
Thèse Robert Attinger, BERN
Point d'injection
Lieu-dit
Reslen
Commune
Wasserauen
Canton
Appenzell
Pays
Suisse
Contexte de l'injection
perte ds Schrattenkalk
Coordonnées injection
0
situation
Caractéristique de l'essai
nature du colorant
Naphtionate
quantité du colorant (kg)
20
Date de l'injection
16.7.1986
Heure de l'injection
09 : 15 : 00
Durée de l'injection (min)
15
Quantité d'eau injectée (l)
200
lieu de détection
Schwendebach EW
Coord lieu de détection
749750238350
Fréqu. des prélèvements
12 fois, 6 et 4 fois par jour
Débit de la source (l/min)
9240
Taux de restitution %
100
Quantité d'eau injectée
Fichiers DATA
Fichier INPUT
ALP9IN.DAT
Fichier OUTPUT
ALP9OUTPUT.DAT
stockage des fichiers
DISK SYQUEST 88MB
fonctions IN et OUTPUT

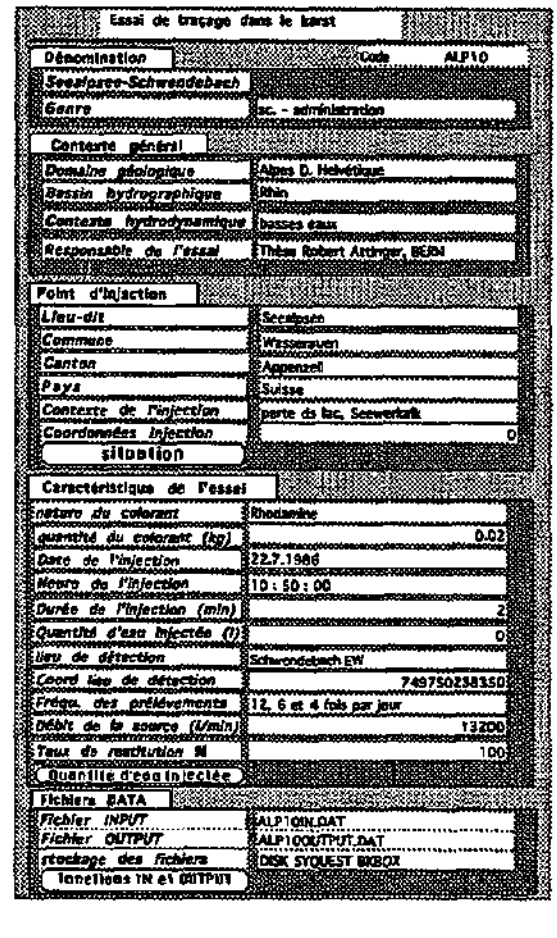
Essai de traçage dans le karst
Dénomination
Code ALP10
Seealpsee-Schwendebach
Genre
sc. - administration
Contexte général
Domaine géologique
Alpes D. Helvétique
Bassin hydrographique
Rhin
Contexte hydrodynamique
basses eaux
Responsable de l'essai
Thèse Robert Attinger, BERN
Point d'injection
Lieu-dit
Seealpsee
Commune
Wasserauen
Canton
Appenzell
Pays
Suisse
Contexte de l'injection
perte ds lac, Seewerkalk
Coordonnées injection
0
situation
Caractéristique de l'essai
nature du colorant
Rhodamine
quantité du colorant (kg)
0.02
Date de l'injection
22.7.1986
Heure de l'injection
10 : 50 : 00
Durée de l'injection (min)
2
Quantité d'eau injectée (l)
0
lieu de détection
Schwendebach EW
Coord lieu de détection
749750238350
Fréqu. des prélèvements
12, 6 et 4 fois par jour
Débit de la source (l/min)
13200
Taux de restitution %
100
Quantité d'eau injectée
Fichiers DATA
Fichier INPUT
ALP10IN.DAT
Fichier OUTPUT
ALP10OUTPUT.DAT
stockage des fichiers
DISK SYQUEST 88MB
fonctions IN et OUTPUT

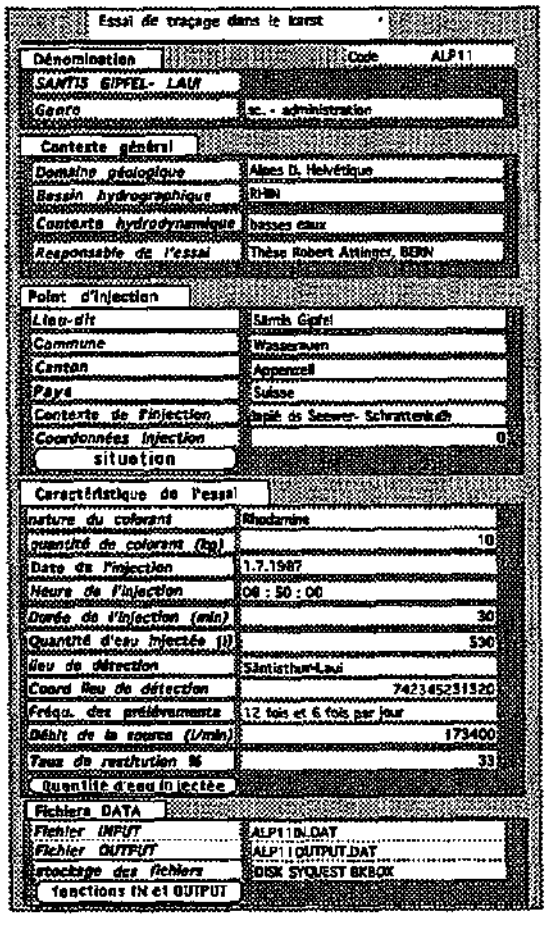

Essai de traçage dans le karst

Dénomination	Code ALP11
SANTIS GIPFEL- LAUI	
Genre	sc. - administration

Contexte général	
Domaine géologique	Alpes D. Helvétique
Bassin hydrographique	RHIN
Contexte hydrodynamique	basses eaux
Responsable de l'essai	Thèse Robert Attinger, BERN

Point d'injection	
Lieu-dit	Sämtis Gipfel
Commune	Wasserauen
Canton	Appenzell
Pays	Suisse
Contexte de l'injection	dolié ds Seewer- Schrattenkalk
Coordonnées injection	0
situation	

Caractéristique de l'essai	
nature du colorant	Rhodamine
quantité de colorant (kg)	10
Date de l'injection	1.7.1987
Heure de l'injection	08 : 50 : 00
Durée de l'injection (min)	30
Quantité d'eau injectée (l)	530
lieu de détection	Sämtisthur-Laui
Coord lieu de détection	742345231520
Fréqu. des prélèvements	12 fois et 6 fois par jour
Débit de la source (l/min)	173400
Taux de restitution %	33
Quantité d'eau injectée	

Fichiers DATA	
Fichier INPUT	ALP11IN.DAT
Fichier OUTPUT	ALP11OUTPUT.DAT
stockage des fichiers	DISK SYQUEST 8XBOX
fonctions IN et OUTPUT	

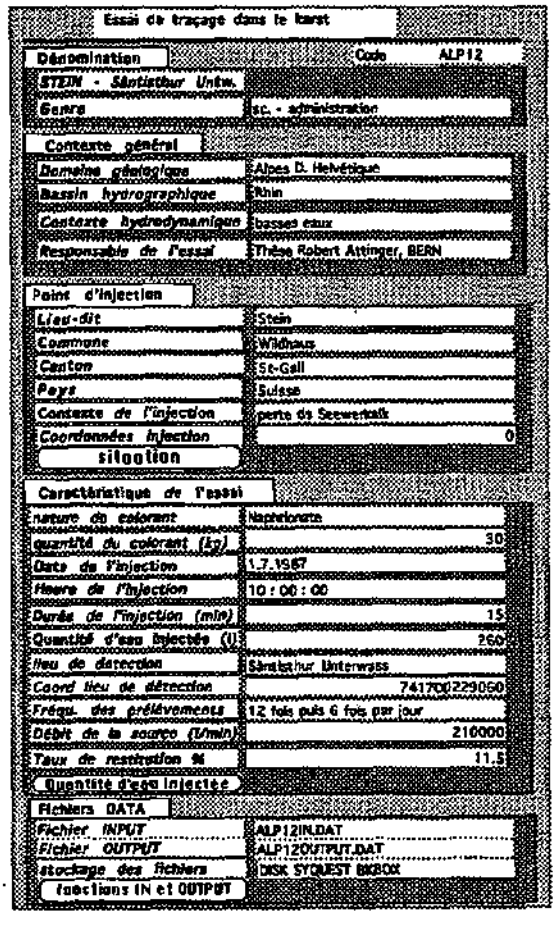

Essai de traçage dans le karst

Dénomination	Code ALP12
STEIN - Sämtisthur Untw.	
Genre	sc. - administration

Contexte général	
Domaine géologique	Alpes D. Helvétique
Bassin hydrographique	Rhin
Contexte hydrodynamique	basses eaux
Responsable de l'essai	Thèse Robert Attinger, BERN

Point d'injection	
Lieu-dit	Stein
Commune	Wildhaus
Canton	St-Gall
Pays	Suisse
Contexte de l'injection	perte ds Seewerkalk
Coordonnées injection	0
situation	

Caractéristique de l'essai	
nature du colorant	Naphtionate
quantité du colorant (kg)	30
Date de l'injection	1.7.1987
Heure de l'injection	10 : 00 : 00
Durée de l'injection (min)	15
Quantité d'eau injectée (l)	260
lieu de détection	Sämtisthur Unterwass
Coord lieu de détection	741700229060
Fréqu. des prélèvements	12 fois puis 6 fois par jour
Débit de la source (l/min)	210000
Taux de restitution %	11.5
Quantité d'eau injectée	

Fichiers DATA	
Fichier INPUT	ALP12IN.DAT
Fichier OUTPUT	ALP12OUTPUT.DAT
stockage des fichiers	DISK SYQUEST 8XBOX
fonctions IN et OUTPUT	

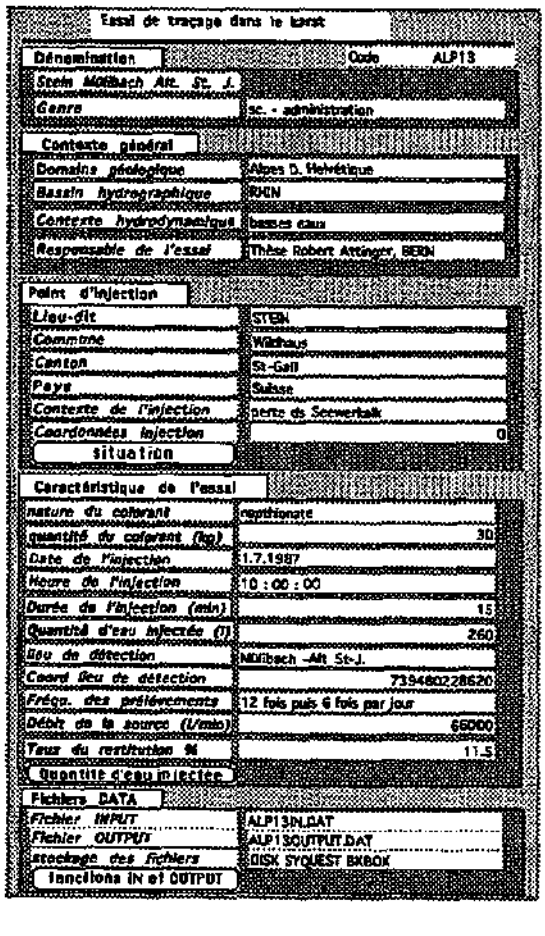

Essai de traçage dans le karst

Dénomination	Code ALP13
Stein Mülibach Alt. St. J.	
Genre	sc. - administration

Contexte général	
Domaine géologique	Alpes D. Helvétique
Bassin hydrographique	RHIN
Contexte hydrodynamique	basses eaux
Responsable de l'essai	Thèse Robert Attinger, BERN

Point d'injection	
Lieu-dit	STEIN
Commune	Wildhaus
Canton	St-Gall
Pays	Suisse
Contexte de l'injection	perte ds Seewerkalk
Coordonnées injection	0
situation	

Caractéristique de l'essai	
nature du colorant	napthionate
quantité du colorant (kg)	30
Date de l'injection	1.7.1987
Heure de l'injection	10 : 00 : 00
Durée de l'injection (min)	15
Quantité d'eau injectée (l)	260
lieu de détection	Mülibach - Alt St-J.
Coord lieu de détection	739480228620
Fréqu. des prélèvements	12 fois puis 6 fois par jour
Débit de la source (l/min)	66000
Taux de restitution %	11.5
Quantité d'eau injectée	

Fichiers DATA	
Fichier INPUT	ALP13IN.DAT
Fichier OUTPUT	ALP13OUTPUT.DAT
stockage des fichiers	DISK SYQUEST 8XBOX
fonctions IN et OUTPUT	

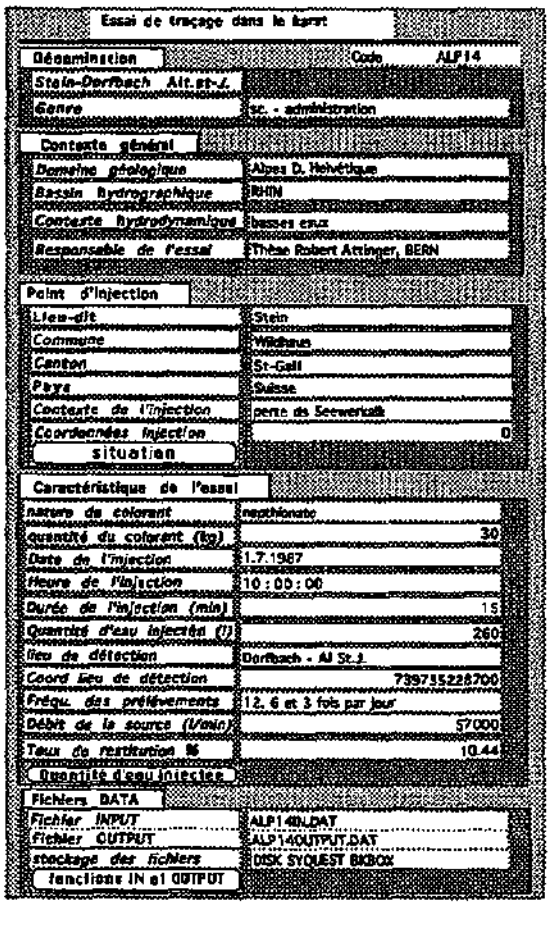

Essai de traçage dans le karst

Dénomination	Code ALP14
Stein-Dorfbach Alt.st-J.	
Genre	sc. - administration

Contexte général	
Domaine géologique	Alpes D. Helvétique
Bassin hydrographique	RHIN
Contexte hydrodynamique	basses eaux
Responsable de l'essai	Thèse Robert Attinger, BERN

Point d'injection	
Lieu-dit	Stein
Commune	Wildhaus
Canton	St-Gall
Pays	Suisse
Contexte de l'injection	perte ds Seewerkalk
Coordonnées injection	0
situation	

Caractéristique de l'essai	
nature du colorant	napthionate
quantité du colorant (kg)	30
Date de l'injection	1.7.1987
Heure de l'injection	10 : 00 : 00
Durée de l'injection (min)	15
Quantité d'eau injectée (l)	260
lieu de détection	Dorfbach - Al St.J.
Coord lieu de détection	739755228700
Fréqu. des prélèvements	12, 6 et 3 fois par jour
Débit de la source (l/min)	57000
Taux de restitution %	10.44
Quantité d'eau injectée	

Fichiers DATA	
Fichier INPUT	ALP14IN.DAT
Fichier OUTPUT	ALP14OUTPUT.DAT
stockage des fichiers	DISK SYQUEST 8XBOX
fonctions IN et OUTPUT	

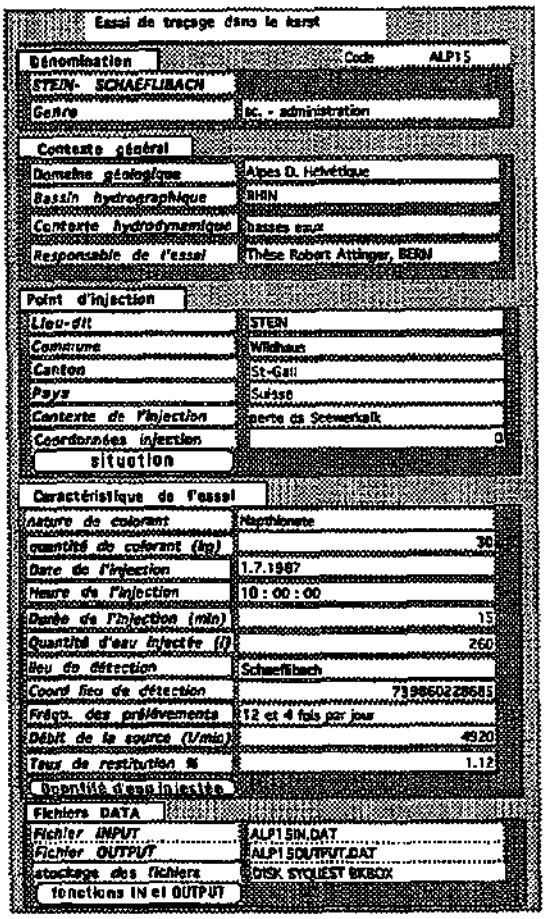
Essai de traçage dans le karst
Dénomination
Code ALP15
STEIN- SCHAEFLIBACH
Genre
sc. - administration
Contexte général
Domaine géologique Alpes O. Helvétique
Bassin hydrographique RHIN
Contexte hydrodynamique basses eaux
Responsable de l'essai Thèse Robert Attinger, BERN
Point d'injection
Lieu-dit STEIN
Commune Wildhaus
Canton St-Gall
Pays Suisse
Contexte de l'injection perte ds Seewerkalk
Coordonnées injection 0
situation
Caractéristique de l'essai
Nature de colorant Naphtionate
quantité de colorant (kg) 30
Date de l'injection 1.7.1987
Heure de l'injection 10 : 00 : 00
Durée de l'injection (min) 15
Quantité d'eau injectée (l) 260
lieu de détection Schaeflibach
Coord lieu de détection 739860228685
Fréqu. des prélèvements 12 et 4 fois par jour
Débit de la source (l/min) 4920
Taux de restitution % 1.12
Quantité d'eau injectée
Fichiers DATA
Fichier INPUT ALP15IN.DAT
Fichier OUTPUT ALP15OUTPUT.DAT
stockage des fichiers DISK SYQUEST 88KBOX
fonctions IN et OUTPUT

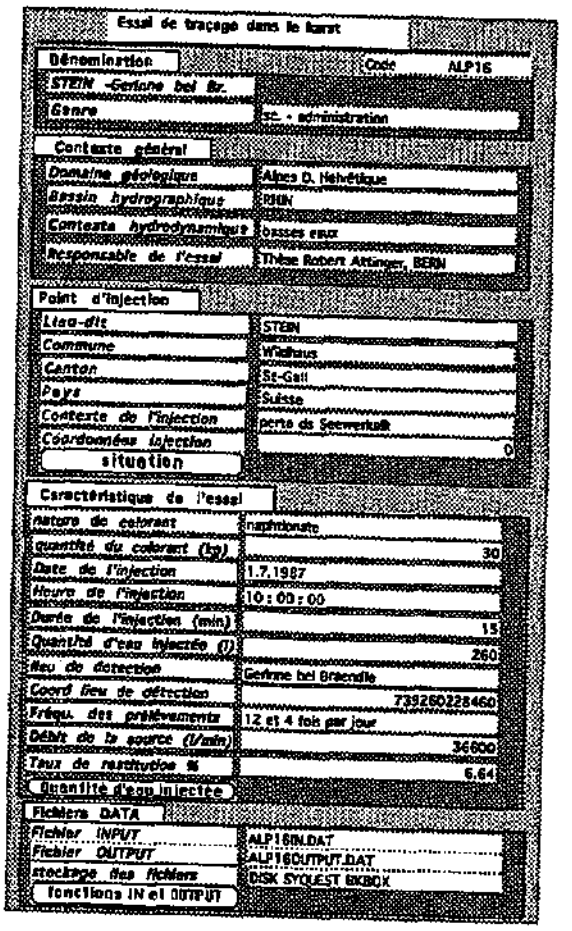
Essai de traçage dans le karst
Dénomination
Code ALP16
STEIN -Gerlone bei Br.
Genre
sc. - administration
Contexte général
Domaine géologique Alpes O. Helvétique
Bassin hydrographique RHIN
Contexte hydrodynamique basses eaux
Responsable de l'essai Thèse Robert Attinger, BERN
Point d'injection
Lieu-dit STEIN
Commune Wildhaus
Canton St-Gall
Pays Suisse
Contexte de l'injection perte ds Seewerkalk
Coordonnées injection 0
situation
Caractéristique de l'essai
Nature de colorant naphtionate
quantité de colorant (kg) 30
Date de l'injection 1.7.1987
Heure de l'injection 10 : 00 : 00
Durée de l'injection (min) 15
Quantité d'eau injectée (l) 260
lieu de détection Gerlone bei Braendle
Coord lieu de détection 739260228460
Fréqu. des prélèvements 12 et 4 fois par jour
Débit de la source (l/min) 36600
Taux de restitution % 6.64
Quantité d'eau injectée
Fichiers DATA
Fichier INPUT ALP16IN.DAT
Fichier OUTPUT ALP16OUTPUT.DAT
stockage des fichiers DISK SYQUEST 88KBOX
fonctions IN et OUTPUT

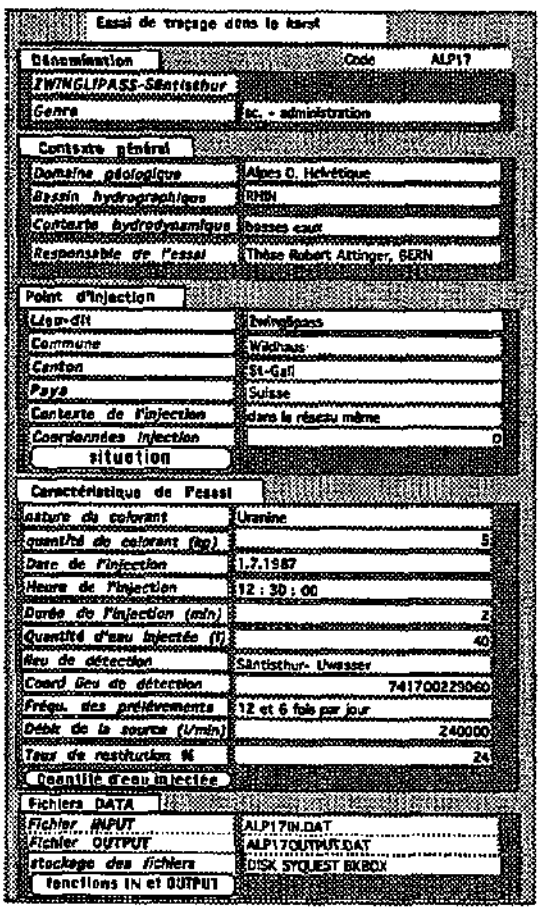
Essai de traçage dans le karst
Dénomination
Code ALP17
ZWINGLIPASS-Säntisthur
Genre
sc. - administration
Contexte général
Domaine géologique Alpes O. Helvétique
Bassin hydrographique RHIN
Contexte hydrodynamique basses eaux
Responsable de l'essai Thèse Robert Attinger, BERN
Point d'injection
Lieu-dit Zwinglipass
Commune Wildhaus
Canton St-Gall
Pays Suisse
Contexte de l'injection dans le réseau même
Coordonnées injection 0
situation
Caractéristique de l'essai
Nature de colorant Uranine
quantité de colorant (kg) 5
Date de l'injection 1.7.1987
Heure de l'injection 12 : 30 : 00
Durée de l'injection (min) 2
Quantité d'eau injectée (l) 40
lieu de détection Säntisthur- Urwasser
Coord lieu de détection 741700229060
Fréqu. des prélèvements 12 et 6 fois par jour
Débit de la source (l/min) 240000
Taux de restitution % 24
Quantité d'eau injectée
Fichiers DATA
Fichier INPUT ALP17IN.DAT
Fichier OUTPUT ALP17OUTPUT.DAT
stockage des fichiers DISK SYQUEST 88KBOX
fonctions IN et OUTPUT

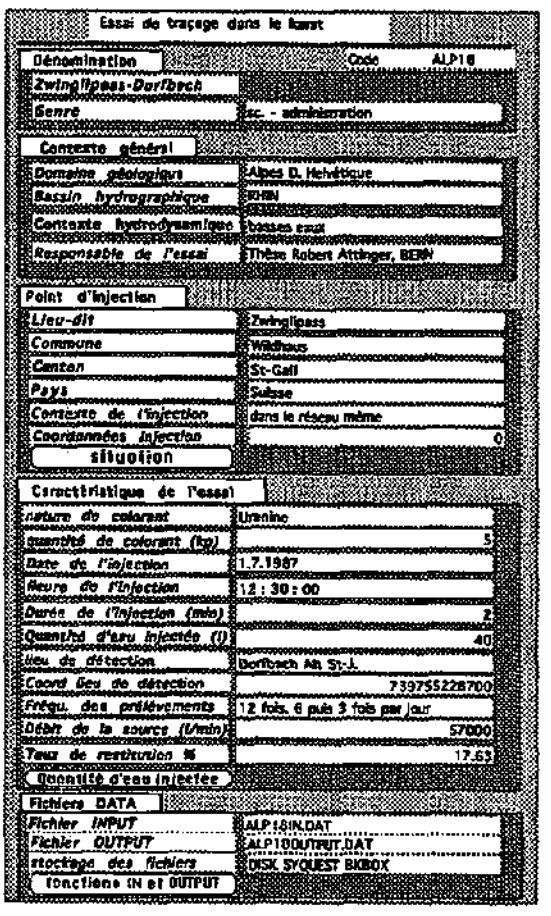
Essai de traçage dans le karst
Dénomination
Code ALP18
Zwinglipass-Dorfbach
Genre
sc. - administration
Contexte général
Domaine géologique Alpes O. Helvétique
Bassin hydrographique RHIN
Contexte hydrodynamique basses eaux
Responsable de l'essai Thèse Robert Attinger, BERN
Point d'injection
Lieu-dit Zwinglipass
Commune Wildhaus
Canton St-Gall
Pays Suisse
Contexte de l'injection dans le réseau même
Coordonnées injection 0
situation
Caractéristique de l'essai
Nature de colorant Uranine
quantité de colorant (kg) 5
Date de l'injection 1.7.1987
Heure de l'injection 12 : 30 : 00
Durée de l'injection (min) 2
Quantité d'eau injectée (l) 40
lieu de détection Dorfbach Alt St-J.
Coord lieu de détection 739755228700
Fréqu. des prélèvements 12 fois, 6 puis 3 fois par jour
Débit de la source (l/min) 57000
Taux de restitution % 17.63
Quantité d'eau injectée
Fichiers DATA
Fichier INPUT ALP18IN.DAT
Fichier OUTPUT ALP18OUTPUT.DAT
stockage des fichiers DISK SYQUEST 88KBOX
fonctions IN et OUTPUT

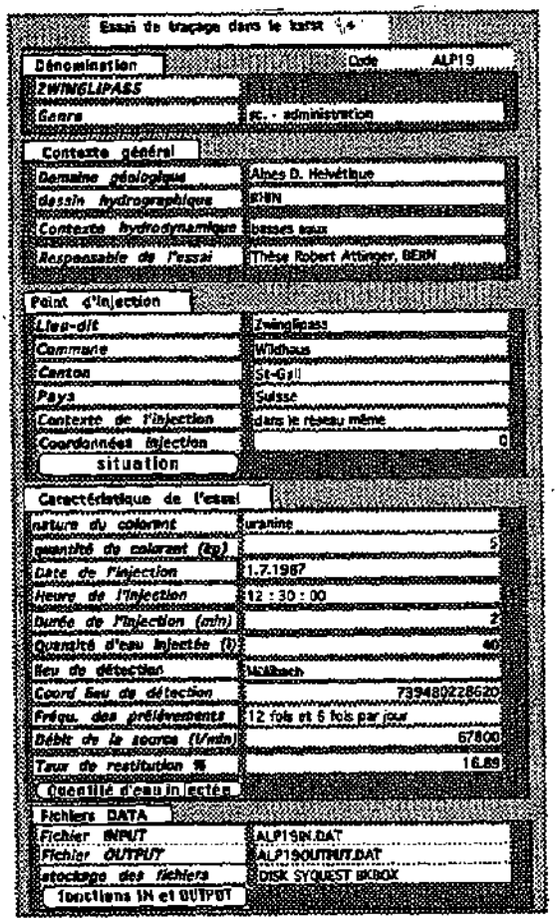

Essai de traçage dans le karst

Dénomination — Code: ALP19

ZWINGLIPASS

Genre: sc. - administration

Contexte général

Domaine géologique	Alpes D. Helvétique
Bassin hydrographique	RHIN
Contexte hydrodynamique	basses eaux
Responsable de l'essai	Thèse Robert Attinger, BERN

Point d'injection

Lieu-dit	Zwinglipass
Commune	Wildhaus
Canton	St-Gall
Pays	Suisse
Contexte de l'injection	dans le réseau même
Coordonnées injection	0

situation

Caractéristique de l'essai

nature du colorant	uranine
quantité de colorant (kg)	5
Date de l'injection	1.7.1987
Heure de l'injection	12 : 30 : 00
Durée de l'injection (min)	2
Quantité d'eau injectée (l)	40
lieu de détection	Mühlbach
Coord lieu de détection	739480228620
Fréqu. des prélèvements	12 fois et 6 fois par jour
Débit de la source (l/min)	67800
Taux de restitution %	16.89

Quantité d'eau injectée

Fichiers DATA

Fichier INPUT	ALP19IN.DAT
Fichier OUTPUT	ALP19OUTPUT.DAT
stockage des fichiers	DISK SYQUEST 88MB

fonctions IN et OUTPUT

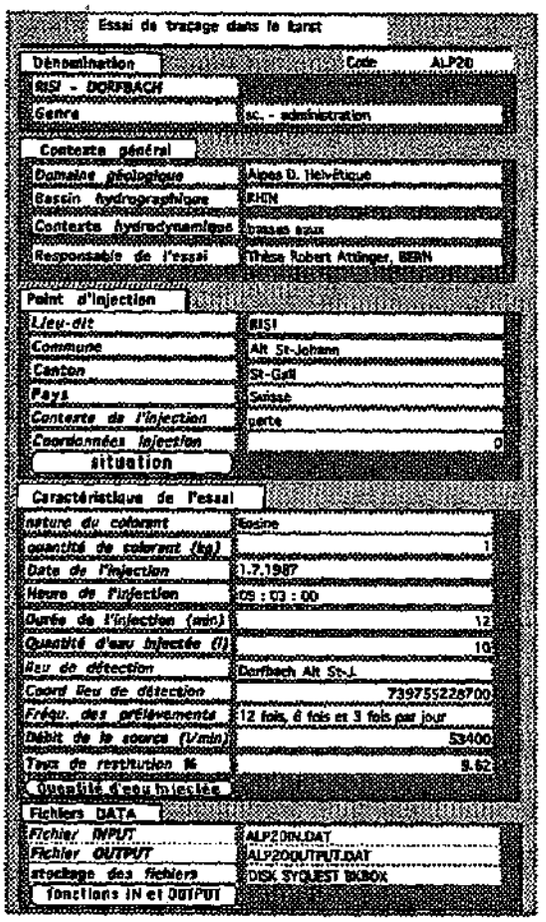

Essai de traçage dans le karst

Dénomination — Code: ALP20

BISI - DORFBACH

Genre: sc. - administration

Contexte général

Domaine géologique	Alpes D. Helvétique
Bassin hydrographique	RHIN
Contexte hydrodynamique	basses eaux
Responsable de l'essai	Thèse Robert Attinger, BERN

Point d'injection

Lieu-dit	BISI
Commune	Alt St-Johann
Canton	St-Gall
Pays	Suisse
Contexte de l'injection	perte
Coordonnées injection	0

situation

Caractéristique de l'essai

nature du colorant	Eosine
quantité de colorant (kg)	1
Date de l'injection	1.7.1987
Heure de l'injection	09 : 03 : 00
Durée de l'injection (min)	12
Quantité d'eau injectée (l)	10
lieu de détection	Dorfbach Alt St-J.
Coord lieu de détection	739755226700
Fréqu. des prélèvements	12 fois, 6 fois et 3 fois par jour
Débit de la source (l/min)	53400
Taux de restitution %	9.62

Quantité d'eau injectée

Fichiers DATA

Fichier INPUT	ALP20IN.DAT
Fichier OUTPUT	ALP20OUTPUT.DAT
stockage des fichiers	DISK SYQUEST 88MB

fonctions IN et OUTPUT

APPENDIX II.7

Datafiles of breakthrough curves of tracer tests

Ju1				Ju2		Ju3		Ju4		Ju5			
Time (min)	Conc. (mg/l)	Time (min)	Conc. (mg/l)	Time (min)	Conc. (mg/l)	Time (min)	Conc. (mg/l)	Time (min)	Conc. (mg/l)	Time (min)	Conc. (mg/l)	Time (min)	Conc. (mg/l)
0	1.10E-07	28100	1.10E-05	0	1.00E-10	1.98E+03	6.00E-05	4.08E+02	2.54E-03	-8.00E+01	1.80E-04	2.54E+04	8.00E-04
12720	1.10E-07	28400	1.00E-06	305	1.00E-10	2.30E+03	6.00E-05	1.30E+03	2.54E-03	1.20E+02	8.90E-04	2.69E+04	8.00E-04
12960	1.34E-07	24640	1.02E-05	1425	1.00E-10	3.42E+03	6.00E-05	1.54E+03	3.54E-03	2.40E+02	1.10E-03	2.84E+04	8.00E-04
13200	2.26E-07	28880	8.22E-06	1730	1.00E-10	3.76E+03	6.00E-05	2.40E+03	3.80E-02	6.00E+02	8.00E-05	2.98E+04	8.00E-04
13440	8.24E-07	27120	9.30E-06	2880	1.00E-10	4.86E+03	6.00E-05	2.65E+03	1.10E+01	1.35E+03	8.00E-05	3.13E+04	8.00E-04
13680	1.03E-06	27360	9.24E-06	3170	1.00E-10	5.16E+03	6.00E-05	2.90E+03	2.40E+01	1.38E+03	8.00E-05	3.28E+04	8.00E-04
13920	1.43E-06	27600	8.38E-06	4260	1.00E-10	6.30E+03	6.00E-05	3.39E+03	2.90E+01	1.44E+03	1.60E-04	3.42E+04	8.00E-04
14160	1.83E-06	27840	8.20E-06	4575	1.20E-09	6.60E+03	6.00E-05	4.01E+03	9.60E-01	1.50E+03	1.00E-04		
14400	5.03E-06	28080	8.02E-06	5750	3.10E-07	7.76E+03	6.00E-05	4.75E+03	4.00E-01	1.68E+03	1.90E-03		
14640	1.23E-05	28320	7.84E-06	6980	3.10E-07	8.95E+03	6.00E-05	5.46E+03	2.10E-01	1.80E+03	6.20E-02		
14880	1.37E-05	28560	7.66E-06	7195	1.89E-07	9.22E+03	1.20E-01	6.14E+03	8.70E-02	1.92E+03	4.30E-01		
15120	1.51E-05	28800	7.30E-06	7480	1.70E-07	9.50E+03	1.80E-01	6.80E+03	8.70E-02	2.04E+03	8.70E-01		
15360	1.85E-05	29040	7.08E-06	8605	6.20E-08	1.07E+04	2.50E-01	7.53E+03	2.80E-02	2.16E+03	8.50E-01		
15600	1.29E-05	29280	6.89E-06	8890	5.10E-08	1.21E+04	2.50E-02	8.40E+03	4.80E-02	2.28E+03	4.10E-01		
15840	2.86E-05	29520	6.71E-06	10080	2.40E-08	1.35E+04	6.60E-03	8.99E+03	1.84E-02	2.40E+03	2.60E-01		
16080	2.32E-05	29760	6.54E-06	10340	2.20E-08	1.63E+04	2.10E-03	9.65E+03	2.34E-02	2.55E+03	1.60E-01		
16320	2.34E-05	30000	6.36E-06	11495	1.30E-08	1.79E+04	1.90E-03	1.04E+04	2.82E-02	2.67E+03	1.00E-01		
16560	2.36E-05	30240	6.02E-06	11800	1.20E-08	1.93E+04	1.80E-03	1.13E+04	3.15E-02	2.79E+03	7.00E-02		
16800	2.38E-05	30480	5.20E-06	12055	9.00E-09	2.07E+04	1.80E-03	1.10E+04	1.40E-02	2.91E+03	4.80E-02		
17040	2.40E-05	30720	5.59E-06	13225	8.30E-09	2.22E+04	2.20E-03	1.27E+04	1.90E-02	3.03E+03	4.30E-02		
17280	2.40E-05	30960	5.38E-06	14350	8.20E-09	2.36E+04	3.00E-03	1.83E+04	1.44E-02	3.15E+03	3.20E-02		
17520	2.41E-05	31200	5.17E-06	15945	5.80E-09	2.51E+04	3.50E-03	1.42E+04	1.46E-02	3.27E+03	3.10E-02		
17760	2.43E-05	31440	4.97E-06	17225	4.00E-08	2.65E+04	2.00E-03	1.47E+04	1.10E-02	3.39E+03	2.60E-02		
18000	2.46E-05	31680	4.77E-06	18725	2.70E-09	2.80E+04	1.30E-03	1.59E+04	1.07E-02	3.51E+03	2.50E-02		
18240	2.47E-05	31920	4.59E-06	20130	1.90E-08	2.94E+04	8.00E-04	1.82E+04	8.30E-03	3.63E+03	1.90E-02		
18480	2.49E-05	32160	4.41E-06	21500	1.80E-09	3.08E+04	7.60E-04	1.71E+04	1.20E-02	3.75E+03	1.50E-02		
18720	2.35E-05	32400	4.23E-06	23020	1.20E-09	3.23E+04	7.30E-04	1.78E+04	5.80E-03	3.87E+03	1.10E-02		
18960	2.30E-05	32640	4.10E-06	24445	1.10E-08	3.66E+04	6.20E-04	1.85E+04	8.50E-03	4.14E+03	7.80E-03		
19200	2.30E-05	32880	3.93E-06	25835	8.60E-10	3.95E+04	8.20E-04			4.50E+03	5.80E-03		
19440	2.30E-05	33120	3.80E-06	27465	8.80E-10	4.23E+04	7.30E-04			4.86E+03	6.30E-03		
19680	2.30E-05	33360	3.80E-06	28800	8.60E-10					5.22E+03	3.90E-03		
19920	9.30E-05	33600	3.80E-06	30305	4.40E-10					5.78E+03	3.00E-03		
20160	2.37E-05	33840	3.80E-06	31680	3.20E-10					6.12E+03	3.50E-03		
20400	2.38E-05	34080	3.80E-06	33275	3.00E-09					6.48E+03	2.80E-03		
20640	2.37E-05	34320	3.00E-06	34660	2.70E-09					6.84E+03	1.90E-03		
20880	2.35E-05	34560	3.80E-06	37420	2.50E-09					7.20E+03	1.80E-03		
21120	2.32E-05	34800	3.80E-06	40305	1.80E-09					7.56E+03	1.30E-03		
21360	9.30E-05	35040	3.80E-06	43280	1.50E-09					7.99E+03	1.50E-03		
21600	2.16E-05	35280	3.80E-06	49150	1.00E-09					9.00E+03	1.00E-03		
21840	2.08E-05	35520	3.80E-06	51760	5.60E-10					9.72E+03	8.00E-04		
22080	2.00E-05	35760	3.80E-06	53250	8.60E-10					1.01E+04	8.00E-04		
22320	1.94E-05	36000	7.08E-06							1.12E+04	8.00E-04		
22560	1.88E-05	36240	8.42E-06							1.19E+04	8.00E-04		
22800	1.82E-05	36480	7.81E-06							1.26E+04	8.00E-04		
23040	1.85E-06	36720	7.15E-06							1.31E+04	8.00E-04		
23280	1.57E-06	36960	6.46E-06							1.34E+04	8.00E-04		
23520	1.55E-06	37200	6.82E-06							1.42E+04	8.00E-04		
23760	1.49E-05	36400	2.61E-06							1.48E+04	8.00E-04		
24000	1.45E-05	36640	1.65E-06							1.56E+04	8.00E-04		
24240	1.40E-05	39600	1.85E-06							1.63E+04	8.00E-04		
24480	1.40E-05	39840	1.84E-06							1.74E+04	8.00E-04		
24720	1.34E-05	40080	1.82E-06							1.84E+04	8.00E-04		
24960	1.29E-05	45120	1.14E-06							1.88E+04	8.00E-04		
25200	1.23E-05	50160	5.03E-07							1.97E+04	8.00E-04		
25440	1.17E-05	55200	4.01E-07							2.12E+04	8.00E-04		
25680	1.11E-05	60000	3.06E-07							2.28E+04	8.00E-04		
25920	1.10E-05	61080	2.73E-07							2.41E+04	8.00E-04		

T1outament				T2outament						T5outament		T5outament				T7outament		T5outament				T10outament	
Time (min)	Conc. (mg/l)	Time (min)	Conc. (mg/l)	Time (min)	Conc. (mg/l)	Time (min)	Conc. (mg/l)	Time (min)	Conc. (mg/l)	Time (min)	Conc. (mg/l)	Time (min)	Conc. (mg/l)	Time (min)	Conc. (mg/l)	Time (min)	Conc. (mg/l)	Time (min)	Conc. (mg/l)	Time (min)	Conc. (mg/l)	Time (min)	Conc. (mg/l)
80	-0.231	1261.2	34.214	90	0	1159.2	52.023	1771.2	5.78	0	0	25	0	845.78	10.5202	0	0	0	0	1100	16.2331	0	0
671.23	0	1271.2	30.289	547.2	0.231	1169.4	49.942	1781.4	5.78	120.9995	0.23121	256	6.46243	855.78	9.52859	50	0.22847	10	4.51E-06	1200	15.8409	346	0.26942?8
681.23	0.231	1281.2	29.595	557.6	0.462	1179.8	48.092	1791.6	5.548	150.9994	14.104	265.996	0.80364	865.76	9.36419	75	0.87778	18	2.23E-05	1300	14.6109	361	4.9179181
691.23	0.231	1291.2	28.902	567.8	0.925	1189.8	46.243	1801.6	5.318	175.9993	138.98	275.997	1.38726	875.76	8.67092	100	1.4752	20	5.52E-04	1400	12.6841	376	29.689017
701.23	0.694	1301.2	28.208	588	1.618	1200	44.393	1812	5.318	200.9992	280.925	285.998	2.31214	885.75	8.43931	110	2.52213	30	0.27934	1450	12.6039	391	21.306532
711.23	1.618	1311.2	27.746	598.2	2.543	1210.2	42.543	1822.2	5.087	225.9991	255.185	295.984	8.89943	895.74	7.74586	120	3.33362	40	0.4625	1500	11.4019	406	12.410405
721.23	2.543	1321.2	27.052	608.4	3.699	1220.4	40.894	1832.4	5.087	240.999	207.63	305.98	5.08871	905.74	7.51445	130	3.95007	50	0.88459	1600	9.27069	421	8.2787988
731.23	4.162	1331.2	26.358	618.6	5.549	1230.6	39.075	1842.6	4.855	250.998	171.561	315.978	8.93842	915.74	7.05202	140	4.72523	60	0.66838	1650	7.22952	439	5.3052023
741.23	5.78	1341.2	25.686	628.8	7.561	1240.8	37.457	1852.8	4.855	265.9989	122.081	325.977	9.01734	925.73	6.82084	150	5.10787	70	0.60357	1700	5.40813	451	3.7179181
751.23	8.009	1351.2	25.202	639	10.636	1251	35.636	1863	4.624	280.9988	83.9308	335.966	11.9205	935.73	6.5856	160	5.81047	80	0.47308	1800	3.35947	466	3.0803468
761.23	10.967	1361.2	24.74	649.2	13.542	1261.2	34.27	1873.2	4.624	290.9988	57.8035	345.964	13.4104	945.72	6.35838	170	6.43692	90	0.45648	1900	2.64859	481	2.3179181
771.23	14.104	1371.2	24.277	659.4	17.341	1271.4	32.601	1883.4	4.624	310.9988	43.8094	358.96	15.7225	955.72	6.12717	180	7.20147	100	0.31788	1950	1.79191	498	2.4242775
781.23	17.803	1381.2	23.815	669.6	21.227	1281.6	31.214	1893.6	4.624	325.9987	33.7572	365.958	16.6347	965.72	6.18407	190	8.02249	110	0.12256	2000	1.33811	511	0.8369942
791.23	21.985	1391.2	23.353	679.8	25.685	1291.8	29.827	1903.8	4.393	340.9986	27.2832	375.952	20.3466	975.71	5.95378	200	8.89544	120	0.22844	2200	0.80364	526	0.4057804
801.23	26.59	1401.2	22.89	690	30.52	1302	28.438	1914	4.393	350.9986	24.9775	385.948	22.4377	985.71	5.48133	210	9.3754	130	0.43704	2250	0.51337	541	0.2057804
811.23	31.445	1411.2	22.478	700.2	35.807	1312.2	27.052	1924.2	4.393	381.9986	18.4971	395.944	24.2775	995.7	5.48133	220	10.1264	140	0.84729	2300	0.25121	1728	0
821.23	36.532	1421.2	21.965	710.4	40.925	1322.4	25.895	1934.4	4.162	370.9985	20.1156	405.94	26.3584	1005.7	5.48133	230	10.9814	150	1.30606	2350	0.33E-02		
831.23	41.816	1431.2	21.503	720.6	46.249	1332.6	24.74	1944.6	4.162	380.9985	18.7283	415.939	28.2081	1105.7	5.87283	240	11.5798	160	2.158	2330	0.10564		
841.23	46.705	1441.2	21.04	730.8	51.782	1342.8	23.584	1954.8	4.162	390.9984	17.8035	425.932	28.9709	1215.6	3.00578	250	12.3798	170	2.82471	2340	7.80E-03		
851.23	51.792	1451.2	20.578	741	57.341	1353	22.428	1965	4.162	400.9984	17.1098	435.929	31.4451	1315.6	2.54333	260	13.1405	180	3.75344	2343	1.75E-03		
861.23	56.416	1461.2	20.347	751.2	62.859	1363.2	21.503	1975.2	3.931	425.9983	15.2601	445.924	32.8324	1405.5	1.90751	270	13.6938	190	4.70135	2411	0.00E+00		
871.23	60.869	1471.2	19.884	761.4	67.748	1373.4	20.578	1985.4	3.931	450.9982	13.6728	455.97	30.269	1505.5	1.6783	280	14.6465	200	5.47208				
881.23	65.202	1481.2	19.422	771.6	72.832	1383.6	19.422	1995.6	3.931	475.9981	12.2168	465.918	35.1445	1605.5	1.7341	290	15.4356	210	8.74978				
891.23	69.871	1491.2	18.96	781.8	77.457	1393.8	18.728	2005.8	3.699	500.998	11.2919	475.912	36.0694	1705.4	1.27168	300	16.0591	220	7.01348				
901.23	71.808	1501.2	18.776	792	81.818	1404	17.803	2016	3.699	550.9978	10.8671	485.908	35.9942	1805.4	0.80925	310	16.6831	230	7.7842				
911.23	74.451	1511.2	18.647	802.2	85.549	1414.2	17.41	2026.2	3.699	575.9977	10.8359	495.904	37.6879	1905.3	0.46243	320	17.3287	240	8.55214				
921.23	78.532	1521.2	15.079	812.4	88.789	1424.4	18.185	2036.4	3.699	825.9975	9.47077	505.9	38.2081	1905.3	0.23121	330	17.8023	250	9.09491				
931.23	78.362	1531.2	13.41	822.6	91.782	1434.6	15.723	2046.6	3.468	850.9974	8.78512	515.896	38.2081	4514.3	0	350	18.5184	260	9.64354				
941.23	79.306	1701.2	12.023	832.8	94.538	1444.8	15.029	2197.8	3.237	867.9972	9.24855	525.892	38.2081			375	19.0329	270	10.2304				
951.23	80.231	1751.2	10.867	843	96.416	1455	14.335	2148.6	3.006			535.888	32.7457			400	19.0329	280	10.7037				
961.23	80.231	1801.2	9.942	853.2	98.035	1465.2	13.873	2220	2.775			545.884	37.052			425	18.6401	290	11.0589				
971.23	80	1851.2	8.249	863.4	99.191	1475.4	13.179	2260.8	2.543			555.88	36.1272			450	17.6879	300	11.607				
981.23	79.306	1901.2	8.555	873.6	99.884	1485.6	12.737	2322	2.312			565.878	34.4711			475	16.6531	310	11.7865				
991.23	78.362	2001.2	7.398	883.8	100.847	1495.8	12.264	2373	2.081			575.872	33.815			500	16.2178	320	12.1519				
1001.2	76.994	3001.2	2.081	894	100.347	1506	11.792	2424	1.85			585.888	32.4277			525	15.4352	330	12.4855				
1011.2	75.376	4001.2	1.618	904.2	100.116	1516.2	11.329	2506.8	1.618			595.884	31.5028			550	14.477	350	12.9734				
1021.2	73.757	5001.2	1.387	914.4	99.422	1526.4	10.867	2566.8	1.387			605.88	30.1158			575	13.3053	375	13.5088				
1031.2	71.445	6001.2	0.694	924.6	98.497	1536.6	10.636	2646.4	1.156			615.859	28.9605			600	11.7317	400	14.4786				
1041.2	69.364	7001.2	0.462	934.8	97.341	1546.8	10.173	2719.8	0.925			625.857	27.6035			625	10.5979	425	15.0296				
1051.2	67.283	8001.2	0.231	945	95.954	1557	9.942	2832	0.694			635.848	26.6474			650	9.63008	450	15.4913				
1061.2	64.971	9001.2	0.231	955.2	94.335	1567.2	9.48	2843.9	0.925			645.844	25.7295			700	7.53097	475	15.9536				
1071.2	62.859	10061	0.462	965.4	92.486	1577.4	9.249	3018.6	0.694			655.84	24.5465			750	5.15879	500	16.4167				
1081.2	60.347			975.6	90.635	1587.6	9.017	3180	0.231			665.836	23.6418			800	3.59978	525	16.8758				
1091.2	57.803			985.8	88.555	1597.8	8.786	3109.2	0.462			675.832	22.7188			875	2.94062	550	17.1185				
1101.2	55.793			996	86.474	1608	8.555	3729.8	0.231			685.826	21.7918			875	1.96359	575	17.3983				
1111.2	53.842			1000.2	84.162	1618.2	8.324					695.824	21.0083			900	1.65705	600	17.6641				
1121.2	51.792			1016.4	82.081	1628.4	8.092					705.82	20.4624			1000	0.82778	625	16.2146				
1131.2	49.842			1028.9	80	1638.6	7.861					715.816	19.7866			1025	0.50827	650	15.3237				
1141.2	48.324			1038.6	77.668	1648.8	7.83					725.812	19.0751			1050	7.54E-02	675	19.3237				
1151.2	46.705			1047	76.376	1659	7.399					735.809	18.3815			1100	0.00E+00	700	18.3938				
1161.2	45.087			1057.2	73.064	1669.2	7.168					745.804	17.9191			1111	0.00E+00	725	18.1859				
1171.2	43.488			1067.4	70.063	1679.4	7.168					755.8	17.2254					750	18.0895				
1181.2	42.081			1077.6	68.671	1689.6	6.936					765.798	16.3006					775	17.9613				
1191.2	40.804			1087.8	66.59	1699.8	6.705					775.792	15.6058					800	17.7778				
1201.2	38.308			1098	64.277	1710	6.474					785.788	14.9135					825	17.6301				
1211.2	37.019			1108.2	62.197	1720.2	6.474					795.784	13.9884					850	17.5483				
1221.2	36.994			1118.4	60.116	1730.4	6.243					805.78	13.2948					875	17.3980				
1231.2	35.838			1128.6	58.035	1740.6	6.243					815.778	12.3699					900	17.1139				
1241.2	34.451			1138.8	56.054	1750.8	6.012					825.772	11.0076					950	18.3812				
1251.2	32.139			1149	53.873	1761	5.78					835.769	10.3827					1000	17.1071				

T11outsmnt				T12outsmnt				T14outsmnt				T15outsmnt				T18outsmnt		T19outsmnt	
Time (min)	Conc. (mg/l)	Time (min)	Conc. (mg/l)	Time (min)	Conc. (mg/l)	Time (min)	Conc. (mg/l)	Time (min)	Conc. (mg/l)	Time (min)	Conc. (mg/l)	Time (min)	Conc. (mg/l)	Time (min)	Conc. (mg/l)	Time (min)	Conc. (mg/l)	Time (min)	Conc. (mg/l)
540	0	1852.5	1.1560894	180	0.346821	810	2.85895954	1440	0.80924855	405	0.5780347	1305	11.445087	0	0	635.997	5.9832701	6	0.2312139	60	0
855.3	0.231214	1894.5	0.9248555	190.5	0.346821	820.5	1.73410405	1450.5	0.80924855	423	3.3526012	1323	10.751445	945.999	2.9816351	845.997	5.9832701	36	0.2312139	210	1.8184971
867	3.809422	1905	0.9248555	201	0.346821	831	1.50289017	1461	0.80924855	436	10.260017	1336	10.289017	255.999	2.9816351	855.997	5.9832701	60	-1.387283	240	35.83815
897.5	5.080705	1915.5	1.1560894	291.5	0.346821	841.5	2.42774566	1471.5	0.80924855	453	23.00578	1353	9.6705896	285.999	5.9449052	865.997	5.9832701	96	0.2312139	270	66.011561
709	6.936416	1926	0.9248555	222	0.346821	852	1.50289017	1482	0.57803468	466	41.965318	1366	9.3641618	275.999	11.02954	875.997	5.9832701	126	0.2312139	300	82.774567
739.5	9.942197	1938.5	0.9248555	232.5	0.346821	862.5	2.42774566	1492.5	0.57803468	483	66.473988	1383	9.139449	285.999	26.834716	885.997	5.9832701	156	0	330	76.375723
750	10.40462	1947	0.3872502	243	0.115607	873	2.42774566	1503	0.80924855	496	93.767776	1396	7.2832247	295.999	44.724529	895.996	5.9832701	168	0	360	64.16185
750.5	10.66705	1989	0.3872839	253.5	0.346821	883.5	2.19653179	1513.5	0.80924855	513	122.65896	1413	6.4393064	305.999	68.577607	906.996	5.9832701	216	-1.387283	390	90.404624
702	11.79191	1999.5	0.3872502	264	0.115607	894	2.19653179	1524	0.57803468	526	150.17341	1426	6.5895954	315.999	92.430687	915.996	5.9832701	246	0	420	84.855491
802.5	12.25434	2010	1.1560894	274.5	0.346821	904.5	2.19653179	1534.5	0.57803468	543	178.76301	1443	7.5144509	326.999	118.38277	926.998	2.9816351	276	-1.387283	450	72.138706
834	13.64162	2020.5	1.1560894	285	0.346821	915	1.96531792	1545	0.57803468	558	201.27168	1458	5.8959538	335.999	140.13685	935.998	2.9816351	306	0	480	58.49711
844.5	13.87283	2062.5	0.9248555	295.5	0.115607	925.5	1.96531792	1555.5	0.57803468	573	223.46821	1473	6.8208093	345.999	159.08339	945.998	2.9816351	336	0	510	46.786127
876	15.0289	2094	1.1560894	306	0.115607	936	2.19653179	1566	0.57803468	588	243.81503	1488	6.5895954	355.999	181.00829	955.998	2.9816351	366	0.2312139	540	42.312139
886.5	15.26012	2104.5	1.1560894	316.5	0.115607	946.5	1.96531792	1576.5	0.57803468	603	264.84971	1503	4.8710983	365.999	183.86993	965.998	2.9816351	396	3.9306358	570	36.812717
918	15.95376	2125.5	0.9248555	327	0.115607	957	2.19653179	1587	0.57803468	618	277.34104	1518	4.5086705	375.999	158.02688	975.998	2.9816351	426	29.901734	600	25.83815
926.3	16.18497	2138	1.1560894	337.5	0.115607	967.5	2.19653179	1597.5	0.34682081	633	290.52023	1533	6.0647399	385.998	152.06336	985.998	5.9832701	456	63.583815	630	34.682081
960	15.6474	2146.5	0.9248555	348	0.578035	978	1.73410405	1608	0.57803468	648	300.46243	1548	4.0462428	395.998	140.13685	1395.99	2.9816351	480	66.329699	660	34.682081
970.5	16.87861	2157	0.9248555	358.5	1.271676	988.5	1.73410405	1618.5	0.57803468	663	308.03642	1563	5.2023121	405.998	128.21031	1275.99	5.9832701	516	98.184971	690	34.913295
981	16.87861	2167.5	1.1560894	369	2.427746	999	1.73410405	1629	0.57803468	678	309.24855	1578	4.8710983	415.998	118.29377	1285.99	2.9816351	546	90.867052	720	34.450867
1012.5	17.34104	2180	1.1560894	378.5	3.352601	1008.5	1.73410405	1639.5	0.57803468	693	307.16763	1593	4.8710983	425.998	104.35723	1005.99	2.9816351	576	80.924855	750	34.682081
1023	17.57225	2209.5	1.1560894	390	4.508671	1020	1.73410405	1650	0.34682081	708	309.23121	1608	4.7398844	435.998	92.430687	1405.99	5.9832701	606	69.82659	780	31.213873
1054.5	17.57225	2220	1.1560894	400.5	5.893064	1030.5	1.73410405	1660.5	0.57803468	723	287.20324	1623	4.7398844	445.998	80.504147	1415.99	2.9816351	630	58.959538	810	26.901734
1065	17.80347	2283	0.6936416	411	7.052023	1041	1.50289017	1671	0.57803468	738	268.78613	1638	4.5086705	455.998	71.339242	1645.99	0	666	49.042197	840	23.121387
1096.5	17.57225	2293.5	0.4624278	421.5	7.978879	1051.5	1.73410405	1681.5	0.57803468	753	249.12717	1653	4.5086705	465.998	62.514336	1655.99	2.9816351	695	49.080925	870	25.202312
1107	17.34104	2304	0.4624278	432	8.67052	1062	1.50289017	1692	0.34682081	768	220	1668	4.5086705	475.998	56.651068	1665.99	0	726	35.83815	900	22.880173
1136.3	18.87861	2314.5	1.1560894	442.5	9.132948	1072.5	0.80924855	1702.5	0.34682081	783	192.94798	1683	4.2774567	485.998	50.867798	1035.99	2.9816351	750	30.751445	930	20.809249
1149	18.6474	2325	0.9248555	453	9.393378	1083	1.50289017	1713	0.57803468	798	166.5896	1698	2.8901734	495.998	44.394526	2385.99	0	786	26.127168	960	19.026902
1180.5	19.95376	2335.5	1.1560894	463.5	9.364162	1093.5	1.2716763	1723.5	0.57803468	813	141.6185	1713	4.0462428	505.999	38.781258	2435.99	2.9816351	816	22.196532	990	11.791908
1212	13.49133	2348	1.3872839	474	9.364162	1104	1.2716763	1734	0.57803468	828	117.57225	1728	4.0462428	515.998	35.779621	2445.99	0	846	18.959538	1020	9.8421965
1222.8	18.26012	2386.5	0.9248555	484.8	8.901734	1114.8	1.2716763	1744.5	0.57803468	843	100	1743	3.4682081	525.998	32.307968	2465.99	2.9816351	876	18.184971	1050	8.7861272
1254	13.87283	2440	1.1560894	495	8.901734	1125	1.2716763	1755	0.34682081	858	84.277457	1758	2.4277457	535.998	28.834716	2475.99	0	906	13.641618	1080	6.0924856
1264.5	13.4104	2419.5	0.9248555	505.5	8.439306	1135.5	1.2716763	1765.5	0.57803468	873	71.32948	1773	3.8150289	545.998	26.834716			926	11.791908	1110	9.2485548
1296	12.02312	2430	1.1560894	518	8.439306	1148	1.04046243	1776	0.57803468	888	60	1788	2.1965318	555.998	23.853081			966	10.17341	1140	7.1676301
1306.5	11.56069	2481	0.9248555	526.8	8.208092	1156.5	1.2716763	1788.5	0.57803468	903	52.136728	1803	3.583815	565.998	20.871448			996	9.017341	1170	6.9364162
1317	10.86705	2484.5	1.1560894	537	7.978879	1167	1.2716763	1797	0.34682081	918	47.514451	1818	1.9653179	575.998	20.671446			1026	8.0346994	1200	5.4739884
1348.5	9.248555	2472	0.6936416	547.5	7.978879	1177.5	1.2716763	1807.5	0.34682081	933	43.921387	1833	3.3526012	585.998	17.88961			1056	7.8612717	1230	6.0115607
1359	8.786127	2493	0.9248555	558	7.283237	1188	0.80924855	1818	0.57803468	948	39.421965	1848	2.3526012	595.998	17.88081			1086	7.3068436	1260	5.549133
1390.5	6.936416	2503.5	0.9248555	568.5	7.978879	1196.5	1.2716763	1826.5	0.57803468	963	35.028902	1863	3.1213873	605.998	14.908175			1116	7.1676301	1290	5.3179191
1401	6.473988	2514	0.5078416	579	7.745665	1208	1.2716763	1838	0.57803468	978	32.710783	1878	3.1213873	615.998	14.908175			1146	6.4739884	1320	4.8554913
1411.5	6.011561	2524.5	0.9248555	589.5	7.514451	1218.8	1.2716768	1848.5	0.34682081	993	32.485549	1893	1.5028902	625.998	11.02654			1176	6.0115607	1350	4.3930636
1443	4.393064			600	7.283237	1230	1.04046243	1860	0.34682081	1008	29.479769	1908	1.5028902	635.997	11.02654			1206	5.0867052	1380	3.9306358
1474.5	3.238994			610.5	7.052023	1240.5	1.2716763	1870.5	0.34682081	1023	29.710983	1923	2.8901734	645.997	11.02654					1410	3.699422
1485	2.774566			621	6.820809	1251	1.2716763	1881	0.57803468	1038	28.554913	1938	2.8901734	655.997	11.02654					1440	3.699422
1518.5	2.080925			631.5	6.358382	1261.5	1.04046243	1891.5	0.57803468	1053	26.242775	1953	2.0589595	665.997	11.02654					1470	3.2369942
1527	1.849711			642	5.895954	1272	1.04046243	1902	0.57803468	1068	25.780347	1968	2.4566595	675.997	11.02654					1500	3.0057804
1537.5	2.080925			652.5	5.433526	1282.5	1.04046243	1912.5	0.57803468	1083	25.780347	1983	1.0404624	685.997	8.8449052					1530	2.7745665
1558	1.618497			663	4.971098	1293	1.2716763	1923	0.57803468	1098	24.653491	1998	2.0589595	695.997	8.8449052					1560	2.7745665
1578.5	1.618497			673.5	4.739884	1303.5	1.04046243	1933.5	0.57803468	1113	24.16185	2013	2.4277457	705.997	8.8449052					1590	2.5433526
1599	1.618497			684	4.277457	1314	1.04046243	1944	0.57803468	1128	21.849711	2028	2.4277457	715.997	8.8449052					1620	2.5433526
1621.5	1.387283			694.5	4.046243	1324.5	1.04046243	1954.5	0.34682081	1143	22.312139	2043	2.1965318	725.997	8.8449052					1650	2.5433526
1632	1.387283			705	3.815029	1335	1.04046243	1965	0.34682081	1158	21.156069	2058	2.1965318	735.997	8.8449052					1680	2.3121387
1642.5	1.387283			715.5	3.583815	1345.5	1.04046243	1975.5	0.57803468	1173	18.843931	2073	0.8092486	745.997	8.8449052					1690	2.3121387
1674	1.156069			726	3.352601	1356	0.80924855	2039.5	0.34682081	1188	19.075145	2088	2.1965318	755.997	8.8449052					1830	2.0809249
1695	1.387283			736.5	3.352601	1366.5	1.04046243	2175	0.57803468	1203	17.919075	2103	1.9653179	765.997	8.8449052					2060	1.849711
1705.9	1.156068			747	2.890173	1377	1.04046243	2185.5	0.34682081	1218	10.353006	2118	0.5780347	775.997	5.9832701					2090	1.849711
1758	1.156069			757.5	3.121387	1387.5	0.80924855	2236	0.11560694	1233	15.606936	2208	0.1156069	785.997	5.9832701					2120	1.849711
1810.5	1.156069			768	2.890173	1398	0.57803468	2246.5	0.34682081	1248	14.682081	2223	0.1156069	795.997	5.9832701					2150	1.849711
1821	-1.15607			778.8	2.890173	1408.5	1.04046243	2301	0.34682081	1263	13.757225	2238	0.1156069	805.997	5.9832701					2160	1.6184971
1831.5	0.924855			780	2.65896	1419	1.04046243	2406	0.11560694	1278	12.83237	2253	1.2716763	815.997	5.9832701					2210	2.7745665
1842	1.156069			799.5	2.65896	1429.5	0.80924855			1293	12.136778			825.997	5.9832701					2240	3.4682081

		T20outlament				T23outlament						T24outlament				T25outlament				T26outlament	
Time (min)	Conc. (mg/l)	Time (min)	Conc. (mg/l)	Time (min)	Conc. (mg/l)	Time (min)	Conc. (mg/l)	Time (min)	Conc. (mg/l)	Time (min)	Conc. (mg/l)	Time (min)	Conc. (mg/l)	Time (min)	Conc. (mg/l)	Time (min)	Conc. (mg/l)	Time (min)	Conc. (mg/l)	Time (min)	Conc. (mg/l)
2270	3.4662081	0	0	1800	0.0358387	0	0	918.7	4.4099817	2538.7	1.0838088	1	-0.346821	201	158.0347	0	0	1702.1	2.1387263	0	0.12584
2280	3.2369942	30	0.040133	1836	0.0849711	69.9	0.0461168	933.7	4.1900465	2553.7	-0.372495	63	0.8092486	203	149.711	22.1	1.818497	1822.1	2.6011561	12	1.783439
2330	3.2369942	60	0.0962659	1860	0.2716763	79.9	2.3665324	946.7	2.5828281	2568.7	-0.592133	65	1.0404624	205	148.9306	52.1	0	1852.1	1.4450867	42	3.038217
2380	3.2369942	90	-0.083815	1890	0.3208093	89.9	38.911603	963.7	3.7501762	2583.7	0.8064289	67	-0.578035	207	137.2254	82.1	0	1882.1	3.0635838	72	2.287994
2390	3.2369942	120	-0.285896	1920	0.3699422	99.9	147.5034	978.7	3.5302411	2598.7	0.8177076	69	1.2716763	209	122.5145	112.1	0	1912.1	2.6011561	102	80.38217
2420	3.0057804	150	-1.604046	1950	0.4190751	109.9	275.46595	993.7	1.6818068	2613.7	0.8289863	91	0.1156069	211	124.7309	142.1	-0.231214	1942.1	2.8323699	132	32.10191
2450	3.0057804	180	-0.398844	1980	0.2369942	119.9	339.0859	1008.7	2.827943	2628.7	0.840265	93	0.8092486	213	117.1098	172.1	1.387283	1972.1	2.6011561	162	14.52229
2480	3.0057804	210	-0.118497	2010	0.2891272	129.9	336.14166	1023.7	1.9455861	2643.7	0.8515436	95	3.3526012	215	109.711	202.1	0	2002.1	2.6011561	192	7.688089
7510	2.7745665	240	-0.300578	2040	0.1040462	139.9	287.52291	1038.7	0.1071679	2658.7	0.8828225	97	3.3526012	217	102.6301	232.1	1.387283	2032.1	2.3699422	222	3.057325
2540	2.7745665	270	10.163479	2070	-0.309248	148.8	282.7365	1156.7	0.4285918	2673.7	-0.513482	99	5.2023121	219	100.9249	262.1	1.387283	2062.1	1.9075145	252	2.547771
2570	2.7745665	300	150.08827	2100	-0.026907	159.9	186.27379	1306.7	0.7725927	2688.7	0.8853799	101	10.057804	221	98.06936	292.1	1.387283	2092.1	1.4450867	282	2.602548
2600	2.7745665	330	421.34971	2130	0.0202312	169.7	106.69143	1456.7	-0.501903	2703.7	0.8866587	103	12.601156	223	96.43931	322.1	-0.231214	2122.1	1.4450867	312	0.254777
2630	2.5433526	360	631.80347	2160	0.0693642	198.7	69.533343	1713.7	0.8459044	2718.7	0.9078374	105	17.456647	225	84.73988	352.1	-0.231214	2152.1	-0.466524	342	2.038217
2660	2.5433526	390	885.95666			213.7	50.122656	1788.7	1.1335419	2733.7	0.9182161	107	23.930636	227	70.65318	382.1	1.156069	2182.1	1.2138728	372	1.019108
2690	2.5433526	420	573.40462			228.7	40.181736	1848.7	0.2537713	2748.7	-0.456788	109	32.254335	229	78.03468	412.1	-0.462428	2212.1	0.882659	402	0.509554
2720	2.3121387	450	449.48532			243.7	33.497815	1863.7	0.26605	2763.7	-0.576724	111	43.121387	231	75.49153	442.1	-0.462428	2242.1	0.982659	432	0.764331
2750	2.3121387	480	293.50289			258.7	27.497535	1878.7	0.2763268	2778.7	0.8530523	113	59.306358	233	72.09312	472.1	0.231214	2272.1	0.982659	462	0.584213
2780	2.3121387	510	241.23988			273.7	24.271817	1893.7	0.8748007	2793.7	-0.654168	115	80.346555	235	68.09249	502.1	4.707868	2302.1	0.6936416		
2810	2.0809249	540	154.67283			288.7	21.739743	1908.7	0.2988862	2808.7	-0.642887	117	87.052023	237	67.88127	532.1	25.60894	2332.1	0.6936416		
2840	2.0809249	570	145.15318			303.7	21.288594	1923.7	1.8974482	2823.7	-0.831609	119	104.84971	239	64.62428	562.1	92.36994	2362.1	0.8930418		
2870	0.4624278	600	88.783005			318.7	18.052879	1938.7	0.3214437	2838.7	0.5357394	121	119.88439	241	59.07514	592.1	97.74586	2392.1	0.6936416		
2900	1.849711	630	83.690751			333.7	16.305371	1953.7	1.7200056	2853.7	0.5470182	123	138.81272	243	59.30836	622.1	125.9538	2422.1	0		
3020	0.2312139	660	51.092121			348.7	17.150581	1968.7	1.5000705	2868.7	0.5562869	125	157.57225	245	54.91329	652.1	137.052	2452.1	0.2312139		
3050	1.6184971	690	36.738994			363.7	18.247004	1983.7	1.5113402			127	170.07515	247	52.13873	682.1	134.2775				
3080	1.6184971	720	30.774667			378.7	13.946144	1998.7	1.5226279			129	188.72832	249	51.6763	712.1	103.9884				
3110	1.3872832	750	24.580926			393.7	14.651064	2013.7	1.5338067			131	218.84393	251	48.20809	742.1	78.24277				
3140	1.1560694	780	22.540133			408.7	14.431129	2028.7	1.5451854			133	232.71676	253	48.38418	772.1	60.28682				
3170	-0.231214	810	20.288127			423.7	13.748786	2043.7	1.5564641			135	251.6763	255	44.27746	802.1	50.34682				
3200	1.1560694	840	16.835836			438.7	13.297817	2058.7	1.5677428			137	262.54335	257	41.50289	832.1	45.64182				
3230	1.1560694	870	15.287686			453.7	11.459185	2073.7	1.5790215			139	282.19653	259	41.7341	862.1	39.01734				
3290	0.9248555	900	10.260116			468.7	10.776822	2088.7	1.5903003			141	295.37572	261	40.57803	892.1	33.46821				
3320	0.9248555	930	10.309248			483.7	11.04417	2103.7	1.601579			143	308.23121	263	37.10983	922.1	27.88786				
3350	0.9248555	960	7.1213873			498.7	11.493021	2118.7	1.3616439			145	309.24856	265	36.41819	952.1	20.76145				
3380	0.9248556	990	6.2456647			513.7	0.854589	2133.7	1.3020226			147	314.79769	267	37.57225	982.1	16.35838				
3410	-0.693642	1020	6.5260116			528.7	9.70344	2148.7	1.4042013			149	310.10075	269	35.40133	1012.1	13.66382				
3440	-0.693642	1050	8.1936416			543.7	10.370788	2163.7	1.41548			151	320.80925	271	35.49133	1042.1	12.19853				
3470	0.9248555	1080	7.549133			558.7	6.6826448	2178.7	1.1955449			153	321.50260	273	32.46555	1072.1	13.19139				
3500	0.6936416	1110	6.0734104			573.7	8.8309176	2193.7	-0.18046			155	320.80925	275	34.33526	1102.1	10.88268				
3850	0.4624278	1140	5.7978079			588.7	9.7109627	2208.7	-0.169181			157	318.95954	277	32.25434	1132.1	10.0578				
3980	0.2312139	1170	5.1531792			603.7	8.1037643	2223.7	-0.157992			159	314.78769	279	28.71098	1162.1	8.62556				
3920	0.2312139	1200	4.7388844			618.7	9.5073262	2238.7	-0.146823			161	308.55491	281	32.02312	1192.1	9.364162				
3950	0.2312139	1230	3.8641618			633.7	9.2823911	2253.7	1.2519385			163	305.08671	283	31.79191	1222.1	8.901734				
4040	0.2312139	1260	1.8323699			648.7	9.0624559	2268.7	1.2832172			165	299.53757	285	30.3237	1252.1	10.0578				
		1290	1.1878613			663.7	9.0737347	2283.7	1.274486			167	290.98266	287	27.59884	1282.1	8.208092				
		1320	2.8558949			678.7	8.8537995	2298.7	1.0545508			169	284.9711	289	27.59884	1312.1	9.595376				
		1350	2.4421965			693.7	7.477795	2313.7	-0.321444			171	277.34104	291	27.18783	1342.1	7.514451				
		1380	2.2801158			708.7	7.2578599	2328.7	1.3083321			173	269.24855	293	28.3237	1372.1	8.67052				
		1410	2.0780347			723.7	8.4252070	2343.7	-0.998866			175	260	295	26.24277	1402.1	6.589595				
		1440	1.6059538			738.7	7.9740589	2358.7	1.0996757			177	253.98644	297	25.78035	1432.1	6.358382				
		1470	1.7138728			753.7	8.3668405	2373.7	1.1109545			179	243.12139	299	26.54013	1462.1	7.514451				
		1500	1.5317919			768.7	7.5341886	2388.7	1.1222332			181	235.49135	301	23.69942	1492.1	5.80474				
		1530	1.349711			783.7	7.3142535	2403.7	-0.253771			183	228.55491	303	23.23688	1522.1	5.209312				
		1560	1.1676301			798.7	7.0943183	2418.7	1.1447906			185	217.88786	305	22.77457	1552.1	4.971098				
		1590	0.9855491			813.7	8.4871	2433.7	1.1660694			187	212.63237	307	22.31214	1582.1	6.358382				
		1620	1.0346821			828.7	6.4232342	2448.7	1.187348			189	202.89017	309	21.84971	1612.1	4.508671				
		1650	0.8528612			843.7	6.203209	2463.7	-0.206556			191	194.10405	311	23.23699	1642.1	4.277457				
		1680	0.9017361			858.7	5.75215	2478.7	0.9566917			193	188.65491	414.864	17.6115	1672.1	3.815029				
		1710	0.9506671			873.7	5.8137177	2493.7	-0.417312			195	182.08093	600	10.3642	1702.1	4.913295				
		1740	0.7687881			888.7	5.0610858	2508.7	0.9612491			197	173.75723	990	3.0312	1732.1	3.063584				
		1770	0.5867052			903.7	4.6299168	2523.7	-0.596755			199	163.81503	1080	0	1762.1	2.801156				

T29outlet		T30outlet				T32outlet		T34outlet		T35outlet		T36outlet		T39outlet		T40outlet		T41outlet			
Time (min)	Conc. (mg/l)	Time (min)	Conc. (mg/l)	Time (min)	Conc. (mg/l)	Time (min)	Conc. (mg/l)	Time (min)	Conc. (mg/l)	Time (min)	Conc. (mg/l)	Time (min)	Conc. (mg/l)	Time (min)	Conc. (mg/l)	Time (min)	Conc. (mg/l)	Time (min)	Conc. (mg/l)	Time (min)	Conc. (mg/l)
0	0.123546	0	0.123546	1772	2.292994	0	0	0	0.254862	0	0	0	0.254862	0	0	0	3.63E-01	0	0	827	1.640711
5	5.2228299	2	5.350316	1809	2.502548	34	0	3	0.764331	12	0	839	0.348821	21	0.057803	10	1.39E+02	28	10.635838	857	1.6184071
86	2.9299353	32	5.859873	1832	2.292994	64	68.34241	33	0.509554	27	0	869	0.578035	51	0.115607	20	3.06E+02	31	42.312139	887	1.649711
95	3.9200393	62	5.350316	1852	2.292994	84	268.5021	63	0.254777	42	0	880	0.578035	61	0.17341	30	4.73E+02	36	166.01156	917	2.0609249
125	4.2038217	92	6.11465	1892	2.547771	124	68.49539	93	0.509554	57	0	729	0	111	0.057803	40	5.37E+02	41	533.41041	947	1.3872832
155	8.0445860	122	5.605096	1922	2.292994	154	52.92528	123	0.509554	72	0	759	0.231214	141	0.115607	50	5.32E+02	46	640.02486	972	1.1580904
185	80.382166	152	5.095541	1952	2.292994	184	32.34121	153	0.509554	87	0	789	0.462429	171	0.115607	60	5.28E+02	51	563.46821	1007	1.3872832
215	123.68427	182	2.547771	1982	3.057325	214	29.81949	183	0.509554	102	0	819	0.693642	201	0.17341	70	4.76E+02	56	527.63008	1037	1.1560904
245	141.27380	212	5.095541	2012	3.057325	244	15.10241	213	0.764331	117	0	849	1.618497	231	0.057803	80	3.94E+02	61	407.39889	1067	1.1568504
275	145.85907	242	5.350316	2042	3.057325	274	8.419927	243	0.764331	132	0	879	3.930636	261	0.115607	90	3.11E+02	66	367.63008	1097	0.9248555
305	138.47134	272	5.095541	2072	3.057325	304	4.811387	273	0.764331	147	0	909	6.554913	291	0.057803	100	2.50E+02	71	329.01734		
335	131.69236	302	3.566879	2102	4.33121	334	3.875839	303	0.509554	327	9.526963	939	15.26012	321	0.057803	110	2.02E+02	76	207.34104		
365	118.09917	332	12.48408	2132	3.699266	364	3.207591	333	0.764331	357	1.027728	969	29.43931	351	0.115607	120	1.54E+02	81	274.68208		
395	91.647134	362	37.86178	2162	3.566879	394	2.139394	363	0	387	2.089341	000	45.85549	381	0.115607	130	1.22E+02	86	301.50269		
425	79.363057	392	75.15924	2192	3.248408	424	1.470148	393	0.764331	417	2.691068	1029	57.87861	411	0.057803	140	9.01E+01	01	267.28324		
455	78.305733	422	66.85096	2222	3.248408	454	1.737945	423	0.764331	462	3.130723	1059	86.51445	441	0.057803	150	7.65E+01	96	245.08871		
485	74.77707	452	93.50318	2252	3.057325	484	2.138394	453	0.254777	507	3.615661	1089	71.75145	471	0	160	6.24E+01	101	188.87052		
515	72.993631	482	80.66153	2282	3.003631	514	2.530343	483	0.254777	612	4.145509	1119	71.52023	501	0.809249	170	5.39E+01	106	168.55491		
545	63.568879	512	78.72611	2312	2.929936	544	2.004745	513	0.254777	627	4.648568	1140	67.12717	531	2.889642	180	4.53E+01	111	167.85127		
575	61.78344	542	84.99815	2342	2.992548	574	2.004745	543	1.013106	717	4.631225	1179	59.49711	591	2.889642	190	3.95E+01	116	174.33586		
605	51.33758	572	80.83694	2372	1.528662	604	1.470148	573	0.764331	777	4.579202	1209	49.62425	561	4.783237	200	3.54E+01	121	161.64971		
635	42.929936	602	53.75796	2402	1.019108	634	1.069197	603	0.764331	837	4.026434	1239	42.22543	621	7.34104	210	3.14E+01	126	135.95375		
665	34.522293	632	47.64381	2432	0.764331	664	1.470148	633	0.509554	927	3.436963	1269	35.84913	651	5.797688	220	2.81E+01	131	102.65886		
695	31.464968	662	44.07643	2462	0.764331	694	1.202847	663	1.528662	1062	2.874853	1299	30.7341	681	5.856765	230	2.52E+01	136	75.63815		
725	27.643312	692	37.70701	2492	0.12354	724	0.666246	693	1.528662	1122	2.393288	1320	27.72532	711	3.952023	240	2.24E+01	141	90.346824		
755	29.976981	722	38.17834			754	0.13365	723	0.509554	1317	1.717087	1350	24.05376	741	7.589593	250	2.07E+01	146	52.254335		
785	25.095541	752	32.36868					753	1.019108	1542	1.187439	1389	20.17341	771	6.791908	260	1.07E+01	151	46.936416		
815	23.312102	782	25.96729					783	1.019108	2022	0.081896	1419	17.63006	801	5.919075	270	1.68E+01	156	42.080925		
845	21.656051	812	25.22293					813	0.509554	2037	0.081896	1440	15.00894	831	4.83237	280	1.77E+01	161	30.306358		
875	21.019108	842	17.83439					843	5.859873	2062	0.081896	1470	13.2948	861	3.803468	290	1.69E+01	166	36.375723		
905	21.019108	872	19.87261					873	5.350316			1500	11.44800	891	4.034682	300	1.55E+01	171	32.83237		
935	20.382166	902	18.59873					903	5.350316			1530	10.00266	921	3.830636	350	1.21E+01	176	30.751445		
965	20.382166	932	18.39873					933	5.350316			1569	10.0578	951	0.537572	400	0.47E+00	181	29.132948		
995	18.745223	962	15.70616					963	5.350316			1599	9.569585	991	0.531792	450	7.51E+00	186	27.052023		
1025	19.10828	992	14.59229					993	5.859873			1628	8.62658	1011	0.323699	500	5.61E+00	191	25.895954		
1055	18.471338	1022	13.24841					1023	1.273885			1659	8.015029	1041	0.323699	550	3.06E+00	196	24.046243		
1085	17.834395	1052	11.87452					1053	2.292994			1689	5.202312	1071	0.184500	600	2.96E+00	201	22.890173		
1115	17.197452	1082	10.44586					1083	4.33121			1718	5.202312	1101	0.011561	650	1.10E+00	206	21.50289		
1145	16.56051	1112	9.036909					1113	5.078433			1749	4.971098	1131	0	675	3.82E-01	211	20.578035		
1175	16.56051	1142	9.171975					1143	3.821656			1779	5.202312			694	0.00E+00	216	19.653179		
1205	15.923567	1172	7.133758					1173	1.021656			1809	3.468208					221	21.040462		
1235	14.640687	1202	6.152866					1203	2.038217			1830	3.699422					257	12.465549		
1265	14.012739	1232	7.388535					1233	1.528662			1869	3.699422					287	10.635838		
1295	13.375796	1262	7.888089					1263	1.528662			1899	3.238994					317	9.4797688		
1325	13.375796	1292	5.905099					1293	1.528662			1920	3.238994					347	8.5549133		
1355	12.738854	1322	6.11465					1323	1.528662			1959	3.468208					377	7.6300578		
1385	12.101911	1352	3.566878					1353	1.273885			1980	3.930636					407	5.7052023		
1415	10.191083	1382	6.11465					1383	1.273885			2019	3.520231					437	5.5491329		
1445	7.0063694	1412	5.905099					1413	1.528662			2049	3.699422					467	4.8554913		
1475	5.7324841	1442	6.380427					1443	1.783439									497	4.6242775		
1505	3.8216561	1472	6.11465					1473	1.783439									527	4.1618497		
1535	1.910828	1502	5.859873					1503	1.783439									557	3.699422		
1565	1.2738854	1532	5.859873					1533	1.783439									587	3.699422		
1595	0.6369427	1562	5.859873					1563	1.528662									617	3.2369942		
1625	0.12546	1582	5.095541					1593	1.783439									647	2.7745665		
		1622	5.605096					1623	2.038217									677	2.5433526		
		1652	5.095541															707	2.3121387		
		1682	4.585987															737	2.3121387		
		1712	4.586987															767	2.0809249		
		1742	4.076433															707	1.849711		

Treatment		Test										T45H50/1	
Time (min)	Conc. (mg/l)	Time (min)	Conc. (mg/l)	Time (min)	Conc. (mg/l)	Time (min)	Conc. (mg/l)	Time (min)	Conc. (mg/l)	Time (min)	Conc. (mg/l)	Time (min)	Conc. (pfu/ml)
0	0	0	0.00E+00	60	1.46E+04	120	8.03E+03	180	3.63E+03	0	0.00E+00	0	1
10	0.5	1	1.55E+03	61	1.38E+04	121	8.44E+03	181	3.33E+03	1	0.00E+00	5	1.6
20	100.75145	2	1.49E+03	62	1.35E+04	122	8.15E+03	182	3.27E+03	2	0.00E+00	15	4700
70	100.60625	3	1.42E+03	63	1.41E+04	123	7.62E+03	183	2.97E+03	3	0.00E+00	25	2300
100	79.537573	4	1.35E+03	64	1.29E+04	124	8.25E+03	184	2.90E+03	4	0.00E+00	35	3787
130	15.722543	5	-7.92E+02	65	1.10E+04	125	7.95E+03	185	2.81E+03	5	0.00E+00	45	2000
160	7.1678301	6	-3.95E+02	66	1.39E+04	126	7.42E+03	186	2.31E+03	6	0.00E+00	55	1567
190	2.3121387	7	-2.30E+02	67	1.25E+04	127	8.05E+03	187	2.24E+03	7	0.00E+00	65	1020
220	1.3872832	8	1.66E+02	68	1.45E+04	128	5.90E+03	188	1.95E+03	8	0.00E+00	75	666.7
250	1.3872832	9	2.16E+03	69	1.07E+04	129	7.02E+03	189	1.65E+03	9	0.00E+00	85	920
280	0.9248555	10	2.00E+02	70	1.13E+04	130	5.31E+03	190	1.58E+03	10	0.00E+00	95	780
		11	3.21E+03	71	1.04E+04	131	7.65E+03	191	1.29E+03	11	0.00E+00	105	1333.3
		12	5.45E+03	72	1.26E+04	132	7.95E+03	192	1.11E+03	12	0.00E+00	115	880.7
		13	1.51E+04	73	1.48E+04	133	7.00E+03	193	9.24E+02	13	0.00E+00	125	870
		14	2.06E+04	74	1.39E+04	134	7.59E+03	194	8.58E+02	14	0.00E+00	135	546.7
		15	2.07E+04	75	1.31E+04	135	7.52E+03	195	1.02E+03	15	0.00E+00	145	420
		16	2.23E+04	76	1.37E+04	136	7.22E+03	196	2.64E+02	16	0.00E+00	155	323.3
		17	2.50E+04	77	1.32E+04	137	7.62E+03	197	1.98E+02	17	0.00E+00	165	233.3
		18	2.40E+04	78	1.43E+04	138	7.78E+03	198	1.32E+02	18	0.00E+00	175	316.7
		19	2.30E+04	79	1.33E+04	139	7.05E+03	199	2.97E+02	19	0.00E+00	185	363.3
		20	2.34E+04	80	1.74E+04	140	7.88E+03	200	0.00E+00	20	0.00E+00	195	156.3
		21	2.10E+04	81	1.20E+04	141	7.12E+03			21	0.00E+00	205	86.7
		22	1.04E+04	82	1.40E+04	142	7.26E+03						
		23	1.66E+04	83	1.30E+04	143	6.99E+03						
		24	1.50E+04	84	1.37E+04	144	8.93E+03						
		25	1.50E+04	85	1.36E+04	145	6.40E+03						
		26	1.49E+04	86	1.33E+04	146	6.56E+03						
		27	1.37E+04	87	1.35E+04	147	6.27E+03						
		28	1.53E+04	88	1.32E+04	148	6.43E+03						
		29	1.59E+04	89	1.30E+04	149	6.14E+03						
		30	1.81E+04	90	1.26E+04	150	6.07E+03						
		31	1.46E+04	91	1.16E+04	151	6.23E+03						
		32	1.67E+04	92	1.20E+04	152	6.17E+03						
		33	2.14E+04	93	1.24E+04	153	5.67E+03						
		34	2.06E+04	94	1.18E+04	154	5.81E+03						
		35	2.31E+04	95	1.20E+04	155	5.74E+03						
		36	2.14E+04	96	9.17E+03	156	3.82E+03						
		37	3.02E+04	97	1.07E+04	157	5.36E+03						
		38	2.08E+04	98	1.23E+04	158	5.31E+03						
		39	2.12E+04	99	1.17E+04	159	5.48E+03						
		40	2.12E+04	100	1.17E+04	160	5.41E+03						
		41	2.33E+04	101	1.16E+04	161	5.81E+03						
		42	2.08E+04	102	1.08E+04	162	5.51E+03						
		43	2.28E+04	103	1.24E+04	163	5.21E+03						
		44	2.07E+04	104	1.12E+04	164	4.92E+03						
		45	1.92E+04	105	8.57E+03	165	5.08E+03						
		46	2.15E+04	106	1.08E+04	166	4.76E+03						
		47	1.86E+04	107	7.75E+03	167	4.72E+03						
		48	2.25E+04	108	1.28E+04	168	4.65E+03						
		49	1.75E+04	109	1.06E+04	169	3.80E+03						
		50	1.71E+04	110	7.09E+03	170	4.06E+03						
		51	1.81E+04	111	8.10E+03	171	3.98E+03						
		52	1.72E+04	112	7.66E+03	172	3.93E+03						
		53	1.52E+04	113	7.36E+03	173	3.86E+03						
		54	1.38E+04	114	5.20E+03	174	3.79E+03						
		55	1.46E+04	115	7.45E+03	175	3.60E+03						
		56	1.53E+04	116	8.06E+03	176	3.20E+03						
		57	1.34E+04	117	8.71E+03	177	3.37E+03						
		58	1.44E+04	118	7.85E+03	178	3.53E+03						
		59	1.36E+04	119	8.11E+03	179	3.70E+03						

T46soil						T47H40/1				T47M67/1						T42soil				T48soil	
Time (min)	Conc. (mg/l)	Time (min)	Conc. (mg/l)	Time (min)	Conc. (mg/l)	Time (min)	Conc. (pfu/ml)	Time (min)	Conc. (pfu/ml)	Time (min)	Conc. (pfu/ml)	Time (min)	Conc. (pfu/ml)	Time (min)	Conc. (pfu/ml)	Time (min)	Conc. (mg/l)	Time (min)	Conc. (mg/l)	Time (min)	Conc. (mg/l)
0	4.62E-04	710	2.78E-02	1390	2.58E-03	0	0.00E+00	590	1.58E+04	0	0.00E+00	600	1.33E+04	1200	2.30E+03	0	3.42E+04	600	2.81E-03	0	0.00E+00
50	9.78E-04	720	2.60E-02	1400	2.51E-03	10	8.25E+03	610	1.19E+04	10	1.81E+03	610	1.31E+04	1210	2.43E+03	10	5.25E+04	610	5.89E-03	5	1.08E-03
100	2.43E-03	730	2.41E-02	1410	2.55E-03	20	1.25E+04	620	9.97E+03	20	3.62E+03	620	1.23E+04	1220	2.48E+03	20	7.03E-04	620	4.86E-03	10	2.69E-04
120	2.67E-03	740	2.26E-02	1440	2.70E-03	30	1.86E+04	630	7.98E+03	30	5.43E+03	630	1.04E+04	1230	2.44E+03	30	7.12E-04	630	4.05E-03	15	4.60E-04
150	2.86E-03	750	2.12E-02	1450	2.70E-03	40	2.50E+04	640	6.90E+03	40	7.25E+03	640	8.60E+03	1240	2.40E+03	40	4.86E-04	640	4.29E-03	20	3.67E-04
160	3.17E-03	760	2.08E-02	1460	2.84E-03	50	3.13E+04	650	5.82E+03	50	9.04E+03	650	6.27E+03	1250	2.38E+03	50	2.64E-04	650	3.75E-03	25	3.77E-03
170	3.20E-03	770	2.01E-02	1420	8.07E-03	60	3.78E+04	660	4.23E+03	60	1.09E+04	660	4.93E+03	1260	2.30E+03	60	2.08E-04	660	3.21E-03	30	4.05E-02
180	2.61E-03	780	1.99E-02	1480	8.30E-03	70	4.38E+04	670	3.65E+03	70	1.27E+04	670	3.10E+03	1270	2.28E+03	70	4.30E-04	670	2.81E-03	35	1.33E-01
190	2.43E-03	800	1.93E-02	1490	8.50E-03	80	5.01E+04	680	2.90E+03	80	1.45E+04	680	2.10E+03	1280	2.20E+03	80	8.21E-04	700	1.92E-03	40	2.54E-01
200	1.88E-02	810	1.88E-02	1500	8.63E-03	90	5.64E+04	690	2.85E+03	90	1.63E+04	690	2.39E+03	1290	2.19E+03	90	2.48E-04	710	1.23E-03	45	3.28E-01
210	5.32E-02	820	1.82E-02	1600	8.62E-03	100	6.28E+04	700	2.40E+03	100	1.81E+04	700	2.60E+03	1300	2.15E+03	100	5.63E-04	720	8.09E-04	50	5.09E-01
220	8.97E-02	830	1.77E-02	1700	8.27E-03	110	6.89E+04	710	2.35E+03	110	1.99E+04	710	2.85E+03	1310	2.11E+03	110	4.39E-04	730	8.09E-04	55	8.18E-01
230	1.24E-01	840	1.73E-02	1800	7.19E-03	120	7.51E+04	720	1.90E+03	120	2.17E+04	720	3.10E+03	1320	2.01E+03	120	5.01E-04	740	8.09E-04	60	8.20E-01
240	1.54E-01	850	1.68E-02	1930	6.57E-03	130	8.14E+04	730	1.65E+03	130	2.35E+04	730	3.35E+03	1330	2.09E+03	130	8.85E-04	750	0.00E+04	65	8.20E-01
250	1.84E-01	860	1.64E-02	1980	5.66E-03	140	8.77E+04	740	1.40E+03	140	2.53E+04	740	3.40E+03	1340	1.95E+03	140	1.23E-03	760	1.24E-03	70	8.39E-01
260	2.04E-01	870	1.61E-02			150	9.39E+04	750	1.15E+03	150	2.21E+04	750	3.15E+03	1350	1.83E+03	150	9.73E-03	770	1.55E-03	75	5.70E-01
270	2.08E-01	880	1.58E-02			160	1.00E+05	760	9.00E+02	160	2.89E+04	760	2.90E+03	1360	1.70E+03	160	3.03E-02	780	2.01E-03	80	4.82E-01
280	2.12E-01	890	1.55E-02			170	1.06E+05	770	6.50E+02	170	3.07E+04	770	2.65E+03	1370	1.58E+03	170	5.00E-02	790	2.21E-03	85	3.93E-01
290	2.13E-01	900	1.53E-02			180	1.13E+05	780	4.00E+02	180	3.25E+04	780	2.40E+03	1380	1.45E+03	180	2.56E-02	800	3.40E-03	90	3.12E-01
300	2.09E-01	910	1.51E-02			190	1.19E+05	790	1.50E+02	190	3.44E+04	790	2.15E+03	1390	1.33E+03	190	1.09E-01	810	4.09E-03	95	2.49E-01
310	2.03E-01	920	1.48E-02			200	1.25E+05	800	1.00E+02	200	3.62E+04	800	2.03E+03	1400	1.20E+03	200	1.37E-01	820	4.46E-03	100	1.93E-01
320	1.07E-01	930	1.45E-02			210	1.31E+05	810	6.00E+02	210	3.80E+04	810	2.12E+03	1410	1.08E+03	210	1.58E-01	830	4.82E-03	105	1.50E-01
330	1.00E-01	940	1.42E-02			220	1.38E+05	820	1.35E+03	220	3.96E+04	820	2.20E+03	1420	9.50E+02	220	1.83E-01	840	5.11E-03	110	1.18E-01
340	1.83E-01	950	1.39E-02			230	1.44E+05	830	1.43E+03	230	4.18E+04	830	2.28E+03	1430	8.25E+02	230	1.68E-01	850	4.86E-03	115	8.95E-02
350	1.24E-01	960	1.36E-02			240	1.50E+05	840	1.27E+03	240	4.24E+04	840	2.32E+03	1440	7.00E+02	240	1.21E-01	860	4.65E-03	120	7.00E-02
360	1.03E-01	970	1.32E-02			250	1.57E+05	850	1.10E+03	250	4.52E+04	850	2.45E+03	1450	5.75E+02	250	1.20E-01	870	4.48E-03	130	4.31E-02
370	1.02E-01	980	1.31E-02			260	1.61E+05	860	9.33E+02	260	4.62E+04	860	2.37E+03	1460	4.83E+02	260	1.69E-01	880	4.20E-03	140	2.87E-02
380	1.43E-01	1010	1.30E-02			270	1.62E+05	900	7.67E+02	270	4.78E+04	870	2.03E+03	1470	4.42E+02	270	1.68E-01	900	4.14E-03	150	1.72E-02
390	1.98E-01	1020	1.28E-02			280	1.63E+05	950	7.83E+02	280	4.88E+04	880	1.70E+03	1480	4.00E+02	280	1.65E-01	900	3.83E-03	160	1.15E-02
400	1.32E-01	1030	1.27E-02			290	1.64E+05	1000	1.00E+03	290	4.95E+04	880	1.37E+03	1490	3.58E+02	290	1.83E-01	910	3.20E-03	170	7.67E-03
410	1.28E-01	1040	1.24E-02			300	1.64E+05	1100	3.33E+01	300	5.05E+04	900	1.03E+03	1500	3.17E+02	300	1.58E-01	920	2.78E-03	180	5.08E-03
420	1.24E-01	1050	1.21E-02			310	1.65E+05	1260	8.58E+02	310	5.14E+04	910	9.00E+02	1510	2.75E+02	310	1.49E-01	930	2.10E-03	190	4.00E-03
430	1.20E-01	1060	1.17E-02			320	1.64E+05	1500	1.42E+03	320	5.14E+04	920	5.67E+02	1520	2.33E+02	320	1.81E-01	940	1.29E-03	200	3.71E-03
440	1.15E-01	1100	1.13E-02			330	1.59E+05	1750	7.75E+02	330	4.98E+04	930	7.33E+02	1530	1.92E+02	330	1.33E-01	950	4.66E-04	210	3.21E-03
450	1.00E-01	1110	1.10E-02			340	1.54E+05	1810	5.00E+02	340	4.83E+04	940	9.00E+02	1540	1.50E+02	340	1.28E-01	960	0.00E+00	220	2.47E-03
460	1.04E-01	1120	1.07E-02			350	1.48E+05			350	4.82E+04	950	1.02E+03	1550	1.08E+02	350	1.23E-01			230	1.07E-03
470	9.84E-02	1130	1.04E-02			360	1.43E+05			360	4.52E+04	960	1.29E+03	1560	6.67E+01	360	1.18E-01			240	2.08E-03
480	9.38E-02	1140	1.01E-02			370	1.38E+05			370	4.38E+04	970	1.40E+03	1570	2.50E+01	370	1.11E-01			250	1.64E-03
490	8.01E-02	1150	0.78E-03			380	1.32E+05			380	4.24E+04	980	1.50E+03	1580	3.33E+01	380	1.04E-01			260	1.21E-03
500	8.54E-02	1160	0.56E-03			390	1.26E+05			390	4.18E+04	990	1.50E+03	1590	1.17E+02	390	0.03E-02			270	0.18E-04
510	8.29E-02	1170	0.40E-03			400	1.19E+05			400	4.08E+04	1000	1.50E+03	1600	2.00E+02	400	9.35E-02			280	8.32E-04
520	8.04E-02	1180	8.41E-03			410	1.13E+05			410	4.00E+04	1010	1.50E+03	1610	2.83E+02	410	8.88E-02			290	7.59E-04
530	7.84E-02	1190	8.24E-03			420	1.08E+05			420	3.93E+04	1020	1.50E+03	1620	3.67E+02	420	8.49E-02			300	7.42E-04
540	7.69E-02	1200	8.03E-03			430	8.98E+04			430	3.85E+04	1030	1.50E+03	1630	4.50E+03	430	7.91E-02			310	8.12E-04
550	7.54E-02	1210	8.82E-03			440	9.30E+04			440	3.77E+04	1040	1.47E+03	1640	5.33E+02	440	7.42E-02			320	0.86E-04
560	7.34E-02	1220	8.44E-03			450	8.82E+04			450	3.71E+04	1050	1.39E+03	1650	6.17E+02	450	6.05E-02			330	1.12E-03
570	7.05E-02	1250	8.29E-03			460	7.04E+04			460	3.04E+04	1060	1.30E+03	1660	7.00E+02	460	8.50E-02			378	7.23E-04
580	6.75E-02	1260	2.90E-03			470	7.26E+04			470	3.83E+04	1070	1.22E+03	1670	7.83E+02	470	6.04E-02			400	2.40E-04
600	6.43E-02	1270	2.51E-03			480	8.59E+04			460	3.51E+04	1080	1.13E+03	1680	8.67E+02	480	5.54E-02			410	8.31E-05
800	6.08E-02	1280	2.41E-03			490	5.91E+04			490	3.44E+04	1090	1.05E+03	1690	9.50E+02	490	4.98E-02			418	0.00E+00
810	5.67E-02	1290	2.71E-03			500	5.35E+04			500	3.22E+04	1100	1.05E+03	1700	0.83E+02	500	4.42E-02				
820	5.33E-02	1300	8.02E-03			510	4.99E+04			510	2.03E+04	1110	1.18E+03	1710	9.42E+02	510	3.88E-02				
830	5.08E-02	1310	8.36E-03			520	4.62E+04			520	2.80E+04	1120	1.30E+03	1720	9.00E+02	520	3.39E-02				
840	4.78E-02	1320	8.75E-03			530	4.25E+04			530	2.27E+04	1130	1.43E+03	1730	8.58E+02	530	2.90E-02				
850	4.49E-02	1330	8.13E-03			540	3.89E+04			540	1.03E+04	1140	1.55E+03	1740	8.17E+02	540	2.47E-02				
860	4.17E-02	1340	8.15E-03			550	3.58E+04			550	1.80E+04	1150	1.68E+03	1750	7.75E+02	550	2.13E-02				
870	3.85E-02	1350	8.81E-03			560	3.14E+04			560	1.39E+04	1160	1.80E+03	1760	7.33E+02	560	1.79E-02				
880	3.56E-02	1360	8.97E-03			570	2.75E+04			570	1.36E+04	1170	1.93E+03	1770	6.92E+02	570	1.48E-02				
890	3.29E-02	1370	2.71E-03			580	2.36E+04			580	1.36E+04	1180	2.05E+03	1780	6.50E+02	580	1.23E-02				
900	3.02E-02	1380	7.84E-03			590	1.07E+04			590	1.34E+04	1190	2.18E+03	1810	5.00E+02	590	0.73E-03				

T49ers				T49salt				T60H40/1				760H0/1				750salt		751H40/
Time (min)	Conc. (1E-09 mg/l)	Time (min)	Conc. (1E-09 mg/l)	Time (min)	Conc. (mg/l)	Time (min)	Conc. (mg/l)	Time (min)	Conc. (pfu/ml)	Time (min)	Conc. (pfu/ml)	Time (min)	Conc. (pfu/ml)	Time (min)	Conc. (pfu/ml)	Time (min)	Conc. (mg/l)	Time (min)
0	7.00E-02	620	1.18E+01	0	1.27E-04	320	1.15E-01	0	0.00E+00	600	1.71E+06	0	0.00E+00	600	5.30E+04	0	6.20E-03	0
10	7.39E-02	630	1.13E+01	5	1.27E-04	330	1.12E-01	10	2.86E+02	610	1.81E+06	10	5.71E+02	610	4.70E+04	10	6.23E-03	10
20	7.78E-02	640	1.06E+01	10	1.31E-04	340	1.08E-01	20	5.71E+02	620	1.48E+06	20	1.14E+03	620	4.39E+04	20	6.25E-03	20
30	8.18E-02	650	9.93E+00	15	1.36E-04	350	1.06E-01	30	8.57E+02	630	1.32E+06	30	1.71E+03	630	4.08E+04	30	6.29E-03	30
40	8.57E-02	660	9.46E+00	20	1.48E-04	360	1.03E-01	40	8.17E+02	640	1.17E+06	40	1.98E+03	640	3.77E+04	40	6.31E-03	40
50	8.98E-02	670	9.01E+00	25	1.57E-04	370	8.98E-02	50	7.50E+02	650	1.03E+06	50	1.88E+03	650	3.48E+04	50	6.30E-03	50
60	9.10E-02	680	8.56E+00	30	1.05E-04	380	9.01E-02	60	5.83E+02	660	8.80E+05	60	1.79E+03	660	3.15E+04	60	6.36E-03	60
70	7.18E-02	690	8.11E+00	35	1.74E-04	390	9.21E-02	70	4.17E+02	670	7.74E+05	70	1.71E+03	670	2.84E+04	70	1.85E-02	70
80	6.10E-02	700	7.66E+00	40	1.82E-04	400	9.81E-02	80	3.50E+02	680	7.06E+05	80	1.63E+03	680	2.63E+04	80	3.08E-02	80
90	5.40E-02	710	7.21E+00	45	1.91E-04	450	9.87E-02	90	8.33E+01	690	8.42E+05	90	1.54E+03	690	2.71E+04	90	4.19E-02	90
100	4.10E-02	720	6.87E+00	50	1.70E-04	475	5.07E-02	100	6.80E+04	700	5.75E+05	100	1.88E+03	700	2.59E+04	100	5.27E-02	100
110	3.10E-02	730	6.55E+00	55	1.49E-04	500	5.06E-02	110	1.47E+05	710	5.09E+05	110	1.18E+04	710	2.48E+04	110	6.98E-02	110
120	1.49E-01	740	6.22E+00	60	1.27E-04	550	3.83E-02	120	2.45E+05	720	6.43E+05	120	1.84E+04	740	2.20E+04	120	7.48E-02	120
130	2.80E-01	750	5.91E+00	65	2.12E-04	600	2.59E-02	130	3.42E+05	730	4.01E+05	130	2.51E+04	750	2.13E+04	130	8.72E-02	130
140	4.12E-01	760	5.68E+00	70	2.97E-04	650	1.56E-02	140	4.40E+05	740	3.82E+05	140	3.19E+04	800	1.83E+04	140	9.94E-02	140
150	5.43E-01	770	5.26E+00	75	3.82E-04	700	8.19E-03	150	5.38E+05	750	3.63E+05	150	3.86E+04	900	1.23E+04	150	1.12E-01	150
160	6.75E-01	780	5.07E+00	80	3.02E-04	710	3.11E-03	160	1.04E+06	760	3.45E+05	160	1.04E+05	1000	1.25E+04	160	1.24E-01	160
170	8.07E-01	790	4.88E+00	85	3.62E-04	720	1.04E-03	170	1.94E+06	770	3.17E+05	170	2.27E+05	1100	6.25E+03	170	1.36E-01	170
180	7.98E+00	800	4.70E+00	90	3.82E-04	725	0.00E+00	180	2.84E+06	800	2.85E+05	180	3.51E+05	1200	7.92E+03	180	1.48E-01	180
190	1.59E+01	850	3.94E+00	95	3.82E-04			190	3.74E+06	850	2.41E+05	190	4.74E+05	1300	7.21E+03	190	1.43E-01	190
200	2.38E+01	900	3.43E+00	100	3.82E-04			200	4.65E+06	875	2.24E+05	200	5.08E+05	1400	5.19E+03	200	1.38E-01	200
210	3.17E+01	950	2.94E+00	105	3.82E-04			210	5.55E+06	900	2.07E+05	210	7.21E+05	1500	3.54E+03	210	1.32E-01	210
220	3.97E+01	1000	2.66E+00	110	3.40E-04			220	8.04E+06	925	1.92E+05	220	7.75E+05	1600	3.05E+03	220	1.27E-01	220
230	4.78E+01	1050	2.25E+00	115	2.97E-04			230	8.13E+06	950	1.76E+05	230	7.60E+05	1700	3.16E+03	230	1.22E-01	230
240	5.01E+01	1100	1.88E+00	120	2.55E-04			240	8.22E+06	1000	1.60E+05	240	7.45E+05	1850	3.39E+03	240	1.16E-01	240
250	6.19E+01	1150	1.41E+00	125	3.40E-04			250	8.30E+06	1025	1.58E+05	250	7.30E+06	2000	3.50E+03	250	1.11E-01	250
260	5.38E+01	1200	7.47E-01	130	4.25E-04			260	8.39E+06	1050	1.40E+05	260	7.15E+06	2200	3.66E+03	260	1.06E-01	260
270	6.67E+01	1300	3.33E-01	135	5.10E-04			270	8.48E+06	1075	1.25E+05	270	7.00E+05	2250	3.93E+03	270	1.01E-01	270
280	5.75E+01	1311	3.20E-01	140	4.67E-04			280	8.58E+06	1100	1.13E+05	280	8.85E+05	2305	4.00E+03	280	9.59E-02	280
290	5.94E+01			145	6.25E-04			290	8.85E+06	1125	1.04E+05	290	8.70E+05			290	9.08E-02	290
300	5.81E+01			150	3.82E-04			300	8.74E+06	1150	9.57E+04	300	8.55E+05			300	8.57E-02	300
310	5.63E+01			155	4.67E-04			310	8.82E+06	1175	8.75E+04	310	8.40E+05			310	8.24E-02	310
320	5.46E+01			160	5.52E-04			320	8.01E+06	1200	7.93E+04	320	8.25E+05			320	7.91E-02	320
330	6.29E+01			165	6.37E-04			330	7.00E+06	1225	7.26E+04	330	8.10E+05			330	7.58E-02	330
340	5.12E+01			170	1.87E-03			340	7.09E+06	1250	6.87E+04	340	5.95E+05			340	7.25E-02	340
350	4.95E+01			175	3.10E-03			350	7.17E+06	1275	6.12E+04	350	5.80E+05			350	6.99E-02	350
360	4.59E+01			180	4.33E-03			360	7.26E+06	1300	5.66E+04	360	5.65E+05			360	6.58E-02	360
380	4.47E+01			185	1.30E-02			370	7.07E+06	1350	4.99E+04	370	5.27E+05			370	6.45E-02	370
400	4.35E+01			190	2.17E-02			380	6.60E+06	1400	4.56E+04	380	4.88E+05			380	6.31E-02	380
410	4.23E+01			195	3.03E-02			390	6.13E+06	1450	3.95E+04	390	4.05E+06			390	6.17E-02	390
420	4.12E+01			200	5.74E-02			400	5.67E+06	1500	2.45E+04	400	3.44E+05			400	6.03E-02	400
430	4.00E+01			205	8.46E-02			410	5.20E+06	1550	2.56E+04	410	2.84E+05			410	5.89E-02	410
440	3.89E+01			210	1.12E-01			420	4.73E+06	1600	2.62E+04	420	2.23E+05			420	5.75E-02	420
450	3.78E+01			215	1.12E-01			430	4.38E+06	1650	2.58E+04	430	1.88E+05			430	5.48E-02	430
460	3.66E+01			220	1.13E-01			440	4.18E+06	1700	2.64E+04	440	1.73E+05			440	5.17E-02	440
470	3.55E+01			225	1.14E-01			450	3.06E+06	1750	2.50E+04	450	1.80E+05			450	4.88E-02	460
480	3.34E+01			230	1.15E-01			460	3.74E+06	1800	2.48E+04	460	1.47E+05			600	3.50E-02	460
490	3.12E+01			235	1.16E-01			470	3.53E+06	1850	2.43E+04	470	1.34E+05			600	2.07E-02	470
500	2.90E+01			240	1.17E-01			480	3.31E+06	1900	2.39E+04	480	1.21E+05			700	1.02E-02	480
510	2.68E+01			245	1.17E-01			490	3.10E+06	1945	2.35E+04	490	1.13E+05			800	1.62E-02	490
520	2.45E+01			250	1.18E-01			500	2.90E+06			500	1.11E+06			800	1.48E-02	500
530	2.23E+01			255	1.19E-01			510	2.68E+06			510	1.00E+05			1000	1.35E-02	510
540	2.09E+01			260	1.20E-01			520	2.49E+06			520	1.07E+05			1150	1.22E-02	520
550	1.95E+01			265	1.21E-01			530	2.29E+06			530	1.05E+05			1300	1.14E-02	530
560	1.81E+01			270	1.22E-01			540	2.08E+06			540	1.03E+05			1450	1.08E-02	540
570	1.68E+01			275	1.22E-01			550	1.96E+06			550	9.80E+04			1850	1.08E-02	550
580	1.54E+01			280	1.23E-01			560	1.81E+06			560	8.00E+04			1826	1.03E-02	560
590	1.40E+01			290	1.24E-01			570	1.66E+06			570	8.00E+04			1850	1.05E-02	570
600	1.33E+01			300	1.21E-01			580	1.61E+06			580	7.10E+04			1920	1.03E-02	580
610	1.28E+01			310	1.18E-01			590	1.76E+06			590	6.20E+04					590

			E51HA/4						261H6/1				TB1a01				203H4/4	
Conc. (pfu/ml)	Time (min)	Conc. (pfu/ml)	Time (min)	Conc. (pfu/ml)	Time (min)	Conc. (pfu/ml)	Time (min)	Conc. (pfu/ml)	Time (min)	Conc. (pfu/ml)	Time (min)	Conc. (pfu/ml)	Time (min)	Conc. (mg/l)	Time (min)	Conc. (mg/l)	Time (min)	Conc. (pfu/ml)
5.00E+02	600	5.29E+08	0	0.00E+00	800	1.18E+09	2010	2.39E+02	0	4.00E+03	600	5.73E+04	0	1.07E-04	600	1.50E-01	0	0.00E+00
3.08E+02	610	5.02E+08	10	1.95E+01	810	1.83E+09	2020	2.61E+02	10	3.62E+03	610	6.23E+04	10	1.07E-04	610	1.40E-01	145	1.83E+04
1.15E+02	620	4.75E+08	20	3.92E+01	820	2.70E+09	2030	2.84E+02	20	3.23E+03	620	6.74E+04	20	1.07E-04	620	1.31E-01	150	9.70E+04
3.33E+01	630	4.47E+08	30	5.88E+01	830	3.48E+09	2040	3.07E+02	30	2.87E+03	630	7.24E+04	30	1.01E-04	630	1.21E-01	160	2.81E+05
1.17E+02	640	4.20E+08	40	7.84E+01	840	4.25E+09	2050	3.30E+02	40	2.53E+03	640	7.75E+04	40	9.46E-05	640	1.11E-01	170	4.24E+05
2.00E+02	650	3.93E+08	50	9.80E+01	850	5.02E+09	2060	3.52E+02	50	2.20E+03	650	8.26E+04	50	8.85E-05	650	1.02E-01	180	5.67E+05
2.03E+02	660	3.68E+08	60	1.18E+02	855	5.41E+09	2070	3.75E+02	60	1.87E+03	660	8.78E+04	60	8.24E-05	660	9.20E-02	190	7.50E+05
3.67E+02	670	3.36E+08	70	1.37E+02	860	5.80E+09	2080	3.98E+02	70	1.53E+03	670	9.27E+04	70	7.64E-05	670	8.69E-02	200	9.13E+05
4.50E+02	680	3.11E+08	80	1.57E+02	870	6.57E+09	2090	4.20E+02	80	1.20E+03	680	9.77E+04	80	7.01E-05	680	8.27E-02	210	1.08E+06
4.67E+02	690	2.84E+08	90	1.76E+02	880	7.38E+09	2100	4.43E+02	90	1.13E+03	690	1.03E+05	90	6.25E-05	690	7.85E-02	220	1.24E+06
5.83E+02	700	2.66E+08	100	1.96E+02	890	8.11E+09	2110	4.66E+02	100	1.47E+03	700	1.02E+05	100	5.40E-05	700	7.44E-02	230	1.40E+06
3.00E+02	710	2.58E+08	110	2.16E+02	700	8.38E+09	2120	4.89E+02	110	1.80E+03	710	9.59E+04	110	4.72E-05	710	7.03E-02	240	1.57E+06
2.17E+02	720	2.50E+08	120	2.35E+02	710	8.09E+09	2125	5.00E+02	120	2.13E+03	720	8.97E+04	120	3.98E-05	720	6.62E-02	250	1.73E+06
1.33E+02	730	2.41E+08	130	2.55E+02	720	7.82E+09	2230	5.00E+02	130	2.47E+03	730	8.34E+04	130	3.20E-05	730	6.24E-02	260	1.89E+06
5.00E+01	740	2.33E+08	140	2.75E+02	730	7.55E+09	2210	5.09E+02	140	2.80E+03	740	7.72E+04	140	2.58E-05	740	6.16E-02	270	2.84E+06
1.83E+01	750	2.25E+08	150	2.94E+02	740	7.27E+09	2250	1.73E+03	150	3.11E+03	750	7.09E+04	150	3.35E-05	750	5.88E-02	280	4.32E+06
6.67E+01	760	2.17E+08	160	3.14E+02	750	7.00E+09	2260	2.55E+03	160	3.39E+03	760	6.46E+04	160	4.11E-05	800	4.88E-02	290	5.60E+06
1.10E+02	770	2.09E+08	170	3.33E+02	760	6.73E+09	2270	3.38E+03	170	3.66E+03	770	5.84E+04	170	4.88E-05	850	4.05E-02	300	7.28E+06
1.56E+02	780	2.00E+08	180	3.53E+02	770	6.45E+09	2280	4.18E+03	180	3.94E+03	780	5.21E+04	180	5.84E-05	900	3.60E-02	310	8.78E+06
2.02E+02	790	1.92E+08	190	3.73E+02	780	6.18E+09	2290	5.00E+03	190	4.21E+03	790	4.59E+04	190	6.40E-05	950	3.28E-02	320	1.02E+07
2.48E+02	800	1.84E+08	200	3.92E+02	790	5.91E+09	2300	5.82E+03	200	4.49E+03	800	3.96E+04	200	7.42E-05	1000	2.98E-02	330	1.12E+07
2.94E+02	810	1.77E+08	210	4.12E+02	800	5.64E+09	2310	6.64E+03	210	4.76E+03	850	3.22E+04	210	1.08E-04	1100	2.40E-02	340	1.17E+07
3.39E+02	820	1.70E+08	220	4.31E+02	810	5.32E+09	2320	7.45E+03	220	5.04E+03	900	2.74E+04	220	1.41E-04	1200	1.89E-02	350	1.23E+07
3.85E+02	830	1.66E+08	230	4.51E+02	820	4.95E+09	2330	8.27E+03	230	5.31E+03	950	2.54E+04	230	1.74E-04	1300	1.40E-02	360	1.28E+07
4.31E+02	840	1.60E+08	240	4.71E+02	830	4.59E+09	2340	9.09E+03	240	5.59E+03	1000	2.45E+04	240	2.08E-04	1400	1.01E-02	370	1.33E+07
4.77E+02	850	1.54E+08	250	4.90E+02	840	4.25E+09	2350	9.07E+03	250	5.86E+03	1050	2.67E+04	250	2.41E-04	1500	6.84E-03	380	1.38E+07
6.00E+05	860	1.49E+08	260	2.70E+03	850	3.86E+09	2360	6.20E+03	260	6.36E+03	1100	2.01E+04	260	2.70E-04	1600	5.40E-03	390	1.30E+07
1.50E+06	870	1.43E+08	270	5.46E+03	860	3.60E+09	2370	7.34E+03	270	7.13E+03	1150	3.08E+04	270	3.01E-04	1700	4.10E-03	400	1.37E+07
2.50E+06	880	1.37E+08	280	8.60E+03	870	3.14E+09	2380	6.48E+03	280	7.89E+03	1200	2.83E+04	280	4.43E-04	1800	3.63E-03	410	1.35E+07
3.50E+06	890	1.31E+08	290	1.21E+04	880	2.77E+09	2385	8.05E+03	290	8.64E+03	1250	2.59E+04	290	6.25E-04	1852	3.28E-03	420	1.32E+07
4.50E+06	900	1.26E+08	300	1.54E+04	880	2.41E+09	2390	5.61E+03	300	9.40E+03	1300	2.49E+04	300	2.54E-03			430	1.30E+07
5.50E+06	910	1.20E+08	310	1.88E+04	900	2.05E+09	2395	5.18E+03	310	1.02E+04	1350	2.30E+04	310	1.34E-02			440	1.28E+07
6.50E+06	920	1.15E+08	320	2.21E+04	910	1.68E+09	2400	4.75E+03	320	1.09E+04	1400	2.21E+04	320	2.70E-02			450	1.22E+07
7.50E+06	930	1.10E+08	330	2.54E+04	920	1.48E+09	2405	4.32E+03	330	1.17E+04	1450	2.05E+04	330	4.05E-02			460	1.14E+07
8.50E+06	940	1.05E+08	340	2.87E+04	930	1.63E+09	2410	3.99E+03	340	1.24E+04	1500	2.10E+04	340	6.40E-02			470	1.06E+07
9.50E+06	950	1.00E+08	350	3.20E+04	940	1.39E+09	2415	3.45E+03	350	1.32E+04	1550	2.48E+04	350	8.76E-02			480	9.76E+06
1.05E+07	960	9.54E+09	360	3.53E+04	950	1.34E+09	2420	3.02E+03	360	1.39E+04	1600	2.27E+04	360	8.11E-02			490	8.94E+06
1.08E+07	970	9.07E+05	370	3.86E+04	960	1.30E+09	2425	2.59E+03	370	2.39E+04	1650	1.81E+04	370	1.95E-01			500	8.13E+06
1.05E+07	980	8.59E+05	380	3.85E+04	970	1.25E+09	2430	2.16E+03	380	4.31E+04	1700	1.29E+04	380	1.31E-01			510	7.54E+06
1.02E+07	990	8.11E+05	390	3.81E+04	980	1.20E+09	2435	1.73E+03	390	6.23E+04	1750	1.74E+04	390	1.57E-01			520	7.11E+06
8.92E+06	1000	7.83E+05	400	3.57E+04	990	1.16E+09	2440	1.30E+03	400	8.15E+04	1800	2.11E+04	400	1.83E-01			530	6.67E+06
8.48E+06	1100	6.27E+05	410	3.54E+04	1000	1.11E+09	2445	8.64E+02	410	1.01E+05	1850	1.88E+04	410	2.00E-01			540	6.24E+06
8.15E+06	1200	4.31E+05	420	3.50E+04	1100	8.30E+02	2450	4.32E+02	420	1.20E+05	1900	1.24E+04	420	2.35E-01			550	5.81E+06
8.81E+06	1300	2.84E+05	430	3.46E+04	1200	6.02E+02	2455	0.00E+00	430	1.39E+05	1950	1.40E+04	430	2.45E-01			560	5.37E+06
8.48E+06	1400	2.04E+05	440	3.43E+04	1300	6.25E+02			440	1.58E+05	2000	1.63E+04	440	2.80E-01			570	4.99E+06
8.14E+06	1500	1.10E+05	450	3.39E+04	1400	6.52E+02			450	1.78E+05	2050	1.84E+04	450	2.55E-01			580	4.64E+06
7.80E+06	1600	9.03E+04	460	3.35E+04	1500	6.41E+02			460	1.07E+05	2100	1.31E+04	460	2.60E-01			590	4.30E+06
7.47E+06	1750	6.80E+04	470	3.32E+04	1600	3.86E+02			470	2.10E+05	2200	1.78E+04	470	0.85E-01			600	3.95E+06
7.23E+06	1900	2.90E+04	480	3.15E+04	1700	0.00E+00			480	0.18E+05	2300	1.64E+04	480	2.71E-01			700	2.83E+06
7.08E+06	2000	3.23E+04	490	9.85E+04	1900	2.27E+00			490	2.02E+06	2400	1.18E+04	490	2.85E-01			800	1.81E+06
6.94E+06	2100	3.07E+04	500	2.55E+04	1910	1.16E+01			500	1.66E+05	2500	1.06E+04	500	2.57E-01			900	1.16E+06
6.79E+06	2200	2.63E+04	510	2.25E+04	1920	3.41E+01			510	1.70E+05	2600	1.10E+04	510	2.50E-01			950	1.22E+06
6.65E+06	2300	2.30E+04	520	1.95E+04	1930	5.88E+01			520	1.54E+05	2650	1.23E+04	520	2.42E-01			1000	1.28E+06
6.50E+06	2400	7.85E+04	530	1.65E+04	1940	7.95E+01			530	1.38E+05	2675	1.30E+04	530	2.34E-01			1050	1.18E+06
6.35E+06	2600	1.54E+04	540	1.35E+04	1950	1.02E+02			540	1.22E+05			540	0.26E-01			1100	9.18E+05
6.21E+06	2675	1.40E+04	550	1.05E+04	1960	1.25E+02			550	1.08E+05			550	2.14E-01			1150	6.93E+05
6.08E+06			560	7.50E+03	1970	1.48E+02			580	0.97E+04			580	2.01E-01			1200	7.00E+05
5.92E+06			570	4.50E+03	1980	1.70E+02			970	7.37E+04			570	1.69E-01			1250	5.88E+05
5.77E+06			580	1.50E+03	1990	1.93E+02			580	6.77E+04			580	1.76E-01			1300	5.17E+05
5.59E+06			590	3.86E+02	2000	2.18E+02			590	6.22E+04			890	1.63E-01			1344	4.80E+05

T5317				T54H40/1		T84pal3				T54H40/1				T5817				T5cf1		T35pcf3	
Time (min)	Conc. (pfu/ml)	Time (min)	Conc. (pfu/ml)	Time (min)	Conc. (pfu/ml)	Time (min)	Conc. (pfu/ml)	Time (min)	Conc. (pfu/ml)	Time (min)	Conc. (pfu/ml)	Time (min)	Conc. (pfu/ml)	Time (min)	Conc. (pfu/ml)	Time (min)	Conc. (pfu/ml)	Time (min)	Conc. (pfu/ml)	Time (min)	Conc. (pfu/ml)
0	7.00E+03	800	4.18E+05	0	0.00E+00	0	3.00E+03	310	1.92E+04	0	0.00E+00	630	1.95E+07	0	1.05E+04	690	9.01E+04	0	0.00E+00	0	5.00E+02
10	8.50E+03	810	3.59E+05	10	0.00E+00	5	1.44E-03	320	1.81E+04	10	1.00E+02	640	1.85E+07	10	1.88E+04	900	8.50E+04	5	1.39E+02	0	6.39E+02
20	3.50E+03	820	3.01E+05	20	5.20E+05	10	7.00E+02	330	1.90E+04	20	3.50E+02	650	1.75E+07	25	2.37E+04	910	7.00E+04	10	2.78E+02	10	7.78E+02
30	4.50E+03	830	2.69E+05	30	7.07E+06	15	1.20E+03	340	1.83E+04	30	5.00E+02	660	1.84E+07	50	2.00E+04	920	7.37E+04	15	4.17E+02	15	9.17E+02
40	5.50E+03	840	2.55E+05	40	1.21E+07	20	2.38E+03	350	1.75E+04	40	5.00E+02	680	1.42E+07	75	2.28E+04	930	5.37E+04	20	1.05E+04	20	5.83E+03
50	4.50E+03	850	2.41E+05	50	1.14E+07	25	2.20E+04	360	1.07E+04	50	4.00E+02	710	1.13E+07	100	2.08E+04	940	9.37E+04	25	3.56E+04	25	1.72E+04
60	6.50E+03	860	2.27E+05	60	1.06E+07	30	9.97E+04	370	1.88E+04	60	3.50E+02	750	4.83E+06	150	2.92E+04	950	1.04E+05	30	6.08E+04	30	2.88E+04
70	9.00E+03	870	2.13E+05	70	9.80E+06	35	1.85E+05	380	1.50E+04	70	0.00E+00	800	3.83E+06	200	2.07E+04	960	1.03E+05	35	8.58E+04	35	4.04E+04
80	7.50E+03	880	1.99E+05	80	9.17E+06	40	1.59E+05	390	1.42E+04	125	0.00E+00	810	3.08E+04	250	2.08E+04	970	9.75E+04	40	1.36E+05	40	2.13E+05
90	8.50E+03	890	1.88E+05	90	8.43E+06	45	1.54E+05	400	1.47E+04	127	2.87E+04	820	3.33E+06	300	2.10E+04	980	9.21E+04	45	4.50E+04	45	6.26E+05
100	1.20E+04	700	1.80E+05	100	7.70E+06	50	1.48E+05	450	1.88E+04	130	1.07E+06	830	3.00E+06	350	2.21E+04	990	8.68E+04	50	7.64E+04	60	1.04E+06
110	1.05E+04	710	1.71E+05	110	6.86E+06	55	1.42E+05	500	1.46E+04	140	3.23E+05	850	9.84E+04	400	3.81E+04	1000	8.06E+04	55	1.06E+07	55	1.45E+06
120	4.50E+03	720	1.63E+05	120	6.22E+06	60	1.38E+05	550	1.18E+04	150	8.28E+05	860	2.75E+06	410	5.80E+04	1100	5.72E+04	60	1.15E+07	80	1.60E+06
130	6.00E+03	730	1.55E+05	140	4.75E+06	65	1.31E+05	600	9.47E+03	160	1.58E+06	870	2.88E+06	420	7.07E+04	1200	5.82E+04	65	8.74E+06	65	1.34E+06
140	9.00E+03	740	1.48E+05	150	4.02E+06	70	1.25E+05	650	7.33E+03	170	1.78E+06	880	2.81E+06	430	1.00E+05	1300	6.03E+04	70	5.93E+06	70	1.06E+06
150	1.42E+04	750	1.41E+05	160	3.00E+06	75	1.18E+05	700	5.45E+03	180	1.28E+06	890	2.57E+06	440	1.44E+05	1350	1.53E+05	75	3.12E+06	75	8.22E+05
160	2.30E+04	760	1.38E+05	170	5.93E+06	80	1.14E+05	750	3.66E+03	190	9.01E+05	900	2.54E+06	450	1.07E+05	1351	1.35E+05	80	1.38E+06	80	6.44E+05
170	3.17E+04	770	1.35E+05	180	3.98E+06	85	1.08E+05	800	2.30E+03	200	7.27E+05	910	2.51E+06	460	2.51E+06	1352	1.36E+05	85	1.25E+06	85	5.56E+05
180	4.04E+04	780	1.31E+05	190	4.80E+06	90	1.02E+05	850	1.05E+03	210	5.72E+05	920	2.41E+06	470	3.04E+05	1353	1.38E+05	90	1.11E+06	80	5.27E+05
100	4.81E+04	800	1.28E+05	200	4.03E+06	95	9.84E+04	900	1.55E+03	220	4.08E+05	930	2.29E+06	480	3.08E+05			95	9.81E+05	95	4.69E+05
200	5.79E+04	810	1.26E+05	210	4.08E+06	100	9.07E+04	950	3.43E+03	230	2.44E+05	940	2.18E+06	490	5.10E+05			100	8.48E+05	100	4.11E+05
210	6.66E+04	820	1.24E+05	220	3.88E+06	105	8.50E+04	1000	4.60E+03	240	1.70E+05	950	2.04E+06	500	6.22E+05			105	7.15E+05	110	2.85E+05
220	7.53E+04	830	1.22E+05	230	3.83E+06	110	7.93E+04	1100	2.30E+03	250	1.58E+05	960	1.94E+06	510	7.33E+05			110	5.82E+05	120	1.78E+05
230	8.40E+04	840	1.21E+05	240	3.70E+06	115	7.35E+04	1200	5.10E+03	260	1.38E+05	970	1.86E+06	520	7.44E+05			115	4.49E+05	130	1.10E+05
240	9.28E+04	850	1.10E+05	250	3.58E+06	120	6.78E+04	1225	3.41E+03	270	1.14E+05	980	1.78E+06	530	7.10E+05			120	3.16E+05	140	6.14E+04
250	1.01E+05	860	1.18E+05	260	3.48E+06	125	6.21E+04	1232	3.50E+03	280	1.11E+05	990	1.69E+06	540	6.77E+05			125	1.83E+05	150	7.23E+04
260	1.10E+05	870	1.16E+05	270	3.30E+06	130	5.84E+04			290	1.15E+05	1000	1.67E+06	550	6.43E+05			130	1.45E+05	160	5.32E+04
270	1.09E+05	880	1.18E+05	280	3.10E+06	135	5.07E+04			300	1.18E+05	1100	1.12E+06	560	6.33E+05			135	1.47E+05	170	4.20E+04
280	3.41E+05	890	1.20E+05	290	2.89E+06	140	4.49E+04			310	1.22E+05	1200	8.39E+05	570	6.33E+05			140	1.26E+05	180	3.87E+04
290	4.83E+05	900	1.21E+05	300	2.69E+06	145	3.92E+04			320	1.17E+05	1300	6.83E+05	580	6.33E+05			145	1.10E+05	190	3.54E+04
300	6.28E+05	910	1.22E+05	310	2.47E+06	150	3.35E+04			330	1.08E+05	1343	5.63E+05	590	6.33E+05			150	9.17E+04	200	3.21E+04
310	2.68E+06	920	1.23E+05	320	2.25E+06	155	3.12E+04			340	9.07E+04			600	7.18E+05			160	5.50E+04	250	3.59E+04
320	9.10E+05	930	1.23E+05	330	2.04E+06	160	3.11E+04			350	9.09E+04			610	8.31E+05			170	4.22E+04	500	6.66E+03
330	1.01E+06	940	1.24E+05	340	1.91E+06	165	3.11E+04			360	9.85E+04			620	9.46E+05			180	5.32E+04	750	1.19E+03
340	1.08E+06	950	1.25E+05	350	1.78E+06	170	3.11E+04			370	1.13E+05			630	1.08E+06			190	6.42E+04	1000	3.04E+03
350	1.15E+06	970	1.26E+05	360	1.67E+06	175	3.10E+04			380	1.28E+05			640	6.80E+05			200	7.52E+04	1125	2.25E+03
360	1.23E+06	980	1.27E+05	370	1.56E+06	180	3.10E+04			390	1.42E+05			650	6.18E+05			250	8.65E+04	1250	1.50E+03
370	1.30E+06	990	1.25E+05	380	1.44E+06	185	3.10E+04			400	5.35E+05			660	6.30E+05			300	3.76E+04	1275	1.50E+03
380	1.37E+06	1000	1.21E+05	390	1.32E+06	190	3.09E+04			410	1.08E+06			670	4.88E+06			400	1.13E+04	1277	1.50E+03
390	1.40E+06	1020	1.13E+05	400	1.20E+06	195	3.09E+04			420	1.85E+06			680	3.09E+05			500	1.28E+04		
400	1.30E+06	1050	1.01E+05	450	1.30E+06	200	3.09E+04			430	2.20E+06			690	3.73E+05			600	8.10E+03		
410	1.39E+06	1100	8.63E+04	500	9.24E+05	205	3.08E+04			440	3.85E+06			700	3.47E+05			750	1.61E+03		
420	1.38E+06	1200	6.32E+04	550	7.03E+05	210	3.08E+04			450	5.47E+06			710	3.21E+05			1000	2.03E+03		
430	1.38E+06	1300	9.81E+04	600	5.80E+05	215	3.03E+04			460	7.30E+06			720	3.09E+05			1100	3.38E+03		
440	1.37E+06	1325	9.62E+04	650	4.97E+05	220	2.93E+04			470	9.12E+06			730	3.00E+05			1200	9.59E+03		
450	1.31E+06	1344	8.30E+04	700	4.22E+05	225	9.84E+04			480	1.07E+07			740	2.93E+05			1250	1.60E+04		
460	1.92E+06			750	3.27E+05	230	2.74E+04			490	1.21E+07			750	2.85E+05			1275	1.92E+04		
470	1.12E+06			800	3.31E+05	235	2.65E+04			500	1.35E+07			760	2.70E+05			1277	1.95E+04		
480	1.03E+06			850	3.20E+05	240	2.55E+04			510	1.49E+07			770	2.52E+05						
490	9.38E+05			900	3.15E+05	250	2.38E+04			520	1.57E+07			780	2.34E+05						
500	8.38E+05			950	2.67E+05	255	2.27E+04			530	1.62E+07			790	2.15E+05						
510	7.83E+05			1000	1.98E+05	260	2.18E+04			540	1.67E+07			800	2.02E+05						
520	7.35E+05			1050	1.90E+05	265	2.08E+04			550	1.72E+07			810	1.90E+05						
530	7.26E+05			1100	1.58E+05	270	1.90E+04			560	1.84E+07			820	1.78E+05						
540	6.98E+05			1112	1.42E+05	275	1.95E+04			570	1.90E+07			830	1.67E+05						
550	6.70E+05					280	1.94E+04			580	2.14E+07			844	1.50E+05						
560	6.41E+05					285	1.94E+04			590	2.29E+07			850	1.46E+05						
570	5.95E+05					290	1.94E+04			600	2.26E+07			860	1.30E+05						
580	5.38E+05					295	1.83E+04			610	2.10E+07			870	1.26E+05						
590	4.77E+05					300	1.93E+04			620	2.06E+07			880	1.13E+05						

T57H40/9	
Time (min)	Conc. (plu/ml)
0	0
48	0
108	0
168	273
196	5450
228	8000
256	6000
288	3200
318	4300
348	8300
378	5300
408	1700
436	2930
501	1870
546	1000
591	630
681	429
771	413
861	417
906	403
951	473
996	410
1041	350
1131	223
1221	173
1311	92
1401	43
1491	43.5
1581	153
1671	126.3

T5711	
Time (min)	Conc. (plu/ml)
0	20.5
48	14.5
108	15.5
168	30.5
196	287.3
228	224.3
256	233.3
288	220
318	230.3
348	57.5
378	27
408	116.5
436	152
501	55
546	23
591	91.5
681	4
771	6.5
861	10.5
906	27
951	25
996	0.5
1041	20.5
1131	2.5
1221	2.5
1311	0.5
1401	1.5
1491	1
1581	1.5
1671	2

T57H6/1	
Time (min)	Conc. (plu/ml)
0	0
48	0
108	0
168	20
196	309
228	490
256	503
288	453
318	417
348	457
378	300
408	283
436	235
501	138
546	80.3
591	62
681	32.5
771	28.5
861	26
906	50
951	79.5
996	34
1041	34
1131	48.5
1221	18
1311	10.5
1401	0.8
1491	11
1581	10.5
1671	17

T5717	
Time (min)	Conc. (plu/ml)
0	30
48	45.5
108	33.5
168	0
196	173
228	280
256	353
288	417
318	282
348	183
378	132
408	109
436	253
501	140
546	123
591	39
681	35
771	11.5
861	38
906	80.5
951	99
996	49
1041	88
1131	32
1221	21
1311	4
1401	14
1491	8
1581	10
1671	14

T23b8me		T24b8me		T25b8me		T26b8me		T30b0me		T31b8me				T32b8me	
Time (min)	Conc. (mg/l)	Time (min)	Conc. (mg/l)	Time (min)	Conc. (mg/l)	Time (min)	Conc. (mg/l)	Time (min)	Conc. (mg/l)	Time (min)	Conc. (mg/l)	Time (min)	Conc. (mg/l)	Time (min)	Conc. (mg/l)
0	0.0145	0	0.00125	0	0.000347	0	0.000543	2	3.47E-05	5	0.0002312	5425	0.2498903	0	0.0133237
7205	0.0288093	8442	0.0034682	563	0.574372	8	0.000853	62	0.12	65	0.0386647	3485	0.3345376	68	0.02615029
7268	0.0288093	8502	0.4001158	623	1.218703	68	0.000853	1022	0.2080116	125	0.0193468	3545	0.1713699	128	0.02615029
7328	0.0059422	8562	2.3854915	683	4.668930	128	0.161237	1082	0.1478362	185	0.0025254	3605	0.3613064	188	0.0133237
7388	1.3455145	9922	4.0178208	743	5.034182	188	0.321615	1142	0.2883006	245	0.0356116	3665	0.4550058	248	0.17300751
7448	0.8718047	9982	3.7453528	803	5.070884	248	0.161237	1202	1.2116763	305	0.0386647	3725	0.2274913	308	12.2175954
7508	2.5126938	9742	4.2054921	863	5.676511	308	0.000853	1262	3.2600604	365	0.0256382	3785	0.1005549	368	39.1954882
7568	2.6842197	9802	4.2280751	923	7.800586	368	0.000853	1322	4.3430280	425	0.0356647	3845	0.2542543	428	48.1005202
7628	0.0288093	9862	3.8070288	983	8.837095	428	0.000853	1382	4.7845054	485	0.0386647	3905	0.3470017	488	48.1005202
7688	1.1080884	9922	4.1206532	1043	4.267771	488	0.01348	1442	5.5473879	545	0.0386647	3965	0.1204393	548	21.5343873
7748	2.3711734	9982	4.2877515	1103	2.340763	548	0.01348	1502	6.9524567	605	0.0002312	4025	0.2140867	608	8.04245087
7808	2.6868786	10042	4.1618003	1163	1.218702	608	0.000853	1562	8.0383237	665	0.0002312	4085	0.2115029	668	4.18648821
7868	4.2759711	10102	3.742815	1223	0.734958	668	0.000853	1622	5.7481387	725	0.0002312	4145	0.4014393	728	2.58284162
7928	4.4224913	10162	3.4703468	1283	0.413788	728	5.62104	1682	1.6933931	785	0.0002312	4205	0.3345607	788	2.10089595
7988	4.5690116	10222	3.1878786	1343	0.413788	788	19.75231	1742	0.5291065	845	0.0002312	4265	0.2576243	848	2.10089595
8048	4.4224913	10282	3.2483988			848	27.62066	1802	1.1313468	905	0.160815	4325	0.2007457	908	2.10089595
8108	3.8688786	10342	2.7994104			908	28.74493	1862	0.0071503	965	0.0640638	4385	0.1338093	968	2.10089595
8168	3.1037861	10402	2.6734682			968	24.73038	1922	0.002354	1025	0.3208364	4446	0.0869306	1028	2.10089596
8228	2.5176936	10462	2.8040462			1028	19.10988			1085	0.0640638	4505	5.78E-05	1088	2.10089596
8288	1.7850809	10522	2.5680083			1088	16.21048			1145	0.0640636			1148	0.08102312
8348	1.4920347	10582	2.4421561			1148	13.65017			1205	0.0640638			1208	0.24180118
8408	1.3455145	10642	2.6091965			1208	10.11735			1265	0.0640638			1268	0.24180118
8468	1.0524682	10702	2.7783006			1268	6.745121			1325	0.4815145			1328	0.08102312
8528	1.1080884	10762	2.2107881			1328	4.338582			1385	0.0640638			1388	0.04887283
8588	0.0059422	10822	2.2313842			1388	3.212301			1445	0.4815145			1448	0.04887283
8648	1.3455145	10882	2.1054162			1448	2.589971			1505	0.0002312			1508	0.00035954
8708	1.1080884	10942	2.1259942			1508	2.248809			1565	0.0640636			1568	0.09304971
8768	1.1080884	11002	2.2030985			1568	2.088225			1625	4.73E-05			1628	0.03804624
8828	1.0524682	11062	1.8740482			1628	1.90044			1685	2.838237			1688	0.03804624
8888	0.0059422	11122	1.8940243			1688	1.445886			1745	0.4840025			1748	0.24180118
8948	0.612886	11182	2.0817283			1748	1.124728			1806	16.295497			1808	0.24180118
9008	0.6128896	11242	1.7892804			1808	1.124728			1865	22.749231			1868	0.40218407
9068	0.3198487	11302	1.8090382			1868	1.124728			1925	28.115335			1928	0.40218407
9128	0.3198487	11362	1.6373699			1928	1.124728			1985	22.722462			1988	0.40218407
9188	0.3198487	11422	1.704474			1988	0.462300			2045	16.453643			2048	0.05881272
9248	0.3198487	11482	1.7249942			2048	0.462300			2105	14.345309			2108	0.37977457
		11542	1.5900462			2108	0.321615			2165	12.485288			2168	0.21010053
		11602	1.328528			2168	0.321615			2225	10.735815			2228	0.05881272
		11662	1.3471561			2228	0.000853			2285	10.04078			2288	0.37977457
		11722	1.2212139			2288	0.000853			2345	9.4743873			2348	0.37977457
		11782	1.2417019			2348	0.321615			2405	8.5777740			2408	0.37977457
		11842	1.1158439			2408	0.000853			2465	7.8417977			2468	0.37977457
		11902	0.8433179			2468	0.01348			2525	7.105785			2528	0.37977457
		11962	0.883898			2528	0.039133			2585	5.7224687			2588	0.37977457
		12022	0.6014355			2588	0.039306			2645	5.152			2648	0.37977457
		12082	0.7585318			2648	0.01348			2705	4.8077746			2708	0.37977457
		12142	0.4880636			2708	0.039133			2765	4.8041222			2768	0.37977457
		12202	0.5801214			2768	0.039133			2825	4.3892601			2828	0.37977457
		12262	0.3808418			2828	0.051985			2885	3.8136831			2888	0.37977457
		12322	0.2548936			2888	0.020306			2946	4.063858			2948	0.37977457
		12382	0.2752717							3005	3.8476821			3008	0.07793084
		12442	0.4473757							3065	2.0975885			3068	0.11986098
		12502	0.4629538							3125	1.0727572			3128	0.10231792
		12562	0.3370068							3185	1.0973084			3188	0.00083237
		12622	0.2110836							3245	0.8824013				
		12682	0.0850678							3305	0.5857019				
		12742	0.1058358							3365	0.0133931				

T14font				T15font				T20font		T23font				T24font		T25font					
Time (min)	Conc. (mg/l)	Time (min)	Conc. (mg/l)	Time (min)	Conc. (mg/l)	Time (min)	Conc. (mg/l)	Time (min)	Conc. (mg/l)	Time (min)	Conc. (mg/l)	Time (min)	Conc. (mg/l)	Time (min)	Conc. (mg/l)	Time (min)	Conc. (mg/l)	Time (min)	Conc. (mg/l)	Time (min)	Conc. (mg/l)
0	5.26E-02	4750	7.26E+00	0	0.00E+00	2800	2.78E+00	0	5.90E-04	0	0.01	3369	1.6184451	0	0.00025	0	0.0722843	1970.8	13.67694	3146.6	1.8540133
1000	5.26E-02	5000	5.19E+00	500	3.47E-02	2700	2.70E+00	2000	5.88E-04	9	0.5305723	3429	2.0841456	3464	0.0002801	1298.6	1.940578	1982.8	13.41965	3158.6	1.5979133
1100	1.95E-02	5250	3.94E+00	750	5.21E-02	2600	2.68E+00	2100	5.90E-04	69	0.0165723	3480	2.5320075	3524	0.0002801	1310.6	0.6555893	1994.8	13.16285	3170.6	1.8122486
1200	1.08E-01	5500	3.24E+00	1000	6.94E-02	2500	2.40E+00	2200	5.89E-04	129	0.1979075	3549	2.9218208	3584	0.1521098	1322.6	0.2272543	2006.8	12.90565	3182.6	1.5122486
1300	6.91E-01	5750	2.78E+00	1025	7.11E-02	2950	2.07E+00	2500	6.01E-04	189	0.1979075	3609	3.361711	3644	0.3360058	1334.6	1.4078133	2018.8	12.79452	3194.6	1.4285838
1400	6.19E-01	6000	2.29E+00	1050	7.29E-02	3000	1.67E+00	2600	6.01E-04	249	0.2735723	3669	3.7158364	3704	0.8382488	1346.6	4.424698	2030.8	12.30619	3206.6	1.2552486
1500	8.91E-01	6250	1.88E+00	1075	7.46E-02	3100	1.23E+00	2700	1.56E-04	309	0.1979075	3729	3.8335087	3764	0.9241445	1358.6	8.1942081	2042.8	11.98353	3218.6	1.0839191
1600	8.91E-01	6500	8.83E-01	1100	7.64E-02	3150	1.06E+00	2750	4.16E-04	369	0.2735723	3789	4.2104104	3824	1.2841503	1370.6	11.877658	2054.8	11.53619	3230.6	1.0895838
1700	5.47E-01	6734	2.12E-01	1125	7.81E-02	3175	9.52E-01	2800	5.79E-04	429	0.358237	3849	4.2367515	3884	1.6325954	1382.6	14.876173	2066.8	11.2782	3242.6	0.9982543
1800	8.20E-01			1150	8.37E-02	3200	0.21E-01	2850	6.16E-04	489	0.4449017	3909	4.1626474	3944	2.088711	1394.6	16.131468	2078.8	10.84986	3254.8	0.9982543
1900	5.20E-01			1175	1.89E-01	3250	1.12E+00	2900	3.93E-01	549	0.7019017	3969	4.3455376	4004	2.4151503	1406.6	22.243468	2090.8	10.50286	3266.8	0.9982543
2000	5.67E-01			1200	2.83E-01	3300	1.18E+00	2950	4.64E-01	609	0.7019017	4029	4.3061156	4064	2.8492659	1418.6	27.554769	2102.8	10.33587	3278.8	0.9125838
2100	4.94E-01			1225	3.83E-01	3350	1.09E+00	3000	5.09E-01	669	0.7019017	4089	4.3234567	4124	3.197211	1430.6	33.380068	2114.8	10.07887	3290.8	0.8289191
2200	4.78E-01			1250	4.82E-01	3400	9.98E-01	3050	7.31E-01	729	0.7019017	4149	4.2782543	4184	3.5403757	1442.6	38.605705	2126.8	9.907532	3302.8	0.8289191
2250	5.08E-01			1268	5.58E-01	3460	9.57E-01	3100	9.12E-01	789	0.7875665	4209	4.0443757	4244	3.7127457	1454.6	42.888017	2138.8	9.584873	3314.8	0.9125838
2300	4.43E-01			1275	6.82E-01	3500	9.13E-01	3150	1.09E+00	849	0.7019017	4269	3.7248324	4304	3.5529789	1466.6	46.315685	2150.8	9.223208	3326.8	0.8289191
2350	3.77E-01			1300	6.82E-01	3550	8.50E-01	3200	1.54E+00	909	0.7019017	4329	3.6082946	4364	3.3969827	1478.6	48.265988	2162.8	9.050473	3338.8	0.7412543
2400	3.72E-01			1325	7.82E-01	3600	5.97E-01	3250	2.25E+00	969	0.7019017	4389	3.3858671	4424	3.4394451	1490.6	49.742312	2174.8	9.708208	3350.8	0.8558898
2450	4.19E-01			1350	9.53E-01	3650	3.19E-01	3300	3.27E+00	1029	0.6305723	4449	3.1204276	4484	3.6512428	1502.6	50.654842	2186.8	9.385543	3362.8	0.4842543
2500	5.56E-01			1375	8.20E-01	4000	2.39E-01	3350	4.81E+00	1089	0.7019017	4509	2.8240058	4544	3.4814882	1514.6	50.841836	2198.8	9.108543	3374.8	0.1415898
2550	8.91E-01			1400	1.00E+00	4050	2.39E-01	3500	9.60E+00	1149	0.7875665	4569	2.5999075	4604	3.4972486	1526.6	51.198836	2210.8	7.785678	3386.8	0.2272543
2600	8.91E-01			1425	1.40E+00	4075	2.39E-01	3600	1.28E+01	1209	0.7019017	4629	2.5391445	4664	3.4972486	1538.6	50.941838	2222.8	7.423214	3398.8	0.2272543
2650	8.91E-01			1450	1.20E+00	4100	1.95E-01	3700	1.60E+01	1269	0.7019017	4689	2.1964798	4724	3.3008266	1550.6	50.513806	2234.8	7.166214	3410.8	0.1415898
2700	4.49E-01			1475	1.27E+00	4110	1.58E-01	3750	1.60E+01	1329	0.7019017	4749	2.054052	4784	3.3008127	1562.8	48.858642	2246.8	6.994664	3422.8	0.0599248
2800	4.17E-01			1500	1.33E+00	4120	1.18E-01	3800	1.55E+01	1389	0.358237	4809	1.7402832	4844	3.2701003	1574.8	46.457316	2258.8	6.737664				
2850	3.72E-01			1525	1.42E+00	4140	3.59E-02	3850	1.71E+01	1449	0.2735723	4869	1.9078555	4904	3.2701008	1586.6	47.000994	2270.8	6.85222				
2900	3.08E-01			1550	1.62E+00	4148	3.99E-03	3900	1.73E+01	1509	0.358237	4929	1.3097572	4964	3.0305316	1598.6	45.287671	2282.8	6.556555				
2950	5.20E-01			1600	1.78E+00	4209	0.00E+00	4000	1.77E+01	1569	0.2735723	4989	1.2958502	5024	2.6139842	1610.6	43.574242	2294.8	6.309555				
3000	8.37E-01			1625	1.89E+00			4100	1.70E+01	1628	0.359237	5049	1.1890068	5084	2.6715805	1622.6	41.889688	2306.8	6.139226				
3050	1.12E+00			1650	1.84E+00			4200	1.55E+01	1688	0.359237	5109	0.8992312	5144	2.617678	1634.6	30.605035	2318.8	5.90589				
3100	1.59E+00			1675	1.98E+00			4300	1.44E+01	1749	0.0165723	5169	1.026133	5204	2.2721367	1646.6	37.749048	2330.8	5.881225				
3150	2.26E+00			1700	2.05E+00			4400	1.32E+01	1808	0.359237	5229	0.8657052	5264	2.0161367	1658.6	36.035723	2342.8	5.824225				
3200	3.04E+00			1750	2.32E+00			4500	1.18E+01	1868	0.5305723	5288	0.7259308	5324	1.8553688	1670.8	34.065308	2354.8	5.624225				
3250	3.97E+00			1800	2.45E+00			4600	1.01E+01	1928	0.5305723	5349	0.7432747	5384	1.8561754	1682.6	31.838075	2366.8	5.45269				
3300	4.83E+00			1850	2.80E+00			4700	8.53E+00	1988	0.4449017	5409	0.5267341	5444	1.2740867	1694.6	30.210423	2378.8	5.281561				
3350	5.84E+00			1900	3.07E+00			4800	7.33E+00	2049	0.358237	5469	0.5808536	5504	0.8284608	1706.6	28.497098	2390.8	5.281561				
3400	6.84E+00			1950	3.19E+00			4900	6.15E+00	2109	0.4449017	5529	0.4616474	5564	0.6148766	1718.6	26.783775	2402.8	5.024681				
3450	7.70E+00			2000	3.19E+00			5000	5.23E+00	2169	0.5305723	5589	0.2303121	5624	1.3886539	1730.6	25.327454	2414.8	4.938896				
3500	8.44E+00			2025	3.19E+00			5250	3.09E+00	2229	0.6305723	5649	0.1619884	5684	1.2067877	1742.6	24.042457	2426.8	4.787581				
3550	9.24E+00			2050	3.19E+00			5500	1.88E+00	2289	0.4449017	5709	0.1908802	5744	0.6188836	1754.6	22.586133	2438.8	4.896231				
3600	1.00E+01			2075	3.19E+00			5750	8.21E-01	2349	0.358237	5769	0.4315896	5804	0.3732543	1766.6	21.388304	2450.8	4.526231				
3650	1.07E+01			2100	3.19E+00			6000	2.99E-01	2400	0.358237	5829	0.2480193	5864	0.2019249	1778.6	20.273145	2462.8	4.598231				
3700	1.12E+01			2125	3.25E+00			6125	1.67E-01	2469	0.358237	5889	0.274815	5924	0.2366869	1790.6	19.50215	2474.8	4.881898				
3750	1.16E+01			2150	3.35E+00			6210	3.11E-02	2529	0.359237	5949	0.2323931	5984	0.3059711	1802.6	18.47416	2486.8	4.787561				
3800	1.20E+01			2175	3.41E+00			6214	2.27E-02	2589	0.358237	6009	0.1786301	6044	1.18E-05	1814.6	17.617491	2498.8	4.853231				
3850	1.21E+01			2200	3.35E+00					2640	0.359237	6609	0.0008266	6104	1.18E-05	1826.6	17.103497	3062.8	2.711572				
3900	1.22E+01			2225	3.29E+00					2700	0.358237	7020	0.1721619	6164	1.10E-05	1838.6	16.419182	3014.8	2.540743				
3950	1.22E+01			2250	3.24E+00					2760	0.358237	7080	0.1721619	6224	1.18E-05	1850.6	16.075497	3026.8	2.540243				
4000	1.22E+01			2275	3.21E+00					2820	0.2735723	7140	0.0864913	6284	1.18E-05	1862.8	15.847188	3038.8	2.187578				
4050	1.20E+01			2300	3.16E+00					2880	0.1979075	7200	0.0008289	6344	1.16E-05	1874.8	15.218838	3050.8	2.111913				
4100	1.19E+01			2325	3.10E+00					2940	0.102237	7260	0.0008266			1886.6	14.961838	3062.8	2.026243				
4150	1.21E+01			2350	3.19E+00					3000	0.0107918	7320	0.0008266			1898.8	14.676173	3074.8	1.759249				
4200	1.17E+01			2375	3.12E+00					3061	0.0118324					1910.8	14.533509	3086.8	1.683578				
4250	1.15E+01			2380	3.08E+00					3129	0.2178439					1922.8	14.190844	3098.8	1.683578				
4300	1.12E+01			2400	3.05E+00					3189	0.482185					1934.8	13.933844	3110.8	1.683578				
4350	1.07E+01			2450	2.98E+00					3249	0.9509799					1946.8	13.676844	3122.8	1.512249				
4500	0.29E+00			2500	2.91E+00					3308	1.2842197					1958.8	13.933844	3134.8	1.597913				

T1salvu				T2salvu		T11salvu		T12salvu		T121salvu				T20salvu				T22salvu	
Time (min)	Conc. (mg/l)	Time (min)	Conc. (mg/l)	Time (min)	Conc. (mg/l)	Time (min)	Conc. (mg/l)	Time (min)	Conc. (mg/l)	Time (min)	Conc. (mg/l)	Time (min)	Conc. (mg/l)	Time (min)	Conc. (mg/l)	Time (min)	Conc. (mg/l)	Time (min)	Conc. (mg/l)
0	3.18E-01	3100	6.05E+00	0	0	0	0	0	0	0	0	3420	8.99312739	0	0.00224855	5357.50128	4.0578302	0	0
500	3.18E-01	3150	6.05E+00	3000	0.9538824	200.5	0.0006824	1044.495	0.081771	60	0.001257	3480	9.82515824	1992.502	0.01389814	5417.50176	3.85141099	23	0.004383
1000	3.18E-01	3200	5.41E+00	3000	1.5977707	260.5	0.0492803	1104.495	0.015485	120	0.0012958	3540	10.2571847	2057.502	0.02138261	5477.50224	2.39450049	83	0.125713
1500	3.18E-01	3250	5.41E+00	3135	2.8849882	320.5	0.0492803	1164.495	0.161318	180	0.144707	3600	10.6378344	2117.501	0.05165078	5537.50128	1.83344725	143	0.650641
1750	3.18E-01	3300	4.78E+00	3195	3.5040784	380.5	0.0492803	1224.495	0.200936	240	0.0474713	3660	11.3753949	2177.502	0.13480955	5597.50176	1.73829624	583	0.015643
2000	3.18E-01	3400	3.50E+00	3240	4.1431847	440.5	0.0006824	1284.495	0.161318	300	0.2419427	3720	11.6871019	2237.502	0.18552303	5657.50224	1.6649294	923	0.038732
2250	3.18E-01	3450	2.82E+00	3315	4.782293	500.5	0.0978981	1344.495	0.112701	360	0.2905605	3780	11.5698662	2297.501	0.14680118	5717.50128	1.77396522	883	0.012694
2300	9.54E-01	3500	2.23E+00	3360	5.4103822	560.5	0.0006824	1404.495	0.033153	420	0.3391783	3840	11.3267771	2357.502	0.12804065	5777.50176	2.03761795	1343	0.11928
2370	9.18E-01	3550	2.00E+00	3405	5.81	620.5	0.1951338	1464.496	0.033153	480	0.3391783	3900	10.9884522	2417.502	0.26166345	5837.50224	2.37880003	1403	1.041057
2380	9.54E-01	3600	2.23E+00	3555	5.41	680.5	0.3409873	1524.495	0.033153	540	0.3877089	3960	10.6113976	2477.501	0.29337892	5897.50128	2.68804013	1463	8.355673
2390	9.55E-01	3650	2.23E+00	3645	4.1431847	740.5	0.3896051	1584.495	0.033153	600	0.5338431	4020	9.38707008	2537.502	0.3250904	5951.50176	2.93170588	1523	11.73418
9400	9.55E-01	3700	1.59E+00	3720	3.5040784	800.5	0.3409873	1644.496	0.081771	660	0.6784966	4080	8.50894904	2597.509	0.51143984	6011.50224	2.88510304	1583	15.48115
9410	1.59E+00	3750	1.59E+00	3750	2.8849882	860.5	0.2923594	1704.495	0.32486	720	0.7281147	4140	7.63183429	2657.501	0.69776595	6071.50128	2.45381184	1643	17.18467
2420	1.59E+00	3800	1.59E+00	3765	2.8849882	920.6	0.2437516	1764.495	0.470713	780	0.8784966	4200	7.19427388	2717.502	0.88413539	6131.50176	1.81553954	1703	17.06036
2430	1.59E+00	3950	1.59E+00	3840	3.5040784	980.5	0.2437516	1824.496	0.616567	840	0.930879	4260	6.2219172	2777.502	1.2588018	6187.50224	1.5885284	1763	16.44478
2440	1.59E+00	3900	9.55E-01	3918	4.1431847	1040.5	0.4382279	1884.495	3.625338	900	0.4850319	4320	5.93021919	2837.501	1.58610288	6257.50128	1.62123987	1823	14.23899
2450	1.59E+00	3950	9.55E-01	4005	4.782293	1100.5	0.2923594	1944.495	1.107745	960	0.4850319	4380	5.15233121	2897.509	1.87519267	6317.50176	1.86513464	1883	10.84098
2460	1.59E+00	4000	3.20E-01	4080	5.5949046	1160.5	0.1465160	2004.495	1.054127	1020	0.4850319	4440	4.8606242	2957.502	1.98457270	6377.50224	1.83930279	1943	7.866383
2470	2.23E+00	4120	3.18E-01	4350	6.5949045	1220.5	0.0492803	2064.495	1.151383	1080	0.2419427	4500	4.81200852	3017.501	2.12514768	6437.50128	1.53597333	2003	5.92872
9480	2.23E+00			4440	7.9068153	1280.5	0.0492803	2124.495	0.966997	1140	0.0985846	4560	4.42306359	3077.502	2.00222538	6497.50176	1.84500848	2063	4.474186
2490	2.23E+00			4455	7.327707	1340.5	0.0492803	2184.496	0.905274	1200	0.0474713	4620	3.83884888	3137.502	2.11126851	6557.50224	1.90887292	2123	3.51465
2500	2.23E+00			4515	6.8865987	1400.6	0.0006824	2244.495	0.70247	1260	0.0980892	4680	3.69658051	3197.501	2.22183902	6617.50128	2.14658365	2183	2.948172
2510	2.23E+00			4580	6.8494805	1460.5	0.0492803	2304.495	0.78242	1320	0.144707	4740	3.61315282	3257.502	2.43240823	6677.50176	2.20409146	2243	2.529086
2520	2.87E+00			4650	5.4103822	1520.5	0.2923594	2364.496	0.618587	1380	0.3391783	4800	2.23528752	3317.502	2.46412221	6737.50224	2.28153592	2303	1.962818
2530	2.23E+00			4740	4.782293	1580.5	0.7299299	2424.495	0.618587	1440	0.3391783	4860	2.08841401	3377.501	2.54736101	6797.50128	1.41008557	2363	1.740057
9540	2.23E+00			4780	4.1431847	1620.6	1.2842281	2484.495	0.619331	1500	0.3391783	4920	2.08841401	3437.502	2.60486547	6857.50176	1.37137838	2423	1.498303
2550	3.50E+00			4860	3.5040784	1680.5	2.3829299	2544.498	0.567948	1560	0.5336433	4980	1.79270701	3497.502	2.78121491	6917.50224	0.88187197	2483	1.344057
2560	2.87E+00			4995	3.25	1740.6	1.9459894	2604.495	0.373478	1620	0.6784966	5040	1.21429299	3557.501	2.90024905	6977.50128	0.14818325	2543	1.022336
2570	2.82E+00			5085	2.8849882	2000.5	2.5287834	2664.495	0.422098	1680	0.5822675	5100	1.06843949	3617.502	2.95773251	7037.50224	0.13229388	2603	0.702414
2580	3.50E+00			5235	2.2958599	2060.5	3.1608153	2724.496	0.422098	1740	0.6784966	5160	0.867895	3677.502	2.98944598	7037.50224	0.08287221	2663	0.470554
2590	4.14E+00			5825	0.9588824	2120.6	3.649768	2784.496	0.213803	1800	0.8739882	5220	0.68745052	3737.501	2.98961413	7097.50128	0.09788929	2723	0.355554
2600	4.14E+00			6165	0.5105541	2180.6	3.7442293	2844.495	0.816587	1860	0.8263903	5280	0.498502	3797.502	2.84978228	7157.50176	0.12032483	2783	0.280382
2610	4.14E+00			6540	0	2240.5	3.7442293	2904.496	0.470713	1920	0.7281147	5340	0.258982	3857.502	3.0845864	7217.50128	0.01514734	2843	0.037618
2620	4.14E+00					2300.5	3.6956115	2964.495	0.32488	1980	0.8739882	5400	0.1256321	3917.501	3.19301819	7277.50176	0.04585561	3903	0.054338
2630	4.14E+00					2360.5	3.4525223	3024.495	0.470713	2040	1.0108217			3977.502	3.0449222	7337.50224	0.09126257	4103	0.002255
2640	4.78E+00					2420.5	3.2094331	3084.496	0.470713	2100	1.1170573			4037.502	3.36013979			4163	0.025344
2650	4.78E+00					2480.5	2.9127761	3144.495	0.32488	2160	1.214293			4097.501	3.82379954				
2660	4.78E+00					2540.5	2.2858943	3204.495	0.227694	2220	1.0684305			4157.502	3.47510898				
2670	5.41E+00					2600.5	1.7022303	3264.496	0.033153	2280	1.1170573			4217.502	3.55836486				
2680	5.41E+00					2660.5	1.2847781	3324.495	0.015485	2340	1.1170573			4277.501	4.58530713				
2690	5.41E+00					2720.5	0.7785478	3384.495	0.112701	2400	1.1656752			4337.502	4.34542399				
2700	5.41E+00					2780.5	0.4868406	3444.496	0.161318	2460	1.1656752			4397.502	4.40090746				
2710	0.05E+00					2840.5	0.0978981	3504.495	0.209936	2520	1.214293			4457.501	4.35530482				
2720	0.05E+00					3000.5	0.0006824	3564.495	0.209936	2580	1.2829108			4517.502	4.41278908				
2770	6.69E+00					3140.5	0.0006824	3624.496	0.161318	2640	1.214293			4577.502	4.39296723				
2780	6.69E+00					3200.5	0.0006824	3684.495	0.209936	2700	0.9212038			4637.501	4.3731253				
2790	0.09E+00							3744.495	0.161318	2760	1.4573822			4697.502	4.45838418				
2800	0.09E+00							3804.496	0.161318	2820	1.8518535			4757.502	4.41078134				
2820	0.09E+00							3864.495	0.209936	2880	2.0407982			4817.501	4.03013558				
2850	7.32E+00							3924.495	0.307172	2940	2.8189815			4877.502	4.20380132				
2900	7.33E+00							3984.496	0.307172	3000	3.5895905			4937.502	4.35128578				
2810	7.05E+00							4044.496	0.047497	3060	4.5202994			4997.501	4.30568284				
2820	7.33E+00							4104.495	0.847497	3120	5.1523312			5057.502	4.2600801				
2830	7.06E+00									3180	6.8810824			5117.502	4.26001924				
2975	7.06E+00									3240	8.0511842			5177.501	4.28773271				
3000	7.32E+00									3300	7.6282094			6237.502	4.4007620				
3050	6.69E+00									3360	8.3124772			5297.502	4.28384335				

T26salvu		T25salvu		T30salvu				T32salvu				T41salvu	
Time (min)	Conc. (mg/l)	Time (min)	Conc. (mg/l)	Time (min)	Conc. (mg/l)	Time (min)	Conc. (mg/l)	Time (min)	Conc. (mg/l)	Time (min)	Conc. (mg/l)	Time (min)	Conc. (mg/l)
0	1.53E-02	0	1.24E-02	0	0.00E+00	1500	1.48E+01	0	0.00E+00	900	1.40E+01	0	1.00E-02
1250	1.06E-01	500	3.51E-01	50	9.61E-03	1510	1.45E+01	50	9.21E-02	950	1.12E+01	250	2.02E-02
1300	2.86E-01	550	3.85E-01	100	1.92E-02	1520	1.44E+01	100	4.43E-02	1000	8.85E+00	500	3.04E-02
1350	2.89E-01	600	4.16E-01	150	2.88E-02	1530	1.42E+01	150	6.11E-02	1100	5.02E+00	750	4.07E-02
1400	3.40E-01	650	4.52E-01	200	3.84E-02	1540	1.39E+01	200	1.18E-01	1150	5.00E+00	1000	8.20E-02
1450	4.03E-01	700	4.88E-01	250	4.80E-02	1550	1.37E+01	210	1.25E-01	1200	4.84E+00	1050	1.62E-01
1500	7.36E-01	750	5.20E-01	300	5.76E-02	1560	1.36E+01	220	1.33E-01	1250	4.19E+00	1075	2.13E-01
1550	1.17E+00	800	2.01E+00	350	6.73E-02	1570	1.32E+01	230	1.40E-01	1300	3.71E+00	1084	2.32E-01
1600	2.03E+00	850	4.08E+00	400	7.69E-02	1580	1.30E+01	240	1.47E-01	1350	3.39E+00	1100	2.78E-01
1650	3.62E+00	900	5.18E+00	450	8.65E-02	1590	1.27E+01	250	1.55E-01	1400	3.32E+00	1125	4.88E-01
1675	5.03E+00	950	6.30E+00	500	9.61E-02	1600	1.24E+01	260	1.62E-01	1500	3.07E+00	1150	7.17E-01
1700	6.38E+00	1000	1.01E+01	550	1.06E-01	1610	1.21E+01	270	1.69E-01	1600	2.82E+00	1175	9.83E-01
1800	1.21E+01	1050	1.15E+01	600	1.15E-01	1620	1.18E+01	280	1.76E-01	1700	2.37E+00	1200	1.27E+00
1900	1.58E+01	1100	1.24E+01	700	2.70E-01	1630	1.15E+01	290	1.69E-01	1800	1.66E+00	1225	1.71E+00
2000	1.80E+01	1150	1.27E+01	750	4.50E-01	1640	1.12E+01	300	1.82E-01	1900	8.51E-01	1250	2.56E+00
2100	1.52E+01	1200	1.28E+01	800	6.29E-01	1650	1.09E+01	310	1.85E-01	2000	7.00E-01	1275	3.40E+00
2200	1.19E+01	1250	1.25E+01	850	8.08E-01	1660	1.04E-01	320	1.47E-01	2100	6.58E-01	1300	3.19E+00
2300	7.82E+00	1300	1.24E+01	900	1.02E+00	1670	1.00E+01	330	1.40E-01	2200	1.03E-01	1325	2.62E+00
2400	4.95E+00	1350	1.17E+01	950	1.10E+00	1680	0.56E+00	340	1.37E-01	2300	9.19E-01	1350	2.56E+00
2500	3.25E+00	1400	1.05E+01	1000	1.35E+00	1690	0.13E+00	350	3.10E-01	2400	2.10E-01	1375	2.47E+00
2600	2.54E+00	1450	9.05E+00	1050	1.52E+00	1700	8.70E+00	360	4.88E-01	2500	2.50E-01	1400	2.36E+00
2700	2.27E+00	1460	8.73E+00	1100	1.70E+00	1710	8.30E+00	370	6.83E-01	2600	2.43E-01	1425	2.24E+00
2800	1.89E+00	1470	8.41E+00	1150	2.14E+00	1720	7.94E+00	380	8.40E-01	2700	3.51E-01	1450	2.12E+00
2900	1.58E+00	1480	8.09E+00	1160	2.23E+00	1730	7.58E+00	390	1.02E+00	2800	3.52E-01	1475	1.05E+00
2950	1.47E+00	1490	7.77E+00	1170	2.65E+00	1740	7.22E+00	400	1.21E+00	2850	3.88E-01	1500	1.76E+00
3000	1.37E+00	1500	7.44E+00	1180	3.05E+00	1750	6.85E+00	410	2.14E+00	2950	3.95E-01	1525	1.55E+00
3100	1.14E+00	1550	5.84E+00	1190	3.56E+00	1760	6.49E+00	420	3.10E+00			1550	1.29E+00
3250	6.17E-01	1600	4.44E+00	1200	4.08E+00	1770	6.09E+00	430	4.05E+00			1575	1.04E+00
3500	1.78E-01	1650	3.55E+00	1210	4.57E+00	1780	5.84E+00	440	5.00E+00			1600	7.88E-01
3750	3.78E-01	1700	2.63E+00	1220	5.07E+00	1790	5.20E+00	450	5.95E+00			1625	5.35E-01
4000	8.08E-02	1750	1.63E+00	1230	5.91E+00	1800	4.76E+00	460	6.92E+00			1650	3.50E-01
4237	6.87E-03	1800	7.08E-01	1240	6.73E+00	1810	4.32E+00	470	8.81E+00			1675	2.09E-01
		1825	3.17E-01	1250	7.65E+00	1820	3.88E+00	480	1.07E+01			1700	1.85E-01
		1840	8.40E-02	1260	8.57E+00	1830	3.81E+00	490	1.26E+01			1725	1.70E-01
		1843	3.74E-02	1270	9.48E+00	1840	3.47E+00	500	1.45E+01			1750	1.61E-01
				1280	1.04E+01	1850	3.34E+00	510	1.64E+01			1775	1.10E-01
				1290	1.12E+01	1860	3.21E+00	520	1.83E+01			1800	5.43E-02
				1300	1.10E+01	1870	3.08E+00	530	1.97E+01			1818	1.91E-02
				1310	1.28E+01	1880	2.95E+00	540	2.11E+01				
				1320	1.32E+01	1890	2.84E+00	550	2.39E+01				
				1330	1.39E+01	1900	2.75E+00	570	2.53E+01				
				1340	1.40E+01	1910	2.60E+00	580	2.67E+01				
				1350	1.51E+01	1920	2.50E+00	590	2.73E+01				
				1360	1.54E+01	1930	2.47E+00	600	2.79E+01				
				1370	1.57E+01	1940	2.30E+00	610	2.86E+01				
				1380	1.60E+01	1950	2.25E+00	620	2.92E+01				
				1390	1.63E+01	1960	2.10E+00	630	2.98E+01				
				1400	1.66E+01	1970	1.94E+00	640	3.04E+01				
				1410	1.65E+01	1980	1.79E+00	650	3.02E+01				
				1420	1.63E+01	1990	1.63E+00	660	2.00E+01				
				1430	1.60E+01	2000	1.48E+00	670	2.97E+01				
				1440	1.57E+01	2010	1.28E+00	680	2.94E+01				
				1450	1.54E+01	2020	1.04E+00	690	2.92E+01				
				1460	1.51E+01	2030	8.10E-01	700	2.89E+01				
				1470	1.49E+01	2040	5.75E-01	750	2.80E+01				
				1480	1.48E+01	2050	3.40E-01	800	2.22E+01				
				1490	1.47E+01	2060	1.10E-02	850	1.63E+01				

Arenav93ur						Arenav93aulio						Arenav93H40/1				Arenav93H40/1(end)		Arenav93H6/1		Arenav93it1	
Time (min)	Conc.(mg/l)	Time (min)	Conc.(mg/l)	Time (min)	Conc.(mg/l)	Time (min)	Conc.(mg/l)	Time (min)	Conc.(mg/l)	Time (min)	Conc.(mg/l)	Time (min)	Conc. (pfu/ml)	Time (min)	Conc. (pfu/ml)	Time (min)	Conc. (pfu/ml)	Time (min)	Conc. (pfu/ml)	Time (min)	Conc. (pfu/ml)
0	9.00E-08	8913	3.00E-08	34805	1.37E-08	0	1.10E-07	8913	5.00E-08	34805	1.11E-08	0	0.00E+00	8913	0.00E+00	34805	1.50E+01	0	0.00E+00	0	0.00E+00
70	9.00E-08	8985	3.00E-08	35805	1.20E-08	70	2.70E-07	8985	1.10E-07	35805	1.11E-08	70	0.00E+00	8985	0.00E+00	35805	1.70E+01	18020	0.00E+00	14820	0.00E+00
310	4.00E-08	9225	3.00E-08	36260	1.14E-08	310	1.10E-07	9225	1.10E-07	36260	1.00E-08	310	0.00E+00	9225	0.00E+00	36260	1.40E+01	18260	1.50E+00	15000	5.00E-01
550	4.00E-08	9485	3.00E-08	37210	1.00E-08	550	1.10E-07	9485	1.10E-07	37210	9.50E-07	500	0.00E+00	9466	0.00E+00	37210	1.50E+01	18500	0.00E+00	15300	0.00E+00
790	4.00E-08	9705	3.00E-08	37885	9.40E-07	790	1.10E-07	9705	5.00E-08	37885	8.60E-07	790	0.00E+00	9705	0.00E+00	37885	0.00E+00	18740	0.00E+00	15540	5.00E-01
1030	4.00E-08	9945	3.00E-08	38550	8.10E-07	1030	1.10E-07	9945	5.00E-08	38550	8.60E-07	1030	0.00E+00	9945	0.00E+00	38830	0.00E+00	18860	1.00E+00	15780	5.00E-01
1270	4.00E-08	10185	3.00E-08	39140	7.60E-07	1270	1.10E-07	10185	1.10E-07	39140	8.20E-07	1270	0.00E+00	10185	0.00E+00	39140	0.00E+00	17220	2.00E+00	16020	5.00E-01
1510	4.00E-08	10425	3.00E-08	40100	7.40E-07	1510	1.10E-07	10425	1.10E-07	40100	8.00E-07	1510	0.00E+00	10425	0.00E+00	40100	0.00E+00	17460	2.50E+00	16260	2.00E+00
1750	4.00E-08	10665	3.00E-08	40585	6.90E-07	1750	1.10E-07	10665	5.00E-08	40585	7.70E-07	1750	0.00E+00	10665	0.00E+00	40085	0.00E+00	17700	8.00E+00	16500	0.00E+00
1990	4.00E-08	10905	3.00E-08	41540	5.90E-07	1990	1.10E-07	10905	5.00E-08	41540	7.70E-07	1990	0.00E+00	10905	0.00E+00	41540	0.00E+00	17940	7.50E+00	16740	0.00E+00
2230	4.00E-08	11145	3.00E-08	42080	4.70E-07	2230	1.10E-07	11145	5.00E-08	42080	6.70E-07	2230	0.00E+00	11145	0.00E+00	42980	0.00E+00	18180	6.00E+00	16980	0.00E+00
2470	4.00E-08	11386	3.00E-08	43475	4.10E-07	2470	1.10E-07	11385	1.10E-07	43475	7.70E-07	2470	0.00E+00	11385	0.00E+00	43475	0.00E+00	18420	8.50E+00	17220	0.00E+00
2710	4.00E-08	11625	3.00E-08	44420	3.20E-07	2710	1.10E-07	11625	5.00E-08	44420	9.70E-07	2710	0.00E+00	11625	0.00E+00	44420	0.00E+00	18660	1.10E+01	17460	5.00E-01
2950	4.00E-08	11865	3.00E-08	44900	2.60E-07	2950	1.10E-07	11865	5.00E-08	44900	5.60E-07	2950	0.00E+00	11886	0.00E+00	44900	0.00E+00	18900	1.50E+01	17700	2.00E+00
3190	4.00E-08	12105	3.00E-08	45870	1.60E-07	3190	1.70E-07	12105	5.00E-08	45870	4.10E-07	3190	0.00E+00	12105	0.00E+00	45870	0.00E+00	18890	2.50E+01	17940	3.00E+00
3325	8.00E-08	12345	3.00E-08	46340	1.80E-07	3325	1.70E-07	12345	1.10E-07	46340	4.10E-07	3325	0.00E+00	12345	0.00E+00	46340	0.00E+00	19230	2.20E+01	18180	1.50E+00
3445	4.00E-08	12585	3.00E-08	47300	1.60E-07	3445	1.10E-07	12585	5.00E-08	47300	5.10E-07	3445	0.00E+00	12585	0.00E+00	47300	0.00E+00	19470	2.90E+01	18420	1.50E+00
3585	4.00E-08	12825	3.00E-08	47780	1.00E-07	3585	1.10E-07	12825	5.00E-08	47780	4.60E-07	3585	0.00E+00	12825	0.00E+00	47780	0.00E+00	19710	3.70E+01	18660	4.00E+00
3685	5.00E-08	13065	3.00E-08	48740	1.60E-07	3685	1.10E-07	13065	5.00E-08	48740	4.10E-07	3685	0.00E+00	13065	0.00E+00	48740	0.00E+00	19950	2.50E+01	18900	0.00E+00
3805	3.00E-08	13140	1.00E-08			3805	1.10E-07	13140	5.00E-08			3805	0.00E+00	13140	0.00E+00			20190	3.50E+01	18960	3.00E+00
3925	3.00E-08	13380	0.00E+00			3925	1.10E-07	13380	0.00E+00			3925	0.00E+00	13380	0.00E+00			20430	4.00E+01	19230	3.00E+00
4045	3.00E-08	13620	1.00E-08			4045	6.00E-08	13620	0.00E+00			4045	0.00E+00	13620	0.00E+00			20670	5.40E+01	19470	2.50E+00
4165	3.00E-08	13800	1.00E-08			4165	6.00E-08	13860	0.00E+00			4165	0.00E+00	13860	0.00E+00			24340	7.00E+00	19710	3.00E+00
4285	3.00E-08	14100	1.00E-08			4285	1.10E-07	14100	0.00E+00			4285	0.00E+00	14100	0.00E+00			28545	3.50E+00	19950	5.00E+00
4405	3.00E-08	14340	1.00E-08			4405	6.00E-08	14340	5.00E-08			4405	0.00E+00	14340	0.00E+00			29025	1.00E+00	20190	4.50E+00
4525	3.00E-08	14580	1.00E-08			4525	6.00E-08	14580	0.00E+00			4525	0.00E+00	14580	0.00E-01			30000	1.50E+00	20430	3.50E+00
4645	3.00E-08	14820	1.00E-08			4645	6.00E-08	14820	0.00E+00			4645	0.00E+00	14820	5.00E-01			30525	1.50E+00	20670	7.00E+00
4765	3.00E-08	15060	1.00E-08			4765	6.00E-08	15060	0.00E+00			4765	0.00E+00	15060	9.00E-01			31440	1.60E+00	21340	2.50E+00
4885	3.00E-08	15300	1.00E-08			4885	6.00E-08	15300	0.00E+00			4885	0.00E+00	15300	6.50E+00			31820	5.00E-01	28545	0.00E+00
5005	4.00E-08	15540	1.00E-08			5005	6.00E-08	15540	0.00E+00			5005	0.00E+00	15540	3.50E+00			32880	1.00E+00	29025	0.00E+00
5125	3.00E-08	15780	1.00E-08			5125	6.00E-08	15780	0.00E+00			5125	0.00E+00	15780	1.50E+01			33375	5.00E-01	30000	5.00E-01
5245	4.00E-08	16020	1.00E-08			5245	6.00E-08	16020	5.00E-08			5245	0.00E+00	16020	2.10E+01			34330	0.00E+00	30525	1.50E+00
5365	3.00E-08	16260	3.00E-08			5365	6.00E-08	16260	0.00E-08			5365	0.00E+00	16260	8.30E+01			34805	1.50E+00	31440	5.00E-01
5485	3.00E-08	16500	3.00E-08			5485	8.00E-08	16500	5.00E-08			5485	0.00E+00	16500	8.00E+01			35805	1.50E+00	31920	0.00E+00
5605	3.00E-08	16740	4.00E-08			5605	8.00E-08	16740	5.00E-08			5605	0.00E+00	16740	1.30E+02			36260	0.00E+00	32880	0.00E+00
5725	3.00E-08	16980	6.00E-08			5725	8.00E-08	16980	1.80E-07			5725	0.00E+00	16980	1.80E+02			37210	1.00E+00	33375	5.00E-01
5845	3.00E-08	17220	7.00E-08			5845	6.00E-08	17220	2.10E-07			5845	0.00E+00	17220	2.50E+02			48740	0.00E+00	34330	5.00E-01
5965	3.00E-08	17460	1.00E-07			5965	8.00E-08	17460	3.70E-07			5965	0.00E+00	17460	3.30E+02					34805	5.00E-01
6033	3.00E-08	17700	1.40E-07			6033	5.00E-08	17700	5.00E-07			6033	0.00E+00	17700	9.00E-01					35805	0.00E+00
6153	3.00E-08	17940	2.20E-07			6153	5.00E-08	17940	0.20E-07			6153	0.00E+00	17940	1.60E+03						
6273	3.00E-08	18180	2.90E-07			6273	1.20E-07	18180	1.08E-06			6273	0.00E+00	18180	5.80E+03						
6393	3.00E-08	18420	4.00E-07			6393	5.00E-08	18420	1.60E-06			6393	0.00E+00	18420	1.40E+03						
6513	3.00E-08	18660	5.00E-07			6513	5.00E-08	18660	2.02E-06			6613	0.00E+00	18660	1.30E+03						
6633	1.30E-07	18900	8.10E-07			6633	5.00E-08	18900	2.45E-06			6633	0.00E+00	18900	9.00E+02						
6753	3.00E-08	18990	1.14E-06			6753	5.00E-08	18990	4.08E-06			6753	0.00E+00	18990	3.20E+03						
6873	3.00E-08	19230	1.23E-06			6873	1.20E-07	19230	4.76E-06			6873	0.00E+00	19230	2.70E+03						
6993	3.00E-08	19470	1.50E-06			6993	5.00E-08	18470	5.81E-06			6993	0.00E+00	19470	2.00E+03						
7113	3.00E-08	19710	1.60E-06			7113	5.00E-08	19710	7.29E-06			7113	0.00E+00	19710	3.70E+03						
7233	3.00E-08	19950	2.10E-06			7233	1.20E-07	19950	8.60E-06			7233	0.00E+00	19950	4.10E+03						
7353	3.00E-08	20190	2.74E-06			7353	5.00E-08	20180	1.07E-05			7353	0.00E+00	20190	4.30E+03						
7473	3.00E-08	20430	3.04E-06			7473	1.20E-07	20430	1.23E-05			7473	0.00E+00	20430	6.40E+03						
7593	3.00E-08	20670	4.34E-06			7593	5.00E-08	20870	1.70E-05			7593	0.00E+00	20670	7.00E+03						
7713	3.00E-08	24340	1.51E-06			7713	5.00E-08	24340	9.08E-06			7713	0.00E+00	24340	1.00E+03						
7833	3.00E-08	28545	4.40E-07			7833	1.20E-07	28545	3.45E-06			7933	0.00E+00	28545	1.40E+03						
7953	3.00E-08	29025	4.30E-07			7953	5.00E-08	28025	2.64E-06			7953	0.00E+00	29025	8.30E+01						
8073	3.00E-08	30000	6.40E-07			8073	1.20E-07	30000	2.21E-06			8073	0.00E+00	30000	0.30E+01						
8193	3.00E-08	30525	6.00E-07			8193	5.00E-08	30525	2.11E-06			8193	0.00E+00	30525	8.30E+01						
8313	3.00E-08	31440	1.00E-06			8313	1.20E-07	31440	1.79E-06			8313	0.00E+00	31440	4.10E+01						
8433	3.00E-08	31920	1.17E-06			8433	5.00E-08	31920	1.53E-06			8433	0.00E+00	31920	3.70E+01						
8553	3.00E-08	32920	1.31E-06			8553	5.00E-08	32880	1.27E-06			8553	0.00E+00	32880	2.80E+01						
8673	3.00E-08	33375	1.21E-06			8673	9.00E-08	33375	1.22E-06			8673	0.00E+00	33375	2.30E+01						
8793	3.00E-08	34330	1.41E-06			8793	5.00E-08	34330	1.16E-06			8793	0.00E+00	34330	1.90E+01						

Tall1Pat2		
Time steps	Time (min)	Conc. (pfu/ml)
1	0	0
18	1965	0
19	2085	500
20	2205	4000
21	2325	5000
22	2445	5000
23	2565	2500
24	2685	0
25	3000	0
26	4000	0
27	5000	0
28	6000	0
29	7430	0

Tall1sulfoG	
Time (min)	Conc. (mg/l)
0	0.25
45	0.36
165	0.51
285	0.25
405	0.31
525	0.14
645	0.28
765	0.31
885	0.28
1005	0.2
1125	0.28
1245	0.25
1365	1.41
1485	3.36
1605	3.73
1725	3.82
1845	3.25
1965	1.30
2085	1.31
2205	0.09
2325	2.31
2445	2.06
2565	1.66
2685	2.09
3000	1.7
4000	0.89
5000	0.18
6000	0.12
7430	0.25

Tall1tum	
Time (min)	Conc. E-09 (mg/l)
0	0.01
45	0.08
165	0.05
285	0.03
405	0.03
525	0.03
645	0.04
765	0.03
885	0.03
1005	0.03
1125	0.03
1245	0.05
1365	0.03
1485	0.04
1605	0.03
1725	0.05
1845	0.39
1965	1.18
2085	3.32
2205	4.78
2325	5.06
2445	4.1
2565	3.28
2685	2.46
3000	1.48
4000	0.5
5000	0.17
6000	0.01
7430	0.01

Tall1H2/1	
Time (min)	Conc. (pfu/ml)
0	0
1245	0
1365	1500
1485	3000
1605	3500
1725	1000
1845	500
1965	1500
2085	500
2205	0
2325	500
2445	0
7430	0

Tall1H40/1	
Time (min)	Conc. (pfu/ml)
0	0
1605	0
1725	2
1845	8700
1905	35700
2085	135000
2205	187000
2325	183000
2445	144300
2585	111000
2685	76300
3000	47800
4000	11250
5000	2810
6000	1800
7430	0

Tall1H4/4	
Time (min)	Conc. (pfu/ml)
0	0
1125	0
1245	3500
1365	109000
1485	266700
1605	153300
1725	103300
1845	48000
1965	26500
2085	6900
2205	9000
2325	5000
2445	22000
9505	9000
2885	17000
3000	12000
4000	8000
5000	6000
6000	2000
7430	0

Tall1H6/1	
Time (min)	Conc. (pfu/ml)
0	0
1725	0
1845	1500
1985	7800
2085	17800
2205	25000
2325	32500
2445	22000
2585	17500
2885	10500
3000	4660
4000	2810
5000	940
6000	400
7430	0

Tall2sulfoG			
Time (min)	Conc. (ppb)	Time (min)	Conc. (ppb)
0	0	23250	1.08
12150	0.06	23430	1.03
12330	0	23610	1.03
12510	0	23700	1.03
12690	0.06	23970	1.03
12870	0.06	24150	0.97
13050	0.24	24330	1.03
13230	0.36	24510	0.97
13452	0.47	24808	0.97
13632	0.47	25048	1.03
13812	0.52	25288	1.03
13992	0.52	25528	1.08
14352	0.52	25708	1.03
14532	0.52	26008	1.08
14712	0.52	26248	1.03
14892	0.47	26488	1.03
15072	0.52	26728	1.03
15252	0.47	26968	0.97
15432	0.52	27208	0.97
15612	0.57	27448	1.08
15792	0.57	27543	1.03
15972	0.57	30000	0
16068	0.57		
16288	0.57		
16271	0.57		
16451	0.57		
16631	0.52		
16811	0.52		
16991	0.52		
17171	0.47		
17351	0.31		
17531	0.28		
17711	0.13		
17891	0.13		
18071	0.13		
18251	0.13		
18431	0.28		
18611	0.28		
18701	0.58		
19113	0.44		
19283	0.44		
19473	0.38		
19653	0.38		
19833	0.38		
20013	0.44		
20193	0.44		
20373	0.5		
20553	0.5		
20733	0.59		
20913	0.55		
21093	0.51		
21273	0.66		
21453	0.71		
21633	0.78		
21816	0.81		
21996	0.92		
22176	1.03		
22356	1.13		
22536	1.15		
22716	1.08		
22896	1.08		
23076	1.15		

Tall2H40/1	
Time (min)	Conc. (pfu/ml)
0	0
12330	0
12510	1
12690	0
12870	8
13050	12
13230	23
13452	14.5
13632	15.5
13812	14.5
13992	16.5
14352	18
14532	8.5
14712	14.5
14892	14.5
15072	12
15252	9
15432	10.5
15612	12
15792	12
15972	12.5
16068	10.5
16258	14
16271	10.5
16451	9.5
16631	10
16811	4.5
16991	6
17171	2.5
17351	4.5
17531	2
17711	1
17891	0
18071	0
18251	0.5
18431	1.5
18611	2
18701	3.5
19113	3.5
19283	3
19473	3
19653	3.5
19833	3.5
20013	4.5
20193	2.5
20373	2
20553	1.5
20733	1.5
20913	1.5
21093	1
21273	0
21453	1
21633	1
21816	1.5
21996	1
22176	1
22356	1
22536	1
22716	0
22896	2
23076	3
23256	0

Tall2surp		Tall2H4/4		Tall2H8/1		Tall3sutfoG		Tall3sutfoG (end)				Tall3H40/1				Tall3H6/1				Tall3H4/4	
Time (min)	Conc. (E-09ng/l)	Time (min)	Conc. (pfu/ml)	Time (min)	Conc. (pfu/ml)	Time (min)	Conc. (ppb)	Time (min)	Conc. (ppb)	Time (min)	Conc. (ppb)	Time (min)	Conc. (pfu/ml)	Time (min)	Conc. (pfu/ml)	Time (min)	Conc. (pfu/ml)	Time (min)	Conc. (pfu/ml)	Time (min)	Conc. (pfu/ml)
0	6.03	0	0	0	0	0	0.25	13835	5.23	24676	0.57	0	0	20588	17.5	0	0	32585	0.5	0	0
17471	6.03	17471	0	17851	0	255	0.2	13955	5.48	24935	0.52	8096	0	20828	18	10428	0.5	33285	0	15626	0.5
17651	6.1	17851	0.5	17931	1	815	0.2	14075	5.17	25295	0.46	8276	2.5	21088	14	10686	0	34005	0	15746	0.5
17831	2.93	17931	0	18011	1	975	0.14	14195	5.17	25655	0.31	8456	2.5	21308	5.5	10908	0	34385	0	18688	6
18011	1.94	18011	1	18191	3.5	1335	0.2	14315	5.12	26015	0.41	8820	5	21515	3	15148	0			18781	71.5
18191	6.03	18191	0	18371	1	1005	0.25	14436	5.07	26376	0.52	9005	37.5	21755	2.5	15386	0.5			18901	80
18371	3.54	18371	1	18551	2.5	2055	0.2	14555	5.07	26735	0.46	10115	72.7	21995	2	15626	0			19021	69
18551	3.9	18551	0.5	18731	0	2415	0.2	14675	4.67	27095	0.41	10235	84.3	22235	2.5	15746	0			19141	61
18731	3.88	18731	5.5	19053	2.5	2655	0.25	14795	4.76	27456	0.46	10355	106.7	22475	0.5	15866	4.5			19261	82
19053	4.55	19053	2.5	19233	3.5	2975	0.2	14916	4.8	27816	0.41	10475	129.7	22715	0.5	15781	1.5			19381	56.5
19233	4.83	19233	3	19413	3.5	3835	0.14	15035	4.48	28176	0.41	10595	135.7	22955	0.5	16001	7			19501	78.5
19413	4.94	19413	2.5	19593	2.5	3805	0.31	15155	4.39	28535	0.36	10715	158.3	23195	1.5	16021	5.5			19621	80.5
19593	4.84	19593	1.5	19773	3.5	4055	0.14	15275	4.28	28852	0.31	10836	178.3	23435	0	16141	8			19741	88
19773	4.53	19773	2.5	19953	3.5	4415	0.2	15395	4.54	29572	0.31	10955	172	23675	0.5	16261	3.5			19861	83.5
19853	4.23	19953	6.5	20133	3	4775	0.14	15515	4.02	30292	0.31	11075	182	23915	0	16381	8			19981	84.5
20133	4.08	20133	1.5	20313	3.5	5135	0.2	15635	3.91	31012	0.25	11195	220	24155	0	16501	2.5			20101	72
20313	3.92	20313	2.5	20493	3.5	5495	0.2	18575	2.91	31732	0.31	11315	242	24395	0.5	16621	6			20221	86.5
20493	3.94	20493	4	20673	2	5675	0.2	18688	3.13	32452	0.31	11435	230	25115	0	16741	8			20341	70.5
20673	3.94	20673	5	20853	5	6035	0.14	18788	3.13	33172	0.31	11555	247.3	25835	1	16861	12			20461	72.5
20853	3.99	20853	4	21033	3.5	6305	0.16	18908	3.17	33892	0.31	11675	274	20555	0.5	16981	7			20581	80
21033	4.53	21033	3	21213	3.5	6755	0.2	19028	3.13			11795	282.3			20101	10			20701	90
21213	4.55	21213	4	21393	3.5	7115	0.14	19148	3.02			11915	273.3			20221	10.5			20821	83.5
21393	5	21393	3	21573	8	7475	0.2	19268	3.17			12035	284.3			20341	11			20941	74
21573	5.14	21573	4	21758	5.5	7655	0.14	19388	2.91			12155	309			20461	10.5			21061	80
21758	5.12	21758	3	21038	2	8735	0.14	19508	3.29			12275	286.7			20581	9			21181	81.5
21038	6.55	21038	1.5	22118	2.5	8015	0.16	19628	2.91			12395	289.7			20701	5.5			21301	88.5
22118	8.91	22118	2.5	22298	5.5	9095	0.14	19748	2.91			12515	270			20821	11			21421	57.5
22298	7.38	22298	2.5	22478	0.5	9275	0.14	19868	2.91			12635	286.3			20941	8.5			21506	84
22478	7.76	22478	4.5	22658	4.5	9455	0.25	19988	2.91			12755	283.7			21001	7			21828	56
22658	7.81	22658	4.5	22838	2	9920	0.14	20108	2.61			12875	200			21181	3.5			21748	43
22838	8.19	22838	1.5	23018	8	9995	0.8	20228	2.66			12995	160			21301	4			21868	46
23016	8.33	23018	1.5	23198	7.5	10115	0.71	20348	2.76			13115	180			21421	2.5			21988	41
23198	8.42	23198	1	23378	9	10235	0.01	20468	2.76			13235	180			21508	0			22108	60
23378	8.49	23378	1.5	23558	10	10355	1.02	20588	2.76			13355	185			21628	6.5			22228	58
23558	8.32	23558	1.5	23738	10	10475	1.23	20708	2.71			13475	110			21868	4.5			22348	50
23736	8.24	23738	6.5	23918	4.5	10595	1.49	20828	2.65			13595	140			21981	5.5			22468	40
23916	8.21	23918	2.5	24098	6	10715	1.55	20948	2.65			13715	120			22348	7.5			22588	40
24096	8.13	24098	3.5	24278	8	10835	1.71	21068	2.76			13835	130			22588	8			22708	41
24276	7.7	24278	3	24458	5.5	10855	1.86	21188	2.65			13955	140			22828	4			22828	96
24456	7.46	24458	2	24748	4	11075	2.07	21308	2.12			14075	110			23048	7			22948	38
24748	9.04	24748	0	25228	4.5	11195	2.39	21388	2.39			14195	100			23308	5			23068	27
24908	7.87	25228	2	25708	1.5	11315	2.54	21515	2.26			14315	115			23548	9			23188	20
25228	7.06	25708	2.5	26188	4	11435	2.68	21636	1.84			14435	105			23788	0			23306	34.5
25468	6.83	26188	2.5	26668	4.5	11555	3.07	21755	1.57			14556	105			24028	7			23428	33
25708	6.3	26668	3	27148	5	11675	3.68	21875	1.48			14675	104			24268	7.5			23548	36
25948	4.05	27148	2	27483	5	11795	3.8	21995	1.31			14795	94.5			24508	1			23668	26
26188	5.35	27483	1	30000	0	11915	3.81	22115	1.28			14915	84			24888	1			23788	27
26428	5.51	30000	0			12035	3.96	22235	1.15			15035	76.5			25228	1			25000	24
26668	5.09					12155	4.18	22356	1.1			15155	62			25588	1.5			24028	23
26908	5.84					12276	4.44	22475	0.99			15276	63.5			25948	1			24148	18
27148	5.89					12395	4.49	22595	0.99			15396	70			26308	0			24268	19
27388	5.58					12515	4.65	22715	0.89			15516	40			26888	0			24388	14
27483	5.29					12635	4.91	22835	0.84			15635	55			27028	0			24508	8.5
30000	0.03					12755	5.07	22955	0.84			15575	25.5			27388	0.5			24988	3.6
						12875	5.17	23075	0.84			18668	25.5			27748	0			25228	3.5
						12995	5.17	23195	0.78			18008	19			28108	0			25588	1.5
						13115	5.17	23315	0.78			19148	23.5			28468	0			25048	8.5
						13235	5.17	23436	0.78			19388	20.5			28985	0			26308	0.5
						13355	5.28	23556	0.73			19628	20			29685	0			26668	0
						13475	5.28	23786	0.73			19868	19.5			30405	0			27028	0
						13595	5.28	24035	0.83			20108	15.5			31125	0			27388	0.5
						13715	5.34	24275	0.83			20348	23			31845	0			27748	0

		Tellijura					
Time (min)	Conc. (pfu/ml)	Time (min)	Conc. (pfu/ml)	Time (min)	Conc. (pfu/ml)	Time (min)	Conc. (pfu/ml)
28108	0	0	0.06	19821	5.73	26288	0.24
28468	0	300	0.06	19741	5.73	26468	0.29
28985	0.5	720	0.06	19881	5.56	26648	0.23
29885	0	1080	0.05	19981	5.73	28865	0.16
30405	0	1440	0.06	20101	5.67	29865	0.14
31125	0	1800	0.06	20221	6.21	30405	0.13
31845	0.5	2160	0.06	20341	5.62	31125	0.12
32565	0	2520	0.06	20461	6.14	31845	0.12
33285	0	2778	0.06	20581	5.79	32565	0.12
34005	0	3060	0.06	20701	6.1	33285	0.11
		3508	0.06	20821	5.76	34006	0.11
		4156	0.06	20941	5.98		
		4528	0.06	21061	5.67		
		4666	0.06	21181	4.87		
		5246	0.06	21301	4.76		
		5606	0.06	21421	5.3		
		5786	0.06	21506	4.82		
		6146	0.06	21626	6.41		
		6506	0.06	21746	7.93		
		6866	0.06	21866	8.84		
		7226	0.06	21986	8.66		
		7586	0.06	22106	8.81		
		8846	0.06	22226	8.9		
		9026	0.06	22346	8.7		
		9206	0.06	22466	7.94		
		9386	0.06	22586	7.01		
		9566	0.06	22706	8.03		
		10033	0.06	22826	5.26		
		10106	0.06	22946	6.01		
		10346	0.06	23066	5.01		
		10586	0.05	23186	5.16		
		10826	0.05	23306	5.25		
		11066	0.06	23426	4.08		
		11306	0.05	23546	4.57		
		11546	0.05	23666	4.14		
		11786	0.05	23786	3.81		
		12026	0.05	23906	3.46		
		12266	0.05	24026	3.14		
		12506	0.05	24146	2.84		
		12746	0.05	24266	2.52		
		12986	0.06	24386	2.2		
		13226	0.05	24506	2.03		
		13466	0.06	24626	1.3		
		13706	0.04	24866	1.05		
		13946	0.06	25046	0.64		
		14186	0.06	25226	0.63		
		14426	0.05	25406	0.59		
		14666	0.05	25586	0.54		
		14906	0.05	25766	0.44		
		15146	0.06	25946	0.64		
		15386	0.06	26126	0.44		
		15506	0.13	26306	0.39		
		15626	0.13	26486	0.34		
		15746	0.18	26606	0.23		
		18086	5.21	26846	0.32		
		18761	4.79	27026	0.28		
		18901	4.94	27206	0.3		
		19021	5.09	27386	0.34		
		19141	5.21	27566	0.24		
		19261	5.44	27746	0.34		
		19381	5.85	27926	0.24		
		19501	5.76	28106	0.22		

NOIR1DUA					
Time (hour)	Conc.(ppb)	Time (hour)	Conc.(ppb)	Time (hour)	Conc.(ppb)
0	0.00E+00	118	9.98E-02	410	5.10E+00
5	2.49E-02	119	4.99E-02	411	5.20E+00
6	5.00E-02	120	0.00E+00	412	5.30E+00
7	7.51E-02	356	2.01E-04	414	5.40E+00
8	1.00E-01	357	2.52E-02	417	5.53E+00
26	1.00E-01	358	5.01E-02	420	5.00E+00
29	7.51E-02	359	7.51E-02	421	5.62E+00
50	5.00E-02	360	1.00E-01	425	5.56E+00
51	2.49E-02	360.1	1.07E-01	500	4.65E+00
52	0.00E+00	361	1.75E-01	250	1.60E-01
37	2.49E-02	362	2.50E-01	709.1	9.05E-02
38	4.98E-02	363	3.25E-01	662	8.34E-02
30	7.48E-02	364	9.99E-01	805	6.67E-02
40	9.98E-02	365	4.50E-01	815	1.12E-02
41	7.51E-02	366	5.00E-01	817	4.48E-05
42	5.00E-02	367	5.50E-01		
43	2.49E-02	368	6.01E-01		
44	2.01E-04	369	7.01E-01		
45	2.52E-02	370	8.00E-01		
46	5.01E-02	371	9.00E-01		
47	7.51E-02	372	1.00E+00		
48	1.00E-01	373	1.10E+00		
49	7.51E-02	324	1.20E+00		
50	5.01E-02	325	1.30E+00		
51	2.52E-02	326	1.40E+00		
52	2.01E-04	327	1.57E+00		
53	2.49E-02	328	1.75E+00		
54	5.00E-02	379	1.93E+00		
55	7.51E-02	380	2.10E+00		
56	9.98E-03	381	2.18E+00		
57	7.48E-02	382	2.26E+00		
58	4.98E-03	383	2.33E+00		
60	2.49E-03	384	2.40E+00		
60	0.00E+00	385	2.55E+00		
112	0.00E+00	386	2.70E+00		
112.1	4.62E-03	387	2.85E+00		
112.2	9.84E-03	388	3.03E+00		
112.3	1.47E-02	389	3.40E+00		
112.4	1.97E-02	390	3.80E+00		
112.5	2.47E-02	391	4.20E+00		
112.6	2.97E-02	392	4.60E+00		
112.7	3.47E-02	393	4.52E+00		
112.8	3.98E-02	394	4.45E+00		
112.9	4.48E-02	395	4.37E+00		
113	4.98E-02	396	4.30E+00		
113.1	5.48E-02	397	4.32E+00		
113.2	5.98E-02	398	4.35E+00		
113.3	6.48E-02	399	4.37E+00		
113.4	6.98E-02	400	4.40E+00		
113.5	7.48E-02	401	4.47E+00		
113.6	7.98E-02	402	4.55E+00		
113.7	8.48E-02	403	4.63E+00		
113.8	9.00E-02	404	4.70E+00		
113.9	9.50E-02	405	4.75E+00		
114	1.00E-01	406	4.80E+00		
115	1.00E-01	407	4.85E+00		
116	2.00E-01	408	4.90E+00		
117	1.50E-01	409	5.00E+00		

NOIR1H4	
Time (hour)	Conc. (ppt/m³)
0	0.00E+00
317	1.29E+02
320	4.85E+02
340	9.98E+02
350	9.98E+02
360	1.00E+04
370	2.10E+04
380	3.20E+04
390	8.95E+04
400	1.02E+05
410	8.85E+04
420	2.10E+04
430	2.03E+04
440	1.40E+04
450	1.15E+04
460	1.05E+04
470	8.75E+03
480	9.00E+03
490	8.25E+03
500	5.00E+03
510	4.85E+03
520	4.81E+03
530	4.36E+03
540	4.11E+03
550	3.87E+03
560	3.62E+03
570	3.38E+03
580	3.13E+03
590	2.88E+03
600	2.64E+03
610	2.30E+03
620	2.15E+03
625	2.09E+03
673	1.98E+03
680	1.87E+03
690	1.72E+03
700	1.58E+03
710	1.40E+03
720	1.24E+03
730	1.09E+03
740	9.29E+02
750	7.72E+02
760	6.14E+02
770	4.57E+02
780	2.99E+02
790	1.42E+02
817	0.00E+00

NOIR1SULFOG	
Time (hour)	Conc. (ppb)
0	0.00E+00
151	0.00E+00
152	8.02E-02
153	1.00E+01
154	2.00E+01
155	2.99E+01
156	3.99E+01
157	4.91E+01
158	5.94E+01
159	6.93E+01
160	7.93E+01
161	8.11E+01
162	8.14E+01
163	8.17E+01
164	8.19E+01
170	8.34E+01
175	8.47E+01
180	8.59E+01
185	8.71E+01
190	8.84E+01
200	9.09E+01
210	9.34E+01
220	9.59E+01
230	9.84E+01
240	8.09E+01
250	8.34E+01
275	1.73E+01
285	2.60E-01
290	2.50E-01
295	1.75E-01
300	1.00E-01
310	1.00E-01
320	1.00E-01
327	1.25E-01
328	1.50E-01
329	1.75E-01
330	2.00E-01
331	1.75E-01
332	1.50E-01
333	1.25E-01
334	1.00E-01
335	1.25E-01
336	1.50E-01
337	1.75E-01
338	2.00E-01
424	9.00E-01
426	1.76E-01
428	1.50E-01
432	1.00E-01
835	1.20E-01
849	1.50E-01
661	1.76E-01
870	1.96E-01
875	1.98E-01
880	1.9eE-01
886	1.89E-01
890	1.88E-01
910	1.70E-01
750	1.39E-01
800	1.00E-01
815	1.00E-01
817	1.00E-01

NOIR1URA	
Time (hour)	Conc. (ppb)
0	2.70E-02
10	1.35E-02
75	1.28E-03
110	2.50E-03
120	7.50E-03
130	1.25E-03
131	6.25E-04
132	0.00E+00
344	2.01E-05
345	2.52E-03
346	5.01E-03
347	7.51E-03
348	1.00E-02
373	1.50E-02
374	2.00E-02
375	2.50E-02
376	3.00E-02
377	2.50E-02
378	2.00E-02
379	1.50E-02
380	1.00E-02
381	1.50E-02
389	2.00E-02
390	2.50E-02
391	3.75E-02
392	4.00E-02
393	4.25E-02
394	4.50E-02
395	4.75E-02
402	1.05E-01
425	6.88E-01
450	1.98E+00
460	2.10E+00
470	2.32E+00
487	2.13E+00
501	2.13E+00
525	1.81E+00
550	1.48E+00
580	1.32E+00
677	1.09E+00
600	7.20E-01
625	4.24E-01
675	9.85E-01
700	5.33E-01
715	5.32E-01
780	4.65E-01
770	4.39E-01
781	4.24E-01
785	4.19E-01
790	4.12E-01
800	3.90E-01
812	3.60E-01

NOIR2DUA			
Time (hour)	Conc. (ppb)	Time (hour)	Conc. (ppb)
0	8.00E-01	369	9.15E-02
10	3.47E-01	370	3.33E-02
25	5.20E-02	371	3.32E-02
28	2.73E-02	372	2.00E-02
27	2.94E-03	373	2.46E-02
21.1	4.90E-04	374	2.07E-02
27.2	0.00E+00	375	1.65E-02
47.1	1.47E-03	376	1.23E-02
48	2.35E-02	377	8.17E-03
49	4.80E-02	378	4.00E-03
50	7.25E-02	379	0.00E+00
59	2.88E+00	456.8	0.00E+00
80	1.25E+01		
85	1.81E+01		
90	1.89E+01		
91	1.81E+01		
93	1.52E+01		
85	5.24E+00		
90	3.33E+00		
95	2.11E+00		
96	1.45E+00		
100	1.11E+00		
105	7.00E-01		
143	8.00E-01		
145	5.48E-01		
150	5.00E-01		
175	4.00E-01		
200	5.00E-01		
250	2.00E-01		
267	0.00E+00		
287.1	0.00E+00		
338.8	0.00E+00		
338.9	1.24E-04		
339	7.48E-04		
340	5.97E-03		
341	1.39E-02		
342	1.94E-02		
343	2.58E-02		
344	3.18E-02		
345	3.81E-02		
346	4.43E-02		
347	5.05E-02		
348	5.67E-02		
349	6.29E-02		
350	6.92E-02		
351	7.54E-02		
352	8.16E-02		
353	8.78E-02		
354	9.40E-02		
355	9.05E-02		
356	8.51E-02		
357	9.15E-02		
358	8.78E-09		
359	8.32E-02		
360	7.90E-03		
361	7.48E-02		
362	7.01E-02		
363	6.65E-02		
364	6.23E-09		
365	5.82E-02		
366	5.40E-02		
367	4.98E-02		
368	4.57E-02		

NOIR2H4	
Time (hour)	Conc. (ppt/m³)
0	0.00E+00
47	0.00E+00
50	9.90E+03
50.1	3.00E+09
52	9.83E+04
53	5.59E+04
54	8.35E+04
55	1.12E+05
56	1.56E+05
57	2.00E+05
58	2.44E+05
59	2.88E+05
60	3.17E+05
61	3.44E+05
62	3.72E+05
63	4.00E+05
64	4.10E+05
65	4.18E+05
70	3.52E+05
75	2.38E+05
80	6.37E+04
85	4.33E+04
90	1.38E+04
92	8.58E+03
95	1.39E+03
100	1.00E+03
103	1.01E+03
105	1.50E+03
107	1.00E+03
110	3.09E+03
115	2.00E+03
117	1.25E+03
118	1.63E+03
119	1.50E+00
120	1.38E+03
121	1.26E+03
122	1.19E+03
123	1.01E+03
124	1.21E+02
125	5.10E+02
128	2.50E+02
127	0.00E+00
443	0.00E+00

HOIR2SULFO			
Time (hour)	Conc. (ppb)	Time (hour)	Conc. (ppb)
0	0.00E+00	305	1.20E-01
22	0.00E+00	306	1.41E-01
30	2.25E-02	307	1.59E-01
31	3.08E-02	308	1.39E-01
32	5.04E-02	309	1.19E-01
33	7.00E-02	310	9.88E-02
34	8.95E-02	315	0.00E+00
35	1.09E-01	347	0.00E+00
36	1.57E+00	348	1.27E-02
37	3.09E+00	349	2.60E-02
38	4.62E+00	350	3.92E-02
39	6.14E+00	351	5.25E-02
40	8.01E+00	352	6.58E-02
41	9.94E+00	353	7.90E-02
42	1.10E+01	354	9.23E-02
43	1.97E+01	355	1.06E-01
44	1.31E+01	360	1.72E-01
45	1.25E+01	362	1.08E-01
46	1.18E+01	366	1.82E-01
47	1.12E+01	370	1.17E-01
48	1.02E+01	375	5.17E-02
49	0.19E+00	377	2.56E-02
50	8.16E+00	327.5	1.91E-02
51	7.12E+00	327.9	1.38E-02
52	6.45E+00	378	1.28E-02
53	5.82E+00	379	0.00E+00
54	5.18E+00	458	0.00E+00
55	4.57E+00		
66	4.26E+00		
67	3.95E+00		
58	3.64E+00		
59	3.33E+00		
60	3.11E+00		
65	2.19E+00		
71	1.58E+00		
75	1.33E+00		
85	9.73E-01		
100	5.65E-01		
125	2.96E-01		
145	3.09E-01		
150	2.47E-01		
163	2.09E-01		
165	1.80E-01		
170	2.52E-02		
175	3.08E-02		
180	6.00E-02		
185	1.00E-01		
189	1.50E-01		
200	9.69E-02		
225	1.48E-01		
230	1.10E-01		
235	5.03E-02		
240	8.82E-02		
246	9.44E-02		
250	5.78E-02		
260	5.00E-02		
284	5.00E-02		
201	0.00E+00		
299	0.00E+00		
300	1.94E-02		
302	5.98E-02		
303	6.00E-02		
304	1.00E-01		

NOIR2T7			
Time (hour)	Conc. (pfu/ml)	Time (hour)	Conc. (pfu/ml)
0	0.00E+00	350	9.27E+01
23.1	2.35E+01	375	8.76E+02
24	2.35E+02	380	9.67E+02
25	4.69E+02	390	6.94E+02
26	7.75E+02	395	4.97E+02
28	9.71E+03	400	3.41E+02
29	1.95E+04	405	1.84E+02
30	2.05E+04	410	7.76E+01
35	5.06E+04	443	0.00E+00
40	3.03E+04		
45	0.50E+03		
46	8.00E+03		
50	8.00E+03		
52	7.77E+03		
55	8.98E+03		
60	4.53E+03		
75	3.03E+03		
80	2.78E+03		
85	5.06E+03		
90	5.50E+03		
95	3.02E+03		
100	2.77E+03		
105	2.00E+03		
115	1.00E+03		
120	1.00E+03		
125	5.10E+02		
130	2.53E+02		
140	1.05E+03		
150	1.02E+03		
160	1.05E+03		
194	1.00E+03		
195	1.01E+03		
200	1.04E+03		
205	2.20E+00		
210	2.88E+00		
225	1.25E+03		
250	1.00E+03		
275	2.40E+00		
285	6.29E+02		
286	8.02E+02		
287	7.55E+02		
288	8.18E+02		
289	8.81E+02		
290	9.44E+02		
291	9.93E+02		
292	9.38E+02		
293	8.68E+02		
294	8.06E+02		
295	7.44E+02		
296	6.82E+02		
297	6.19E+02		
298	5.57E+02		
299	4.95E+02		
300	4.33E+02		
325	8.78E+02		
332	4.34E+02		
333	3.71E+02		
334	3.08E+02		
337	1.19E+02		
338	5.58E+01		
338.8	5.58E+00		
347	0.00E+00		
347.1	3.01E+00		

NOIR2UBA			
Time (min)	Conc. (ppb)	Time (min)	Conc. (ppb)
0	0.23	16732.6	0.76
662.4	0.22	16877.6	0.80
1137.6	0.22	17222.4	0.84
1627.2	0.21	17482.6	0.67
2102.4	0.21	17607.6	0.5
2577.6	0.21	17942.4	0.40
3087.2	0.21	18172.8	0.46
3207.6	0.21	18417.6	0.44
3542.4	0.24	18662.4	0.42
3767.2	0.25	18692.8	0.39
4017.6	0.20	19137.6	0.36
4269.4	0.24	19382.4	0.35
4507.2	0.23	19612.8	0.36
4737.6	0.22	19857.6	0.36
4982.4	0.21	20102.4	0.34
5227.2	0.19	20932.8	0.36
5457.6	0.21	20577.6	0.32
5702.4	0.23	20822.4	0.34
5947.2	0.34	21207.6	0.34
6177.6	0.56	21772.8	0.34
6422.4	1.41	22287.4	0.31
6667.2	2.51	22737.6	0.31
6907.6	3.65	23212.8	0.27
7149.4	5.39	23702.4	0.26
7387.2	6.76	24177.6	0.25
7617.6	7.55	24652.8	0.23
7862.4	8.13	25142.4	0.23
8092.8	8.36	25617.6	0.22
8337.6	7.96	26587.8	0.19
8562.4	7.22	27532.8	0.10
8812.8	5.81		
9057.6	4.70		
9302.4	4.19		
9532.8	3.75		
9777.6	3.14		
10022.4	2.67		
10252.8	2.07		
10497.6	1.86		
10742.4	1.71		
10972.8	1.5		
11217.6	1.31		
11462.4	0.99		
11692.8	0.74		
11937.6	0.59		
12182.4	0.66		
12412.8	0.83		
12657.6	1.29		
12902.4	1.78		
13132.8	2.22		
13377.6	2.49		
13622.4	2.61		
13852.8	2.64		
14097.6	2.67		
14342.4	2.51		
14572.8	2.23		
14817.6	1.83		
15062.4	1.61		
15292.8	1.60		
15537.6	1.5		
15782.4	1.32		
16012.8	1.09		
16757.6	0.94		
16502.4	0.84		

ALP12		ALP13				ALP14				ALP15				ALP16		ALP17		ALP18
Time (min)	Conc. (mg/l)	Time (min)	Conc. (mg/l)	Time (min)	Conc. (mg/l)	Time (min)	Conc. (mg/l)	Time (min)	Conc. (mg/l)	Time (min)	Conc. (mg/l)	Time (min)	Conc. (mg/l)	Time (min)	Conc. (mg/l)	Time (min)	Conc. (mg/l)	Time (min)
240.04942	3.35E-05	5.6350165	1.23E-05	9820.77229	5.00E-04	7.43252	4.63E-05	8517.2156	2.00E-03	7.9304039	5.79E-06	4421.6904	1.28E-02	0.573871817	2.02E-06	0	7.81E-07	11.9259998
853.08748	2.30E-05	485.73052	1.23E-06	10060.1838	3.93E-04	501.4016	5.26E-05	8025.9133	2.10E-03	561.47256	5.74E-06	4492.3094	1.24E-02	630.2027603	5.77E-06	400.6069803	6.25E-06	666.934(391
1024.5065	1.95E-05	1066.3418	1.35E-05	10143.9923	3.61E-04	1447.4443	6.81E-05	6767.1274	1.11E-03	1104.0096	5.21E-05	4529.316	1.13E-02	1435.403099	4.04E-05	1063.429439	5.86E-06	1362.30701
1343.8332	3.14E-05	1707.095	1.92E-05	10262.4748	3.46E-04	1811.828	1.25E-04	6883.2574	1.52E-03	1473.0977	2.61E-05	4545.1756	1.08E-02	1876.682248	4.62E-05	1178.059181	5.87E-06	1403.589041
1467.4825	2.86E-05	1982.9221	1.31E-04	10383.9008	4.42E-04	1695.0416	2.28E-04	6999.6641	1.90E-03	1722.7096	3.10E-05	4571.6135	9.63E-03	1966.244434	8.08E-05	1209.104704	1.67E-03	1470.557669
1749.0999	2.79E-05	2476.1811	8.92E-04	10507.9704	3.12E-04	2004.8693	7.02E-04	7141.5305	1.95E-03	1035.0185	2.08E-04	4595.9334	9.13E-03	2062.589233	3.95E-04	1250.075873	2.85E-03	1541.19581
1806.4093	2.55E-04	2266.2278	1.10E-03	10660.5767	3.71E-04	2191.4685	1.58E-03	7271.5981	2.10E-03	2024.3679	5.68E-04	4634.526	7.99E-09	2178.10982	3.72E-04	1330.107260	4.87E-03	1597.082111
1862.1848	4.08E-04	2949.7437	2.87E-03	10883.3286	3.08E-04	2187.4503	2.45E-03	7501.089	1.84E-03	2098.3849	8.40E-04	4646.1593	7.54E-03	2220.513087	1.20E-03	1411.229135	4.84E-03	1695.041802
1920.9498	5.30E-04	2412.0417	4.42E-03	11137.3491	4.08E-04	2224.1216	3.50E-03	7804.1824	1.87E-03	2169.3202	1.08E-03	4660.5244	6.41E-03	2355.856841	8.51E-03	1492.261002	4.66E-03	1890.726409
1963.5744	9.04E-04	7471.0897	8.33E-03	11253.9358	2.20E-04	2274.2898	4.65E-03	7979.5246	1.48E-03	2199.3663	2.35E-03	4252.1649	6.53E-03	2508.179782	1.10E-02	1565.128983	4.54E-03	1755.862380
2060.8552	1.40E-03	2509.9319	8.13E-03	11688.5302	2.13E-04	2356.0454	6.88E-03	8237.7877	1.34E-03	2237.96	3.02E-03	4946.9859	7.02E-03	2636.594988	1.58E-02	1723.520486	4.05E-03	1801.731292
2096.1359	1.88E-03	2866.4292	1.03E-02	11834.0258	1.83E-04	2390.4199	6.91E-03	8325.1274	1.46E-03	2259.1977	5.10E-03	5018.3595	7.13E-03	2746.583205	2.00E-02	1777.23824	3.77E-03	1879.706461
2158.7616	2.75E-03	2580.5	1.22E-02	12130.7058	2.23E-04	2424.2044	1.07E-02	8576.7554	1.53E-03	2269.1659	6.73E-03	5062.5261	7.26E-03	2827.453324	2.42E-02	1786.342944	3.57E-03	1897.132904
2201.4694	3.58E-03	2619.8836	1.38E-02	12407.4805	3.73E-04	2452.6656	1.24E-02	8706.0338	1.49E-03	2320.4362	8.32E-03	5226.8048	6.67E-03	2838.253087	2.59E-02	1859.180577	3.49E-03	2066.018809
2248.5923	4.40E-03	2651.163	1.69E-02	12606.5313	3.96E-04	2484.4724	1.49E-02	8868.105	9.77E-04	2356.3873	1.00E-02	5301.7393	6.65E-03	2956.983954	2.78E-02	1953.882486	3.41E-03	2206.377844
2288.4671	5.19E-03	2668.2338	1.81E-02	12820.5003	6.75E-04	2516.8403	1.71E-02	9187.2786	9.75E-04	2399.7402	1.22E-02	5404.1836	8.16E-03	3018.725629	2.84E-02	2083.156297	2.59E-03	2287.115659
2351.7082	6.03E-03	2716.461	2.01E-02	13102.2818	7.85E-04	2552.0729	2.09E-02	9477.137	6.67E-04	2450.4949	1.50E-02	5556.6146	5.94E-03	3164.321468	2.90E-02	2185.129903	2.00E-03	2377.844984
2433.203	6.72E-03	2782.0028	2.24E-02	13470.6603	7.83E-04	2599.1035	2.40E-02	9556.1954	6.20E-04	2483.8028	1.68E-02	5750.0715	5.49E-05	3340.814801	2.68E-02	2225.189681	1.82E-03	2454.904754
2540.2979	7.50E-03	2828.4127	2.40E-02	13599.868	7.81E-04	2631.9703	2.77E-02	9704.7519	7.80E-04	2521.3397	1.92E-02	6830.4329	6.17E-03	3467.701283	2.49E-02	2239.757208	1.64E-03	2537.486615
2582.9281	7.77E-03	2841.206	2.30E-02	13808.365	6.37E-04	2668.8416	3.15E-02	9820.8618	6.15E-04	2563.2421	2.15E-02	8037.1521	4.63E-03	3663.846585	2.19E-02	2425.493174	1.32E-03	2562.024631
2605.1805	8.22E-03	3080.5434	2.50E-02	13932.5867	6.31E-04	2726.7324	2.78E-02	9824.9343	4.85E-04	2656.1566	2.48E-02	8105.8823	4.46E-03	3943.602406	1.85E-02	2540.317147	1.05E-03	2852.129827
2650.4178	8.11E-03	3180.5429	2.29E-02	14159.1251	6.12E-04	2748.2422	2.45E-02	10057.797	4.78E-04	2724.3581	2.81E-02	8293.0398	3.87E-03	4014.899129	1.55E-02	2590.529075	1.04E-03	2943.867472
2928.8247	7.68E-03	3307.0818	2.34E-02	14426.4215	5.42E-04	2825.3788	2.55E-02	10200.859	3.59E-04	2755.9323	2.87E-02	8357.5404	3.76E-03	4166.531624	1.29E-02	2602.427921	7.88E-04	3098.904432
2968.1441	7.55E-03	3651.6295	1.98E-02	14597.9841	5.27E-04	2901.5088	3.01E-02	10406.035	4.82E-04	2799.7801	3.18E-02	8595.0381	3.48E-03	4430.980985	1.48E-02	3030.955894	4.68E-04	3105.22917
3115.653	7.23E-03	3729.8271	1.72E-02	14777.1295	5.50E-04	3005.5813	2.70E-02	10703.47	4.17E-04	2849.4305	3.18E-02	8665.2401	3.36E-03	4530.004074	1.41E-02	3060.091047	4.61E-04	3520.698523
3225.9259	6.78E-03	3854.9446	1.55E-02			3235.8489	3.00E-02	10823.652	2.86E-04	2859.1249	3.30E-02	8883.0619	3.08E-03	4677.880892	9.84E-03	3161.138068	4.13E-04	3607.862665
3356.2568	8.53E-03	3993.3321	1.37E-02			3266.0145	2.54E-02	11035.137	3.40E-04	2889.8392	3.34E-02	8968.1363	2.93E-03	4827.501178	7.83E-03	3285.867709	3.78E-04	3901.240163
3461.0359	8.24E-03	4094.753	1.19E-02			3339.8988	2.11E-02	11157.77	1.47E-04	2934.7781	3.44E-02	7150.9309	2.69E-03	5086.581036	4.30E-03	3436.115326	2.93E-04	4148.385368
3599.6325	8.73E-03	4214.1833	1.14E-02			3459.0351	2.23E-02	11301.772	1.47E-04	2982.6892	3.48E-02	7248.3891	2.53E-03	5082.908358	3.97E-09	3636.230757	2.35E-04	4256.638048
3705.5204	5.27E-03	4310.885	1.11E-02			3506.3138	2.01E-02	11392.818	2.89E-04	3029.9552	3.50E-02	7451.9362	2.30E-03	5231.211366	3.39E-03	4097.115044	1.84E-04	4419.012033
3841.3451	4.99E-03	4518.4462	1.02E-02			3611.1785	1.88E-02	11501.615	1.63E-04	3143.8121	3.46E-02	7640.2156	2.12E-03	6332.183138	3.28E-03	4263.733928	1.35E-04	4641.01782
4045.1313	4.12E-03	4564.7964	9.83E-03			3657.8305	1.84E-02	11639.013	2.61E-04	3215.0431	3.42E-02	7752.7626	1.86E-03	6770.458125	2.73E-03	4433.990386	1.24E-04	4782.111577
4229.4156	3.41E-03	4860.8251	8.85E-03			3730.0956	1.03E-02	11857.338	3.10E-04	3267.4187	3.92E-02	7832.0889	1.77E-03	7182.740709	2.28E-03	4620.837329	1.24E-04	4891.481839
4412.0128	2.88E-03	4930.292	7.89E-03			3858.3031	1.49E-02	11952.1	9.29E-04	3310.8263	3.27E-02	7917.7152	1.65E-03	7230.557686	1.69E-03	4879.210926	9.72E-05	5304.094171
4452.8936	2.54E-03	4985.7460	8.25E-03			3981.8664	1.38E-02	12400.826	7.82E-04	3356.7904	3.16E-02			7800.751844	1.30E-03	5291.562974	6.35E-05	5728.111093
4523.5706	2.28E-03	5078.7355	6.37E-03			4025.5303	1.11E-02	12652.526	9.36E-04	3387.3386	3.11E-02					5956.39748	6.59E-05	6129.005479
4688.2093	2.09E-03	5337.3968	4.84E-03			4058.9258	7.72E-03	12672.776	1.02E-03	3441.2686	3.00E-02					6415.684877	5.19E-05	6210.852182
4826.4902	2.05E-03	5676.2674	4.22E-03			4066.205	5.17E-03	13242.539	1.03E-03	3467.1226	2.95E-02					7132.92519	4.65E-05	6720.714565
4940.584	1.87E-03	5719.3842	3.81E-03			4214.1254	3.94E-03	13687.107	8.87E-04	3524.9715	2.94E-02					7731.744718	3.90E-05	7203.255664
5054.3431	1.74E-03	5848.3974	3.58E-03			4234.6643	4.45E-03	14140.918	7.38E-04	3555.4644	2.79E-02					8209.848255	2.81E-05	7889.486237
5109.7818	1.42E-03	5958.2448	3.42E-03			4266.8368	6.51E-03	14534.115	6.67E-04	3607.2764	2.66E-02					8823.141123	3.26E-05	8346.14097
5166.5466	1.01E-03	6169.849	3.57E-03			4338.7587	1.13E-02			3636.8269	2.63E-02					9630.955994	9.37E-08	10048.98101
5295.6101	1.40E-03	6331.7914	3.07E-03			4456.463	1.01E-02			3706.1421	2.52E-02					10773.59636	6.64E-06	11806.87225
5420.7927	1.39E-03	6449.238	3.00E-03			4592.0763	1.01E-02			3825.7037	2.49E-02					11435.50835	2.73E-08	14403.75917
5580.4881	1.23E-03	6700.4188	2.34E-03			4845.2	6.80E-03			3706.5095	2.37E-02					12274.05169	7.81E-08	
5766.1395	1.04E-03	6822.4319	2.26E-03			4729.7426	7.42E-03			3912.4005	2.32E-02					13139.98648	8.59E-08	
5936.3723	9.08E-04	7040.7083	1.81E-03			4821.7176	6.74E-03			3976.4962	2.21E-02					13978.30048	1.05E-08	
6103.7921	7.22E-04	7186.8707	1.77E-03			4863.0833	3.82E-03			3904.4022	2.16E-02					14219.35352	1.95E-08	
6142.8041	6.58E-04	7305.101	1.35E-03			4934.1314	1.15E-03			3963.0872	2.06E-02							
6283.0727	6.20E-04	7443.5373	1.36E-03			5001.0223	2.27E-03			3994.2801	2.01E-02							
6406.4922	6.57E-04	8053.9621	1.24E-03			5072.9584	4.63E-03			4040.3668	1.89E-02							
6539.3346	4.62E-04	8172.1835	1.26E-03			5208.1882	4.86E-03			4087.8586	1.85E-02							
6679.384	3.44E-04	8312.7236	1.13E-03			5314.1988	4.38E-03			4140.7262	1.24E-02							
7099.1195	2.30E-04	8431.2103	1.12E-03			5446.8196	3.04E-03			4169.2771	1.69E-02							
7240.8441	1.85E-04	8593.2942	9.90E-04			5550.065	1.20E-03			4203.2498	1.58E-02							
7460.4795	7.80E-05	8999.9259	9.04E-04			5685.7248	3.95E-03			4261.799	1.54E-02							
7620.0253	5.30E-05	9122.4363	1.02E-03			5781.4159	2.91E-03			4273.4303	1.52E-02							
7758.0868	7.67E-05	9200.9188	8.13E-04			5924.4881	3.54E-03			4400.6455	1.45E-02							
		9543.0494	6.48E-04			6023.8954	3.37E-03			4427.2001	1.43E-02							
		9837.8359	6.87E-04			6160.4642	3.36E-03			4433.0958	1.40E-02							

	ALP10		ALP20			
Conc. (mg/l)	Time (min)	Conc. (mg/l)	Time (min)	Conc. (mg/l)	Time (min)	Conc. (mg/l)
2.34E-06	0.913620360	3.56E-06	0	0.00E+00	10994.407	2.05E-05
5.48E-05	554.8413700	3.20E-05	1442.5547	0.00E-07	11016.388	2.71E-05
7.41E-05	1220.76772	1.16E-04	3447.7428	2.43E-05	11054.350	3.79E-05
3.20E-04	1244.214743	1.87E-04	3809.1587	3.75E-04	11079.038	5.00E-05
1.88E-06	1965.932173	6.87E-04	3785.0582	5.78E-04	11087.71	6.11E-05
7.28E-03	1285.589911	0.02E-04	3792.7015	6.01E-04	11103.634	4.40E-05
1.25E-02	1318.991586	1.03E-03	3829.5953	6.14E-04	11230.751	3.16E-05
2.15E-02	1328.307341	2.64E-03	3891.3827	6.85E-04	11323.685	3.54E-05
2.16E-02	1352.166762	3.78E-03	3965.1897	7.37E-04	11377.182	3.59E-05
2.24E-02	1373.630120	4.79E-03	4046.0085	7.51E-04	11449.388	4.07E-05
2.15E-02	1396.183631	6.82E-03	4211.448	7.36E-04	11563.496	3.41E-05
1.88E-02	1418.697133	8.88E-03	4297.2265	8.86E-04	11619.759	2.67E-05
1.44E-02	1438.958527	1.09E-02	4412.5202	6.21E-04	11671.411	1.73E-05
1.13E-02	1466.71867	1.28E-02	4556.8720	5.84E-04	11731.384	9.98E-07
6.77E-03	1485.993134	1.49E-02	4675.3698	6.47E-04	12356.883	9.11E-06
5.32E-03	1508.526836	1.59E-02	4816.5093	6.28E-04	12565.188	8.67E-06
5.05E-03	1547.808012	1.69E-02	4878.0961	5.47E-04	12882.037	6.92E-06
4.33E-03	1594.093044	1.70E-02	5116.2729	4.82E-04	12868.778	8.55E-06
3.91E-03	1627.895298	1.65E-02	5204.8184	4.52E-04	13010.661	9.54E-06
2.88E-03	1680.508321	1.54E-02	5312.7333	4.29E-04	13157.318	8.74E-06
1.71E-03	1698.64336	1.45E-02	5443.707	3.86E-04	13502.275	4.30E-06
1.45E-03	1725.839977	1.35E-02	5536.8643	3.57E-04	13886.730	6.23E-06
1.35E-03	1748.650048	1.25E-02	5677.8638	3.63E-04	14065.63	2.08E-06
1.42E-03	1773.447543	1.15E-02	5859.0868	3.52E-04	14225.397	2.68E-08
7.84E-04	1801.462188	1.06E-02	6043.2142	3.19E-04	14273.895	3.49E-08
6.08E-04	1828.179286	9.47E-03	6280.278	3.12E-04		
5.11E-04	1858.709445	8.53E-03	6534.8465	2.81E-04		
4.95E-04	1897.0773	7.50E-03	6644.6061	2.53E-04		
3.76E-04	1932.704595	6.54E-03	6780.1815	2.20E-04		
4.70E-04	1985.660778	5.56E-03	6914.8545	1.91E-04		
4.19E-04	2027.406206	4.90E-03	7014.4582	1.81E-04		
3.02E-04	2085.480555	4.77E-03	7067.8845	1.81E-04		
3.26E-04	2132.745555	4.19E-03	7147.2566	1.00E-04		
2.77E-04	2170.218861	3.88E-03	7263.5028	7.85E-05		
2.42E-04	2220.903221	3.52E-03	7305.6634	7.22E-05		
2.20E-04	2286.677539	3.13E-03	7523.8062	6.88E-05		
1.74E-04	2300.863303	3.00E-03	7621.3742	6.03E-05		
1.79E-04	2338.003132	2.86E-03	7740.3573	6.49E-05		
1.17E-04	2375.15288	2.20E-03	7870.4086	6.04E-05		
8.77E-05	2382.20534	1.94E-03	7875.5565	5.29E-05		
5.07E-05	2440.712058	1.80E-03	8121.2077	5.03E-05		
1.56E-05	2500.914284	1.80E-03	8226.4355	5.15E-05		
2.73E-05	2548.635351	1.47E-03	8319.5928	3.88E-05		
3.90E-06	2612.886258	1.33E-03	8485.3241	4.05E-05		
	2681.486781	1.26E-03	8571.3943	2.91E-05		
	2744.024203	1.10E-03	8835.1662	3.13E-05		
	2816.383206	1.06E-03	8927.4212	2.48E-05		
	2825.910248	8.79E-04	9098.0782	2.77E-05		
	3065.165346	7.12E-04	9337.8667	1.94E-05		
	3213.155845	6.12E-04	9484.5203	2.31E-05		
	3363.688508	5.00E-04	9564.7647	2.74E-05		
	3521.02553	4.32E-04	9685.5925	1.93E-05		
	3670.220337	3.82E-04	9834.0269	2.82E-05		
	3802.376284	3.42E-04	10102.495	2.77E-05		
	3983.100031	3.05E-04	10262.081	1.87E-05		
	4085.185843	3.20E-04	10304.499	1.48E-05		
	4312.729863	2.19E-04	10574.737	2.15E-05		
	4545.677367	1.87E-04	10684.497	3.48E-05		
	4750.441124	1.57E-04	10782.268	3.60E-05		
	4985.385162	1.80E-04	10865.278	2.52E-05		
	5047.800054	1.69E-04	10951.058	2.21E-05		

APPENDIX II.8

Hydrogramms of the Milandrine, the Font, the Bâme and the Saivu with tracer tests events

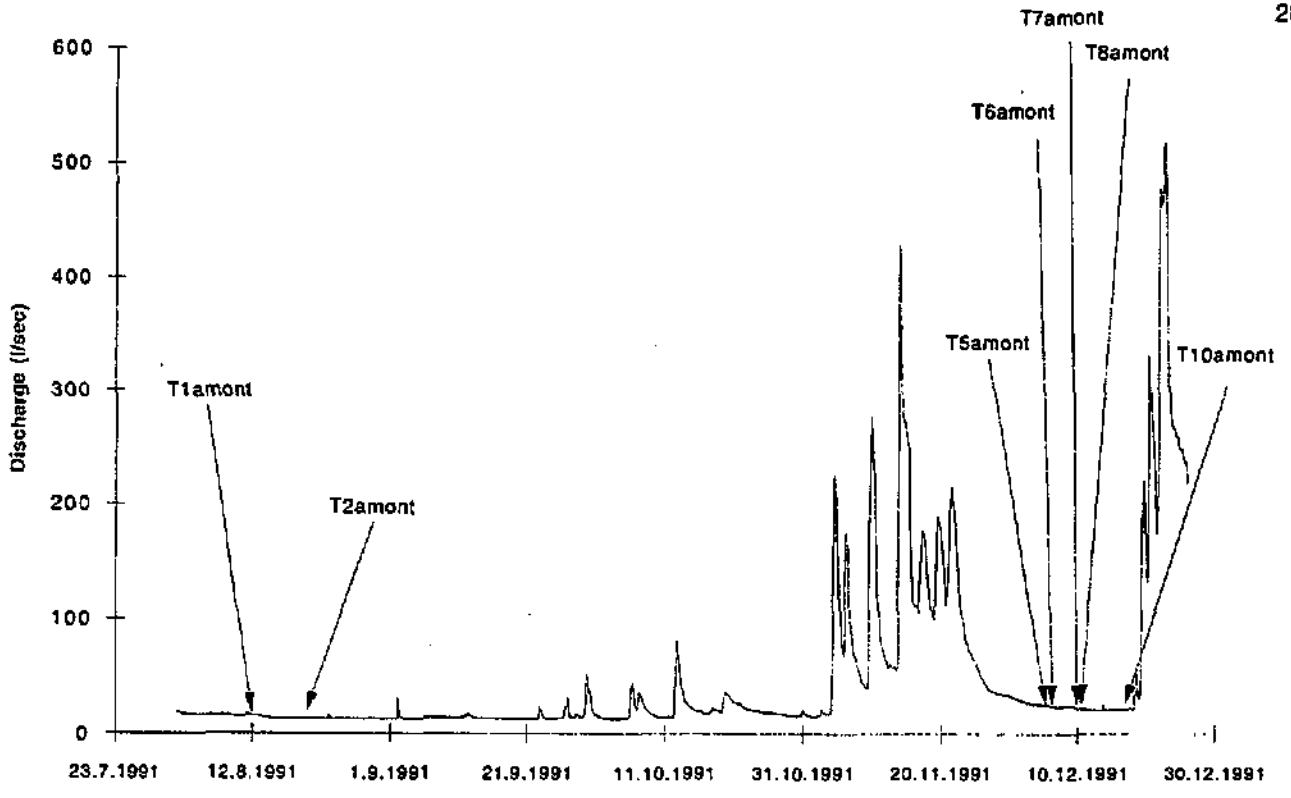
Discharge (l/sec)
600
500
400
300
200
100
0
T1amont
T2amont
T5amont
T6amont
T7amont
T8amont
T10amont
23.7.1991
12.8.1991
1.9.1991
21.9.1991
11.10.1991
31.10.1991
20.11.1991
10.12.1991
30.12.1991

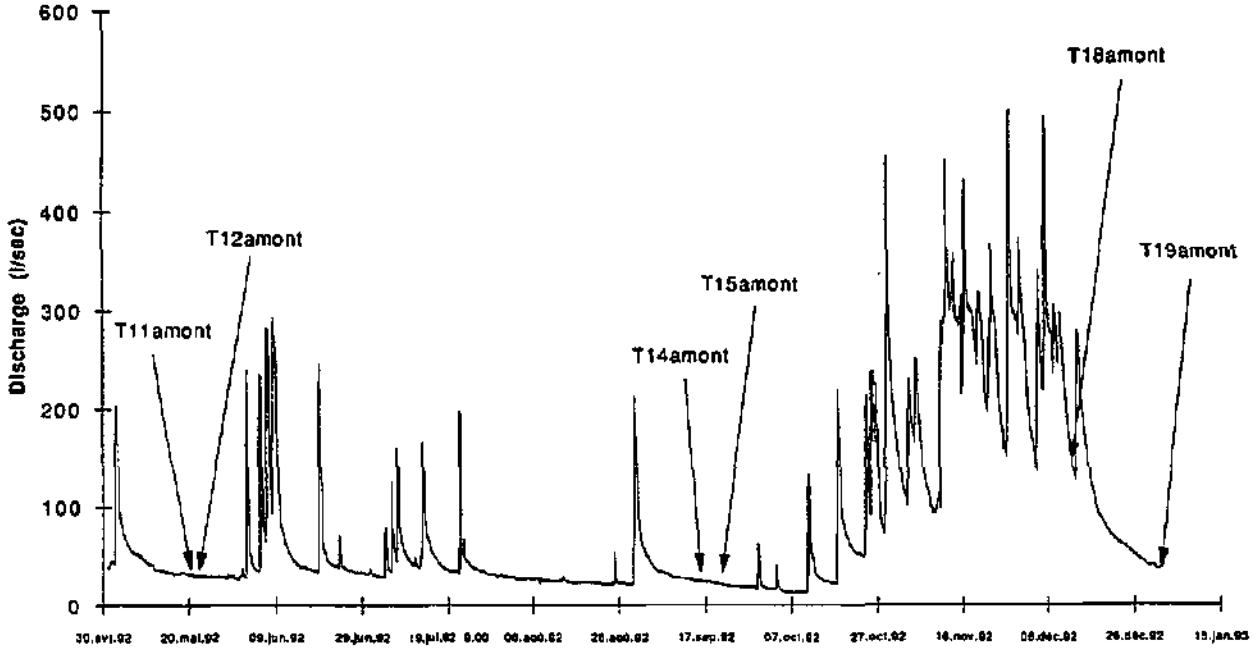
Discharge (l/sec)
600
500
400
300
200
100
0
T11amont
T12amont
T14amont
T15amont
T18amont
T19amont

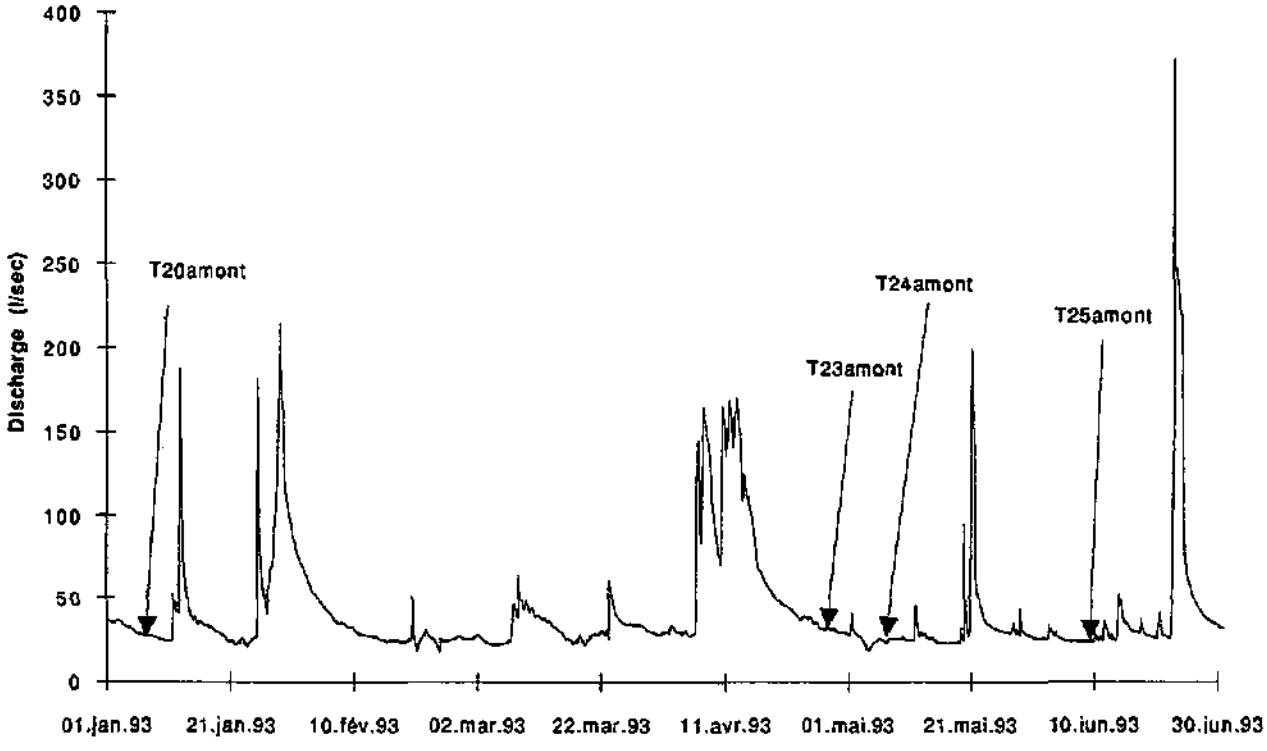
Discharge (l/sec)
400
350
300
250
200
150
100
50
0
T20amont
T24amont
T25amont
T23amont
01.jan.93
21.jan.93
10.fév.93
02.mar.93
22.mar.93
11.avr.93
01.mai.93
21.mai.93
10.jun.93
30.jun.93

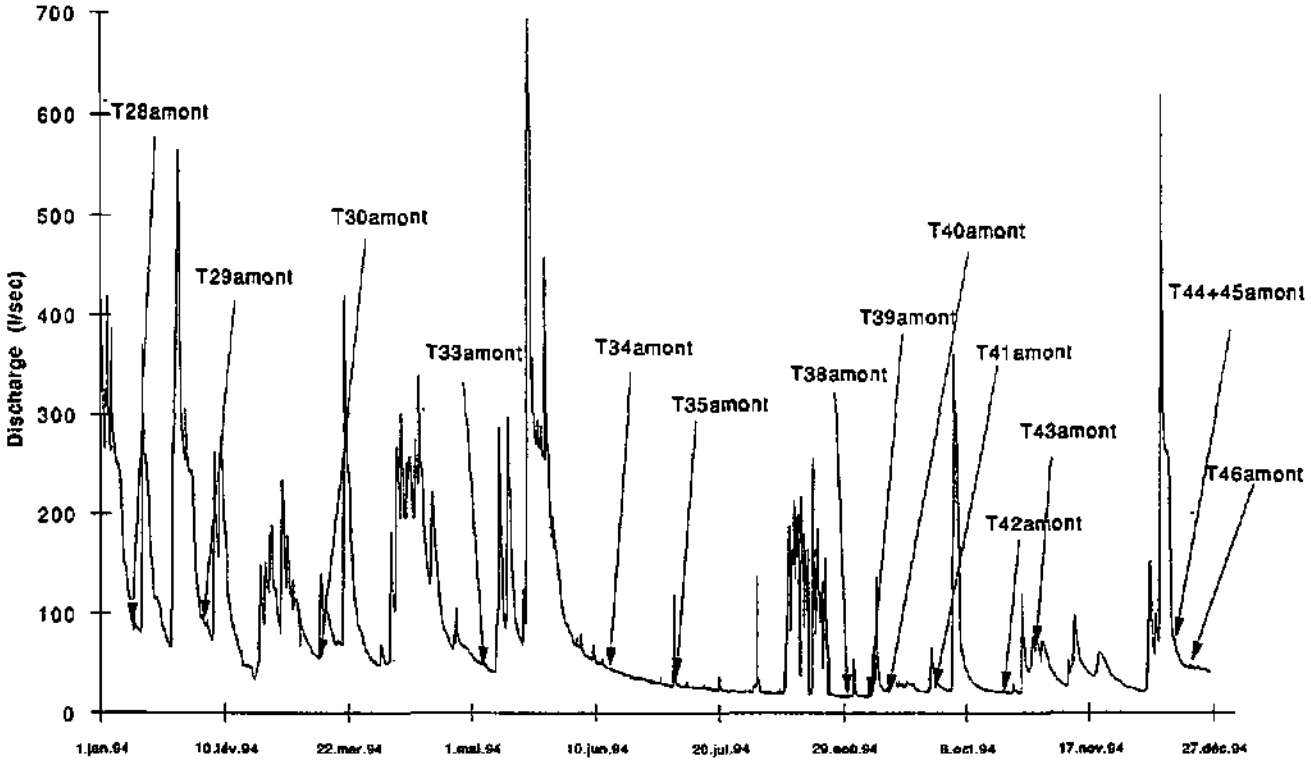
Discharge (l/sec)
700
600
500
400
300
200
100
0
T28amont
T29amont
T30amont
T33amont
T34amont
T35amont
T38amont
T39amont
T40amont
T41amont
T42amont
T43amont
T44+45amont
T46amont
1.jan.94
10.fév.94
22.mar.94
1.mai.94
10.jun.94
20.jul.94
29.aoû.94
8.oct.94
17.nov.94
27.déc.94

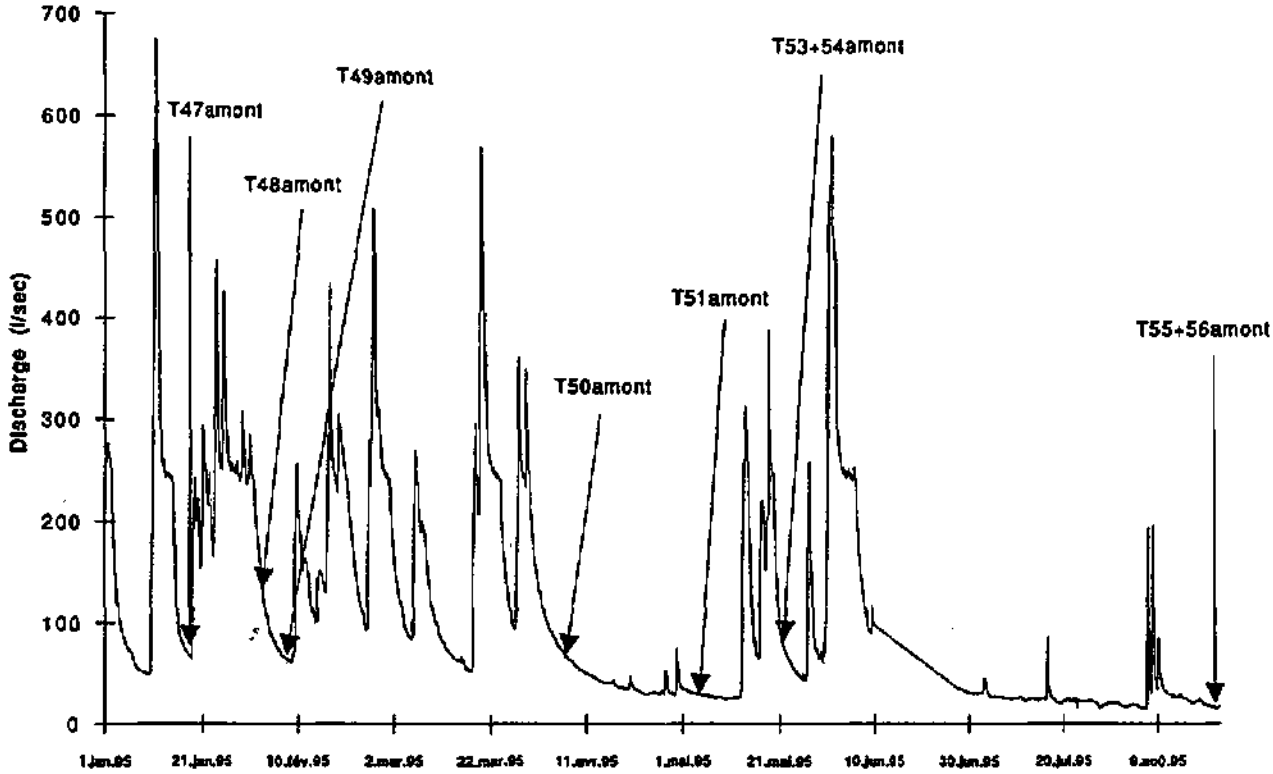
Discharge (l/sec)
700
600
500
400
300
200
100
0
T47amont
T48amont
T49amont
T50amont
T51amont
T53+54amont
T55+56amont

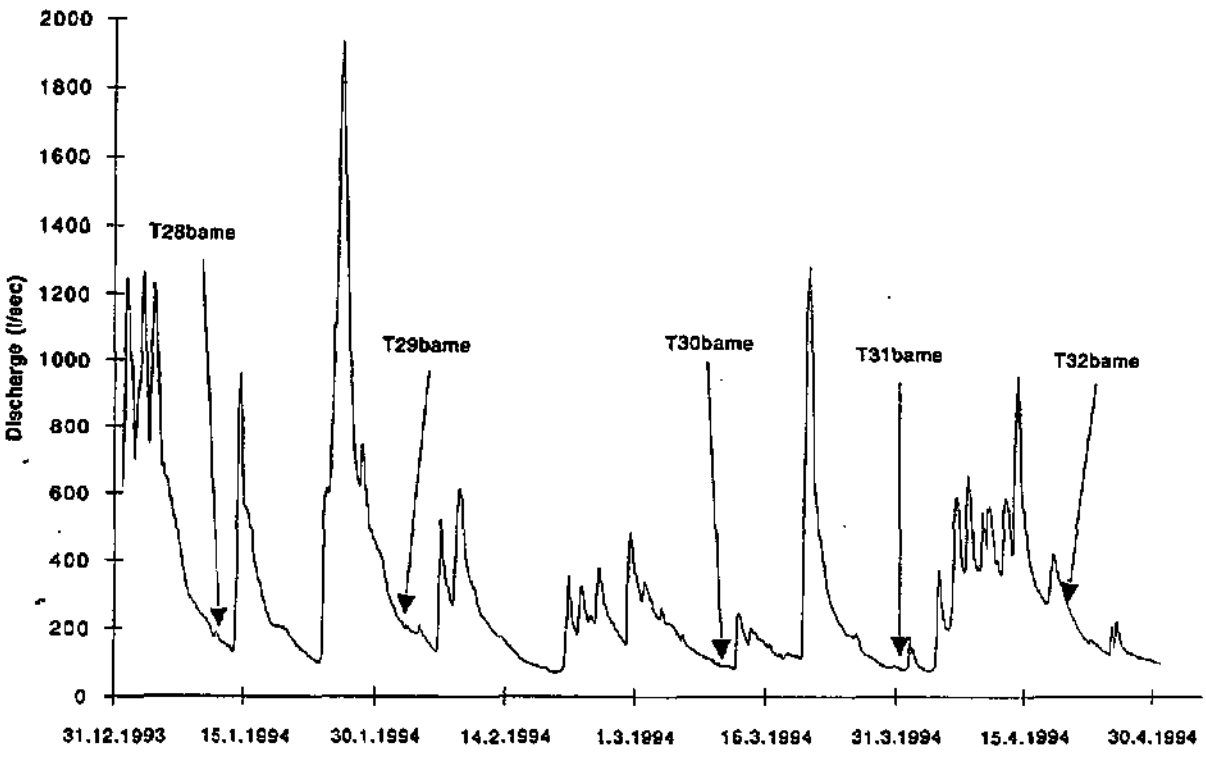
Discharge (l/sec)
2000
1800
1600
1400
1200
1000
800
600
400
200
0
T28bame
T29bame
T30bame
T31bame
T32bame
31.12.1993
15.1.1994
30.1.1994
14.2.1994
1.3.1994
16.3.1994
31.3.1994
15.4.1994
30.4.1994

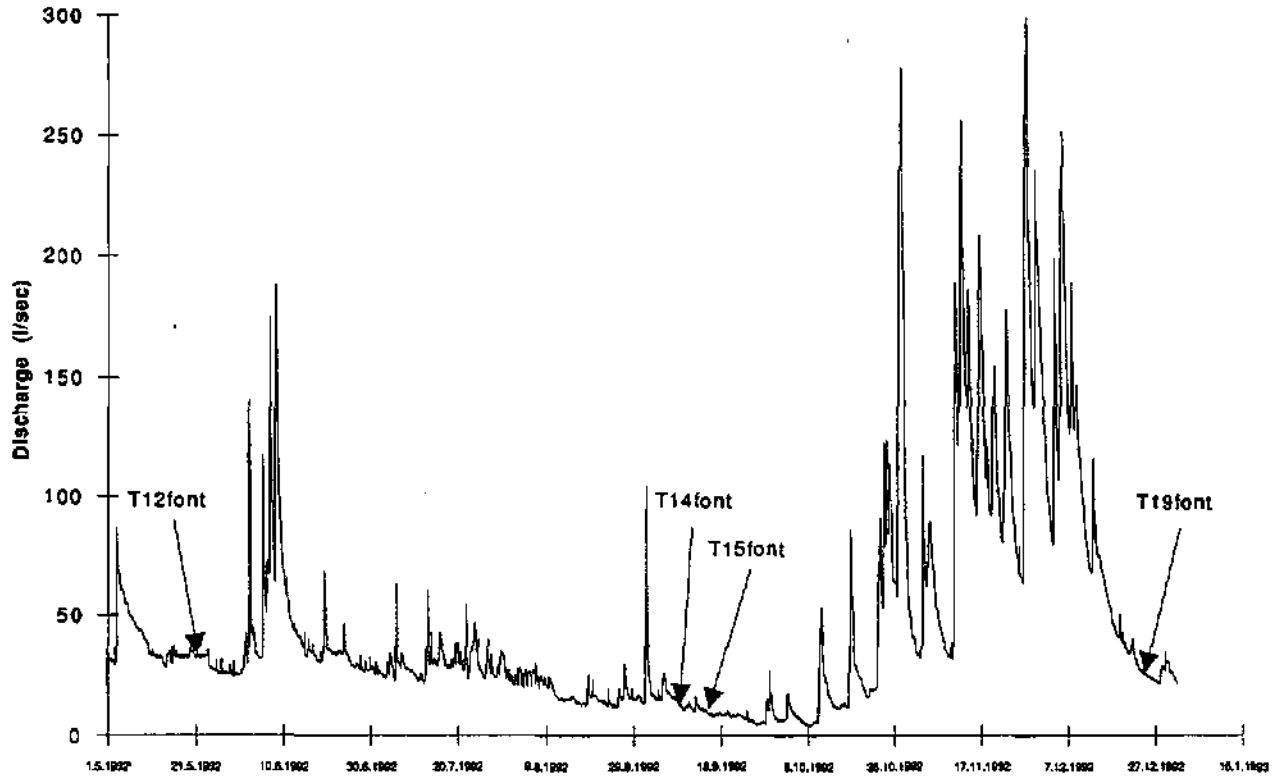
Discharge (l/sec)
300
250
200
150
100
50
0
T12font
T14font
T15font
T19font
1.5.1992
21.5.1992
10.6.1992
30.6.1992
20.7.1992
9.8.1992
29.8.1992
18.9.1992
8.10.1992
28.10.1992
17.11.1992
7.12.1992
27.12.1992
16.1.1993

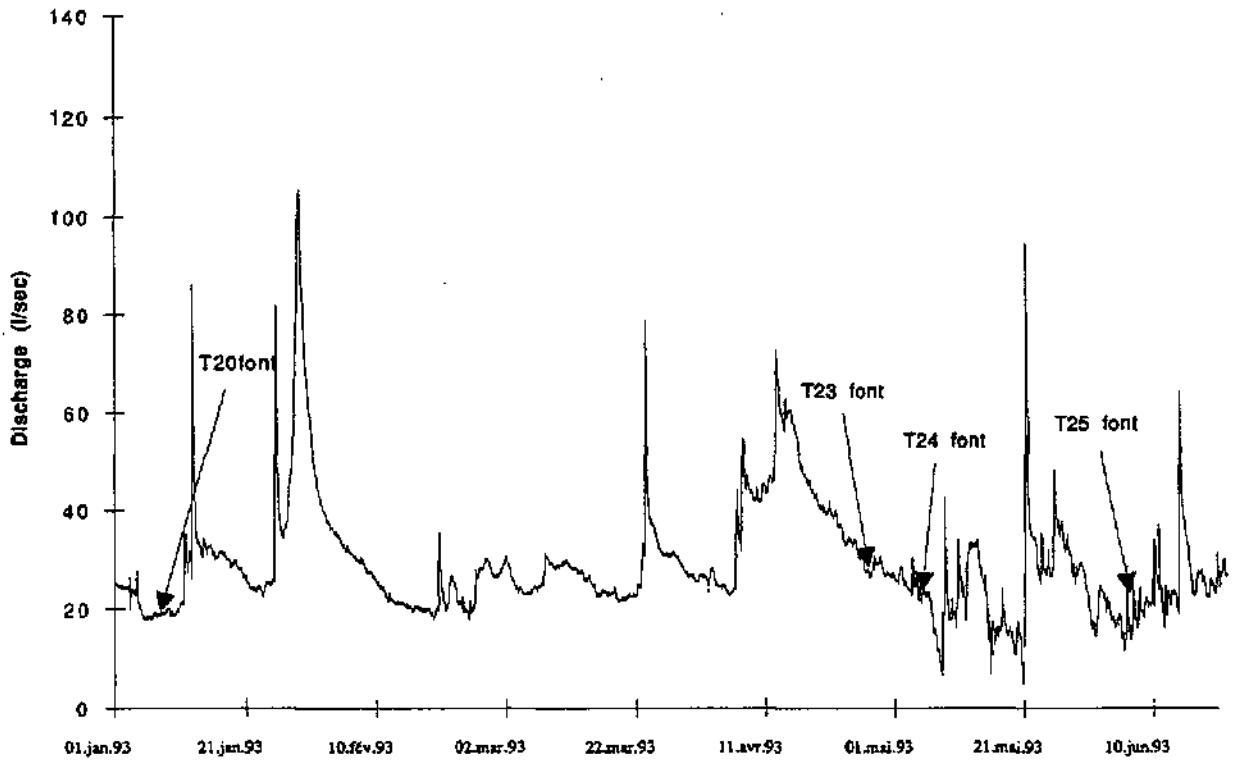
Discharge (l/sec)
140
120
100
80
60
40
20
0
T20font
T23 font
T24 font
T25 font
01.jan.93
21.jan.93
10.fév.93
02.mar.93
22.mar.93
11.avr.93
01.mai.93
21.mai.93
10.jun.93

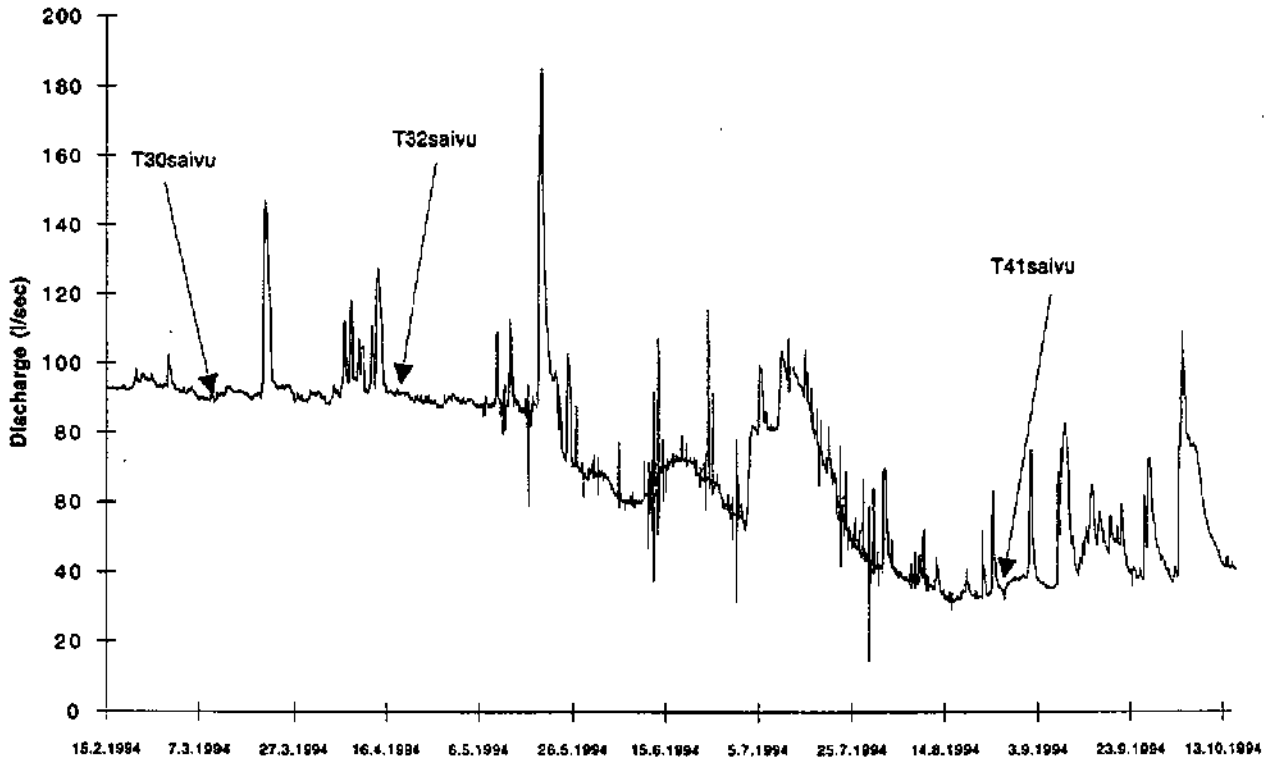
Discharge (l/sec)
T30saivu
T32saivu
T41saivu

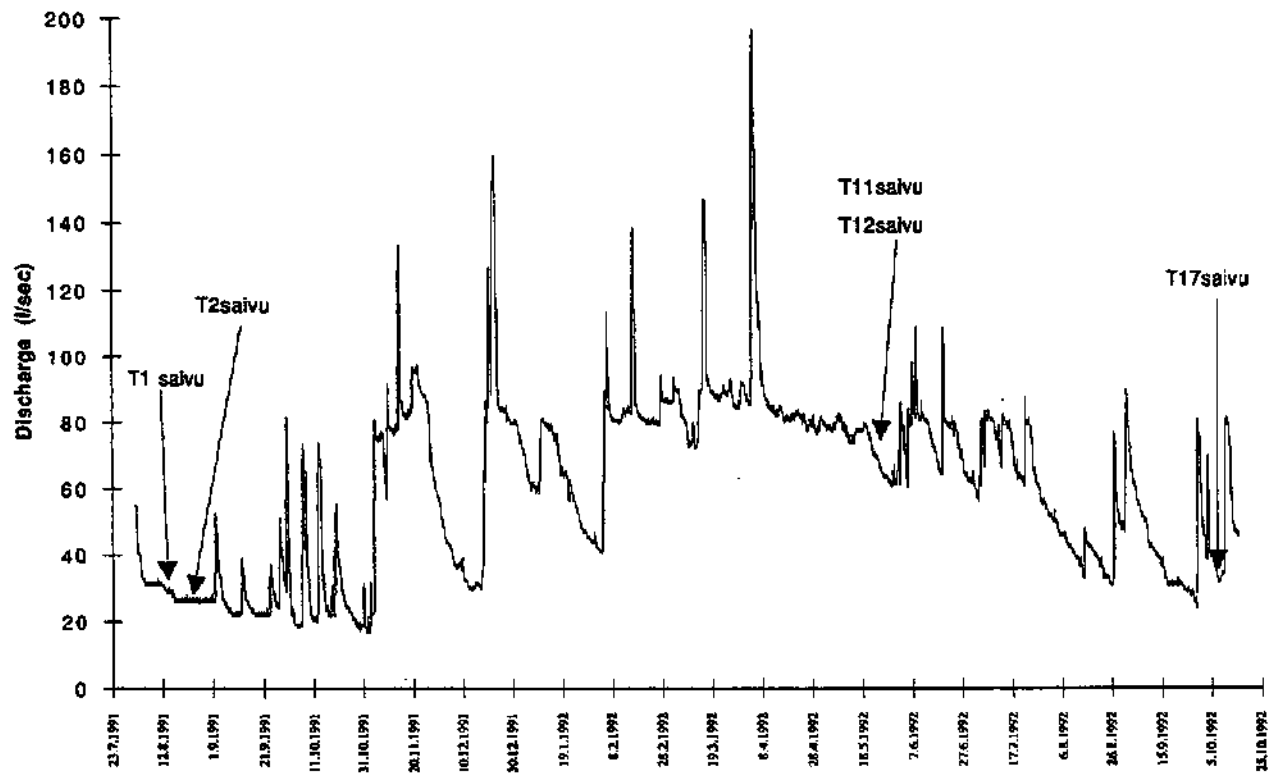
Discharge (l/sec)
T1 saivu
T2saivu
T11saivu
T12saivu
T17saivu

APPENDIX II.9

Tracer tests breakthrough curves of the Alpstein with discharge level

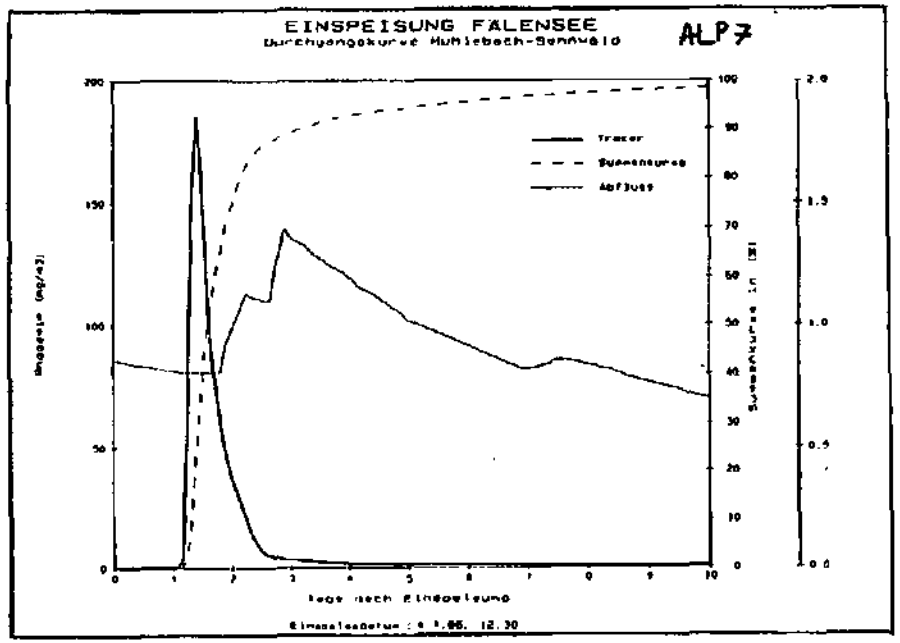
EINSPEISUNG FÄLENSEE
ALP7
Tracer
Summenkurve
Abfluss
Tage nach Einspeisung

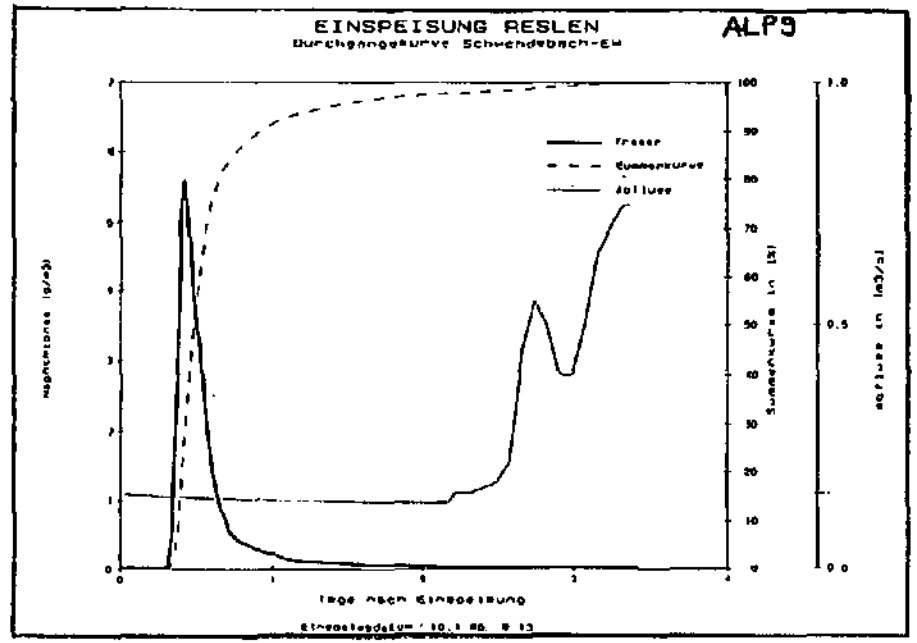
EINSPEISUNG RESLEN
ALP9
Tracer
Summenkurve
Abfluss
Tage nach Einspeisung

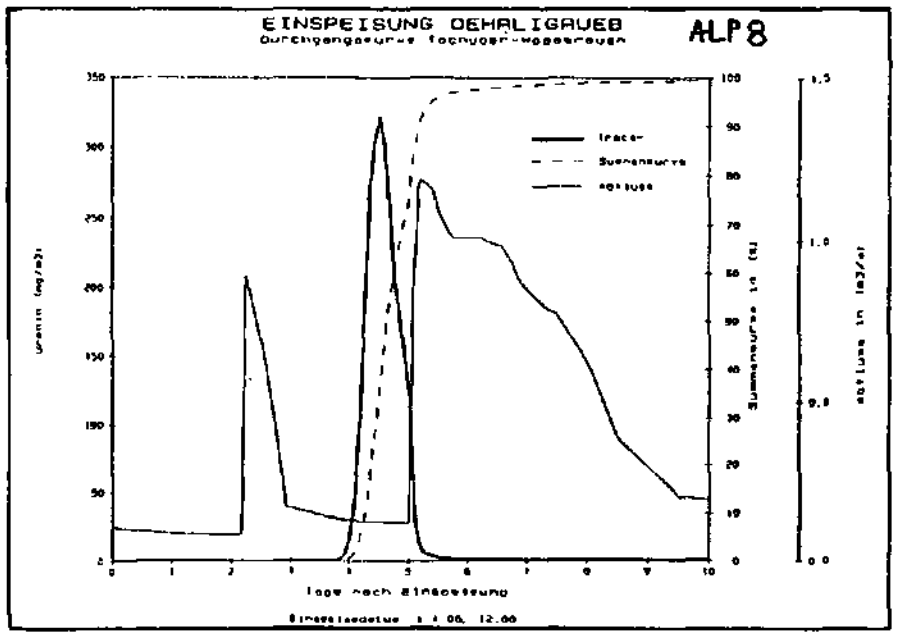
EINSPEISUNG OEHLIGRUEB
ALP8
Tracer
Summenkurve
Abfluss
Tage nach Einspeisung

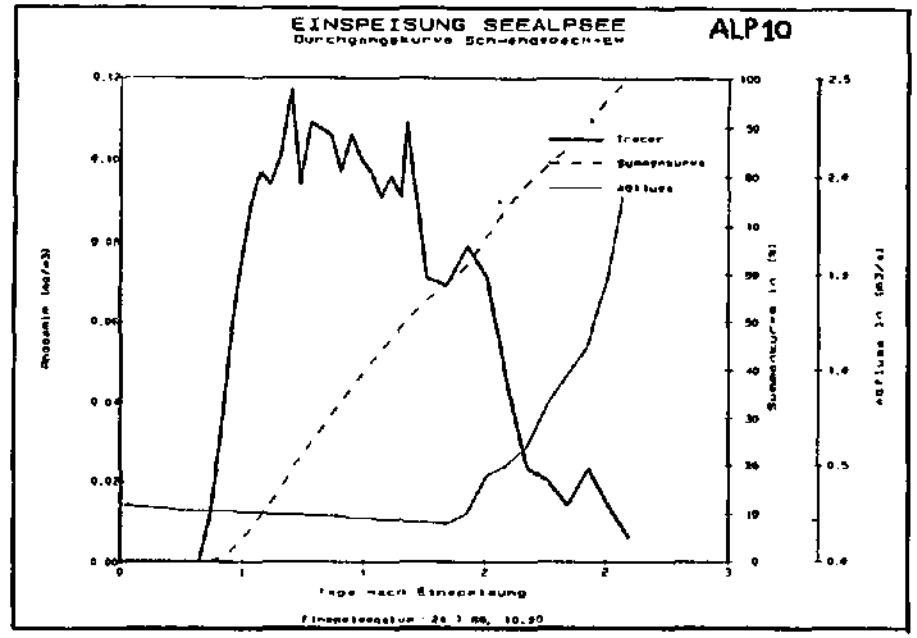
EINSPEISUNG SEEALPSEE
ALP10
Tracer
Summenkurve
Abfluss
Tage nach Einspeisung

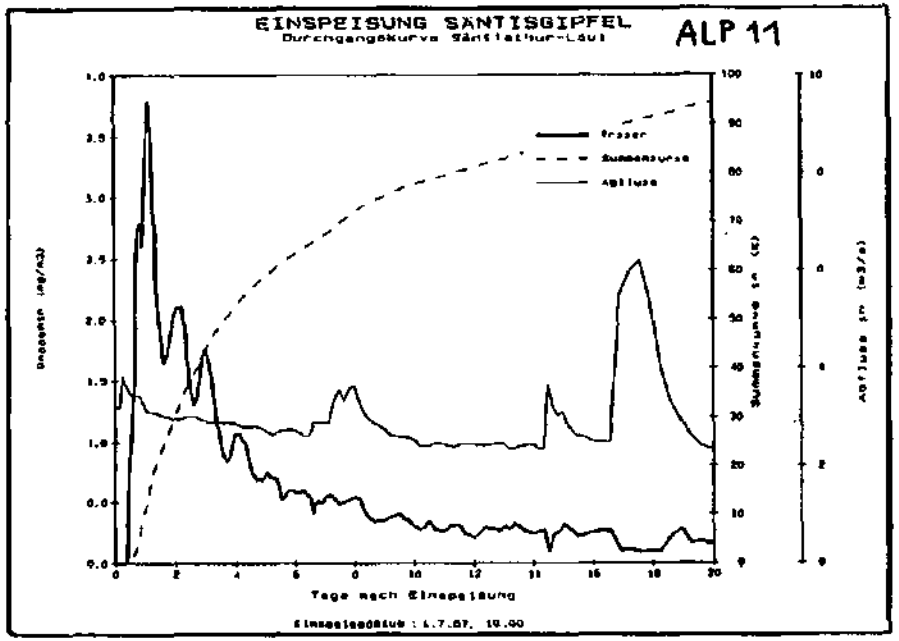
EINSPEISUNG SANTISGIPFEL
ALP 11
Tage nach Einspeisung

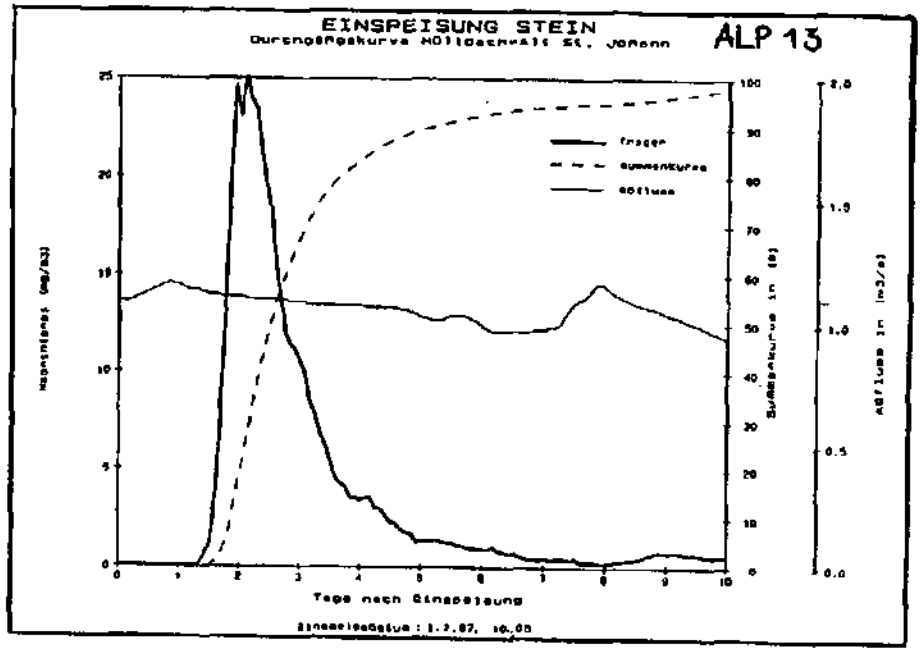
EINSPEISUNG STEIN
ALP 13
Tage nach Einspeisung

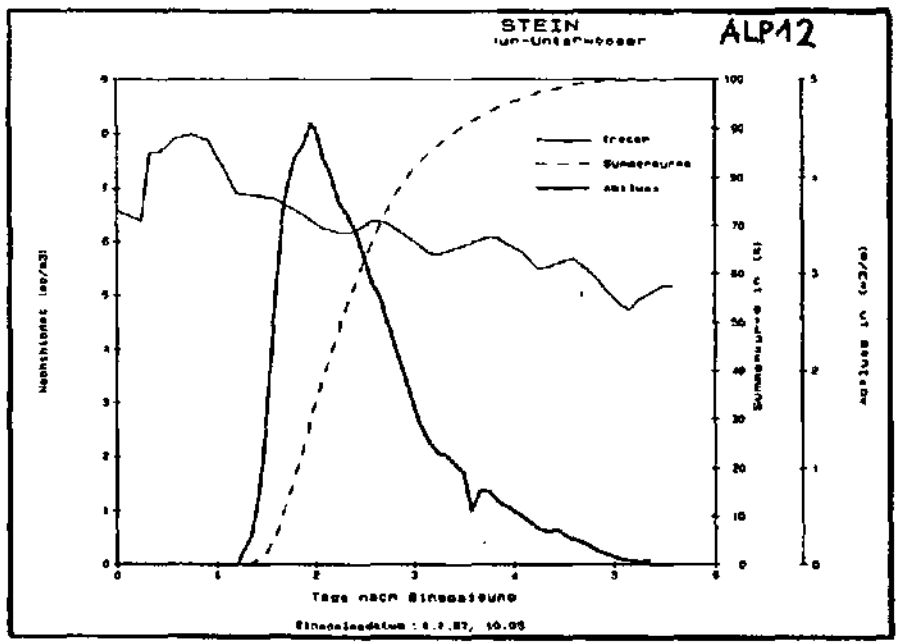
STEIN
ALP12
Tage nach Einspeisung

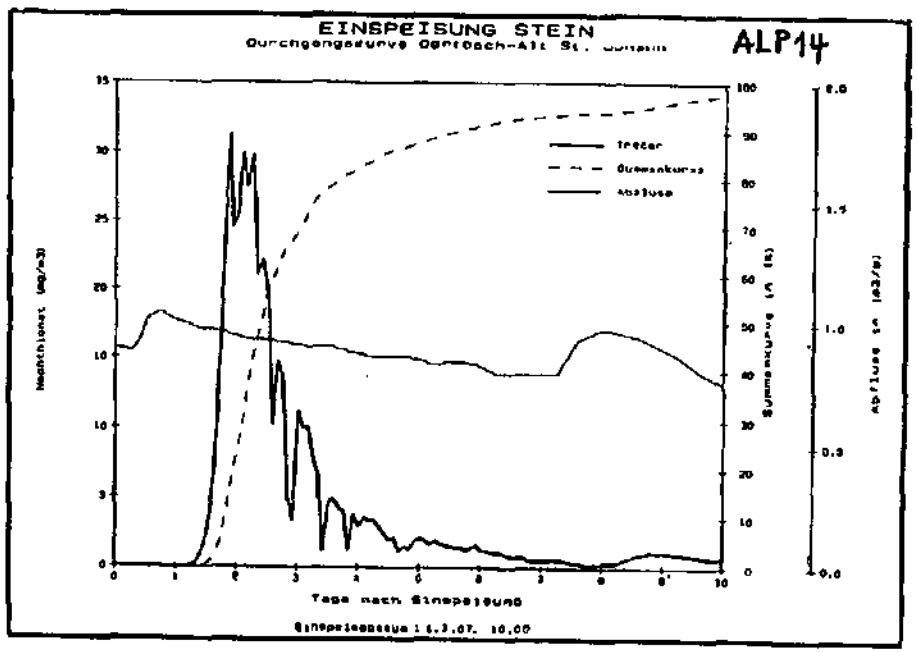
EINSPEISUNG STEIN
ALP14
Tage nach Einspeisung

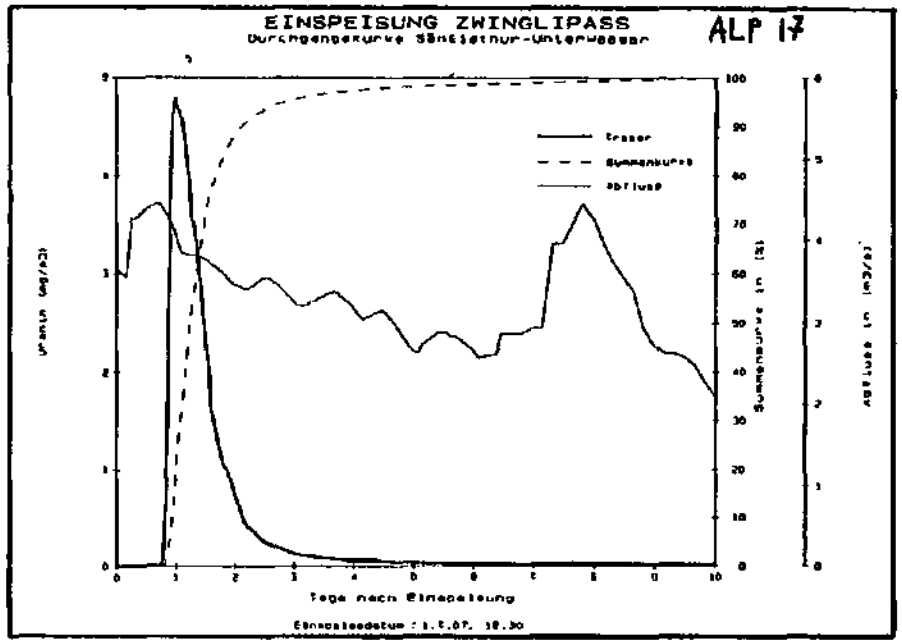
EINSPEISUNG ZWINGLIPASS
Durchgangskurve Sänetlehnur-Unterwasser
ALP 17
Tracer
Summenkurve
Abfluss
Tage nach Einspeisung

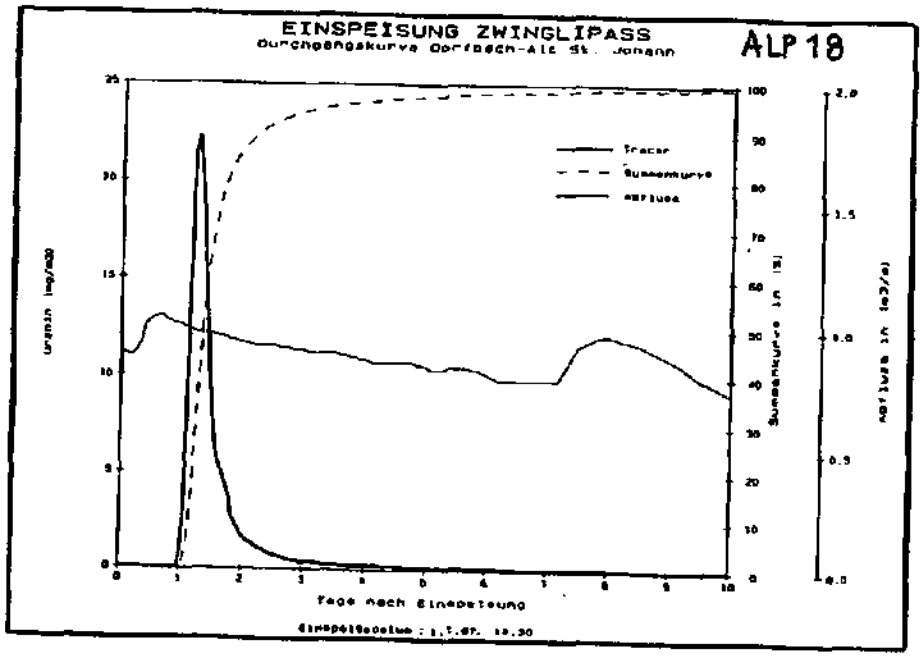
EINSPEISUNG ZWINGLIPASS
Durchgangskurve Dorfbach-Alt St. Johann
ALP 18
Tracer
Summenkurve
Abfluss
Tage nach Einspeisung

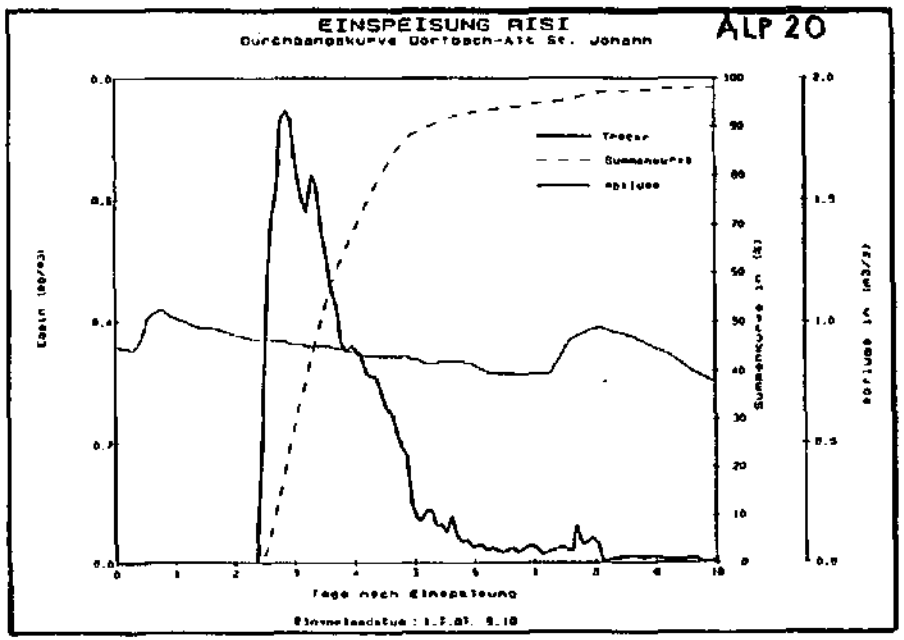
EINSPEISUNG RISI
Durchgangskurve Dorfbach-Alt St. Johann
ALP 20
Tracer
Summenkurve
Abfluss
Tage nach Einspeisung

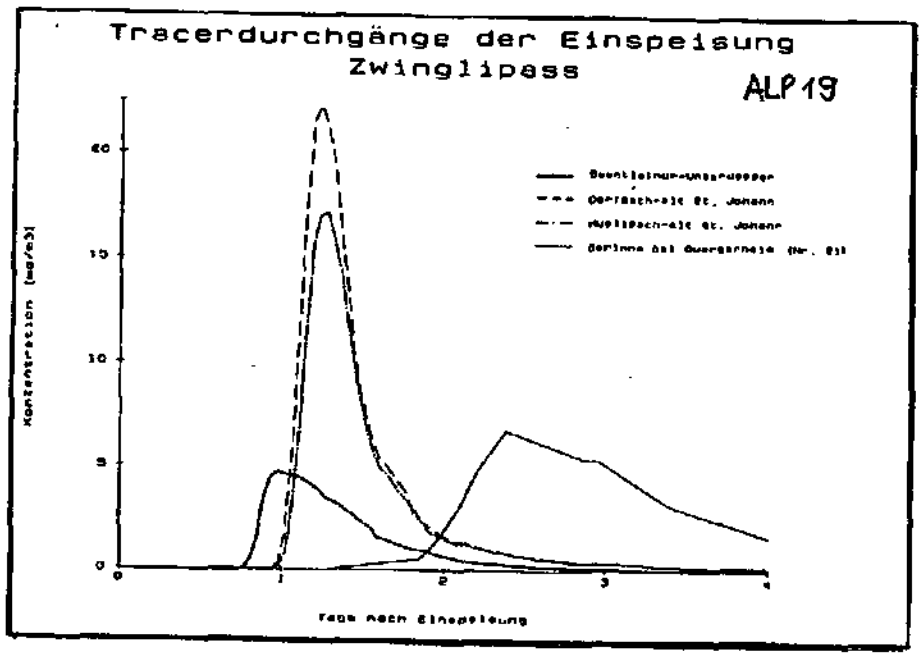
Tracerdurchgänge der Einspeisung
Zwinglipass
ALP 19
Tage nach Einspeisung

APPENDIX II.10

Microbiological tracers

Appendix II.10.

Microbiological tracers

a) why microbiological tracers ?

The use of bacteriophages as artificial tracers for surface and subsurface waters dates back to 1972 (Winpenny et al.). In the 1980's, the Microbiology Laboratory associated to the Centre of Hydrogeology of the University of Neuchâtel had accomplished several encouraging experiments. A detailed research on the use of the bacteriophages ac biological tracers has been undertaken by Rossi (1994).

The bacteriophages, bacteria viruses, are nm range of size and are not dangerous for the Environment. They, thus, can be used a artificial tracers. These biological tracers are inert organisms; their impact on the environment is insignificant.

The bacteriophages as all viruses, are not able to self - multiply; they do need to physically get integrated to a specific host-bacteria, whose metabolism is misappropriated to the benefit of the intracellular multiplication. They possess a capside - head - containing the genetic code. Some phages have a tail (more or less long and flexible, sometimes retractile) on whose extremity are located the specific recognition sites of the host cell (Rossi, 1995).

The bacteriophages respond to the expected characteristics of an artificial tracer for the subsurface water; according to Keswick et al., 1982, they are the following:

Table 1
Characteristics of bacteriophages

- they are not pathogeneous (i.e. not able to induce diseases for human beings, animals or plants)
- they are not present naturally in the subsurface waters or at least are distinguished with the present micro-organisms.
- they do not modify the subsurface water flow systems.
- they are stable in the traced environment for a time period relatively long (till 1 to 2 months)
- due to their density, they behave as water molecules. The selected bacteriophages interact only weakly with the environment (adsorption, absorption, destruction and inactivation)
- the detection limit is low (< 1 pfu* / ml)
- they do not react with other organisms that occur in the aquifer and do not induce any modifications of the environment or of the organisms properties; their host-bacteria are not present in the traced environment
- in the case of multitracing experiments, they are easily identifiable individually, as they possess their own specific host-bacteria.

* *pfu: plaque forming units is equivalent to the virus or bacteriophage per ml.*

An interesting advantage is specially for the use of tracers in urban environment, due to the fact that the bacteriophages are unseen at the outlet of the tracing system.

For several years, the laboratory of Microbiology of the university of Neuchâtel has developed the production and analyses methodology of various bacteriophages, testing in particular their physic-chemical properties (electric charge, adsorption, mechanical resistance). Several experimants in porous and karstic fissured aquifer had been carried out and had given some very positive results that had encouraged the hydrogeologists to use this type of tracer (Rossi, 1994).

The isolation and production technology of the seven phages had been developed taking into consideration the physiological properties of the host-bacteria and the physic-chemical characteristics of the phages. Among these seven virions, four had been isolated out of marine

environments (Atlantic ocean and North sea). None of them are naturally found in the aquifers.

Some toxicity tests on trout and daphnies and their eggs had been carried out after a tracing experiment accomplished in a river - the Arausa (NE) - by Rossi (1995): all of them were negative. No fish were dead, after bathing in bacteriophages solutions with 10, 3, 1 and 0.3 per thousand and for tests duration of 24 to 96 hours.

b) used bacteriophages: physic-chemical characteristics

The seven different bacteriophages had been used in some double and repeated tracing tests in Bure, Areuse-Brévina and Noiraigue watercatchment basins. The scientific denomination and the name of the host-bacteria are in the following table:

Table 2.3.1.

Bacteriophages and host-bacteria listings

Bacteriophages	**Host bacteria (ATCC)**
f1	*Escherichia coli K12* (ATCC 15766)
T7	*Escherichia coli B* (ATCC 11303)
H40/1	*H40* Bacterial strains not yet registered
H6/1	*H6* Bacterial strains not yet registered
H4/4	*H4* Bacterial strains not yet registered
H2/1	*H2* Bacterial strains not yet registered
Psf2	*Pseudomonas fluorescens* (ATCC 27663)

ATCC: American Type Culture Collection

The bacteriophages H4/4, H6/1, H40/1 and H2/1 are marine bacteriophage; they were isolated during marine exploration campaigns in the Atlantic by K. Moebus (Moebus K., Hermann F., 1987; Moebus K., Nattkemper H., 1989, Moebus K., 1989,. Moebus K., 1992). H40/1 belongs to the Siphoviridae family. It has an icosahedral head and a flexible noncontractile tail. H6/1 is an icosahedron without a tail; it is member of the Leviviridae family.

The bacteriophage Psf2 belongs to the Siphoviridae family of the type B1; its head is polyhedral (icosahadron) and its tail flexible and noncontractile. It was isolated from waster water of the water treatment plant.

The phages T7 and f1 belong to the collections of the Laboratory of Microbiology of the University of Neuchâtel. They possess the same host-bacteria Escherichia coli, but belong to two different morphological groups. T7 is a phage of small size; it is member of the Podoviridae family characterised by a polyhedral head and a small noncontractile tail. The phage f1 is a filament shape phage of the Inoviridae family (Ackermann and DuBow, 1987).

The structure of the bacteriophages induce an interaction with their environment. In the more common value of pH of karstic groundwater, they are strongly negatively charged.

Two phenomenons may be differentiated: the **inactivation** of phages due to the agitation of the tracing system (turbulent flows, torrential or laminar), and the **adsorption**.

The adsorption according Lipson et al, 1985, is a reversible process. It is characterised by a dynamic equilibrium, established between the phage population and the adsorption sites (suspended particles, aquifer material). This equilibrium is called Quasi-Equilibrium Adsorption (QEA) by Grant et al. (1993). From theoretical cases, three stages can be differentiated:

- *Quasi-Equilibrium Adsorption* (QEA): the phage is not influenced by the presence of adsorbent material. Adsorption, if it occurs, is irreversible. The adsorption on the particle does not influence the virulence of the bacteriophage.
- *Quasi-Equilibrium Adsorption and Reduced Inactivation* (QEARI): the adsorption of viruses on colloids or on substrate induces a protector effect (reduced inactivation).

- *Quasi-Equilibrium Adsorption* and *Surface Sink* (QEASS):the solid surface acts as a trap for the viruses. The inactivation rate of adsorbed phages is higher than that of the free-floating phage. Several authors had shown that a great percentage of adsorbed phages on particles retain their virulence (Payment et al., 1974, Lipson and Stolzky, 1985).

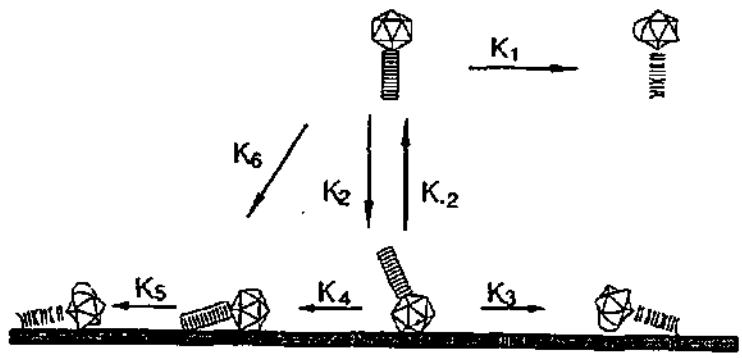

theoretical model of the phages behaviour.

In this figure a homogenous population of phages is subdivided into several fractions

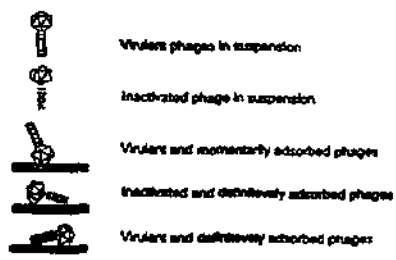

Figure 1: Quasi-Equilibrium adsorption (modified after Grant et al., 1993). Open circles: Inactivation reaction; Filled circles: Inactivation and adsorption reaction (in Rossi, 1994).

According to the work of Rossi on the processes study on some phages used as artificial tracers in karstic environment, the following comments can be made:

- More than 90% of phages (f1, Pef2, H40/1 et T7) react in similar manner to the inactivation by shaking : they are inactivated in great rate after 180 minutes of strong shaking. This inactivation follows a decreasing exponential law. This rapid decreasing is function of physical factors such as the temperature; it is independent therefore of the pH and of the ionic concentrations. The phage H6/1 is an exception: it is more resistant.
- After accomplishing experiments of adsorption with the phage T7, one deduces that the phage T7 gets adsorbed on the positively chargad sites of the clays. The physic-parameters (pH, ionic concentration) and the presence of organic matter influence strongly the adsorption. The experiments with other phages give evidence that phages react each specifically and differently to a particular adsorbent. This behaviour allows to distinguish three types of phages categories according to Grant et al., (1993):
    - Psf2, H40/1, H4/4 and H6/1 do not react practically to colloids minerals in laboratory. They have a behaviour of QEA or QEARI type, depending on the nature of the colloids. They are the best potential tracers.

- f1 is the only one that behaves under the QEASS type. Adsorbed on mineral suspended material, it loses its virulence. This can be explained by its filament morphology.
- The bacteriophage T7 has a behaviour of QEARI type. It reacts strongly with the mineral colloids. A great number of phages are inactivated quickly after a first stage of reaction. The reaction produces consequantly a strong protection of the phage regarding the inactivation.

c) phages production and analyses principles

Production

It is necessary to produce suspensions of phages in large quantities; the suspensions contain in average 10^{+13} phages. This means a production of 10 litres of phages in order to achieve some long distance tracing experiments (5 to 10 km) and of 1 to 2 litres for kilometre range distance. The production can be made in Petri dishes or in liquid phase, as it is described by Rossi (1994).

Analysea

The analyse is carried out under two phases. The first one consists in the test of the presence or the absence of the phages in the water samples. It gives a good estimation of the dilution's order to be accomplished in the second phase. This second phase is about the accurate counting of phages (Rossi, 1994).

APPENDIX II.11

Breakthrough curves of bacteriophages tracer tests

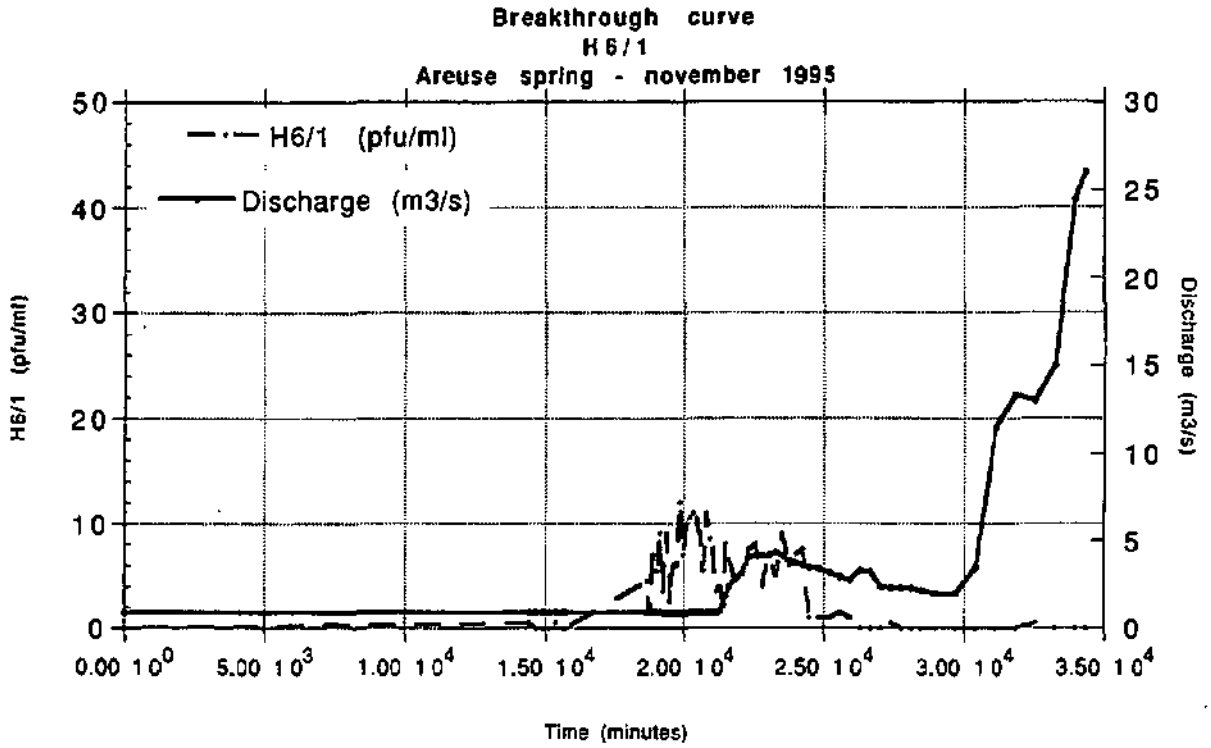
Breakthrough curve
H 6 / 1
Areuse spring - november 1995
H6/1 (pfu/ml)
Discharge (m3/s)
H6/1 (pfu/ml)
Discharge (m3/s)
Time (minutes)
0.00 10^0
5.00 10^3
1.00 10^4
1.50 10^4
2.00 10^4
2.50 10^4
3.00 10^4
3.50 10^4

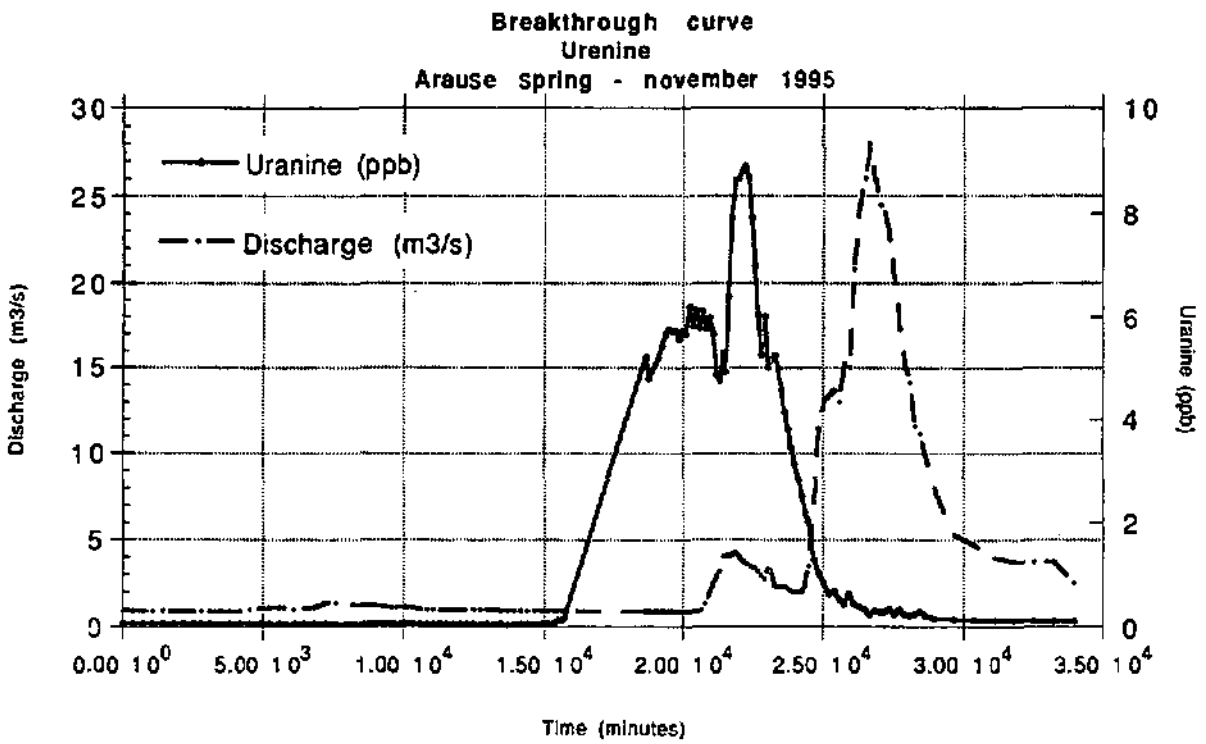
Breakthrough curve
Urenine
Arause spring - november 1995
Uranine (ppb)
Discharge (m3/s)
Discharge (m3/s)
Uranine (ppb)
Time (minutes)
0.00 10^0
5.00 10^3
1.00 10^4
1.50 10^4
2.00 10^4
2.50 10^4
3.00 10^4
3.50 10^4

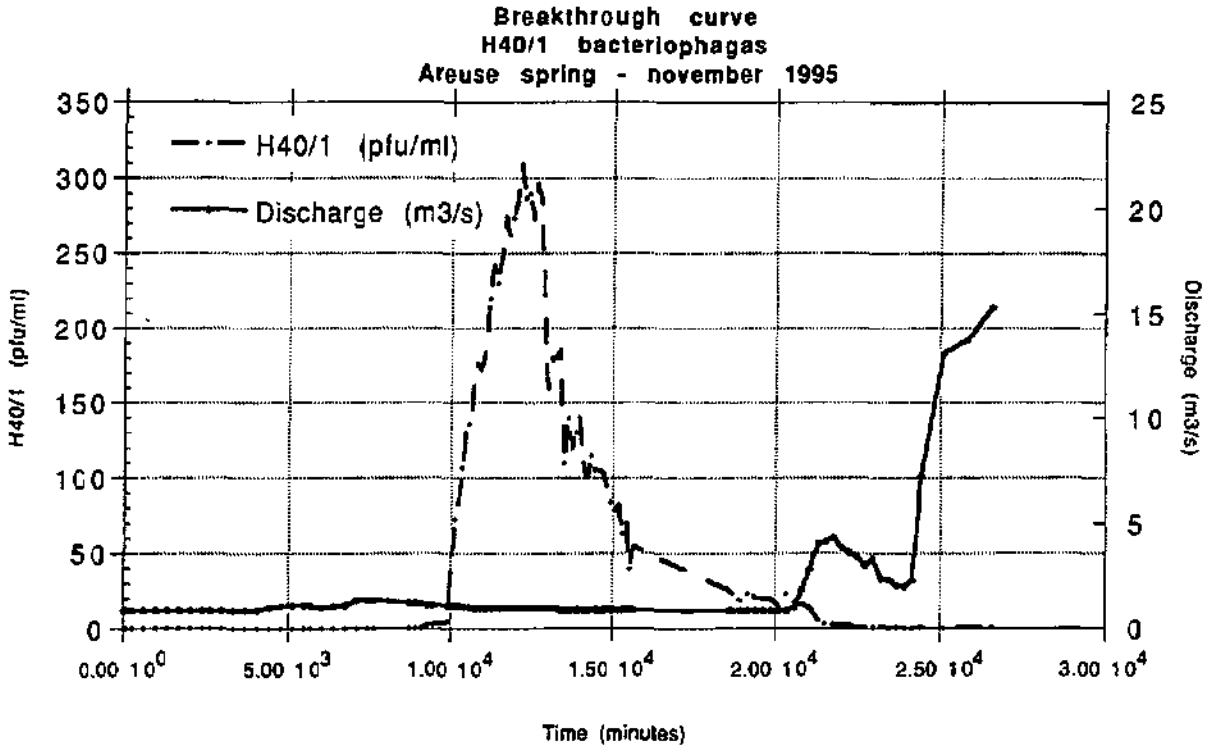
Breakthrough curve
H40/1 bacteriophagas
Areuse spring - november 1995
H40/1 (pfu/ml)
Discharge (m3/s)
H40/1 (pfu/ml)
Discharge (m3/s)
Time (minutes)
0.00 10^0
5.00 10^3
1.00 10^4
1.50 10^4
2.00 10^4
2.50 10^4
3.00 10^4

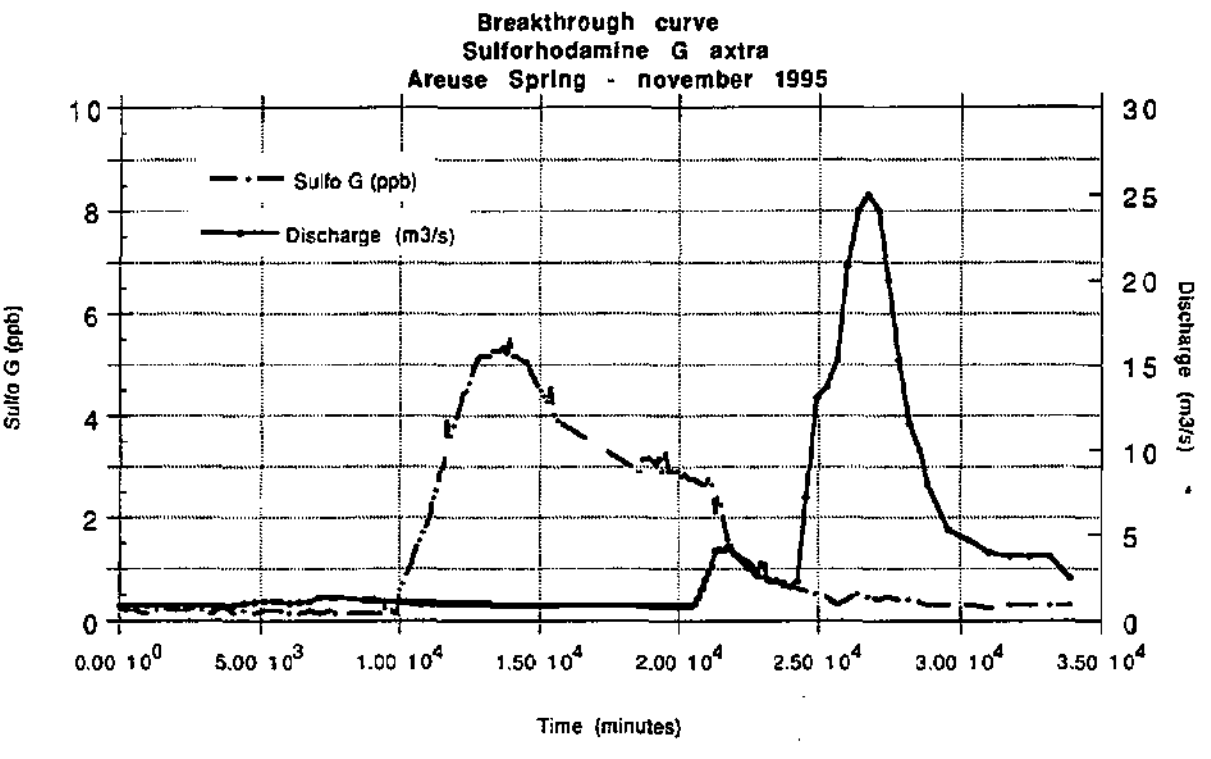
Breakthrough curve
Sulforhodamine G axtra
Areuse Spring - november 1995
Sulfo G (ppb)
Discharge (m3/s)
Sulfo G (ppb)
Discharge (m3/s)
Time (minutes)
0.00 10^0
5.00 10^3
1.00 10^4
1.50 10^4
2.00 10^4
2.50 10^4
3.00 10^4
3.50 10^4

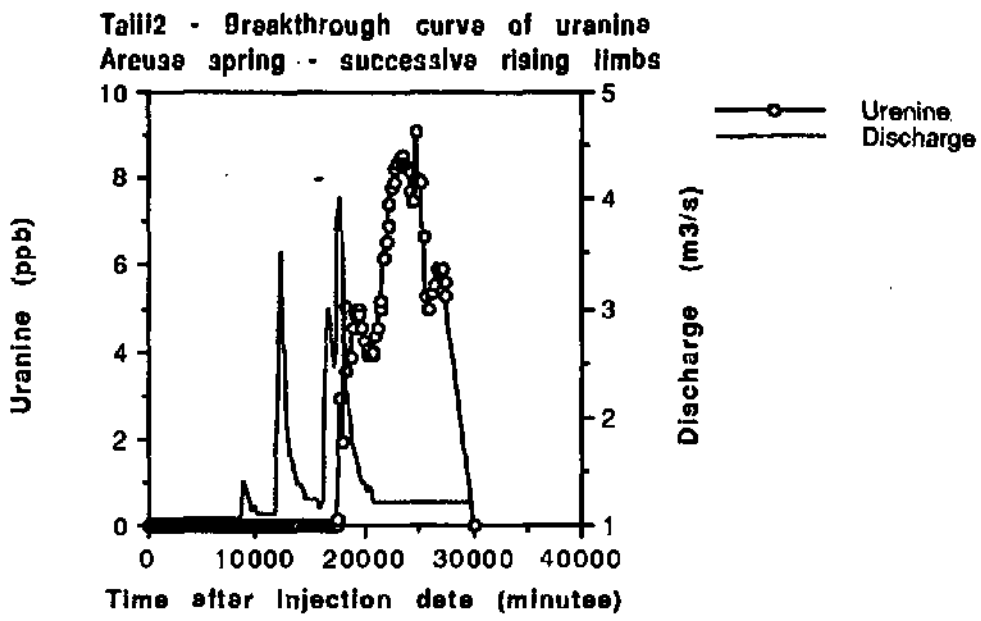
Taill2 - Breakthrough curve of uranine
Areuse spring - successive rising limbs
Uranine (ppb)
Discharge (m3/s)
Urenine
Discharge
Time after injection date (minutes)

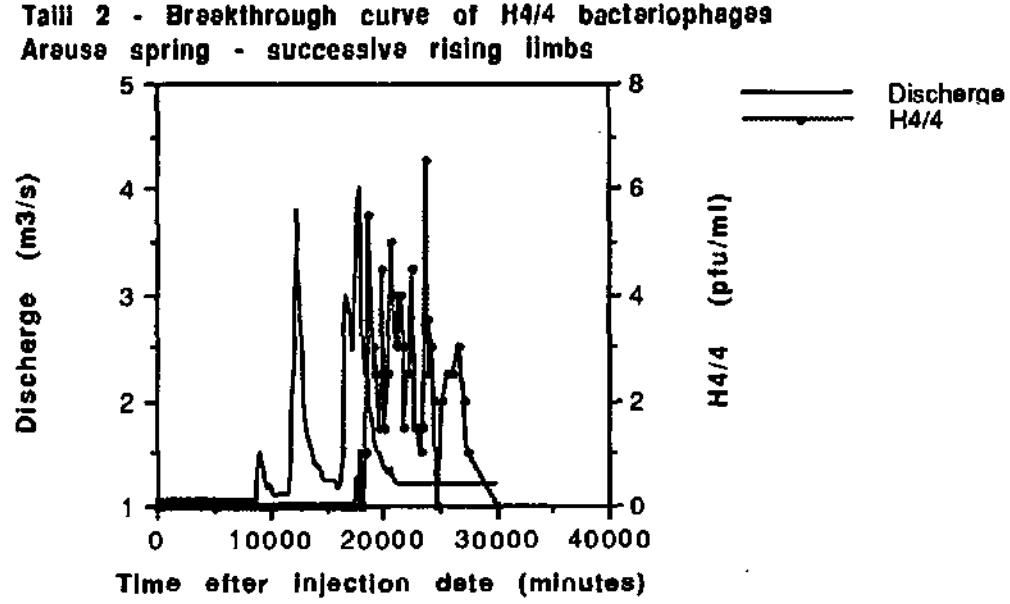
Taill 2 - Breakthrough curve of H4/4 bacteriophages
Areuse spring - successive rising limbs
Discherge (m3/s)
H4/4 (pfu/ml)
Discherge
H4/4
Time after injection date (minutes)

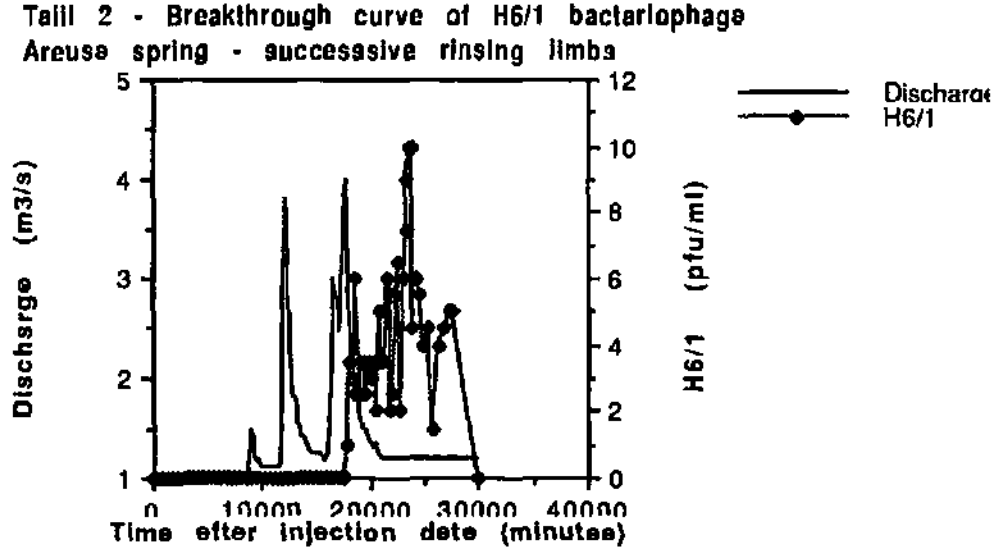
Taill 2 - Breakthrough curve of H6/1 bacteriophage
Areuse spring - successive rinsing limbs
Dischsrge (m3/s)
H6/1 (pfu/ml)
Discharge
H6/1
Time after injection date (minutes)

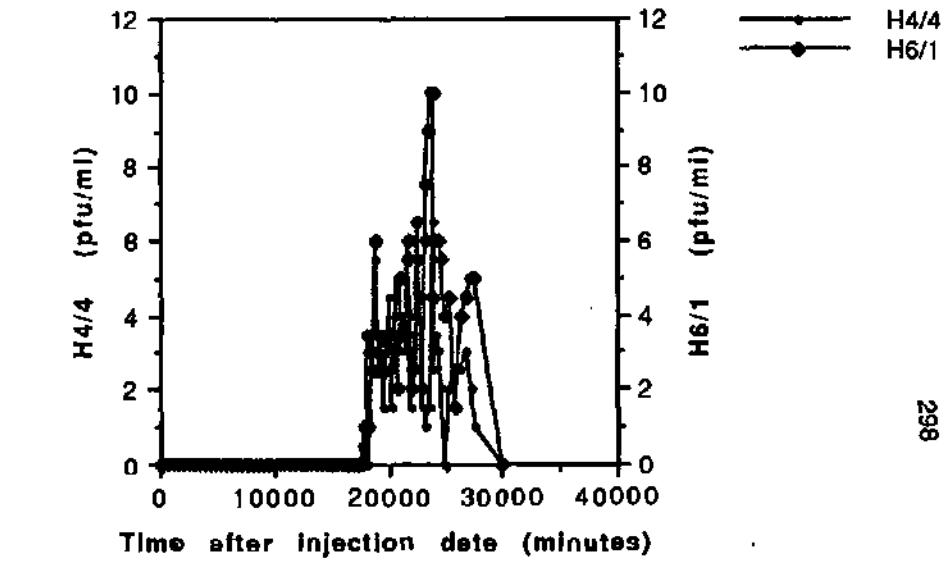
Breakthrough curves of bacteriophages H4/1 and H6/1
Areuse spring - Taill2
H4/4 (pfu/ml)
H6/1 (pfu/ml)
H4/4
H6/1
Time after injection date (minutes)

Teill2 - Breakthrough curve of sulforhodemine G extra
Areuse spring - Successive rising limbs

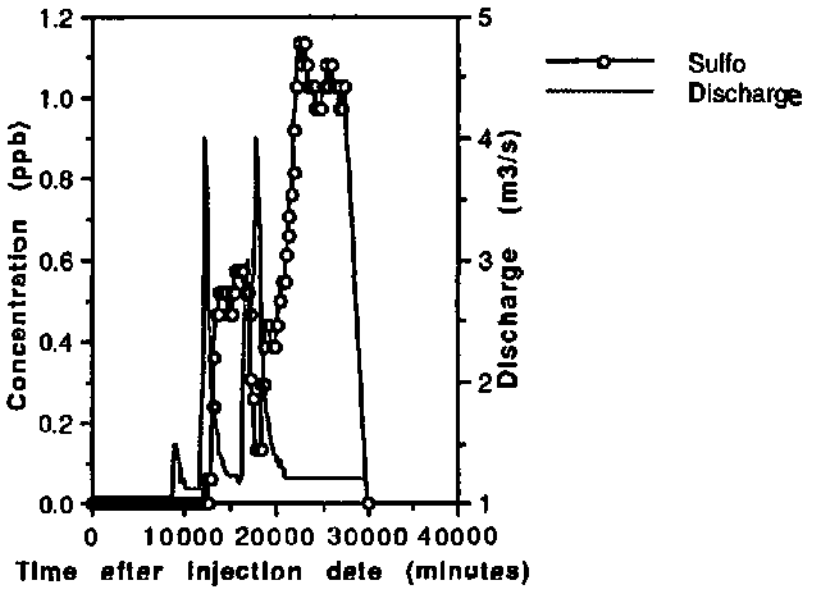

Teill2 - Breakthrough curve of becteriphage H40/1
Areuse epring - euccessive rinsing limbs

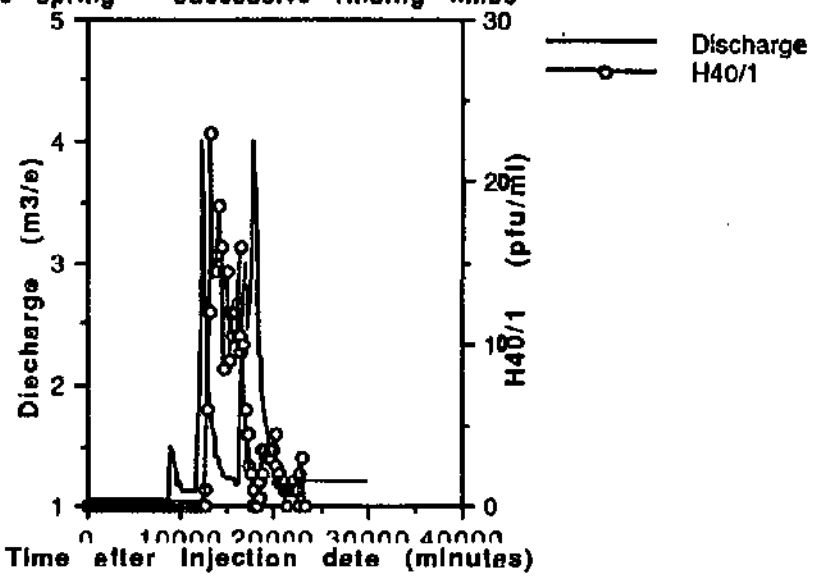

Teill2 - Breakthrough curves of sulfoG and bacteriophages H40/1
Areuse spring

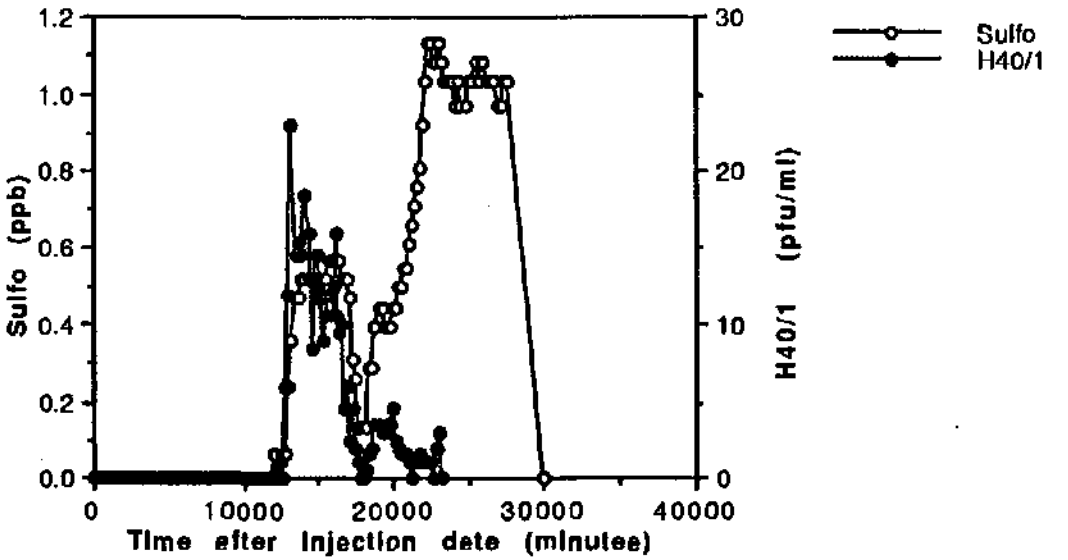

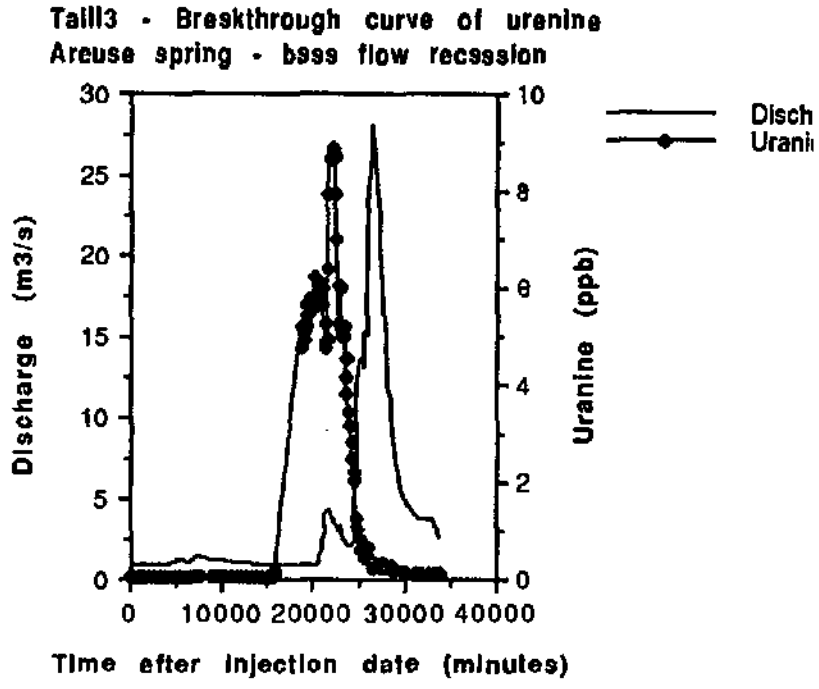
Taill3 - Breskthrough curve of urenine
Areuse spring - bsss flow recssion
Disch
Urani
Discharge (m3/s)
Uranine (ppb)
Time after injection date (minutes)

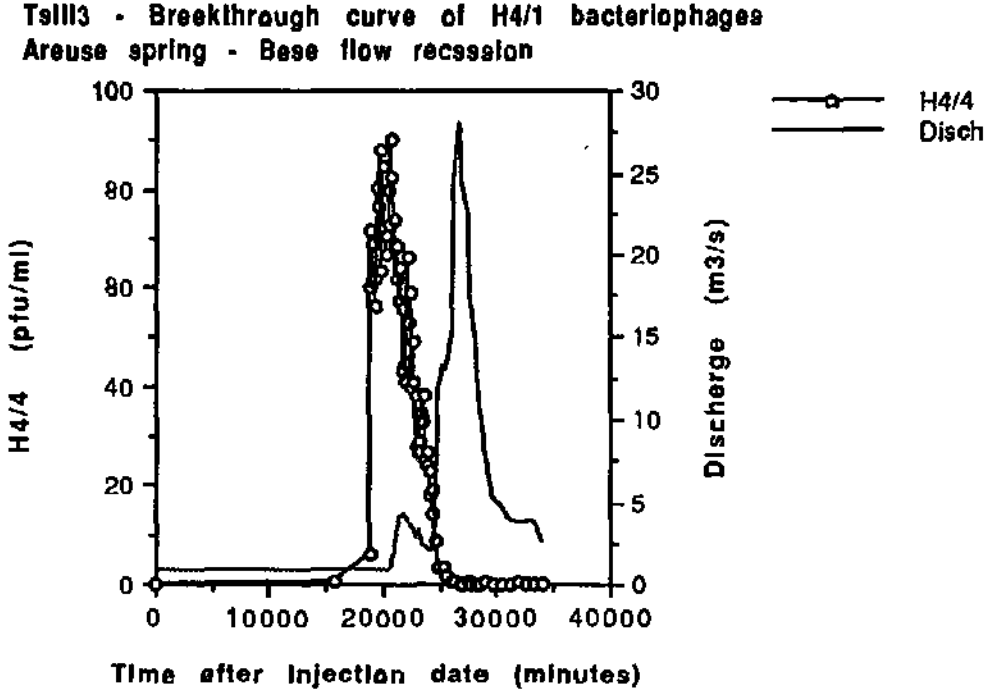
Tsill3 - Breekthrough curve of H4/1 bacteriophages
Areuse spring - Bese flow recession
H4/4
Disch
H4/4 (pfu/ml)
Discherge (m3/s)
Time after injection date (minutes)

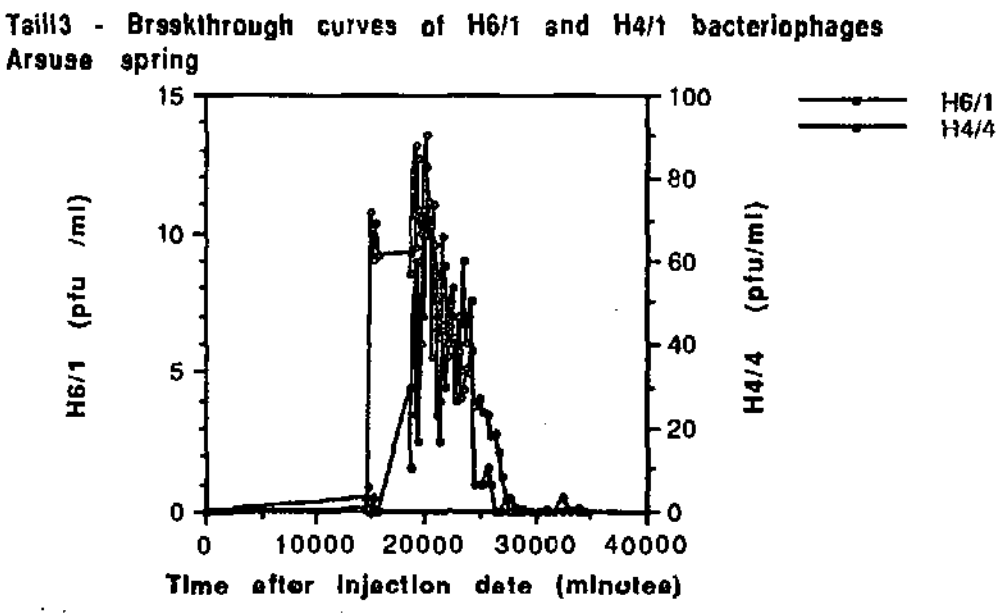
Taill3 - Brsskthrough curves of H6/1 and H4/1 bacteriophages
Arsuse spring
H6/1
H4/4
H6/1 (pfu /ml)
H4/4 (pfu/ml)
Time after injection date (minutes)

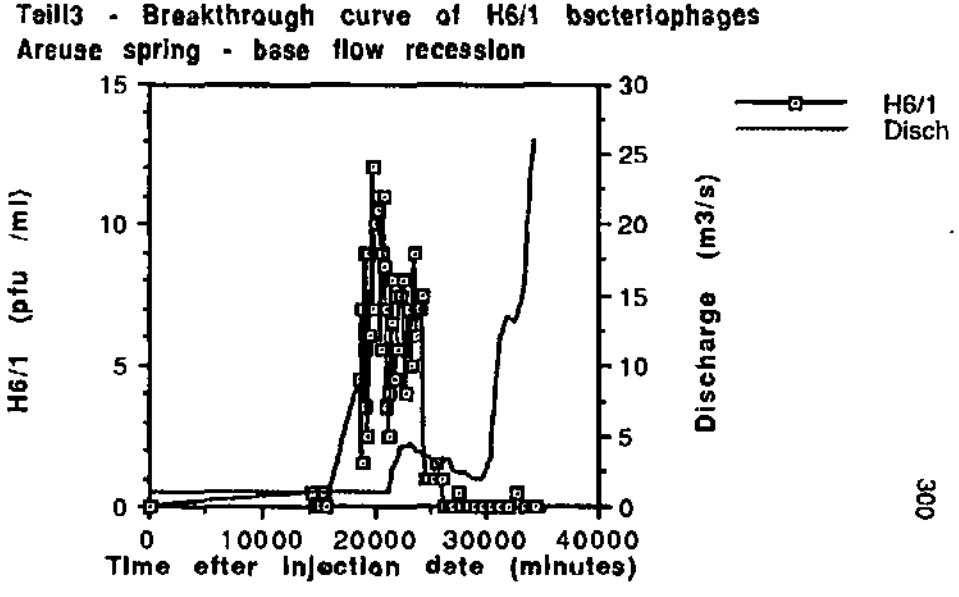
Teill3 - Breakthrough curve of H6/1 bacteriophages
Areuse spring - base flow recession
H6/1
Disch
H6/1 (pfu /ml)
Discharge (m3/s)
Time after injection date (minutes)

APPENDIX II.12

Table of tracer tests with phages

Tracing tests carried out on the Bure Plateau (Ajola, Swiss Jura)

Classical and microbiological tracing tests

Ament = Up-underground karstic network

Injection date	Code	TRACER	Mass (KG OU PFU)	Recovery %	Discharge (l/s)	Injection duration	Injection site	Surface of WCS	Position on hydrograph	Tracing distance (m)
2.11.1994	T43outamont.dat	NaCl	350	91	85	triang. 15'	surface point 1	5 km2	Falling limb	20
2.11.1994	T43Boutamont.dat	Uranine	7.26E+10	13	85	triang. 15'	surface point 1	5 km2	Falling limb	20
12.12.1994	T44outamont.dat	naphtionate	2.00	0%	85	.	borehole MIL9	5 km2	rising limb / before rising up	435
12.12.1994	T44Boutamont.dat	HBF1	6.21E+08	0%	85	.	borehole MIL9	5 km2	small falling limb / before rising up	435
12.12.1994	T45outamont.dat	NaCl	100	78.6	235.5	triang. 15'	surface point 1	5 km2	Falling limb	20
12.12.1994	T45Boutamont.dat	HADF1	4.03E+10	9	235.5	triang. 15'	surface point 1	5 km2	Falling limb	20
18.1.1995	T47outamont.dat	NaCl	250	69	87.75	triang. 15'	borehole MIL3	5 km2	Base flow recession	432
18.1.1995	T47Boutamont.dat	HBF1	1.43E+12	8	87.75	triang. 15'	borehole MIL3	5 km2	Base flow recession	432
18.1.1995	T47Boutamont.dat	HADF1	5.93E+11	30	87.75	triang. 15'	borehole MIL3	5 km2	Base flow recession	432
4.4.1995	T50outamont.dat	NaCl	300	98	87.3	triang. 10'	borehole MIL3	5 km2	Falling limb	432
4.4.1995	T50Boutamont.dat	HBF1	4.41E+12	23	87.9	triang. 10'	borehole MIL3	5 km2	Falling limb	432
4.4.1995	T50Boutamont.dat	HADF1	7.26E+12	160	87.9	triang. 10'	borehole MIL3	5 km2	Falling limb	432
4.5.1995	T51Boutamont.dat	HBF1	5.45E+12	3	29.93	triang. 14'	borehole MIL3	5 km2	Base flow recession	432
4.5.1995	T51Boutamont.dat	HBF4	3.63E+11	6	29.93	triang. 14'	borehole MIL3	5 km2	Base flow recession	432
4.5.1995	T51Boutamont.dat	HADF1	1.57E+13	40	29.93	triang. 14'	borehole MIL3	5 km2	Base flow recession	432
4.5.1995	T51outamont.dat	NaCl	250	65	29.93	triang. 14'	borehole MIL3	5 km2	Base flow recession	432
21.8.1995	T53Boutamont.dat	T7	6.25E+13	2	45	triang. 13'	borehole MIL3	5 km2	Base flow recession	432
21.8.1995	T53Boutamont.dat	HBF1	2.01E+12	négatif	45	triang. 13'	borehole MIL3	5 km2	Base flow recession	432
21.8.1995	T53Boutamont.dat	HBF4	5.04E+13	23	45	triang. 13'	borehole MIL3	5 km2	Base flow recession	432
21.8.1995	T54Boutamont.dat	Pst2	1.27E+12	6	45	triang. 9'	surface point 1	5 km2	Base flow recession	20
21.8.1995	T54outamont.dat	HADF1	9.31E+15	16	45	triang. 9'	surface point 1	5 km2	Base flow recession	20
21.8.1995	T55Boutamont.dat	HADF1	8.30E+12	60	19.21	triang. 34'	borehole MIL3	5 km2	Base flow recession	432
21.8.1995	T55outamont.dat	T7	6.11E+13	9.5	19.21	triang. 34'	borehole MIL3	5 km2	Base flow recession	432
21.8.1995	T56Boutamont.dat	T1	4.98E+13	0.75	19.21	triang. 13'	surface point 1	5 km2	Base flow recession	20
21.8.1995	T56Boutamont.dat	Pst2	3.32E+11	21	19.21	triang. 13'	surface point 1	5 km2	Base flow recession	20
22.8.1995	T57Boutamont.dat	T1	6.50E+12	0.5	66.87	triang. 13'	borehole MIL3	5 km2	Falling limb	432
22.8.1995	T57Boutamont.dat	T7	3.88E+13	1.3	66.87	triang. 13'	borehole MIL3	5 km2	Falling limb	432
22.8.1995	T57Boutamont.dat	HBF1	4.10E+12	13	66.87	triang. 13'	borehole MIL3	5 km2	Falling limb	432
22.8.1995	T57Boutamont.dat	HADF1	8.98E+12	73.5	66.87	triang. 13'	borehole MIL3	5 km2	Falling limb	432
22.8.1995	T57woutamont.dat	uranine	0.45	94	66.87	triang. 13'	borehole MIL3	5 km2	Falling limb	432
22.8.1995	T57wouamont.dat	uranine	0.45	90	66.87	triang. 13'	borehole MIL3	5 km2	Falling limb	432

		Transfert functions - Kernel function				S transfert functions		
Code	Step time	MAX (Ligne)	Max. step time number	Step time at Cg	MODE	Gradient at 0.3	Gradient at 0.5	Gradient at 0.8
T43outamont.dat	1	1.77E-09	278	71.7	unimodal	89	87	87
T43Boutamont.dat	1	3.30E-03	200	66.5	bimodal	87.5	87	76
T44outamont.dat	.	.	.	.	.	.	.	.
T44Boutamont.dat	.	.	.	.	.	.	.	.
T45outamont.dat	1	2.57E-09	102	59.6	unimodal	88	87.5	86
T45Boutamont.dat	1	3.14E-02	187	55.5	unimodal	90	87.5	87.5
T46outamont.dat	1	4.00E-03	1651	329.7	unimodal	48.9	86.5	82
T47outamont.dat	1	3.5aE-09	992	308.4	unimodal	85	84	82
T47Boutamont.dat	1	2.93E-03	1803	318.5	unimodal	85.5	86.5	82
T50outamont.dat	1	2.26E-03	1802	552.8	unimodal	84	86	58
T50Boutamont.dat	1	4.38E-03	2296	308.8	unimodal	87	85	80
T50outamont.dat	1	3.17E-03	1838	305.5	unimodal	85	83	78
T51outamont.dat	1	2.26E-03	1811	889.3	bimodal	89	90	85
T51Boutamont.dat	1	3.00E-03	2552	707.6	bimodal	87	87	86
T51Boutamont.dat	1	3.00E-03	2802	973.2	unimodal	85	84	72
T51outamont.dat	1	3.00E-03	1795	634.85	unimodal	88.5	84	86.5
T53Boutamont.dat	1	3.00E-03	1332	525.5	unimodal	87	85	76
T53Boutamont.dat	1	.	.	.	.	.	.	.
T53Boutamont.dat	1	3.34E-03	1932	517	unimodal	87	85	70
T54Boutamont.dat	1	6.48E-03	1324	275.75	bimodal	88	83	71
T54outamont.dat	1	5.56E-03	1104	244.5	bimodal	83	80	75
T55Boutamont.dat	1	8.55E-03	1525	639.2	unimodal	88.5	85	78
T55outamont.dat	1	4.20E-03	1310	855	unimodal	86.5	85	76
T56Boutamont.dat	1	4.98E-03	1905	78	unimodal	90	90	88
T56outamont.dat	1	3.50E-03	1385	112	unimodal	90	90	47
T57Boutamont.dat	1	3.60E-03	1859	388	bimodal	87	86.5	80
T57Boutamont.dat	1	3.88E-03	1859	521.5	bimodal	85	83.5	73
T57outamont.dat	1	3.3aE-03	1838	483.5	bimodal	89	87	78
T57Boutamont.dat	1	4.5aE-03	1859	422.67	bimodal	88	85	79
T57wouamont.dat	1	3.10E-03	1784	456.25	bimodal	86	87	76
T57wouamont.dat	1	3.10E-03	1704	456.75	bimodal	88	87	78

Tracing tests carried out on the Bure Plateau (Ajoie, Swiss Jura)

Velocities

Code	Mean transit velocity (m/h)	Modal velocity (m/h)	Max. velocity (m/h)
T42oulamont.dat	17	22.5	60
T43Boutamont.dat	18	27.3	54.5
T44oulamont.dat	-	-	-
T44Boutamont.dat	-	-	-
T45oulamont.dat	10	63.5	216
T45Boutamont.dat	33	72	216
T47oulamont.dat	124	115	195
T47Boutamont.dat	70	66	161
T47Boutamont.dat	85	89	161
T50B1oulamont.dat	74	131	271
T50B2oulamont.dat	68	126	271
T50oulamont.dat	50	94	271
T51Boutamont.dat	28	57	78
T51Boutamont.dat	38	74	78
T51Boutamont.dat	47	74	108
T51oulamont.dat	43	85	150
T53Boutamont.dat	32	70	123
T53Boutamont.dat	-	-	-
T53Boutamont.dat	33	70	123
T54Boutamont.dat	8	34	72
T54oulamont.dat	5	34	50
T55Boutamont.dat	42	46	59
T55Boutamont.dat	41	43	58
T56Boutamont.dat	15	19	29
T56Boutamont.dat	11	19	29
T57Boutamont.dat	66	102	271
T57Boutamont.dat	52	66	271
T57Boutamont.dat	59	104	244
T57Boutamont.dat	64	104	244
T57ureetamont.dat	60	79	250
T57ureutamont.dat	60	79	250

Tracing tests carried out on the Noiraigue watercatchment basin (Swiss Jura)

Injection date	Code	TRACER	Mass [KG OU PFU]	Recovery %	Discharge (l/s)	Injection duration	Injection site	Surface of WCB	Position on hydrograph	Tracing distance (m)
28.7.1995	NOIR1DUA	Duasino	2.8	85%	1000	15 min	Brot dessus-swallowhole	70 km2	Falling limb	695
28.7.1995	NOIR1H4	H4/1, bacteriophages	3.68E+13	51%	1000	15min	Brot dessus-swallowhole	70 km2	Falling limb	695
28.7.1995	NOIR1SULFOG	Sulforhodamine G extra	3.18	32%	800	10min	R. Berthoud - Swallowhole	70 km2	Base flow recession	2441
28.7.1995	NOIR1URA	Uranine	3.00E+99	min 35%	1000	45min	Voisinage- swallowhole	70 km2	Base flow recession	3920
28.7.1995	NOIR2DUA	Duasino	3.00E+99	98%	1850	15min	Brot dessus-swallowhole	70 km2	Falling limb	695
28.7.1995	NOIR2H4	H4/, bacteriophages	1.69E+14	34%	1950	15min	Brot dessus-swallowhole	70 km2	Falling limb	695
28.7.1995	NOIR2SULFO	Sulforhodamine G extra	3.18E+00	65%	2500	10min	R. Berthoud - swallowhole	70 km2	Falling limb	2343
28.7.1995	NOIR2T7	T7, bacteriophages	4.34E+14	2%	2500	5min	Combe Varin - swallowhole	70 km2	Falling limb	2441
28.7.1995	NOIR2URA	Uranine	3	85%	1300	45min	Voisinage- swallowhole	70 km2	Base flow - rising and falling limb	3920

Transfert functions - Kernel function | *S transfert functions*

	Code	Step time at Gavity center	MAX (1/hour)	Max. step time numbers	Step time	MODE	Gradient at 0.2	Gradient at 0.5	Gradient at 0.8
20.9.1995	NOIR1DUA	4774.75	6.23E-04	8188	0.1 hour	unimodal	93	83	60
20.9.1995	NOIR1H4	4337	2.99E-03	8188	0.1 hour	unimodal	97	87	77
20.9.1995	NOIR1SULFOG	228.8	1.04E-03	8188	0.1 hour	(plurl) unimodal	92	83	64
20.9.1995	NOIR1URA	5536.1	6.07E-04	8163	0.1 hour	unimodal	93.5	83.5	60
20.9.1995	NOIR2DUA	861.5	3.78E-03	4565	0.1 hour	unimodal	88	87	75
20.9.1995	NOIR2H4	874.75	8.47E-03	4428	0.1 hour	unimodal	89	88	89
20.9.1995	NOIR2SULFO	893.54	5.12E-03	4579	0.1 hour	unimodal	89	86	76
20.9.1995	NOIR2T7	849.14	6.82E-03	4430	0.1 hour	unimodal	88	87	50
20.9.1995	NOIR2URA	407.15	2.23E-03	2192	0.1 hour	bimodal	87	86	80

	Code	Mean transit velocity (m/h)	Model velocity (m/h)	Max. velocity (m/h)
28.7.1995	NOIR1DUA	1.45	1.65	2
28.7.1995	NOIR1H4	1.6	1.75	2.15
28.7.1995	NOIR1SULFOG	11	30	68.5
28.7.1995	NOIR1URA	7.1	8.15	11.25
20.9.1995	NOIR2DUA	8	11.1	41
20.9.1995	NOIR2H4	10.5	11.1	66
20.9.1995	NOIR2SULFO	35	81	66
20.9.1995	NOIR2T7	27.6	75.8	14.5
20.9.1995	NOIR2URA	27.6	28.6	14.5

APPENDIX GC.1.

Theoretical background of the 1D numerical analytical transport method - various cases of 1D transport simulation

Appendix GC.1.

Theoretical background of the 1D numerical analytical transport model (Mermoud, 1982).

The purpose of a dispersion-advection model is to find analytical solutions for various initiel and boundary conditions of the following equation:

$$\frac{\partial C}{\partial t} = \alpha u \left(\frac{\partial^2 C}{\partial t^2} \right) - \left(\frac{\partial C}{\partial x} \right) \quad (1)$$

The solution of this equation (1) considering fixed flux conditions [step injection] in the case of an one-dimensionnal semi-infiniyt environment is written as following:

$$C(x,t) = \frac{Co}{2} \exp\left(\frac{x}{2\alpha}\right) \left[\exp\left(\frac{-x}{2\alpha}\right) erfc\left(\frac{(x-ut)}{2\sqrt{(\alpha ut)}}\right) + \left(\frac{2ut}{\sqrt{2\Pi\, \alpha ut}}\right) \exp\left(\frac{\left(-x^2 + u^2 t^2\right)}{4\alpha ut}\right) - \left(1 + \frac{x}{\alpha} + \frac{ut}{\alpha}\right) \exp\left(\frac{x}{2\alpha}\right) erfc\left(\frac{(x+ut)}{2\sqrt{\alpha ut}}\right) \right]$$

whith C= concentration [kg/m^3]

X= distance from the origin [m]

t= time [s]

u = flow velocity [m/s]

α= dispersivity [m]

$$C_0 = \left(\frac{\Delta M}{\Delta t}\right) \frac{1}{(L e m_e u)} \quad [kg/m^3]$$

where $\frac{\Delta M}{\Delta t}$ = fixed mass flux [kg/s]

L = " widness " of the aquifer [m]

e = " thickness " of the aquifer [m]

m_e = efficient porosity [1]

u= flow velocity [m/s]

with the tollowing initiel conditions:

$$Cu - \left(\alpha u \frac{\partial C}{\partial t}\right) = C_0 u \quad when \quad t \geq 0$$

the tollowing flux conditions:

$$C(\infty, t) = 0 \quad when \quad t \geq 0$$

Various cases of 1D transport simulation

The various cases of simulation presented herebelow, take into account coherant values of dispersivity, flow velocity end tracing distence with tracing tests performed in karstic environment.

The considered dispersivity velues are in the renge 1 to 100m. Some measured velues of dispersivity from the interpretation of tracing tests carried out in Belgium karstic aquifers, with dispersion-edvection models (Seuty, 1988) and with an ADTS model (diffusion, exchange with immobile weter, without absorption) (Raven et al., 1988) are in the range 2 to 200m (Meus, 1994). Accarding Rossier et el., 1992 these values of dispersivity,

resulting of computering such models, are affected of a scale effect and are quite often overestimated, as the models do not consider the hydraulic source term. Nevrethless, these values give the scale of sizes of plausible dispersivity values in a karstic environment. They are the following: 1m (α1), 5m (α2), 10m (α3), 50m (α4) and 100m (α5). .

The flow velocities are choosen from the mean transit velocities of tracing tests carried out in low and high discharge rates in karstic aquifers. The scale of sizes of these velocities is similar than those measured within a karstic aquifer - narrow pass, small waterpathways, large rooms - for some tracing tests in the Milandrine and in the Hölloch karstic system (Bögli, 1980).

We hold the following values for the velocity:

V_1 = 0.0015m/s ; V_2= 0.003m/s; V_3=0.007m/s; V_4=0.03m/s; V_5=0.1m/s.

The tracing distances are also plausible distances with the experimental situations: 20m, 200m and 5000m.

Other parameters remain fixed for all simulations:

C_0= fixed mass flux when x=0 is 50 kg/m^3 (for example, the section can be 2m x 1m and the efficient porosity between 0.5 to 5).

Duration of the simulation: 20 hours = 72'000 seconds.

Table 1

1D simulations cases

Co= 50 kg/m3 ; d1=20m; Tbegin=0sec; Tend =72'000sec.

Flow velocity [m/s]	Dispersivity α1 1m	Disparsivity α2 5m	Disparsivity α3 10m	Dispersivity α4 50m	Disparsivity α5 100m
V1=0.0015	Tav1d1a1	Tav1d1a2	Tav1d1a3	Tav1d1a4	Tav1d1a5
V2= 0.003	Tav2d1a1	Tav2d1a2	Tav2d1a3	Tav2d1a4	Tav2d1a5
V3= 0.007	Tav3d1a1	Tav3d1a2	Tav3d1a3	Tav3d1a4	Tav3d1a5
V4= 0.03	-	Tav4d1a2	Tav4d1a3	Tav4d1a4	Tav4d1a5
V5= 0.1	-	Tav5d1a2	Tav5d1a3	Tav5d1a4	Tav5d1a5

Table 2

1D simulations cases

Co= 50 kg/m3 ; d2=200m; Tbegin=0sec; Tend =72'000sec.

Flow velocity [m/s]	Disparsivity α1 1m	Dispersivity α2 5m	Dispersivity α3 10m	Dispersivity α4 50m	Dispersivity α5 100m
V1=0.0015	-	Tav1d2a2	Tav1d2a3	Tav1d2a4	Tav1d2a5
V2= 0.003	-	Tav2d2a2	Tav2d2a3	Tav2d2a4	Tav2d2a5
V3= 0.007	Tav3d2a1	Tav3d2a2	Tav3d2a3	Tav3d2a4	Tav3d2a5
V4= 0.03	Tav4d2a1	Tav4d2a2	Tav4d2a3	Tav4d2a4	Tav4d2a5
V5= 0.1	Tav5d2a1	Tav5d2a2	Tav5d2a3	Tav5d2a4	Tav5d2a5

Table 3

1D simulations cases

Co= 50 kg/m3 ; d3=5000m; Tbegin=0sec; Tend =72'000sec.

Flow velocity [m/s]	Dispersivity α1 1m	Dispersivity α2 5m	Dispersivity α3 10m	Dispersivity α4 50m	Dispersivity α5 100m
V1=0.0015	-	-	-	-	-
V2= 0.003	-	-	-	-	-
V3= 0.007	-	-	-	-	-
V4= 0.03	-	-	-	-	-
V5= 0.1	-	-	-	Tav5d3a4	Tav5d3a5

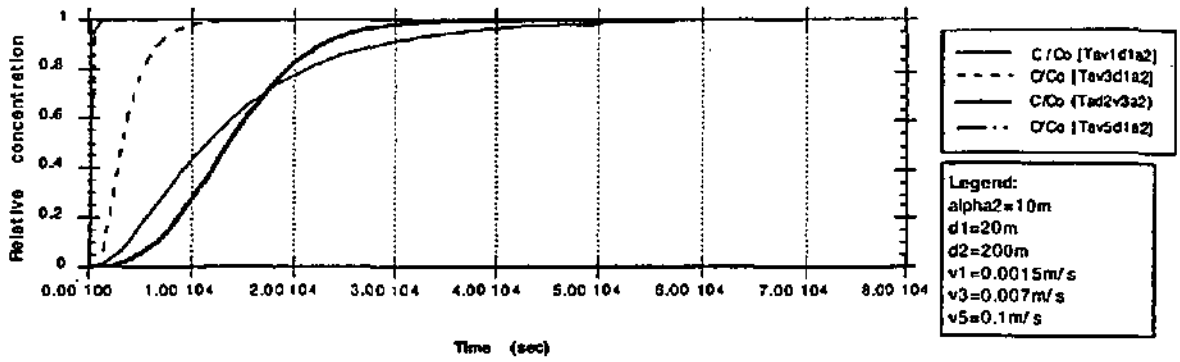

Fig. GC1: Effect of distance and velocity on transfer curve

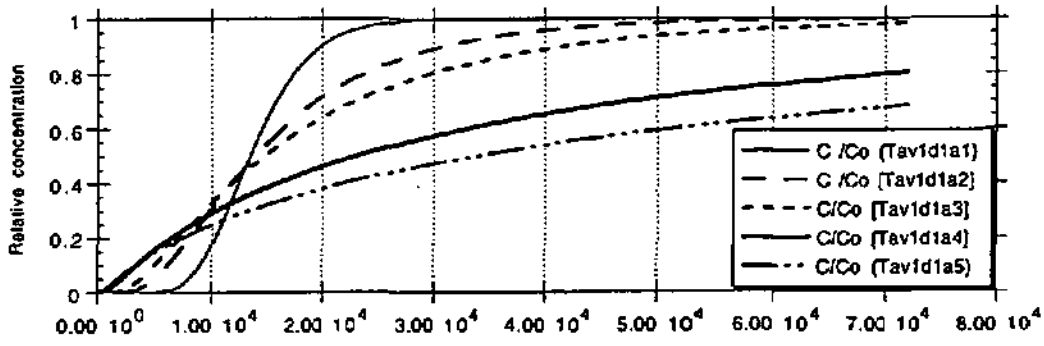

Fig. GC2: Effect of dispersivity on transfer curve

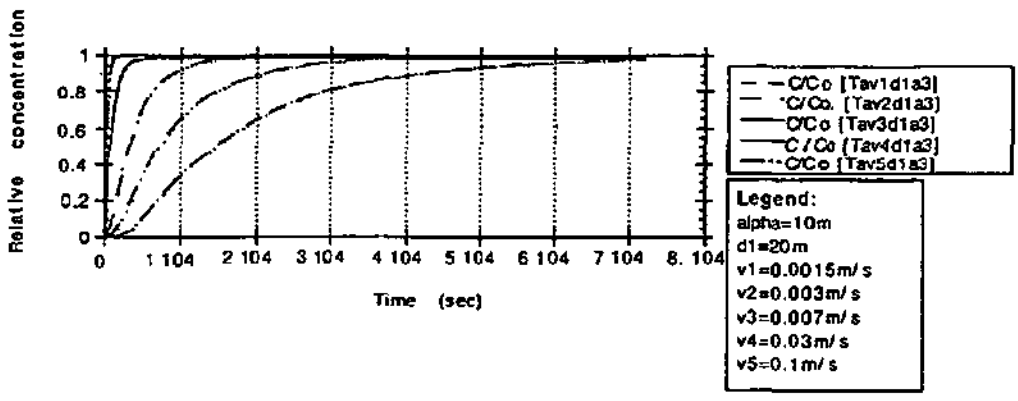

Fig. GC3: Effect of flow velocity on transfer curve

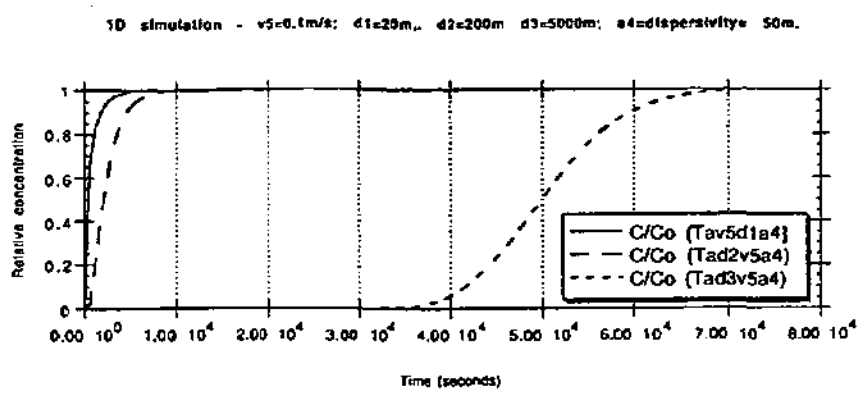

Fig. GC4: Effect of distance on transfer curve

Advances in karst groundwater protection strategy from the artificial tracer tests analysis and multiattribute vulnerability mapping (EPIK method)

by

Nathalie DOERFLIGER

University of Neuchâtel, Center of Hydrogeology, Switzerland

Key words: *Groundwater protection, karst aquifers, artificial tracer tests, input-response model, transfer functions, parametric conceptual model, vulnerability, multiattribute overlay method.*

Karst groundwater protection is a major issue in environmental concern at the end of the 20th century. Karst areas provide large quantities of water for water supply at springs and wells in Europe as well as in Switzerland. Karst environment can be troublesome water sources in certain cases, due either to an accident in a very sensitive area or also to inappropriate protection zones and corresponding regulations.

Karst aquifers are characterized generally by on the one hand, highly heterogeneous structure with the existence of a high hydraulic conductivity karst network more or less connected, developed and surrounded by an important volume of fissured rocks with a low hydraulic conductivity. On the other hand, diffuse and concentrated infiltration with limited filtering and auto-purification action of the contaminants occurs.

In matter of karst groundwater protection, therefore, specific strategy has to be developed as required by the Federal Office of the Environment, Forest and Landscape and the dependent Swiss National Hydrological and Geological survey. Two approaches referring to specific conceptual models had been used in the framework of this thesis in order to answer to the following questions on the one hand: does exist a mean transfer function based on artificial tracer tests, that characterizes a given water catchment basin or a part of it and can we use this transfer function to establish some contaminant predicting scheme in the framework of a hydrogeological impact assessment ? And on the other hand, to suggest an appropriated method to outline the groundwater protection zones of karst water catchment basin, as concentric protection zones are not suitable in karst environment due to its specific hydrological features.

Considering the tracing-system (tracing pathway) as an input-response model (black box model), artificial tracer tests are interpreted in terms of transfer functions - impulse response and / or indicial response. The transfer function as impulse response is obtained by deconvolution of the tracer breakthrough curve by its corresponding input function. The indicial response corresponds to the convolution of the impulse response by a step-unit function. In order to determine mean transfer function to specific parts of a water catchment basin or the whole water catchment basin, a study of variability of the transfer functions by variance and multivariance analyses on the gradients at given percentiles of the indicial response and on the modal velocity based on around 100 artificial tracer tests (fluorescent dyes, NaCl salt) carried out in various karst aquifers in Switzerland (Tabular and Folded Jura, Alps (Helvetic realm)) and in various hydrological conditions has been led to, determine the validity of a mean transfer function. The following parameters had been taken into consideration in the variance analysis: geological context, water catchment size, injection site's nature, hydrological conditions, tracing distance and discharge level.

Results of this variability study show that mean transfer functions for a water catchment basin do not exist ! No significant difference of the considered parameters is relevant. Nevertheless, mean transfer functions from tracer tests corresponding to a given geological context or to a given injection point's nature can be differentiated. The validity of the transfer functions intra-water catchment basin is important and depends principally to the injection sites. At the scale of a water catchment basin, tracer tests are not the single tool used to protect the groundwater: a multiattribute approach has to be applied to assess the vulnerability.

In order to outline groundwater protection zones of a water catchment basin an input-response method for tracing-pathway characterizing is not sufficient. An original multiattribute approach based on a parametric conceptual model of the karst aquifer, the EPIK method has been specifically developed for outlining and rating the water catchment basin taking into account the groundwater sensitivity to all kinds of contaminants. EPIK for Epikarst, Protective cover, Infiltration conditions and Karst network development has been applied on two test-sites in the Swiss Jura (St-Imier's springs water catchment basin in the Folded Jura and the Font, Saivu and Bâme's water catchment basin in the Tabular Jura (Bure)) to assess the vulnerability. The resulting vulnerability maps were the basis for outlining the groundwater protection zones according to the Swiss water and environment regulations.

By applying this method on these two test-sites using a GIS, it appears that outlining karst groundwater protection zones from the multiattribute vulnerability mapping is feasible in a reasonable time invest. If the weighting of key attribute into protection factor appears to be logical, the obtained values may dangerously hide the weakness of the method in a simple index. Although the concept underlying these new vulnerability mapping approach is clear nowadays, further developments are still needed to appreciate fully its pertinence, specifically regarding the epikarst, the protective cover attributes and the validation of the weighting system that is still problematic. On critical points in a water catchment basin, tracer tests may be carried out.

In the framework of hydrological impact assessment, it remains useful to carry out repeated tracer tests, at least three, in various and/or extreme hydrological conditions to define characteristic transfer functions, used to establish contaminant forecasting.